frontiers | Research Topics

Neural responses for rehabilitation of the elderly: Evidence from the micro, meso to macro scale

Edited by
Le Li, Chuhuai Wang, Howe Liu, Sheng Li and Wenxin Niu

Published in
Frontiers in Aging Neuroscience

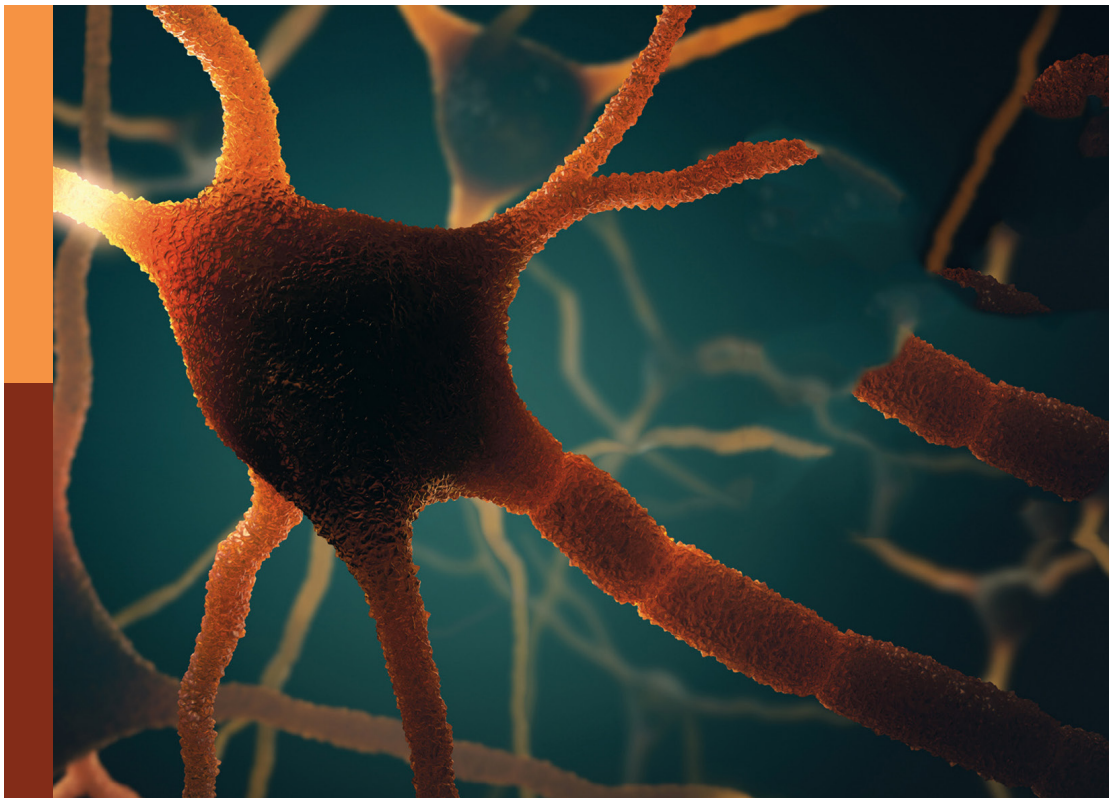

ISSN 1664-8714
ISBN 978-2-8325-2561-6
DOI 10.3389/978-2-8325-2561-6

About Frontiers

Frontiers is more than just an open access publisher of scholarly articles: it is a pioneering approach to the world of academia, radically improving the way scholarly research is managed. The grand vision of Frontiers is a world where all people have an equal opportunity to seek, share and generate knowledge. Frontiers provides immediate and permanent online open access to all its publications, but this alone is not enough to realize our grand goals.

Frontiers journal series

The Frontiers journal series is a multi-tier and interdisciplinary set of open-access, online journals, promising a paradigm shift from the current review, selection and dissemination processes in academic publishing. All Frontiers journals are driven by researchers for researchers; therefore, they constitute a service to the scholarly community. At the same time, the *Frontiers journal series* operates on a revolutionary invention, the tiered publishing system, initially addressing specific communities of scholars, and gradually climbing up to broader public understanding, thus serving the interests of the lay society, too.

Dedication to quality

Each Frontiers article is a landmark of the highest quality, thanks to genuinely collaborative interactions between authors and review editors, who include some of the world's best academicians. Research must be certified by peers before entering a stream of knowledge that may eventually reach the public - and shape society; therefore, Frontiers only applies the most rigorous and unbiased reviews. Frontiers revolutionizes research publishing by freely delivering the most outstanding research, evaluated with no bias from both the academic and social point of view. By applying the most advanced information technologies, Frontiers is catapulting scholarly publishing into a new generation.

What are Frontiers Research Topics?

Frontiers Research Topics are very popular trademarks of the *Frontiers journals series*: they are collections of at least ten articles, all centered on a particular subject. With their unique mix of varied contributions from Original Research to Review Articles, Frontiers Research Topics unify the most influential researchers, the latest key findings and historical advances in a hot research area.

Find out more on how to host your own Frontiers Research Topic or contribute to one as an author by contacting the Frontiers editorial office: frontiersin.org/about/contact

Neural responses for rehabilitation of the elderly: Evidence from the micro, meso to macro scale

Topic editors

Le Li — Northwestern Polytechnical University, China
Chuhuai Wang — Sun Yat-sen University, China
Howe Liu — Allen College, United States
Sheng Li — University of Texas Health Science Center at Houston, United States
Wenxin Niu — Tongji University, China

Citation

Li, L., Wang, C., Liu, H., Li, S., Niu, W., eds. (2023). *Neural responses for rehabilitation of the elderly: Evidence from the micro, meso to macro scale*. Lausanne: Frontiers Media SA. doi: 10.3389/978-2-8325-2561-6

Table of contents

frontiers | Frontiers in Aging Neuroscience

TYPE Editorial
PUBLISHED 15 May 2023
DOI 10.3389/fnagi.2023.1208578

OPEN ACCESS

EDITED AND REVIEWED BY
Kristy A. Nielson,
Marquette University, United States

*CORRESPONDENCE
Le Li
✉ lile5@nwpu.edu.cn

RECEIVED 19 April 2023
ACCEPTED 02 May 2023
PUBLISHED 15 May 2023

CITATION
Li L, Li S, Liu H, Niu W and Wang C (2023) Editorial: Neural responses for rehabilitation of the elderly: evidence from the micro, meso to macro scale.
Front. Aging Neurosci. 15:1208578.
doi: 10.3389/fnagi.2023.1208578

Editorial: Neural responses for rehabilitation of the elderly: evidence from the micro, meso to macro scale

Le Li[1]*, Sheng Li[2], Howe Liu[3], Wenxin Niu[4] and Chuhuai Wang[5]

[1]Institute of Medical Research, Northwestern Polytechnical University, Xi'an, China, [2]McGovern Medical School, University of Texas Health Science Center at Houston, Houston, TX, United States, [3]Department of Physical Therapy, Allen College, Waterloo, IA, United States, [4]School of Medicine, Shanghai Yangzhi Rehabilitation Hospital, Tongji University, Shanghai, China, [5]Department of Rehabilitation Medicine, First Affiliated Hospital, Sun Yat-sen University, Guangzhou, China

KEYWORDS

rehabilitation, elderly, stroke, Parkinson's disease, motor function, neuromodulation

Editorial on the Research Topic
Neural responses for rehabilitation of the elderly: evidence from the micro, meso to macro scale

The 19 articles in the Research Topic "*Neural Responses for Rehabilitation of the Elderly: Evidence from the Micro, Meso, to Macro Scale*" cover a variety of neural responses after motor exercise and rehabilitation intervention in older adults as well as in people with neurological disease. Among them, three original research articles addressed the impact of noninvasive brain stimulation, such as repetitive transcranial magnetic stimulation (rTMS) and continuous and intermittent theta burst stimulation (iTBS), on the functions of post-stroke and Parkinson's disease (PD). One review article examined the effect of rTMS on Alzheimer's disease and another provided a summary of non-invasive brain stimulation (NIBS) for osteoarthritis (OA). Moreover, four other articles highlight the effects of exercise therapy, such as Tai Chi, on mild cognitive impairment in the elderly, dance movement therapy (DMT) for neurodegenerative diseases, exercise intervention on social distancing in middle-aged and elderly patients with chronic low back pain, as well as robotic-assisted rehabilitation treatment of hand function. Further, nine articles covered various topics related to applied basic research on the elderly, including four articles on functional near-infrared spectroscopy (fNIRS) for subacute stroke, age-related differences in response to visual stimuli from EEG, the relationship between motor imagery (MI) and age-related fatigue, and post-stroke sensory deficiency in response to cold stimulation from EEG as well as five articles focused on the peripheral neuromuscular system, such as dual-task gait analysis in middle-aged to older people, the role of the diaphragm in postural stability and visceral function in PD, H-Reflex from lateral gastrocnemius among elderly people with peripheral neuropathy, and sarcopenia related to body composition and gait analysis. Last but not least, one basic research article covered the association between mitochondrial function and rehabilitation of PD by exosomal mRNA and lncRNA expression profiles.

Exercise interventions

Tai Chi is a form of light-to-moderate-intensity mind-body exercise for seniors. In a review, Wang, Liu et al. showed that Tai Chi can improve cognitive functions and alleviate the accompanying symptoms of mild cognitive impairment in the elderly by potentially activating the expression of signals in different brain regions, altering their neural connectivity, increasing the brain volume, and modulating brain-derived neurotropic and inflammation factors. However, more studies are required to determine the frequency and duration of training to optimize the beneficial effects of Tai Chi on mild cognitive impairment.

DMT is the psychotherapeutic use of movement as a process that promotes the emotional, social, cognitive, and physical integration of the individual. In a systematic review, Wu et al. discussed the effects of DMT on motor function, cognitive deficit, mood, and quality of life in people with neurodegenerative diseases. This review showed that DMT can effectively improve motor function and cognitive deficits in neurodegenerative diseases. Future research on the effects of DMT on Alzheimer's disease requires scientific design, large sample size, long-term comprehensive intervention, and clear reporting standards. The same team also investigated the effect of exercise on social distancing in middle-aged and elderly patients with chronic low back pain. The authors concluded that the 8-week exercise intervention cannot only shorten the social distance and improve the abnormal behavior of social distancing regulation of middle-aged and elderly patients with chronic low back pain, but can also relieve pain, disability, and negative emotions. More studies may be needed to explore the long-term effects of exercise intervention, and further work is required to determine whether this new finding equally applies to other types of exercise.

Li, Zhang et al. implemented a hybrid brain computer interface (BCI) paradigm based on MI and steady-state visual evoked potential (SSVEP). In this study, EEG data from 12 healthy participants were collected, and the activation regions of THE MI-SSVEP paradigm were identified by power spectral density. This study verified the clinical effect of THE MI-SSVEP intervention paradigm for 61 stroke patients by applying robot assisted therapy with the MI-SSVEP intervention paradigm, which demonstrated significant functional improvement in these patients.

Non-invasive brain stimulation

In various neurological diseases, NIBS has been actively explored. It is believed that NIBS induces excitatory changes in the underlying cerebral cortex in a non-invasive manner and lasting changes in neuroplasticity. Cao et al. conducted a randomized, case-control study of rTMS combined with respiratory muscle training for pulmonary rehabilitation after ischemic stroke. The authors found that the combined intervention showed a stronger increase in lung function detection indexes than respiratory muscle training alone and that the combined intervention could improve lung functionality after acute ischemic stroke. As a special kind of rTMS, iTBS has been proved to recover the function balance in stroke patients when conducted on the cerebellar vermis (Wang, Huang et al.). Zheng, Chen et al. designed and proposed a study protocol on cerebellar continuous theta burst stimulation (cTBS) for aphasia rehabilitation, which may further help researchers to investigate the efficacy of cTBS treatment on the right cerebellum in augmenting language recovery in chronic post-stroke aphasia. In order to analyze the effects of rTMS on global cognitive function in Alzheimer's disease, Zhang, Sui et al. conducted a systematic review and meta-analysis. The authors found that rTMS is a safe, potentially effective treatment and can induce long-lasting effects for cognitive impairment in AD. Another review from Zhu et al. summarized the therapeutic effects and mechanisms of different NIBS techniques (including TMS, electrical stimulation, ultrasound stimulation, and random noise stimulation) in OA, and clarified the potential of NIBS as a treatment choice for OA, which may provide prospects and suggestions for further research.

Signal processing in aging or related disease: from central nervous system to peripheral neuromuscular system

Li, Chen et al. investigated EEG characteristics during MI by comparing young and elderly participants, and studied convolutional neural networks (CNN) classification for the elderly population in terms of fatigue analysis in both frontal and parietal regions. The authors demonstrated that the elderly are less affected by the level of cognitive fatigue during MI compared to the young subjects as the controls. The deep learning method also provides a potentially feasible option for the application of MI-BCI in the elderly by considering ERD and fatigue. Zhang, Jiang et al. also analyzed age-related differences in the transient EEG response in visual BCIs from visual evoked potential (VEP)/motion onset VEP (mVEP) and SSVEP/SSMVEP between the younger group and the elderly group. Their findings showed that the amplitudes of P1 elicited by motion onset are significantly higher in the senior group, which might be a potential advantage for seniors if mVEP-based BCIs is used. EEG could also be applied to study reduced elementary somatosensation after stroke. Huang et al. designed a new configuration for the measurement of post-stroke elementary thermal sensation by non-painful cold stimulation and the post-stroke cortical responses were investigated and compared with unimpaired persons. The results revealed that post-stroke cortical responses during stimulation and sensory deficiency were characterized by a wide distribution of representative EEG relative spectral power bands, lowered resolution toward different temperatures, and extensive activated sensory cortical areas. As well as EEG, fNIRS was also proved to be a useful tool to investigate reorganization of the brain network after stroke. Yuan et al. analyzed hemispheric dominance differences in the task-state motor network properties of subacute stroke by fNIRS and the results revealed that the changes in macroscale cortical network indicators were similar between the left hemisphere stroke (LHS) and the right hemisphere stroke (RHS) groups, while those of the mesoscale indicators were different. The authors revealed that the brain network characteristics of RHS were affected by the severity of the dysfunction.

Meanwhile, quantitative evaluations of peripheral neuromuscular systems also attract researchers' interests.

Zheng, Lang et al. applied dual-task, three-dimensional gait analysis to mild cognitive impairment and age-matched controls, and principal component analysis was conducted to select the key biomechanical indexes from spatial-temporal parameters. Their results showed that there were significant differences in dual-task cost cadence during walking calculation tasks between the two groups, which may prove the potential value for application in the early identification of mild cognitive impairment in the clinic. Age-induced sarcopenia may negatively affect walking stability and increases the risk of falls, which represents the leading cause of accidental death in the elderly. Fan et al. analyzed and contrasted body the composition and gait characteristics of those with sarcopenia in relation to health controls. In the study, significant differences were found in certain gait parameters between elderly with sarcopenia and normal elderly participants, which were related to absolute muscle strength, suggesting that sarcopenia was a disease mainly caused by decreased muscle mass.

In an opinion article, Chen et al. reviewed the development of the motor unit number estimation (MUNE) method and discussed the feasibility and challenges of simulation-free MUNE, which is important to study motor units related to basic organizational and functional elements of neuromuscular control. The hoffmann reflex (H-reflex) assesses peripheral neuropathy (PN) adaptation in aged people, and Song et al. tried to find a reliable muscle among triceps surae during standing and walking in the PN population. Their results showed that LG was more reliable than SO and MG.

In patients with PD, Yu et al. found that gender and Hoehn and Yahr stages play significant roles in diaphragm thickness and exertion during resting breathing. The diaphragm's functionality is significantly correlated with the patient's postural stability, vocal capability, as well as with the respiratory, gastrointestinal, and urological functions. From the same lab, a randomized controlled trial study conducted on two small groups (intervention vs. control) compared how exosomal mRNA and lncRNA expression profiles may change after a 2-week rehabilitation intervention. The study revealed that the exosomal mRNA can be significantly upregulated while the lncRNAs can be significantly downregulated after the 2-week rehabilitation in comparison with the control group or in pre- and post-comparison within the PD patients; however, how the diaphragm might response to the rehabilitation was not assessed. The mRNA is related to mitochondrial respiration and lncRNA to pathogenesis of the disease. This may provide micro-level evidence why rehabilitation is beneficial to patients with PD.

Author contributions

All authors listed have made a substantial, direct, and intellectual contribution to the work and approved it for publication.

Conflict of interest

The authors declare that the research was conducted in the absence of any commercial or financial relationships that could be construed as a potential conflict of interest.

Publisher's note

All claims expressed in this article are solely those of the authors and do not necessarily represent those of their affiliated organizations, or those of the publisher, the editors and the reviewers. Any product that may be evaluated in this article, or claim that may be made by its manufacturer, is not guaranteed or endorsed by the publisher.

frontiers in Aging Neuroscience

ORIGINAL RESEARCH
published: 23 December 2021
doi: 10.3389/fnagi.2021.785020

The Role of the Diaphragm in Postural Stability and Visceral Function in Parkinson's Disease

Xin Yu[1†], Hong-ying Jiang[2†], Chen-xi Zhang[2], Zhao-hui Jin[3], Lei Gao[3], Rui-dan Wang[3], Jin-ping Fang[3], Yuan Su[3], Jia-ning Xi[2] and Bo-yan Fang[3*]*

[1] Beijing Rehabilitation Medical College, Beijing Rehabilitation Hospital, Capital Medical University, Beijing, China,
[2] Department of Respiratory Rehabilitation Center, Beijing Rehabilitation Hospital, Capital Medical University, Beijing, China,
[3] Parkinson Medical Center, Beijing Rehabilitation Hospital, Capital Medical University, Beijing, China

OPEN ACCESS

Edited by:
Chuhuai Wang,
Sun Yat-sen University, China

Reviewed by:
Dianyou Li,
Shanghai Jiao Tong University, China
Jung Hung Chien,
University of Nebraska Medical Center, United States

***Correspondence:**
Bo-yan Fang
fangboyanv@ccmu.edu.cn
Jia-ning Xi
xijn888@sina.com

[†] These authors have contributed equally to this work

Specialty section:
This article was submitted to Parkinson's Disease and Aging-related Movement Disorders, a section of the journal Frontiers in Aging Neuroscience

Received: *28 September 2021*
Accepted: *29 November 2021*
Published: *23 December 2021*

Citation:
Yu X, Jiang H-y, Zhang C-x, Jin Z-h, Gao L, Wang R-d, Fang J-p, Su Y, Xi J-n and Fang B-y (2021) The Role of the Diaphragm in Postural Stability and Visceral Function in Parkinson's Disease. Front. Aging Neurosci. 13:785020. doi: 10.3389/fnagi.2021.785020

Background: In normal subjects, the diaphragm plays a key functional role in postural stability, articulation, respiration, defecation, and urination.

Objectives: The aim of this study was to investigate the role of the diaphragm in postural stability and visceral function in patients with Parkinson's disease (PD) and to compare the diaphragm function by gender, Hoehn and Yahr (H&Y) staging, and motor subtypes.

Methods: In total, 79 patients were enrolled in this cross-sectional study. The severity of the disease was assessed by the Movement Disorder Society-Unified Parkinson's Disease Rating Scale III and by H&Y staging. Postural stability was quantitatively recorded, and respiratory function was evaluated by spirometry. Several scales were used to evaluate visceral function in patients with PD. In addition, diaphragm ultrasound was used to measure the excursion, contraction velocity, and thickness of the diaphragm during quiet breathing, deep breathing, and the sniff test. Significant features were selected by the least absolute shrinkage and selection operator (LASSO) regression and fitted in the multivariate linear regression and Pearson's correlation analysis.

Results: Diaphragm thickness and excursion during quiet breathing were significantly different between men and women and between H&Y stage 1–2 and stage 2.5–3, whereas the diaphragm function was not influenced by motor subtypes. It was shown that the diaphragmatic function was significantly correlated with postural stability, voice function, respiratory function, constipation, and urological function to varying degrees in patients with PD.

Conclusion: The diaphragmatic function is associated with dysfunction in PD although it remains unclear as to whether the observed changes in the diaphragm are primary or secondary.

Keywords: Parkinson's disease, diaphragm, postural stability, visceral function, motor subtypes

INTRODUCTION

Parkinson's disease (PD) is a common neurodegenerative disease that is associated with major motor symptoms, including resting tremors, rigidity, bradykinesia, and postural instability. Patients with postural instability are more likely to fall, leading to reduced mobility and life expectancy (Fasano et al., 2017). PD involves the accumulation of α-synuclein in multiple visceral systems which play essential roles in the non-motor symptoms (Pfeiffer, 2020), including dysarthria (Schalling et al., 2017), delayed gastric emptying and constipation (Fasano et al., 2015), urinary urgency, and nocturia (Jia et al., 2020). If not treated appropriately, the combination of motor and non-motor symptoms can significantly reduce the quality of life (QoL; Schapira et al., 2017). In addition, researchers have discovered abnormalities in the respiratory center during the early stages of PD that appear to arise from α-synuclein accumulation in the dorsolateral pons and ventrolateral medulla (Zhang et al., 2019).

The diaphragm is a muscle pump that plays a key role in generating negative intrathoracic pressures for ventilation and positive intra-abdominal pressures for expulsive behaviors and venous return. The non-ventilation function of diaphragm has been discussed the diaphragm generates no more than 30% of the maximal transdiaphragmatic pressure to maintain ventilation requirements during exercise while to perform expulsive maneuvers such as defecation and parturition, diaphragm generates almost maximal transdiaphragmatic pressures, which suggest the reserved capacity of the diaphragm for certain functions (Fogarty and Sieck, 2019). Specifically, although limits of stability (LOS) were significantly reduced in the elderly compared to the healthy young group, the diaphragm was thicker in the elderly, and the muscle thickness also had a positive correlation with LOS. The abovementioned findings from previous research may indicate the compensatory role of the diaphragm in postural stabilization (Özkal et al., 2019). Regarding the role of the diaphragm in phonation, the posterior and middle diaphragm is the main part to elevate and act as one functional unit to keep constant subglottic pressure during phonation (Traser et al., 2017). In terms of visceral function, the diaphragm, pelvic floor muscles, and abdominal muscles synergistically operate to maintain intra-abdominal pressure and accommodate to the changes in the abdominal cavity, for example, with increasing gas load in the colon, the diaphragm relaxes whereas the anterior abdominal wall increased the tone to enlarge intra-abdominal volume in healthy volunteers (Villoria et al., 2011). Besides, diaphragmatic breathing training in combination with strength training has also been demonstrated to improve overactive bladder, which may be associated with the activation of deeper muscle and the reduction of detrusor pressure (Hagovska et al., 2020).

Parkinson's disease is also a heterogeneous disease that could be classified into tremor dominant (TD) subtypes/indeterminate subtypes/postural instability and gait disorders (PIGD) subtypes according to the Movement Disorder Society-Unified Parkinson's Disease Rating Scale (MDS-UPDRS; Stebbins et al., 2013). Researches have demonstrated that such classification is more suitable in that it comprehensively reveals significant differences between different motor subtypes related to the activity of daily living, motor symptom severity, and cardiovascular and gastrointestinal symptoms (Ren et al., 2020). The progression of PD is often described using the Hoehn and Yahr (H&Y) staging, which weighted the bilateral motor symptoms involvement and balance control as the principal mark of disease severity (Hoehn and Yahr, 1967). The modified version of the H&Y scale introduced 0.5 increments to evaluate disease progression (Goetz et al., 2004).

Diaphragm function is characterized by diaphragm thickness during tidal breathing, diaphragm excursion during three maneuvers (i.e., quiet breathing, sniff test, and deep breathing), and diaphragm contraction velocity during quiet breathing and sniff test. The criteria of normal diaphragm function are based on the research from Sarwal et al. (2013) and Tuinman et al. (2020), in which male and female subjects always exhibit different standards. The objective of this study was to (1) compare the diaphragm function in patients with PD by gender, motor subtypes, and disease staging and (2) investigate the correlation between the diaphragm and postural stability, articulation, respiration, defecation, and urination in patients with PD.

MATERIALS AND METHODS

Participants

This cross-sectional study is part of an ongoing project (active and passive biofeedback and neuromodulation collaborative therapy system evaluation and clinical validation, ChiCTR1900020771, registered on January 19, 2019). In brief, we screened 436 patients between February 2019 and December 2020 from outpatient and the internet. Of note, 81 eligible patients were included in the project of the Parkinson's Medical Center, Beijing Rehabilitation Hospital, Capital Medical University, and two patients were dropped out (**Supplementary Figure 1**). We recruited patients between 30 and 75 years of age and in accordance with the clinical diagnostic criteria from the MDS (Postuma et al., 2015), including clinically established PD and probable PD with H&Y stage $\leq$3. The study was approved by the Ethics Committee of Beijing Rehabilitation Hospital of Capital Medical University (2018bkky022), and each patient signed an informed consent form.

We excluded patients with atypical Parkinsonism and those who had comorbidities, including cardiac diseases, respiratory diseases, and neurological diseases. A range of baseline information was collected including age, course of the disease, gender, H&Y stage, and 39-item Parkinson's Disease Questionnaire (PDQ-39). Motor subtypes were determined according to the method proposed by Stebbins et al. (2013), patients were characterized as TD subtypes if TD/PIGD ratio $\geq$1.15, if TD/PIGD ratio $\leq$0.9 then patients were considered as PIGD subtypes, and patients with a ratio between 0.9 and 1.15 were indeterminate.

Evaluation of Motor Function and Postural Stability

Motor function was evaluated by the MDS-UPDRS III with the same qualified physiotherapist. Postural stability was evaluated

by the Stability and Balance Learning Environment (STABLE) system (Motek, Amsterdam/Culemborg, Netherlands) without visual feedback. The mean velocity of the center of pressure (COP) was determined in the following three conditions during the "ON" state: standing on both feet with eyes open, standing on both feet with eyes closed, and tandem standing. During the evaluation, the patients were instructed to look ahead and to avoid using handrails. These evaluation methods provide us with information on static balance and postural stability in the patient's standing posture.

Evaluation of Visceral Function

Evaluation of respiratory function: All patients with PD were seated and wore nose clips to perform pulmonary function tests delivered by a skilled respiratory physician. Forced vital capacity (FVC) maneuver and vital capacity (VC) maneuver were conducted in accordance with the guidelines from the American Thoracic Society and the European Respiratory Society (Graham et al., 2019). VC, FVC, forced expiratory volume during the first second (FEV_1), and FEV_1/FVC were recorded.

Evaluation of voice function: The Voice Handicap Index-10 (VHI-10) is commonly used to evaluate voice function in patients with PD, which consists of five physical, three functional, and two emotional items (Sunwoo et al., 2014). Participants were scored based on the frequency of symptoms ranging from 0 (never happened) to 4 (always happens); therefore, a higher score indicated that the perceived symptoms were more severe. Due to the cultural differences between eastern and western societies, the physiological aspect accounts for a greater proportion in the simplified Chinese version (Li et al., 2012).

Evaluation of intestinal function: The Bowel Function Index (BFI) is a physician-scored assessment incorporating defecation difficulty, the perception of incomplete evacuation, and the overall judgment of constipation over the last week (Ducrotté and Caussé, 2012). Patients arbitrarily chose any number from 0 to 100 according to the severity of constipation for each question. The BFI is the mean score of three questions. The Patient Assessment of Constipation Quality of Life (PAC-QoL) is a 5-point Likert-type scale that consists of four subscales, including worries and concerns, physical suffering, mental suffering, and dissatisfaction (Marquis et al., 2005). A higher score in BFI or PAC-QoL indicated that the subjective judgment of constipation or related burden was more severe.

Evaluation of urological function: The International Consultation on Incontinence Questionnaire for Overactive Bladder (ICIQ-OAB) was used to evaluate the severity of lower urinary tract symptoms in patients with PD, including domains related to frequency, urgency, nocturia, and urinary incontinence (McDonald et al., 2020). The International Prostate Symptom Score (IPSS) was also used to evaluate the filling (three items) and voiding (four items) phases in patients with PD (Brusa et al., 2020). For both of these questionnaires, a higher score implied more severe symptoms in the lower urinary tract.

Ultrasound of the Diaphragm

Diaphragm ultrasound (GE, LOGIQ e, Germany) was performed by a skilled respiratory physician with ultrasound experience to measure bilateral excursion and contraction velocity as well as the thickness of the diaphragm during different maneuvers. Patients remained in the supine position during the examination. The thickness of the diaphragm was determined with a 10–15 MHz linear transducer placed perpendicular to the skin over the zone of apposition to the rib cage, between the midaxillary and antero-axillary line on both sides (**Figure 1A**; Vivier et al., 2012). In the zone of the apposition, the abdominal organs were observed to reach the bottom of the rib cage where the diaphragm was bounded by two echogenic layers (i.e., peritoneum and the diaphragmatic pleurae) (**Figure 1B**). The thickness of the diaphragm was defined as the distance between the peritoneum and the diaphragmatic pleurae. We recorded diaphragm thickness at end-expiration (DTEE) and end-inspiration (DTEI) until at least three breathing cycles had been captured. The diaphragm thickening fraction (DTF) was calculated by the following equation.

$$\mathrm{DTF} = \frac{(\mathrm{DTEI} - \mathrm{DTEE})}{\mathrm{DTEE}} \times 100\% \quad (1)$$

Diaphragm excursion was determined with a 2–5 MHz curved-array probe under the costal margin in the midclavicular line and perpendicular to the diaphragmatic dome on both sides of the body where the liver and spleen served as the acoustic window (**Figure 1C**). M mode was chosen to demonstrate the diaphragm excursion during quiet breathing (DE_{QB}), the sniff test (DE_{Sniff}), and deep breathing (DE_{DB}) (**Figure 1D**). The excursion was defined as the maximal perpendicular distance of diaphragm movement. We also determined the diaphragmatic contraction velocity during quiet breathing (DV_{QB}) and the sniff test (DV_{sniff}).

Statistical Analysis

Numerical variables were described as means ± SD or as medians and interquartile ranges according to the results of Kolmogorov–Smirnov or Shapiro–Wilk normality tests. Mean imputation was applied for missing values. Differences in the diaphragmatic parameters between gender and motor subtypes were assessed by the Mann–Whitney *U* test and the Kruskal–Wallis test; differences between H&Y stage 1–2 and stage 2.5–3 were also compared using the independent *t*-test or the Mann–Whitney *U* test; $p < 0.05$ was regarded as being statistically significant; and 95% CI was also analyzed. Statistical analysis was carried out with SPSS version 25.0 (IBM, Armonk, NY, United States). To overcome the data overfitting and select the main diaphragmatic variables, the least absolute shrinkage and selection operator (LASSO) regression was performed using the "glmnet" R package (Friedman et al., 2010). The regression model was determined when the penalty parameter lambda (λ) was minimum or plus one standard error. In one model related to postural stability (tandem standing), significant features were first fitted into the principal component analysis to exclude collinearity. Pearson's correlation analysis and multivariate linear regression were also used to determine the correlation between the diaphragmatic parameters and the dependent variables (i.e., postural stability, VHI-10, spirometry test, BFI, PAC-QoL, ICIQ-OAB, and IPSS).

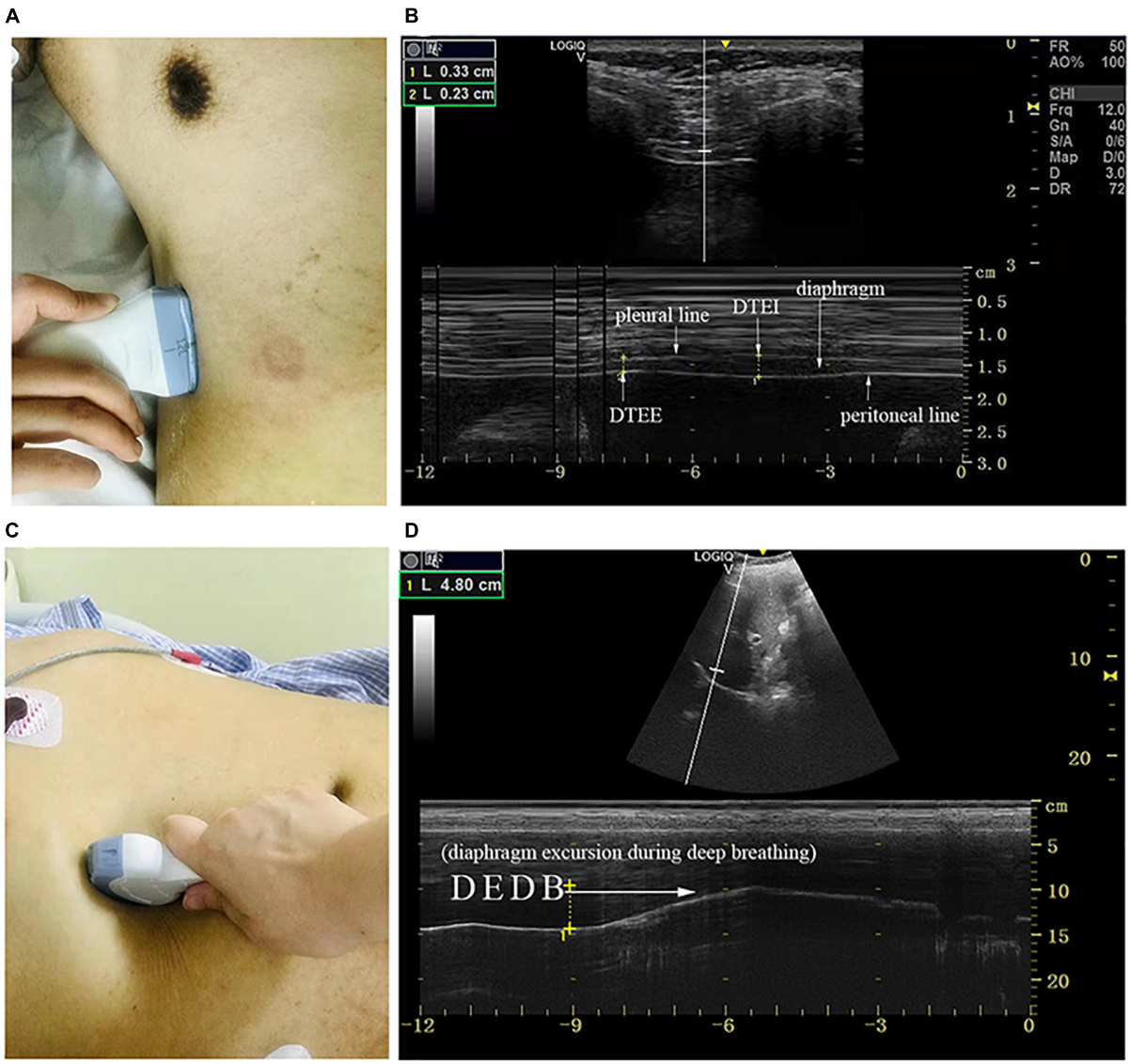

FIGURE 1 | The measurement of diaphragmatic thickness and excursion. **(A)** A 10–15 MHz probe was placed at the zone of apposition. **(B)** The non-echogenic layer between the yellow markers indicates the thickness of the diaphragm at the end of expiration and inspiration. **(C)** A 2–5 MHz curved-array probe was placed under the costal margin. **(D)** The bright line indicates diaphragmatic excursion during deep breathing. DTEE, diaphragm thickness at end-expiratory; DTEI, diaphragm thickness at end-inspiration; DE_{DB}, diaphragmatic excursion during deep breathing.

RESULTS

A total of 81 patients with PD were enrolled; two patients were dropped out. Demographic baseline information, such as disease duration, H&Y stages, and PDQ-39 score, was summarized in **Table 1**. The means of MDS-UPDRS III scores in the OFF and ON states were 38.87 and 30.57, respectively. The similar scores could be related to the fact that mild-to-moderate patients with PD may not manifest with motor fluctuations. Motor function and visceral function were also presented in **Table 1**.

Diaphragmatic parameters were divided into three categories, namely, thickness, excursion, and velocity. We not only presented the data from the overall cohort but also compared the data by gender (**Table 1**), H&Y stage (**Figure 2**), and motor subtypes (**Supplementary Table 1**). Compared with women, both diaphragmatic thickness and excursion during quiet breathing were significantly higher in men. The diaphragm function of patients with PD was beyond the pathological values. Patients in H&Y stage 1–2 presented significantly higher diaphragm thickness at the end of inspiration (0.38 ± 0.12 vs. 0.32 ± 0.09, $p = 0.025$), higher diaphragm excursion [1.46 (0.52) vs. 1.03 (0.57), $p = 0.007$], and higher contraction velocity during quiet breathing [1.09 (0.33) vs. 1 (0.34), $p = 0.03$] (**Figure 2**). In contrast, we did not find any significant differences in diaphragm function between motor subtypes. In addition, the

TABLE 1 | Clinical features and diaphragm function in patients with Parkinson's disease.

Characteristic	Overall Cohort (*n* = 79)	Male	Female	*P* value	Abnormal value
Demographic characteristics					
Age (year)	61.5 (9)	64 (13)	61 (8)	0.2	/
Disease duration (months)	78 (60)	6 (5.42)	7 (4.3)	0.5	/
Gender (male), n (%)	35 (44.3%)	35 (44.3%)	44 (55.7%)		/
Hoehn & Yahr stage, n (%)				0.6	/
Stage 1–1.5	6 (7.6%)	4	2		/
Stage 2	39 (49.4%)	18	21		/
Stage 2.5	16 (20.3%)	7	9		/
Stage 3	18 (22.8%)	6	12		/
PDQ-39 (score)	23.07 (13.46)	21.15 (11.3)	25.96 (12.83)	**0.02***	/
MDS-UPDRS III-ON (score)	30.57 ± 12.48	31.17 ± 13	30.67 ± 11	0.9	/
MDS-UPDRS III-OFF (score)	38.87 ± 14.17	37.68 ± 12.2	38.12 ± 14.6	0.9	/
Postural stability (COP)					
Eyes open (cm/s)	2.78 (0.98)	2.5 (1.1)	2.8 (0.9)	0.2	/
Eyes closed (cm/s)	2.83 (0.86)	2.7 (1.0)	2.9 (0.7)	0.14	/
Tandem standing (cm/s)	4.16 (1.90)	5.3 (2.3)	3.8 (1.1)	<0.001*	/
Voice function					
VHI-10 (score)	8 (7)	9 (8)	7 (7)	0.14	>7.5
Respiratory function					
VC (% of predicted)	100.48 ± 18.76	93.67 ± 14.56	105.89 ± 27.8	**0.02***	<80
FVC (% of predicted)	95.47 ± 15.40	92.23 ± 14.22	98.03 ± 22.5	0.1	<80
FEV_1 (% of predicted)	91.10 ± 14.82	90.36 ± 13.67	91.61 ± 15.81	0.7	<80
FEV_1/FVC (%)	78.12 ± 4.94	75.8 (6.5)	79.7 (5.2)	0.2	<70
Intestinal function					
BFI (score)	46.67 (53.33)	56.7 (53.3)	40 (48.75)	0.2	>29
PAC-QoL (score)	48 (20.05)	54 (37)	47 (31)	0.5	/
Urological function					
ICIQ-OAB (score)	4 (3)	4.8 (4)	4 (2)	0.4	Mild: 0–7; Moderate: 8–19; Severe: >20
IPSS (score)	8 (13)	8 (13)	/	/	
Diaphragm function					
DTEE (cm)	**0.21 (0.09)**	**0.23 (0.06)**	**0.20 (0.08)**	**0.005***	Men: <0.17; Women: <0.13
DTEI (cm)	**0.34 (0.14)**	**0.4 (0.15)**	**0.30 (0.13)**	**<0.001***	
DTF (%)	62 (43)	68 (56)	57.5 (42)	0.26	<20
DE_{QB} (R) (cm)	**1.2 (0.65)**	**1.45 (0.6)**	**1.13 (0.54)**	**0.028***	Men: <1; Women: <0.9
DE_{Sniff} (R) (cm)	4.35 ± 1.47	4.63 ± 1.51	4.12 ± 1.42	0.13	Men: <1.8; Women: <1.6
DE_{DB} (R) (cm)	4.89 ± 1.32	5.20 ± 1.43	4.64 ± 1.19	0.06	Men: <4.7; Women: <3.7
DV_{QB} (R) (cm/s)	1.07 (0.32)	1.09 (0.32)	1.02 (0.30)	0.13	/
DV_{Sniff} (R) (cm/s)	3.77 (1.8)	3.98 (2.34)	3.66 (1.39)	0.40	/
DE_{QB} (L) (cm)	1.24 (0.53)	1.33 (0.74)	1.21 (0.48)	0.24	/
DE_{Sniff} (L) (cm)	3.96 ± 1.3	4.02 ± 1.39	3.92 ± 1.24	0.74	/
DE_{DB} (L) (cm)	4.19 ± 1.23	4.16 ± 1.34	4.22 ± 1.15	0.82	/
DV_{QB} (L) (cm/s)	1.05 (0.41)	1.05 (0.49)	1.05 (0.37)	0.64	/
DV_{Sniff} (L) (cm/s)	3.78 (1.62)	3.57 (1.97)	3.78 (1.26)	0.45	/

*Data are expressed as means ± SD if normally distributed; otherwise, data are shown as medians with interquartile ranges (IQRs). *p < 0.05 (two-tailed) defined as being statistically significant and was shown in bold. n, number; PDQ-39, 39-item Parkinson's Disease Questionnaire; MDS-UPDRS, Movement Disorder Society-Unified Parkinson's Disease Rating Scale; COP, center of pressure; VHI-10, Voice Handicap Index-10; VC, vital capacity; FVC, forced vital capacity; FEV_1, forced expiratory volume during the first second; BFI, Bowel Function Index; PAC-QoL, Patient Assessment of Constipation Quality of Life; ICIQ-OAB, International Consultation on Incontinence Questionnaire for Overactive Bladder; IPSS, International Prostate Symptom Score; R, right; L, left; DTEE, diaphragm thickness at end-expiratory; DTEI; diaphragm thickness at end-inspiration; DTF, diaphragm thickening fraction; DE_{QB}, diaphragmatic excursion during quiet breathing; DE_{Sniff}, diaphragmatic excursion during sniff test; DE_{DB}, diaphragmatic excursion during deep breathing; DV_{QB}, diaphragm velocity during quiet breathing; DV_{Sniff}, diaphragm velocity during sniff test.*

right-to-left ratio during quiet breathing was within the normal but was higher in several patients during deep breathing (**Supplementary Table 2**).

In a further analysis, we selected several principal features through the LASSO regression (**Supplementary Figure 2** and **Supplementary Table 3**) and entered those features in the

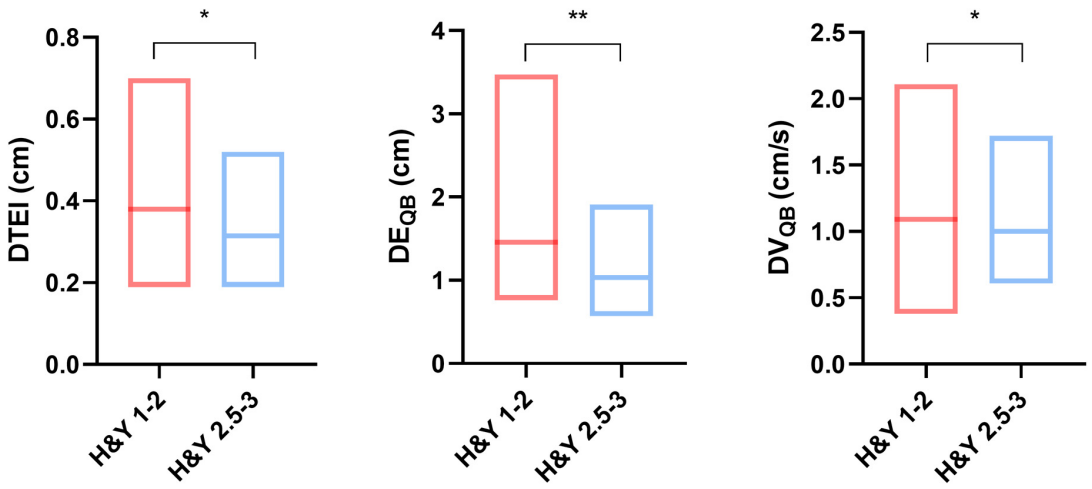

FIGURE 2 | Comparison of diaphragm function between different Hoehn and Yahr (H&Y) stages. *$p < 0.05$; **$p < 0.01$. DTEI, diaphragm thickness at end-inspiration; DE_{QB}, diaphragmatic excursion during quiet breathing; DV_{QB}, diaphragm velocity during quiet breathing.

multivariate linear regression analysis (**Table 2**). Diaphragm function was a significant predictor for static balance, voice, and respiratory function, while diaphragm together with age was determined as the significant predictors for intestinal and urological function. Pearson's correlation analysis (**Figure 3** and **Supplementary Table 4**) revealed that the contraction velocity of the diaphragm was positively correlated with postural stability during eyes open (r/p 0.29/0.009) and eyes closed (r/p 0.28/0.01). The diaphragmatic principal component extracted from excursion and contraction velocity was also positively correlated with postural stability during tandem standing (r/p 0.4/0.0003). In contrast, VHI-10 showed a negative correlation with a diaphragmatic excursion (r/p −0.3/0.007; −0.22/0.05). Besides, we also found significant correlation between diaphragm and respiratory function [i.e., FVC (r/p: −0.29/0.01) and FEV_1 (r/p: −0.25/0.03)], BFI (r/p −0.22/0.05), and PAC-QoL (r/p −0.26/0.02; −0.24/0.04). Furthermore, diaphragm contraction velocity was also positively correlated with the ICIQ-OAB scores (r/p 0.33/0.003) whereas thickness was negatively correlated with the IPSS scores (r/p −0.39/0.02).

DISCUSSION

In this study, we found that diaphragm function was influenced by gender in PD, which is consistent with other researches (Spiesshoefer et al., 2020; Tuinman et al., 2020). We also discovered that diaphragm function showed significant differences between H&Y stages, instead of motor subtypes in patients with PD. The result may be related to the fact that the diaphragm function in the earlier stage of PD showed more compensation ability than that in the later stage. The significant difference in diaphragm function in the progression of the disease may provide insight into the time window of rehabilitation. Besides, we identified correlations not only between the diaphragm and respiratory function but also between postural stability, voice, and intestinal and urological function in our cohort of patients. In the following, we would discuss how the diaphragm gets involved in the abovementioned physiological behaviors in sequence.

The result of the pulmonary function test showed that these patients should not be diagnosed with restrictive or obstructive ventilation dysfunction according to the Global Initiative for Chronic Obstructive Lung Disease (GOLD; Vogelmeier et al., 2017). Respiration is controlled by the active contraction of the diaphragm to expand the chest and lung and decrease the intrapulmonary pressure lower than atmospheric pressure. Obstructive and restrictive ventilation dysfunction may occur in patients with PD due to the reduced compliance of the rib cage or dystonia of the upper airway (Sabaté et al., 1996; Tsai et al., 2016). Considering the negative correlation between the right diaphragm contraction velocity and FVC or FEV_1, we deemed that diaphragm may indirectly compensate for relatively poorer respiratory function. Therefore, advanced PD patients with respiratory dysfunction may benefit from diaphragm training.

Postural instability may be related to the increased flexor muscle tone of the trunk which interferes with the projection of the center of mass to the base of support (Schoneburg et al., 2013); a reduction of proprioception and an increase of fatigue of the musculoskeletal system may also involve (Schoneburg et al., 2013; Moretto et al., 2021). In our study, the regression model suggested that diaphragm contraction velocity and excursion were higher in patients with poorer levels of control. Contraction velocity is an indicator of respiratory muscle strength (Sarwal et al., 2013) while increased mobility may elevate intra-abdominal pressure to stabilize the trunk and stimulate mechanoreceptors in the diaphragm crura (Hodges and Gandevia, 2000; Kocjan et al., 2018). The diaphragm may alter to activate core muscles and compensate for flexed posture in patients with PD. Soilemezi et al. (2020) also reported that

TABLE 2 | Main diaphragmatic parameters associated with postural stability and visceral function selected by the least absolute shrinkage and selection operator (LASSO) regression and the principal component analysis and fitted in the multivariate linear regression.

	Adjusted R^2	Standard β coefficient	*p* value
Postural stability (COP)			
Eyes open	0.08		
DV_{sniff} (R)		0.29	**0.009***
Eyes close	0.06		
DV_{sniff} (R)		0.28	**0.01***
Tandem standing	0.15		
PC 1		0.4	**<0.001***
Voice function	0.08		
DE_{sniff} (R)		−0.3	**0.007***
Respiratory function			
FVC	0.09		
DV_{QB} (L)		−0.27	**0.01***
Gender		0.16	0.14
FEV_1	0.09		
DV_{QB} (L)		−0.34	**0.005***
DV_{QB} (R)		0.25	**0.036***
Bowel function			
BFI	0.26		
Age		0.26	**0.02***
DV_{QB} (L)		−0.26	**0.02***
DE_{Sniff} (L)		−0.46	**0.001***
PAC-QoL	0.06		
DE_{DB} (L)		0.19	0.09
Age		0.27	**0.02***
Urological function			
ICIQ-OAB	0.26		
DV_{sniff} (L)		0.41	**<0.001***
Age		0.34	**0.001***
IPSS	0.32		
DTEE		−0.34	**0.02***
Age		0.45	**0.003***

**p < 0.05 presented in bold. COP, center of pressure; L, left; R, right; DV_{Sniff}, diaphragm velocity during sniff test; PC, principal component; DE_{Sniff}, diaphragmatic excursion during sniff test; FVC, forced vital capacity; DV_{QB}, diaphragm contraction velocity during quiet breathing; FEV_1, forced expiratory volume during the first second; DE_{DB}, diaphragmatic excursion during deep breathing; BFI, Bowel Function Index; PAC-QoL, Patient Assessment of Constipation Quality of Life; ICIQ-OAB, International Consultation on Incontinence Questionnaire for Overactive Bladder; IPSS, International Prostate Symptom Score; DTEE, diaphragm thickness at end-expiratory.*

patients who failed a weaning trial exhibited a higher peak transdiaphragmatic pressure and peak contraction velocity than healthy volunteers. They hypothesized that such alterations may compensate for diaphragmatic perfusion and were beneficial for recovering optimal muscle length to initiate the following contraction. Similarly, Özkal et al. (2019) indicated that the diaphragm was thicker in the elderly compared with the younger adults to compensate for atrophic lower limbs and maintain balance. The relationship between diaphragm function and balance function was further confirmed in longitudinal clinical trials: diaphragmatic breathing training or dynamic neuromuscular stabilization was able to promote balance function (Stephens et al., 2017; Yoon et al., 2020).

The score of VHI-10 indicated general dysphonia in this cohort of patients (Ng et al., 2020). PD can cause numerous changes in a patient's voice, including hypokinetic dysarthria and monotonic articulation (Ma et al., 2020). These deficits are due to incomplete closure of the glottis, rigidity of the laryngeal muscle, and the reduction of the expulsion of lung air volume per syllable (Hammer, 2013; Ma et al., 2020). Earlier studies proposed that the diaphragm could be regarded as separate functional units during phonation (Hammer, 2013; Traser et al., 2017, 2020). The posterior diaphragm was elevated to reduce lung volume during exhalation whereas the anterior diaphragm and rib cage remained in inhalation position. In this study, we found that VHI-10 decreased by 0.3 points for every unit increase in diaphragm excursion. The positive correlation between diaphragm and voice function implied that the patients with dysphonia tend to amplify diaphragmatic excursion to facilitate subglottal pressure or respiratory drive to enhance voice function.

The BFI score indicated that constipation was quite common among our cohort of patients (Madeo et al., 2015). Constipation appears to be caused by delayed colonic transit and paradoxical movements of the pelvic floor muscles in PD. In this study, we found that patients with less burden tend to reserve better diaphragm function. The impaired diaphragmatic function may be caused by the dysfunction of pelvic floor muscles in PD. The pelvic floor muscles operate with other synergistic muscles, such as the diaphragm and deep erectors, to maintain intra-abdominal pressure (Szczygiel et al., 2018; Hwang et al., 2021). It is reasonable to suggest that paradoxical movement of the pelvic floor muscles might impact the diaphragm. Correlations between the diaphragm and defecation have also been reported. For example, patients with diaphragm weakness often experience defecation difficulty; diaphragm pacing has also been shown to improve defecation in quadriplegic patients (Perry et al., 2010). PD Patients with constipation could benefit from respiratory rehabilitation by improving diaphragm excursion or contraction velocity, and an increase in contraction velocity may help to recruit diaphragmatic motor units and compensate for lower gastrointestinal peristalsis (Fogarty and Sieck, 2020).

The loss of dopaminergic neurons in the substantia nigra pars compacta is known to lead to the disinhibition of the micturition reflex in the pons, thus resulting in an overactive bladder in patients with PD (Jost, 2012; Pfeiffer, 2020). The role of the diaphragm in reducing urinary incontinence has been demonstrated in a randomized clinical trial which assigned patients with radical prostatectomy to diaphragm training or pelvic floor muscle training, and researchers observed comparable effects between groups (Zachovajeviene et al., 2019). The diaphragm, abdominal muscles, and pelvic floor muscles are known to be functionally linked by numerous myofascial connections (Mazur-Bialy et al., 2020). Previous studies have reported that the combination of pelvic floor muscle exercise and urge suppression and voiding schedules effectively reduced the frequency of micturition and the severity of OAB and also improved the QoL (McDonald et al., 2020).

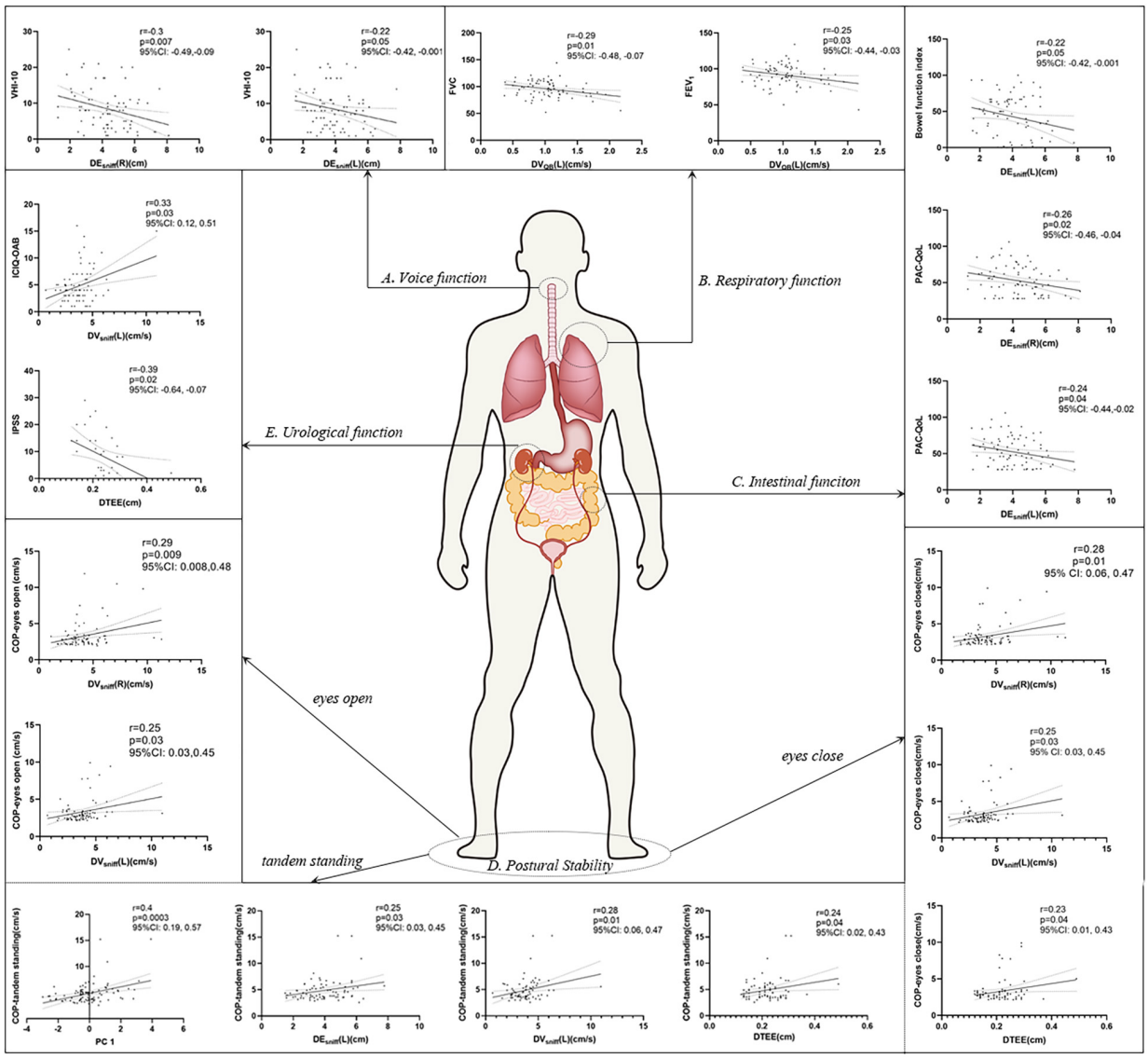

FIGURE 3 | Pearson's correlation analysis between the diaphragm and voice **(A)**, respiratory **(B)**, intestinal **(C)**, postural stability **(D)**, and urological function **(E)**. $p < 0.05$ was considered to be statistically significant. VHI-10, voice handicap index-10; PC, principal component; FVC, forced vital capacity; FEV_1, forced expiratory volume during the first second; BFI, Bowel Function Index; PAC-QoL, Patient Assessment of Constipation Quality of Life; ICIQ-OAB, International Consultation on Incontinence Questionnaire for Overactive Bladder; IPSS, International Prostate Symptom Score; COP, center of pressure.

Other researchers have found that reducing abdominal fat and practicing diaphragmatic breathing could improve the severity of overactive bladders in young women (Hagovska et al., 2020). The underlying principle of these observations relates to the reduction of detrusor pressure, an increase in urethral pressure, and the inhibition of the urination reflex. We found that patients with higher OAB score tended to show better diaphragm function. We assumed that OAB in PD may stimulate the potential of the diaphragm to function as a whole to compensate for the impairment. With regard to IPSS, the diaphragm was thinner in patients with a severer symptom. Training of the diaphragm or pulmonary rehabilitation may be considered for patients with PD who suffered from urinary dysfunction.

Our data indicated that the diaphragm plays a role in postural stability and visceral function in PD. However, there are some limitations in our study. First, although diaphragm ultrasound has been used extensively in patients with respiratory disorders, this technique is not routinely applied for patients with PD. Consequently, the reliability and reproducibility of this technique need to be evaluated in patients with PD. Second, the diaphragm ultrasound was taken during the ON state; whether the diaphragm exerts different effects during the OFF state still needs to be clarified. Third, this study was exploratory; future longitudinal studies should be rigorously designed and recruit a larger number of participants to fully confirm the potential role of the diaphragm in PD.

CONCLUSION

The diaphragm was influenced by gender and disease progression but not motor subtypes in patients with PD. Our investigations also demonstrated the correlations between the diaphragm and postural stability, vocal function, respiratory function, intestinal function, and urological function in PD.

DATA AVAILABILITY STATEMENT

The raw data supporting the conclusions of this article will be made available by the authors, without undue reservation.

ETHICS STATEMENT

The studies involving human participants were reviewed and approved by the Ethics Committee of Beijing Rehabilitation Hospital of Capital Medical University (2018bkky022). The patients/participants provided their written informed consent to participate in this study.

AUTHOR CONTRIBUTIONS

B-YF, J-NX, H-YJ, and XY conceived and designed the study. Z-HY, LG, and C-XZ performed the experiments. R-DW, J-PF, YS, and C-XZ collected patients' data. XY and B-YF performed the statistical analysis. XY wrote the first draft of the manuscript. B-YF, J-NX, and H-YJ reviewed and edited the manuscript. All authors contributed to the manuscript revision and read and approved the submitted version.

FUNDING

This study was supported by the National Key R&D Program of China (No. 2018YFC0115405) to B-YF and the Science and Technology Development Fund of Beijing Rehabilitation Hospital, Capital Medical University (2019R-006 to Z-HY and 2020-069 to B-YF). The funding body had no role in protocol design, statistical analysis, and manuscript preparation.

ACKNOWLEDGMENTS

We are grateful to all the patients and the medical staff of the Neurological Rehabilitation Center of Beijing Rehabilitation Hospital who contributed to this project.

SUPPLEMENTARY MATERIAL

The Supplementary Material for this article can be found online at: https://www.frontiersin.org/articles/10.3389/fnagi.2021.785020/full#supplementary-material

REFERENCES

Brusa, L., Ponzo, V., Stefani, A., Ceravolo, R., Palermo, G., Agrò, E. F., et al. (2020). Extended release levodopa at bedtime as a treatment for nocturiain Parkinson's disease: an open label study. *J. Neurol. Sci.* 410:116625. doi: 10.1016/j.jns.2019.116625

Ducrotté, P., and Caussé, C. (2012). The bowel function index: a new validated scale for assessing opioid-induced constipation. *Curr. Med. Res. Opin.* 28, 457–466. doi: 10.1185/03007995.2012.657301

Fasano, A., Canning, C. G., Hausdorff, J. M., Lord, S., and Rochester, L. (2017). Falls in parkinson's disease: a complex and evolving picture. *Mov. Disord.* 32, 1524–1536. doi: 10.1002/mds.27195

Fasano, A., Visanji, N. P., Liu, L. W. C., Lang, A. E., and Pfeiffer, R. F. (2015). Gastrointestinal dysfunction in Parkinson's disease. *Lancet Neurol.* 14, 625–639.

Fogarty, M. J., and Sieck, G. C. (2019). Evolution and functional differentiation of the diaphragm muscle of mammals. *Compr. Physiol.* 9, 715–766. doi: 10.1002/cphy.c180012

Fogarty, M. J., and Sieck, G. C. (2020). Spinal cord injury and diaphragm neuromotor control. *Expert Rev. Respir. Med.* 14, 453–464. doi: 10.1080/17476348.2020.1732822

Friedman, J., Hastie, T., and Tibshirani, R. (2010). Regularization paths for generalized linear models via coordinate descent. *J. Stat. Softw.* 33, 1–22.

Goetz, C. G., Poewe, W., Rascol, O., Sampaio, C., Stebbins, G. T., Counsell, C., et al. (2004). Movement disorder society task force report on the hoehn and yahr staging scale: status and recommendations. *Mov. Disord.* 19, 1020–1028. doi: 10.1002/mds.20213

Graham, B. L., Steenbruggen, I., Miller, M. R., Barjaktarevic, I. Z., Cooper, B. G., Hall, G. L., et al. (2019). Standardization of spirometry 2019 update. an official american thoracic society and european respiratory society technical statement. *Am. J. Respir. Crit. Care Med.* 200, e70–e88. doi: 10.1164/rccm.201908-1590ST

Hagovska, M., Švihra, J., Buková, A., Draèková, D., Horbacz, A., and Nagyová, I. (2020). Effect of an exercise programme for reducing abdominal fat on overactive bladder symptoms in young overweight women. *Int. Urogynecol. J.* 31, 895–902.

Hammer, M. J. (2013). Aerodynamic assessment of phonatory onset in Parkinson's disease: evidence of decreased scaling of laryngeal and respiratory control. *J. Parkinsons Dis.* 3, 173–179. doi: 10.3233/JPD-130180

Hodges, P. W., and Gandevia, S. C. (2000). Changes in intra-abdominal pressure during postural and respiratory activation of the human diaphragm. *J. Appl. Physiol.* 89, 967–976. doi: 10.1152/jappl.2000.89.3.967

Hoehn, M. M., and Yahr, M. D. (1967). Parkinsonism: onset, progression and mortality. *Neurology* 17, 427–442. doi: 10.1212/wnl.17.5.427

Hwang, U. J., Lee, M. S., Jung, S. H., Ahn, S. H., and Kwon, O. Y. (2021). Effect of pelvic floor electrical stimulation on diaphragm excursion and rib cage movement during tidal and forceful breathing and coughing in women with stress urinary incontinence: a randomized controlled trial. *Medicine* 100:e24158. doi: 10.1097/MD.0000000000024158

Jia, C., Cui, X., Yoshimura, N., Mao, W., Xu, E., Wang, Q., et al. (2020). Assessment and management of urinary dysfunction in 187 patients with parkinson's disease. *J. Parkinsons Dis.* 10, 993–1001. doi: 10.3233/JPD-191806

Jost, W. H. (2012). Urological problems in Parkinson's disease: clinical aspects. *J. Neural Transm.* 120, 587–591. doi: 10.1007/s00702-012-0914-8

Kocjan, J., Gzik-Zroska, B., Nowakowska, K., Burkacki, M., Suchoń, S., Michnik, R., et al. (2018). Impact of diaphragm function parameters on balance maintenance. *PLoS One* 13:e0208697. doi: 10.1371/journal.pone.0208697

Li, H., Huang, Z., Hu, R., Zhang, L., and Xu, W. (2012). Study on the simplified chinese version of the voice handicap index. *J. Voice* 26, 365–371. doi: 10.1016/j.jvoice.2011.01.002

Ma, A., Lau, K. K., and Thyagarajan, D. (2020). Voice changes in Parkinson's disease: what are they telling us? *J. Clin. Neurosci.* 72, 1–7. doi: 10.1016/j.jocn.2019.12.029

Madeo, G., Schirinzi, T., Natoli, S., Pierantozzi, M., Stefani, A., Dauri, M., et al. (2015). Efficacy and safety profile of prolonged release oxycodone in combination with naloxone (OXN PR) in Parkinson's disease patients with chronic pain. *J. Neurol.* 262, 2164–2170. doi: 10.1007/s00415-015-7823-3

Marquis, P., De La Loge, C., Dubois, D., McDermott, A., and Chassany, O. (2005). Development and validation of the patient assessment of constipation quality of life questionnaire. *Scand. J. Gastroenterol.* 40, 540–551. doi: 10.1080/00365520510012208

Mazur-Bialy, A. I., Kolomanska-Bogucka, D., Nowakowski, C., and Tim, S. (2020). Urinary Incontinence in Women: modern methods of physiotherapy as a support for surgical treatment or independent therapy. *J. Clin. Med.* 9:1211. doi: 10.3390/jcm9041211

McDonald, C., Rees, J., Winge, K., Newton, J. L., and Burn, D. J. (2020). Bladder training for urinary tract symptoms in Parkinson disease. *Neurology* 94, e1427–e1433. doi: 10.1212/WNL.0000000000008931

Moretto, G. F., Santinelli, F. B., Penedo, T., Mochizuki, L., Rinaldi, N. M., and Barbieri, F. A. (2021). Prolonged standing task affects adaptability of postural control in people with parkinson's disease. *Neurorehabil. Neural Repair* 35, 58–67. doi: 10.1177/1545968320971739

Ng, E., Law, T., Tang, E. C., Ho, F. N., Tong, M. C., and Lee, K. Y. (2020). The cutoff point and diagnostic accuracy of the voice handicap index in cantonese-speaking population. *J. Voice* 35, 163–168. doi: 10.1016/j.jvoice.2020.09.021

Özkal, Ö, Kara, M., Topuz, S., Kaymak, B., Bakı, A., and Özçakar, L. (2019). Assessment of core and lower limb muscles for static/dynamic balance in the older people: an ultrasonographic study. *Age Ageing* 48, 881–887. doi: 10.1093/ageing/afz079

Perry, S. F., Similowski, T., Klein, W., and Codd, J. R. (2010). The evolutionary origin of the mammalian diaphragm. *Respir. Physiol. Neurobiol.* 171, 1–16. doi: 10.1016/j.resp.2010.01.004

Pfeiffer, R. F. (2020). Autonomic dysfunction in parkinson's disease. *Neurotherapeutics* 17, 1464–1479.

Postuma, R. B., Berg, D., Stern, M., Poewe, W., Olanow, C. W., Oertel, W., et al. (2015). MDS clinical diagnostic criteria for Parkinson's disease. *Mov. Disord.* 30, 1591–1601. doi: 10.1002/mds.26424

Ren, J., Hua, P., Li, Y., Pan, C., Yan, L., Yu, C., et al. (2020). Comparison of three motor subtype classifications in de novo parkinson's disease patients. *Front. Neurol.* 11:601225. doi: 10.3389/fneur.2020.601225

Sabaté, M., González, I., Ruperez, F., and Rodríguez, M. (1996). Obstructive and restrictive pulmonary dysfunctions in Parkinson's disease. *J. Neurol. Sci.* 138, 114–119. doi: 10.1016/0022-510x(96)00003-2

Sarwal, A., Walker, F. O., and Cartwright, M. S. (2013). Neuromuscular ultrasound for evaluation of the diaphragm. *Muscle Nerve* 47, 319–329. doi: 10.1002/mus.23671

Schalling, E., Johansson, K., and Hartelius, L. (2017). Speech and communication changes reported by people with parkinson's disease. *Folia Phoniatr. Logop.* 69, 131–141.

Schapira, A. H. V., Chaudhuri, K. R., and Jenner, P. (2017). Non-motor features of Parkinson disease. *Nat. Rev. Neurosci.* 18, 435–450.

Schoneburg, B., Mancini, M., Horak, F., and Nutt, J. G. (2013). Framework for understanding balance dysfunction in Parkinson's disease. *Mov. Disord.* 28, 1474–1482. doi: 10.1002/mds.25613

Soilemezi, E., Savvidou, S., Sotiriou, P., Smyrniotis, D., Tsagourias, M., and Matamis, D. (2020). Tissue doppler imaging of the diaphragm in healthy subjects and critically Ill patients. *Am. J. Respir. Crit. Care Med.* 202, 1005–1012. doi: 10.1164/rccm.201912-2341OC

Spiesshoefer, J., Herkenrath, S., Henke, C., Langenbruch, L., Schneppe, M., Randerath, W., et al. (2020). Evaluation of respiratory muscle strength and diaphragm ultrasound: normative values, theoretical considerations, and practical recommendations. *Respiration* 99, 369–381. doi: 10.1159/000506016

Stebbins, G. T., Goetz, C. G., Burn, D. J., Jankovic, J., Khoo, T. K., and Tilley, B. C. (2013). How to identify tremor dominant and postural instability/gait difficulty groups with the movement disorder society unified Parkinson's disease rating scale: comparison with the unified Parkinson's disease rating scale. *Mov. Disord.* 28, 668–670. doi: 10.1002/mds.25383

Stephens, R. J., Haas, M., Moore, W. L. III, Emmil, J. R., Sipress, J. A., and Williams, A. (2017). Effects of diaphragmatic breathing patterns on balance: a preliminary clinical trial. *J. Manip. Physiol. Ther.* 40, 169–175. doi: 10.1016/j.jmpt.2017.01.005

Sunwoo, M. K., Hong, J. Y., Lee, J. E., Lee, H. S., Lee, P. H., and Sohn, Y. H. (2014). Depression and voice handicap in Parkinson disease. *J. Neurol. Sci.* 346, 112–115. doi: 10.1016/j.jns.2014.08.003

Szczygiel, E., Blaut, J., Zielonka-Pycka, K., Tomaszewski, K., Golec, J., Czechowska, D., et al. (2018). The impact of deep muscle training on the quality of posture and breathing. *J. Mot. Behav.* 50, 219–227. doi: 10.1080/00222895.2017.1327413

Traser, L., Burk, F., Ozen, A. C., Burdumy, M., Bock, M., Blaser, D., et al. (2020). Respiratory kinematics and the regulation of subglottic pressure for phonation of pitch jumps - a dynamic MRI study. *PLoS One* 15:e0244539. doi: 10.1371/journal.pone.0244539

Traser, L., Özen, A. C., Burk, F., Burdumy, M., Bock, M., Richter, B., et al. (2017). Respiratory dynamics in phonation and breathing—a real-time MRI study. *Respir. Physiol. Neurobiol.* 236, 69–77. doi: 10.1016/j.resp.2016.11.007

Tsai, C. C., Wu, M. N., Liou, L. M., and Chang, Y. P. (2016). Levodopa reverse stridor and prevent subsequent endotracheal intubation in Parkinson disease patients with bilateral vocal cord palsy: a case report. *Medicine* 95:e5559. doi: 10.1097/MD.0000000000005559

Tuinman, P. R., Jonkman, A. H., Dres, M., Shi, Z. H., Goligher, E. C., Goffi, A., et al. (2020). Respiratory muscle ultrasonography: methodology, basic and advanced principles and clinical applications in ICU and ED patients-a narrative review. *Intensive Care Med.* 46, 594–605. doi: 10.1007/s00134-019-05892-8

Villoria, A., Azpiroz, F., Burri, E., Cisternas, D., Soldevilla, A., and Malagelada, J. R. (2011). Abdomino-phrenic dyssynergia in patients with abdominal bloating and distension. *Am. J. Gastroenterol.* 106, 815–819. doi: 10.1038/ajg.2010.408

Vivier, E., Mekontso Dessap, A., Dimassi, S., Vargas, F., Lyazidi, A., Thille, A. W., et al. (2012). Diaphragm ultrasonography to estimate the work of breathing during non-invasive ventilation. *Intensive Care Med.* 38, 796–803. doi: 10.1007/s00134-012-2547-7

Vogelmeier, C. F., Criner, G. J., Martinez, F. J., Anzueto, A., Barnes, P. J., Bourbeau, J., et al. (2017). Global strategy for the diagnosis, management, and prevention of chronic obstructive lung disease 2017 report. GOLD executive summary. *Am. J. Respir. Crit. Care Med.* 195, 557–582.

Yoon, H. S., Cha, Y. J., and You, J. S. H. (2020). Effects of dynamic core-postural chain stabilization on diaphragm movement, abdominal muscle thickness, and postural control in patients with subacute stroke: a randomized control trial. *NeuroRehabilitation* 46, 381–389. doi: 10.3233/NRE-192983

Zachovajeviene, B., Siupsinskas, L., Zachovajevas, P., Venclovas, Z., and Milonas, D. (2019). Effect of diaphragm and abdominal muscle training on pelvic floor strength and endurance: results of a prospective randomized trial. *Sci. Rep.* 9:19192. doi: 10.1038/s41598-019-55724-4

Zhang, W., Zhang, L., Zhou, N., Huang, E., Li, Q., Wang, T., et al. (2019). Dysregulation of respiratory center drive (P0.1) and muscle strength in patients with early stage idiopathic parkinson's disease. *Front. Neurol.* 10:724. doi: 10.3389/fneur.2019.00724

Conflict of Interest: The authors declare that the research was conducted in the absence of any commercial or financial relationships that could be construed as a potential conflict of interest.

frontiers in Aging Neuroscience

OPINION
published: 11 February 2022
doi: 10.3389/fnagi.2022.799676

Motor Unit Number Estimation (MUNE) Free of Electrical Stimulation or M Wave Recording: Feasibility and Challenges

Maoqi Chen[1], *James Bashford*[2] *and Ping Zhou*[1]*

[1] *Faculty of Rehabilitation Engineering, University of Health and Rehabilitation Sciences, Qingdao, China,* [2] *Department of Basic and Clinical Neuroscience, UK Dementia Research Institute, Maurice Wohl Clinical Neuroscience Institute, Institute of Psychiatry, Psychology and Neuroscience, King's College London, London, United Kingdom*

Keywords: EMG-electromyogram, motor unit number estimate (MUNE), electrical stimulation, compound muscle action potential (CMAP), motor unit (MU)

OPEN ACCESS

Edited by:
Chuhuai Wang,
Sun Yat-sen University, China

Reviewed by:
Guang H. Yue,
Kessler Foundation, United States
Wens Hou,
Chongqing University, China
Yong Hu,
The University of Hong Kong, Hong Kong SAR, China

***Correspondence:**
Ping Zhou
dr.ping.zhou@outlook.com

Specialty section:
This article was submitted to Neurocognitive Aging and Behavior, a section of the journal Frontiers in Aging Neuroscience

Received: *21 October 2021*
Accepted: *10 January 2022*
Published: *11 February 2022*

Citation:
Chen M, Bashford J and Zhou P (2022) Motor Unit Number Estimation (MUNE) Free of Electrical Stimulation or M Wave Recording: Feasibility and Challenges. Front. Aging Neurosci. 14:799676. doi: 10.3389/fnagi.2022.799676

INTRODUCTION

The motor unit is the basic organizational and functional element for neuromuscular control. In motor neuron diseases, such as amyotrophic lateral sclerosis and spinal muscular atrophy, motor neurons progressively degenerate, resulting in a reduced number of motor units. Loss of motor units is also a major factor in development of sarcopenia (Gilmore et al., 2017). Although motor unit loss can be partially compensated by axonal branching and muscle fiber reinnervation, such compensation becomes insufficient with disease progression. As a result, patients suffer from progressive muscle weakness and loss of function. The number of motor units provides an important biomarker for diagnosing neuromuscular disease, tracking disease progression, and evaluating the effect of treatments and therapies (Olney and Lomen-Hoerth, 2000; Cudkowicz et al., 2006; Neuwirth et al., 2015). This has led to significant efforts in the past 50 years toward motor unit number estimation (MUNE).

OVERVIEW OF EXISTING MUNE METHODS

The first MUNE method was introduced by McComas et al. (1971) based on recording and measuring the compound muscle action potential (CMAP) and individual surface recorded motor unit potentials (SMUPs). The MUNE can then be calculated as dividing the CMAP by the mean SMUP of a sample of motor units:

$$MUNE = \frac{max\ CMAP}{mean\ SMUP}$$

A range of MUNE methods has been developed based on the above rationale, with each method having its advantages and limitations (Gooch et al., 2014; Carvalho et al., 2018). For all MUNE methods, it is necessary to apply supramaximal electrical stimulation of the motor nerve to record the maximal CMAP, which is derived from all motor units within the recording territory of the surface electrode. The essential difference among different MUNE methods lies in how the mean SMUP is estimated. In most MUNE methods, the mean SMUP is estimated from averaging a sample of approximately 10 motor units. For example, a sample of motor units can be obtained from incremental stimulation or multiple point stimulation of the motor nerve (Shefner et al., 2011).

It can also be estimated from identification of F wave repeaters (Li et al., 2016), or spike-triggered averaging of surface electromyography (EMG) based on simultaneously recorded intramuscular EMG decomposition (Doherty et al., 2009). Recent development in high-density surface EMG provides another approach to MUNE, taking advantage of the spatial information extracted from an electrode array (van Dijk et al., 2008). High-density surface EMG decomposition can be used to estimate SMUPs without applying an invasive needle EMG electrode (Peng et al., 2016). Other MUNE methods also include Bayesian MUNE based on the CMAP scan (Ridall et al., 2006). The CMAP scan records electrical activity of a muscle in response to a full spectrum of transcutaneous stimulations of the motor nerve in approximately 500 fine steps (Visser and Blok, 2009).

Most of the existing MUNE methods are time-consuming and not automated. So far, two MUNE methods have attracted most attention in clinical application because they are automatic and quick to implement. One is called motor unit number index (MUNIX) developed by Nandedkar and colleagues (Nandedkar et al., 2004, 2010). MUNIX is based on a mathematical model, which involves analysis of the CMAP and surface EMG interference patterns taken from different levels of voluntary contraction. The other method is called MScanFit, recently developed by Bostock et al. and based on the CMAP scan (Bostock, 2016; Jacobsen et al., 2018a). It involves analysis of a large number of stimulus responses, using a progressively improved model, which takes into account the probabilistic nature of motor unit discharge.

An essential procedure of all the existing MUNE methods is to record and measure the CMAP with supramaximal stimulation of the motor nerve. This remains true regardless of the method used to estimate the mean SMUP or which signal processing approach is used. Although efforts have been made to reduce the number of electrical stimuli for estimating motor unit number (such as MUNIX and EMG decomposition-based MUNE, which only require measurement of the CMAP with supramaximal stimulation), to the best of our knowledge no attempt has been made toward a MUNE method free of electrical stimulation. Not only would this approach improve patient tolerance, but it would simplify the experimental setup, leading to greater accessibility.

STIMULATION-FREE MUNE

While reviewing the existing MUNE methods, we note that only SMUP waveform (area, amplitude) information is used. This is also the case for EMG decomposition-based MUNE approaches (i.e., those based on spike-triggered averaging and high-density surface EMG decomposition), even though information regarding the motor unit firing rate is available. Indeed, it is not difficult to understand that CMAP plays an indispensable role in MUNE if solely relying on SMUP waveform information. However, with EMG decomposition both the SMUP waveform and the temporal discharge information of the decomposed motor units can be obtained. By making rational use of such information, we argue that it is feasible to perform MUNE without any electrical stimulation.

EMG signal can be considered as a linear superposition of different motor unit action potential trains (MUAPTs). Consider the *i*th MUAPT as a random variable s_i, EMG signal can be expressed as:

$$\mathrm{EMG} = \sum s_i + n$$

where n denotes the noise component. Due to the sparsity of MUAPT, any two MUAPTs can be considered uncorrelated, i.e.,

$$E\left\{s_i \cdot s_j\right\} = 0 \ \textit{for}\ i \neq j.$$

Meanwhile, noise n can also be considered uncorrelated to any MUAPT, i.e.,

$$E\left\{s_i \cdot n\right\} = 0 \ \textit{for any}\ i.$$

Consider the second moment of the EMG signal, we have

$$m_2\left(EMG\right) = E\left\{EMG^2\right\} = E\left\{\left(\sum_i s_i + n\right)^2\right\} =$$
$$\sum_i E\left\{s_i^2\right\} + E\left\{n^2\right\} = \sum_i m_2\left(s_i\right) + m_2\left(n\right)$$

where $m_2(x)$ represents the second moment of random variable x. The above equation indicates that the second moment of the EMG signal can be expressed as a summation of the second moments of its constituent individual MUAPTs and the noise component.

For maximum voluntary contraction (MVC), all motor units of the examined muscle are active. If the mean second moment of the MUAPTs is known, MUNE can be performed in a similar strategy to previous MUNE methods (based on CMAP and mean SMUP), i.e.,

$$MUNE = \frac{m_2\left(EMG\right) - m_2\left(n\right)}{mean\ m_2\left(s\right)}$$

where $m_2(EMG)$ can be calculated from surface EMG recorded during MVC and $m_2(n)$ can be calculated from the baseline (rest period) of the surface EMG signal. Calculation of $m_2(EMG)$ and $m_2(n)$ is straightforward. The key procedure of the proposed approach is to obtain the mean $m_2(s)$, which can be estimated from the MUAPTs of different motor units extracted by EMG decomposition (Holobar et al., 2009; Chen and Zhou, 2016). For each of the decomposed motor units, the second moment of its MUAPT can be calculated. The mean $m_2(s)$ can then be estimated by averaging the second moment of all the available MUAPTs from EMG decomposition.

CHALLENGES

Most of the MUNE methods use the rationale of maximum CMAP divided by mean motor unit size. Therefore, the accuracy

is reliant on a representative sample of motor units. This imposes a major challenge for MUNE development, especially given a large range of motor unit size distribution in a muscle. The strategy of the proposed method is similar to previous CMAP-based MUNE methods in the way that it divides the second moment of maximum voluntary surface EMG by the mean second moment of the MUAPTs of a sample of individual motor units (obtained from EMG decomposition). The main difference is to replace CMAP with maximum voluntary surface EMG, and to replace SMUP area (or amplitude) with the second moment of the MUAPT. The challenge of the proposed method will also be similar to previous CMAP-based MUNE, that is, how to obtain the mean second moment of MUAPTs representative of the examined muscle? This determines the reliability of the MUNE.

For EMG decomposition, the decomposed motor units tend to have a relatively large amplitude (compared to those that cannot be decomposed in the superimposed EMG signal). It was reported that the EMG decomposition-based MUNE tends to have lower values using motor unit samples from decomposition of EMG signals at relatively high muscle contraction levels (Doherty et al., 2009). For example, in a previous EMG decomposition-based MUNE study involving M wave and voluntary surface EMG recordings (Peng et al., 2016), the estimated motor unit number with the mean motor unit size derived from 10% MVC was nearly 2–3 times the number derived from 20 and 30% MVC. A similar situation is expected for the proposed method. The mean second moment of the MUAPTs tends to be large for motor units sampled from relatively high muscle contraction levels. This will cause an underestimation of motor unit number. Because of this, it is more favorable to perform EMG decomposition at different contraction levels to obtain a less biased sample of motor units than from a single muscle contraction level. It is also helpful to increase the decomposition yield (i.e., extracting a larger number of motor units) to have a more representative motor unit sample. It is worth noting that for previous EMG decomposition-based MUNE, for each motor unit a partial decomposition would be sufficient to obtain SMUP waveform template. For the proposed method, a complete decomposition is required for decomposed motor units to calculate the second moment of MUAPTs.

CONCLUDING REMARKS

By proposing a novel strategy to perform MUNE without recording the CMAP, we argue that stimulation-free MUNE is feasible. The challenge remains in the acquisition of representative motor unit samples for calculation of the mean second moment of MUAPTs, which is critical for the performance of the proposed MUNE method. The performance is also affected by other complex neurophysiological factors such as motor unit distribution and the level of motor unit synchronization, and thus requires further investigation. Our future work will involve both surface EMG simulation and experimental approaches for evaluating the performance of the stimulation-free MUNE approach, in terms of diagnostic accuracy or sensitivity, as compared with CMAP-based MUNE methods (Blok et al., 2005; Major and Jones, 2005; Boekestein et al., 2012; Li et al., 2012; Jacobsen et al., 2018b). Since there is a lack of 'ground truth' regarding the real motor unit number in human subjects, it is difficult to experimentally quantify a MUNE method's accuracy in terms of absolute motor unit number (especially given the uncertainty of the muscle volume a surface electrode can record from). Therefore, like various existing MUNE methods, such investigation should focus on the sensitivity of following disease progression when serial investigations are performed, rather than the absolute numerical result. If the stimulation-free MUNE proves to be reasonably sensitive to motor unit number changes, it provides a novel biomarker for monitoring disease progression and holds value for clinical trials. Importantly, the advent of a stimulation-free approach would facilitate home-based MUNE assessments, leading to notable practical and analytical advantages.

AUTHOR CONTRIBUTIONS

MC wrote the first draft. JB and PZ revised the manuscript. All authors contributed to the conception and design of the work and approved the submitted version.

FUNDING

The study was supported by the Shandong Provincial Natural Science Foundation under grant nos. ZR2021QH053 and ZR2020KF012. JB was supported by a National Institute for Health Research Clinical Lectureship in Neurology.

REFERENCES

Blok, J. H., Visser, G. H., Graaf, d. e., Zwarts, S., and Stegeman, M. J. D. F. (2005). Statistical motor number estimation assuming a binomial distribution. *Muscle Nerve* 31, 182–191. doi: 10.1002/mus.20256

Boekestein, W. A., Schelhaas, H. J., van Putten, M. J., Stegeman, D. F., Zwarts, M. J., and van Dijk, J. P. (2012). Motor unit number index (MUNIX) versus motor unit number estimation (MUNE): a direct comparison in a longitudinal study of ALS patients. *Clin. Neurophysiol.* 123, 1644–1649. doi: 10.1016/j.clinph.2012.01.004

Bostock, H. (2016). Estimating motor unit numbers from a CMAP scan. *Muscle Nerve* 53, 889–896. doi: 10.1002/mus.24945

Carvalho, d. E., Barkhaus, M., Nandedkar, P. E., and Swash, S. D. M. (2018). Motor unit number estimation (MUNE): where are we now? *Clin. Neurophysiol.* 129, 1507–1516. doi: 10.1016/j.clinph.2018.04.748

Chen, M., and Zhou, P. (2016). A Novel Framework Based on FastICA for High Density Surface EMG Decomposition. *IEEE Trans. Neural Syst. Rehabil. Eng.* 24, 117–127. doi: 10.1109/TNSRE.2015.2412038

Cudkowicz, M. E., Shefner, J. M., Schoenfeld, D. A., Zhang, H., Andreasson, K. I., Rothstein, J. D., et al. (2006). Trial of celecoxib in amyotrophic lateral sclerosis. *Ann. Neurol.* 60, 22–31. doi: 10.1002/ana.20903

Doherty, T. J., Stashuk, D. W., and Boe, S. G. (2009). Decomposition-enhanced spike triggered averaging MUNE: validity, reliability, and impact of contraction force. *Suppl. Clin. Neurophysiol.* 60, 119–127. doi: 10.1016/S1567-424X(08)00011-1

Gilmore, K. J., Morat, T., Doherty, T. J., and Rice, C. L. (2017). Motor unit number estimation and neuromuscular fidelity in 3 stages of sarcopenia. *Muscle Nerve*. 55, 676–684. doi: 10.1002/mus.25394

Gooch, C. L., Doherty, T. J., Chan, K. M., Bromberg, M. B., Lewis, R. A., Stashuk, D. W., et al. (2014). Motor unit number estimation: a technology and literature review. *Muscle Nerve*. 50, 884–893. doi: 10.1002/mus.24442

Holobar, A., Farina, D., Gazzoni, M., Merletti, R., and Zazula, D. (2009). Estimating motor unit discharge patterns from high-density surface electromyogram. *Clin. Neurophysiol.* 120, 551–562. doi: 10.1016/j.clinph.2008.10.160

Jacobsen, A. B., Bostock, H., and Tankisi, H. (2018a). CMAP Scan MUNE (MScan) - a novel motor unit number estimation (MUNE) method. *J. Vis. Exp.* 136, 56805. doi: 10.3791/56805

Jacobsen, A. B., Kristensen, R. S., Witt, A., Kristensen, A. G., Duez, L., Beniczky, S., et al. (2018b). The utility of motor unit number estimation methods versus quantitative motor unit potential analysis in diagnosis of ALS. *Clin. Neurophysiol.* 129, 646–653. doi: 10.1016/j.clinph.2018.01.002

Li, X., Fisher, M., Rymer, W. Z., and Zhou, P. (2016). Application of the F-response for estimating motor unit number and amplitude distribution in hand muscles of stroke survivors. *IEEE Trans. Neural Syst. Rehabil. Eng.* 24, 674–681. doi: 10.1109/TNSRE.2015.2453274

Li, X., Rymer, W. Z. and Zhou, P. (2012). A simulation-based analysis of motor unit number index (MUNIX) technique using motoneuron pool and surface electromyogram models. *IEEE Trans. Neural Syst. Rehabil. Eng.* 20, 297–304. doi: 10.1109/TNSRE.2012.2194311

Major, L. A., and Jones, K. E. (2005). Simulations of motor unit number estimation techniques. *J. Neural Eng.* 2, 17–34. doi: 10.1088/1741-2560/2/2/003

McComas, A. J., Fawcett, P. R., Campbell, M. J., and Sica, R. E. (1971). Electrophysiological estimation of the number of motor units within a human muscle. *J. Neurol. Neurosurg. Psychiatry* 34, 121–131. doi: 10.1136/jnnp.34.2.121

Nandedkar, S. D., Barkhaus, P. E., and Stålberg, E. V. (2010). Motor unit number index (MUNIX): principle, method, and findings in healthy subjects and in patients with motor neuron disease. *Muscle Nerve* 42, 798–807. doi: 10.1002/mus.21824

Nandedkar, S. D., Nandedkar, D. S., Barkhaus, P. E., and Stalberg, E. V. (2004). Motor unit number index (MUNIX). *IEEE Trans. Biomed. Eng.* 51, 2209–2211. doi: 10.1109/TBME.2004.834281

Neuwirth, C., Barkhaus, P. E., Burkhardt, C., Castro, J., Czell, D., Carvalho, d. M., et al. (2015). Tracking motor neuron loss in a set of six muscles in amyotrophic lateral sclerosis using the Motor Unit Number Index (MUNIX): a 15-month longitudinal multicentre trial. *J. Neurol Neurosurg. Psychiatry* 86, 1172–1179. doi: 10.1136/jnnp-2015-310509

Olney, R. K., and Lomen-Hoerth, C. (2000). Motor unit number estimation (MUNE): how may it contribute to the diagnosis of ALS? *Amyotroph. Lateral Scler. Other Motor Neuron. Disord.* 1(Suppl. 2):S41–S44. doi: 10.1080/146608200300079473

Peng, Y., He, J., Yao, B., Shenh, L., Zhou, P., and Zhang, Y. (2016). Motor unit number estimation based on high-density surface electromyography decomposition. *Clin. Neurophysiol.* 127, 3059–3065. doi: 10.1016/j.clinph.2016.06.014

Ridall, P. G., Pettitt, A. N., and Henderson, R. D., McCombe, P. A. (2006). Motor unit number estimation–a Bayesian approach. *Biometrics* 62, 1235–1250. doi: 10.1111/j.1541-0420.2006.00577.x

Shefner, J. M., Watson, M. L., Simionescu, L., Caress, J. B., Burns, T. M., Maragakis, N. J., et al. (2011). Multipoint incremental motor unit number estimation as an outcome measure in ALS. *Neurology* 77, 235–241. doi: 10.1212/WNL.0b013e318225aabf

van Dijk, J. P., Blok, J. H., Lapatki, B. G., van Schaik, I. N., Zwarts, M. J., and Stegeman, D. F. (2008). Motor unit number estimation using high-density surface electromyography. *Clin. Neurophysiol.* 119, 33–42. doi: 10.1016/j.clinph.2007.09.133

Visser, G. H., and Blok, J. H. (2009). The CMAP scan. *Suppl. Clin. Neurophysiol.* 60, 65–77. doi: 10.1016/S1567-424X(08)00006-8

Conflict of Interest: The authors declare that the research was conducted in the absence of any commercial or financial relationships that could be construed as a potential conflict of interest.

Publisher's Note: All claims expressed in this article are solely those of the authors and do not necessarily represent those of their affiliated organizations, or those of the publisher, the editors and the reviewers. Any product that may be evaluated in this article, or claim that may be made by its manufacturer, is not guaranteed or endorsed by the publisher.

frontiers in Aging Neuroscience

ORIGINAL RESEARCH
published: 11 March 2022
doi: 10.3389/fnagi.2022.800698

Hoffmann Reflex Measured From Lateral Gastrocnemius Is More Reliable Than From Soleus Among Elderly With Peripheral Neuropathy

*Qipeng Song[1,2], Mengzi Sun[2,3], Kelsey Lewis[2], Jung Hun Choi[4], Brad Manor[5,6,7] and Li Li[2]**

[1] Biomechanics Laboratory, College of Sports and Health, Shandong Sport University, Jinan, China, [2] Department of Health Sciences and Kinesiology, Georgia Southern University, Statesboro, GA, United States, [3] Biomechanics Laboratory, Beijing Sport University, Beijing, China, [4] Department of Mechanical Engineering, Georgia Southern University, Statesboro, GA, United States, [5] Hinda and Arthur Marcus Institute for Aging Research, Hebrew SeniorLife, Boston, MA, United States, [6] Harvard Medical School, Boston, MA, United States, [7] Division of Gerontology, Department of Medicine, Beth Israel Deaconess Medical Center, Boston, MA, United States

OPEN ACCESS

Edited by:
Le Li,
Northwestern Polytechnical University, China

Reviewed by:
Tung-Wu Lu,
National Taiwan University, Taiwan
Xiyao Shan,
Aichi Medical University, Japan

***Correspondence:**
Li Li
lili@georgiasouthern.edu

Specialty section:
This article was submitted to Neuroinflammation and Neuropathy, a section of the journal Frontiers in Aging Neuroscience

Received: *23 October 2021*
Accepted: *09 February 2022*
Published: *11 March 2022*

Citation:
Song Q, Sun M, Lewis K, Choi JH, Manor B and Li L (2022) Hoffmann Reflex Measured From Lateral Gastrocnemius Is More Reliable Than From Soleus Among Elderly With Peripheral Neuropathy. Front. Aging Neurosci. 14:800698. doi: 10.3389/fnagi.2022.800698

Introduction: Peripheral neuropathy (PN) affects up to 20% of the population over the age of 60. Hoffmann reflex (H-reflex) may assess PN adaptation by measuring the function of the peripheral neural system and central nervous system (CNS) modulation. This project aimed to find a reliable muscle among triceps surae muscles during standing and walking among the PN population.

Materials and Methods: Sixteen older adults (> 65 years of age) diagnosed with PN were recruited in this study. The H-reflex test was conducted on the muscle belly of the soleus (SOL), the medial (MG), and lateral gastrocnemius (LG) during standing and walking (heel contact, midstance, and toe-off phases). All measurements were collected on two occasions, separated by at least 7 days. Intraclass correlation coefficients (ICCs) and their confidence intervals (CIs) were used to examine the consistency of the H-reflex outcome variables in the repeated tests for all three tested muscles.

Results: The ICCs of H-index during standing and the three walking phases were poor to moderate in SOL (0.486∼0.737) and MG (0.221∼0.768), and moderate to high in LG (0.713∼0.871). The ICCs of H/M ratio were poor to moderate in SOL (0.263∼0.702) and MG (0.220∼0.733), and high in LG (0.856∼0.958).

Conclusion: The H-reflex of LG was more reliable than SOL and MG during standing and walking among older adults with peripheral neuropathy. It is crucial for future studies in this population to study H-reflex of LG, not SOL and MG, for more reliable results.

Keywords: H-reflex, peripheral nerve, postural control, postural balance, central nervous modulation, peripheral nervous system diseases

INTRODUCTION

Peripheral neuropathy (PN) is estimated to affect 20% of the population over 60 (Suzuki, 2013). As a neurodegenerative disease, PN damages the nerve endings, axons, and myelin of peripheral nerves in a distal to proximal manner (Azhary et al., 2010). Patients often exhibit neural impairments and associated abnormal sensations, including tingling, pricking, burning, and numbness in the lower extremities (Richardson, 2002). Together, these impairments and symptoms decrease postural control (Dixit, 2015), increase the likelihood of falls in older adults (Richardson et al., 1992), along with increased mortality (Kan et al., 2009). Although PN is viewed as a peripheral nerve pathology, the central nervous system (CNS) modulation occurs with the progress of the disease. The CNS alters the latency and amplitude of the monosynaptic stretch reflex by modifying the sensitivity and threshold of excitability of the spinal interneurons (Li et al., 2019).

One of the most common assessments of PN is sensory nerve conduction velocity (NCV), which tests the velocity and amplitude of action potentials in peripheral sensory fibers, most typically the sural nerve (Richardson, 2002). Although decreased sural NCV is the leading assessment of sensory nerve impairment (Richardson, 2002), PN often results in significant sural nerve fiber density degeneration without a decrease in sural NCV (Periquet et al., 1999). Sensory NCV may thus not adequately assess the degeneration of peripheral sensory fibers (Li and Manor, 2010; Grewal et al., 2015), the level of CNS modulation that occurs in the presence of peripheral nerve deterioration, nor the impact of this disease on the function within this vulnerable population.

Hoffmann reflex (H-reflex) has traditionally been used as a window to look into how the CNS modulates the peripheral nervous system. The H-index represents the latency of the monosynaptic peripheral sensory fibers reflexive loop (Knikou, 2008). It is an essential diagnostic tool in neurological impairments because it provides an estimated conduction velocity of an entire monosynaptic reflex arc (Zhang et al., 2015). The H/M ratio between the amplitudes of the maximum reflex response and the maximum direct motor wave is commonly used to estimate the reflex excitability level of the motor neuron pool (Mynark, 2005; Zhang et al., 2015). It helps elucidate the effect of somatosensory reweighting on postural control in many participants with PN vs. healthy individuals with impaired sensation (Li et al., 2019).

Differences between postures may be susceptible to PN-related changes during weight-bearing activities. The amplitude modulation of the H-reflex may vary between different forms or phases of locomotion among older adults with PN. The H-reflex was up to 3.5 times during standing than during walking, and during walking (Capaday and Stein, 1986; Simonsen et al., 2013) or running (Capaday and Stein, 1987; Simonsen et al., 2013), the H-reflex increased progressively during the stance phase, and decreased rapidly at the end of the stance phase and was absent during the swing phase. Soleus (SOL) H-reflex has been proven reliable during standing or walking among healthy individuals (Simonsen and Dyhre-Poulsen, 2011). However, the changed peripheral nerve properties caused by PN may influence H-reflex outcomes (Mynark, 2005; Grewal et al., 2015; Zhang et al., 2015). PN has a progression route from the distal to the proximal direction (Li et al., 2019), so gastrocnemius may have better reliability since it is physically more proximal to the SOL.

Somatosensory reweighting occurs with diseases such as PN, and H-reflex can help to elucidate the impact of somatosensory reweighting on postural control among patients with PN. An intact somatosensory system provides the most accurate information to assist postural control, but it has been established that alternative sources of sensory information can be used to compensate for those who have been impaired (Merabet and Pascual-Leone, 2010). Among patients with PN, proprioception can compensate for their impaired cutaneous sensation (Dixit et al., 2016). Proprioception could be improved by exercise (Zhang et al., 2021) or stretching (Song et al., 2020), identifying the somatosensory reweighting among patients with PN during different postures can help find appropriate rehabilitation methods for this population. To our best knowledge, no studies measured test-retest reliability during standing or walking among older adults with PN. The purpose of this study was to examine the test-retest reliability of H-reflex testing in SOL, MG, and LG during both standing and walking conditions among older adults with PN.

MATERIALS AND METHODS

Participants

Sixteen volunteers (6 women, 10 men, age: 72.3 ± 5.2 years, height: 170.4 ± 10.4 cm, body mass: 91.0 ± 22.6 kg) participated in this project. Inclusion criteria were: (1) age 65 years and older; (2) physician-diagnosed peripheral neuropathy; and (3) impaired foot sole cutaneous sensation as defined by the inability to detect the 5.07-gauge monofilament at three or more of 10 total tested sites (five on each foot sole). Individuals were excluded with one or more of the following: (1) Self-reported history or evidence of central nervous system dysfunction; (2) self-reported trauma or disease that may significantly affect gait or postural control; (3) evidence of foot sole ulcer(s); (4) with a cardiac pacemaker; (5) global cognitive impairment defined by a Mini-Mental State Exam (MMSE) score < 24; and (6) contraindications to physical activity determined by the Physical Activity Readiness Questionnaire Plus (PAR-Q+), i.e., (a) heart condition; (b) high blood pressure; (c) spinal cord disease; (d) lose balance because of dizziness or lost consciousness within the past 12 months; (e) bone, joint, or soft tissue problem that could be made worse by becoming more physically active; (f) only do medically supervised physical activity. An apriori power analysis (G*Power Version 3.1) indicated that a minimum of 11 participants is needed to obtain the alpha level of 0.05 and the beta level of 0.80 based on our previous report (Zhang et al., 2015). All individuals gave written informed consent before participating in the study. Human participation was approved (Nov. 11, 2019) by the University Institutional Review Board (Chair Person: Dr. Andrew Hensen) of Georgia Southern University (H20076) and was in accordance with the Declaration of Helsinki.

Protocol

All testing procedures were completed during two visits to the lab, with at least 1 week in between. On the first visit, after providing informed consent, individuals completed a medical history, MMSE, the PAR-Q+, and a test of cutaneous sensation to determine eligibility. Height and weight were then recorded. H-reflex testing was completed during standing and then walking conditions, as described below. During the second visit, H-reflex testing was repeated using identical procedures. The skin temperature at the right gastrocnemius was measured each time before the initiation of the H-reflex tests (IRT0421, Infrared Thermometer, Kintrex, Tx, United States).

Cutaneous Sensation Test

A foot sole cutaneous sensation test was performed with participants in a supine position on an exam table, with a 5.07-gauge Semmes–Weinstein monofilament (North Coast Medical, Inc., Morgan Hill, CA, United States). The testing sites included the heel, midsole, bases of first/fifth metatarsals, and hallux. A score of "1" was given when a "yes" response accompanied the detected pressure, "0" with a "no" response. Each site was tested three times. Then, the score from each site was added. The site was reassigned to "1" if the total score was two or greater; otherwise, the site was reassigned to "0."

H-Reflex Test

Surface electromyography (EMG) electrodes (Trigno Wireless EMG System with Avanti Sensors; Delsys Inc., MA, United States) were placed on the muscle belly of SOL, MG, and LG along with the orientation of the muscle fibers (**Figure 1**). Before the EMG electrodes placement, the skin was shaved and cleaned with alcohol pads. EMG data were collected using EMGWorks (Delsys Inc., MA, United States) at a sampling rate of 2,000 Hz. The optimal site of tibial nerve stimulation in the popliteal fossa (located at the back of the knee) was determined using a hand-held electrode that comes with the stimulator (Digitimer model DS7A, Digitimer Ltd., Welwyn Garden City, England, United Kingdom) at low stimulation intensities. A disposable electrodes (2 cm in diameter) cathode (negative electrode) was placed on the skin at the determined site (**Figure 1**), and the 5 cm × 8 cm anode (positive electrode) was placed over the patella (kneecap) of the same limb.

Two testing conditions were used for the H-reflex test, standing and walking. For the standing condition, the standard stimulation protocol was used to estimate H-index and H/M ratio (Chen and Zhou, 2011). During this test, participants were instructed to stand with their feet shoulder-width apart, relax their arms by their sides, and have their vision fixated on a point in their field of view. A 500 μs square-pulse single stimulus elicited H-reflex. Stimulation started at 5 mA and increased with 2 mA increments until the maximum M-wave was reached. Approximately 30 stimuli were executed, with at least 10 s break in between each stimulation. The participants were instructed to limit talking and movement and relax as much as possible during the process. Noise-canceling headphones were used during the test (see **Figure 2** for the exemplar recruitment curve). After this test, the participants rested for 10 min or longer upon their request.

Before the walking test, participants completed a 5-min familiarization of treadmill walking at their preferred pace. H-reflex was collected during the three phases in the walking condition, at 5, 20, and 55% of the gait cycle, to represent the heel contact, midstance, and toe-off phases (Querry et al., 2008; Knikou et al., 2011), respectively. A consistent stimuli intensity was applied during all three walking phases, equivalent to the stimulus intensity that elicited 15% of each individual's maximum M-wave during stance. The stimulation intensity was chosen since it has been demonstrated that M-waves below 15% stimulation level present problems due to the underlying EMG during voluntary muscle activity in the stance phase, and about 25% result in lower H-wave (Simonsen and Dyhre-Poulsen, 1999). The gait cycle was confirmed by a custom-made footswitch system and defined by two consecutive right heel contacts with the ground. A pressure sensor was taped under the right heel of the shoe to detect and record heel contacts during walking. The footswitch system was connected to the stimulator through a LabVIEW board. Heel contact information was detected through footswitch and collected through a customized LabVIEW program at 1,000 Hz. The gait cycle duration was calculated using the average duration of 10 strides before the start of the stimulation. The participants walked on the treadmill for less than 5,min during testing. At least fifteen stimulations were administered in each phase. The H-reflex was estimated using the average of ten recordings for further analysis (see **Figure 3** for details).

H-reflex tests were performed during each visit for each participant in a standing-walking fixed order. All measurements were collected on two separate occasions with at least 7 days in between. In this study, a treadmill was used instead of ground walking to improve the safety of participants by using a safety belt fixed above the treadmill and to improve the timing accuracy of the stimulations by using a more consistent walking speed on the treadmill.

Variables

Raw EMG data were used to estimate H-reflex parameters without filtering and any other types of conditioning. The measurements of interest for this study were the H-index and H/M ratio. H/M ratio during standing was defined as the ratio of magnitudes of maximum peak-to-peak H- and M-waves, i.e., the H/M ratio was as Hmax/Mmax (i.e., the period between the onsets of the H- and M-waves, see **Figure 4**). H/M ratio during walking was defined as the mean magnitudes of peak-to-peak H-wave across 10 strides over Mmax during standing (**Figure 5**). H-index was defined as the relative latency between H- and M-waves and was calculated as follows (Li and Manor, 2010):

$$\text{H-index} = \left[\frac{\text{Height (cm)}}{\Delta t_H - \Delta t_M}\right]^2 * 2$$

Data Analysis

Statistical analysis was performed using the statistical package SPSS 22.0 (SPSS Inc., Chicago, Illinois). The test-retest reliability

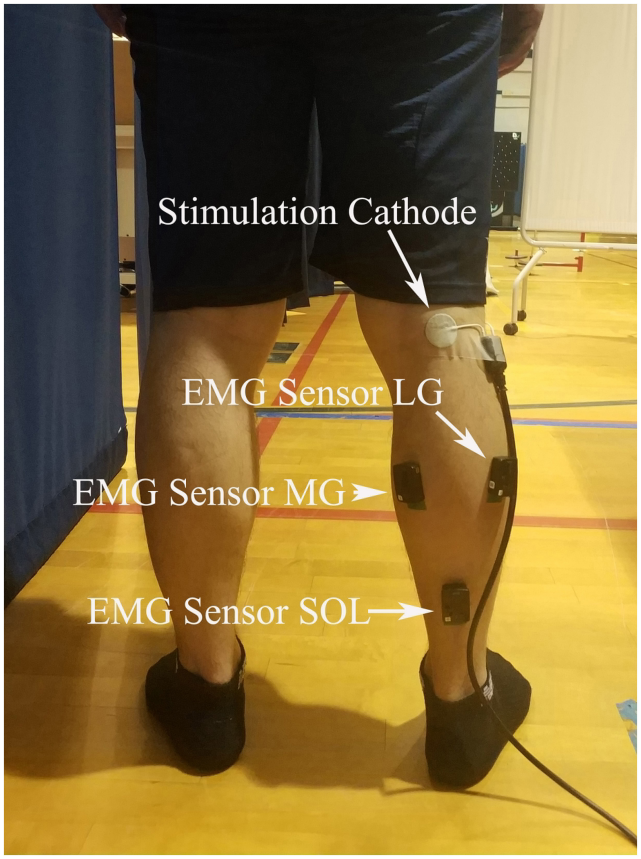

FIGURE 1 | EMG and stimulation locations. Surface electromyography (EMG) electrodes were placed on the muscle belly of soleus (SOL), the medial (MG), and lateral gastrocnemius (LG), and a disposable electrodes cathode was placed on the skin at popliteal fossa.

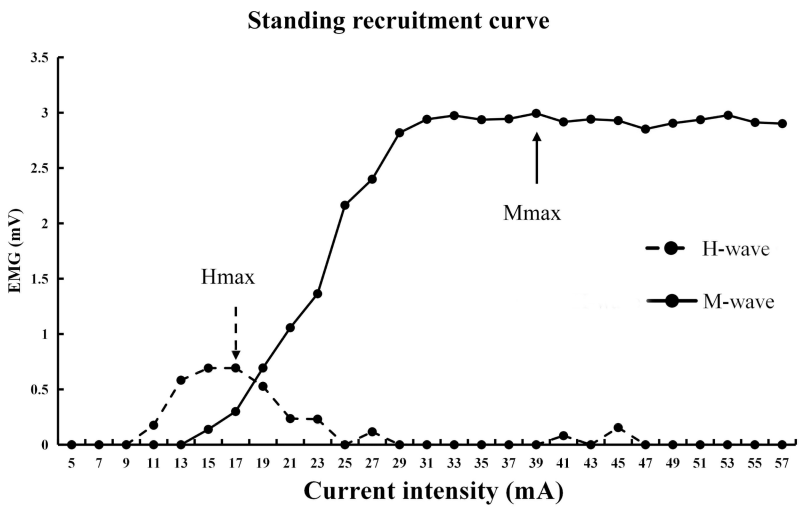

FIGURE 2 | Exemplar H-reflex recruitment curse during standing.

of the H-index and H/M ratio was examined using intraclass correlation coefficients (ICC) with a two-way mixed model. The 95% confidence intervals (CIs) of ICCs were also computed. ICC values < 0.60 were considered poor, those between 0.60 and 0.80 were considered moderate, and those > 0.80 were deemed high (Cicchetti and Sparrow, 1981).

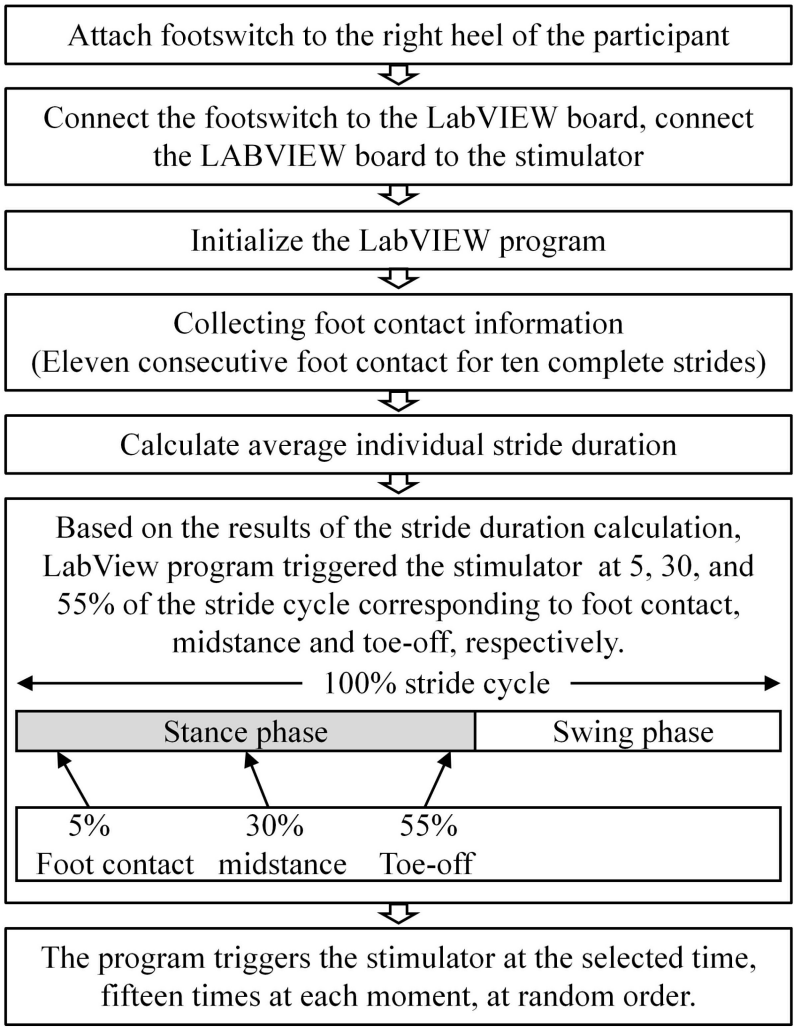

FIGURE 3 | Flowchart of the customized stimulation control during walking using LabVIEW and footswitch. The connection from the footswitch to the LabVIEW board, and from the LabVIEW board to the stimulator were tethered. Heel strike information was detected though footswitch and collected through a customized LabVIEW program at 1,000 Hz. Stride length was calculated from 10 (11) consecutive strides (foot strikes).

RESULTS

The H-reflex during both standing and walking was successfully elicited from 12 of 16 participants (5 women, 7 men, age: 71.5 ± 4.8 years, height: 170.0 ± 10.0 cm, body mass: 89.3 ± 21.4 kg). In one of these 12 participants (ID#1), the H-reflex was elicited only during walking. The total foot sole sensitivity test score of these 12 participants ranged from 0 to 7 (two scored 0, one scored 1, 4 or 7, respectively, three scored 5, and four scored 6). Skin temperature at the test site was consistent within participants, between the two testing visits, during the tests of both standing (test: 85.5 ± 2.6, retest: 84.7 ± 2.9°F, ICC = 0.60) and walking (test: 84.7 ± 2.9, retest: 85.8 ± 2.7°F, ICC = 0.75).

Table 1 presents the mean and standard deviation, ICCs and their 95%CIs, of the H-index. The ICCs of H-index during standing and heel contact, midstance, and toe-off phases were poor to moderate in SOL (0.486∼0.737) and MG (0.221∼0.768), and moderate to high in LG (0.713∼0.871).

Table 2 presents the mean and standard deviation, ICCs and their 95% CIs, of the H/M ratio. The ICCs of H/M ratio during standing and heel contact, midstance, and toe-off phases were poor to moderate in SOL (0.263∼0.702) and MG (0.220∼0.733), and high in LG (0.856∼0.958).

DISCUSSION

The present study indicates that h-reflex measured from LG was more reliable than from SOL and MG. Previous studies have reported high reliability in H-reflex in the upper (Stowe et al., 2008) and lower (Mynark, 2005) limb muscles during lying prone and standing among younger and older populations (Mynark, 2005). This study further indicated that the H-reflex in LG, rather

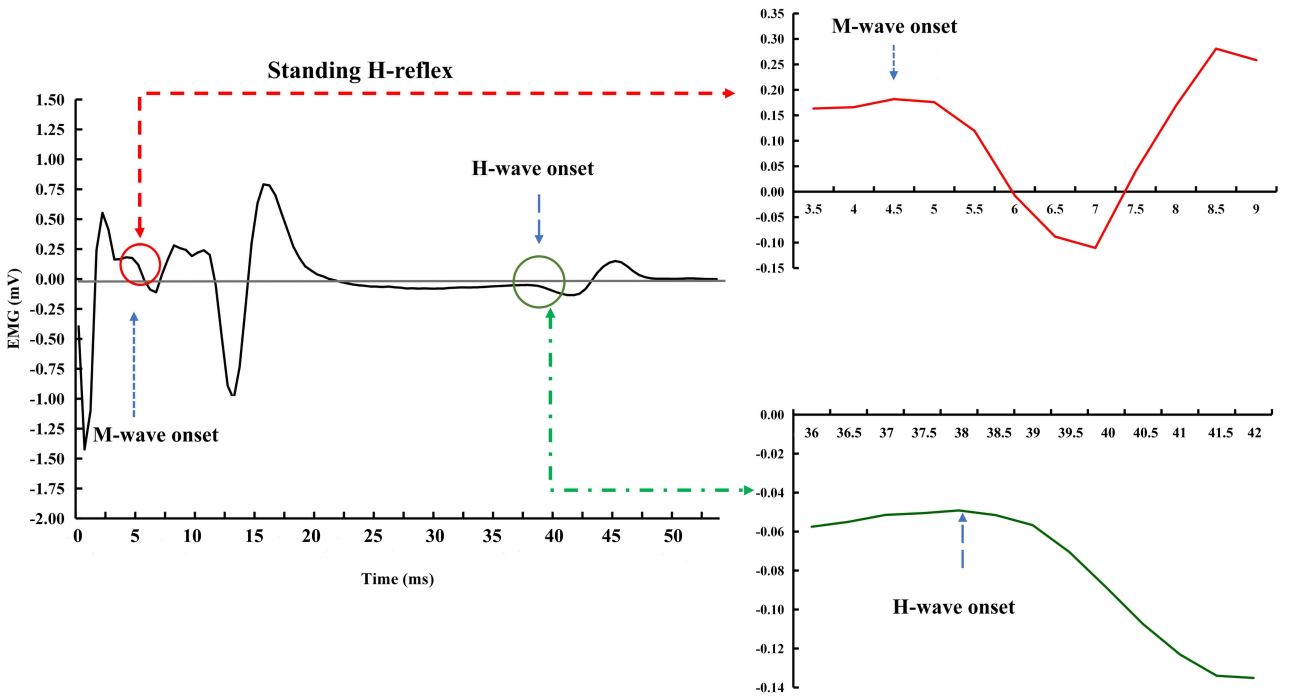

FIGURE 4 | Exemplar H-reflex recordings with standing condition. The onsets of the M- and H-waves were identified based on a single recording. There was a short period of stabled signal in after the stimulation artifact and before the onset of the M-wave. A much more extended period of the stable signal was observed between the end of the M-wave and the beginning of the H-wave.

than MG and SOL, can be reliably measured during standing and walking among older adults with peripheral neuropathy, despite chronic PN pathology and related CNS adaptation in this population.

In the present study, 75% (12/16) of participants successfully elicited the H-wave. The age, height, and body mass of the four exceptions were within the range of the others, yet they had worse foot sole cutaneous sensation (i.e., lower total foot sole sensitivity test score; median: 1 of the 4 vs. 5 of the 12). The eliciting rate of H-wave in this study is fully consistent with a previous study among older adults with PN (75%, 12/16) (Zhang et al., 2015). Among healthy older adults, the rate was 79% (11/14) (Scaglioni et al., 2002) to 90% (18/20) (Chen et al., 2015), and among healthy middle-aged (Raffalt et al., 2015) or young (Chen et al., 2015) individuals, the rate was 100%. Antidromic action potential could be one reason that partially explained the unsuccessful trials (Palmieri et al., 2004). Other mechanisms by which H-waves cannot be excited in each individual are unknown. It is inferred from the limited information above that the inability of the four participants in our study to excite H-waves was due to their aging and PN. Loss of myelinated and unmyelinated nerve fibers has been reported in the elderly (Verdu et al., 2000), and PN further damaged the axons and myelin of peripheral nerves (Li et al., 2019). The overlapping damage to the peripheral nervous system among older adults with PN may be associated with their low H-wave excitation rates. The H-reflex intensity was determined using approximately 30 stimulations during one standing testing trial. Then the walking trial data were estimated using ten trials. More testing trials during standing and walking can potentially increase the reliability of our observations. However, our participants were elderly with PN, and more trials could lead to exhaustion and failed data collection sessions.

H/M ratio modulation is highly correlated with postural sway and postural stability among adults (average age = 31) (Tokuno et al., 2008). It decreased with increased body sway during the stance phase of walking (Earles et al., 2000) and was amplified after balance training (Taube et al., 2008). The inhibition mechanisms associated with the H/M ratio are not fully understood yet, but are believed to occur at the presynaptic level (Chen and Zhou, 2011). The effect of presynaptic inhibition decreases the H/M ratio under challenging conditions to prevent the overdrive of motor fibers' autogenic excitation and alter the saturation of motor fiber excitability for receiving CNS commands (Chalmers and Knutzen, 2002). The ability to maintain posture control is related to the complex interactions between peripheral sensory input and motor process modulated by CNS; the functional adaptation of CNS may explain the postural control improvement after different exercise training (Li and Manor, 2010; Grewal et al., 2013, 2015) to training tasks (Taube et al., 2008). From this perspective, the H-reflex in LG, which assesses the function of sensory and motor fibers, CNS modulation, and the influence of postural control, should be better used as a functional assessment tool for older adults with PN.

The LG H-reflex was much more reliable than that of the MG and SOL, especially during walking. LG, MG, and SOL

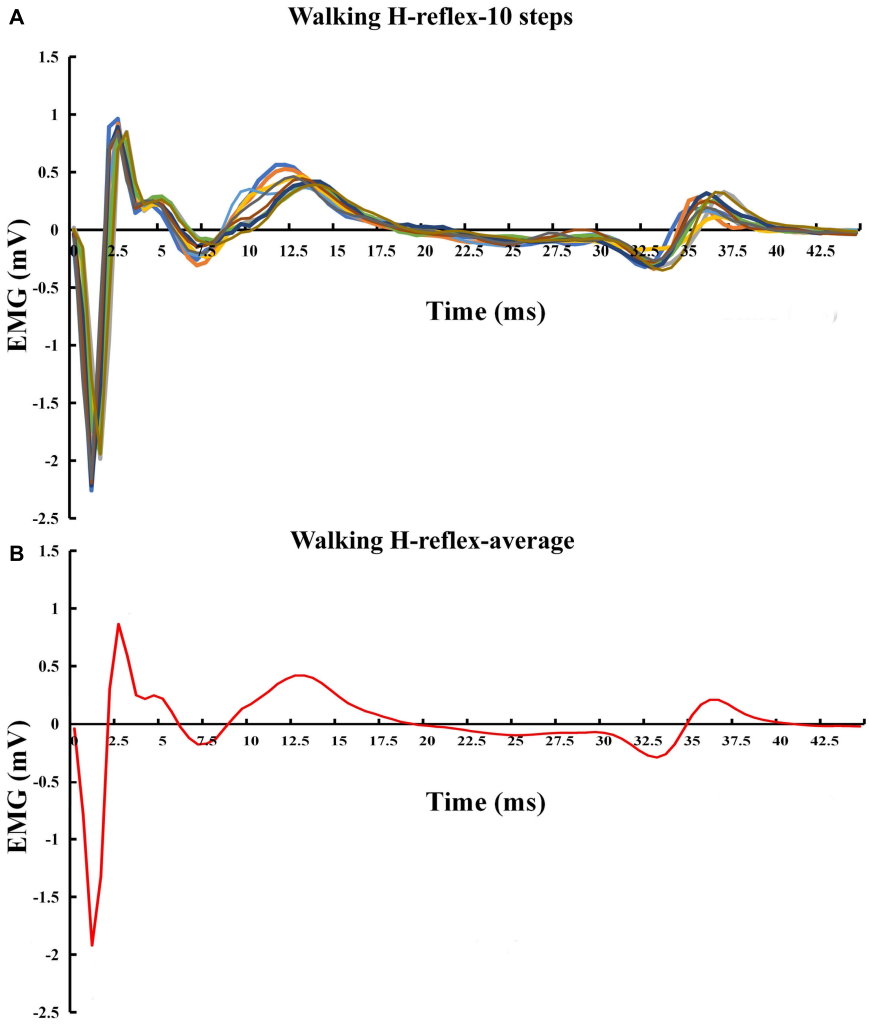

FIGURE 5 | Exemplar H-reflex recordings with walking condition. **(A)** Walking H-reflex in 10 steps. **(B)** Average of the 10 steps.

muscles' mechanical behaviors are different during walking (Orendurff et al., 2005). Aging differentially affects the triceps surae muscles, with age-related network deficits of 38% for the gastrocnemius and 66% for the SOL in all walking speeds. Ebrahimi et al. (2020) inferred that the musculoskeletal function of the SOL is impaired more rapidly with age than that of the gastrocnemius. Moreover, most of the PN has a progression route from distal to proximal direction (Li et al., 2019), i.e., starting from the nerve ending at the bottom of the big toe and growing upwards. Our participants may have different degrees of PN, where cases of SOL nerve ending impairments exist, but the LG nerve endings for most participants were intact. This and other potential mechanisms should be explored further in the future to understand the differential effects of aging and PN on triceps surae H-reflex.

It is worth noting that the reliability of the H-reflex measured from the triceps surae is improved partially due to the advancement of the technology. Compared to the stimulator used before (e.g., Zhang et al., 2015), the present study used a 0.5 ms square wave from a constant current stimulator. They have measured the H-reflex reliability of the LG muscle in a prone position for the same population. The reliability of the H/M ratio was poor, although the H-index reliability is comparable to the current project. The shorter stimulation time (0.5 vs. 1 ms) potentially reduced the possibility of antidramatic interference with the reflexive responses. The constant current (not controllable in the cited paper) provided less variability in the stimulation signals than the previous technology.

This study has several limitations. Antidramatic action potential could be one of the reasons for failing to observe H-reflex among 4 of the 16 participants during walking. And also, we have limited the numbers of our testing trials (one standing and 10 walking) due to the advanced age of our participants with PN. More trials could potentially increase the reliability of the observations. Furthermore, the footswitch sensor was taped under the right heel of the shoe to detect heel contact during walking. However, the shapes and texture of the participant's shoes were different, leading to inconsistent

TABLE 1 | Test-retest reliability of H-index (cm^2/s^2), includes the mean, standard deviation (SD), standard error of measurement (SEM), intraclass correlation coefficients (ICC), and 95% confidence intervals (CI) of the H-index.

		Standing		Heel Contact		Midstance		Toe off	
		Test	**Re-test**	**Test**	**Re-test**	**Test**	**Re-test**	**Test**	**Re-test**
Soleus	Mean	64.2	60.3	63.4	59.6	56.3	59.5	59.3	61.5
	SD	19.9	8.9	10.3	8.8	6.7	7.7	13.2	11.8
	SEM	5.74	2.57	2.99	2.55	1.94	2.22	3.81	3.41
	ICC	0.507		0.486		**0.737**		**0.725**	
	95%CI	–0.065∼0.828		–0.091∼0.819		**0.243∼0.928**		**0.218∼0.924**	
Medial gastrocnemius	Mean	61.4	60.4	60.1	62.0	61.8	63.2	64.2	67.4
	SD	14.26	15.47	10.00	11.04	10.11	9.13	13.88	9.56
	SEM	4.1	4.47	2.89	3.19	2.92	2.63	4.01	2.76
	ICC	0.221		0.223		**0.768**		**0.621**	
	95%CI	–0.378∼0.690		–0.396∼0.713		**0.334∼0.932**		**0.070∼0.882**	
Lateral gastrocnemius	Mean	63.3	64.9	65.4	62.1	65.4	61.5	63.4	61.6
	SD	10.18	10.50	12.47	10.27	12.47	11.13	10.36	9.92
	SEM	2.94	3.03	3.60	2.97	3.60	3.21	2.99	2.86
	ICC	**0.759**		**0.713**		**0.724**		**0.871**	
	95%CI	**0.325∼0.929**		**0.265∼0.908**		**0.295∼0.912**		**0.612∼0.961**	

Bolded ICC and 95% CI indicate moderate or high reliability.

TABLE 2 | Test-retest reliability of H/M ratio, includes the mean, standard deviation (SD), standard error of measurement (SEM), intraclass correlation coefficients (ICC), and 95% confidence intervals (CI) of the H/M ratio.

		Standing		Heel Contact		Midstance		Toe off	
		Test	**Re-est**	**Test**	**Re-test**	**Test**	**Re-test**	**Test**	**Re-test**
Soleus	Mean	0.32	0.36	0.23	0.26	0.22	0.32	0.249	0.341
	SD	0.18	0.22	0.17	0.14	0.15	0.16	0.18	0.43
	SEM	0.05	0.06	0.05	0.04	0.04	0.05	0.05	0.12
	ICC	**0.702**		**0.700**		0.396		0.263	
	95%CI	**0.243∼0.904**		**0.239∼0.903**		–		–0.402∼0.747	
Medial gastrocnemius	Mean	0.11	0.11	0.09	0.09	0.08	0.10	0.08	0.10
	SD	0.05	0.06	0.06	0.05	0.05	0.06	0.04	0.08
	SEM	0.01	0.02	0.02	0.02	0.01	0.02	0.01	0.02
	ICC	0.220		**0.666**		**0.733**		0.582	
	95%CI	–0.379∼0.689		**0.179∼0.891**		**0.304∼0.915**		0.010∼0.867	
Lateral gastrocnemius	Mean	0.18	0.21	0.13	0.15	0.12	0.15	0.11	0.12
	SD	0.15	0.15	0.13	0.17	0.13	0.14	0.13	0.14
	SEM	0.04	0.04	0.04	0.05	0.04	0.04	0.04	0.04
	ICC	**0.885**		**0.883**		**0.856**		**0.958**	
	95%CI	**0.631∼0.968**		**0.645∼0.965**		**0.576∼0.956**		**0.860∼0.988**	

Bolded ICC and 95% CI indicate high reliability. M-waves used in calculating both H/M ratio during standing and walking were the maximum M-waves for each collection during standing. The H/M ration calculations used maximum H-wave during standing, but H-wave magnitudes during walking were from the stimulation intensive as 15% of that needed for maximum M-wave during standing.

heel contact detection. Standard testing shoes for the participants in future projects would help to avoid the potential problem. However, the participants in this project wore the same pair of shoes for the test-retest; the results of the reliability examination should not be affected. Finally, the 5-min treadmill walking allotted for each participant to familiarize them with the treadmill setting may not be sufficiently long for an older adult who has never walked on a treadmill before. The familiarization period should only end after the participants feel comfortable walking on the treadmill. A more extended resting period might also be needed if the familiarization led to potential fatigue.

CONCLUSION

The H-reflex in LG could be reliably measured. LG provides the most reliable window than the MG and traditional SOL on central modulation of the peripheral nervous system through

H-reflex during standing and walking among older adults with peripheral neuropathy.

DATA AVAILABILITY STATEMENT

The original contributions presented in the study are included in the article/supplementary material, further inquiries can be directed to the corresponding author/s.

ETHICS STATEMENT

The studies involving human participants were reviewed and approved by Institutional Review Board (Chair Person: Dr. Andrew Hensen) of Georgia Southern University (Approval #H20076). The patients/participants provided their written informed consent to participate in this study.

AUTHOR CONTRIBUTIONS

QS, MS, and KL participated in the design of the study, contributed to data collection, data reduction and analysis. JC participated in the design of the study and contributed to data collection. BM participated the design and interpretation of results of the study. LL participated in the design of the study, contributed to data analysis, and interpretation of results. All authors contributed to the manuscript writing, read and approved the final version of the manuscript and agreed with the order of presentation of the authors.

ACKNOWLEDGMENTS

We thank all volunteers who participated in this study.

REFERENCES

Azhary, H., Farooq, M. U., Bhanushali, M., Majid, A., and Kassab, M. Y. (2010). Peripheral neuropathy: differential diagnosis and management. *Am. Fam. Phys.* 81, 887–892.

Capaday, C., and Stein, R. B. (1986). Amplitude modulation of the soleus H-reflex in the human during walking and standing. *J. Neurosci.* 6, 1308–1313. doi: 10.1523/JNEUROSCI.06-05-01308.1986

Capaday, C., and Stein, R. B. (1987). Difference in the amplitude of the human soleus H reflex during walking and running. *J. Neurosci.* 392, 513–522. doi: 10.1113/jphysiol.1987.sp016794

Chalmers, G. R., and Knutzen, K. M. (2002). Soleus H-reflex gain in healthy elderly and young adults when lying, standing, and balancing. *J. Gerontol. Ser. A Biol. Sci. Med. Sci.* 57, B321–B329. doi: 10.1093/gerona/57.8.b321

Chen, Y. S., and Zhou, S. (2011). Soleus H-reflex and its relation to static postural control. *Gait Posture* 33, 169–178. doi: 10.1016/j.gaitpost.2010.12.008

Chen, Y. S., Zhou, S., and Cartwright, C. (2015). Modulation of soleus H-reflex during shortening and lengthening muscle actions in young and older adults. *Chin. J. Physiol.* 58, 9–18. doi: 10.4077/CJP.2015.BAC240

Cicchetti, D. V., and Sparrow, S. A. (1981). Developing criteria for establishing interrater reliability of specific items: applications to assessment of adaptive behavior. *Am. J. Ment. Defic.* 86, 127–137.

Dixit, S. (2015). Postural sway in diabetic peripheral neuropathy among Indian elderly. *Indian J. Med. Res.* 142, 713–720. doi: 10.4103/0971-5916.174562

Dixit, S., Maiya, A., Shastry, B. A., and Guddattu, V. (2016). Analysis of postural control during quiet standing in a population with diabetic peripheral neuropathy undergoing moderate intensity aerobic exercise training: a single blind, randomized controlled trial. *Am. J. Phys. Med. Rehabil.* 95, 516–524. doi: 10.1097/PHM.0000000000000426

Earles, D. R., Koceja, D. M., and Shively, C. W. (2000). Environmental changes in soleus H-reflex excitability in young and elderly subjects. *Int. J. Neurosci.* 105, 1–13. doi: 10.3109/00207450009003261

Ebrahimi, A., Martin, J. A., Schmitz, D. G., and Thelen, D. G. (2020). Shear wave tensiometry reveals an age-related deficit in triceps surae work at slow and fast walking speeds. *Front. Sports Act. Living* 2:69. doi: 10.3389/fspor.2020.00069

Grewal, G. S., Sayeed, R., Schwenk, M., Bharara, M., Menzies, R., Talal, T. K., et al. (2013). Balance rehabilitation: promoting the role of virtual reality in patients with diabetic peripheral neuropathy. *J. Am. Podiatr. Med. Assoc.* 103:498. doi: 10.7547/1030498

Grewal, G. S., Schwenk, M., Lee-Eng, J., Parvaneh, S., Bharara, M., Menzies, R. A., et al. (2015). Sensor-Based interactive balance training with visual joint movement feedback for improving postural stability in diabetics with peripheral neuropathy: a randomized controlled trial. *Gerontology* 61, 567–574. doi: 10.1159/000371846

Kan, G. a. V., Rolland, Y., Andrieu, S., Bauer, J., Beauchet, O., Bonnefoy, M., et al. (2009). Gait speed at usual pace as a predictor of adverse outcomes in community-dwelling older people an International Academy on Nutrition and Aging (IANA) Task Force. *J. Nutr. Health Aging* 13, 881–889. doi: 10.1007/s12603-009-0246-z

Knikou, M. (2008). The H-reflex as a probe: pathways and pitfalls. *J. Neurosci. Methods* 171, 1–12. doi: 10.1016/j.jneumeth.2008.02.012

Knikou, M., Hajela, N., Mummidisetty, C. K., Xiao, M., and Smith, A. C. (2011). Soleus H-reflex phase-dependent modulation is preserved during stepping within a robotic exoskeleton. *Clin. Neurophysiol.* 122, 1396–1404. doi: 10.1016/j.clinph.2010.12.044

Li, L., and Manor, B. (2010). Long term Tai Chi exercise improves physical performance among people with peripheral neuropathy. *Am. J. Chin. Med.* 38, 449–459. doi: 10.1142/S0192415X1000797X

Li, L., Zhang, S., and Dobson, J. (2019). The contribution of small and large sensory afferents to postural control in patients with peripheral neuropathy. *J. Sport Health Sci.* 8, 218–227. doi: 10.1016/j.jshs.2018.09.010

Merabet, L. B., and Pascual-Leone, A. (2010). Neural reorganization following sensory loss: the opportunity of change. *Nat. Rev. Neurosci.* 11, 44–52. doi: 10.1038/nrn2758

Mynark, R. G. (2005). Reliability of the soleus H-reflex from supine to standing in young and elderly. *Clin. Neurophysiol.* 116, 1400–1404. doi: 10.1016/j.clinph.2005.02.001

Orendurff, M. S., Segal, A. D., Aiona, M. D., and Dorociak, R. D. (2005). Triceps surae force, length and velocity during walking. *Gait Posture* 21, 157–163. doi: 10.1016/j.gaitpost.2004.01.009

Palmieri, R. M., Ingersoll, C. D., and Hoffman, M. A. (2004). The hoffmann reflex: methodologic considerations and applications for use in sports medicine and athletic training research. *J. Athl. Train.* 39, 268–277.

Periquet, M. I., Novak, V., Collins, M. P., Nagaraja, H. N., Erdem, S., Nash, S. M., et al. (1999). Painful sensory neuropathy: prospective evaluation using skin biopsy. *Neurology* 53, 1641–1641. doi: 10.1212/wnl.53.8.1641

Querry, R. G., Pacheco, F., Annaswamy, T., Goetz, L., Winchester, P. K., and Tansey, K. E. (2008). Synchronous stimulation and monitoring of soleus H reflex during robotic body weight-supported ambulation in subjects with spinal cord injury. *J. Rehabil. Res. Dev.* 45, 175–186. doi: 10.1682/jrrd.2007.02.0028

Raffalt, P. C., Alkjaer, T., and Simonsen, E. B. (2015). Changes in soleus H-reflex during walking in middle-aged, healthy subjects. *Muscle Nerve* 51, 419–425. doi: 10.1002/mus.24279

Richardson, J. K. (2002). Factors associated with falls in older patients with diffuse polyneuropathy. *J. Am. Geriatr. Soc.* 50, 1767–1773. doi: 10.1046/j.1532-5415.2002.50503.x

Richardson, J. K., Ching, C., and Hurvitz, E. A. (1992). The relationship between electromyographically documented peripheral neuropatny and falls. *J. Am. Geriatr. Soc.* 40, 1008–1012. doi: 10.1111/j.1532-5415.1992.tb04477.x

Scaglioni, G., Ferri, A., Minetti, A. E., Martin, A., Van Hoecke, J., Capodaglio, P., et al. (2002). Plantar flexor activation capacity and H reflex in older adults: adaptations to strength training. *J. Appl. Physiol.* 92, 2292–2302.

Simonsen, E. B., Alkjaer, T., and Raffalt, P. C. (2013). Influence of stimulus intensity on the soleus H-reflex amplitude and modulation during locomotion. *J. Electromyogr. Kinesiol.* 23, 438–442. doi: 10.1016/j.jelekin.2012.10.019

Simonsen, E. B., and Dyhre-Poulsen, P. (1999). Amplitude of the human soleus H reflex during walking and running. *J. Physiol.* 515, 929–939.

Simonsen, E. B., and Dyhre-Poulsen, P. (2011). Test-retest reliability of the soleus H-reflex excitability measured during human walking. *Hum. Mov. Sci.* 30, 333–340. doi: 10.1016/j.humov.2010.02.009

Song, Q., Shen, P., Mao, M., Sun, W., Zhang, C., and Li, L. (2020). Proprioceptive neuromuscular facilitation improves pain and descending mechanics among elderly with knee osteoarthritis. *Scand. J. Med. Sci. Sports* 30, 1655–1663. doi: 10.1111/sms.13709

Stowe, A. M., Hughes-Zahner, L., Stylianou, A. P., Schindler-Ivens, S., and Quaney, B. M. (2008). Between-day reliability of upper extremity H-reflexes. *J. Neurosci. Methods* 170, 317–323. doi: 10.1016/j.jneumeth.2008.01.031

Suzuki, M. (2013). Peripheral neuropathy in the elderly. *Handb. Clin. Neurol.* 115:803.

Taube, W., Gruber, M., and Gollhofer, A. (2008). Spinal and supraspinal adaptations associated with balance training and their functional relevance. *Acta Physiol.* 193, 101–116. doi: 10.1111/j.1748-1716.2008.01850.x

Tokuno, C. D., Garland, S. J., Carpenter, M. G., Thorstensson, A., and Cresswell, A. G. (2008). Sway-dependent modulation of the triceps surae H-reflex during standing. *J. Appl. Physiol.* 104, 1359–1365. doi: 10.1152/japplphysiol.00857.2007

Verdu, E., Ceballos, D., Vilches, J. J., and Navarro, X. (2000). Influence of aging on peripheral nerve function and regeneration. *J. Peripher. Nerv. Syst.* 5, 191–208. doi: 10.1046/j.1529-8027.2000.00026.x

Zhang, S., Holmes, M., and Li, L. (2015). Reliability of nerve function assessments for people with peripheral neuropathy. *Int. J. Neurosci.* 125, 201–207. doi: 10.3109/00207454.2014.920332

Zhang, T., Mao, M., Sun, W., Li, L., Chen, Y., Zhang, C., et al. (2021). Effects of a 16-week Tai Chi intervention on cutaneous sensitivity and proprioception among older adults with and without sensory loss. *Res. Sports Med.* 29, 406–416. doi: 10.1080/15438627.2021.1906673

Conflict of Interest: The authors declare that the research was conducted in the absence of any commercial or financial relationships that could be construed as a potential conflict of interest.

Publisher's Note: All claims expressed in this article are solely those of the authors and do not necessarily represent those of their affiliated organizations, or those of the publisher, the editors and the reviewers. Any product that may be evaluated in this article, or claim that may be made by its manufacturer, is not guaranteed or endorsed by the publisher.

frontiers | Frontiers in Aging Neuroscience

ORIGINAL RESEARCH
published: 08 April 2022
doi: 10.3389/fnagi.2022.870871

Robot Assisted Treatment of Hand Functional Rehabilitation Based on Visual Motor Imagination

Long Li[1,2,3], Yanlong Zhang[4], Liang Huang[1,2,3], Jie Zhao[1,2,3], Jue Wang[1,2,3] and Tian Liu[1,2,3]**

[1] The Key Laboratory of Biomedical Information Engineering of Ministry of Education, School of Life Sciences and Technology, Xi'an Jiaotong University, Xi'an, China, [2] The Key Laboratory of Neuro-Informatics and Rehabilitation Engineering of Ministry of Civil Affairs, Institute of Health and Rehabilitation Science, School of Life Sciences and Technology, Xi'an Jiaotong University, Xi'an, China, [3] National Engineering Research Center of Health Care and Medical Devices, Xi'an, China, [4] Key Laboratory for Artificial Intelligence and Cognitive Neuroscience of Language, Xi'an International Studies University, Xi'an, China

This pilot study implements a hybrid brain computer interface paradigm based on motor imagery (MI) and steady-state visual evoked potential (SSVEP), in order to explore the neural mechanism and clinical effect of MI-SSVEP intervention paradigm on upper limb functional rehabilitation. In this study, EEG data of 12 healthy participants were collected, and the activation regions of MI-SSVEP paradigm were identified by power spectral density (PSD). By analyzing the inter trial phase consistency (ITPC) of characteristic regions and the causal relationship of brain network, the motor cognitive process including high-level somatosensory joint cortex in the intervention process of MI-SSVEP was studied. Subsequently, this study verified the clinical effect of MI-SSVEP intervention paradigm for 61 stroke patients. The results show that the robot assisted therapy using MI-SSVEP intervention paradigm can more effectively improve the rehabilitation effect of patients.

Keywords: steady-state visual evoked potential (SSVEP), motor imagery (MI), inter trial phase locking consistency (ITPC), robot assisted therapy, electroencephalogram

OPEN ACCESS

Edited by:
Wenxin Niu,
Tongji University, China

Reviewed by:
Rohit Bose,
University of Pittsburgh, United States
Jing Jin,
East China University of Science and Technology, China

****Correspondence:***
Jue Wang
juewang_xjtu@126.com
Tian Liu
tianliu@xjtu.edu.cn

Specialty section:
This article was submitted to Neurocognitive Aging and Behavior, a section of the journal Frontiers in Aging Neuroscience

Received: *07 February 2022*
Accepted: *07 March 2022*
Published: *08 April 2022*

Citation:
Li L, Zhang Y, Huang L, Zhao J, Wang J and Liu T (2022) Robot Assisted Treatment of Hand Functional Rehabilitation Based on Visual Motor Imagination. Front. Aging Neurosci. 14:870871. doi: 10.3389/fnagi.2022.870871

INTRODUCTION

Stroke is one of the leading causes of motor dysfunction and death worldwide. It affects more than 17 million people every year, and most stroke patients have motor dysfunction, which seriously affects the daily life of stroke survivors (Uzdensky, 2020). Due to the existence of brain neural plasticity (Hummel and Cohen, 2005), many studies have found that patients' motor ability can be significantly restored through rehabilitation training (Becerra-Calixto and Cardona-Gomez, 2017). This phenomenon supports most repetitive, goal-based rehabilitation practices, because imitating natural motion patterns may lead to rewiring and strengthening motor neural networks to restore normal motor function. Therefore, how to "mobilize" the brain to produce similar natural movement patterns is the main goal of clinical rehabilitation of stroke.

Robot assisted rehabilitation therapy is one of the widely used interventions in clinical stroke rehabilitation therapy (Jihun and Jaehyo, 2017). With the development of brain science, the brain-computer interface method based on visual stimulation has gradually entered clinical robot assisted rehabilitation training (Grimm et al., 2016), and the rehabilitation therapy aimed at improving

patients' willingness to actively recover has gradually entered clinical applications, and previous studies have shown that the effect of traditional passive robot assisted rehabilitation training is not significant, compared with active rehabilitation training (Yang et al., 2021). At present, the brain-computer interface paradigm used in most clinical trials involves two types of methods, steady state visual evoked (SSVEP) and motor imagery (MI) (Stefano Filho et al., 2021).

Steady state visual evoked refers to visual periodic stimulation with a certain frequency, and the EEG of cerebral cortex also contains signal characteristics with the same frequency, which is referred to as SSVEP for short (Cheng et al., 2002). Light arrives at the retina through the human eye structure to form an image. This image information is transmitted to the visual cortex of the nerve center through the optic nerve. The change of ganglion cell activity leads to the change of potential, so that regular EEG signals can be detected in the occipital lobe, the whole process of visual evoked and its physiological structure. At present, SSVEP is widely used in brain computer interface control in clinical robot assisted rehabilitation. In general, the process of steady-state visual induction is closer to the human body's own neural function response, and has less correlation with active intention.

The physiological basis of motor imagery (MI) is due to the existence of mirror neurons in humans (Carrillo-de-la-Pena et al., 2008). Existing studies have shown that sensorimotor regions can be activated through motor imagination tasks (Hummel and Cohen, 2005; Rizzolatti and Craighero, 2004). At the same time, the motor imagination task will also activate the contralateral brain region, improve the blood flow and oxygen supply, and produce the phenomenon of desynchronization, while the ipsilateral brain energy increases and the synchronization is enhanced (Li et al., 2015). For stroke patients, motor imagery can activate mirror neurons in the contralateral motor area when the nerves in the motor area of the brain are damaged or the neuronal connections are abnormal (Figueroa-Garcia et al., 2014). Meanwhile, repeated activation of contralateral motor area neurons can promote nerve germination and nerve facilitation (Kim and Choe, 2009). However, motor imagery needs long-term training, and it is difficult for untrained people to directly desynchronize (Maksimenko et al., 2018).

Although both SSVEP and MI are used in robot assisted rehabilitation, these two methods have some defects in clinical application. Firstly, although the traditional motor imagination can activate motor mirror neurons, its classification rate is not high and needs to be trained in advance. Some people can not obtain the ideal classification effect of motor imagination even through training (Sitaram et al., 2007). Secondly, training only through SSVEP method cannot effectively activate mirror neurons, which makes the actual rehabilitation effect not ideal. At the same time, after long-term induced stimulation, it is easy to lead to patients' inattention and increase the degree of visual fatigue, thus affecting the rehabilitation effect (Amiri and Fazelrezai, 2013). During the clinical experiment, it is found that the rehabilitation effect is often better when the two methods are combined.. Therefore, some researchers have designed a hybrid brain computer interface paradigm based on MI-SSVEP and verified its feasibility. Mcgeady et al. (2019) used three different hand action photos to guide the motor imagination, and made one of the pictures flicker at a certain frequency to achieve the effect of mixed stimulation. Mcgeady et al. (2019) show that the system can be used for neural rehabilitation training. Similar studies show that compared with the simple brain computer interface of motor imagination, users using MI-SSVEP method can have higher resolution and robustness without motor imagination training. Previous studies on MI-SSVEP method mainly focused on the classification success rate of EEG signals. However, the neural mechanism of MI-SSVEP is not clear. At the same time, we believe that the previous paradigm of MI-SSVEP method still has defects and needs to be further improved. Static arrows or pictures and other guidance methods cannot well induce the occurrence of motion imagination, while dynamic motion animation can often better induce its occurrence (Yao et al., 2015). In this study, we designed an active training program of motor task steady-state visual evoked (MI-SSVEP) hand function, hoping to study the effect of MI-SSVEP stimulation paradigm through this program, and verify whether this paradigm can effectively affect the motor function of participants. We hypothesized that MI-SSVEP stimulation paradigm could activate major brain regions related to motor function and change the activation pattern of the brain in motor tasks. Firstly, we used normal subjects to observe the brain power spectral density distribution under the intervention of MI-SSVEP paradigm and the consistent spectral distribution between active brain regions. At the same time, we observed the causal connection between different brain regions to analyze the neural mechanism of MI-SSVEP intervention paradigm on the rehabilitation of upper limb function. Then we used this paradigm to verify the clinical effect, and followed 84 stroke patients with rehabilitation training.

MATERIALS AND METHODS

Participants

Neural Mechanism Validation Participants

Twelve healthy right-handed volunteers (average age 22 years; range 18–21 years; five men and seven women) who had no depression or other types of neurological diseases, and no history of medication for mental illness. Before the start of the experiment, they were not informed of the purpose, intention, and detailed process of the experiment. None of the 12 subjects had undergone motor imagination training in advance. There was no significant difference in the average Fugl-Meyer (FMA-UE hand function test item) scores of the 12 subjects. All subjects signed an informed consent form, which was approved by the ethics committee of Xi'an Jiaotong University.

Clinical Trial Participants

The inclusion criteria of rehabilitation training were the patients with hand motor dysfunction after stroke, the length of illness was within six months, no shoulder dislocation, no cognitive impairment, and the age was between 30 and 70 years old. There were 84 patients in total. We divided the subjects into two

groups with 42 people in each group. Due to the intervention design, the inclusion and exclusion criteria of patients are as follows:

Inclusion criteria: (1) Between 30 and 70 years old; (2) Unilateral stroke with onset time less than 6 months (based on the results of head CT or MRI); (3) The neuro-nutrition, drugs to promote the recovery of brain function and daily rehabilitation methods taken by stroke patients were similar.

Exclusion criteria: (1) History of previous stroke; (2) Neuroradiological evidence of hemispheric involvement; (3) Dementia or aphasia is serious enough to affect the patient's compliance with the experiment; (4) In addition to stroke, there are other neurological diseases; (5) The hands cannot complete subtle flexion movement, that is, the EMG signal cannot be recorded when performing the experimental task (this article is only applicable to the exclusion criteria in the second part of the experiment).

All subjects signed informed consent and were approved by the ethics committee of Xi'an Jiaotong University.

Experimental Paradigm

Neural Mechanism Validation Paradigm

The MI-SSVEP experiment combines motor imagination and visual evoker to give the subjects visual guidance on grasping actions. The stimulation contains frequency information and action guidance. Frequency stimulation can induce the subjects' occipital area of the visual cortex EEG to appear related frequencies information. Motion guidance can activate mirror neurons in the sensorimotor area. Visual stimuli in EEG are generally stable and robust, so this paradigm can complete the collection of highly robust EEG signals that activate motor mirror neurons. In order to study the difference between MI and MI-SSVEP, this article selects the grasping action as the goal of motor imagination task. The specific experimental process is as follows: the subject sits on a chair, maintains a comfortable sitting posture and eyes level, the front chest is about 30 cm away from the desktop, and the screen resolution used for visual stimulation is 60 Hz. The EEG acquisition device uses a 32-lead Neuroscan EEG acquisition device. Before the experiment, make sure that the impedance of all leads is below 5 KΩ, and check whether the EEG signal amplitude and rhythm are normal. The whole experiment contains two groups of experiments, each group contains 80 trials, a trial has a total duration of 8 s, and each trial contains 2 s of rest time and 6 s of stimulation time. The MI group stimulus pictures are black and white hand grasping movements, and the MI-SSVEP stimulus pictures are also black and white hand grasping movements. During the stimulation process, the picture will flash at a frequency of 10 Hz, and the rest time of each group of stimulation is displayed. In the picture, REST is marked with black font on the image for three seconds. The screen background is gray, the foreground of the stimulus image is black, and the background is white. The matching of black and white is to give the subjects the maximum color visual difference. All 12 subjects received MI stimulation and MI-SSVEP stimulation, and the order of stimulation was given in a random alternating manner. The detailed experimental process is shown in **Figure 1**.

Clinical Trial Paradigm

In the clinical experiment, in order to verify whether the MI-SSVEP method can effectively improve the traditional hand function robot assisted therapy, we divided the subjects into two groups with 42 people in each group. Group A was treated with manual robot assisted therapy based on MI-SSVEP intervention paradigm, and group B was treated with hand functional robot assisted therapy. Both groups received two hours of upper and lower limb training every day, six times a week. Base on routine treatments, the patients of the two groups will increase intervention training three times a week. Each intervention training lasts for 30 min, with a rest adjustment of about one minute every 5 min. Each person continued training for 2 weeks and made tracking records.

Recordings

All experiments are carried out in electromagnetic shielding room. EEG data was recorded using SynAmps2 system (EI Paso Neuroscan). According to the extended 10–20 system, a flexible cap with 32 Ag/AgCI electrodes is located. This system is usually used to detect brain electrical activity records with the parietal lobe as a reference. The electrode impedance is kept below 5 KΩ. All data are based on the electrode centered between Fz and Cz. EEG data is band-pass filtered (0.5–100 Hz). All signals are sampled to the hard disk at a frequency of 1,000 Hz, and stored on the hard disk together with event markers for offline analysis.

Data Analysis

First, we use Neuroscan's EDIT4.3 to preprocess the original EEG data, mainly using 50 Hz notch filter and ocular wake removal. In order to capture the differences between the prefrontal cortex, the motor sensory cortex, and the occipital visual cortex under different stimulation paradigms, the power spectrum analysis, time-frequency phase coherence and brain network connection analysis of all EEG channels were performed. The main analysis work in the research was carried out in the Matlab environment. Our analysis program was written using an open-source toolbox Field-Trip, and neurophysiological data analysis was carried out through this program.

Power Estimated of EEG

This chapter uses the multi-cone method to calculate the power spectrum of the EEG signal, and normalizes the power of the EEG to the sum of the total power of each frequency (0–50 Hz). This calculation is an estimate of the power ratio for the main research frequency band. In the calculation process, the EEG electrodes corresponding to the brain regions of this study were selected. They include: left motor function cortex (lM), right motor function cortex (rM), somatosensory motor cortex (fM), occipital visual cortex (oM). The calculated data segment only includes the 6-s period during which visual stimulation occurs, and the EEG during the rest period is not included in the analysis process.

Inter-Trial Coherence Calculation

Observing the desynchronization and synchronization of EEG signals is an important way to judge the overall effect of motor

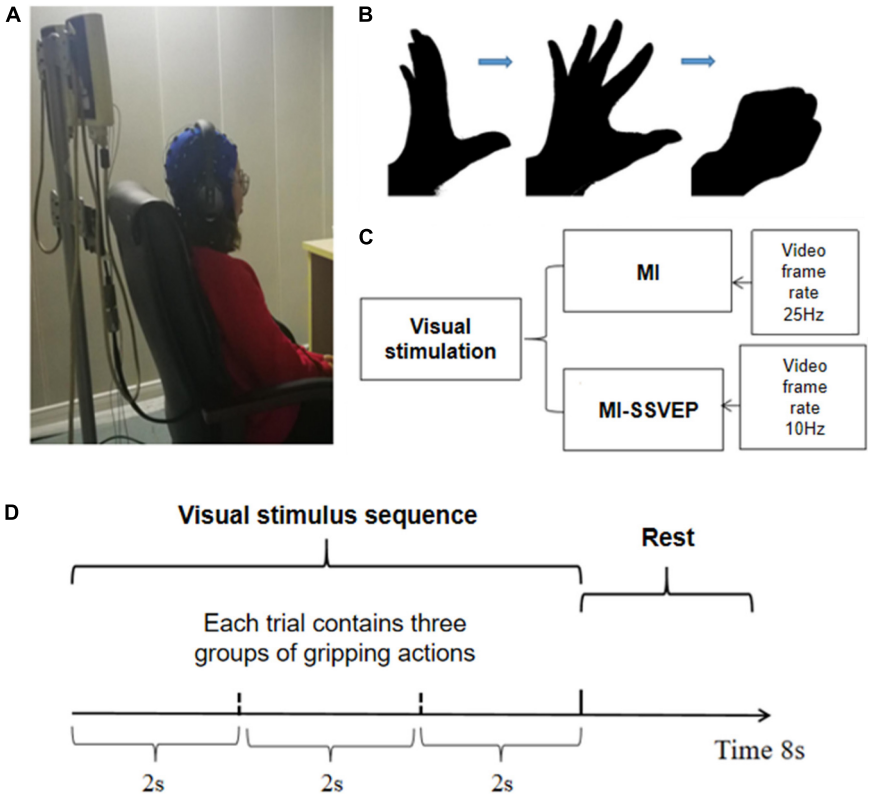

FIGURE 1 | Task design. **(A)** The picture of the experimental environment, the subjects kept sitting relaxed with their hands flat on their legs. **(B)** The screen plays the animation of grasping action stimulation. The whole grasping action is divided into 50 pictures and played continuously in two seconds; **(C)** The experimental stimulation group was divided into MI stimulation group and MI-SSVEP stimulation group. The MI-SSVEP stimulation group added 10 Hz strobe when playing animation; **(D)** Each trial has a total of 8 s, and a total of three complete grasping movements are played during the stimulation time.

imagination. The synchronization and desynchronization effects can be viewed intuitively and comprehensively by using the time-frequency analysis method. Most research on hearing uses ITPC to calculate the correlation between signals, but for visual stimuli, ITLC can preserve the linear correlation between signals, more so, the two calculations in this chapter Calculated separately. First, a time-frequency analysis of the original data in EEGLAB was carried out one by one. And use the "newtimef" function to calculate inter-group correlation linear coherence (ITLC) and inter-group phase coherence (ITPC):

$$\mathrm{ITLC}\left(\mathrm{f},\mathrm{t}\right) = \frac{\sum_{i=1}^{n} F_k(f,t)}{\sqrt{n\sum_{i=1}^{n}\left|F_k(f,t)\right|^2}}$$

$$\mathrm{ITPC}\left(\mathrm{f},\mathrm{t}\right) = \frac{1}{n}\sum_{k=1}^{n}\frac{F_k(f,t)}{\left|F_k(f,t)\right|}$$

In this function, $F_k(f, t)$ is the spectral estimate of trial k at frequency f and time t obtained using short-time Fourier transformation (STFT), and || represents the complex norm of trial k. The modified STFT (with Hanning tapers) in EEGLAB uses overlapping sliding windows that are adaptive to the target frequency bins (i.e., the time window decreases linearly as frequency increases), which is recommended to overcome limitations of conventional fixed window in estimating low frequency activities. The frequency range analyzed was 0.5–50 Hz. Zero-padding was applied to windows without sufficient number of sample points with a pad-ratio of 16 with a frequency spacing of 0.5 Hz. ITPC value of a given frequency at a given time point can range from 0 to 1. Larger ITPC values indicate higher phase consistency across trials, and smaller values indicate lower consistency or larger neural "jittering." For the calculation of theta ITPC, the ITPC data were first averaged across the frequencies for further processing.

Convergent Cross Mapping

Identifying causal networks is important for dynamic mechanism for coordinating neural activity across neuronal networks and controlling the timing of neuronal firing. In this study, we use convergent cross mapping (CCM) to estimate causal relationship between sensorimotor area, frontoparietal lobe and visual cortex. CCM is a new method, based on nonlinear state space reconstruction, that can distinguish causality from correlation (Sugihara et al., 2012). The CCM result usually expressed as a normalized quantity between −1 and 1. The calculation process and method of CCM are described briefly below:The image space reconstruction is the first

step in the non-linear dynamic analysis of EEG and EMG signals.$X(k)$ and $Y(k)$,$k = 1, 2, \cdots N$ denotes the time series which we study. Its m-dimensional delay vector can be expressed as $X(n) = \{x(n), x(n-\tau), x(n-2\tau), \cdots, x(n-(m-1)\tau)\}$, m denotes embedding dimension, τ denotes time delay. $X(n)$ denotes the reconstructed manifold M_X. Next step is to generate a cross-mapped estimate of $Y(\mathrm{n})$, denoted by $\widehat{Y}(n) \Big| M_X$.

$$\widehat{Y}(n) \Big| M_X = \sum w_i Y(n_i) i = 1 \ldots m+1$$

The w_i is a weighting based on the distance between $x(n)$ and its ith nearest neighbor on M_X and $Y(\mathrm{n_i})$ are the contemporaneous values of Y. The w_i can be expressed as

$$w_i = u_i / \sum u_j j = 1 \ldots m+1$$

where

$$u_i = \exp\{-d[\underline{x}(n), \underline{x}(n_i)]/d[\underline{x}(n), \underline{x}(n_1)]\}$$

$d[\underline{x}(n), \underline{x}(n_i)]$ is the Euclidean distance between two vectors.

The last step is to calculate the correlation coefficient ρbetween predicted and observed X.

Clinical Application Validation

This part of the work is completed by Xi'an trade union hospital to evaluate and record all the tested data. The subjects were tested with Fugl-Meyer, Wolf and ARAT. After two weeks of intervention, the two groups were evaluated with the scale again and recorded statistically. Cases such as transfer, discomfort caused by high muscle tone and withdrawal from the experiment were excluded. Secondly, the EEG data is filtered (0.5–100 Hz) to manually remove the disturbed data segments such as eye electricity. After preprocessing, EEG data is converted into a data structure suitable for field trip toolbox through the built-in interface function between EEG lab toolbox and field trip toolbox for subsequent processing and calculation.

RESULTS

Topographic Map of EEG Power Spectrum

In the experiment, we compared the distribution characteristics of EEG power and power spectrum under MI stimulation group and MI-SSVEP stimulation group to judge whether there is a differential distribution of brain activity under the traditional paradigm spontaneous motor imagination task and SSVEP induced motor imagination characters. During the analysis, we superimposed and averaged the data of 12 subjects in order to analyze the characteristics of brain activity under different tasks. As shown in **Figure 2**, we found that the main areas of brain activation in traditional motor imagination tasks are frontal parietal lobe (fM) and right motor cortex (rM). As shown in **Table 1**, the active areas of the brain in the motor imagination task guided by SSVEP were significantly different from those in the simple motor imagination task, and were significantly activated in the occipital lobe (oM) and left motor cortex (lM).

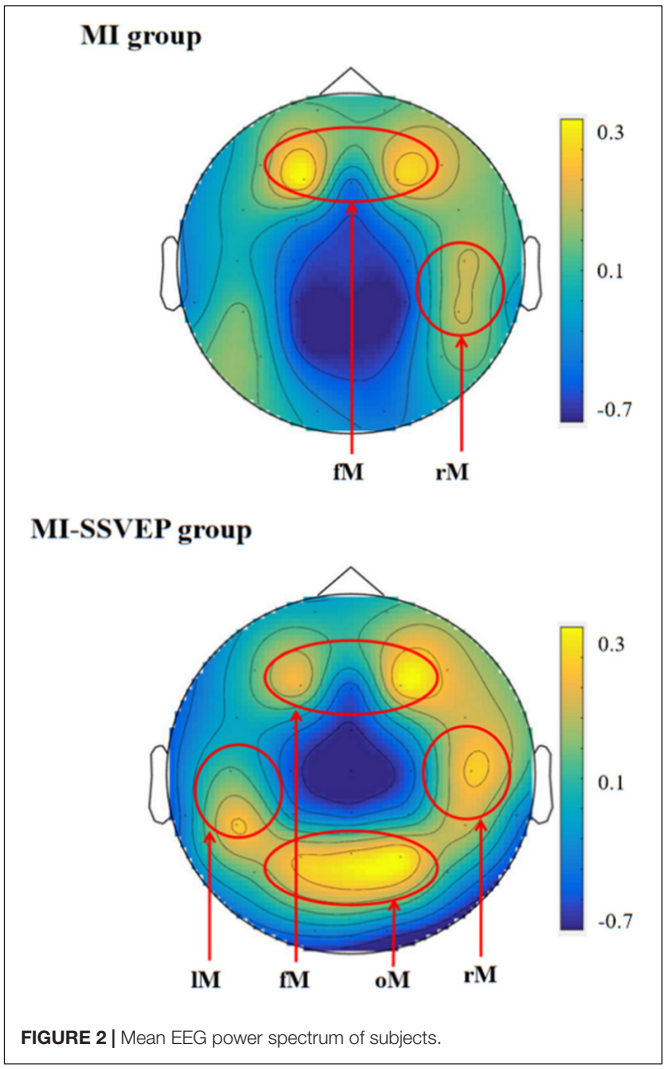

FIGURE 2 | Mean EEG power spectrum of subjects.

TABLE 1 | The statistical analysis result of EEG power spectrum.

Area	F	df	P-value
fM	1.231	1	0.275
lM	6.274	1	0.017
rM	2.067	1	0.161
oM	5.408	1	0.031

Frontal parietal lobe (fM), left motor cortex (lM), right motor cortex (rM), occipital lobe (oM).

Inter-Trial Phase Coherence

As two time-frequency measurement methods, ITLC / ITPC observe the phase correlation and signal amplitude linear correlation between signals, respectively. ITLC / ITPC are widely used to study the relationship between EEG evoked potential and spontaneous EEG oscillation phase, and display the relevant cognitive processes in the brain. In this chapter, we analyzed the distribution characteristics of ITLC / ITPC in prefrontal lobe (**Figure 3**), left (**Figure 4**) and right parietal motor cortex (**Figure 5**) and occipital visual cortex (**Figure 6**).

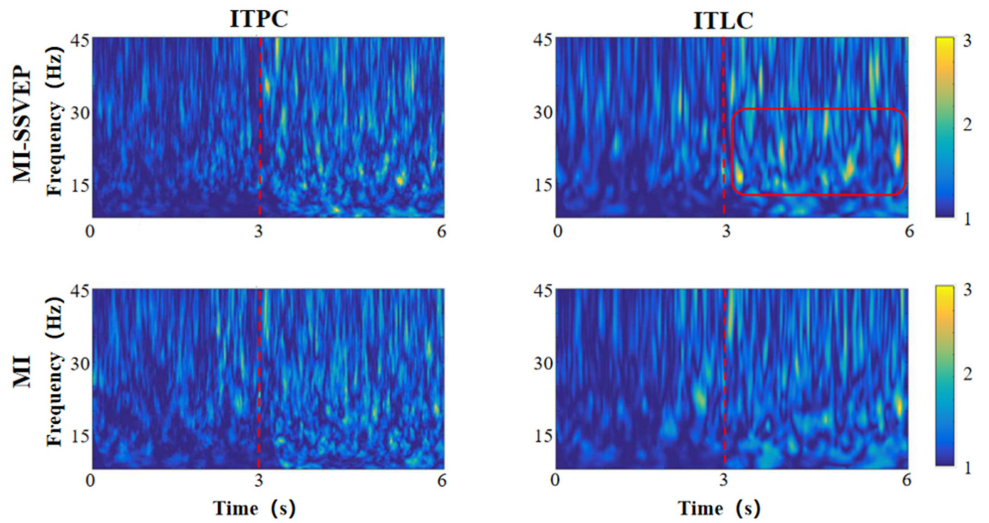

FIGURE 3 | Time frequency distribution of frontal parietal ITLC / ITPC.

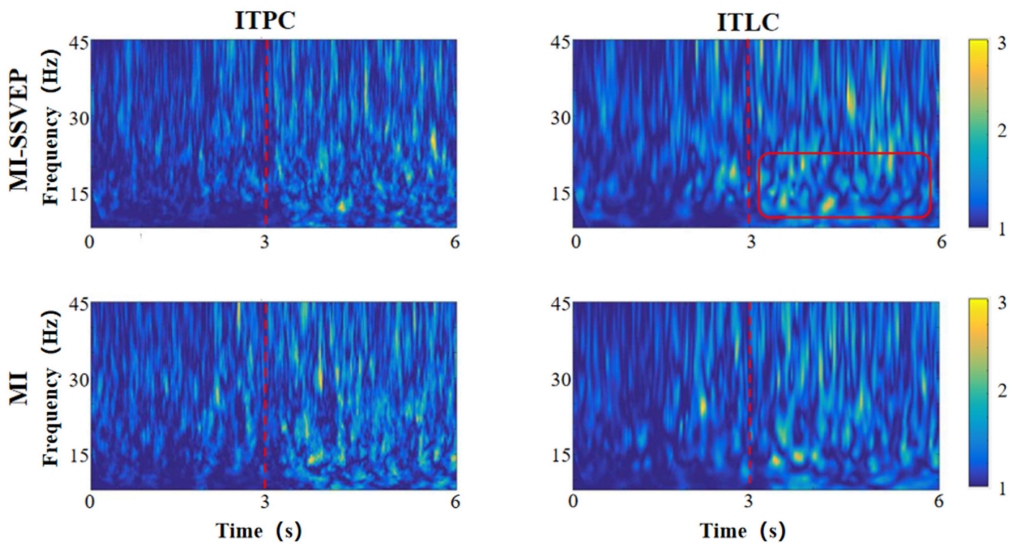

FIGURE 4 | Time frequency distribution of ITLC / ITPC in left motor cortex.

It can be found from the figure that the consistency change caused by motion imagination has an obvious gradual process in time distribution. Whether the MI stimulation group or the MI-SSVEP stimulation group, the consistency of each brain region is at a low level within 1–3 s after the beginning of the experiment. The consistency of each brain region gradually increases within 3–6 s, and the consistency level reaches the highest when the stimulation lasts around 5 s. There are also some obvious differences in the consistent frequency domain distribution. In the stimulation of MI-SSVEP group in fM region, there is a high consistent distribution in the beta frequency band within 3–6 s, but there is no such feature in the MI stimulation group. In the lM region, both MI-SSVEP stimulation and MI stimulation showed a high consistent distribution in the beta band within 3–4 s, and then the consistent distribution of MI-SSVEP shifted to the low gamma band. In the rM region, the MI stimulation group had a significantly high consistent distribution in the gamma band. In the oM region, the alpha band of MI-SSVEP stimulation showed a significantly high consistent distribution in 4–6 s.

Convergent Cross Mapping

The dynamic mechanism of neural activity coordination among neural networks during tactile stimulation was studied by using convergent cross mapping (CCM) analysis method. We selected the frontal parietal lobe (fM), left and right motor cortex (lM, rM) and occipital lobe (oM) as the main focus areas of CCM analysis,

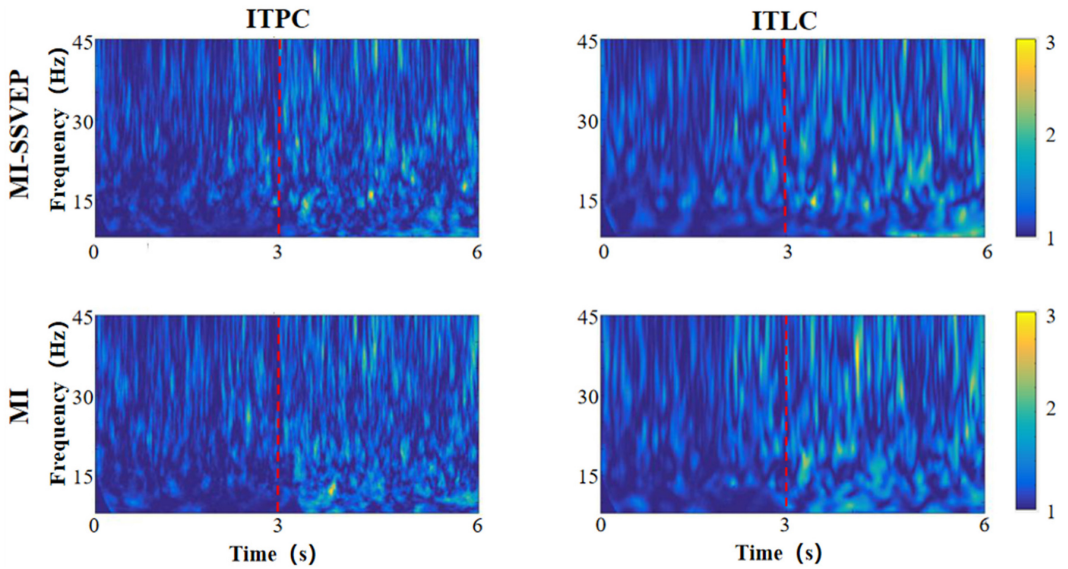

FIGURE 5 | Time frequency distribution of ITLC / ITPC in right motor cortex.

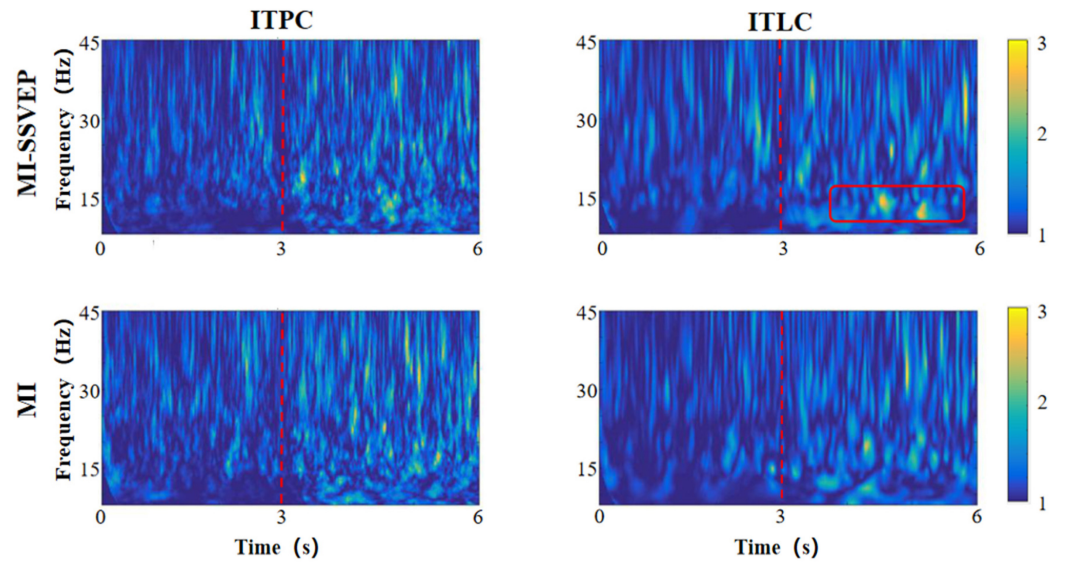

FIGURE 6 | Time frequency distribution of ITLC / ITPC in occipital cortex.

and calculated their two-way causality. The results are shown in **Table 2**.

Clinical Trial Results

In the clinical experiment, 84 patients were divided into two groups on average. Group A adopted the traditional clinical rehabilitation intervention method combined with manual robot assisted therapy using the "peripheral central peripheral" loop intervention paradigm, and group B adopted the traditional clinical rehabilitation intervention method and manual robot assisted therapy. Among them, 30 patients in group A and 31 patients in group B finally completed the experiment. We recorded the Fugl-Meyer, Wolf and ARAT scores of patients before and after two weeks of intervention.

We compared the differences between groups and within groups on the statistical results of group ab. the differences between groups mainly compared the differences between group A and group B, which were divided into two stages before and after the intervention. It should be emphasized that the grouped variables here are groups, and the compared variables are pre-test data and post-test data. In this section, in order to confirm whether the effect of the statistical experimental group is obvious, the difference between the two groups before and after intervention is also compared. The intra group difference is

TABLE 2 | The statistical analysis result of CCM.

Group		Df	F	P-value
1	lM_fM	23	0.15	0.702
2	fM_lM	23	0.001	0.977
3	rM_fM	23	0.428	0.52
4	fM_rM	23	0.006	0.937
5	lM_oM	23	0.006	0.94
6	oM_lM	23	0.005	0.943
7	rM_oM	23	0.438	0.515
8	oM_rM	23	0.625	0.438
9	oM_fM	23	1.378	0.253
10	fM_oM	23	14.581	0.001

Frontal parietal lobe (fM), left motor cortex (lM), right motor cortex (rM), occipital lobe (oM) "lm_fm" in the tableindicates the one-way causal connection from lM brain area to fM brain area, "fm_lm" indicates the one-way causal connection from fM brain area to lM brain area.
Other expressions are similar.

mainly compared with the control comparison before and after intervention in group A and group B. here is to compare the difference between pre-test and post-test in group A or group B. here, paired sample *t*-test is used. The statistical results are shown in **Tables 3**, **4**.

It can be seen from the table that there are significant differences between group A with "peripheral central peripheral" loop intervention and group B with manual energy robot assisted treatment, indicating that the two experimental paradigms have certain rehabilitation effects after intervention. The comparison results between groups can show that there is no difference between group A and group B before the intervention, and the prognosis and rehabilitation effect of group A is significantly better than that of group B.

We superimposed and averaged the CMC values on the frontoparietal cognitive area (fMl) and contralateral motor cortex area (lMl) of five subjects during the stable maintenance period. The results are shown in the figure. It can be seen from **Figure 7** and **Table 5** that the CMC coupling strength of patients is still at a low level (CMC < 0.2). Comparing the fMl region and lMl region before and after the intervention, it can be found that the CMC coupling of patients after the intervention is significantly improved in the beta band, but not in the gamma band.

Then we statistically analyzed the frequency bands of CMC values in the frontal parietal cognitive region and contralateral motor cortex. The statistical results are shown in the **Table 4**. In fMl area, the brain muscle coupling of beta band was significantly improved after patient intervention, and in lMl area, the brain muscle coupling of beta band was significantly improved after patient intervention. There was no significant difference before and after gamma band intervention.

DISCUSSION

By comparing the distribution characteristics of EEG power spectrum during MI and MI-SSVEP motor imagination tasks, we found that the right-hand motor imagination task induced by visual SSVEP stimulation can cause greater power response in the left motor cortex (lM) and occipital visual cortex (oM). The phenomenon of occipital lobe (oM) region is consistent with the experimental expectation and the previous research results on motor imagination task. At the same time, the power intensity of left and right motor cortex, occipital visual cortex and prefrontal cognitive cortex of MI and MI-SSVEP were compared. It was found that the activation intensity of occipital visual cortex and prefrontal cognitive cortex stimulated by MI-SSVEP was significantly higher than that of traditional motor imagination task. Mcgeady et al. (2019) studied a hybrid brain computer interface system. They tried to infer the effect of measuring multiple brain signals in motor imagination (MI) tasks. In addition to sensory motor rhythms (SMRs), they also introduced steady-state visual evoked potentials (SSVEP) to obtain additional information related to user intention. Their research results show that the hybrid brain computer interface with SSVEP has significantly improved the classification accuracy, but similar to the research of Jochunsen et al. they cannot obtain the internal neural mechanism of BCI induced neural plasticity from statistical experiments (Jochumsen et al., 2015). According to our existing research results, we infer that SSVEP visual stimulation under MI-SSVEP stimulation can

TABLE 3 | Statistical analysis of differences between groups.

Assessment scale	T	df	P	Average difference	Standard error
FM_after	2.31	59.00	0.02	1.85	0.80
FM_before	−0.91	59.00	0.37	−0.56	0.62
FM_D	3.51	59.00	0.00	2.41	0.69
wolf_after	4.02	59.00	0.00	2.21	0.55
wolf_before	0.11	59.00	0.91	0.03	0.29
wolf_D	3.98	51.00	0.00	2.18	0.55
ARAT_after	1.27	59.00	0.21	1.60	1.26
ARAT_before	0.34	59.00	0.74	0.39	1.15
ARAT_D	3.01	59.00	0.00	1.21	0.40

Fugl-Meyer test before and after (FM_before, FM_after), Wolf test before and after (lM_before, lM_after), ARAT test before and after (ARAT_before, ARAT_after).
FM_D represents the difference between the scores of FM scale after intervention and before intervention.
Wolf_D and ARAT_D scales are expressed in the same way.

TABLE 4 | Statistical analysis of differences before and after.

Group	classification	Average	T	df	P
A	FM_before and FM_after	−9.63	−18.15	29	0.00
	wolf_before and wolf_after	−5.47	−12.04	29	0.00
	ARAT_before and ARAT_after	−5.47	−16.50	29	0.00
B	FM_before and FM_after	−7.22	−16.45	30	0.00
	wolf_before and wolf_after	−3.29	−10.79	30	0.00
	ARAT_before and ARAT_after	−4.25	−18.38	30	0.00

A stands for experimental group A, FM_ before and FM_ Afte indicates the result of comparing the difference before andafter using FM scale score. Other evaluation criteria are expressed in the same way.

enhance the activation of occipital cortex and motor imagination tasks. At the same time, in our experiment, we also found that the prefrontal cognitive cortex was always activated at a high level. Therefore, we speculate that visual stroboscopic can enhance the activation of frontal parietal lobe in motor imagination task by affecting the connection between occipital lobe and cognitive cortex.

Most neurological diseases have adverse effects on cognitive and motor functions. These injuries will not only change the measured values of EEG power spectrum and event-related potential, but also affect the consistency of EEG amplitude and phase (ITLC / ITPC) (Rosenblum et al., 2000). Therefore, observing ITLC / ITPC can reflect the ability of neural response and timely synchronization of related events (Makeig et al., 2004), so as to optimize information processing (Palva, 2005). In this study, we found the phase / linear consistency of motor imagination evoked potentials in different brain regions and different frequency bands under visual guidance. At the same time, there is a certain regularity in the distribution of phase / linear consistency between motor imagination tasks stimulated by MI-SSVEP and those without stroboscopic visual MI stimulation. The results show that: (1) the consistency change caused by motor imagination has an obvious gradual process in time distribution, which shows that the "coordination" between brain neurons can be improved after the start of motor imagination task, and this "coordination" represents the improvement of brain efficiency in information processing. From the experimental results, it can be concluded that the improvement of efficiency is a gradual process. The brain needs a "pre-treatment" process to adapt to the activation effect of motor imagination task; (2) When subjects performed motor imagination tasks under MI-SSVEP stimulation, there was a high consistency distribution in the beta band of frontal parietal lobe within 3–6 s, but this feature did not appear in the MI stimulation group. At the same time, there was a significant high consistency distribution in the alpha band of MI-SSVEP stimulation within 4–6 s in the occipital region. This shows that MI-SSVEP stimulation can more effectively cause the information processing efficiency of frontoparietal cortex, and the power of this region is also significantly improved. The consistency difference of frontal parietal lobe region shows that the motor imagination task guided by stroboscopic stimulation is a complex feedback process, which may be related to the activation of occipital lobe; (3) At the same time, in the LM region, both MI-SSVEP stimulation and Mi stimulation have a high consistency distribution in the beta frequency band within 3–4 s, and then the MI-SSVEP consistency distribution shifts to the low gamma frequency band. Papenberg et al. (2016) studied the characteristics of linear consistency distribution in different frequency bands. They believe that the linear consistency of low gamma frequency band is related to the improvement of motor function, The improvement of consistency shows the change of response time variability of motor cortex to motor task in motor task. The faster the response time, the higher the consistency. That is, stroboscopic stimulation enhances motor imagination response (Papenberg et al., 2013).

Convergent cross mapping (Ye et al., 2015) based on EEG data is a new computational method to study the connectivity of human brain network (Clark et al., 2015). In our study, the visual evoked motor imagination task under stroboscopic stimulation was introduced. We found that the unidirectional causal relationship between motor sensory cortex and EMG channels increased significantly during MI-SSVEP stimulation compared with visual evoked motor imagination alone. We believe that in the current study, the causal difference between occipital cortex and parietal cognitive cortex reflects the interactive intervention mechanism between occipital cortex and parietal cognitive cortex in MI-SSVEP induced motor imagination tasks.

Combined with previous studies and the findings on the linear consistency between groups and CCM causality in this chapter's experiments, we speculate that the principle of this intervention may come from two aspects: (1) stroboscopic motion picture stimulation improves the subjects' attention concentration in the process of motion observation and motion imagination; (2) Similar to the process of human brain processing film, human photosensitive system can distinguish up to 48 flashes per second. If the frequency continues to increase, the conversion between light and dark will not be detected (Watson and Ahumada, 1985), For motion pictures, humans will keep the images they see for 100–400 ms. Therefore, when people see motion pictures with a frame rate of more than 15, they will think that they are continuous motion movements (Crick et al., 1981). In our experiment, the frame rate of MI-SSVEP is 10, so it will lead to an "involuntary" motion imagination process in the cerebral cognitive cortex to supplement the missing pictures. This "involuntary" motor imagination process may lead to the cognitive cortex group not only in the process of motor imagination, but also constantly "waiting" or "grasping" the "new" picture information coming from the occipital visual cortex. This process of "waiting" or "grasping" directly leads to the enhancement of causality between the two cortexes.

In the clinical study, we used two different intervention methods to treat 84 stroke patients. From the clinical experiment, we found that: (1) after two weeks of intervention, the traditional robot assisted rehabilitation therapy and "MI-SSVEP" intervention can effectively improve the scores of multiple scales; (2) Comparing the therapeutic effects of the two intervention paradigms, "MI-SSVEP" intervention can more effectively

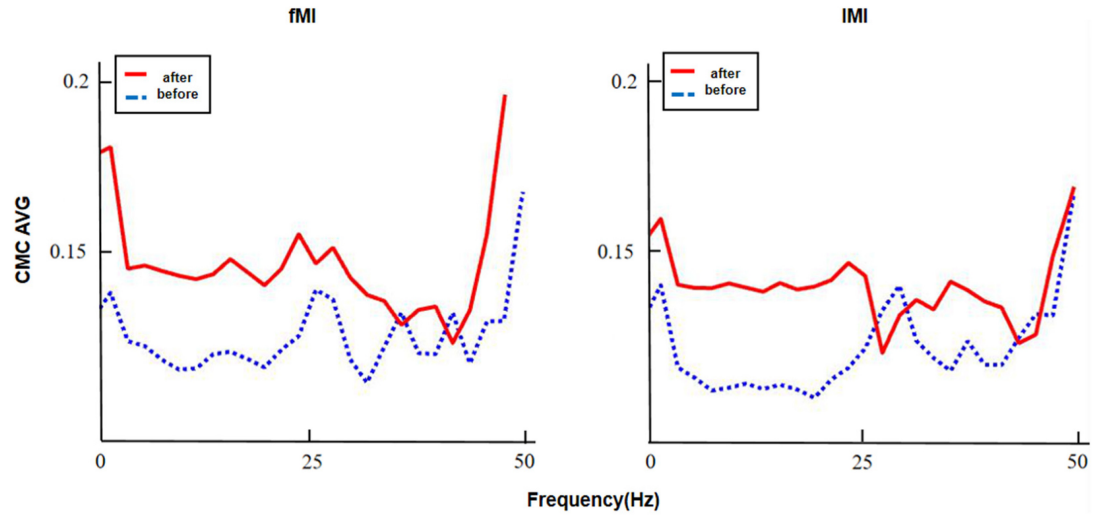

FIGURE 7 | Mean value of cortical muscle coupling of 5 subjects before and after intervention.

TABLE 5 | Statistical analysis of cmc value in frequency division.

Area	Band	Mean differences	T	df	P
fMI	Beta	−0.024	−4.23	4	0.013
	Gamma	0.087	0.84	4	0.449
lMI	Beta	−0.127	−29.793	4	0.00
	Gamma	−0.003	−1.58	4	0.19

fMI and lMI represent frontal parietal lobe cognitive region and contralateral motor cortex region, respectively.

improve the rehabilitation effect of patient intervention. (3) "MI-SSVEP" intervention can effectively improve the brain muscle coupling effect of beta band in patients, indicating that it does have a neural mechanism to improve the effect of rehabilitation treatment. The significant effect of robot assisted therapy on clinical intervention is completely within the expected range. A large number of previous studies on robot assisted therapy have proved the effectiveness of this therapy (Rodgers et al., 2017). We analyzed deeply the scores of patients with "peripheral central peripheral" motor loop nerve intervention treatment scheme integrated with peripheral feedback in Fugl-Meyer, Wolf and ARAT evaluation scales. It was found that compared with traditional robot assisted treatment, patients with new treatment scheme had relatively high scores in fine motor and muscle tension. Combined with the follow-up visit to patients in clinical experiments, we believe that this improvement is mainly due to the following reasons: (1) in the process of patient intervention, compared with the traditional robot assisted passive treatment, MI-SSVEP intervention paradigm can mobilize the attention concentration of patients' rehabilitation and make patients more focused during training time. (2) The real-time effect of visual stimulus input can change the CMC distribution of primary motor somatosensory cortex and contralateral motor cortex. This effect not only has real-time effect, but also has prognostic effect. (3) MI-SSVEP guided motor imagination task can more effectively improve the intervention effect of motor imagination in the training process, and can stimulate motor imagination activities more directly.

DATA AVAILABILITY STATEMENT

The original contributions presented in the study are included in the article/supplementary material, further inquiries can be directed to the corresponding author/s.

ETHICS STATEMENT

The studies involving human participants were reviewed and approved by the Ethics Committee of Xi'an Jiaotong University. The patients/participants provided their written informed consent to participate in this study. Written informed consent was obtained from the individual(s) for the publication of any potentially identifiable images or data included in this article.

AUTHOR CONTRIBUTIONS

LL participated to study design, data collection and analysis, and manuscript writing. YZ participated to study design, data collection and analysis, and manuscript definition.

LH participated to data analysis. JZ participated in the data collection. JW and TL participated to study design. All authors read and approved the final manuscript.

FUNDING

This work was supported by the National Natural Science Foundation of China (Grant No. U1913216) and the National Natural Science Foundation of China (Grant No. 61431012), a National Key Research and Development Program of China (Nos. 2017YFB1300303 and 2018YFC2002601). 2019 Ministry of Education in China (MOE) Youth Foundation Project of Humanities and Social Sciences (Grant No. 19YJC740119).

ACKNOWLEDGMENTS

We would like to thank YZ for his help in subject recruitment and syllable stimulation, as well as Professor TL, Professor JW and LH for their help in the revision of the article.

REFERENCES

Amiri, A. S., and Fazelrezai, R. (2013). "A review of P300, SSVEP, and hybrid P300 / SSVEP brain- computer interface systems," in *Brain-Computer Interface Systems – Recent Progress and Future Prospects*, ed. R. Fazel-Rezai (London: IntechOpen).

Becerra-Calixto, A., and Cardona-Gomez, G. P. (2017). The role of astrocytes in neuroprotection after brain stroke: potential in cell therapy. *Front. Mol. Neurosci.* 10:88. doi: 10.3389/fnmol.2017.00088

Carrillo-de-la-Pena, M. T., Galdo-Alvarez, S., and Lastra-Barreira, C. (2008). Equivalent is not equal: primary motor cortex (MI) activation during motor imagery and execution of sequential movements. *Brain Res.* 1226, 134–143. doi: 10.1016/j.brainres.2008.05.089

Cheng, M., Gao, X., Gao, S., and Xu, D. (2002). Design and implementation of a brain-computer interface with high transfer rates. *IEEE Trans. Biomed. Eng.* 49, 1181–1186. doi: 10.1109/tbme.2002.803536

Clark, T., Ye, H., Isbell, F., Deyle, E. R., Cowles, J., Tilman, G. D., et al. (2015). Spatial convergent cross mapping to detect causal relationships from short time series. *Ecology* 96, 1174–1181. doi: 10.1890/14-1479.1

Crick, F. H. C., Marr, D. C., and Poggio, T. (1981). "An information processing approach to understanding the visual cortex," in *Neurosciences Research Program Colloquium on Cerebral Cortex*, ed. F. Schmitt (Cambridge, MA: MIT Press).

Figueroa-Garcia, I., Aguilar-Leal, O., Hernandez-Reynoso, A. G., Madrigal, J., Fuentes, R. Q., Huegel, J. C., et al. (2014). Platform for the study of virtual task-oriented motion and its evaluation by EEG and EMG biopotentials. *Annu. Int. Conf. IEEE Eng. Med. Biol. Soc.* 2014, 1174–1177. doi: 10.1109/EMBC.2014.6943805

Grimm, F., Walter, A., Spuler, M., Naros, G., Rosenstiel, W., and Gharabaghi, A. (2016). Hybrid neuroprosthesis for the upper limb: combining brain-controlled neuromuscular stimulation with a multi-joint arm exoskeleton. *Front. Neurosci.* 10:367. doi: 10.3389/fnins.2016.00367

Hummel, F. C., and Cohen, L. G. (2005). Drivers of brain plasticity. *Curr. Opin. Neurol.* 18, 667–674. doi: 10.1097/01.wco.0000189876.37475.42

Jihun, K., and Jaehyo, K. (2017). Robot-assisted mirroring exercise as a physical therapy for hemiparesis rehabilitation. *Annu. Int. Conf. IEEE Eng. Med. Biol. Soc.* 2017, 4243–4246. doi: 10.1109/EMBC.2017.8037793

Jochumsen, M., Niazi, I. K., Taylor, D., Farina, D., and Dremstrup, K. (2015). Detecting and classifying movement-related cortical potentials associated with hand movements in healthy subjects and stroke patients from single-electrode, single-trial EEG. *J. Neural Eng.* 12:056013. doi: 10.1088/1741-2560/12/5/056013

Kim, J. I., and Choe, M. A. (2009). [Effects of unilateral sciatic nerve injury on unaffected hindlimb muscles of rats]. *J. Korean Acad. Nurs.* 39, 393–400. doi: 10.4040/jkan.2009.39.3.393

Li, L., Wang, J., Xu, G., Li, M., and Xie, J. (2015). The study of object-oriented motor imagery based on EEG suppression. *PLoS One* 10:e0144256. doi: 10.1371/journal.pone.0144256

Makeig, S., Debener, S., Onton, J., and Delorme, A. (2004). Mining event-related brain dynamics. *Trends Cogn. Sci.* 8, 204–210. doi: 10.1016/j.tics.2004.03.008

Maksimenko, V. A., Pavlov, A., Runnova, A. E., Nedaivozov, V., and Hramov, A. E. (2018). Nonlinear analysis of brain activity, associated with motor action and motor imaginary in untrained subjects. *Nonlinear Dyn.* 91, 2803–2817. doi: 10.1007/s11071-018-4047-y

Mcgeady, C., Vuckovic, A., and Puthusserypady, S. (2019). "A hybrid MI-SSVEP based brain computer interface for potential upper limb neurorehabilitation: a pilot study," in *Proceedings of the 2019 7th International Winter Conference on Brain-Computer Interface (BCI)*, (Piscataway, NJ: IEEE).

Palva, J. M. (2005). Phase synchrony among neuronal oscillations in the human cortex. *J. Neurosci.* 25, 3962–3972. doi: 10.1523/JNEUROSCI.4250-04.2005

Papenberg, G., Ferencz, B., Mangialasche, F., Mecocci, P., Cecchetti, R., Kalpouzos, G., et al. (2016). Physical activity and inflammation: effects on gray—matter volume and cognitive decline in aging. *Hum. Brain Mapp.* 37, 3462–3473. doi: 10.1002/hbm.23252

Papenberg, G., Hämmerer, D., Müller, V., Lindenberger, U., and Li, S. C. (2013). Lower theta inter-trial phase coherence during performance monitoring is related to higher reaction time variability: a lifespan study. *Neuroimage* 83, 912–920. doi: 10.1016/j.neuroimage.2013.07.032

Rizzolatti, G., and Craighero, L. (2004). The mirror-neuron system. *Annu. Rev. Neurosci.* 27, 169–192. doi: 10.1146/annurev.neuro.27.070203.144230

Rodgers, H., Shaw, L., Bosomworth, H., Aird, L., Alvarado, N., Andole, S., et al. (2017). Robot assisted training for the upper limb after stroke (RATULS): study protocol for a randomised controlled trial. *Trials* 18:340. doi: 10.1186/s13063-017-2083-4

Rosenblum, M., Tass, P., Kurths, J., Volkmann, J., and Freund, H. J. (2000). "Detection of phase locking from noisy data: application to magnetoencephalography," in *Proceedings of the Workshop*, (Bonn: University of Bonn).

Sitaram, R., Zhang, H., Guan, C., Thulasidas, M., Hoshi, Y., Ishikawa, A., et al. (2007). Temporal classification of multichannel near-infrared spectroscopy signals of motor imagery for developing a brain-computer interface. *Neuroimage* 34, 1416–1427. doi: 10.1016/j.neuroimage.2006.11.005

Stefano Filho, C. A., Attux, R. R. F., and Castellano, G. (2021). Motor imagery practice and feedback effects on functional connectivity. *J. Neural Eng.* 18:066048. doi: 10.1088/1741-2552/ac456d

Sugihara, G., May, R., Ye, H., Hsieh, C. H., Deyle, E., Fogarty, M., et al. (2012). Detecting causality in complex ecosystems. *Science* 338, 496–500. doi: 10.1126/science.1227079

Uzdensky, A. B. (2020). Regulation of apoptosis in the ischemic penumbra in the first day post-stroke. *Neural Regen. Res.* 15, 253–254. doi: 10.4103/1673-5374.265546

Watson, A. B., and Ahumada, A. J. (1985). Model of human visual-motion sensing. *J. Opt. Soc. Am. A* 2, 322–341. doi: 10.1364/josaa.2.000322

Yang, Z., Guo, S., Hirata, H., and Kawanishi, M. (2021). A mirror bilateral neuro-rehabilitation robot system with the sEMG-based real-time patient active participant assessment. *Life (Basel)* 11:1290. doi: 10.3390/life11121290

Yao, L., Meng, J., Sheng, X., Zhang, D., and Zhu, X. (2015). A novel calibration and task guidance framework for motor imagery BCI via a tendon vibration induced sensation with kinesthesia illusion. *J. Neural Eng.* 12:016005. doi: 10.1088/1741-2560/12/1/016005

Ye, H., Deyle, E. R., Gilarranz, L. J., and Sugihara, G. (2015). Distinguishing time-delayed causal interactions using convergent cross mapping. *Sci. Rep.* 5:14750. doi: 10.1038/srep14750

Conflict of Interest: The authors declare that the research was conducted in the absence of any commercial or financial relationships that could be construed as a potential conflict of interest.

Publisher's Note: All claims expressed in this article are solely those of the authors and do not necessarily represent those of their affiliated organizations, or those of the publisher, the editors and the reviewers. Any product that may be evaluated in this article, or claim that may be made by its manufacturer, is not guaranteed or endorsed by the publisher.

frontiers | Frontiers in Aging Neuroscience

STUDY PROTOCOL
published: 29 April 2022
doi: 10.3389/fnagi.2022.881311

Effects of the Intermittent Theta Burst Stimulation of the Cerebellar Vermis on Balance Recovery After Stroke: A Study Protocol for a Randomized Controlled Trial

Lin Wang[1†], Guilan Huang[2†], Li Zhang[2], Jinyu Yang[2], Caili Ren[3], Chengpan Liang[2], Ying Shen[4] and Bin Su[2,1*]*

[1] School of Kinesiology, Shanghai University of Sport, Shanghai, China, [2] Department of Rehabilitation, Wuxi Tongren Rehabilitation Hospital, Wuxi, China, [3] Department of Neurorehabilitation, Wuxi Tongren Rehabilitation Hospital, Wuxi, China, [4] Rehabilitation Medicine Center, The First Affiliated Hospital of Nanjing Medical University, Nanjing, China

OPEN ACCESS

Edited by:
Wenxin Niu,
Tongji University, China

Reviewed by:
Jack Jiaqi Zhang,
The Hong Kong Polytechnic University, Hong Kong SAR, China
Zhongfei Bai,
The Hong Kong Polytechnic University, Hong Kong SAR, China
Qiang Gao,
Sichuan University, China

***Correspondence:**
Ying Shen
shenying@njmu.edu.cn
Bin Su
13951585359@163.com

[†] These authors have contributed equally to this work and share first authorship

Specialty section:
This article was submitted to Parkinson's Disease and Aging-related Movement Disorders, a section of the journal Frontiers in Aging Neuroscience

Received: 22 February 2022
Accepted: 28 March 2022
Published: 29 April 2022

Citation:
Wang L, Huang G, Zhang L, Yang J, Ren C, Liang C, Shen Y and Su B (2022) Effects of the Intermittent Theta Burst Stimulation of the Cerebellar Vermis on Balance Recovery After Stroke: A Study Protocol for a Randomized Controlled Trial. Front. Aging Neurosci. 14:881311. doi: 10.3389/fnagi.2022.881311

Background: The recovery of balance function is a critical segment in the rehabilitation treatment of stroke. The cerebellum is considered as the key structure involved in balance and motor control. The cerebellar vermis plays an important role in integrating vision, proprioception, and sensory skin input and may be a candidate stimulation target for regulating the motor network related with balance. However, evidence that the intermittent theta burst stimulation (iTBS) of cerebellar vermis can promote the recovery of balance function after stroke remains insufficient. Therefore, this study aims to explore the efficacy of the cerebellar vermis iTBS for the treatment of balance function in patients with stroke.

Methods and Analysis: Forty patients with stroke will be recruited in this prospective, randomized, sham-controlled trial. Participants will be randomized in a 1:1 ratio to receive either 15 sessions of cerebellar vermis iTBS (600 pulses) or sham stimulation. Additionally, a routine rehabilitation therapy follows the intervention. The primary outcome is the Berg Balance Scale, and the secondary outcomes are the Fugl–Meyer assessment of the lower extremity and modified Barthel index. The above outcomes will be assessed before intervention and at the end of each week. Pre- and post-iTBS resting-state functional magnetic resonance imaging (rs-fMRI) will be acquired, and the regional homogeneity, fractional amplitude of low-frequency fluctuation and functional connectivity will be calculated and analyzed.

Discussion: This protocol holds promise as a potential method to improve balance function in patients with stroke. If the outcomes of patients improve after the intervention, the study will provide new insights into improving balance function.

Ethics and Dissemination: This study has been approved by the Medical Research Ethics Committee of Wuxi Mental Health Center (Wuxi Tongren Rehabilitation Hospital).

Results will be disseminated through (open-access) peer-reviewed publications, networks of scientists, professionals, and the public and presented at conferences.

Clinical Trial Registration Number: www.chictr.org.cn, identifier ChiCTR2100052590.

Keywords: study protocol, stroke, intermittent theta burst stimulation, cerebellar vermis, RCT

INTRODUCTION

Every year, over 15 million people in the world suffer from stroke (Van Lieshout et al., 2017). Balance problem is a common dysfunction that arises after stroke and is usually due to poor proprioception, decreased motor control, and abnormal integration of nervous system (Xiong et al., 2019). Moreover, the balance problem may be the main cause of poor walking ability and increased risk of falls in patients with stroke (Zhang et al., 2020). About 15–37% of patients with stroke fall down at least once due to balance dysfunction during hospitalization (Rabadi et al., 2012). Falls appear to be frequent after discharge, with approximately 40% falling within 6–12 months of stroke (Wada et al., 2007). Therefore, balance plays a significant role in the rehabilitation process of stroke. However, pharmacotherapy (Mead et al., 2013) and conventional rehabilitation treatments, including core strength exercises (Chung et al., 2014), visual feedback training (Zhang et al., 2020), neurodevelopmental therapy (Langhammer and Stanghelle, 2011), and proprioceptive neuromuscular facilitation (Eng and Tang, 2007) performed unsatisfactory results on balance recovery among stroke patients.

In recent years, repetitive transcranial magnetic stimulation (rTMS), a non-invasive brain stimulation technology, has been widely used in various nervous system diseases (Ren et al., 2019; Yin et al., 2020). rTMS induces a current in the cerebral cortex through a coil that generates a magnetic field, thereby regulating the excitability of the cerebral cortex and affecting neuroplasticity (Brown et al., 2021). Theta burst stimulation (TBS), a novel pattern of rTMS, has the characteristics of lower stimulation intensity and a shorter stimulation session (2–3 min or less) (Pinto et al., 2018), the relatively low stimulation intensity reduces the risk of adverse reactions especially the risk of epileptic seizures (Gutierrez-Muto et al., 2020). Huang and Rothwell (2004) were the first to investigate the neurophysiological effects of TBS in healthy human subjects, founded that 600-pulse intermittent TBS (iTBS) can enhance cortical excitability.

The cerebellum plays an important role in maintaining postural position, regulating the muscle tension associated with postural movements, and coordinating voluntary movements (Manto et al., 2011). To date, studies on the effects of cerebellar rTMS on balance rehabilitation are still limited. As pointed out in neurophysiological research, the cerebellar activity in patients with stroke is positively correlated with the recovery of walking function (Bijsterbosch et al., 2011). Low-frequency rTMS in the cerebellum can improve walking ability in patients with spinocerebellar degeneration (Svenja et al., 2017). Furthermore, a meta-analysis suggested that cerebellar stimulation may affect corticospinal excitability (Zelda et al., 2016). Koch et al. (2018) also found that the iTBS of the unaffected cerebellum promotes the excitability of the posterior parietal cortex and improves the balance and gait function in patients with chronic stroke (over 6 months).

Notably, the choice of the rTMS target has a remarkable influence on its therapeutic effect. However, an agreement on how to select the best targets for patients with balance dysfunctions is limited until now. Primary motor cortex (M1) area is one of the most common targets. Kim et al. (2014) used low-frequency rTMS to act on the M1 area of the patient's lower extremities and found that the 10 min walking speed and Berg Balance Scale (BBS) are improved. Additionally, the supplementary motor area (SMA) (Richard et al., 2017) and dorsal prefrontal cortex (Harris et al., 2018) have been implicated to be critical in balance tasks. With deepening research, recent studies demonstrated that the cerebellum is also one of the effective targets of rTMS. The cerebellar vermis is a major part of the cerebellum. Notably, patients with cerebellar vermis lesions present with balance dysfunction (Harris et al., 2018), whereas cerebellar hemisphere lesions focus on global coordination dysfunctions (Carass et al., 2018; Maas et al., 2020). A recent study that used fNIRS technology found that after a single iTBS on the cerebellar vermis in healthy individuals, the HBO_2 values in bilateral SMA regions are increased. These results indicated a potential link between the cerebellar vermis and SMA (Tan et al., 2021). The cerebellar vermis may be a new target for iTBS to intervene with balance function and deserves further exploration.

A randomized controlled clinical trial will be conducted to investigate the rehabilitation effect of the cerebellar vermis intervened by iTBS in stroke patients with balance dysfunctions. Furthermore, the resting-state functional magnetic resonance imaging (rs-fMRI) will be used to analyze the functional connections between cerebellar vermis and other areas of the cerebral cortex, and clarify the neural remodeling mechanism. We propose a hypothesis that iTBS of cerebellar vermis can promote the recovery of balance function after stroke. This study may provide new insights into the therapeutic efficacy and underlying neuroplasticity mechanisms of cerebellar vermis intervention.

MATERIALS AND METHODS

Study Design

This study will be carried out in the Department of Rehabilitation, Tongren Rehabilitation Hospital, Wuxi, China. Before the conduct of formal experiments, a research coordinator who is responsible for recruitment will arrange a conversation with

potential participants to discuss some details, including research purpose, procedures, and the potential risks and benefits. Once informed consent is signed by the patient or their legal guardians (if the patient cannot write independently or consider consent), a questionnaire and baseline assessment will be arranged.

All participants will be randomly assigned to real or sham iTBS and then receive routine rehabilitation treatment, and they will be assessed using the BBS, Fugl–Meyer assessment of the lower extremity (FMA-LE), and modified Barthel index (MBI). Moreover, rs-fMRI scans will be performed at baseline and 3 weeks after treatment. The study flow chart is shown in **Figure 1**. All baseline data gathering, follow-up assessment, and interventions will be carried out by well-trained researchers with the support of academic staff. This study has been approved by ethics committees (WXMHCIRB2021LLky132) and registered on www.chictr.org.cn on 27 October 2021 under the number ChiCTR2100052590. Details are shown in **Table 1**.

Participants

Inclusion Criteria

The inclusion criteria are as follows. Participants who (a) have a diagnosis of stroke confirmed by CT and/or MRI, (b) have their first-ever unilateral ischemic stroke between 1 and 6 months of onset, (c) are 40–75 years old, (d) presented with a balance dysfunction with a Berg score between 0 and 40, (e) can follow simple verbal commands or instructions, and (f) can cooperate in signing informed consent forms.

Exclusion Criteria

Participants (a) with contraindications involving TMS and fMRI (e.g., intracranial implant, cardiac pacemaker, implanted drug pumps, and pregnancy), (b) with cerebellum or brainstem stroke, (c) with balance dysfunction before stroke, (d) with serious diseases that may contribute to condition progression, (e) with severe deficits in communication or executing commands that prevent cooperation with assessment and treatment, (f) who are taking psychotropic drugs, and (g) who are currently enrolled in other clinical trials will be excluded from the study.

Sample Size

The sample size was calculated using a G*power of 3.1.4. The effect size was calculated as 0.28 based on the BBS from a study reported by Koch et al. (2018). To achieve 95% power with an alpha error of 5%, a sample size of 30 patients will be required. Allowing for a dropout rate of 20%, at least 38 patients are necessary. To ensure enough power to detect this typical difference, we will aim to recruit 40 patients (20 patients per group).

Randomization

All participants will be prestratified into two subgroups (i.e., poor balance on 0–20 scores vs. acceptable balance on 21–40 scores) on the basis of their balance function to ensure a relatively even distribution between groups (Lisa and Nicol, 2008) (**Figure 2**). After obtaining informed consent, a random sequence will be generated using the computer, 40 participants will be randomly allocated in a 1:1 ratio to each group and will receive either real or sham iTBS. The advantage of this type of assignment process, which is designed in our study, is that detect effects can be improved especially for studies involving small samples.

Blind

This study is a participants and assessors-blinded study. Given the nature of the iTBS intervention, blinding the physicians performing the intervention is impossible. The intervention team needs to be separated into blinded physicians performing routine rehabilitation treatment, and unblinded physicians exclusively applying iTBS. However, patients, outcome assessors, research assistants, and statisticians will be blinded. For urgent unblinding, researchers can use sealed envelopes labeled with the patients' randomization numbers. To maintain the quality of the trial, a patient's allocation must be unblinded only in exceptional circumstances when knowledge of the actual treatment is essential for the management of the patient.

Intervention

Patients recruited in this study will receive a 60 min routine rehabilitation treatment immediately after completing real or sham iTBS therapy. The rehabilitation program focuses on the exercise designed to promote recovery of balance function, including trunk control, weight bearing, task oriented intervention, and balance training, which will be designed by physicians according to the patient's balance function. Patients in both groups will be required to attend 15 sessions [one session per day, five times per week (Monday to Friday) for three consecutive weeks]. Enrollment, intervention, and assessment procedures are shown in **Figure 3**.

Cerebellar iTBS: We use the Magneuro 100 (Vishee Medical Technology Co., Ltd., Nanjing, China) equipped with a double-cone coil (each coil is 70 mm in diameter) to stimulate the cerebellum vermis. iTBS is performed by the physician in accordance with the TMS guidelines (Groppa et al., 2012; Klooster et al., 2016). Before intervention, active motor threshold (AMT) for the tibialis anterior muscle in the unaffected side will be measured. The AMT is defined as the minimum output of stimulation that produced a motor evoked potential (MEP) of $>200\ \mu V$ in at least 5 out of 10 trials with 10% maximal voluntary contraction (Liao et al., 2020). Stimulation will be administered at 80% of AMT. The iTBS paradigm consisting of three pulses at 50 Hz repeated at 5 Hz frequency will be used, with 8-s rest after each 2-s stimulus, generating a total of 600 pulses in 200 s. The coil will be positioned tangentially to the scalp over the cerebellum vermis (at 1 cm below the highest point of the occipital protuberance) (Cattaneo et al., 2014; Tan et al., 2021). Sham iTBS will be performed with a customized sham coil and at the same location, frequency and intensity so that all participants are exposed to a similar clicking noise.

Outcome Assessment

Primary Outcome

The BBS is a clinical test commonly used to assess the patients' static and dynamic balance performance and can determine whether a patient is at risk of falls with an inter-rater reliability of 0.98 (Maeda et al., 2015; Meseguer-Henarejos et al., 2019).

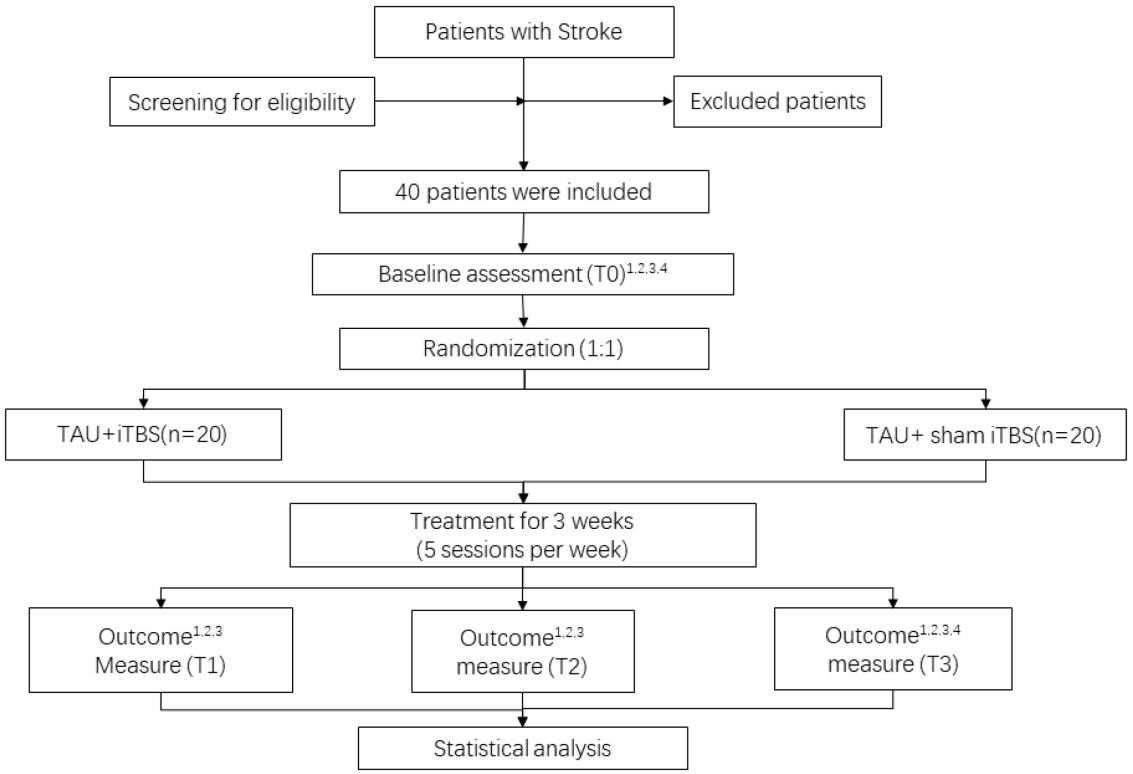

FIGURE 1 | Study flow diagram. [1]BBS, [2]FMA-LE, [3]MBI, and [4]fMRI. TAU, treatment as usual; iTBS, intermittent theta burst stimulation. T0, before intervention; T1, at the end of first week of post-intervention; T2, at the end of second week of post-intervention; T3, at the end of third week of post-intervention.

The BBS consists of 14 items, and the score for each item is 0–4 points with an overall score of 0–56 points. Good completion results in high score.

Secondary Outcomes

In addition to the BBS scores, FMA-LE, MBI, and rs-fMRI will be measured with the following tests.

Fugl–Meyer assessment of the lower extremity has been widely used in the assessment of the motor function of patients with stroke and has good prediction, reliability, and sensitivity to interventions (Balasubramanian et al., 2016). In addition, the reliability of the FMA scale is >75% between different raters and >88% within the same rater (Hernández et al., 2021). The FMA-LE consists of 17 items, with each item scoring a minimum of 0 and a maximum of 2 points, resulting in a maximum total score of 34 points. A high score results in good motor function of the lower extremity.

The MBI, one of the main scales used to measure the patients' abilities to perform activities of daily living, has a reliability of 88% in patients with ischemic stroke (Yang et al., 2021). The MBI consists of 10 items, with a full score of 100 points. A high score results in good independence of the patient's life.

All subjects will undergo rs-fMRI scans. Regional homogeneity (ReHo), fractional amplitude of low-frequency fluctuation (fALFF), and functional connectivity (FC) will be calculated to measure the local and global FC networks related to motion function. All images will be acquired by professional personnel in a 3.0T, 8-channel MRI scanner (Siemens Skyra, Germany). During scanning, subjects will be required to keep awake, breathe quietly, lie flat on the bed, fix their heads to minimize the movement of their heads and other parts, and try not to do any active thinking activity. It will take approximately 40 min to complete the test. Conventional T1 structural image parameters are as follows: repetition time (TR) = 2,000 ms, echo time (TE) = 20 ms, field of view (FOV) = 240 mm × 240 mm, slice thickness = 4 mm, slice spacing = 4 mm, flip angle (FA) = 90°, and 36 slices. Functional images will be acquired using T1-weighted gradient echo planar imaging (EPI) sequence in the axial plane with the following parameters: TR = 2,000 ms, TE = 30 ms, FOV = 240 mm × 240 mm, slice thickness = 4 mm, FA = 90°, and 35 slices.

Statistical Analysis

Clinical Data Analysis

The SPSS (version 22.0, Chicago, IL, United States) statistical software will be used for data analysis. The difference will be considered statistically significant when the P-value ≤ 0.05 in two-tailed test. The assumption of normality will be verified by normal probability plots and the Shapiro–Wilk test. Continuous variables with normal distribution will be described as the mean (standard deviation) and analyzed by an independent-samples t-test. For abnormally distributed variables, the data will be

TABLE 1 | Trial registration data.

Data category	Trial information
Primary registry and trial identifying number	ChiCTR2100052590
Date of registration in primary registry	27 October 2021
Secondary identifying numbers	N/A
Source(s) of monetary or material support	This project is being supported by Wuxi Taihu Talent Project (WXTTP2020008), the Nanjing Municipal Science and Technology Bureau (2019060002), the Major Scientific Research Project of Wuxi Health Committee (Z202013), Top Talent Support Program for Young and Middle-Aged People of Wuxi Health Committee (HB2020079), Scientific and Technological Development Fund from Wuxi Science and Technology Bureau (Y20212008), Wuxi Municipal Health Commission Scientific Project (T201144), and Jiangsu Geriatrics Clinical Technology Application Research Project (LR2021040).
Primary sponsor	N/A
Secondary sponsor(s)	N/A
Contact for public queries	Bin Su, 13951585359@163.com
Contact for scientific queries	Bin Su, 13951585359@163.com
Public title	Effect of cerebellar vermis iTBS on the balance dysfunction of stroke patients and the brain remodeling mechanism
Scientific title	Effect of cerebellar vermis iTBS on the balance dysfunction of stroke patients and the brain remodeling mechanism
Countries of recruitment	China
Healthy conditions(s) or problem(s) studied	Stroke with hemiparesis, including balance dysfunction
Intervention(s)	Active comparator: iTBS (application of 600 pulses with a frequency of 50 Hz, in a theta-rhythm of 5 Hz for 200 s) will be applied to the cerebellum vermis positioned tangentially to the scalp combined with routine rehabilitation treatment. Sham comparator: Sham stimulus will be applied to same location with a customized sham coil, also combined with routine rehabilitation treatment.
Key inclusion and exclusion criteria	Inclusion criteria: (a) have a diagnosis of stroke confirmed by CT and/or MRI, (b) have their first-ever unilateral ischemic stroke between 1 and 6 months of onset, (c) are 40–75 years old, (d) presented with a balance dysfunction with a Berg score between 0 and 40, (e) can follow simple verbal commands or instructions, and (f) can cooperate in signing informed consent forms. Exclusion criteria: (a) with contraindications involving TMS and fMRI (e.g., intracranial implant, cardiac pacemaker, implanted drug pumps, and pregnancy), (b) with cerebellum or brainstem stroke, (c) with balance dysfunction before stroke, (d) with serious diseases that may contribute to condition progression, (e) with severe deficits in communication or executing commands that prevent cooperation with assessment and treatment, (f) who are taking psychotropic drugs, and (g) who are currently enrolled in other clinical trials.
Study type	Interventional Allocation: randomized intervention model Masking: participants and assessors-blinded Assignment: parallel Primary purpose: treatment
Date of first enrolment	Not yet started
Target sample size	40
Recruitment status	Recruiting
Primary outcome(s)	Berg balance scale
Key secondary outcome(s)	Lower extremity of the Fugl–Meyer assessment; modified Barthel index; regional homogeneity, fractional amplitude of low frequency fluctuation and functional connectivity analyses from rs-fMRI.

described as medians with ranges and compared by Mann–Whitney U test (non-parametric tests). Categorical variables will be expressed as frequency (percentage) and Chi-square test or Fisher's exact test will be used. Repeated measures analysis of variance (ANOVA) will be used to analyze value changes of BBS, FMA-LE, and MBI across four testing time points (weeks 0, 1, 2, and 3). When the interaction is significant, *post hoc* analysis will be conducted, and the Bonferroni adjustment will be used for paired comparisons. Data on clinical scales will be based on per-protocol (PP) and intention-to-treat (ITT) analyses (Sanchez and Xun, 2010). The PP is usually defined as subjects who complete at least 80% of the treatment protocol (Zhao et al., 2021). An ITT analysis include all the patients recruited in the study, irrespective of whether they completed the study period or not. The missing values will be imputed using a multiple imputation method.

Functional Magnetic Resonance Imaging Data Analysis

On the MATLAB R2013b (Mathworks, Natick, MA, United States) platform, the statistical parametric graph software (SPM12.0[1]) and data processing assistant for rs-fMRI

[1]http://www.fil.ion.ucl.ac.uk/spm/

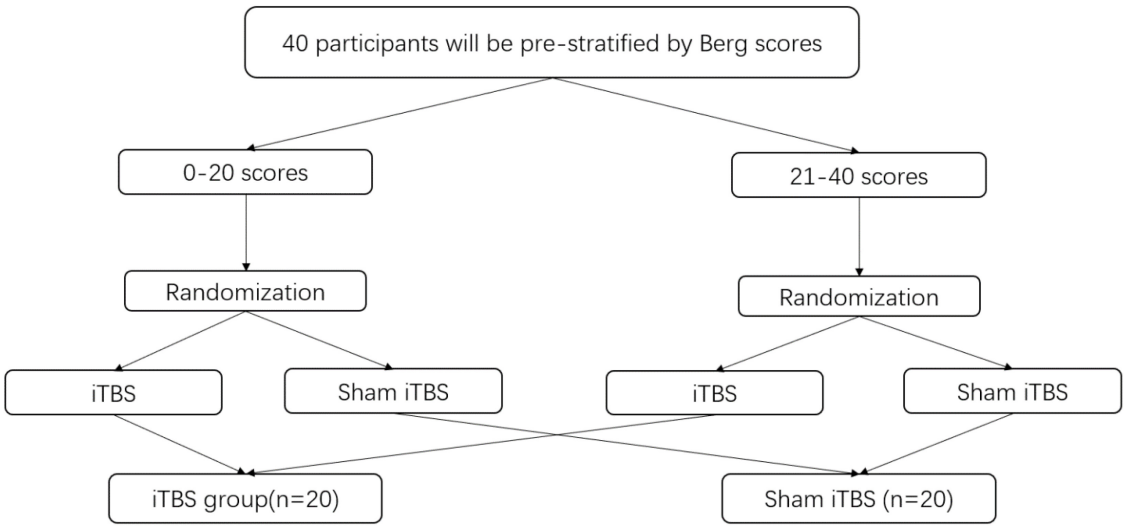

FIGURE 2 | Flow chart of random grouping procedure.

	Study Period					
	Enrollment	Allocation	Post-allocation			
TIME POINT	W-1	0	AFT	W1	W2	W3
ENROLLMENT:			×			
Eligibility screen	×					
Informed consent	×					
Rondomization	×					
Allocation		×				
INTERVENTIONS:						
iTBS			←	—	—	→
sham iTBS			←	—	—	→
ASSESSMENTS:						
Baseline data			×			
BBS			×	×	×	×
FMA-LE			×	×	×	×
MBI			×	×	×	×
fMRI			×			×

FIGURE 3 | Schedule of participant enrollment, interventions, and assessments. BBS, Berg Balance Scale; FMA-LE, lower extremity of the Fugl–Meyer assessment; MBI, modified Barthel index; fMRI, functional magnetic resonance imaging.

software (DPARSF[2]) will be used for data processing and analysis. DPARSF is a SPM-based rs-fMRI data processing software (Yan et al., 2016). Preprocessing steps include (Lv et al., 2018; Ll et al., 2020): (a) removing the first 10–20 time points and slice timing, (b) head movement correction (head movement exceeding 2 mm in any direction or head rotation exceeding 2° will be ruled out), (c) normalization (in accordance with the Montreal Neurological Institute EPI template, each voxel is resampled to 3 mm × 3 mm × 3 mm), (d) delinear drift, (e) removal covariate (confounding effects of head movement parameters, white matter, and cerebrospinal fluid signals), (f) filter (0.01–0.1 Hz), and (g) smooth (8 mm full-width half-maximum Gaussian).

[2]http://rfmri.org/dpabi

Then, the ReHo, fALFF, and FC values will be calculated. The ReHo analysis is a voxel-based measurement that calculates the Kendall coefficient of concordance between a voxel and its surrounding 26 voxels, which is the ReHo value of that voxel (Zang et al., 2004). The ReHo analysis determines the synchrony of adjacent regions, and high values indicate high consistency of regional brain activity. The ALFF measurement is the root mean square of the power spectrum of the BOLD signal in the range of 0.01–0.1 Hz for each voxel. Afterward, the ALFF value of each voxel divided by the full-band ALFF sum is the fALFF value, which can reflect the strength of brain self-activity (Toole et al., 2005). FC was examined by using a seed voxel correlation approach. The cerebellar vermis will be selected as the seed region based on the stimulation target. In SPM12, after bandpass filtering and linear-trend removal, a reference time series for the seed will be extracted by averaging the fMRI time series of voxels. Then, correlations will be computed between the seed reference and the rest of the brain in a voxelwise manner. Finally, an individual relativity value (r-value) map will be created, and the correlation coefficients in each voxel will be transformed to z values by using Fisher's r-to-z transformation to improve normality before performing random effect t-tests. The AlphaSim will be used for correction to obtain the adjustment statistical threshold value of $P < 0.05$. Data will be analyzed by the independent-samples (between-group comparison) or paired (within-group comparison) t-test.

Safety

Operation procedures will strictly follow the latest safety guidelines for TMS (Rossi et al., 2009), and participants will be screened strictly in accordance with the inclusion and exclusion criteria to minimize the risk of adverse event. Common adverse events of TMS include (but are not limited to) headache, dizziness, tinnitus, and seizures. If mild headache, discomfort caused by noise, and scalp irritation occur, they are usually self-healing and transient. Hence, before testing or intervention, the patient should be informed of the risks in advance. Seizures, the most severe TMS-related adverse event with a crude risk of approximately 0.02% (Rossi et al., 2009), are expected to occur only during or immediately after stimulation. In addition, any adverse event occurring within 24 h after MRI will be reported. If a serious incident occurs, it will be immediately reported to the principal researcher and ethics committee. The ethics committee will assess whether the patient should receive further treatment. If the patients suffer from syncope, seizures, and other conditions that may affect the subject's health during the treatment, we will stop the assigned intervention. Once the participants are injured during this trial, they will be compensated. All adverse events from TMS will be reported by the researcher and recorded on the case report form. The researchers will record the date, duration, and severity of adverse events.

Patient and Public Involvement

During the trial, patients will not participate in the design, implementation, or outcome assessment of the study. However, we plan to publicize our research proposal to participants and the public through the official website of the hospital (such as WeChat official account) and lectures at major academic conferences.

Ethics and Dissemination

The study has been approved by the Medical Research Ethics Committee of Wuxi Mental Health Center (Wuxi Tongren Rehabilitation Hospital). Before entering the study, all participants will be informed that their participation are entirely voluntary and that they can withdraw from the trial at any time without consequence. During the trial, the welfare and rights of participants should be satisfied, and the privacy of patients should be guaranteed. Any change in the key aspects of the protocol, such as inclusion criteria, observation indicators, and statistical analysis, will be submitted to the Medical Research Ethics Committee. Results will be presented at conferences and submitted to peer-reviewed journals.

Research Quality Assurance and Management

Researchers should perform their respective responsibilities. Including the following contents:

1. The principal researcher establishes unified experimental test indices, standard operating procedures, and quality control procedures.
2. Researchers participating in our trials must have professional expertise and the ability to conduct clinical trials. Moreover, invariability of personnel involving in this research should be guaranteed.
3. The interveners and evaluators need to participate in standardized training before the trial, they should adopt standard operating procedures to ensure the quality of clinical trials.
4. The principal researcher shall appoint an inspector to ensure that the rights and interests of participants are protected, that the trial follows approved protocols, and that reports are accurate.

DISCUSSION

This 3-week randomized controlled clinical trial aims to study whether cerebellar vermis iTBS can improve balance function in patients with stroke. In this perspective of experiment design, our study puts forward some methodological concerns that should be discussed, including the large variation in balance function among enrolled patients. Therefore, a stratification approach will be adopted in this study to divide all participants into two subgroups in accordance with the BBS. In addition, we set a sham stimulation group to eliminate the placebo effect of iTBS intervention. After careful consideration of all factors, including the feasibility of the study and the treatment time pattern of the hospital where the experiment will be conducted, we set sessions from Monday to Friday for 3 weeks. Also, outcome will be evaluated at pre-intervention, the end of first, second, and third week of post-intervention. We want to compare the efficacy at different time points, and to explore the earliest time when

the treatment can take effect. Our study will use rs-fMRI rather than task state fMRI for measuring the iTBS-induced effects, although task state fMRI can reflect the fMRI images of the brain when performing specific tasks. What we considering is that our subjects are post-stroke patients with motor dysfunction, there may be great differences in the quality of tasks completed by stroke patients, which may affect the results.

In this study, we expect that the cerebellar vermis iTBS can promote the recovery of balance function after stroke. This hypothesis is based on the following evidence.

Maintaining balance depends upon a complex coordination and integration of multiple systems in the body, including the visual system, vestibular system, and auditory system. As pointed out in fMRI research, the cerebellar vermis and the visual network have a strong functional connection (Kellermann et al., 2012; Li et al., 2012). Recent evidence displayed that the vermis coordinates eye and body movements, and provides visual and auditory input related to balance (Fujita et al., 2020). In addition, studies have shown that the vermis participates in regulating vestibular system and maintaining head position (Lam et al., 2016). Balance is best maintained when all inputs are integrated together. Therefore, the cerebellar vermis plays an essential role in the active maintenance of body balance.

In addition, the process of maintaining balance involves a close cooperation between the cerebellum and the cerebrum. These interconnections are facilitated by white-matter tracts with the following connective pathways: the cortico-ponto-cerebellar pathway and cerebello-thalamo-cortical (CTC) pathway (Iwata and Ugawa, 2005; Opie and Semmler, 2020), which have been proven to be involved in motor coordination (Spampinato et al., 2020). As pointed out in an animal experiment, the reduction of ipsilateral cerebral cortical activity can lead to the reduction of contralateral cerebellar activity and metabolism (Baek et al., 2020). Previous studies similarly confirmed that the cerebellum establishes strong anatomical and functional connections with the M1 area through the cerebellum–thalamic–M1 circuit (Maurer et al., 2016). The cerebellum has three functional areas, the spinocerebellum, the cerebrocerebellum and the vestibulocerebellum. The vermis classically belongs to the "spinocerebellum" and to receive somatic sensory input from ascending spinal pathways. Cattaneo et al. (2014) pointed out that compared to cerebellar hemispheres, cerebellar vermis takes a more prominent role in continuous visual processing in visual feedback loops. Interestingly, in Coffman et al.'s (2011) study, the rabies virus was injected into the lobule of the vermis, and retrograde transneuronal transport of the virus was used to define disynaptic inputs to it. It was found that large numbers of neurons in the primary motor cortex and other motor areas on the medial wall of the hemisphere project to the vermis. This implicates that there is potential connection between cerebellum vermis and motor area of cerebral cortex. Therefore, iTBS may improve balance by regulating the excitability of the cerebellar vermis, then promoting excitability changes in motor areas of the cerebral cortex.

In current studies, the depth of coil stimulation is an important factor affecting the efficacy of rTMS. Recent studies showed that an eight-figure coil has mostly been used for iTBS (Li et al., 2018). This coil is characterized by small stimulation area, shallow stimulation depth, and good focusing. The range of the magnetic field induced by rTMS attenuates with increasing distance from the scalp surface (Deng et al., 2013). However, the cerebellum is located in the posterior fossa and covered by the tentorium cerebellum, which is deeper from the skull. Previous studies found that the double-cone coil can achieve deeper stimulation effects (Deng et al., 2013) and generate stronger electric field than the eight-figure coil (Mai and Ueno, 2017), confirming good reliability and validity. In addition, Hardwick et al. (2014) showed that the double-cone coil causes the most evident cerebellar brain effect in magnetic stimulation with the same parameters compared with the eight-figure and airfoil coils, suggesting that the double-cone coil may be suitable for studies of TMS over the cerebellum.

In our trial, the location of cerebellar vermis is consistent with similar literatures (Cattaneo et al., 2014; Tan et al., 2021), In Cattaneo's study, the accuracy of this localization method was further verified by using a neuronavigation system in some subjects for whom structural MRIs were available. The results shown that the scalp coordinate 1 cm below the inion indeed corresponded to the cerebellar vermis (Cattaneo et al., 2014). This research is the first study to explore the effect of cerebellar vermis iTBS on balance dysfunction after stroke by using the double-cone coil. This protocol proposes a rigorous randomized parallel controlled trial design that meets the methodological requirements of full concealment, randomization, and placebo control.

Intermittent theta burst stimulation has the advantages of short stimulation time, easy promotion, and relatively easy application. We hope that the results of this study can shed light on this potential effect. We believe that the current protocol and our results will have important implications for the treatment of post-stroke patients with balance dysfunction.

ETHICS STATEMENT

The studies involving human participants were reviewed and approved by the Medical Research Ethics Committee of Wuxi Mental Health Center (Wuxi Tongren Rehabilitation Hospital) (No. WXMHCIRB2021LLky132): Effect of cerebellar vermis iTBS on the balance dysfunction of stroke patients and the brain remodeling mechanism. The patients/participants provided their written informed consent to participate in this study.

AUTHOR CONTRIBUTIONS

GH designed the trial protocol, with scientific insight and contributions from YS and BS. JY prepared the human research ethics. LZ provided iTBS and routine rehabilitation training programs. LZ and CL were involved in the overall research design and selection of outcome measure. CR calculated the sample size and designed the statistical analysis plan. LW and GH prepared the first draft of this manuscript and it was reviewed by YS and BS. LW performed the revisions. All authors read and approved the final manuscript.

FUNDING

This project was being supported by Wuxi Taihu Talent Project (WXTTP2020008), the Nanjing Municipal Science and Technology Bureau (2019060002), the Major Scientific Research Project of Wuxi Health Committee (Z202013), Top Talent Support Program for Young and Middle-Aged People of Wuxi Health Committee (HB2020079), Scientific and Technological Development Fund from Wuxi Science and Technology Bureau (Y20212008), Wuxi Municipal Health Commission Scientific Project (T201144), and Jiangsu Geriatrics Clinical Technology Application Research Project (LR2021040).

ACKNOWLEDGMENTS

We are grateful to all the participants for their contributions in completing this study.

REFERENCES

Baek, H., Sariev, A., Lee, S., Dong, S. Y., and Kim, H. (2020). Deep cerebellar low-intensity focused ultrasound stimulation restores interhemispheric balance after ischemic stroke in mice. *IEEE Trans. Neural Syst. Rehabil. Eng.* 28, 2073–2079. doi: 10.1109/TNSRE.2020.3002207

Balasubramanian, C. K., Li, C. Y., Bowden, M. G., Duncan, P. W., Kautz, S. A., and Velozo, C. A. (2016). Dimensionality and item-difficulty hierarchy of the lower extremity fugl-meyer assessment in individuals with subacute and chronic stroke. *Arch. Phys. Med. Rehabil.* 97, 582.e–589.e. doi: 10.1016/j.apmr.2015.12.012

Bijsterbosch, J. D., Lee, K. H., Hunter, M. D., Tsoi, D. T., Lankappa, S., Wilkinson, I. D., et al. (2011). The role of the cerebellum in sub- and supraliminal error correction during sensorimotor synchronization: evidence from fMRI and TMS. *J. Cogn. Neurosci.* 23, 1100–1112. doi: 10.1162/jocn.2010.21506

Brown, J. C., Yuan, S., Devries, W. H., Armstrong, N. M., Korte, J. E., Sahlem, G. L., et al. (2021). Nmda-receptor agonist reveals ltp-like properties of 10-hz rtms in the human motor cortex. *Brain Stimul.* 14, 619–621. doi: 10.1016/j.brs.2021.03.016

Carass, A., Cuzzocreo, J. L., Han, S., Hernandez-Castillo, C. R., Rasser, P. E., Ganz, M., et al. (2018). Comparing fully automated state-of-the-art cerebellum parcellation from magnetic resonance images. *Neuroimage* 183, 150–172. doi: 10.1016/j.neuroimage.2018.08.003

Cattaneo, Z., Renzi, C., Casali, S., Silvanto, J., Vecchi, T., Papagno, C., et al. (2014). Cerebellar vermis plays a causal role in visual motion discrimination. *Cortex* 58, 272–280. doi: 10.1016/j.cortex.2014.01.012

Chung, E., Lee, B. H., and Hwang, S. (2014). Core stabilization exercise with real-time feedback for chronic hemiparetic stroke: a pilot randomized controlled trials. *Restor. Neurol. Neurosci.* 32, 313–321. doi: 10.3233/RNN-130353

Coffman, K. A., Dum, R. P., and Strick, P. L. (2011). Cerebellar vermis is a target of projections from the motor areas in the cerebral cortex. *Proc. Natl. Acad. Sci. U.S.A.* 108, 16068–16073. doi: 10.1073/pnas.1107904108

Deng, Z. D., Lisanby, S. H., and Peterchev, A. V. (2013). Electric field depth–focality tradeoff in transcranial magnetic stimulation: simulation comparison of 50 coil designs. *Brain Stimul.* 6, 1–13. doi: 10.1016/j.brs.2012.02.005

Eng, J. J., and Tang, P. F. (2007). Gait training strategies to optimize walking ability in people with stroke: a synthesis of the evidence. *Expert Rev. Neurother.* 7, 1417–1436. doi: 10.1002/pri.474

Fujita, H., Kodama, T., and du Lac, S. (2020). Modular output circuits of the fastigial nucleus for diverse motor and nonmotor functions of the cerebellar vermis. *eLife* 9:2209. doi: 10.7554/eLife.58613

Groppa, S., Oliviero, A., Eisen, A., Quartarone, A., Cohen, L. G., Mall, V., et al. (2012). A practical guide to diagnostic transcranial magnetic stimulation: report of an IFCN committee. *Clin. Neurophysiol.* 123, 858–882. doi: 10.1016/j.clinph.2012.01.010

Gutierrez-Muto, A. M., Castilla, J., Freire, M., Oliviero, A., and Tornero, J. (2020). Theta burst stimulation: technical aspects about TMS devices. *Brain Stimul.* 13, 562–564. doi: 10.1016/j.brs.2020.01.002

Hardwick, R. M., Lesage, E., and Miall, R. C. (2014). Cerebellar transcranial magnetic stimulation: the role of coil geometry and tissue depth. *Brain Stimul.* 7, 643–649. doi: 10.1016/j.brs.2014.04.009

Harris, D. M., Rantalainen, T., Muthalib, M., Johnson, L., Duckham, R. L., Smith, S. T., et al. (2018). Concurrent exergaming and transcranial direct current stimulation to improve balance in people with Parkinson's disease: study protocol for a randomised controlled trial. *Trials* 19:387. doi: 10.1186/s13063-018-2773-6

Hernández, E. D., Forero, S. M., Galeano, C. P., Barbosa, N. E., Sunnerhagen, K. S., and Murphy, M. A. (2021). Intra- and inter-rater reliability of fugl-meyer assessment of lower extremity early after stroke. *Braz. J. Phys. Ther.* 25, 709–718. doi: 10.1016/j.bjpt.2020.12.002

Huang, Y., and Rothwell, J. C. (2004). The effect of short-duration bursts of high-frequency, low-intensity transcranial magnetic stimulation on the human motor cortex. *Clin. Neurophysiol.* 115, 1069–1075. doi: 10.1016/j.clinph.2003.12.026

Iwata, N. K., and Ugawa, Y. (2005). The effects of cerebellar stimulation on the motor cortical excitability in neurological disorders: a review. *Cerebellum* 1, 218–223. doi: 10.1080/14734220500277007

Kellermann, T., Regenbogen, C., De Vos, M., Moßnang, C., Finkelmeyer, A., and Habel, U. (2012). Effective connectivity of the human cerebellum during visual attention. *J. Neurosci.* 32, 11453–11460. JNEUROSCI.0678-12.2012 doi: 10.1523/

Kim, W., Jung, S., Oh, M., Min, Y., Lim, J., and Paik, N. (2014). Effect of repetitive transcranial magnetic stimulation over the cerebellum on patients with ataxia after posterior circulation stroke: a pilot study. *J. Rehabil. Med.* 46, 418–423. doi: 10.2340/16501977-1802

Klooster, D., Louw, A. D., Aldenkamp, A. P., Besseling, R., Mestrom, R., Carrette, S., et al. (2016). Technical aspects of neurostimulation: focus on equipment, electric field modeling, and stimulation protocols. *Neurosci. Biobehav. Rev.* 65, 113–141. doi: 10.1016/j.neubiorev.2016.02.016

Koch, G., Bonnì, S., Casula, E. P., Losa, M., Paolucci, S., Pellicciari, M. C., et al. (2018). Effect of cerebellar stimulation on gait and balance recovery in patients with hemiparetic stroke a randomized clinical trial. *JAMA Neurol.* 76, 170–178. doi: 10.1001/jamaneurol.2018.3639

Lam, C. K., Tokuno, C. D., Staines, W. R., and Bent, L. R. (2016). The direction of the postural response to a vestibular perturbation is mediated by the cerebellar vermis. *Exp. Brain Res.* 234, 3689–3697. doi: 10.1007/s00221-016-4766-6

Langhammer, B., and Stanghelle, J. K. (2011). Can physiotherapy after stroke based on the bobath concept result in improved quality of movement compared to the motor relearning programme. *Physiother. Res. Int.* 16, 69–80. doi: 10.1002/pri.474

Li, S., Wen, Q., Yong, L., Wei, H., Zhang, Y., Jiang, T., et al. (2012). Resting-state functional connectivity of the vermal and hemispheric subregions of the cerebellum with both the cerebral cortical networks and subcortical structures. *Neuroimage* 61, 1213–1225. doi: 10.1016/j.neuroimage.2012.04.011

Li, Y., Fan, J., Yang, J., He, C., and Li, S. (2018). Effects of repetitive transcranial magnetic stimulation on walking and balance function after stroke: a systematic review and meta-analysis. *Am. J. Phys. Med. Rehabil.* 97, 773–781. doi: 10.1097/PHM.0000000000000948

Liao, L. Y., Xie, Y. J., Chen, Y., and Gao, Q. (2020). Cerebellar theta-burst stimulation combined with physiotherapy in subacute and chronic stroke patients: a pilot randomized controlled trial. *Neurorehabil. Neural Repair* 35, 23–32. doi: 10.1177/1545968320971735

Lisa, B., and Nicol, K. B. (2008). Usefulness of the berg balance scale in stroke rehabilitation: a systematic review. *Phys. Ther.* 88, 559–566. /ptj.20070205 doi: 10.2522

Ll, A., Rh, C., Xl, B., Bao, F. B., Wl, B., and Rong, S. (2020). Reduced complexity in stroke with motor deficits: a resting-state fMRI study. *Neuroscience* 434, 35–43. doi: 10.1016/j.neuroscience.2020.03.020

Lv, H., Wang, Z., Tong, E., Williams, L. M., Zaharchuk, G., Zeineh, M., et al. (2018). Resting-state functional mri: everything that nonexperts have always wanted to know. *AJNR Am. J. Neuroradiol* 39, 1390–1399. doi: 10.3174/ajnr.A5527

Maas, R., Helmich, R. C. G., and van de Warrenburg, B. P. C. (2020). The role of the cerebellum in degenerative ataxias and essential tremor: insights from noninvasive modulation of cerebellar activity. *Mov. Disord.* 35, 215–227. doi: 10.1002/mds.27919

Maeda, N., Urabe, Y., Murakami, M., Itotani, K., and Kato, J. (2015). Discriminant analysis for predictor of falls in stroke patients by using the berg balance scale. *Singapore Med. J.* 56, 280–283. doi: 10.11622/smedj.2015033

Mai, L., and Ueno, S. (2017). Comparison of the induced fields using different coil configurations during deep transcranial magnetic stimulation. *PLoS One* 12:e0178422. doi: 10.1371/journal.pone.0178422

Manto, M., Bower, J. M., Conforto, A. B., Delgado-García, J. M., da Guarda, S. N. F., Gerwig, M., et al. (2011). Consensus paper: roles of the cerebellum in motor control-the diversity of ideas on cerebellar involvement in movement. *Cerebellum* 11, 457–487. doi: 10.1007/s12311-011-0331-9

Maurer, C. W., LaFaver, K., Ameli, R., Epstein, S. A., Hallett, M., and Horovitz, S. G. (2016). Impaired self-agency in functional movement disorders: a resting-state fMRI study. *Neurology* 87, 564–570. doi: 10.1212/WNL.0000000000002940

Mead, G. E., Hsieh, C. F., and Lee, R. (2013). Selective serotonin reuptake inhibitors for stroke recovery: a systematic review and meta-analysis. *Stroke Mar.* 44, 844–850. doi: 10.1161/STROKEAHA.112.673947

Meseguer-Henarejos, A. B., Aparicio, M. R., López-Pina, J. A., Carles-Hernández, R., and Conesa, A. G. (2019). Characteristics that affect score reliability in the berg balance scale: a meta-analytic reliability generalization study. *Eur. J. Phys. Rehabil. Med.* 55, 570–584. doi: 10.23736/S1973-9087.19.05363-2

Opie, G. M., and Semmler, J. G. (2020). Characterising the influence of cerebellum on the neuroplastic modulation of intracortical motor circuits. *PLoS One* 1:e0236005. doi: 10.1371/journal.pone.0236005

Pinto, N., Duarte, M., Gonçalves, H., Silva, R., Gama, J., and Pato, M. V. (2018). Bilateral theta-burst magnetic stimulation influence on event-related brain potentials. *PLoS One* 13:e0190693. doi: 10.1371/journal.pone.0190693

Rabadi, M. H., Rabadi, F. M., and Peterson, M. (2012). An analysis of falls occurring in patients with stroke on an acute rehabilitation unit. *Rehabil. Nurs.* 33, 104–109. doi: 10.1002/j.2048-7940.2008.tb00213.x

Ren, C., Zhang, G., Xu, X., Hao, J., and Gao, F. (2019). The effect of rTMS over the different targets on language recovery in stroke patients with global aphasia: a randomized sham-controlled study. *Biomed Res. Int.* 2019:4589056. doi: 10.1155/2019/4589056

Richard, A., Van Hamme, A., Drevelle, X., Golmard, J. L., Meunier, S., and Welter, M. L. (2017). Contribution of the supplementary motor area and the cerebellum to the anticipatory postural adjustments and execution phases of human gait initiation. *Neuroscience* 358, 181–189. doi: 10.1016/j.neuroscience.2017.06.047

Rossi, S., Hallett, M., Rossini, P. M., and Pascual-Leone, A. (2009). Safety, ethical considerations, and application guidelines for the use of transcranial magnetic stimulation in clinical practice and research. *Clin. Neurophysiol.* 120, 2008–2039. doi: 10.1016/j.clinph.2009.08.016

Sanchez, M. M., and Xun, C. (2010). Choosing the analysis population in non-inferiority studies: per protocol or intent-to-treat. *Stat. Med.* 25, 1169–1181. doi: 10.1002/sim.2244

Spampinato, D., Ibanez, J., Spanoudakis, M., Hammond, P., and Rothwell, J. C. (2020). Cerebellar transcranial magnetic stimulation: the role of coil type from distinct manufacturers. *Brain Stimul.* 13, 153–156. doi: 10.1016/j.brs.2019.09.005

Svenja, D. K., Eva, M. P., Anna, S. S., Anne, K. R., Simon, B. E., Gereon, R. F., et al. (2017). Interindividual differences in motor network connectivity and behavioral response to iTBS in stroke patients. *NeuroImage Clin.* 15, 559–571. doi: 10.1016/j.nicl.2017.06.006

Tan, H., Wei, Q., Chen, Y., Xie, Y., Guo, Q., He, L., et al. (2021). The Immediate effects of intermittent theta burst stimulation of the cerebellar vermis on cerebral cortical excitability during a balance task in healthy individuals: a pilot study. *Front. Hum. Neurosci.* 15:748241. doi: 10.3389/fnhum.2021.748241

Toole, T., Maitland, C. G., Warren, E., Hubmann, M. F., and Panton, L. (2005). The effects of loading and unloading treadmill walking on balance, gait, fall risk, and daily function in parkinsonism. *Neurorehabilitation* 20, 307–322. doi: 10.3233/NRE-2005-20406

Van Lieshout, E. C. C., Visser-Meily, J. M. A., Neggers, S. F. W., Bart, V. D. W. H., and Dijkhuizen, R. M. (2017). Brain stimulation for arm recovery after stroke (b-stars): protocol for a randomised controlled trial in subacute stroke patients. *BMJ Open* 7:e016566. doi: 10.1136/bmjopen-2017-016566

Wada, N., Sohmiya, M., Shimizu, T., Okamoto, K., and Shirakura, K. (2007). Clinical analysis of risk factors for falls in home-living stroke patients using functional evaluation tools. *Arch Phys. Med. Rehabil.* 88, 1601–1605. doi: 10.1016/j.apmr.2007.09.005

Xiong, X., Peng, T., and Luo, Y. (2019). Effect of core muscle group training on motor recovery in patients with post-stroke balance dysfunction. *Med. Forum* 23, 3570–3572. doi: 10.19435/j.1672-1721.2019.25.010

Yan, C., Wang, X., Zuo, X., and Zang, Y. (2016). Dpabi: data processing & analysis for (resting-state) brain imaging. *Neuroinformatics* 14, 339–351. doi: 10.1007/s12021-016-9299-4

Yang, H., Chen, Y., Wang, J., Wei, H., Chen, Y., and Jin, J. (2021). Activities of daily living measurement after ischemic stroke: rasch analysis of the modified barthel index. *Medicine* 100:e24926. doi: 10.1097/MD.0000000000024926

Yin, M., Liu, Y., Zhang, L., Zheng, H., and Hu, X. (2020). Effects of rTMS treatment on cognitive impairment and resting-state brain activity in stroke patients: a randomized clinical trial. *Front. Neural Circuit* 14:563777. doi: 10.3389/fncir.2020.563777

Zang, Y., Jiang, T., Lu, Y., He, Y., and Tian, L. (2004). Regional homogeneity approach to fmri data analysis. *Neuroimage* 22, 394–400. doi: 10.1016/j.neuroimage.2003.12.030

Zelda, D., Riccardo, M., Jessica, M., Nicoletta, C., Davide, B., Edgardo, C., et al. (2016). Repetitive TMS on left cerebellum affects impulsivity in borderline personality disorder: a pilot study. *Front. Hum. Neurosci.* 10:582. doi: 10.3389/fnhum.2016.00582

Zhang, M., You, H., Zhang, H., Zhao, W., Han, T., Liu, J., et al. (2020). Effects of visual feedback balance training with the pro-kin system on walking and self-care abilities in stroke patients. *Medicine* 99:e22425. doi: 10.1097/MD.0000000000022425

Zhao, J., Chen, M., Wang, X., Ye, K., Shi, S., Li, H., et al. (2021). Efficacy of acupuncture in refractory irritable bowel syndrome: study protocol for a randomised controlled trial. *BMJ Open* 11:e045655. doi: 10.1136/bmjopen-2020-045655

Conflict of Interest: The authors declare that the research was conducted in the absence of any commercial or financial relationships that could be construed as a potential conflict of interest.

Publisher's Note: All claims expressed in this article are solely those of the authors and do not necessarily represent those of their affiliated organizations, or those of the publisher, the editors and the reviewers. Any product that may be evaluated in this article, or claim that may be made by its manufacturer, is not guaranteed or endorsed by the publisher.

frontiers | Frontiers in Aging Neuroscience

ORIGINAL RESEARCH
published: 11 May 2022
doi: 10.3389/fnagi.2022.866272

Electroencephalographic Measurement on Post-stroke Sensory Deficiency in Response to Non-painful Cold Stimulation

*Yanhuan Huang[1], Jiao Jiao[2], Junyan Hu[2], Chihchia Hsing[1], Zhangqi Lai[1], Yang Yang[1], Zengyong Li[3] and Xiaoling Hu[1,4,5,6]**

[1] Department of Biomedical Engineering, The Hong Kong Polytechnic University, Hong Kong, Hong Kong SAR, China, [2] Institute of Textiles and Clothing, The Hong Kong Polytechnic University, Hong Kong, Hong Kong SAR, China, [3] Beijing Key Laboratory of Rehabilitation Technical Aids for Old-Age Disability, National Research Centre for Rehabilitation Technical Aids Beijing, Beijing, China, [4] University Research Facility in Behavioral and Systems Neuroscience (UBSN), The Hong Kong Polytechnic University, Hong Kong, Hong Kong SAR, China, [5] The Hong Kong Polytechnic University Shenzhen Research Institute, Shenzhen, China, [6] Research Institute for Smart Ageing (RISA), The Hong Kong Polytechnic University, Hong Kong, Hong Kong SAR, China

OPEN ACCESS

Edited by:
Le Li,
Northwestern Polytechnical University, China

Reviewed by:
Qiuhua Yu,
Sun Yat-sen University, China
Sio Hang Pun,
University of Macau, Macao SAR, China

***Correspondence:**
Xiaoling Hu
xiaoling.hu@polyu.edu.hk

Specialty section:
This article was submitted to Neurocognitive Aging and Behavior, a section of the journal Frontiers in Aging Neuroscience

Received: *31 January 2022*
Accepted: *08 April 2022*
Published: *11 May 2022*

Citation:
Huang YH, Jiao J, Hu JY, Hsing CC, Lai ZQ, Yang Y, Li ZY and Hu XL (2022) Electroencephalographic Measurement on Post-stroke Sensory Deficiency in Response to Non-painful Cold Stimulation. Front. Aging Neurosci. 14:866272. doi: 10.3389/fnagi.2022.866272

Background: Reduced elementary somatosensation is common after stroke. However, the measurement of elementary sensation is frequently overlooked in traditional clinical assessments, and has not been evaluated objectively at the cortical level. This study designed a new configuration for the measurement of post-stroke elementary thermal sensation by non-painful cold stimulation (NPCS). The post-stroke cortical responses were then investigated during elementary NPCS on sensory deficiency *via* electroencephalography (EEG) when compared with unimpaired persons.

Method: Twelve individuals with chronic stroke and fifteen unimpaired controls were recruited. A 64-channel EEG system was used to investigate the post-stroke cortical responses objectively during the NPCS. A subjective questionnaire of cold sensory intensity was also administered *via* a numeric visual analog scale (VAS). Three water samples with different temperatures (i.e., 25, 10, and 0°C) were applied to the skin surface of the ventral forearm for 3 s *via* glass beaker, with a randomized sequence on either the left or right forearm of a participant. EEG relative spectral power (RSP) and topography were used to evaluate the neural responses toward NPCS with respect to the independent factors of stimulation side and temperature.

Results: For unimpaired controls, NPCS initiated significant RSP variations, mainly located in the theta band with the highest discriminative resolution on the different temperatures ($P < 0.001$). For stroke participants, the distribution of significant RSP spread across all EEG frequency bands and the temperature discrimination was lower than that observed in unimpaired participants ($P < 0.05$). EEG topography showed that the NPCS could activate extensive and bilateral sensory cortical areas after stroke. Significant group differences on RSP intensities were obtained in each EEG band ($P < 0.05$). Meanwhile, significant asymmetry cortical responses in RSP toward different upper limbs were observed during the NPCS in both unimpaired controls and

participants with stroke ($P < 0.05$). No difference was found between the groups in the VAS ratings of the different temperatures ($P > 0.05$).

Conclusion: The post-stroke cortical responses during NPCS on sensory deficiency were characterized by the wide distribution of representative RSP bands, lowered resolution toward different temperatures, and extensive activated sensory cortical areas.

Keywords: stroke, sensory deficiency, electroencephalography, elementary somatosensation, thermal sensation, non-painful cold stimulation

INTRODUCTION

Reduced somatosensation is common after stroke, with one in two stroke survivors experiencing this sensory deficit (Carey et al., 2018). It mainly impairs their discrimination in sensations of thermal, touch, and pain and further affects their ability of functional independence and overall quality of life (Carey, 1995; Kessner et al., 2016). Due to the learned non-use of the sensory affected limb, post-stroke motor restoration was reported to be hindered by the impaired somatosensation, which is typically represented by slower recovery, reduced movement control, and even lesser rehabilitation outcomes (Wu et al., 2006; De Diego et al., 2013; Serrada et al., 2019). Despite the high prevalence and apparent importance of somatosensation in post-stroke motor restoration, sensory deficiency and its functional evaluation received little attention, compared to those of the motor function (De Diego et al., 2013; Carey et al., 2016; Serrada et al., 2019).

To evaluate the sensory impairment, quantitative and precise measurement of somatosensory functions is crucial. It is known that the somatosensory functions could be divided into two subtypes, the elementary and the intermediate (Takeda et al., 2000; Satoh et al., 2002; Dijkerman and De Haan, 2007; Matsuda et al., 2020). The elementary somatosensory functions mainly consist of light touch, pain, thermal sensation, joint position sense, and vibration sense (Matsuda et al., 2020). The intermediate somatosensory functions are usually the integration of the multiple tactile related functions, including 2-point discrimination, tactile localization, weight, texture, and shape perceptions (Matsuda et al., 2020). The traditional clinical practices on post-stroke sensory evaluation were mainly focused on the intermediate somatosensation because it is generally believed that brain lesions, e.g., stroke, or brain trauma, mainly leads to the impairment of intermediate somatosensation (Head and Holmes, 1911; Takeda et al., 2000) rather than the elementary ones. For instance, the two-point discrimination (Dellon et al., 1987) and the Semmes-Weinstein monofilament tests (Bell-Krotoski and Tomancik, 1987) are two typical assessments widely used in clinical practice for multiple integrated sensory functions. Recently, evidence was found that brain lesions also led to disturbances of the elementary somatosensation. For example, infarction at the postcentral gyrus would cause disturbance of thermal sensation (Satoh et al., 2002). However, the measurement of elementary sensation is underdeveloped in traditional clinical sensory assessments. A challenge is the configuration of the measurement with minimum introduction of other unrelated sensory inputs, when performing an elementary somatosensory evaluation. In the current clinical measurements for stroke rehabilitation, both elementary and intermediate somatosensory functions, as well as the motor functions, are usually evaluated in a mixture related to daily tasks, e.g., the Fugl-Meyer Assessment (FMA) (Fugl-Meyer et al., 1974). Among them, somatosensory measurements are oversimplified in these mixed scales with limited resolution by subjective ordinal scales (Dellon et al., 1987). For example, although the Rivermead assessment of somatosensory performance contains the item on thermal sensation, it only has two grades of "warm" and "cold," and requires the intact cognition of a subject to give subjective verbal response in the measurement as in most of the clinical somatosensory assessments (Steimann et al., 2012). Therefore, objective measurements with more precise control on the stimulation to evoke elementary somatosensory responses are preferred in the understanding of the related impairment after stroke.

The cortical responses to external sensory inputs could be objectively captured by brain imaging and electrophysiological technologies, e.g., functional magnetic resonance imaging (fMRI) and electroencephalography (EEG). fMRI has been applied in exploration of tactile, thermal, and pain stimulations to unimpaired persons with the advantage of its high spatial resolution (Chen et al., 2002; Mazzola et al., 2012). Relatively static spatial segregations in relation to these sensory inputs were observed (Chen et al., 2002; Mazzola et al., 2012). However, fMRI is hard to detect transient responses because of its lower temporal resolution compared to other modalities, e.g., EEG (Lystad and Pollard, 2009; Caliandro et al., 2017). EEG features represented by somatosensory evoked potential (SSEP) in time domain (Misra et al., 2008) and selected frequency components in EEG power spectra (Ahn et al., 2016) have been applied in objective measurement on cortical responses to sensory stimulations. SSEP parameters, e.g., onset value, peak intensity, duration, etc., have been widely used to determine the afferent neural integrity (Hwang et al., 2016; Yoon et al., 2018), based on the detection of the whole SSEP waveform with high repetitions to achieve a high signal-to-noise ratio (SNR) (Society, 2015). On the other hand, frequency features in the EEG power spectra, e.g., alpha and beta powers, could be less affected by the background noises to demonstrate the cortical responses to the sensory inputs, because of the less overlapped distribution between the selected power bands and those of the noises in the frequency domain (Thut and Miniussi, 2009). Therefore, EEG frequency features could be obtained with less repetitions, compared to those SSEP detections in the time domain (Thut and Miniussi, 2009). EEG spectral

patterns also have been introduced to investigate the neural activities during the touch (Singh et al., 2014; Ahn et al., 2016) and thermal (Chang et al., 2005; Shao et al., 2012) stimulations in both unimpaired and stroke persons. Based on the study conducted by Singh et al. (2014), beta oscillation was found to be highly related to touch sensations, and its power changes could differentiate pleasant stimuli from unpleasant stimuli with different textile fabrics on a single trial basis. However, similar to the clinical manual assessments, the configurations in cortical measurements of elementary sensations were mixed with intermediate somatosensation in the reported EEG and fMRI studies (Kwan et al., 2000; Tseng et al., 2010; Mazzola et al., 2012; Ansari et al., 2018), e.g., the application of contact thermode with fastening belts for thermal stimulation to the skin would introduce multiple tactile and pressure stimuli, besides the thermal stimulation in the experiment (Kwan et al., 2000; Tseng et al., 2010).

In this study, we designed a new configuration for the measurement of post-stroke elementary thermal sensation by non-painful cold stimulation (NPCS), with minimized introduction of other sensations, such as tactile sensations with different textures and shapes. During thermal stimulation, pain sensation could be triggered and mixed with the thermal sensation according to an individual's temperature threshold and the stimulus duration (Chang et al., 2005). Additionally, heat stimulation without pain (warm) is prone to make one drowsy, disturbing the cortical responses to the sensory inputs and lowering the efficiency of cortical network processing (Slater, 2008). Therefore, NPCS was selected to investigate the elementary thermal sensation in this study, with the purpose of minimizing the involvements of elementary pain sensation and potential disturbance from sleepiness. Then, we used quantitative EEG power spectra to investigate the cortical responses during the elementary NPCS on post-stroke sensory deficiency, when compared with unimpaired individuals.

METHODS

In this study, the post-stroke neural responses during the NPCS were investigated using EEG. A visual analog scale (VAS) questionnaire was administered to collect the subjective perceptions of cold stimulation. Three water samples, each at a different temperature, were applied to the forearm *via* glass beakers to induce the NPCSs in both stroke survivors and unimpaired individuals, with minimized disturbance of other sensory inputs. EEG power spectra and topography were used to evaluate the neural responses toward NPCSs.

Participants

Before conducting the experiment, an approval was obtained from the Human Subjects Ethics Sub-Committee of the Hong Kong Polytechnic University. Twelve participants from local districts who entered the chronic stage after stroke were recruited to the "stroke group." The following inclusion criteria were applied: (1) at least 6 months post-onset of a singular and unilateral brain lesion due to stroke; (2) the stroke-induced lesions occurred in the subcortical area; (3) an absence of visual, cognitive or attention deficits that would prevent participants from following instructions or performing the experimental procedures (assessed using the Mini-Mental State Examination (MMSE) score > 21) (Roselli et al., 2009); (4) presence of moderate-to-severe motor disability in the paretic limb [$13 <$ Fugl-Meyer Assessment (FMA) < 47 (Fugl-Meyer et al., 1974; Woytowicz et al., 2016)] and muscle spasticity at the wrist and elbow [Modified Ashworth Score (MAS) ≤ 2 (Bohannon and Smith, 1987)]; (5) moderate-to-severe sensory impairment of their affected forearm, with a score of 1 as measured by the sensation part of light touch in FMA (Fugl-Meyer et al., 1974); (6) without symptom of central post-stroke pain (CPSP). The rationale for recruiting persons with chronic stroke was that their sensorimotor functions were relatively stable and were representative of a large population of stroke survivors. Meanwhile, to ensure the accessibility of cortical EEG responses, particularly those of the sensorimotor cortex, subjects with stroke and lesions in subcortical areas were recruited, since their cerebral cortex were not directly impaired due to stroke. Stroke patients with CPSP (overall prevalence around 6–8%; Krause et al., 2016) were excluded from this study to minimize bias, because patients with CPSP frequently show impairments of thermal and pain sensations that are different from patients without CPSP (Krause et al., 2016). The stroke group was subdivided into the "stroke affected group" and the "stroke unaffected group" according to the hemiplegic sides of the participants with stroke.

Fifteen unimpaired adults from local districts were recruited to the "control group." They had no history of neurological, psychiatric, cognitive and/or cardiovascular diseases. All recruited participants gave written consent before the start of the experiment. The demographic characteristics of the participants are presented in **Table 1**. In this study, the recruited participants were mainly middle aged [45–65 years-old (Dictionary, 2016)], with a mean age of 55.13 years for the stroke group and 46.40 years for the control group. The difference in age was not statistically significant ($p = 0.192$, $t = 1.341$, independent t-test). However, significant difference in gender was found between the stroke participants and unimpaired controls ($p = 0.005$, Fisher's exact test). In addition, all unimpaired participants and stroke survivors before their stroke onset were right-handed.

Electroencephalography Measurement of Cortical Response During Non-painful Cold Stimulation

Experimental Setup

The experiment was conducted in a lab which was controlled on temperature and humidity. The room temperature was maintained at 25 ± 1°C and the relative humidity was fixed at 60 ± 5%. **Figure 1A** shows the experimental setup. Each participant was comfortably seated in front of a table with both forearms placed on the table. Each participant wore an eye mask and ear plugs to minimize the disturbances from visual and audio

TABLE 1 | Demographic characteristics of the participants.

Characteristics	Stroke group (n = 12)	Control group (n = 15)	P-values
Age in years[a] (mean ± SD)	55.13 ± 16.04	46.40 ± 17.39	0.192
Gender[b] (male/female)	11/1	5/10	0.005
Handedness before stroke[b] (right/left)	12/0	15/0	1
Affected side (right/left)	6/6	Nil	Nil
Type of stroke (ischemic/hemorrhagic)	10/2	Nil	Nil
Times since stroke in years (mean ± SD)	14.92 ± 5.79	Nil	Nil
MAS elbow (mean ± SD)	1.08 ± 0.69	Nil	Nil
FMA full score for upper extremity (mean ± SD)	42.5 ± 15.17	Nil	Nil
FMA for light touch on forearm (mean ± SD)	1 ± 0	Nil	Nil

[a] *Independent t-test.*
[b] *Fisher's exact test.*

stimuli from the surroundings. A 64-channel EEG system (BP-01830, Brain Products Inc.) was mounted on the scalp of each participant based on the standard 10–20 system, which was used to record the whole brain EEG with the skin impedance of each channel under 5 KΩ (Nuwer et al., 1999). The whole brain EEG recording was adopted because cold stimulation could activate multiple brain cortices in addition to the primary somatosensory cortex (Singh et al., 2014). The recording sampling frequency was set at 1,000 Hz.

Non-painful Cold Stimulation

In this study, the configuration for the measurement of post-stroke elementary thermal sensation using NPCS is shown in **Figure 1B** *via* glass beaker with different temperatures of water. During the stimulation, the glass beaker was designed to statically attach to the skin surface without friction, or load of weight. The selection of glass beaker was mainly due to its smooth surface and the monocomponent in the material, and these features could minimize the unnecessary sensory inputs of tactile sensations with different textures and shapes, when compared with the contact thermode fastened by belts used in the literature (Kwan et al., 2000; Tseng et al., 2010). The static attachment without friction and weight loading during the stimulation could further limit the introduction of friction sensation and weight perception. The NPCSs were delivered by three water samples with different temperatures of 25, 10, and 0°C, and the three temperatures could provoke weak to strong non-painful cold sensations, respectively. In the clinical application, 25°C usually acts as the adaptation temperature for control. The 10°C is frequently used for cool stimulation (Shao et al., 2012; Ansari et al., 2018), where the 0°**C** is a typical temperature for cold-induced pain. As mentioned above, pain sensation is related with the intensity and duration of the thermal stimulation (Chang et al., 2005). In unimpaired adults, exposing the skin to 0°C will evoke cold pain in 5 s (Rebbeck et al., 2015). To avoid the cold pain during the 0°C water stimulus, a 3-s short stimulation duration was used in this study. The target temperature was achieved by mixing room temperature water and different quantities of ice. The 0°C water was maintained as a mixture of ice and water during the whole experiment. Before applying each stimulus, a thermometer was used to ensure that the water temperature was within ±0.1°C of the target temperature. The NPCS with different temperatures was delivered to the skin surface of ventral forearm around the muscle belly of the *flexor carpi radialis* (FCR) and *flexor digitorum* (FD) muscles by the same experimenter. The FCR and FD muscles were selected because they were not only a common area to use in studies investigating the cold sensation for unimpaired participants (Chang et al., 2005), but also related to the wrist-hand flexion, which could promote post-stroke upper limb sensorimotor restoration for wrist-hand joints with appropriate stimulation (Lin et al., 2017). The estimated size of the contact area was around 3 cm × 3 cm.

Electroencephalography Measurement Protocol

The timeline of EEG measurement during the NPCS is summarized in **Figure 2**. Each single trial of EEG measurement consisted of a 30-s baseline test, and three 3-s cold stimuli, which were separated by two 90-s resting times. Each participant was asked to keep their eyes closed, place both forearms on the table while remaining relaxed and still (**Figure 1A**). During the baseline test, no stimulation was applied to the participants, and they were required to remain awake without mental activity. During each NPCS, the glass beaker with a target temperature was statically attached to the skin surface around the FCR and FD muscles (**Figure 1B**), i.e., without friction, for 3 s. There was a computer program with timer to instruct the operator to deliver each NPCS. The operator would receive beep sounds though a headphone for instructions to start and stop. A countdown of the instruction would also be displayed on the computer screen as a reminder. Whether the stimulus was placed on the participant's right or left forearm was determined by a randomized sequence. Participants were asked not to perform active cognition toward the cold stimuli during the EEG recording. The 90-s duration of rest was selected based upon the average clearance of cortical responses to cold stimulation in unimpaired persons (Garkavenko et al., 2008; Shao et al., 2012; De Pascalis et al., 2019). The cycles of EEG measurement for each participant were repeated three times on each forearm. The neural responses of both forearms were evaluated because the post-stroke cortical responses between different sides were varied during both sensory and motor tasks. This could be due to the different handedness before the stroke (Özcan et al., 2005; Dirnberger et al., 2011), and this asymmetric cortical response was also observed in our previous work in post-stroke fine touch to textile fabrics (Huang et al., 2020).

Electroencephalography Data Processing

After acquiring the targeted EEG data, the signals were processed off-line with a band-pass filter from 0.1 to 100 Hz, and a notch filter from 49 to 51 Hz to eliminate the 50 Hz noise from the environment. Following this, the EEG signals were divided into individual segments containing the baseline and cold stimulation periods. Then, the relative powers of each EEG frequency band,

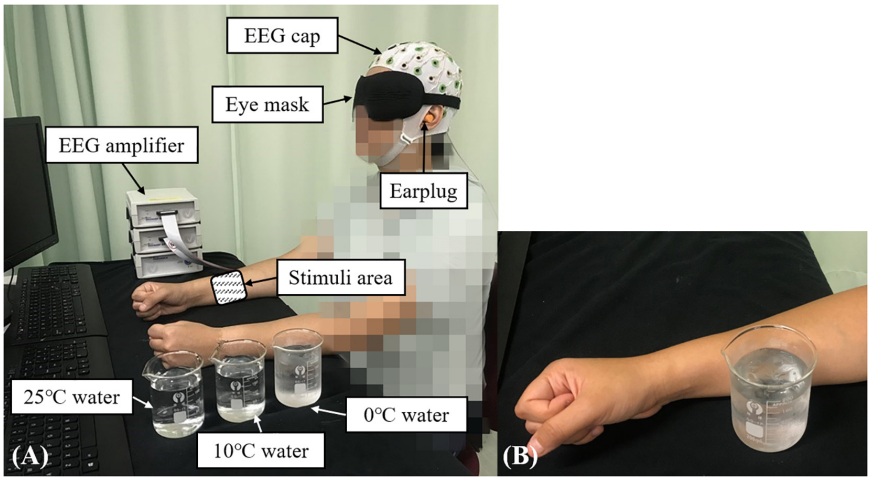

FIGURE 1 | The experimental setup for the EEG evaluation during the non-painful cold stimulation (NPCS): **(A)** participant in the recording position; **(B)** demonstration of the NPCS.

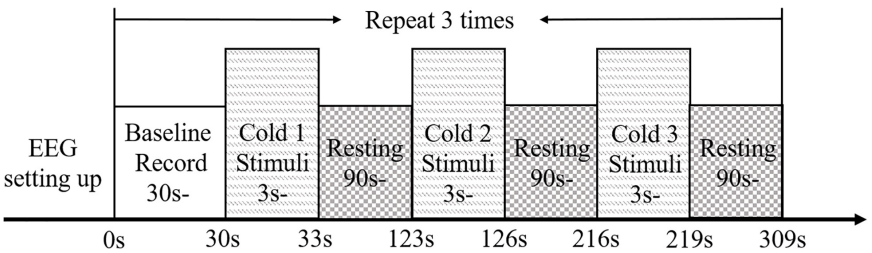

FIGURE 2 | The experimental protocol for EEG evaluation presented with the timeline.

were calculated [i.e., Delta (δ, 0.1–4 Hz), Theta (θ, 4–8 Hz), Alpha (α, 8–13 Hz), Beta (β, 13–30 Hz), and Gamma (γ, 30–100 Hz) (Lebeau, 2010; Ahmed et al., 2012)]. The following equation was used:

$$\mathbf{P}_{\mathbf{Relative/band}} = \frac{\int_{\mathbf{F_1}}^{\mathbf{F_2}} \mathbf{p}\,(\mathbf{f})\,\mathbf{df}}{\int_{\mathbf{0.1}}^{\mathbf{100}} \mathbf{p}\,(\mathbf{f})\,\mathbf{df}} - \frac{\int_{\mathbf{F_1}}^{\mathbf{F_2}} \mathbf{p}_{\mathbf{Baseline}}\,(\mathbf{f})\,\mathbf{df}}{\int_{\mathbf{0.1}}^{\mathbf{100}} \mathbf{p}_{\mathbf{Baseline}}\,(\mathbf{f})\,\mathbf{df}} \quad (1)$$

where, the $P_{Relative/band}$ is the relative spectral power (RSP) of a frequency band; p(f) is the power spectral density of an EEG segment for a cold stimulation event, which is estimated by Fast Fourier Transform. F_1 and F_2 are the cutoff frequencies of a EEG frequency band, as stated above; and $p_{Baseline}(f)$ is the power spectral density of the EEG segments in the baseline tests of each trial. Similar analysis methods were adopted in our previous study (Huang et al., 2020).

Non-painful Cold Sensation Evaluated by Questionnaire

The subjective evaluation of sensory intensities to the three cold stimuli were assessed using a numeric visual analog scale (VAS, range from 0 to 10), and it was conducted half an hour after the EEG measurement. Scores of 0–5 indicate no sensation to maximum non-painful cold sensation, while 6–10 score denotes minimum to maximum cold pain. During the VAS questionnaire, a non-painful cold stimulus was applied to the participants' skin surface around the FCR and FD muscles, i.e., without friction, for 3 s. After removing the stimulus, participants were asked to rate the intensity of the cold sensation caused by the applied stimulus. The sequence for each cold stimulus was randomized. The subjective evaluation of cold sensations was also repeated three times on each forearm. Both forearms were assessed for the stroke participants, while only the dominant forearm (the right forearm in this study) was assessed for those unimpaired participants.

Statistical Analysis

The normality tests for the EEG data and VAS scores were first evaluated using the Lilliefors method (Razali and Wah, 2011); the probabilities were statistically insignificant ($P > 0.05$), and the data obeyed normal distribution. During the intragroup comparisons, two-way repeated ANOVA was used to evaluate the RSP differences with respect to the independent factors of the stimulation side (i.e., left side and right side) and temperature (i.e., 25, 10, and 0°C) for each EEG frequency band. Then an independent *t*-test was used to evaluate the RSP differences with respect to the independent factor of stimulation side. One-way repeated measure ANOVA was conducted to investigate the RSP differences with respect to the independent factor of

temperature with Bonferroni *post-hoc* test. During the intergroup comparisons, RSP differences of each EEG frequency band for each stimulation side with respect to the independent factors of the group and temperature were evaluated *via* mixed-model repeated measure ANOVA. Following this, one-way ANOVA was conducted to compare the group differences of RSPs on each stimulation side, with Bonferroni *post-hoc* test or Dunnett's T3 *post-hoc* test. The selection of which *post-hoc* test to use was based on the homogeneity of the variance test. Specifically, for equal variance, the Bonferroni *post-hoc* test was adopted, otherwise, Dunnett's T3 *post-hoc* test was used (Shingala and Rajyaguru, 2015). In addition, the intragroup VAS differences with respect to the independent factor of temperature were evaluated by one-way repeated measure ANOVA, while the intergroup differences of the VAS scores were calculated by one-way ANOVA, and both of them used Bonferroni *post-hoc* test. In this work, the level of statistical significance was set at 0.05, and the significance at levels 0.01 and 0.001 were also indicated.

RESULTS

Figure 3 shows the EEG RSPs in response to the cold stimuli for each group at different EEG frequency bands. **Table 2** presents the two-way repeated ANOVA probabilities and predicted effect sizes (EFs) with respect to the independent factors of the stimulation side and temperature. **Table 3** provides a summary of the detailed values, means, and 95% CIs for each RSP, in addition to the one-way repeated ANOVA and independent *t*-test probabilities and EFs. In the control group (**Figure 3A**), significant RSP differences with respect to the temperatures were detected at all EEG frequency bands ($P < 0.001$, two-way repeated ANOVA, **Table 2**). In terms of the stimulation sides, significant differences were observed in the delta ($P = 0.047$, two-way repeated ANOVA, **Table 2**) and alpha ($P = 0.001$, two-way repeated ANOVA, **Table 2**) bands. Significant interactions between the temperature and the stimulation side were detected in the alpha ($P = 0.042$, two-way repeated ANOVA, **Table 2**) and gamma ($P < 0.001$, two-way repeated ANOVA, **Table 2**) bands. The theta RSPs of both sides in response to the 0°C water were significantly higher than those for 25 and 10°C stimuli ($P < 0.001$, one-way repeated ANOVA, **Table 3**), and the theta RSPs of both sides to 10°C water were significantly higher than those for 25°C water ($P < 0.001$, one-way repeated ANOVA, **Table 3**). The alpha and beta RSPs in response to 25°C were significantly lower than those in response to the 10 and 0°C water when the right side was stimulated ($P < 0.001$, one-way repeated ANOVA, **Table 3**). When the left side was stimulated, the beta and gamma RSPs in response to 0°C were found to be significantly higher than those at the 10 and 25°C water ($P < 0.001$, one-way repeated ANOVA, **Table 3**). Meanwhile, independent *t*-test established significant RSP differences in the delta, alpha, beta, and gamma bands for the different stimulation sides ($P < 0.05$, **Table 3**). The RSP of the right side was significantly lower than the left side in the delta band, while significantly higher in the alpha ($P < 0.01$, independent *t*-test, **Table 3**) and beta ($P < 0.05$, independent *t*-test, **Table 3**) bands. The gamma RSP for the right side was significantly higher than that for the left side when stimulated by the 10°C water ($P = 0.012$, independent *t*-test, **Table 3**), and significantly lower when stimulated by the 0°C water ($P = 0.004$, independent *t*-test, **Table 3**).

In the stroke unaffected group (**Figure 3B**), two-way repeated ANOVA identified significant RSP differences with respect to the temperatures observed at all EEG frequency bands ($P < 0.01$, **Table 2**). Meanwhile, significant differences with respect to the stimulation sides were detected at the delta, beta, and gamma bands ($P < 0.01$, two-way repeated ANOVA, **Table 2**). In terms of the interaction between the temperature and the stimulation side, significances were found at the delta, alpha, beta, and gamma bands ($P < 0.05$, two-way repeated ANOVA, **Table 2**). One-way repeated ANOVA showed the RSPs of 25°C in the theta, beta, and gamma bands were significantly lower than that of 10 and 0°C for right-side stimulation ($P < 0.01$, **Table 3**). When the left side was stimulated, the significant variations between the RSPs of 10 and 0°C were observed in the alpha, beta, and gamma bands ($P < 0.05$, one-way repeated ANOVA, **Table 3**). Furthermore, significant differences were detected in all EEG frequency bands for the stroke unaffected group in respect of stimulation sides ($P < 0.05$, independent *t*-test, **Table 3**). Furthermore, the RSPs of the right side were significantly higher in the delta and alpha bands ($P < 0.05$, independent *t*-test, **Table 3**), and lower in theta, beta, and gamma bands ($P < 0.05$, independent *t*-test, **Table 3**), when compared with the left side.

In the stroke affected group (**Figure 3C**), significant differences with respect to the stimulation sides were detected at the theta ($P = 0.019$, two-way repeated ANOVA, **Table 2**) and gamma ($P = 0.002$, two-way repeated ANOVA, **Table 2**) bands. In terms of the temperature factor, significant differences were observed in all EEG frequency bands ($P < 0.001$, two-way repeated ANOVA, **Table 2**). No significant interactions between the temperature and the stimulation side was captured ($P > 0.05$, two-way repeated ANOVA, **Table 2**). One-way repeated ANOVA showed significant RSP variations in the delta ($P < 0.001$, one-way repeated ANOVA, **Table 3**), theta ($P < 0.001$, one-way repeated ANOVA, **Table 3**) and gamma ($P = 0.001$, one-way repeated ANOVA, **Table 3**) bands when the left side was stimulated with 25 and 10°C water. Additionally, significant RSP variations between the 25 and 0°C were found at the delta ($P < 0.001$, one-way repeated ANOVA, **Table 3**), theta ($P < 0.001$, one-way repeated ANOVA, **Table 3**), alpha ($P < 0.001$, one-way repeated ANOVA, **Table 3**), and beta ($P = 0.006$, one-way repeated ANOVA, **Table 3**) bands. When the right side was stimulated, the 25°C RSPs were significantly lower than those RSPs of 10 and 0°C in the theta, alpha, and beta bands ($P < 0.001$, one-way repeated ANOVA, **Table 3**). The gamma RSP for 0°C was significantly higher than that of both 25 and 10°C ($P < 0.001$, one-way repeated ANOVA, **Table 3**). Furthermore, there were significant RSP variations between the right side and the left side at theta, alpha, beta, and gamma bands, as determined by the independent *t*-test ($P < 0.05$, **Table 3**).

Figure 4 compares the group differences of RSPs in response to the cold stimuli at each EEG frequency band with respect to the stimulation sides. **Table 4** displays the values of statistical results including probabilities and EFs of the mixed-model

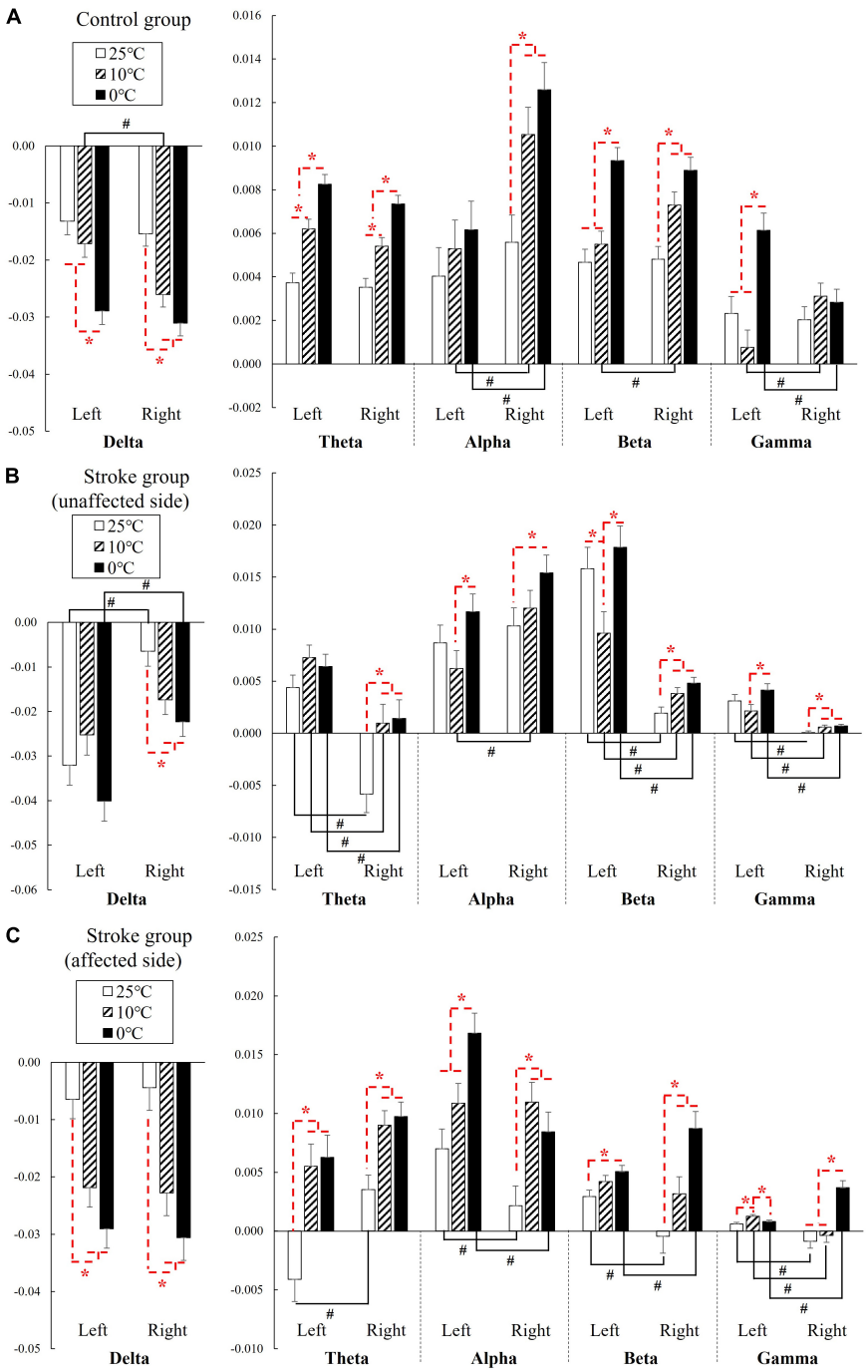

FIGURE 3 | The EEG relative spectral power in response to the NPCSs on the left and right forearms for **(A)** control group, **(B)** stroke group-unaffected side, and **(C)** stroke group-affected side on the whole brain at the delta, theta, alpha, beta, and gamma band presented as mean value with SE (error bar). The significant intragroup differences are indicated by "*" ($p < 0.05$, one-way repeated ANOVA with Bonferroni *post-hoc* tests), and the significant intergroup differences are indicated by "#" ($p < 0.05$, independent *t*-test).

repeated measure ANOVA and one-way ANOVA. Significant differences between both factors of groups and temperatures were found in the mixed-model repeated measure ANOVA for all the EEG frequency bands ($P < 0.05$, **Table 4**) on both stimulation sides. Significant interactions between the temperature factor and the group were recorded at delta and alpha band on the left side ($P < 0.05$, mixed-model repeated measure ANOVA, **Table 4**), as well as the theta, beta, and gamma bands on both sides ($P < 0.05$, mixed-model repeated measure ANOVA, **Table 4**). In comparison to the control group, when the left

TABLE 2 | Comparisons on the whole brain relative spectral power on each EEG frequency band.

		Two-way repeated ANOVA					
		Temperature		Stimulation side		Temperature × Stimulation side	
Bands	**Groups**	**P (Partial η^2)**	**F**	**P (Partial η^2)**	**F**	**P (Partial η^2)**	**F**
Delta	Control group	<0.001▲▲▲ (0.030)	30.939	0.047▲ (0.004)	3.956	0.137 (0.002)	1.993
	Stroke group-affected side	<0.001▲▲▲ (0.062)	24.698	0.206 (0.004)	1.605	0.467 (0.002)	0.763
	Stroke group-unaffected side	<0.001▲▲▲ (0.033)	12.465	0.006▲▲ (0.020)	7.638	0.001▲▲ (0.020)	7.454
Theta	Control group	<0.001▲▲▲ (0.049)	50.654	0.058 (0.004)	3.595	0.593 (0.001)	0.523
	Stroke group-affected side	<0.001▲▲▲ (0.069)	27.437	0.019▲ (0.015)	5.547	0.395 (0.002)	0.929
	Stroke group-unaffected side	<0.001▲▲▲ (0.034)	13.102	0.255 (0.003)	1.301	0.097 (0.006)	2.336
Alpha	Control group	<0.001▲▲▲ (0.010)	10.323	0.001▲▲ (0.012)	11.554	0.042▲ (0.003)	3.178
	Stroke group-affected side	<0.001▲▲▲ (0.037)	14.302	0.490 (0.001)	0.477	0.232 (0.004)	1.463
	Stroke group-unaffected side	0.006▲▲ (0.014)	5.079	0.334 (0.003)	0.934	<0.001▲▲▲ (0.021)	7.938
Beta	Control group	<0.001▲▲▲ (0.033)	33.607	0.370 (0.001)	0.805	0.077 (0.003)	2.567
	Stroke group-affected side	<0.001▲▲▲ (0.034)	12.872	0.212 (0.004)	1.564	0.716 (0.001)	0.335
	Stroke group-unaffected side	<0.001▲▲▲ (0.037)	14.432	<0.001▲▲▲ (0.067)	26.648	<0.001▲▲▲ (0.020)	7.744
Gamma	Control group	<0.001▲▲▲ (0.010)	10.248	0.526 (0.000)	0.403	<0.001▲▲▲ (0.009)	9.436
	Stroke group-affected side	<0.001▲▲▲ (0.031)	11.943	0.002▲▲ (0.025)	9.379	0.099 (0.006)	2.319
	Stroke group-unaffected side	<0.001▲▲▲ (0.058)	23.024	<0.001▲▲▲ (0.034)	12.901	0.001▲▲ (0.018)	6.885

Differences with statistical significance are marked with "▲" ($p < 0.05$, two-way repeated ANOVA intragroup tests on the temperature and stimulation side effects). Significant levels are indicated as, 1 superscript for < 0.05, 2 superscripts for < 0.01, 3 superscripts for < 0.001.

side was stimulated, the RSPs of the stroke affected group were significantly lower at the theta, beta, and gamma bands ($P \leq 0.001$, one-way ANOVA, **Table 4**), and higher in the alpha band ($P = 0.001$, one-way ANOVA, **Table 4**). Meanwhile, when the right side was stimulated, the RSPs of the stroke affected group were significantly lower at the beta ($P < 0.001$, one-way ANOVA, **Table 4**) and gamma ($P = 0.002$, one-way ANOVA, **Table 4**) bands, and higher in the delta and theta bands ($P < 0.001$, one-way ANOVA, **Table 4**). Furthermore, significant RSP differences between the stroke affected group and the stroke unaffected group were noted in response to different temperatures across all frequency bands ($P < 0.05$, one-way ANOVA, **Table 4**). During the right-side stimulation, the alpha RSP of the stroke affected group was significantly lower than that of the unaffected group ($P < 0.001$, one-way ANOVA, **Table 4**), while the theta and gamma RSPs of the stroke affected group were significantly higher than those of the unaffected group ($P < 0.05$, one-way ANOVA, **Table 4**). During the left-side stimulation, the RSPs of the stroke affected group at theta, beta, and gamma bands were significantly lower than those of the unaffected group ($P < 0.001$, one-way ANOVA, **Table 4**), while the alpha RSPs of the stroke affected group were significantly higher than that of the unaffected group ($P < 0.001$, one-way ANOVA, **Table 4**). A comparison of the RSP values of the control group and the stroke unaffected group revealed significant differences in the theta, alpha, beta, and gamma bands ($P \leq 0.001$, one-way ANOVA, **Table 4**) during the right-side stimulation. Similarly, significant differences were found in the delta, beta, and gamma bands ($P < 0.05$, one-way ANOVA, **Table 4**) during the left-side stimulation.

Figure 5 demonstrates the whole brain EEG topography of the mean RSPs in all EEG frequency bands for each group with respect to the independent factors of temperature and stimulation side. Hotspots of significant RSPs in all EEG frequency bands were captured bilaterally, mainly in the parietal, frontal, and occipital regions of both stroke and unimpaired participants. In the control group, there were increased theta power (**Figure 5B**) in the parietal and occipital regions bilaterally. The powers of high frequency bands (i.e., beta and gamma bands, **Figures 5D,E**) were increased not only in the parietal and occipital regions, but also in the occipital lobe. For stroke participants who had experienced right-side brain lesions (left hemiplegia), theta activity was increased in the bilateral parietal areas and decreased in the paramedian central area for both stimulation sides. Brain activity in the beta band (**Figure 5D**) only slightly increased in the bilateral parietal regions for both stimulation sides. In contrast, for participants with stroke who had experienced left-side brain lesions (right hemiplegia), theta activity (**Figure 5B**) increased in the left hemisphere of the brain when the unaffected left forearms were stimulated, while a remarkable increase in theta activity could be observed over the frontal, parietal, and occipital lobes when their affected right forearms were stimulated. In terms of the high frequency bands (i.e., beta and gamma bands, **Figures 5D,E**), brain activity in the central areas were significantly increased for the affected right forearms, where the 0°C stimulus initiated greater brain activity than the 25 and 10°C stimuli. Meanwhile, high frequency brain activities increased significantly almost over the whole brain when the unaffected left forearms were stimulated.

Table 5 presents the means and 95% CIs of each NPCS evaluated by VAS, in addition to the statistical probabilities and the EFs. The results demonstrated that the three temperatures of cold water could provoke weak to strong non-painful cold sensations in both stroke and unimpaired participants.

TABLE 3 | The whole brain relative spectral power of each non-painful cold stimuli for each group.

			25°C	10°C	0°C	One-way repeated ANOVA	
Bands	**Groups**	**Stimulation side**	**Mean (95% confidence interval, E-03)**			**P (Partial η^2)**	**F**
Delta	Control group	Left forearm	–13.22 (–17.90 to –8.55)	–17.15 (–21.83 to –12.48)	–28.92 (–33.60 to –24.25)	<0.001*** (0.016)	16.457
		Right forearm	–15.37 (–19.73 to –11.02)	–26.04 (–30.39 to –21.69)	–31.08 (–35.43 to –26.73)	<0.001*** (0.017)	17.242
		Independent *t*-test P (Cohen's d)	0.437 (0.036)	0.007## (0.120)	0.554 (0.027)		
	Stroke group-affected side	Left forearm	–6.46 (–13.07 to –0.16)	–21.88 (–28.49 to –15.26)	–29.06 (–35.67 to –22.44)	<0.001*** (0.042)	16.459
		Right forearm	–4.42 (–12.24 to 3.41)	–22.78 (–30.61 to –14.95)	–30.60 (–38.43 to –22.77)	<0.001*** (0.042)	16.202
		Independent *t*-test P (Cohen's d)	0.644 (0.035)	0.860 (0.013)	0.797 (0.018)		
	Stroke group-unaffected side	Left forearm	–32.00 (–40.87 to –23.14)	–25.27 (–34.13 to –16.40)	–40.10 (–48.97 to –31.24)	0.012* (0.012)	4.489
		Right forearm	–6.50 (–13.00 to 0.01)	–17.39 (–23.90 to –10.89)	–22.32 (–28.83 to –15.81)	<0.001*** (0.023)	8.728
		Independent *t*-test P (Cohen's d)	<0.001### (0.367)	0.147 (0.107)	0.004## (0.209)		
Theta	Control group	Left forearm	3.72 (2.85–4.60)	6.20 (5.32–7.07)	8.25 (7.38–9.13)	<0.001*** (0.030)	30.250
		Right forearm	3.53 (2.74–4.31)	5.40 (4.61–6.19)	7.35 (6.56–8.13)	<0.001*** (0.025)	25.899
		Independent *t*-test P (Cohen's d)	0.651 (0.021)	0.204 (0.057)	0.198 (0.064)		
	Stroke group-affected side	Left forearm	–4.10 (–7.80 to –0.39)	5.52 (1.82–9.22)	6.28 (2.57–9.98)	<0.001*** (0.045)	17.637
		Right forearm	3.54 (1.12–5.95)	9.01 (6.60–11.42)	9.75 (7.34–12.16)	<0.001*** (0.029)	11.133
		Independent *t*-test P (Cohen's d)	<0.001### (0.334)	0.137 (0.109)	0.188 (0.097)		
	Stroke group-unaffected side	Left forearm	4.39 (2.07–6.72)	7.27 (4.95–9.60)	6.40 (4.08–8.73)	0.119 (0.006)	2.144
		Right forearm	–5.82 (–9.37 to –2.28)	0.97 (–2.58 to 4.51)	1.41 (–2.13 to 4.96)	<0.001*** (0.036)	14.033
		Independent *t*-test P (Cohen's d)	<0.001### (0.401)	0.004## (0.211)	0.038# (0.153)		
Alpha	Control group	Left forearm	4.02 (1.43–6.62)	5.29 (2.69–7.88)	6.16 (3.56–8.75)	0.295 (0.001)	1.222
		Right forearm	5.58 (3.13–8.03)	10.53 (8.09–12.98)	12.59 (10.14–15.04)	<0.001*** (0.011)	11.449
		Independent *t*-test P (Cohen's d)	0.320 (0.046)	0.006## (0.123)	0.001## (0.146)		
	Stroke group-affected side	Left forearm	7.00 (3.70–10.31)	10.88 (7.57–14.19)	16.84 (13.53–20.15)	<0.001*** (0.031)	11.694
		Right forearm	2.17 (–1.13 to 5.46)	10.96 (7.67–14.26)	8.44 (5.14–11.73)	<0.001*** (0.025)	9.568
		Independent *t*-test P (Cohen's d)	0.017# (0.174)	0.972 (0.003)	0.002## (0.226)		
	Stroke group-unaffected side	Left forearm	8.69 (5.35–12.03)	6.22 (2.88–9.56)	11.67 (8.33–15.02)	0.034* (0.009)	3.433
		Right forearm	10.31 (6.93–13.70)	12.01 (8.62–15.39)	15.40 (12.01–18.78)	0.026* (0.010)	3.679
		Independent *t*-test P (Cohen's d)	0.496 (0.049)	0.013# (0.182)	0.146 (0.106)		
Beta	Control group	Left forearm	4.67 (3.48–5.85)	5.50 (4.32–6.68)	9.34 (8.15–10.52)	<0.001*** (0.020)	20.709
		Right forearm	4.81 (3.64–5.97)	7.30 (6.14–8.47)	8.90 (7.73–10.06)	<0.001*** (0.016)	16.625

(Continued)

TABLE 3 | (Continued)

Bands	Groups	Stimulation side	25°C	10°C	0°C	One-way repeated ANOVA	
			Mean (95% confidence interval, E-03)			P (Partial η^2)	F
		Independent *t*-test P (Cohen's d)	0.851 (0.006)	0.028# (0.099)	0.647 (0.019)		
	Stroke group-affected side	Left forearm	2.95 (1.92–3.98)	4.21 (3.19–5.24)	5.06 (4.03–6.08)	0.006** (0.013)	5.074
		Right forearm	–0.43 (–3.28 to 2.42)	3.18 (0.33–6.03)	8.72 (5.87–11.57)	<0.001*** (0.036)	14.015
		Independent *t*-test P (Cohen's d)	0.013# (0.184)	0.461 (0.052)	0.046# (0.144)		
	Stroke group-unaffected side	Left forearm	15.81 (11.79–19.82)	9.62 (5.61–13.63)	17.86 (13.85–21.87)	<0.001*** (0.024)	9.215
		Right forearm	1.94 (0.79–3.08)	3.81 (2.67–4.96)	4.80 (3.66–5.95)	<0.001*** (0.021)	7.909
		Independent *t*-test P (Cohen's d)	<0.001### (0.482)	0.001## (0.248)	<0.001### (0.387)		
Gamma	Control group	Left forearm	2.32 (0.77–3.86)	0.77 (-0.78 to 2.31)	6.13 (4.59–7.68)	<0.001*** (0.014)	13.633
		Right forearm	2.03 (0.86–3.21)	3.11 (1.93–4.28)	2.83 (1.65–4.01)	0.286 (0.001)	1.251
		Independent *t*-test P (Cohen's d)	0.752 (0.015)	0.012# (0.111)	0.004## (0.130)		
	Stroke group-affected side	Left forearm	0.60 (0.34–0.86)	1.27 (1.01–1.53)	0.81 (0.54–1.07)	0.001** (0.020)	7.695
		Right forearm	–0.86 (–2.02 to 0.31)	–0.37 (–1.53 to 0.80)	3.69 (2.52–4.85)	<0.001*** (0.054)	21.076
		Independent *t*-test P (Cohen's d)	0.001## (0.244)	0.001## (0.264)	0.001## (0.257)		
	Stroke group-unaffected side	Left forearm	3.11 (1.92–4.31)	2.16 (0.96–3.35)	4.16 (2.96–5.36)	0.004** (0.015)	5.701
		Right forearm	0.07 (–0.27 to 0.41)	0.61 (0.27–0.94)	0.71 (0.37–1.05)	0.003** (0.016)	5.978
		Independent *t*-test P (Cohen's d)	<0.001### (0.366)	0.006## (0.207)	<0.001### (0.353)		

Differences with statistical significance are marked with superscripts beside the P-values ("" for one-way repeated ANOVA intragroup tests with Bonferroni post-hoc tests, "#" for independent t-test). Significant levels are indicated as, 1 superscript for < 0.05, 2 superscripts for < 0.01, and 3 superscripts for < 0.001.*

Significant VAS variations with respect to the different temperatures were observed for each group *via* one-way repeated ANOVA ($P < 0.001$, **Table 5**). No statistical difference was found in the intergroup comparison for each cold stimulus ($P > 0.05$, one-way ANOVA, **Table 5**).

DISCUSSION

This study designed a novel configuration for the measurement of post-stroke elementary thermal sensation with NPCS. We utilized glass beaker with different temperatures of water, which statically attached to the skin surface without friction and load, to deliver the NPCSs with different intensities. In the literature, cold stimuli were mainly delivered by thermal pack (Mazzola et al., 2012; Ansari et al., 2018), thermode (Kwan et al., 2000; Tseng et al., 2010), or direct contact with the water (Maihöfner et al., 2002; Fardo et al., 2017), and these approaches unavoidably introduced mixed sensory inputs other than the thermal sensation. For example, direct contact with the water would mix the thermal sensation and the wetness sensation, while thermal pack and thermode with fasteners would introduce the intermediate texture, shape, or even weight perceptions. In comparison with those configurations in the literature, the involvements of other unrelated sensory inputs like texture, shape, wetness, and weight perceptions were effectively minimized with the configuration of this study. Meanwhile, the pain sensation was also avoided in the configuration with the precise 3 s stimulus duration. The NPCSs of this study were further verified by the VAS questionnaire (**Table 5**), where the VAS scores of all stroke and unimpaired participants were lower than 6 indicating without cold pain.

We measured the post-stroke sensory deficiency on the elementary non-painful cold sensation using both EEG RSP and VAS questionnaire. The VAS scores indicated that both stroke and unimpaired participants could distinguish the different NPCSs with statistical significance (**Table 5**). However, there was no significant intergroup difference in VAS scores between the stroke and unimpaired participants (**Table 5**), which could not further assess the post-stroke sensory alteration on thermal sensation. The insignificant intergroup VAS result could be due to the compensation of voluntary cognition toward sensory inputs for those stroke participants, leading to high thermal discrimination (Barulli and Stern, 2013). During the VAS

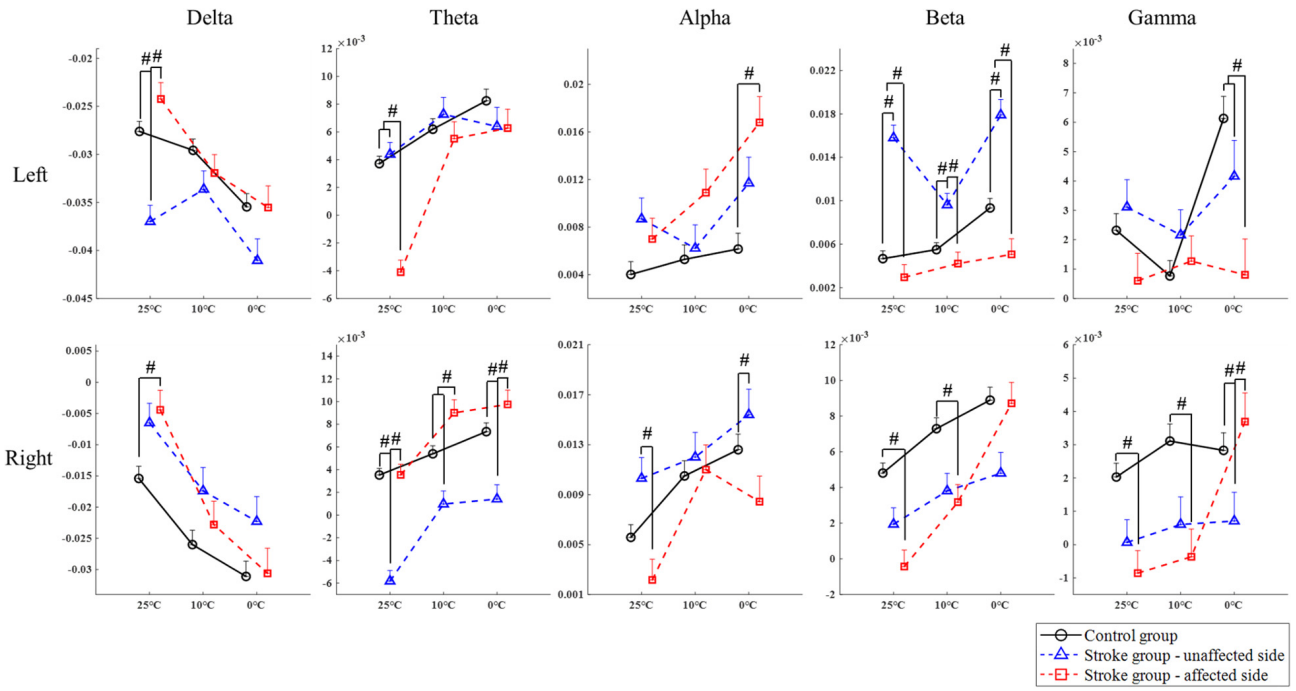

FIGURE 4 | The EEG overall relative spectral power in response to the non-painful cold stimuli on the left and right forearms for each group at the delta, theta, alpha, beta, and gamma band, respectively, presented as mean value with SE (error bar). The significant intergroup differences are indicated by "#" ($P < 0.05$, one-way ANOVA with Bonferroni *post-hoc* tests or Dunnett's T3 *post-hoc* tests).

questionnaire, participants were asked to rate the cold sensation provoked by each NPCS. This cognitive process could be related to the individual experiences, and mainly consisted of four primary elements including comprehension, retrieval, judgment, and response (Sudman et al., 1997; Tourangeau et al., 2000). On the contrary, significant group differences in cortical responses were found between the stroke and unimpaired groups toward different NPCSs. That is because the cortical responses captured by EEG RSPs were associated with involuntary attention drawn by the NPCS. During the EEG recording, to minimize the bias caused by the participants' active cognitive process, the participants were requested to remain awake yet mentally inactive. Therefore, the EEG RSP could reveal much more preliminary cortical response on the post-stroke sensory deficiency than the compensated cognitive process during the VAS questionnaire rating.

The EEG results of the unimpaired participants (**Figure 3A**) highlighted that different NPCSs could induce significant RSP variations across the target frequency bands (i.e., theta, alpha, and beta bands). These three bands were activated with increased power during the NPCS. In line with our observations of enhanced EEG beta RSP in both fronto-temporal and parietal brain regions (**Figure 5D**), it has been reported in the literature that beta activity increased bilaterally in the fronto-temporal cortex in unimpaired people during the cold stimulation, especially during the cold pain (Chang et al., 2002; De Pascalis et al., 2019). Chang et al. (2002) suggested that the increased beta power was related to the frontal and temporal muscle activities in response to cold stimulation, caused by situational tension factors like stress or pain. The increased beta activities were then suspected to associate with residual muscle artifact, as EEG artifact. However, the increased beta power of this study was mainly located in sensorimotor cortex (**Figure 5D**), not closely to the frontal or temporal muscles, which could not be accounted as muscle artifact. In addition, the present results also found that beta RSP intensities were increased with the increase of stimulus intensities. De Pascalis et al. (2019) reported a similar observation during the cold pain, and they found that the higher EEG beta power in the left frontal, midline central, posterior temporal cortices were correlated with the higher cold pain scores (De Pascalis et al., 2019). Together with the increased beta power during the NPCS in this work, it implied that the beta power could be proportional to the intensities of cold stimulations whether it was painful or non-painful. It was also observed that both theta and alpha RSPs were increased during the NPCS. It could be the involuntary attention aroused during the non-painful thermal stimulation, i.e., outside events attract spontaneous attentional processes (Eimer et al., 1996; Iannetti et al., 2008; Wang et al., 2010), for example, to process the different NPCSs in this work. Chen et al. (2017) reported that the intensity of attentive oscillation (i.e., theta and alpha bands) increased with the difficulty of sensory tasks. The attentive oscillation would be relatively low when processing an easy task, while its intensity would be higher when a difficult task lasts for a longer duration to obtain more information (Chen et al., 2017). These are consistent with our findings (**Figure 3A**),

TABLE 4 | Intergroup comparisons on the whole brain relative spectral power of each EEG frequency band.

			One-way ANOVA		Mixed-model repeated measure ANOVA					
			P (partial η^2)	F	Temperature		Group		Temperature × Group	
Bands	Stimulation side	Temperature			P (partial η^2)	F	P (partial η^2)	F	P (partial η^2)	F
Delta	Left forearm	25°C	<0.001$^{\#\#\#}$ (0.018)	15.943	<0.001$^{\Delta\ \Delta\ \Delta}$ (0.013)	22.970	<0.001$^{\Delta\ \Delta\ \Delta}$ (0.009)	7.724	0.017$^{\Delta}$ (0.003)	3.008
		10°C	0.165 (0.002)	1.801						
		0°C	0.090 (0.003)	2.414						
	Right forearm	25°C	0.003$^{\#\#}$ (0.007)	5.804	<0.001$^{\Delta\ \Delta\ \Delta}$ (0.021)	37.990	0.012$^{\Delta}$ (0.005)	4.456	0.315 (0.001)	1.186
		10°C	0.140 (0.002)	1.967						
		0°C	0.160 (0.002)	1.836						
Theta	Left forearm	25°C	<0.001$^{\#\#\#}$ (0.038)	34.097	<0.001$^{\Delta\ \Delta\ \Delta}$ (0.023)	40.855	0.002$^{\Delta\ \Delta}$ (0.007)	6.121	<0.001$^{\Delta\ \Delta\ \Delta}$ (0.009)	7.892
		10°C	0.587 (0.001)	0.532						
		0°C	0.328 (0.001)	1.117						
	Right forearm	25°C	<0.001$^{\#\#\#}$ (0.043)	38.554	<0.001$^{\Delta\ \Delta\ \Delta}$ (0.028)	50.435	<0.001$^{\Delta\ \Delta\ \Delta}$ (0.030)	26.779	0.003$^{\Delta\ \Delta}$ (0.005)	3.993
		10°C	<0.001$^{\#\#\#}$ (0.014)	12.355						
		0°C	<0.001$^{\#\#\#}$ (0.014)	11.969						
Alpha	Left forearm	25°C	0.052 (0.003)	2.961	<0.001$^{\Delta\ \Delta\ \Delta}$ (0.007)	11.405	0.001$^{\Delta\ \Delta}$ (0.008)	7.058	0.011$^{\Delta}$ (0.004)	3.260
		10°C	0.053 (0.003)	2.949						
		0°C	<0.001$^{\#\#\#}$ (0.011)	9.322						
	Right forearm	25°C	0.002$^{\#\#}$ (0.007)	6.088	<0.001$^{\Delta\ \Delta\ \Delta}$ (0.009)	15.911	0.022$^{\Delta}$ (0.004)	3.842	0.180 (0.002)	1.569
		10°C	0.818 (0.000)	0.200						
		0°C	0.051 (0.003)	2.985						
Beta	Left forearm	25°C	<0.001$^{\#\#\#}$ (0.044)	40.099	<0.001$^{\Delta\ \Delta\ \Delta}$ (0.011)	19.707	<0.001$^{\Delta\ \Delta\ \Delta}$ (0.039)	35.077	<0.001$^{\Delta\ \Delta\ \Delta}$ (0.008)	6.772
		10°C	<0.001$^{\#\#\#}$ (0.009)	7.685						
		0°C	<0.001$^{\#\#\#}$ (0.024)	20.947						
	Right forearm	25°C	<0.001$^{\#\#\#}$ (0.015)	12.796	<0.001$^{\Delta\ \Delta\ \Delta}$ (0.020)	35.387	<0.001$^{\Delta\ \Delta\ \Delta}$ (0.013)	11.568	0.002$^{\Delta\ \Delta}$ (0.005)	4.222
		10°C	<0.001$^{\#\#\#}$ (0.010)	8.586						
		0°C	0.009$^{\#\#}$ (0.005)	4.683						
Gamma	Left forearm	25°C	0.143 (0.002)	1.949	0.002$^{\Delta\ \Delta}$ (0.003)	6.022	0.013$^{\Delta}$ (0.005)	4.371	0.003$^{\Delta\ \Delta}$ (0.005)	3.985
		10°C	0.382 (0.001)	0.962						
		0°C	0.001$^{\#\#}$ (0.008)	7.010						
	Right forearm	25°C	<0.001$^{\#\#\#}$ (0.009)	7.791	<0.001$^{\Delta\ \Delta\ \Delta}$ (0.005)	8.678	0.001$^{\Delta\ \Delta}$ (0.008)	7.079	0.001$^{\Delta\ \Delta}$ (0.006)	4.817
		10°C	<0.001$^{\#\#\#}$ (0.009)	7.770						
		0°C	0.038$^{\#}$ (0.004)	3.288						

Differences with statistical significance are marked with superscripts beside the P-values ("#" for one-way ANOVA intergroup tests with Bonferroni post-hoc tests or Dunnett's T3 post-hoc tests, "Δ" for mixed-model repeated measure ANOVA intergroup tests on the temperature and group effects). Significant levels are indicated as, 1 superscript for < 0.05, 2 superscripts for < 0.01, 3 superscripts for < 0.001.

among the three stimuli, the 0°C stimulus obtained the highest RSP intensity, and the RSP of 10°C was higher than that of the 25°C stimulus. Of the three representative frequency bands, the theta band showed the highest sensitivity in distinguishing different cold stimuli in unimpaired participants, because theta RSP obtained statistical differences between three cold stimuli for both stimulation sides. The limited sensitivity toward cold stimuli in the alpha and beta RSPs were possibly due to the dominance of the theta band during involuntary attention evoked by the sensory stimulation, as designed in this work.

Post-stroke neural responses of the elementary cold sensation induced by NPCS were also investigated for both affected and unaffected sides in the stroke participants. In the stroke unaffected group, the sensitive EEG RSPs of distinguishing different cold stimuli were concentrated in the beta and gamma bands (**Figure 3B**). Varied with the control group, the theta band was no longer the dominant frequency band toward cold stimuli in the stroke unaffected group, and it only remained limited resolution to different temperatures during the right-side stimulation. Instead, significant variations were observed in beta and gamma RSPs during the NPCS on both stimulation sides, whereas its thermal resolution was also limited. For example, both beta and gamma RSPs of the right side could not distinguish the difference between the 10°C and the 0°C water. The sensory deficiency in the unaffected upper limb of stroke survivors was frequently overlooked in routine stroke clinical practice. Recently, it has been pointed out that sensorimotor deficits frequently occurring in the unaffected upper limb were mainly due to the transcallosal interactions between the hemispheres (Grefkes and Fink, 2011), and decreased sensory discrimination

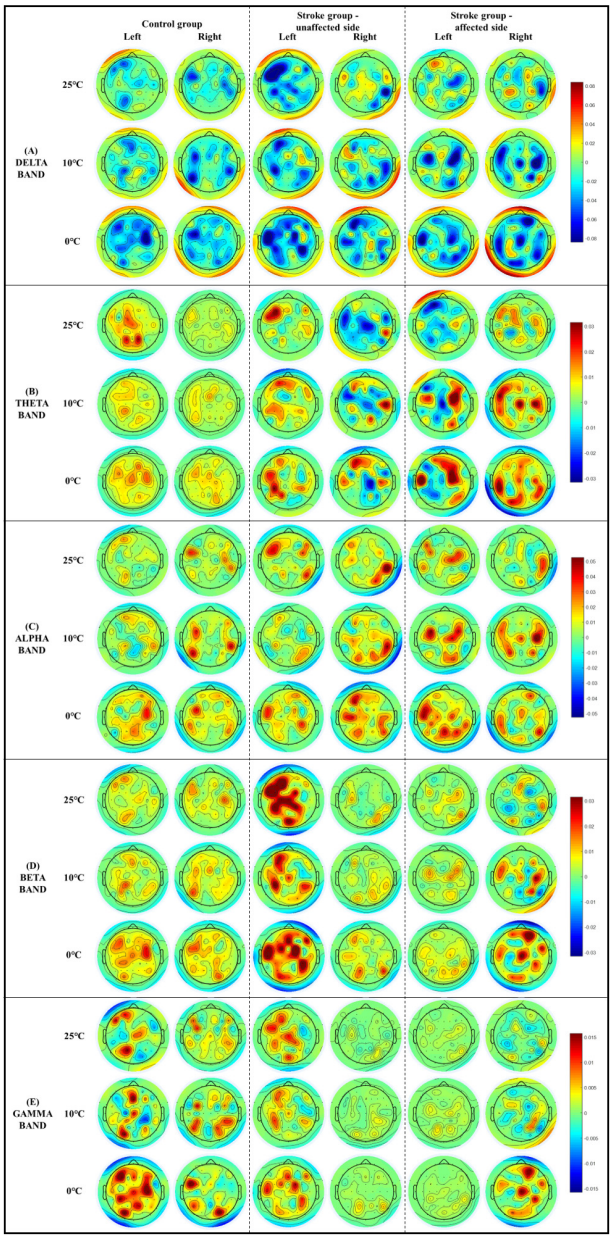

FIGURE 5 | The whole brain EEG topography on the mean relative spectral power of **(A)** delta, **(B)** theta, **(C)** alpha, **(D)** beta, **(E)** gamma in response to the non-painful cold stimuli with respect to the stimulation side.

is one of the representative symptoms for sensory deficiency in the unaffected upper limb. In this study, the reduced sensory discrimination toward elementary cold sensation for the unaffected side of the stroke participants was captured.

For the stroke affected group, in comparison with both unimpaired participants and the unaffected side of stroke survivors, a wider distribution of representative RSP across the whole spectrum toward NPCSs was observed, and all EEG frequency bands showed significant RSP differences toward the different cold stimuli (**Figure 3C**). These broadly activated EEG frequency responses could be related to the excessive cortical effort after stroke. It indicated that the desired sensory responses were challenging for chronic stroke survivors, even after the recovery period of pathological reorganization (Thibaut et al., 2017). It was widely reported that excessive cortical effort was required in post-stroke motor recovery when a task became more complex (Jones and Adkins, 2015; Thibaut et al., 2017). In this work, we observed the similar additional cortical effort in the sensory experiences during the NPCS. Meanwhile, although significant RSP variations toward different cold stimuli could be obtained in EEG frequency bands for the affected sides, their thermal resolutions on different temperatures represented by EEG RSP were low. For example, in unimpaired participants, the theta RSP demonstrated the highest sensitivity in distinguishing the three cold stimuli on both sides, while the theta RSP did not show a significant difference between the 10°C and the 0°C water on both sides for the stroke affected group. Another finding related to the power spectrum was the involvement of high frequency gamma band during the NPCS to the affected limbs of the stroke participants (**Figure 3C**). It could be due to the compensation of the impaired afferent proprioception and efferent control in sensorimotor system (Chen et al., 2018). Increased unconscious employments of higher-level attention and behavioral processes were usually observed in stroke survivors, when compared with the unimpaired individuals (Bannister et al., 2015; Chen et al., 2018). Previous studies also highlighted the contributions of post-stroke gamma activation, i.e., contributed to cognitive motor tasks (Gross and Gotman, 1999; Meador et al., 2002), and acted as a coding feature for functional prevalence in hand sensory areas (Tecchio et al., 2003, 2004). In our previous studies on post-stroke sensory deficiency during mechanical tactile stimulation (i.e., textile fabric stimulations), similar engagements of high frequency bands (i.e., beta and gamma bands) were observed in persons with chronic stroke (Huang et al., 2020). It further indicated the importance of gamma oscillation for somatosensory functions, including thermal and tactile sensations, following a stroke.

We also investigated the variations of neural responses during the NPCS between the left and right sides for each group. These variations were mainly investigated from two aspects, which included the RSP intensity and its resolution. From the resolution aspect, the RSP resolutions of the control and stroke affected group toward different cold stimuli between the left and right sides were comparable (**Figures 3A,C**). From the intensity aspect, the control group obtained significantly higher RSP intensities in the relative high frequency bands (i.e., alpha, beta, and gamma bands) during the right-side stimulation than left-side stimulation (**Figure 3A**). This could be related to the higher amplitude of cortical potentials during the dominant hand movement, in comparison with the non-dominant hand (Tarkka and Hallett, 1990). In this study, all the unimpaired participants were right-handed. In the stroke affected group, the right-side stimulation achieved significant higher RSP intensities in the relative high frequency bands (i.e., alpha, beta, and gamma bands) during the strong NPCS (i.e., 0°C) than the left-side stimulation, while the right-side stimulation obtained significant lower RSP intensities during the weak NPCS (i.e.,

TABLE 5 | Non-painful cold sensation evaluated by visual analog scale.

Groups	25°C	10°C	0°C	One-way repeated ANOVA	
	Mean (95% confidence interval)			P (partial η^2)	F
Control group	1.40 (1.12–1.68)	3.27 (2.99–3.55)	4.60 (4.32–4.88)	<0.001*** (0.888)	110.480
Stroke group-unaffected side	1.42 (1.09–1.74)	3.25 (2.92–3.58)	4.67 (4.17–4.83)	<0.001*** (0.893)	91.432
Stroke group-affected side	1.50 (1.14–1.86)	3.67 (3.30–4.03)	4.92 (4.55–5.28)	<0.001*** (0.920)	125.673
One-way ANOVA					
P (Partial η^2)	0.871 (0.008)	0.181 (0.091)	0.180 (0.091)		
F	0.138	1.795	1.797		

Differences with statistical significance are marked with "" beside the P-values (one-way repeated ANOVA intragroup tests with Bonferroni post-hoc tests). Significant levels are indicated as, 1 superscript for < 0.05, 2 superscripts for < 0.01, 3 superscripts for < 0.001.*

25°C) (**Figure 3C**). It might imply that the affected left forearm is more sensitive to a weak stimulus, where the affected right forearm is more sensitive to a high stimulus. This particular finding could be related to the lateralization of brain function, which result in the differences of behavior and recovery outcome between the left hemiplegia and right hemiplegia (Chen et al., 2000; Park and Lee, 2011; Frenkel-Toledo et al., 2019). For example, patients with left-hemisphere stroke often develop a slow and cautious behavioral style; on the contrary, those patients with right-hemisphere stroke usually present a quick and overly curious behavior (Hayn and Fisher, 1997). Owing to the superiority of controlling complex motor movements in the left hemisphere (Serrien and Spapé, 2009), it was also reported that patients with right hemiplegia had slower motor restoration in gait functions (Laufer et al., 2003; Gama et al., 2017). However, few works have been done on the differences in sensory impairment after the left- and right-hemisphere lesions, which necessitate further investigations (Goodin et al., 2018).

When it comes to the stroke unaffected group, asymmetric neural responses from both aspects were observed in all EEG frequency bands, especially in the high frequency bands (i.e., beta and gamma bands, **Figures 3B**, **5**). Firstly, the thermal resolution of different temperatures for right unaffected forearms was higher than those of the left. In the theta band, significant RSP variation toward different cold stimuli was only observed during the right-side stimulation. In the gamma band, the RSP of the right forearm could significantly distinguish the 25°C stimulus from the other two stimuli, where the RSP of the left forearm could not. Secondly, the RSP intensities (theta, beta, and gamma bands) were significantly higher for the left unaffected forearms than the right ones (**Figures 3B**, **5**). This excessive neural response suggested that additional cortical efforts were needed during the neural processing of thermal inputs for the unaffected left forearms. The imbalance of neural responses toward thermal stimulation for the stroke unaffected group could be related to the handedness alteration after stroke. Typically, dominant hands have better sensorimotor performance during single-handed tasks, like better manual dexterity during motor movements, and higher sensation thresholds for touch and pain than non-dominant hands (Özcan et al., 2005; Dirnberger et al., 2011). Most stroke survivors will use their unaffected forearms to perform sensorimotor tasks in their daily lives after stroke. In some stroke survivors with affected right dominant forearms, the unaffected left forearms will gradually become their new dominant upper limbs (Harris and Eng, 2006). However, it can be difficult for stroke survivors during the handedness alteration, with the unaffected left forearms presenting low sensation resolution and poor control over voluntary motor tasks, compared to their original dominant right arms. In this study, all stroke survivors were right-handed before their stroke onset. Among them, half were right hemiplegics, who had experienced handedness alteration after stroke. The RSP results of this study further verified the thermal sensitivity during the NPCS for the unaffected left forearm was lower than the unaffected right ones. In line with our previous study (Huang et al., 2020), the unaffected right forearms also showed better touch discrimination to the different fabrics during the tactile stimulation when compared with the unaffected left forearms.

Significant intergroup differences of RSP intensities were also observed (**Figure 4**). Significant variation on RSP intensity between the stroke unaffected group and control group was mainly captured in the beta band (**Figure 4**). When the left sides were stimulated, the intensity of beta RSP in the unaffected group was significantly higher than that in the control group. This might also be related to the alteration in handedness after stroke. When compared with the control group, the stroke affected group displayed sensory deficiency related to attenuated cortical responses during the weak cold stimuli (i.e., 10 and 25°C). When the right side was stimulated with the 10 and 25°C water, the RSP intensities of high frequency bands (i.e., beta and gamma bands, **Figure 4**) in the stroke affected group were significantly lower than the control group; however, the RSP intensities between the two groups were comparable when stimulated by 0°C. The cortical activation in the stroke affected group was relatively low during the processing of weak to moderate NPCSs (i.e., 10 and 25°C), while strong NPCS (i.e., 0°C stimulus) could initiate high cortical activation. It implied that the reduced somatosensation after stroke was mainly characterized as the insensitivity to those weak sensory inputs and their discriminations.

The sensory cortical centers in response to elementary thermal stimulation for both stroke and unimpaired participants were revealed by the whole-brain RSP topography (**Figure 5**). For those unimpaired participants, multiple brain regions were activated bilaterally during the NPCS, which included the

primary sensorimotor cortex, insula cortex, occipital cortex, prefrontal, and frontal cortices. These findings were in line with the literature (Chang et al., 2002, 2005; De Pascalis et al., 2019), and further verified the cortical processing of thermal stimulation was a distributed system, rather than a strict somatotopic arrangement (Berman et al., 1998; Chang et al., 2005). In several fMRI studies, innocuous thermal-related activations in the anterior cingulate cortex and lateral-thalamus pathway were also reported (Davis et al., 1998; Kwan et al., 2000; Mazzola et al., 2012). For stroke survivors, the brain cortices that process non-painful cold sensation were also activated bilaterally in multiple brain regions as seen in unimpaired individuals, where the activated regions were more extensive with higher intensity. Similar distribution of post-stroke cortical activation after thermal stimulation was reported by one fMRI study (Chen et al., 2020). They observed that brain activations promoted by thermal stimuli were in the inferior-middle frontal cortex, superior-middle temporal cortex, insula, and primary sensorimotor cortex (Chen et al., 2020).

One of the concerns in the EEG measurements is the high signal to noise ratio (SNR) to ensure the signal quality, and it could be achieved by ensemble mean *via* repetitions (Väisänen and Malmivuo, 2009). In this study, we preferred EEG power spectra to investigate the cortical responses to NPCS, since it requires less repetition or signal length than the measurement of intact waveform of SSEP in the time domain. It is because the frequency components are less affected by the background noises, e.g., environmental noise (50 Hz power line) and spontaneous EEG unrelated to the stimulation, as the target EEG frequency features may not be overlapped with the noise features in the spectrum (Thut and Miniussi, 2009). For instance, the SSEP waveform detection usually requires averaging over 250–1,000 repetitions to obtain a reasonable SNR (Society, 2015), while Singh et al. (2014) only used a single trial to achieve the significant power changes between the pleasant and unpleasant touch stimuli.

The small sample size was one of the limitations of this study. However, under the current small sample size, significant differences in EEG RSP between the unimpaired population and the chronic stroke population had been obtained. Another limitation of this study was the significant gender differences between the two groups (p = 0.005, Fisher exact test, **Table 1**). In this study, we focused on the investigation of the impairment in elementary thermal sensation introduced by the neurological lesion after stroke, rather than the difference of gender. Gender differences in post-stroke sensory impairment, e.g., thermal sensation, has not been investigated yet. In future work, more stroke participants in different recovery stages, gender, age groups, and lesion sites will be investigated for a more comprehensive understanding.

CONCLUSION

The contribution of this study was the objective and quantitative evaluation of post-stroke elementary thermal impairment toward non-painful cold stimulation *via* EEG RSP analysis, with a new configuration minimizing the unnecessary sensory inputs. The characteristics of cortical responses during the NPCS following a stroke were (1) wide distribution of representative RSP bands, (2) limited sensitivity toward different thermal stimuli, (3) more extensive sensory cortical areas, when compared with the EEG RSP features of the unimpaired control. Meanwhile, the post-stroke somatosensation of unaffected side was also impaired, which was represented by lower resolution toward different NPCSs and asymmetric RSP intensities toward different stimulation sides. EEG RSP pattern could quantify the neural responses of elementary thermal sensation after stroke, and enhance the understanding of post-stroke sensory deficiency on elementary thermal sensation.

DATA AVAILABILITY STATEMENT

The datasets presented in this article are not readily available because it has been stated in the consent approved by the Human Subjects Ethics Sub-Committee of the Hong Kong Polytechnic University that the results of the experiment may be published, but the individual results should be kept confidentially for each subject. Requests to access the datasets should be directed to XLH, xiaoling.hu@polyu.edu.hk.

ETHICS STATEMENT

The studies involving human participants were reviewed and approved by the Human Subjects Ethics Sub-Committee of the Hong Kong Polytechnic University. The patients/participants provided their written informed consent to participate in this study.

AUTHOR CONTRIBUTIONS

YHH contributed to the experimental design, data analysis, and manuscript drafting. JYH and ZYL contributed to the experimental design. JJ, CCH, ZQL, and YY contributed to the subject management and experimental process. XLH conceived of the study and coordinated the whole project, including the study design, human subject experiments, and manuscript revising. All authors read and approved the final manuscript.

FUNDING

This project was funded by the National Natural Science Foundation of China (NSFC 81771959), University Grants Committee Research Grants Council, Hong Kong (GRF 15207120), and Science and Technology Innovation Committee of Shenzhen, China (2021Szvup142).

ACKNOWLEDGMENTS

We would like to thank the participants of this study.

REFERENCES

Ahmed, S. A., Rani, D. E., and Sattar, S. A. (2012). Alpha activity in EEG and intelligence. *Int. J. Adv. Inf. Technol.* 2:27. doi: 10.5121/ijait.2012.2103

Ahn, S.-N., Lee, J.-W., and Hwang, S. (2016). Tactile perception for stroke induce changes in electroencephalography. *Hong Kong J. Occupat. Therapy* 28, 1–6. doi: 10.1016/j.hkjot.2016.10.001

Ansari, Y., Remaud, A., and Tremblay, F. (2018). Variations in corticomotor excitability in response to distal focal thermal stimulation. *Somatosens Mot. Res.* 35, 69–79. doi: 10.1080/08990220.2018.1460263

Bannister, L. C., Crewther, S. G., Gavrilescu, M., and Carey, L. M. (2015). Improvement in touch sensation after stroke is associated with resting functional connectivity changes. *Front. Neurol.* 6:165–165. doi: 10.3389/fneur.2015.00165

Barulli, D., and Stern, Y. (2013). Efficiency, capacity, compensation, maintenance, plasticity: emerging concepts in cognitive reserve. *Trends Cogn. Sci.* 17, 502–509. doi: 10.1016/j.tics.2013.08.012

Bell-Krotoski, J., and Tomancik, E. (1987). The repeatability of testing with semmes-weinstein monofilaments. *J. Hand Surgery* 12, 155–161. doi: 10.1016/S0363-5023(87)80189-2

Berman, H. H., Kim, K. H., Talati, A., and Hirsch, J. (1998). Representation of nociceptive stimuli in primary sensory cortex. *Neuroreport* 9, 4179–4187. doi: 10.1097/00001756-199812210-00033

Bohannon, R. W., and Smith, M. B. (1987). Interrater reliability of a modified Ashworth scale of muscle spasticity. *Physical Therapy* 67, 206–207. doi: 10.1093/ptj/67.2.206

Caliandro, P., Vecchio, F., Miraglia, F., Reale, G., Della Marca, G., La Torre, G., et al. (2017). Small-world characteristics of cortical connectivity changes in acute stroke. *Neurorehabilitation Neural Repair* 31, 81–94. doi: 10.1177/1545968316662525

Carey, L. M. (1995). Somatosensory Loss after Stroke. *Crit. Rev. Phys. Rehabil. Med* 7, 51–91. doi: 10.1615/CritRevPhysRehabilMed.v7.i1.40

Carey, L. M., Lamp, G., and Turville, M. (2016). The state-of-the-science on somatosensory function and its impact on daily life in adults and older adults, and following stroke: a scoping review. *OTJR (Thorofare N J)* 36, 27s–41s. doi: 10.1177/1539449216643941

Carey, L. M., Matyas, T. A., and Baum, C. (2018). Effects of somatosensory impairment on participation after stroke. *Am. J. Occup. Ther.* 72, 7203205100p7203205101-7203205100p7203205110. doi: 10.5014/ajot.2018.025114

Chang, P. F., Arendt-Nielsen, L., and Chen, A. C. (2002). Dynamic changes and spatial correlation of EEG activities during cold pressor test in man. *Brain Res. Bull.* 57, 667–675. doi: 10.1016/s0361-9230(01)00763-8

Chang, P. F., Arendt-Nielsen, L., and Chen, A. C. (2005). Comparative cerebral responses to non-painful warm vs. cold stimuli in man: EEG power spectra and coherence. *Int J Psychophysiol* 55, 73–83. doi: 10.1016/j.ijpsycho.2004.06.006

Chen, A., Wang, A., Wang, T., Tang, X., and Zhang, M. (2017). Behavioral oscillations in visual attention modulated by task difficulty. *Front. Psychol.* 8:1630. doi: 10.3389/fpsyg.2017.01630

Chen, C.-L., Tang, F.-T., Chen, H.-C., Chung, C.-Y., and Wong, M.-K. (2000). Brain lesion size and location: Effects on motor recovery and functional outcome in stroke patients. *Archiv. Physical Med. Rehabil.* 81, 447–452. doi: 10.1053/mr.2000.3837

Chen, J.-I., Ha, B., Bushnell, M. C., Pike, B., and Duncan, G. H. (2002). Differentiating noxious-and innocuous-related activation of human somatosensory cortices using temporal analysis of fMRI. *J. Neurophysiology* 88, 464–474. doi: 10.1152/jn.2002.88.1.464

Chen, S. C.-J., Hsu, M.-J., Kuo, Y.-T., Lin, R.-T., Lo, S.-K., and Lin, J.-H. (2020). Immediate effects of noxious and innocuous thermal stimulation on brain activation in patients with stroke. *Medicine* 99:e19386. doi: 10.1097/MD.0000000000019386

Chen, X., Xie, P., Zhang, Y., Chen, Y., Cheng, S., and Zhang, L. (2018). Abnormal functional corticomuscular coupling after stroke. *NeuroImage Clin.* 19, 147–159. doi: 10.1016/j.nicl.2018.04.004

Davis, K. D., Kwan, C. L., Crawley, A. P., and Mikulis, D. J. (1998). Functional MRI study of thalamic and cortical activations evoked by cutaneous heat, cold, and tactile stimuli. *J. Neurophysiology* 80, 1533–1546. doi: 10.1152/jn.1998.80.3.1533

De Diego, C., Puig, S., and Navarro, X. (2013). A sensorimotor stimulation program for rehabilitation of chronic stroke patients. *Restor. Neurol. Neurosci.* 31, 361–371. doi: 10.3233/rnn-120250

De Pascalis, V., Scacchia, P., Papi, B., and Corr, P. J. (2019). Changes of EEG band oscillations to tonic cold pain and the behavioral inhibition and fight-flight-freeze systems. *Personal. Neurosci.* 2:e12. doi: 10.1017/pen.2019.9

Dellon, A. L., Mackinnon, S. E., and Crosby, P. M. (1987). Reliability of two-point discrimination measurements. *J. Hand Surgery* 12, 693–696. doi: 10.1016/S0363-5023(87)80049-7

Dictionary, O. (2016). *Middle Age: Definition Of Middle Age In Oxford Dictionary (American English) (Us) [Online]*. Available online at: https://www.lexico.com/en/definition/middle_age (accessed April 26, 2022).

Dijkerman, H. C., and De Haan, E. H. F. (2007). Somatosensory processes subserving perception and action. *Behav. Brain Sci.* 30, 189–201. doi: 10.1017/S0140525X07001392

Dirnberger, G., Duregger, C., Lindinger, G., and Lang, W. (2011). On the regularity of preparatory activity preceding movements with the dominant and non-dominant hand: a readiness potential study. *Int. J. Psychophysiol.* 81, 127–131. doi: 10.1016/j.ijpsycho.2011.04.008

Eimer, M., Nattkemper, D., Schröger, E., and Prinz, W. (1996). "Chapter 5 Involuntary attention," in *Handbook of Perception and Action*, eds O. Neumann and A. F. Sanders (Cambridge: Academic Press), 155–184. doi: 10.1016/s1874-5822(96)80022-3

Fardo, F., Vinding, M. C., Allen, M., Jensen, T. S., and Finnerup, N. B. (2017). Delta and gamma oscillations in operculo-insular cortex underlie innocuous cold thermosensation. *J Neurophysiol.* 117, 1959–1968. doi: 10.1152/jn.00843.2016

Frenkel-Toledo, S., Fridberg, G., Ofir, S., Bartur, G., Lowenthal-Raz, J., Granot, O., et al. (2019). Lesion location impact on functional recovery of the hemiparetic upper limb. *PLoS One* 14:e0219738. doi: 10.1371/journal.pone.0219738

Fugl-Meyer, A. R., Jääskö, L., Leyman, I., Olsson, S., and Steglind, S. (1974). The post-stroke hemiplegic patient. 1. a method for evaluation of physical performance. *Scand. J. rehabil. Med.* 7, 13–31.

Gama, G. L., Larissa, C. D. L., Brasileiro, A.C.D.a.L, Silva, E. M. G. D. S., Galvão, , ÉR. V. P., Maciel, , ÁC., et al. (2017). Post-stroke hemiparesis: does chronicity, etiology, and lesion side are associated with gait pattern? *Top Stroke Rehabil* 24, 388–393. doi: 10.1080/10749357.2017.1304865

Garkavenko, V. V., Man'kovskaya, O. P., Omel'chenko, T. G., Gorkovenko, A. V., and Shevko, A. N. (2008). Effect of cold stimulation of the arm fingers on the spectral/coherent EEG characteristics in humans. *Neurophysiology* 40, 228–230. doi: 10.1007/s11062-008-9041-4

Goodin, P., Lamp, G., Vidyasagar, R., McArdle, D., Seitz, R. J., and Carey, L. M. (2018). Altered functional connectivity differs in stroke survivors with impaired touch sensation following left and right hemisphere lesions. *NeuroImage Clin.* 18, 342–355. doi: 10.1016/j.nicl.2018.02.012

Grefkes, C., and Fink, G. R. (2011). Reorganization of cerebral networks after stroke: new insights from neuroimaging with connectivity approaches. *Brain* 134, 1264–1276. doi: 10.1093/brain/awr033

Gross, D. W., and Gotman, J. (1999). Correlation of high-frequency oscillations with the sleep–wake cycle and cognitive activity in humans. *Neuroscience* 94, 1005–1018. doi: 10.1016/s0306-4522(99)00343-7

Harris, J. E., and Eng, J. J. (2006). Individuals with the dominant hand affected following stroke demonstrate less impairment than those with the nondominant hand affected. *Neurorehabil. Neural Rep.* 20, 380–389. doi: 10.1177/1545968305284528

Hayn, M. A., and Fisher, T. R. (1997). Stroke rehabilitation: salvaging ability after the storm. *Nursing* 27:40.

Head, H., and Holmes, G. (1911). Sensory disturbances from cerebral lesions 1. *Brain* 34, 102–254. doi: 10.1093/brain/34.2-3.102

Huang, Y., Jiao, J., Hu, J., Hsing, C., Lai, Z., Yang, Y., et al. (2020). Measurement of sensory deficiency in fine touch after stroke during textile fabric stimulation by electroencephalography (EEG). *J. Neural Eng.* 17:045007. doi: 10.1088/1741-2552/aba160

Hwang, P., Sohn, M. K., Kim, C. S., and Jee, S. (2016). Tibial somatosensory evoked potential can prognosticate for ambulatory function in subacute hemiplegic stroke. *J. Clin Neurosci.* 26, 122–125. doi: 10.1016/j.jocn.2015.05.070

Iannetti, G. D., Hughes, N. P., Lee, M. C., and Mouraux, A. (2008). Determinants of laser-evoked EEG responses: pain perception or stimulus saliency? *J. Neurophysiol.* 100, 815–828. doi: 10.1152/jn.00097.2008

Jones, T. A., and Adkins, D. L. (2015). Motor system reorganization after stroke: stimulating and training toward perfection. *Physiology (Bethesda, Md.)* 30, 358–370. doi: 10.1152/physiol.00014.2015

Kessner, S. S., Bingel, U., and Thomalla, G. (2016). Somatosensory deficits after stroke: a scoping review. *Topics Stroke Rehabil.* 23, 136–146. doi: 10.1080/10749357.2015.1116822

Krause, T., Asseyer, S., Geisler, F., Fiebach, J. B., Oeltjenbruns, J., Kopf, A., et al. (2016). Chronic sensory stroke with and without central pain is associated with bilaterally distributed sensory abnormalities as detected by quantitative sensory testing. *Pain* 157, 194–202. doi: 10.1097/j.pain.0000000000000354

Kwan, C. L., Crawley, A. P., Mikulis, D. J., and Davis, K. D. (2000). An fMRI study of the anterior cingulate cortex and surrounding medial wall activations evoked by noxious cutaneous heat and cold stimuli. *Pain* 85, 359–374. doi: 10.1016/s0304-3959(99)00287-0

Laufer, Y., Sivan, D., Schwarzmann, R., and Sprecher, E. (2003). Standing balance and functional recovery of patients with right and left hemiparesis in the early stages of rehabilitation. *Neurorehabil. Neural Rep.* 17, 207–213. doi: 10.1177/0888439003259169

Lebeau, F. (2010). Gamma oscillations and the cellular components of consciousness? New Horiz. *Neurosci. Consci.* 79, 29–37. doi: 10.1075/aicr.79.07leb

Lin, R., Hsu, M. J., Lin, R. T., Huang, M. H., Koh, C. L., Hsieh, C. L., et al. (2017). No difference between noxious and innocuous thermal stimulation on motor recovery of upper extremity in patients with acute stroke: a randomized controlled trial with 6-month follow-up. *PMR* 9, 1191–1199. doi: 10.1016/j.pmrj.2017.05.012

Lystad, R. P., and Pollard, H. (2009). Functional neuroimaging: a brief overview and feasibility for use in chiropractic research. *J. Can. Chiropr. Assoc.* 53, 59–72. doi: 10.4324/9780203938904-12

Maihöfner, C., Kaltenhäuser, M., Neundörfer, B., and Lang, E. (2002). Temporo-spatial analysis of cortical activation by phasic innocuous and noxious cold stimuli–a magnetoencephalographic study. *Pain* 100, 281–290. doi: 10.1016/s0304-3959(02)00276-2

Matsuda, K., Satoh, M., Tabei, K.-I., Ueda, Y., Taniguchi, A., Matsuura, K., et al. (2020). Impairment of intermediate somatosensory function in corticobasal syndrome. *Sci. Rep.* 10:11155. doi: 10.1038/s41598-020-67991-7

Mazzola, L., Faillenot, I., Barral, F.-G., Mauguière, F., and Peyron, R. (2012). Spatial segregation of somato-sensory and pain activations in the human operculo-insular cortex. *NeuroImage* 60, 409–418. doi: 10.1016/j.neuroimage.2011.12.072

Meador, K. J., Ray, P. G., Echauz, J. R., Loring, D. W., and Vachtsevanos, G. J. (2002). Gamma coherence and conscious perception. *Neurology* 59, 847–854. doi: 10.1212/WNL.59.6.847

Misra, U. K., Kalita, J., and Kumar, B. (2008). A study of clinical, magnetic resonance imaging, and somatosensory-evoked potential in central post-stroke pain. *J. pain* 9, 1116–1122. doi: 10.1016/j.jpain.2008.06.013

Nuwer, M. R., Comi, G., Emerson, R., Fuglsang-Frederiksen, A., Guerit, J.-M., Hinrichs, H., et al. (1999). *Recommendations For The Practice Of Clinical Neurophysiology: Guidelines Of The International Federation Of Clinical Physiology, Electroencephalography and Clinical Neurophysiology Supplement*. Amsterdam: Elsevier.

Özcan, A., Ozdirenç, M. M., and Akln, F. (2005). Light touch and pain sensation differences between dominant and non-dominant hands of healthy subjects. *British J. Hand Ther.* 10, 76–79. doi: 10.1177/1758998305010003-401

Park, S. Y., and Lee, I. H. (2011). The influence of age, lesion side and location on rehabilitation outcome after stroke. *J. Physic. Ther. Sci.* 23, 817–819. doi: 10.1080/09297040701792383

Razali, N. M., and Wah, Y. B. (2011). Power comparisons of shapiro-wilk, kolmogorov-smirnov, lilliefors and anderson-darling tests. *J. Stat. Model. Anal.* 2, 21–33.

Rebbeck, T., Moloney, N., Azoory, R., Hübscher, M., Waller, R., Gibbons, R., et al. (2015). Clinical ratings of pain sensitivity correlate with quantitative measures in people with chronic neck pain and healthy controls: cross-sectional study. *Phys. Ther.* 95, 1536–1546. doi: 10.2522/ptj.20140352

Roselli, F., Tartaglione, B., Federico, F., Lepore, V., Defazio, G., and Livrea, P. (2009). Rate of MMSE score change in alzheimer's disease: influence of education and vascular risk factors. *Clin. Neurol. Neurosurg.* 111, 327–330. doi: 10.1016/j.clineuro.2008.10.006

Satoh, M., Terada, S., Onouchi, K., Takeda, K., and Kuzuhara, S. (2002). Somatosensory and skin temperature disturbances caused by infarction of the postcentral gyrus: a case report. *J. Neurol.* 249, 1404–1408. doi: 10.1007/s00415-002-0853-7

Serrada, I., Hordacre, B., and Hillier, S. L. (2019). Does sensory retraining improve sensation and sensorimotor function following stroke: a systematic review and meta-analysis. *Front. Neurosci.* 13:402–402. doi: 10.3389/fnins.2019.00402

Serrien, D. J., and Spapé, M. M. (2009). The role of hand dominance and sensorimotor congruence in voluntary movement. *Exp. Brain Res.* 199, 195–200. doi: 10.1007/s00221-009-1998-8

Shao, S., Shen, K., Yu, K., Wilder-Smith, E. P., and Li, X. (2012). Frequency-domain EEG source analysis for acute tonic cold pain perception. *Clin. Neurophysiol.* 123, 2042–2049. doi: 10.1016/j.clinph.2012.02.084

Shingala, M. C., and Rajyaguru, A. (2015). Comparison of post hoc tests for unequal variance. *Int. J. New Technol. Sci. Eng.* 2, 22–33.

Singh, H., Bauer, M., Chowanski, W., Sui, Y., Atkinson, D., Baurley, S., et al. (2014). The brain's response to pleasant touch: an EEG investigation of tactile caressing. *Front. Human Neurosci.* 8:893. doi: 10.3389/fnhum.2014.00893

Slater, J. D. (2008). A definition of drowsiness: One purpose for sleep? *Med. Hypotheses* 71, 641–644. doi: 10.1016/j.mehy.2008.05.035

Society, A. C. N. (2015). *Guideline 11b: Recommended Standards For Intraoperative Monitoring Of Somatosensory Evoked Potentials. 2009. Retrieved from Acns. Org*. Hauppauge: Nova Science.

Steimann, L., Missala, I., Van Kaick, S., Walston, J., Malzahn, U., Heuschmann, P. U., et al. (2012). Rivermead assessment of somatosensory performance. *Der. Nervenarzt* 83, 1632–1637. doi: 10.1007/s00115-012-3614-6

Sudman, S., Bradburn, N., and Schwarz, N. (1997). Thinking about answers: the application of cognitive processes to survey methodology. *Psyccritiques* 42, 652–652. doi: 10.1023/A:1025127424627

Takeda, K., Shozawa, Y., Sonoo, M., Shimizu, T., and Kaminaga, T. (2000). The rostrocaudal gradient for somatosensory perception in the human postcentral gyrus. *J. Neurol. Neurosurg. Psychiatry* 69, 692–693. doi: 10.1136/jnnp.69.5.692

Tarkka, I. M., and Hallett, M. (1990). Cortical topography of premotor and motor potentials preceding self-paced, voluntary movement of dominant and non-dominant hands. *Electroencephalogr Clin Neurophysiol.* 75, 36–43. doi: 10.1016/0013-4694(90)90150-i

Tecchio, F., Babiloni, C., Zappasodi, F., Vecchio, F., Pizzella, V., Romani, G. L., et al. (2003). Gamma synchronization in human primary somatosensory cortex as revealed by somatosensory evoked neuromagnetic fields. *Brain Res.* 986, 63–70. doi: 10.1016/s0006-8993(03)03171-8

Tecchio, F., De Lucia, M., Salustri, C., Montuori, M., Bottaccio, M., Babiloni, C., et al. (2004). District-related frequency specificity in hand cortical representation: dynamics of regional activation and intra-regional synchronization. *Brain Res.* 1014, 80–86. doi: 10.1016/j.brainres.2004.04.028

Thibaut, A., Simis, M., Battistella, L. R., Fanciullacci, C., Bertolucci, F., Huerta-Gutierrez, R., et al. (2017). Using brain oscillations and corticospinal excitability to understand and predict post-stroke motor function. *Front. Neurol.* 8:187–187. doi: 10.3389/fneur.2017.00187

Thut, G., and Miniussi, C. (2009). New insights into rhythmic brain activity from TMS–EEG studies. *Trends Cogn. Sci.* 13, 182–189. doi: 10.1016/j.tics.2009.01.004

Tourangeau, R., Rips, L. J., and Rasinski, K. (2000). *The Psychology Of Survey Response*. Cambridge: Cambridge University Press.

Tseng, M. T., Tseng, W. Y., Chao, C. C., Lin, H. E., and Hsieh, S. T. (2010). Distinct and shared cerebral activations in processing innocuous versus noxious contact heat revealed by functional magnetic resonance imaging. *Hum. Brain Mapp.* 31, 743–757. doi: 10.1002/hbm.20902

Väisänen, O., and Malmivuo, J. (2009). Improving the SNR of EEG generated by deep sources with weighted multielectrode leads. *J. Physiol. Paris* 103, 306–314. doi: 10.1016/j.jphysparis.2009.07.003

Wang, A.-L., Mouraux, A., Liang, M., and Iannetti, G. D. (2010). Stimulus novelty, and not neural refractoriness, explains the repetition suppression of laser-evoked potentials. *J. Neurophysiol.* 104, 2116–2124. doi: 10.1152/jn.01088.2009

Woytowicz, E., Rietschel, J., Goodman, R., Conroy, S., Sorkin, J., Whitall, J., et al. (2016). Determining levels of upper extremity movement impairment by

applying cluster analysis to upper extremity fugl-meyer assessment in chronic stroke. *Arch. Phys. Med. Rehabil.* 98, 456–462. doi: 10.1016/j.apmr.2016.06.023

Wu, C. W., Seo, H. J., and Cohen, L. G. (2006). Influence of electric somatosensory stimulation on paretic-hand function in chronic stroke. *Arch .Phys. Med. Rehabil.* 87, 351–357. doi: 10.1016/j.apmr.2005.11.019

Yoon, H. S., Cha, Y. J., Sohn, M. K., and You, J. S. H. (2018). Effect of rehabilitation on the somatosensory evoked potentials and gait performance of hemiparetic stroke patients. *Technol. Health care* 26, 145–150. doi: 10.3233/THC-174432

Conflict of Interest: The authors declare that the research was conducted in the absence of any commercial or financial relationships that could be construed as a potential conflict of interest.

Publisher's Note: All claims expressed in this article are solely those of the authors and do not necessarily represent those of their affiliated organizations, or those of the publisher, the editors and the reviewers. Any product that may be evaluated in this article, or claim that may be made by its manufacturer, is not guaranteed or endorsed by the publisher.

frontiers | Frontiers in Aging Neuroscience

STUDY PROTOCOL
published: 02 June 2022
doi: 10.3389/fnagi.2022.909733

Cerebellar Continuous Theta Burst Stimulation for Aphasia Rehabilitation: Study Protocol for a Randomized Controlled Trial

Kai Zheng[1,2,3†], Mingyun Chen[1†], Ying Shen[4†], Xinlei Xu[2,3], Fanglan Gao[2,3], Guilan Huang[2,3], Yingying Ji[2,3], Bin Su[2,3], Da Song[2,3], Hui Fang[2,3], Peng Liu[1] and Caili Ren[2,3*]*

[1] Department of Rehabilitation Medicine, The First Affiliated Hospital, Sun Yat-sen University, Guangzhou, China, [2] Department of Neurorehabilitation, Wuxi Tongren Rehabilitation Hospital, Wuxi, China, [3] The Affiliated Wuxi Mental Health Center of Nanjing Medical University, Wuxi, China, [4] Rehabilitation Medicine Center, The First Affiliated Hospital of Nanjing Medical University, Nanjing, China

OPEN ACCESS

Edited by:
Wenxin Niu,
Tongji University, China

Reviewed by:
Jack Jiaqi Zhang,
The Hong Kong Polytechnic University, Hong Kong SAR, China
Isabel Catarina Duarte,
Coimbra Institute for Biomedical Imaging and Translational Research (CIBIT), Portugal

***Correspondence:**
Caili Ren
rencaili@njmu.edu.cn
Peng Liu
liupeng2@mail.sysu.edu.cn

† These authors have contributed equally to this work

Specialty section:
This article was submitted to Neurocognitive Aging and Behavior, a section of the journal Frontiers in Aging Neuroscience

Received: *31 March 2022*
Accepted: *03 May 2022*
Published: *02 June 2022*

Citation:
Zheng K, Chen M, Shen Y, Xu X, Gao F, Huang G, Ji Y, Su B, Song D, Fang H, Liu P and Ren C (2022) Cerebellar Continuous Theta Burst Stimulation for Aphasia Rehabilitation: Study Protocol for a Randomized Controlled Trial. Front. Aging Neurosci. 14:909733. doi: 10.3389/fnagi.2022.909733

Background: Language recovery is limited in moderate to severe post-stroke aphasia patients. Repetitive transcranial magnetic stimulation (rTMS) has emerged as a promising tool in improving language dysfunctions caused by post-stroke aphasia, but the treatment outcome is as yet mixed. Considerable evidence has demonstrated the essential involvement of the cerebellum in a variety of language functions, suggesting that it may be a potential stimulation target of TMS for the treatment of post-stroke aphasia. Theta burst stimulation (TBS) is a specific pattern of rTMS with shorter stimulation times and better therapeutic effects. The effect of continuous TBS (cTBS) on the cerebellum in patients with aphasia with chronic stroke needs further exploration.

Methods: In this randomized, sham-controlled clinical trial, patients (n = 40) with chronic post-stroke aphasia received 10 sessions of real cTBS (n = 20) or sham cTBS (n = 20) over the right cerebellar Crus I+ a 30-min speech-language therapy. The Western Aphasia Battery (WAB) serves as the primary measure of the treatment outcome. The secondary outcome measures include the Boston Diagnostic Aphasia Examination, Boston Naming Test and speech acoustic parameters. Resting-state fMRI data were also obtained to examine treatment-induced changes in functional connectivity of the cerebro-cerebellar network. These outcome measures are assessed before, immediately after, and 12 weeks after cerebellar cTBS intervention.

Discussion: This protocol holds promise that cerebellar cTBS is a potential strategy to improve language functions in chronic post-stroke aphasia. The resting-state fMRI may explore the neural mechanism underlying the aphasia rehabilitation with cerebellar cTBS.

Keywords: study protocol, aphasia, continuous theta burst stimulation, cerebellum, randomized controlled trial (RCT)

INTRODUCTION

Aphasia is an acquired language disorder caused by ischemic or hemorrhagic stroke (Engelter et al., 2006), characterized by impairments in verbal fluency, language comprehension, word repetition, and picture naming as well as reading/writing skills. Approximately, one-third of post-stroke patients develops aphasia (Engelter et al., 2006), which persists in approximate 20% of long-term stroke survivors (Berthier, 2005). Patients with post-stroke aphasia suffer from decreased quality of life, limited independence, and substantial long-term disability (Cruice et al., 2011; Ellis et al., 2012). To date, speech-language therapy (SLT) is considered as the standard protocol for the treatment of post-stroke aphasia and produce beneficial effects on language functions, but the effect size is somewhat small that results in modest improvements (Brady et al., 2012). Therefore, it is important to develop other therapeutic approaches to improve the effectiveness of SLT for aphasia treatment.

In recent years, repetitive transcranial magnetic stimulation (rTMS) has emerged as a promising non-invasive neuromodulation method to augment the treatment of post-stroke non-fluent aphasia (Hartwigsen and Saur, 2017; Fisicaro et al., 2019; Ren et al., 2019). Generally, low-frequency rTMS ($\leq$1 Hz) is considered to decrease cortical excitability, while high-frequency rTMS ($\geq$5 Hz) produces the opposite effect (Chen and Seitz, 2001). The majority of recent studies have shown naming improvements in post-stroke non-fluent aphasia by delivering inhibitory low-frequency rTMS over the intact right inferior frontal gyrus (IFG) (the right hemisphere homolog of Broca's area) (Hara et al., 2015; Harvey et al., 2017; Ren et al., 2019; Kim et al., 2020). Similar beneficial effects on post-stroke aphasia were also observed when excitatory high-frequency rTMS was applied over the left perilesional cortex (Broca's area) or right intact IFG (Hara et al., 2017; Hu et al., 2018). Alternatively, applying rTMS over other cortical regions is also beneficial for post-stroke aphasia, as evidenced by improvement in speech perception and auditory comprehension following low-frequency rTMS over the right posterior superior temporal gyrus (pSTG) (Kawamura et al., 2019; Ren et al., 2019). Nevertheless, it is noteworthy that the evidence for beneficial effects of rTMS on post-stroke aphasia is not unequivocal (Breining and Sebastian, 2020). Some studies reported null results when low-frequency rTMS was applied over the right hemisphere, showing that rTMS did not add to the effect of SLT on post-stroke aphasia (Santos et al., 2017; Heikkinen et al., 2018). Among many possible resources of the inconsistencies across the studies investigating the efficacy of rTMS for post-stroke aphasia are type of stimulation modality (inhibitory or excitatory), laterality of brain hemisphere (left or right), and choice of stimulation target (Broca's area, STG, etc.) (Breining and Sebastian, 2020). Particularly, the optimal protocol of rTMS over the right hemisphere remains controversial for aphasia rehabilitation (Anglade et al., 2014), which is due to the limited knowledge about the causal links between cortical brain regions and language functions. Accordingly, developing a novel stimulation protocol with other potential targets that are significantly involved in language processing is important for improving effectiveness of TMS in augmenting the treatment of post-stroke aphasia.

The present study protocol proposes a research protocol that stimulates the right cerebellum with TMS to augment SLT for patients with post-stroke aphasia. Multiple lines of evidence have demonstrated significant contributions of the right cerebellum to a variety of language functions, including word retrieval and generation, verbal working memory, language learning, and semantic processing (Gordon, 1996; Desmond and Fiez, 1998; Murdoch, 2010; Stoodley, 2012; Mariën and Borgatti, 2018). Clinical evidence has shown deficits in a variety of language tasks as a result of damage to the right cerebellum (Marien et al., 1996, 2001; Silveri et al., 1998). Moreover, a growing body of empirical and clinical studies using transcranial direct current stimulation (tDCS) has established a causal link between the right cerebellum and language functions. For example, applying tDCS over the right cerebellum in healthy individuals exerts modulatory effects on various speech/language tasks, such as verbal generation (Pope and Miall, 2012), verbal fluency (Turkeltaub et al., 2016), semantic prediction (D'Mello et al., 2017), and speech motor learning (Lametti et al., 2018). Clinically, several recent studies showed augmentation of SLT in post-stroke aphasia with tDCS over the right cerebellum (Sebastian et al., 2016, 2020; Marangolo et al., 2018). For example, one randomized, double-blind, sham-controlled study found significant improvement in verbal generation in patients with post-stroke aphasia following 4-week cathodal tDCS over the right cerebellum coupled with SLT (Marangolo et al., 2018). In another randomized, double-blind, sham-controlled study (Sebastian et al., 2020), both cathodal and anodal tDCS over the right cerebellum led to improved picture naming in chronic post-stroke aphasia, while greater gains were noted for patients receiving cathodal cerebellar tDCS. Taken together, these studies provide evidence suggesting that the cerebellum may be an optimal site of neuromodulation for the treatment of post-stroke aphasia.

On the other hand, continuous theta burst stimulation (cTBS) is applied over the right cerebellum in the present study protocol. As a specific form of rTMS, cTBS produces an inhibitory effect on cortical excitability for up to 60 min after less than 1-min of stimulation (Huang et al., 2005). In addition to modulating cerebellar activity (Koch, 2010), cTBS over the right cerebellum exerts modulatory effects on speech/language production (Arasanz et al., 2012; Sheu et al., 2019). Cerebellar TBS is safe and tolerable and has reported no serious adverse effects (Hurtado-Puerto et al., 2020). The previous studies have shown that the cerebellar cTBS modulates motor cortical excitability and improves motor symptoms (e.g., gait ataxia and dyskinesia) in a variety of neurodegenerative diseases, such as Parkinson's disease (PD) and spinocerebellar ataxia (SCA) (Koch et al., 2009, 2014; Benussi et al., 2020; Maas et al., 2020). Moreover, one recent study on patients with SCA showed that single-session c-TBS over the right cerebellum produces facilitatory effects on their abnormalities in auditory-motor integration for vocal pitch regulation (Lin et al., 2022). Therefore, it is plausible to assume that stimulating the right cerebellum with inhibitory cTBS coupled with SLT leads to beneficial effects on chronic post-stroke aphasia, which is yet to be answered.

To this end, the purpose of the present study is to investigate the short- and long-term effectiveness of cTBS over the right cerebellum in augmenting language recovery in chronic post-stroke aphasia in a randomized, sham-controlled design. In addition to aphasia test batteries and speech acoustic analyses for evaluation of treatment outcome, the resting-state functional magnetic resonance (RS-fMRI) is also used to explore the neural mechanisms underlying aphasia rehabilitation. The previous studies have shown associations between improved spelling or phonemic fluency and increased resting-state functional connectivity between the cerebellum and language-related cortical regions for patients with chronic post-stroke aphasia or healthy individuals following tDCS over the right cerebellum (Sebastian et al., 2016; Turkeltaub et al., 2016). Accordingly, we hypothesize that, following cTBS over the right cerebellum, patients with chronic post-stroke aphasia will exhibit improved language functions and increased functional connectivity within the cerebro-cerebellar language network. This randomized, sham-controlled study provides significant new insights into the therapeutic efficacy of cTBS over the right cerebellum to augment SLT for post-stroke aphasia and the underlying neuroplastic mechanisms.

METHODS

Study Design

This is a prospective, randomized, sham-controlled, single-center study (Registration number: ChiCTR210049828) that will be conducted in the Department of Neurorehabilitation, Wuxi Tongren Rehabilitation Hospital, China. Hospitalized patients with chronic post-stroke aphasia are recruited to participate in the study. They are randomly assigned with a ratio of 1:1 to a real or sham stimulation group. Details about the study design and data collection are shown in **Figure 1** and **Table 1**. On the day of enrollment (T0), after the end of cerebellar cTBS intervention (T1), and 12 weeks post-treatment completion (T2), aphasia test batteries and speech acoustic analyses are performed to evaluate language functions in post-stroke aphasia. Also, RS-fMRI data are collected before and after the end of the intervention. This study has been approved by the Ethics Committee of Wuxi Mental Health Center and Wuxi Tongren Rehabilitation Hospital (WXMHCIRB2021LLky078).

Participants

The inclusion and exclusion criteria of the present study correspond to the guidelines for using rTMS in clinics and research (Wassermann, 1998; Rossi et al., 2009; Rossini et al., 2015). Participant inclusion criteria are: (1) patients aged 40–80 years; (2) first-ever unilateral ischemic stroke on the left hemisphere; (3) longer than 6 months post-stroke; (4) non-fluent aphasia as confirmed by the Western Aphasia Battery (WAB); (5) right-handed, native-Chinese speakers without experience of professional vocal or instrumental training; (6) Boston Diagnostic Aphasia Examination (BDAE) Grades I–III; and (7) elementary education level and above, with normal or corrected to normal vision. Participant exclusion criteria are: (1) history of substance or alcohol abuse, premorbid seizures, or neuropsychiatric diseases; (2) contraindications involving TMS and fMRI (e.g., skull defect or skin damage at the stimulation site, intracranial implant, cardiac pacemaker, and implanted drug pumps); (3) history of neurosurgical treatment; (4) unable to cooperate with assessment and treatment due to severe cognitive impairment; and (5) other neurological disease. All participants provide written informed consent prior to participating in the study.

Sample Size

The sample size was calculated using PASS software (v.15.0) on the basis of previous studies. With an effect size of 0.5 based on the WAB-AQ (Hu et al., 2018), we expect that the target effect size had 80% of power with a type I error of 5% ($\alpha = 0.05$). Thus, the sample size of each group is at least 16. With an assumption of 20% dropout rate, a sample size of 20 participants will be targeted for each group.

Randomization and Blinding

Once the inclusion criteria are satisfied, the participant is allocated to one real or sham cTBS group using the network-based random sequence generator to receive real or sham cTBS over the right cerebellum coupled with SLT. Based on the previous studies, patients will receive a 10-day cerebellar cTBS within 2 weeks (Thiel et al., 2013; Wang et al., 2014; Hara and Abo, 2021). The concealment of allocation is performed using sealed envelopes with numbers. The participants and physicians performing the SLT or the data collection/processing are blinded to the grouping. Note that physicians conducting the cTBS intervention cannot be blinded due to the nature of the cTBS intervention and are thus not involved in the research process. The designer and the staff responsible for allocation concealment will not participate in the whole intervention.

Interventions

The application of cerebellar cTBS is administered using Magneuro 100 (Vishee Medical Technology Co., Ltd., Nanjing, China) equipped with a figure 8-shaped coil (7 cm out diameter). Before intervention, a single-pulse TMS will be applied over the right primary motor cortex to determine active motor threshold (AMT). The AMT is defined as the lowest stimulus intensity that produces a motor evoked potential (MEP) of $>200\ \mu V$ in at least 5–10 consecutive trials with 10% maximal voluntary contraction of the first dorsal interosseous muscle of the non-paretic hand (Koch et al., 2020). Each participant receives real or sham cTBS over the Crus I of the right lateral cerebellum (3 cm right and 1 cm inferior to the inion) at 80% of AMT (Lin et al., 2022). A standard cTBS protocol consists of bursts of 3 pulses at 50 Hz that are repeatedly presented at 5 Hz, resulting in a total of 600 pulses in 40 s. The coil is oriented vertically to the target with the handle pointing superiorly during real stimulation; while the stimulation face of the coil is turned 90°, so that the side of the coil is placed on the target during sham stimulation (Rastogi et al., 2017). Immediately following real or sham cerebellar cTBS, all participants receive a 30-min SLT that includes training on comprehension, expression of spoken language, semantic, and

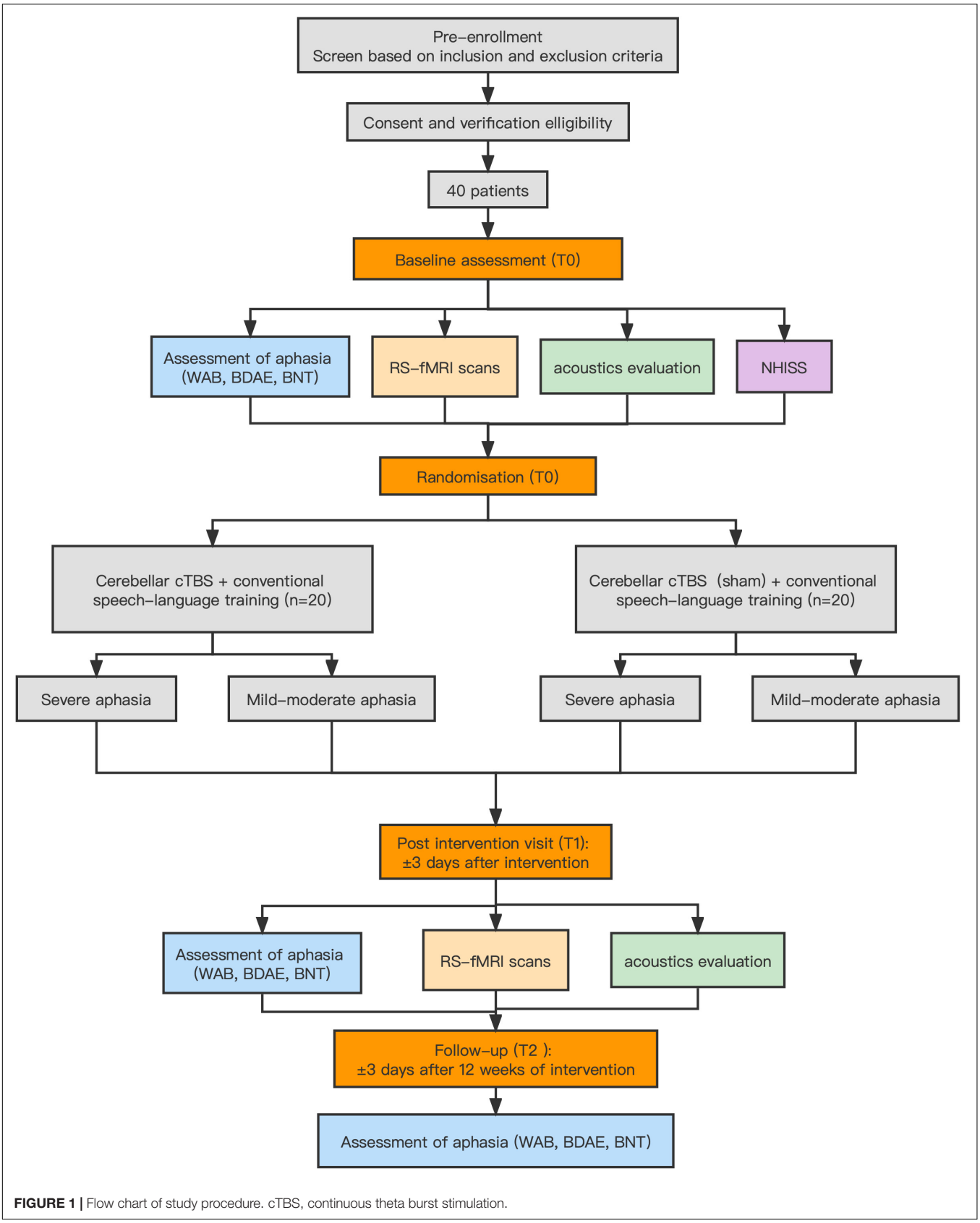

FIGURE 1 | Flow chart of study procedure. cTBS, continuous theta burst stimulation.

TABLE 1 | Overview of data collection and study timings.

Study period visits	Pre-enrollment	T0	T1	T2
Relative start of treatment days	−1 week	Day 0	±3 days after intervention	±3 days after 12 weeks of intervention
Screening (in-/exclusion criteria)	×			
Written informed consent	×			
Medical history	×			
Randomization		×		
NIHSS		×		
WAB		×	×	×
BDAE		×	×	×
BNT		×	×	×
Acoustic evaluation		×	×	×
RS-fMRI		×	×	

phonological processing. The content of SLT will be modified based evaluation of language function on an individual level. Totally, each participant receives 10 sessions of cerebellar cTBS coupled with SLT (5 sessions per week) within 2 weeks.

Outcome Measures

The primary outcome measure is the WAB assessment that is divided into four subitems including spontaneous speech, auditory verbal comprehension, repetition, and naming. The original scores of the four items are 20, 200, 100, and 100, respectively. An aphasia quotient (AQ) is calculated using the following formula: AQ = (spontaneous speech + auditory verbal comprehension/20 + repetition/10 + naming/10) × 2. The AQ indicates the severity of aphasia and can be used as an index for evaluating the improvement and deterioration of aphasia. The highest AQ score is 100, and the normal range is 98.4–99.6. AQ <93.8 is considered as aphasia.

In addition to the WAB scores, there are several secondary measures of treatment outcome including BDAE, Boston Naming Test (BNT), speech acoustic parameters, and RS-fMRI. BDAE is used to measure the severity of impaired language function that can be divided into five grades from severe to mild. The BNT is an assessment tool to measure the confrontational word naming of 30 object pictures. The speech acoustic parameters include fundamental frequency, intensity, speaking rate, maximum phonation time, range of voice features, and speech intelligibility. Speech signals are recorded using a laptop at sampling frequency 44.1 K Hz and Praat software is used to extract acoustic parameters.

RS-fMRI data are acquired using a 3.0 T MAGNETOM Skyra scanner (Siemens, Germany). The participants are instructed to lie still with their eyes closed and think of nothing. Functional images are obtained using echo-planar imaging (EPI) pulse sequence with the following parameters: repetition time (TR) = 2,000 ms; echo time (TE) = 30 ms; 35 slices, field of view (FOV) = 224 mm × 224 mm; slice thickness = 3.5 mm; layer spacing 0.7 mm; flip angle (FA) = 90°; acquisition matrix 64 × 64; voxel size = 3.5 mm × 3.5 mm × 3.5 mm. For registration purposes, a set of high-resolution structural images are acquired through a T1-weighted sequence: 192 sagittal slices; slice thickness = 1 mm; TR = 6.6 ms; TE = 3.1 ms; FA = 12°; FOV = 256 mm × 256 mm. The scanning lasted for 8 min and produced 240 brain volumes.

Data Analysis

Repeated-measures analysis of variances (RM-ANOVAs) are performed to examine differences in the WAB, BDAE, and BNT scores as well as speech parameters across the conditions, with a within-subject factor of phase (pre- vs. post-treatment) and a between-subject factor of group (real vs. sham cTBS). In the *post hoc* analysis, multiple comparisons are corrected with Bonferroni adjustment. Prior to entering the data into the RM-ANOVAs, Kolmogorov–Smirnov test is used to verify whether they are normally distributed. For non-normally distributed measures, the Wilcoxon Signed Rank Test is used for comparison across the conditions. The intention-to-treat (ITT) analysis is used when there are missing data.

The preprocessing of RS-fMRI data is conducted using DPABI software (v. 6.1) on the MATLAB platform (Mathworks, Natick, MA, United States) (Yan et al., 2016). The main steps are as follows: (1) use MRIConvert software (v. 2.1.0, Lewis Center, Eugene, OR, United States) to convert raw data in DICOM format to NIFI format; (2) remove the first 10 slices and correct the remaining 230 slices for slice timing; (3) correct head motion exceeding 3 mm in any direction or head rotation exceeding 3°; (4) spatially normalize the functional images to a standard Montreal Neurological Institute (MNI) space and resample them to a voxel size of 3 mm × 3 mm × 3 mm; (5) apply a band-pass filter (0.01–0.08) for each voxel to reduce the influence of low frequency fluctuation and high-frequency noise (Lv et al., 2018); and (6) smooth the functional data with a 6-mm full width at half maximum (FWHM) Gaussian kernel.

After the preprocessing, regional homogeneity (ReHo), degree centrality (DC), and seed-to-voxel analyses are conducted to measure the local and global functional connectivity within the language networks. ReHo is calculated based on the Kendall's coefficient of concordance (KCC), which measures the consistency of the time signal between a voxel and surrounding voxels. Higher ReHo values represent better consistency between the local voxel and the regional brain activities. DC values reflect the network connection intensity between a certain voxel and all of the brain, indicating the importance of this voxel as

the network node (Zang et al., 2004). One-way ANOVAs are conducted on the ReHo and DC values to explore differences across the conditions within the predefined gray matter mask. The ANOVA F maps are corrected using Gaussian random field (GRF) correction (single voxel $p < 0.001$, cluster level $p < 0.05$). The ReHo and DC values of the peak voxels in the surviving clusters are extracted and entered into SPSS (v. 22) for further analysis. Seed-to-voxel analyses are conducted with *a priori* regions of interest (ROI). The ROIs consist of language-related regions in cerebellar Crus I; IFG pars opercularis; IFG pars triangularis; primary motor cortex (M1); anterior and posterior STG; angular gyrus; anterior and posterior supramarginal gyrus (SMG), which are selected from the AAL atlas (Tzourio-Mazoyer et al., 2002). These ROI-based functional connectivity maps are statistically compared between pre- and post-treatment and between real cTBS and sham stimulation group. Differences across the conditions are considered significant when $p < 0.05$ at the voxel level, with a false discovery rate (FDR) cluster corrected $p < 0.05$.

Safety

Adverse effects are defined as any negative experiences that occur to the patients who underwent the cerebellar cTBS or MRI scanning. All adverse effects will be reported by the investigator during the treatment and within 1 week after the end of treatment. Particularly, seizures that are the most severe TMS-related adverse effects with a risk of approximately 0.02%, are only expected to occur during or immediately after cerebellar cTBS. In addition, adverse effects that occur during the MRI scanning will be reported within 24 h. Earplugs will be provided to patients to protect their hearing against noise. Any serious incident will be immediately reported to the Medical Research Ethics Committee of Wuxi Tongren Rehabilitation Hospital.

DISCUSSION

This randomized, sham-controlled clinical trial investigates the neural and behavioral effects of cTBS over the right cerebellum on chronic post-stroke aphasia. We hypothesize that stimulating the right cerebellum with inhibitory cTBS can produce beneficial effects in augmenting SLT for language recovery in post-stroke aphasia by regulating functional connectivity between the right cerebellum and the cerebral cortical regions involved in language processing. These results can provide supportive evidence that the right cerebellum may be a potential optimal stimulation target for the treatment of chronic post-stroke aphasia.

Variability in lesion location and size in brain reorganization for post-stroke aphasia complicate efforts to determine the optimal stimulation strategy at the cortical level (Breining and Sebastian, 2020). Right cerebellar stimulation, in contrast, can potentially serve as a single target site that can be used across patients with post-stroke aphasia with varying site and size of lesion in the left hemisphere (Turkeltaub et al., 2016). The present study proposes a new stimulation protocol for language recovery in chronic post-stroke aphasia by applying inhibitory cTBS over the right cerebellum, since this region has been demonstrated to be essentially involved in a variety of language functions (Gordon, 1996; Desmond and Fiez, 1998; Murdoch, 2010; Stoodley, 2012; Mariën and Borgatti, 2018) and damage to this region leads to impaired language performance (Marien et al., 1996, 2001; Silveri et al., 1998). More importantly, several clinical studies reported improvement in verbal generation or naming functions in the patients with chronic post-stroke aphasia following anodal or cathodal tDCS over the right cerebellum (Sebastian et al., 2016, 2020; Marangolo et al., 2018), providing further evidence in support of the right cerebellum as an optimal stimulation site for neuromodulation in aphasia. On the other hand, Sebastian et al. (2020) found greater beneficial effects on naming functions (relative to sham) when chronic post-stroke patients received cathodal tDCS over the right cerebellum than when they received anodal cerebellar tDCS. And applying inhibitory cTBS over the right cerebellum led to facilitatory effects on impaired vocal motor control in patients with SCA (Lin et al., 2022). As compared to rTMS, cTBS induces robust, long-lasting changes in activation in much shorter periods. Therefore, cTBS over the right cerebellum proposed in the present study protocol may be a promising technique to augment SLT for language recovery in chronic post-stroke aphasia.

The present study protocol also investigates the neural effects of cTBS over the right cerebellum on chronic post-stroke aphasia with RS-fMRI. The majority of previous studies reported behavioral performance assessed by aphasia test batteries following stimulation with rTMS or tDCS (Sebastian et al., 2020), but little is known about the underlying neural mechanisms (Sebastian et al., 2016). In a case report study that combined tDCS and RS-fMRI, Sebastian et al. (2016) found that improvement in spelling induced by anodal tDCS over the right cerebellum was accompanied by increased functional connectivity of the cerebro-cerebellar network. In another study on healthy individuals (Turkeltaub et al., 2016), in addition to improved phonemic fluency, increased resting-state functional connectivity between the cerebellum and speech-motor areas and within the left-lateralized network involved in cognitive aspects of language and motor aspect of speech production were found following tDCS over the right posterolateral cerebellum. Moreover, cerebellar cTBS can modulate activity in the neural pathway that reciprocally links the cerebellum and prefrontal and parietal regions involved in language production (O'Reilly et al., 2010; Stoodley, 2012) by altering short- and long-intracortical inhibition (Koch et al., 2008). Therefore, it is possible that c-TBS over the right cerebellum is effective in an augmenting chronic post-stroke aphasia by altering functional connectivity of the cerebro-cerebellar network.

The present study applies a figure-of-8 coil to the cerebellum. This coil has been shown to be a flat coil model with increased trial tolerances (Hardwick et al., 2014) that can stimulate the superficial layers of the cerebellar cortex (Li et al., 2019). The reported average depth of the lateral cerebellar gray matter is approximately 14.6–14.7 mm from the scalp surface, which is within a range of ∼30 mm at 100% peak output of the figure-of-8 coil (Hardwick et al., 2014). Several studies have successfully

applied rTMS or TBS over the cerebellum with a figure-of-8 coil to change motor or speech performance (Theoret et al., 2001; Koch et al., 2008; Popa et al., 2010; Demirtas-Tatlidede et al., 2011; Lin et al., 2022). On the other hand, the present study protocol performs acoustic signal analysis to extract speech parameters for the evaluation of language function with the WAB, BDAE, and BNT scores. The previous research has shown impaired abilities of speech production and motor control in patients with non-fluent aphasia (e.g., Broca's aphasia) (Hillis, 2007; Behroozmand et al., 2018). Therefore, performing speech acoustic analysis has the potential to comprehensively elucidate the mechanisms underlying the treatment of post-stroke aphasia with cTBS over the right cerebellum coupled with SLT.

CONCLUSION

In conclusion, the present study protocol proposes a randomized, sham-controlled clinical trial to investigate the efficacy of cTBS over the right cerebellum in augmenting language recovery in chronic post-stroke aphasia and the neural mechanisms underlying the treatment outcome. If this intervention study produces a significant positive effect as expected, the findings will provide valuable evidence for establishing a novel and feasible stimulation protocol to promote language recovery from chronic post-stroke aphasia.

ETHICS STATEMENT

The studies involving human participants were reviewed and approved by the Medical Research Ethics Committee of Wuxi Mental Health Center (Wuxi Tongren Rehabilitation Hospital). The patients/participants provided their written informed consent to participate in this study.

AUTHOR CONTRIBUTIONS

CR and PL designed the study. CR, MC, YS, PL, and KZ drafted the protocol. MC coordinated the trial. FG, HF, YJ, and DS performed data acquisition and clinical evaluation. GH and BS conducted the interventions. CR, YS, and MC revised the manuscript. All authors read and approved the final manuscript.

FUNDING

This work was supported by the National Natural Science Foundation of China (No. 81772439), Natural Science Foundation of Jiangsu Province (No. BK20201138), Wuxi Taihu Talent Project (No. WXTTP2020008), and Top Talent Support Program for Young and Middle-Aged People of Wuxi Health Committee and General Project from Wuxi Health Commission (No. MS201911).

SUPPLEMENTARY MATERIAL

The Supplementary Material for this article can be found online at: https://www.frontiersin.org/articles/10.3389/fnagi.2022.909733/full#supplementary-material

REFERENCES

Anglade, C., Thiel, A., and Ansaldo, A. I. (2014). The complementary role of the cerebral hemispheres in recovery from aphasia after stroke: a critical review of literature. *Brain Inj.* 28, 138–145. doi: 10.3109/02699052.2013.859734

Arasanz, C. P., Staines, W. R., and Schweizer, T. A. (2012). Isolating a cerebellar contribution to rapid visual attention using transcranial magnetic stimulation. *Front. Behav. Neurosci.* 6:55. doi: 10.3389/fnbeh.2012.00055

Behroozmand, R., Phillip, L., Johari, K., Bonilha, L., Rorden, C., Hickok, G., et al. (2018). Sensorimotor impairment of speech auditory feedback processing in aphasia. *Neuroimage* 165, 102–111. doi: 10.1016/j.neuroimage.2017.10.014

Benussi, A., Pascual-Leone, A., and Borroni, B. (2020). Non-invasive cerebellar stimulation in neurodegenerative ataxia: a literature review. *Int. J. Mol. Sci.* 21:1948. doi: 10.3390/ijms21061948

Berthier, M. L. (2005). Poststroke aphasia : epidemiology, pathophysiology and treatment. *Drugs Aging* 22, 163–182. doi: 10.2165/00002512-200522020-00006

Brady, M. C., Kelly, H., Godwin, J., and Enderby, P. (2012). Speech and language therapy for aphasia following stroke. *Cochrane Database Syst. Rev.* 2016:Cd000425.

Breining, B. L., and Sebastian, R. (2020). Neuromodulation in post-stroke aphasia treatment. *Curr. Phys. Med. Rehabil. Rep.* 8, 44–56. doi: 10.1007/s40141-020-00257-5

Chen, R., and Seitz, R. J. (2001). Changing cortical excitability with low-frequency magnetic stimulation. *Neurology* 57, 379–380.

Cruice, M., Worrall, L., and Hickson, L. (2011). Reporting on psychological well-being of older adults with chronic aphasia in the context of unaffected peers. *Disabil. Rehabil.* 33, 219–228. doi: 10.3109/09638288.2010.503835

Demirtas-Tatlidede, A., Freitas, C., Pascual-Leone, A., and Schmahmann, J. D. (2011). Modulatory effects of theta burst stimulation on cerebellar nonsomatic functions. *Cerebellum* 10, 495–503. doi: 10.1007/s12311-010-0230-5

Desmond, J. E., and Fiez, J. A. (1998). Neuroimaging studies of the cerebellum: language, learning and memory. *Trends Cogn. Sci.* 2, 355–362. doi: 10.1016/s1364-6613(98)01211-x

D'Mello, A. M., Turkeltaub, P. E., and Stoodley, C. J. (2017). Cerebellar tDCS modulates neural circuits during semantic prediction: a combined tDCS-fMRI study. *J. Neurosci.* 37, 1604–1613. doi: 10.1523/JNEUROSCI.2818-16.2017

Ellis, C., Simpson, A. N., Bonilha, H., Mauldin, P. D., and Simpson, K. N. (2012). The one-year attributable cost of poststroke aphasia. *Stroke* 43, 1429–1431. doi: 10.1161/STROKEAHA.111.647339

Engelter, S. T., Gostynski, M., Papa, S., Frei, M., Born, C., Ajdacic-Gross, V., et al. (2006). Epidemiology of aphasia attributable to first ischemic stroke: incidence, severity, fluency, etiology, and thrombolysis. *Stroke* 37, 1379–1384.

Fisicaro, F., Lanza, G., Grasso, A. A., Pennisi, G., and Pennisi, M. (2019). Repetitive transcranial magnetic stimulation in stroke rehabilitation: review of the current evidence and pitfalls. *Ther. Adv. Neurol. Disord.* 12:175628641987831. doi: 10.1177/1756286419878317

Gordon, N. (1996). Speech, language, and the cerebellum. *Eur. J. Disord. Commun.* 31, 359–367.

Hara, T., and Abo, M. (2021). New treatment strategy using repetitive transcranial magnetic stimulation for post-stroke aphasia. *Diagnostics* 11:1853. doi: 10.3390/diagnostics11101853

Hara, T., Abo, M., Kakita, K., Mori, Y., Yoshida, M., and Sasaki, N. (2017). The effect of selective transcranial magnetic stimulation with functional near-infrared spectroscopy and intensive speech therapy on individuals with post-stroke aphasia. *Eur. Neurol.* 77, 186–194. doi: 10.1159/000457901

Hara, T., Abo, M., Kobayashi, K., Watanabe, M., Kakuda, W., and Senoo, A. (2015). Effects of low-frequency repetitive transcranial magnetic stimulation combined with intensive speech therapy on cerebral blood flow in post-stroke aphasia. *Transl. Stroke Res.* 6, 365–374. doi: 10.1007/s12975-015-0417-7

Hardwick, R. M., Lesage, E., and Miall, R. C. (2014). Cerebellar transcranial magnetic stimulation: the role of coil geometry and tissue depth. *Brain Stimul.* 7, 643–649. doi: 10.1016/j.brs.2014.04.009

Hartwigsen, G., and Saur, D. (2017). Neuroimaging of stroke recovery from aphasia – Insights into plasticity of the human language network. *Neuroimage* 190, 14–31. doi: 10.1016/j.neuroimage.2017.11.056

Harvey, D. Y., Podell, J., Turkeltaub, P. E., Faseyitan, O., Coslett, H. B., and Hamilton, R. H. (2017). Functional reorganization of right prefrontal cortex underlies sustained naming improvements in chronic aphasia via repetitive transcranial magnetic stimulation. *Cogn. Behav. Neurol.* 30, 133–144. doi: 10.1097/WNN.0000000000000141

Heikkinen, P. H., Pulvermuller, F., Makela, J. P., Ilmoniemi, R. J., Lioumis, P., Kujala, T., et al. (2018). Combining rTMS with intensive language-action therapy in chronic aphasia: a randomized controlled trial. *Front. Neurosci.* 12:1036. doi: 10.3389/fnins.2018.01036

Hillis, A. E. (2007). Aphasia: progress in the last quarter of a century. *Neurology* 69, 200–213. doi: 10.1212/01.wnl.0000265600.69385.6f

Hu, X. Y., Zhang, T., Rajah, G. B., Stone, C., Liu, L. X., He, J. J., et al. (2018). Effects of different frequencies of repetitive transcranial magnetic stimulation in stroke patients with non-fluent aphasia: a randomized, sham-controlled study. *Neurol. Res.* 40, 459–465. doi: 10.1080/01616412.2018.1453980

Huang, Y. Z., Edwards, M. J., Rounis, E., Bhatia, K. P., and Rothwell, J. C. (2005). Theta burst stimulation of the human motor cortex. *Neuron* 45, 201–206.

Hurtado-Puerto, A. M., Nestor, K., Eldaief, M., and Camprodon, J. A. (2020). Safety considerations for cerebellar theta burst stimulation. *Clin. Ther.* 42, 1169–1190.e1. doi: 10.1016/j.clinthera.2020.06.001

Kawamura, M., Takahashi, N., and Kobayashi, Y. (2019). Effect of repetitive transcranial magnetic stimulation on the right superior temporal gyrus for severe aphasia caused by damage to the left inferior frontal gyrus. *Case Rep. Neurol.* 11, 189–198. doi: 10.1159/000500669

Kim, W. J., Rosselin, C., Amatya, B., Hafezi, P., and Khan, F. (2020). Repetitive transcranial magnetic stimulation for management of post-stroke impairments: an overview of systematic reviews. *J. Rehabil. Med.* 52:jrm00015. doi: 10.2340/16501977-2637

Koch, G. (2010). Repetitive transcranial magnetic stimulation: a tool for human cerebellar plasticity. *Funct. Neurol.* 25, 159–163.

Koch, G., Brusa, L., Carrillo, F., Lo Gerfo, E., Torriero, S., Oliveri, M., et al. (2009). Cerebellar magnetic stimulation decreases levodopa-induced dyskinesias in Parkinson disease. *Neurology* 73, 113–119. doi: 10.1212/WNL.0b013e3181ad5387

Koch, G., Esposito, R., Motta, C., Casula, E. P., Di Lorenzo, F., Bonni, S., et al. (2020). Improving visuo-motor learning with cerebellar theta burst stimulation: behavioral and neurophysiological evidence. *Neuroimage* 208:116424. doi: 10.1016/j.neuroimage.2019.116424

Koch, G., Mori, F., Marconi, B., Codeca, C., Pecchioli, C., Salerno, S., et al. (2008). Changes in intracortical circuits of the human motor cortex following theta burst stimulation of the lateral cerebellum. *Clin. Neurophysiol.* 119, 2559–2569. doi: 10.1016/j.clinph.2008.08.008

Koch, G., Porcacchia, P., Ponzo, V., Carrillo, F., Cáceres-Redondo, M. T., Brusa, L., et al. (2014). Effects of two weeks of cerebellar theta burst stimulation in cervical dystonia patients. *Brain Stimul.* 7, 564–572. doi: 10.1016/j.brs.2014.05.002

Lametti, D. R., Smith, H. J., Freidin, P. F., and Watkins, K. E. (2018). Cortico-cerebellar networks drive sensorimotor learning in speech. *J. Cogn. Neurosci.* 30, 540–551. doi: 10.1162/jocn_a_01216

Li, W., Zhuang, J., Guo, Z., Jones, J. A., Xu, Z., and Liu, H. (2019). Cerebellar contribution to auditory feedback control of speech production: evidence from patients with spinocerebellar ataxia. *Hum. Brain Mapp.* 40, 4748–4758. doi: 10.1002/hbm.24734

Lin, Q., Chang, Y., Liu, P., Jones, J. A., Chen, X., Peng, D., et al. (2022). Cerebellar continuous theta burst stimulation facilitates auditory-vocal integration in spinocerebellar ataxia. *Cereb. Cortex* 32, 455–466. doi: 10.1093/cercor/bhab222

Lv, H., Wang, Z., Tong, E., Williams, L. M., Zaharchuk, G., Zeineh, M., et al. (2018). Resting-state functional MRI: everything that nonexperts have always wanted to know. *AJNR Am. J. Neuroradiol.* 39, 1390–1399. doi: 10.3174/ajnr.A5527

Maas, R., Helmich, R. C. G., and van de Warrenburg, B. P. C. (2020). The role of the cerebellum in degenerative ataxias and essential tremor: insights from noninvasive modulation of cerebellar activity. *Mov. Disord.* 35, 215–227. doi: 10.1002/mds.27919

Marangolo, P., Fiori, V., Caltagirone, C., Pisano, F., and Priori, A. (2018). Transcranial cerebellar direct current stimulation enhances verb generation but not verb naming in poststroke aphasia. *J. Cogn. Neurosci.* 30, 188–199. doi: 10.1162/jocn_a_01201

Mariën, P., and Borgatti, R. (2018). Language and the cerebellum. *Handb. Clin. Neurol.* 154, 181–202.

Marien, P., Engelborghs, S., Fabbro, F., and De Deyn, P. P. (2001). The lateralized linguistic cerebellum: a review and a new hypothesis. *Brain Lang.* 79, 580–600. doi: 10.1006/brln.2001.2569

Marien, P., Saerens, J., Nanhoe, R., Moens, E., Nagels, G., Pickut, B. A., et al. (1996). Cerebellar induced aphasia: case report of cerebellar induced prefrontal aphasic language phenomena supported by SPECT findings. *J. Neurol. Sci.* 144, 34–43. doi: 10.1016/s0022-510x(96)00059-7

Murdoch, B. E. (2010). The cerebellum and language: historical perspective and review. *Cortex* 46, 858–868. doi: 10.1016/j.cortex.2009.07.018

O'Reilly, J. X., Beckmann, C. F., Tomassini, V., Ramnani, N., and Johansen-Berg, H. (2010). Distinct and overlapping functional zones in the cerebellum defined by resting state functional connectivity. *Cereb. Cortex* 20, 953–965. doi: 10.1093/cercor/bhp157

Popa, T., Russo, M., and Meunier, S. (2010). Long-lasting inhibition of cerebellar output. *Brain Stimul.* 3, 161–169. doi: 10.1016/j.brs.2009.10.001

Pope, P. A., and Miall, R. C. (2012). Task-specific facilitation of cognition by cathodal transcranial direct current stimulation of the cerebellum. *Brain Stimul.* 5, 84–94. doi: 10.1016/j.brs.2012.03.006

Rastogi, A., Cash, R., Dunlop, K., Vesia, M., Kucyi, A., Ghahremani, A., et al. (2017). Modulation of cognitive cerebello-cerebral functional connectivity by lateral cerebellar continuous theta burst stimulation. *Neuroimage* 158, 48–57. doi: 10.1016/j.neuroimage.2017.06.048

Ren, C., Zhang, G., Xu, X., Hao, J., Fang, H., Chen, P., et al. (2019). The effect of rTMS over the different targets on language recovery in stroke patients with global aphasia: a randomized sham-controlled study. *Biomed. Res. Int.* 2019:4589056. doi: 10.1155/2019/4589056

Rossi, S., Hallett, M., Rossini, P. M., and Pascual-Leone, A. (2009). Safety, ethical considerations, and application guidelines for the use of transcranial magnetic stimulation in clinical practice and research. *Clin. Neurophysiol.* 120, 2008–2039.

Rossini, P. M., Burke, D., Chen, R., Cohen, L. G., Daskalakis, Z., Di Iorio, R., et al. (2015). Non-invasive electrical and magnetic stimulation of the brain, spinal cord, roots and peripheral nerves: basic principles and procedures for routine clinical and research application. An updated report from an I.F.C.N. Committee. *Clin. Neurophysiol.* 126, 1071–1107. doi: 10.1016/j.clinph.2015.02.001

Santos, M. D. D., Cavenaghi, V. B., Mac-Kay, A., Serafim, V., Venturi, A., Truong, D. Q., et al. (2017). Non-invasive brain stimulation and computational models in post-stroke aphasic patients: single session of transcranial magnetic stimulation and transcranial direct current stimulation. A randomized clinical trial. *Sao Paulo Med. J.* 135, 475–480. doi: 10.1590/1516-3180.2016.0194060617

Sebastian, R., Kim, J. H., Brenowitz, R., Tippett, D. C., Desmond, J. E., Celnik, P. A., et al. (2020). Cerebellar neuromodulation improves naming in post-stroke aphasia. *Brain Commun.* 2:fcaa179. doi: 10.1093/braincomms/fcaa179

Sebastian, R., Saxena, S., Tsapkini, K., Faria, A. V., Long, C., Wright, A., et al. (2016). Cerebellar tDCS: a novel approach to augment language treatment post-stroke. *Front. Hum. Neurosci.* 10:695. doi: 10.3389/fnhum.2016.00695

Sheu, Y. S., Liang, Y., and Desmond, J. E. (2019). Disruption of cerebellar prediction in verbal working memory. *Front. Hum. Neurosci.* 13:61. doi: 10.3389/fnhum.2019.00061

Silveri, M. C., Di Betta, A. M., Filippini, V., Leggio, M. G., and Molinari, M. (1998). Verbal short-term store-rehearsal system and the cerebellum. Evidence from a patient with a right cerebellar lesion. *Brain* 121(Pt 11), 2175–2187. doi: 10.1093/brain/121.11.2175

Stoodley, C. J. (2012). The cerebellum and cognition: evidence from functional imaging studies. *Cerebellum* 11, 352–365. doi: 10.1007/s12311-011-0260-7

Theoret, H., Haque, J., and Pascual-Leone, A. (2001). Increased variability of paced finger tapping accuracy following repetitive magnetic stimulation of the

cerebellum in humans. *Neurosci. Lett*. 306, 29–32. doi: 10.1016/s0304-3940(01)01860-2

Thiel, A., Hartmann, A., Rubi-Fessen, I., Anglade, C., Kracht, L., Weiduschat, N., et al. (2013). Effects of noninvasive brain stimulation on language networks and recovery in early poststroke aphasia. *Stroke* 44, 2240–2246. doi: 10.1161/STROKEAHA.111.000574

Turkeltaub, P. E., Swears, M. K., D'Mello, A. M., and Stoodley, C. J. (2016). Cerebellar tDCS as a novel treatment for aphasia? Evidence from behavioral and resting-state functional connectivity data in healthy adults. *Restor. Neurol. Neurosci*. 34, 491–505. doi: 10.3233/RNN-150633

Tzourio-Mazoyer, N., Landeau, B., Papathanassiou, D., Crivello, F., Etard, O., Delcroix, N., et al. (2002). Automated anatomical labeling of activations in SPM using a macroscopic anatomical parcellation of the MNI MRI single-subject brain. *Neuroimage* 15, 273–289.

Wang, C. P., Hsieh, C. Y., Tsai, P. Y., Wang, C. T., Lin, F. G., and Chan, R. C. (2014). Efficacy of synchronous verbal training during repetitive transcranial magnetic stimulation in patients with chronic aphasia. *Stroke* 45, 3656–3662. doi: 10.1161/STROKEAHA.114.007058

Wassermann, E. M. (1998). Risk and safety of repetitive transcranial magnetic stimulation: report and suggested guidelines from the International Workshop on the Safety of Repetitive Transcranial Magnetic Stimulation, June 5-7, 1996. *Electroencephalogr. Clin. Neurophysiol*. 108, 1–16. doi: 10.1016/s0168-5597(97)00096-8

Yan, C. G., Wang, X. D., Zuo, X. N., and Zang, Y. F. (2016). DPABI: data processing & analysis for (resting-state) brain imaging. *Neuroinformatics* 14, 339–351.

Zang, Y., Jiang, T., Lu, Y., He, Y., and Tian, L. (2004). Regional homogeneity approach to fMRI data analysis. *Neuroimage* 22, 394–400. doi: 10.1016/j.neuroimage.2003.12.030

Conflict of Interest: The authors declare that the research was conducted in the absence of any commercial or financial relationships that could be construed as a potential conflict of interest.

Publisher's Note: All claims expressed in this article are solely those of the authors and do not necessarily represent those of their affiliated organizations, or those of the publisher, the editors and the reviewers. Any product that may be evaluated in this article, or claim that may be made by its manufacturer, is not guaranteed or endorsed by the publisher.

frontiers | Frontiers in Aging Neuroscience

ORIGINAL RESEARCH
published: 16 June 2022
doi: 10.3389/fnagi.2022.909622

Association Between Mitochondrial Function and Rehabilitation of Parkinson's Disease: Revealed by Exosomal mRNA and lncRNA Expression Profiles

Yixuan Wang[1†], *Yonghong Liu*[1†], *Zhaohui Jin*[1], *Cui Liu*[1], *Xin Yu*[2], *Keke Chen*[2], *Detao Meng*[1], *Aixian Liu*[1*] and *Boyan Fang*[1*]

[1] Parkinson Medical Center, Beijing Rehabilitation Hospital, Capital Medical University, Beijing, China, [2] Beijing Rehabilitation Medical College, Capital Medical University, Beijing, China

OPEN ACCESS

Edited by:
Howe Liu,
University of North Texas Health Science Center, United States

Reviewed by:
Ying Shen,
The First Affiliated Hospital of Nanjing Medical University, China
Wanlin Yang,
Southern Medical University, China

***Correspondence:**
Aixian Liu
lax721@163.com
Boyan Fang
fangboyanv@ccmu.edu.cn
orcid.org/0000-0002-9935-433X

[†] These authors have contributed equally to this work

Specialty section:
This article was submitted to Parkinson's Disease and Aging-related Movement Disorders, a section of the journal Frontiers in Aging Neuroscience

Received: 31 March 2022
Accepted: 10 May 2022
Published: 16 June 2022

Citation:
Wang Y, Liu Y, Jin Z, Liu C, Yu X, Chen K, Meng D, Liu A and Fang B (2022) Association Between Mitochondrial Function and Rehabilitation of Parkinson's Disease: Revealed by Exosomal mRNA and lncRNA Expression Profiles. Front. Aging Neurosci. 14:909622. doi: 10.3389/fnagi.2022.909622

Rehabilitation has been proposed as a valid measure complementary to the management of Parkinson's disease (PD). However, the mechanism underlying is not clear yet. The differential expressions of exosomal messenger RNA (mRNA) and long noncoding RNAs (lncRNAs) may play a critical role in PD progression and rehabilitation. To compare the differential expressions of exosomal mRNAs and lncRNAs, patients with PD (PWPs, Hoehn and Yahr stages 1.5-2.5, $n = 6$) and age- and sex-matched healthy controls (HCs, $n = 6$) were included in this study. All PWPs received a 2-week rehabilitation treatment in the hospital, which seemingly led to improvement in both the motor and non-motor functions. A set of differentially expressed mRNAs (DEmRNAs) and differentially expressed lncRNAs (DElncRNAs) extracted from exosomes in blood samples *via* next-generation sequencing (NGS) was screened out. Compared to HCs, 2,337 vs. 701 mRNAs and 1,278 vs. 445 lncRNAs were significantly upregulated and significantly downregulated, respectively, in pre-rehabilitation (pre-rehab) PWPs; 2,490 vs. 629 mRNAs and 1,561 vs. 370 lncRNAs were significantly upregulated and significantly downregulated, respectively, in post-rehabilitation (post-rehab) PWPs. Compared to pre-rehab PWPs, 606 vs. 1,056 mRNAs and 593 vs. 1,136 lncRNAs were significantly upregulated and significantly downregulated, respectively, in post-rehab PWPs. Overall, 14 differentially expressed mRNAs (DEmRNAs) and 73 differentially expressed lncRNAs (DElncRNAs) were expressed in the blood exosomes of HCs, pre- and post-rehab PWPs, simultaneously. Gene Ontology (GO) and Kyoto Encyclopedia of Genes and Genomes (KEGG) pathway enrichment analyses identified 243 significantly co-expressed lncRNA-mRNA pairs. One DEmRNA of interest (ENSG00000099795, NDUFB7) and three corresponding DElncRNAs (ENST00000564683, ENST00000570408, and ENST00000628340) were positively related. Quantitative real-time polymerase chain reaction (qRT-PCR) validated that the expression levels of NDUFB7 mRNA and the 3 DElncRNAs increased significantly in pre-rehab PWPs, but decreased significantly in post-rehab PWPs compared to HCs. NDUFB7 mRNA is a marker related to mitochondrial respiration. It is reasonably believed that mitochondrial function is

associated with PD rehabilitation, and the mitochondrial pathway may involve in the pathogenesis of PD.

Keywords: Parkinson's disease, rehabilitation, exosome, messenger RNA, NDUFB7, mitochondrial function, long noncoding RNAs

INTRODUCTION

Parkinson's Disease (PD) is one of the fastest-growing neurological disorders characterized by bradykinesia, rigidity, and tremor (Bloem et al., 2021). The primary pathological changes underlying PD are the degeneration of dopaminergic neurons in the substantia nigra and significant decreases of dopamine in the striatum (Ntetsika and Papathoma, 2021). The neurodegenerative pathogenesis may be related to oxidative stress (Puspita and Chung, 2017), genetic predisposition (Pinnell et al., 2021), apoptosis (Venderova and Park, 2012), and neuroinflammation (Tansey and Goldberg, 2010). Increasing evidence has indicated that rehabilitation might be a promising supplementary therapy to prevent PD development and delay PD progression (Xu et al., 2019). However, the potential mechanisms of PD, especially the mechanism underlying PD rehabilitation, are not clear yet. High-quality, objective biomarkers are needed for accurate PD evaluation.

Exosomes (EXOs) are intracellular membrane-based vesicles with diverse compositions involved in biological and pathological processes (Doyle and Wang, 2019), including intercellular communication, the regulation of cellular function, and waste management (Van Der Pol et al., 2012). Various important cell signaling molecules, such as messenger RNA (mRNA), long non-coding RNAs (lncRNA), and proteins can be transported and transmitted by EXOs (Cheng et al., 2021). The contents of exosomes are stable and can be transported into receiver cells to exert their biological roles (Cheng et al., 2021). Therefore, exosomes are considered potential biomarkers for diagnosing various diseases, such as PD, e.g., miR-133b variant, a marker involved in dopamine neuron survival in mice (Kim et al., 2007; Lee et al., 2019). A previous study suggested that lnc-MKRN2-42:1 may be involved in the occurrence and development of PD (Wang et al., 2020). Considering the properties of exosomes, it is appropriate to use RNA-based biomarkers from EXOs to study PD.

Mitochondrial dysfunction has been observed in PD (Macdonald et al., 2018). The nigral neurons are highly susceptible to mitochondrial dysfunction due to high basal rates of oxidative phosphorylation leading to increased oxidative stress (Haddad and Nakamura, 2015). Mitochondrial dysfunction, especially reductions in complex I activity has been evidenced in both familial and sporadic forms of PD (Haddad and Nakamura, 2015). Complex I activity may become an essential marker of the development and assessment of PD. However, the expression of mRNAs and lncRNAs, and their interactions underlying mitochondrial mechanisms in peripheral blood exosomes of PWPs before and after rehabilitation remains unknown.

In this study, we aimed to compare the expression profiles of exosomal lncRNA and mRNA in the peripheral blood between healthy controls (HCs), pre-and post-rehab PWPs for the purpose to elucidate their potential association with PD pathogenesis and rehabilitation. The differentially expressed mRNAs (DEmRNAs) and differentially expressed lncRNAs (DElncRNAs) of interest were characterized to identify their potential function and signaling pathways in PD rehabilitation.

MATERIALS AND METHODS

Subjects and Sample Collection

We included 80 PWPs between June 2020 and December 2020 in the Parkinson Medical Center of Beijing rehabilitation hospital. Six PWPs who met the inclusion criteria and were willing to participate in the project were included. Six age- and sex-matched healthy subjects were also included as HCs. Most HCs were life partners or caregivers of the PWPs.

All PWPs met the clinical diagnosis of PD based on the Movement Disorder Society (MDS) diagnostic criteria for primary PD (Postuma et al., 2015), with a disease severity rating of stage 1.5 to 2.5 on the Hoehn and Yahr (H&Y) scale (1 to 5 points from mild to severe) during the "ON" stage (Hoehn and Yahr, 1967); <75 years of age; without comorbidities requiring treatment; without deep brain stimulation therapy; Mini-Mental State Exam (MMSE) score >24 if education level $\geq$ secondary school or >20 if education level $\leq$ primary school (Folstein et al., 1975); stable medication use; and the ability to walk and stand without assistance.

The PWPs were excluded if they had a history of other neurological, psychological, or medical conditions, including atypical PD; history of head injury (stroke, depression, or learning disability); debilitating conditions other than PD (e.g., hearing or vision impairment); or significantly abnormal laboratory tests (including hematology, electrolytes, renal and liver function tests).

Peripheral blood sample (5 ml) was taken from each participant under fasting conditions between 6 am and 7 am on Day 2 of hospitalization. All samples were stored at −80°C for later assay. The study protocol was approved by the Ethics Committee of Beijing Rehabilitation Hospital, Capital Medical University (approval No. 2020bkky010). All participants voluntarily signed informed consent. Flow chart of the study is shown in **Figure 1**.

Rehabilitation Procedure

Rehabilitation was administered as previously described (Chen K. K. et al., 2021). Briefly, three to four patients with PD were admitted to hospital simultaneously for a two weeks rehabilitation covering four daily sessions, five days a week in hospital. The four sessions consisted of (1) one on one physical therapy; (2) balance and gait training using C-MiLL (Motekforce

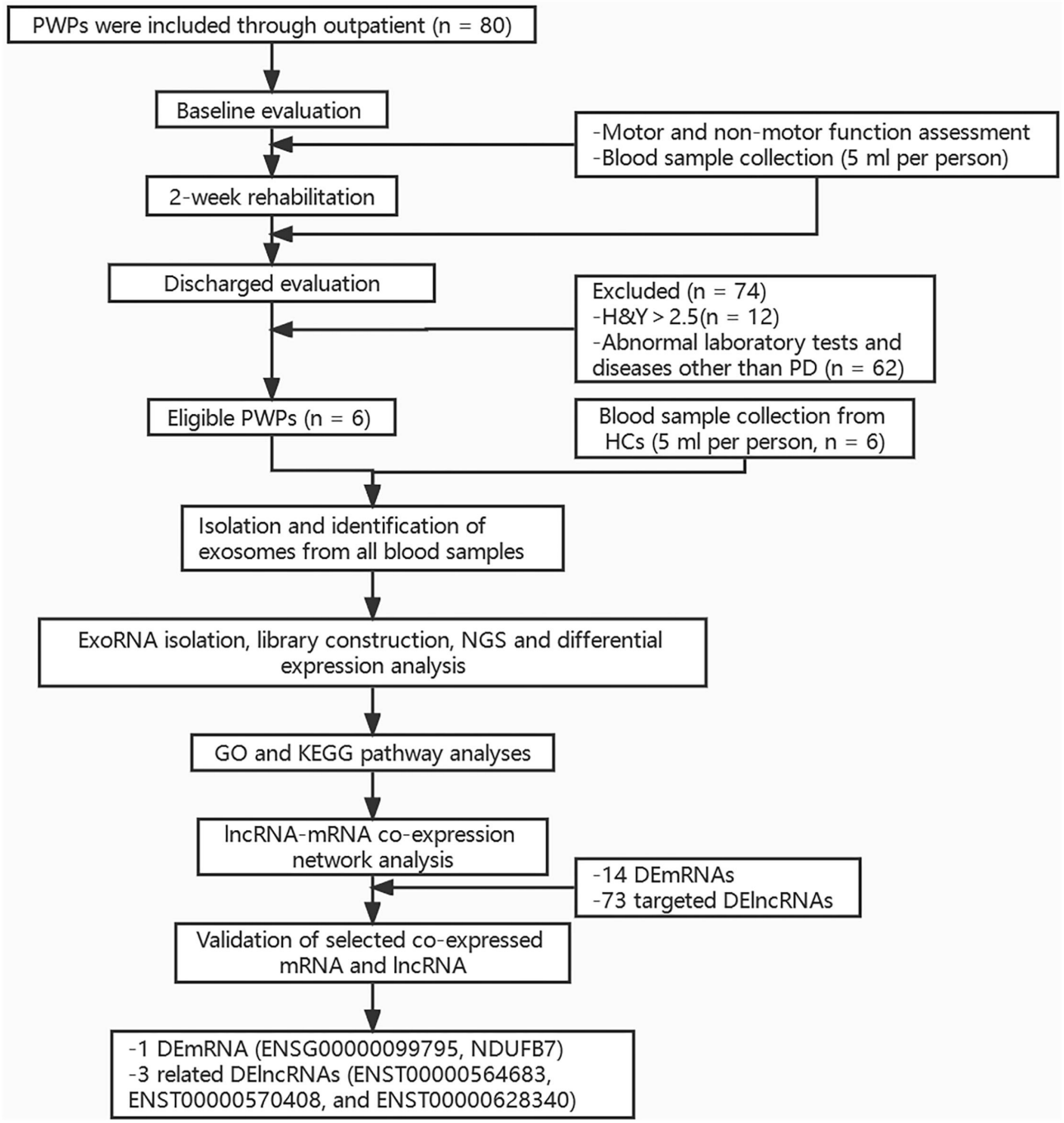

FIGURE 1 | Flow chart of the study. PWPs, patients with Parkinson's disease; H and Y, Hoehn and Yahr; PD, Parkinson's disease; HCs, healthy controls; NGS, Next-generation sequencing; GO, Gene ontology Ontology; KEGG, Kyoto Encyclopedia of Genes and Genomes; DEmRNAs, differentially expressed mRNAs; DElncRNAs, differentially expressed lncRNAs.

link, Culemburg, Netherlands) and Balance Tutor (Meditouch, Netanya, Israel); (3) aerobic training using upper and lower limb trainer (T5XR; Nustep, Ann Arbor, MI, USA); (4) speech therapy. Each session lasted for 30 to 60 min and run by one well-trained physical (for session1, 2, and 3) or speech therapist (for session 4) respectively to keep the consistency.

The total intervention time is 2.5 h per day. All sessions were divided and completed in the morning and afternoon (1–1.5 h for half a day). For example, the therapists conducted the C-Mill treadmill training (30 min) and one-on-one PT session (30 min) in the morning and conducted the balance tutor training (30 min), aerobic training (30 min), and speech therapy training

(30 min) in the afternoon. The interval between sessions was at least 30–60 min, and the patients can get enough rest for the upcoming training. In addition, they will be asked if any discomfort appears on the next day such as muscle soreness. No feelings of fatigue were reported. Especially, we screened for cardiovascular endurance by cardiopulmonary exercise test for each patient before intervention to avoid risk. The whole study process lasted for about 1 year. The rehabilitation procedure for patients with PD is shown in **Table 1**.

Clinical and Neuropsychological Assessment

Demographic data were collected, including gender, age, and disease duration. All PWPs underwent a battery of assessments under "ON" medication state (1 h after taking their regular antiparkinsonian medication and having a good therapeutic effect) at baseline (pre-rehabilitation) and on Day 1 after a 14-day rehabilitation (post-rehabilitation). The assessments included motor function, cognitive function, quality of life, and neuropsychological symptoms necessary for the evaluation of PD motor and non-motor functions. The Movement Disorders Society–Unified Parkinson's Disease Rating Scale Part III (MDS-UPDRS-III; Chung et al., 2020), the 10-m walk test (10MWT; Tao et al., 2021), the 6-min walk test (6MWT; Koyanagi et al., 2021), the Five Times Sit-to-Stand Test (FTSST; Duncan et al., 2011), the Timed Up-and-Go Test (TUG; Giardini et al., 2018), and the Mini Balance Evaluation System Test (Mini-BESTest; Conradsson et al., 2015) were used to assess walking and balance function. The Mini-mental State Examination (MMSE; Zhao et al., 2020) and the Montreal Cognitive Assessment (MoCA; Van Steenoven et al., 2014) were used to assess cognitive function. The Hamilton Anxiety Scale (HAMA; Sumec et al., 2017) and the Hamilton depression scale (HAMD; Sumec et al., 2017) were used to evaluate psychiatric symptoms. The Parkinson's Disease Questionnaire (PDQ-39; Meng et al., 2022) was used to measure perceived health in terms of physical, mental, and social functions. The evaluations were performed randomly and patients were given short breaks between assessments.

ExoRNA Isolation, Library Construction, and Next-Generation Sequencing (NGS)

ExoRNA isolation, library construction, and high-throughput sequencing were carried out by CloudSeq Biotech Inc. (Shanghai, China). Briefly, total RNAs were extracted, followed by the removal of ribosomal RNAs (rRNAs) using TRIzol reagent (Invitrogen, Carlsbad, CA, USA) and NEBNext® rRNA Depletion Kit (New England Biolabs, Inc., Massachusetts, USA) according to the manufacturer's instructions. The TruSeq Stranded Total RNA Library Prep Kit (Illumina, USA) was used for the construction of RNA libraries. The RNA libraries underwent quantitative and quantitative evaluation on the Agilent 2100 Analyzer (Agilent Technologies, USA). Ten pM libraries were denatured to single-stranded DNA molecules and were then captured on Illumina flow cells, amplified *in situ* as clusters, and sequenced with 150 cycles on Illumina NovaSeq 6000 sequencer following the manufacturer's protocol.

Differential Expression Analysis

The raw reads were generated by Illumina NovaSeq 6000 sequencer. Low-quality reads were removed using fastp software (v0.20.0). STAR software (v2.7.9a) was used to align the high-quality clean reads to the human reference genome (GRCh38/hg38). Featurecount software (v2.0.2) and HTSeq software (v0.13.5) were used to obtain the raw read counts of mRNA gene level and lncRNA transcript level as the mRNA and lncRNA expression profiles, respectively. The fold change and *P*-value between two groups of samples were calculated using the DESeq2 R package, and the fold change $\geq$2.0 and a $p \leq 0.05$ were categorized as the threshold for DEmRNA and DElncRNA screening.

Gene Ontology (GO) and Kyoto Encyclopedia of Genes and Genomes (KEGG) Pathway Analyses

The GO and KEGG analyses were carried out for the DEmRNAs. GO analysis provides a controlled vocabulary for annotating and inferring the functions of DEmRNAs. The GO terms covered the common terms of biological process (BP), molecular function (MF), and cellular component (CC). The KEGG pathway analysis was used to speculate on the biological functions involved in DEmRNAs. In brief, the Ensembl human GTF gene annotation database (v104) was used to annotate the DEmRNAs. GO and KEGG pathway enrichment analyses were performed with clusterProfiler R package (v3.18.1) based on the DEmRNAs. A $p < 0.05$ was considered statistically significant.

lncRNA–mRNA Co-expression Network Analysis

A co-expression network was constructed to evaluate relationships between DE mRNAs and DElncRNAs. The Pearson's correlation coefficient (PCC) between coding and non-coding genes was calculated. The mRNA–lncRNA pairs were selected if PCC $\geq$ 0.990. The network of lncRNA–mRNA interactions was visualized using the Cytoscape software (http://www.cytoscape.org/).

Experimental Validation of Selected Co-expressed mRNA and lncRNA

The expression of selected lncRNA and mRNA was validated by qRT-PCR. Total RNA was reverse transcribed into cDNA using the PrimeScript RT Reagent Kit (Perfect Real Time; TaKaRa, Osaka, Japan) following kit instructions. cDNA was then subjected to qRT-PCR analysis on a QuantStudio 5 Real-Time PCR System using qPCR SYBR Green master mix (CloudSeq). The data were then normalized to the β-actin expression level. The relative expression ratios of selected co-expressed mRNA and lncRNA were calculated using the $\Delta\Delta$Ct method. The experiment was repeated three times. qRT-PCR primers of selected co-expressed mRNA and lncRNA are shown in **Table 2**.

TABLE 1 | Illustration of rehabilitation procedure for patients with PD.

Intervention	Description and dose	Selection and adjustment of intervention
One on one physical therapy	This session was conducted by one well-trained therapist for 30 minutes per day: 1. warm-up activities (5 minutes): Stretching all the joints and major muscle 2. Active and passive exercises (20 min): 2.1 Stretching: extremities and spine stretching, ROM traction 2.2 Strength training: isometric training, isotonic training, resistance training 2.3 Balance training: tandem, one leg stance, inclined ramp 2.4 Gait training: external cueing (visual or auditory cues), dual-task training 2.5 Adjustment /control of posture: antigravity trunk extension 3 Cool-down (5 min): Stretching all the joints	• H and Y stage 1-2: Items 2.2, 2.3, and 2.4 are required. Difficulty was raised according to patients' adaptation to the intervention. For example, balance training performed on different surfaces like foam and inclined ramp and less cues were provided during gait training. • H and Y stage>2:All items are required. Difficulty was reduced according to the severity of symptoms.
Balance and gait training	The training was conducted by one well-trained therapist using automatized and standardized program supported by C-Mill (conducted in the morning for 30 min per day) and Balance Tutor (conducted in the afternoon for 30 min per day).	Difficulty was adjusted according to the severity of symptoms. For example, more reaction times or cues were provided for patients with worse function of gait or balance.
Aerobic training	The training was conducted by one well-trained therapist using upper and lower limb trainer (T5XR; Nustep, Ann Arbor, MI, USA) for 30 min per day.	Difficulty was adjusted according to patients' adaptation to the intervention. For example, increased resistance level was set for patients with good adaptation to the training.
Speech therapy	Three possible kinds of interventions were conducted by one speech therapist for 30 min per day: (1) counseling for the management of swallowing and language problems; (2) individual swallowing training (3) speech therapy to treat hypokinetic dysarthria	The determination of speech therapies for patients with PD was mainly based on their complaints and symptoms, as well as the results of swallowing angiography: • For patients with PD with mild dysphagia or dysarthria, only one kind of intervention was needed. • For patients with PD with both dysphagia and dysarthria, we gave two kinds of intervention (2 and 3).
Home exercise program	A platform of home exercise program for patients with PD was established by Beijing Rehabilitation Hospital, which consisted of several home exercise video courses.	patients with PD keep doing exercise at home and sign up every day after 2-week rehabilitation.

PD, Parkinson's disease; ROM, range of motion; H and Y, Hoehn and Yahr.

TABLE 2 | Primers for mRNA and lncRNAs.

Genes	Type of primers	Sequences (5′-3′)
mRNA		
ENSG00000099795	1-Forward	ACAGCTTCCCCAACTTCCTG
	1-Reverse	AACTCTGCCGCCTTCTTCTC
lncRNA		
ENST00000564683	1-Forward	GTCTTGAACTCCTGGGCTCA
	1-Reverse	GTGCCTCCGTTTTCCTCATC
ENST00000570408	1-Forward	AGGGAAGCAGAAACGAGACA
	1-Reverse	AGTTAATTCCGTGGGGCTCT
ENST00000628340	1-Forward	GCCAAACCCATAACAGTGCT
	1-Reverse	CCTCTCCTTCCTCAACGTCA

Statistical Analysis

Graphs were plotted and analyses were performed by GraphPad Prism 8 software (San Diego, CA, USA). The statistical difference in relative expression ratios of the selected co-expressed mRNA and lncRNA between multiple groups was evaluated by one-way ANOVA followed by Tukey's multiple comparison test. The level of significance was set at $P < 0.05$.

RESULTS

Demographic and Laboratory Test Data

The demographic and laboratory test data of 6 PWPs and 6 age- and sex-matched HCs are shown in **Table 3**. The PWPs were 52–68 years of age at early-stage (Hoehn and Yahr score 1.5–2.5) of PD for more than 2 years(range of 2–9 years). All laboratory tests of PWPs and HCs were within normal range.

The clinical and neuropsychological assessments of pre-and post-rehab PWPs are shown in **Table 4**. Post-rehab PWPs showed better and improved motor function (velocity and mean time of 10MWT, FTSST, 6MWT, TUG, the score of Mini-BESTest), cognition (the score of MMSE, MoCA), quality of life (the score of PDQ-39), and neuropsychological function (the score of HAMA, HAMD) compared with the pre-rehab PWPs.

Differential Expression of Exosomal mRNAs and lncRNAs

The DEmRNAs and DElncRNAs are visually displayed in the form of scatter plots and volcano maps. Fold change $\geq$2.0 and $p \leq 0.05$ were used as the thresholds for significantly differential expression. Compared with the HCs, there were 3,038 (including 2337 upregulated and 701 downregulated mRNAs) and 3,119

TABLE 3 | Clinical characteristics and blood biochemical features in PWPs and HCs.

	PD-01	PD-02	PD-03	PD-04	PD-05	PD-06	HC-01	HC-02	HC-03	HC-04	HC-05	HC-06
Sex (male/female)	Fmale	Male	Fmale	Fmale	Male	Fmale	Fmale	Male	Fmale	Male	Fmale	Fmale
Age (y)	67	55	68	62	52	66	65	52	67	55	62	64
Duration (y)	8	8	9	7	9	2	–	–	–	–	–	–
H and Y (score)	2.5	2	2.5	2	1.5	2	–	–	–	–	–	–
UPDRS III-off (score)	48	31	53	28	25	18	–	–	–	–	–	–
SBP (mmHg)	91	155	117	125	117	127	–	–	–	–	–	–
DBP (mmHg)	61	91	79	70	73	57	–	–	–	–	–	–
RBC (10^{12}/L)	4.7	4.92	4.39	4.48	4.74	4.32	–	–	–	–	–	–
Hb (g/L)	140	153	127	135	154	130	–	–	–	–	–	–
WBC (10^9/L)	6.85	6.45	5.67	7.44	4.6	7.68	–	–	–	–	–	–
NC (104^9/L)	55.6	4.34	3.16	5.01	2.54	4.66	–	–	–	–	–	–
NR (%)	3.8	67.2	55.7	67.5	55.3	60.6	–	–	–	–	–	–
Plt (10^9/L)	191	231	240	242	226	223	–	–	–	–	–	–
Na (mmol/L)	145	140	141	141	143	145	–	–	–	–	–	–
K (mmol/L)	4.2	3.8	3.7	4.1	4	4.1	–	–	–	–	–	–
Ca (mmol/L)	2.36	2.54	2.47	2.24	2.32	2.35	–	–	–	–	–	–
ALT (U/L)	12	20	26	15	24	9	–	–	–	–	–	–
AST (U/L)	18	16	19	18	22	17	–	–	–	–	–	–
TBIL (umol/L)	15.1	19.8	15.9	11.6	9.5	14.5	–	–	–	–	–	–
GHb (%)	6.6	7.1	6.6	5.9	5.4	5.8	–	–	–	–	–	–
Cre (umol/L)	64.8	62.2	61	60.1	80.3	72.6	–	–	–	–	–	–
BUN (mmol/L)	5.7	4.3	6.1	4.5	4.1	5.1	–	–	–	–	–	–

PWPs, patients with PD; HCs, Healthy controls; H and Y, HoehnandYahr; UPDRS, Unified Parkinson Disease Rating Scale; SBP, systolic blood pressure; DBP, diastolic blood pressure; RBC, red blood cell count; Hb, hemoglobin; WBC, white blood cell count; NC, neutrophil count; NR, neutrophil ratio; Plt, platelet; Na, sodium ion; K, potassium ion; Ca, calcium ion; ALT, alanine transaminase; AST, aspartate aminotransferase; TBIL, total bilirubin; GHb, glycated hemoglobin; Cre, creatinine; BUN, blood urea nitrogen.

TABLE 4 | The results of motor, cognitive, quality of life, and neuropsychological assessment in the pre- and post-rehabilitation PWPs.

Case No.	PD-01		PD-02		PD-03		PD-04		PD-05		PD-06	
	Pre-	Post-	Pre-	Post-	Pre-	Post-	Pre-	Post-	Pre-	Post-	Pre-	Post-
Motor functional assessment												
10MV-V_{CGS} (m/s)	1.14	1.15	0.97	0.97	1.05	1.19	1.01	1.47	1.4	1.41	1.23	1.34
10MV-MT_{CGS} (s)	8.76	8.69	10.26	10.25	9.51	8.37	9.89	6.76	7.13	7.04	8.08	7.42
10MV-V_{MGS} (m/s)	1.82	1.87	1.86	1.43	1.61	1.68	1.24	1.91	2.04	2.42	1.54	1.95
10MV-MT_{MGS} (s)	5.46	5.34	5.35	6.96	6.18	5.94	8.02	5.22	4.88	4.12	6.46	5.1
FTSST (s)	9.37	10.03	12.1	9.91	9.09	10.99	10.61	8.9	6.92	5.49	8.72	7.87
6MWT (m)	522	527	445	520	466	446	509	536	559	591	464	498
TUG (s)	8.15	7.34	10.15	8.43	9.58	10.08	8.48	7.36	8.85	6.57	8.14	7.16
Mini-BESTest (score)	22	25	25	25	22	25	22	25	23	27	25	26
Cognitive assessment												
MMSE (score)	26	27	27	30	25	27	25	30	24	30	29	30
MoCA (score)	27	30	27	28	22	25	21	27	23	29	29	30
Quality of life assessment												
PDQ-39 (score)	39.74	23.71	23.07	14.1	20.51	18.58	14.1	13.46	21.15	14.74	17.3	12.17
Neuropsychological assessment												
HAMA (score)	15	4	4	4	5	9	10	9	6	6	12	8
HAMD (score)	12	4	7	4	2	8	5	3	6	1	8	4

Pre-, pre- rehabilitation; Post-, post-rehabilitation; 10MWT-VCGS, the velocity of 10-m walk test in comfortable gait speed; 10 MWT-MTCGS, the mean time of 10-m walk test in comfortable gait speed; 10MWT -VMGS, the velocity of 10-m walk test in maximum gait speed; 10MWT -MTMGS, the mean time of 10-m walk test in maximum gait speed; FTSST, the Five Times Sit-to-Stand Test; 6MWT, the six-minute walk test; TUG, the time up and go; Mini-BESTest, Mini Balance Evaluation System Test; HAMA, Hamilton Anxiety Scale; HAMD, Hamilton depression scale; MMSE, Mini-mental State Examination; MoCA, Montreal Cognitive Assessment; PDQ-39, The Parkinson's Disease Questionnaire.

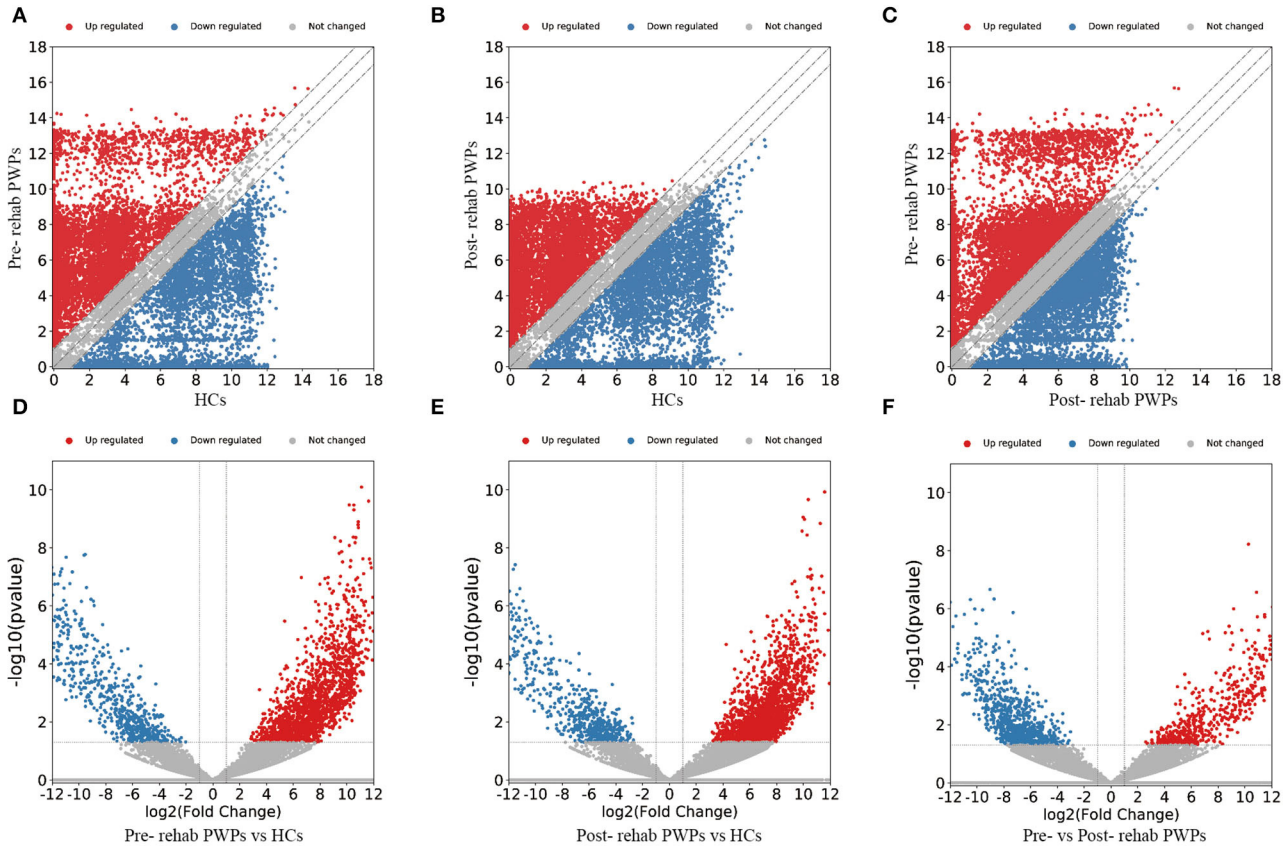

FIGURE 2 | Changes in the mRNA expression profiles of the HCs, pre- and post-rehab PWPs. The scatter plot **(A)** and volcanic map **(D)** reveal that a significant difference existed in the distribution of mRNAs between pre-rehab PWPs and the HCs. The scatter plot **(B)** and volcanic map **(E)** reveal that a significant difference existed in the distribution of mRNAs between Post-rehab PWPs and the HCs. The scatter plot **(C)** and volcanic map **(F)** reveal that a significant difference existed in the distribution of mRNAs between pre- and post-rehab PWPs. Red represents upregulation, while green represents downregulation. Pre-rehab, pre-rehabilitation; Post-rehab, post-rehabilitation; PWPs, patients with Parkinson's disease.

(including 2,490 upregulated and 629 downregulated mRNAs) DEmRNAs in the blood exosomes of pre-rehab (**Figures 2A,D**) and post-rehab PWPs (**Figures 2B,E**), respectively. Compared with pre-rehab PWPs, mRNA expression levels of post-rehab PWPs (**Figures 2C,F**) revealed 1,662 DEmRNAs, of which 606 and 1,056 were up and downregulated, respectively. In addition, lncRNA expression profiles revealed that, compared with the HCs, a total of 1,723 (including 1,278 upregulated and 445 downregulated lncRNAs) and 1,931 (including 1,561 upregulated and 370 downregulated lncRNAs) DElncRNAs were identified in the blood exosomes of pre- rehab (**Figures 3A,D**) and post-rehab (**Figures 3B,E**) PWPs, respectively. Compared with pre-rehab PWPs, lncRNA expression levels of post-rehab PWPs (**Figures 3C,F**) revealed 1,729 DElncRNAs, of which 593 and 1,136 were up and downregulated, respectively.

GO Analysis of DEmRNAs

Gene ontology enrichment analysis was performed to investigate the role of the DEmRNAs in the process of rehabilitation (**Figure 4**). GO analysis between HCs and pre-rehab PWPs revealed that the upregulated DEmRNAs were significantly enriched in biological processes related to thymus development, protein autophosphorylation, and extracellular matrix organization (**Figure 4A**), while the downregulated DEmRNAs were enriched in protein localization to the endoplasmic reticulum, establishment of protein localization to the endoplasmic reticulum, SRP–dependent cotranslational protein targeting the membrane (**Figure 4D**).

Gene ontology analysis between HCs and post-rehab PWPs revealed that the upregulated DEmRNAs were significantly enriched in post–translational protein modification, positive regulation of apoptotic signaling pathway, and negative regulation of mitochondrion organization (**Figure 4B**). The downregulated mRNAs were enriched in protein localization to the endoplasmic reticulum, protein K48–linked ubiquitination, SRP-dependent cotranslational protein targeting the membrane (**Figure 4E**).

Gene ontology analysis between pre-and post-rehab PWPs revealed that the upregulated DEmRNAs were significantly enriched in collagen metabolic process, skin morphogenesis, and RNA stabilization (**Figure 4C**). These downregulated DEmRNAs are involved in proteasome-mediated ubiquitin-dependent

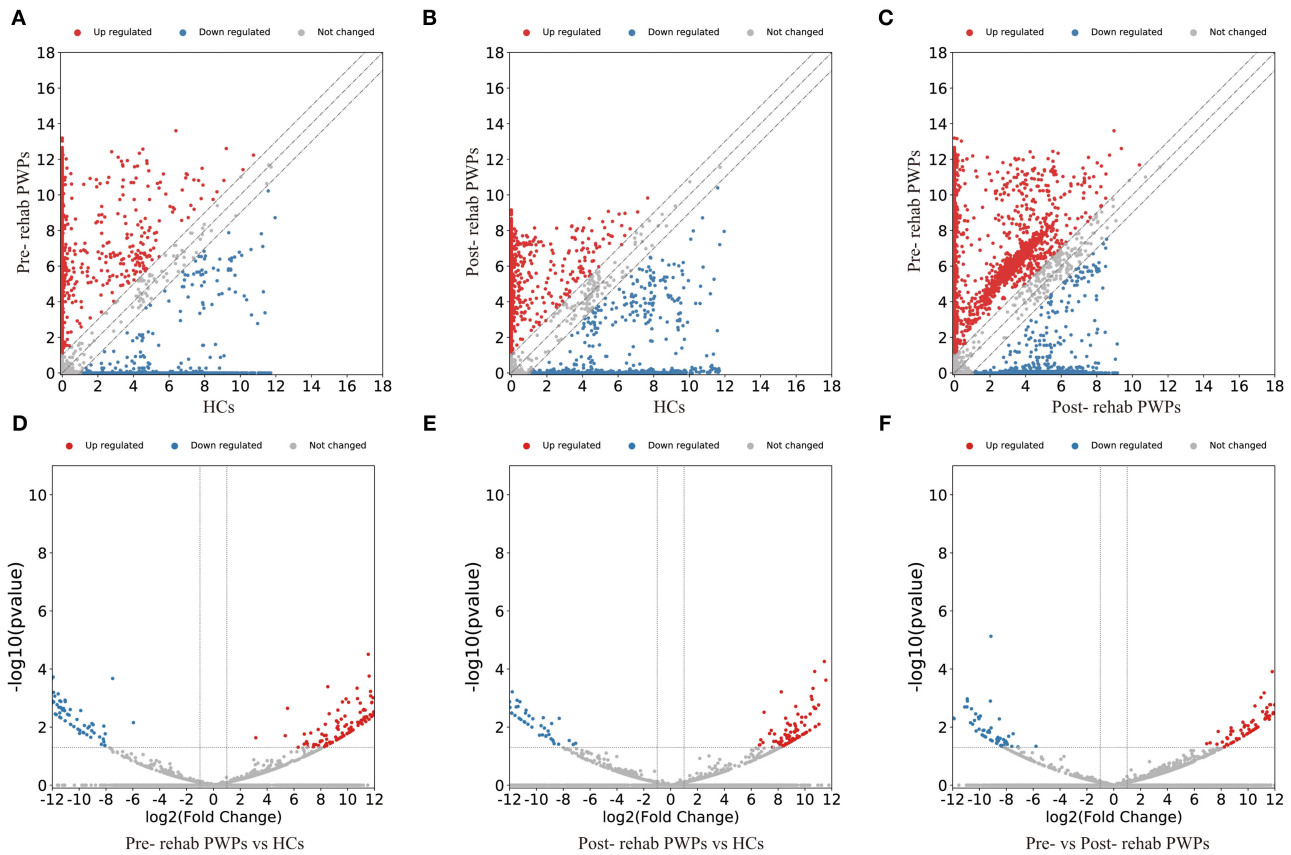

FIGURE 3 | Changes in the lncRNA expression profiles of the HCs, pre- and post-rehab PWPs. The scatter plot **(A)** and volcanic map **(D)** reveal that a significant difference existed in the distribution of lncRNAs between pre-rehab PWPs and HCs. The scatter plot **(B)** and volcanic map **(E)** reveal that a significant difference existed in the distribution of lncRNAs between post-rehab PWPs and the HCs. The scatter plot **(C)** and volcanic map **(F)** reveal that a significant difference existed in the distribution of lncRNAs between Pre- and Post-rehab PWPs. Red represents upregulation, while green represents downregulation. Pre-rehab, pre-rehabilitation; Post-rehab, post-rehabilitation; PWPs, patients with Parkinson's disease.

protein catabolic process, proteasomal protein catabolic process, and the regulation of innate immune response (**Figure 4F**).

Pathway Analysis of DEmRNAs

KEGG pathway analysis identified the pathways influenced by exosomal DEmRNAs of HCs, pre- and post-rehab PWPs. The pathways of upregulated DEmRNAs between HCs and pre-rehab PWPs are involved in "axon guidance," "Fc epsilon RI signaling pathway," "B cell receptor signaling pathway" (**Figure 5A**), while the pathways of downregulated DEmRNAs are involved in "long–term potentiation," "ribosome," and "neurotrophin signaling pathway" (**Figure 5D**).

Compared to the HCs, the pathways associated with upregulated DEmRNAs in post-rehab PWPs are involved in "lysosome," "natural killer cell mediated cytotoxicity," "calcium signaling pathway" (**Figure 5B**), while the pathways associated with downregulated DEmRNAs are involved in the "mRNA surveillance pathway," "mTOR signaling pathway," and "protein export" (**Figure 5E**). Then compared to the pre-rehab PWPs, the pathways associated with upregulated DEmRNAs of the post-rehab group are involved in the "B cell receptor signaling pathway," "ubiquitin-mediated proteolysis," "VEGF signaling pathway" (**Figure 5C**), while the pathways associated with downregulated DEmRNAs are involved in the "MAPK signaling pathway," "neurotrophin signaling pathway," and "proteasome" (**Figure 5F**).

Co-expression of DElncRNAs and DEmRNAs

The potential functions of mRNA can be inferred from lncRNA–mRNA co-expression networks. We screened all DEmRNA and DElncRNA, and 14 DEmRNAs and 73 DElncRNAs of interest were expressed simultaneously in HCs, pre-and post-rehab PWPs. The lncRNA–mRNA co-expression revealed that the interaction network comprised 87 nodes, including 14 DEmRNAs and 73 targeted DElncRNAs. These nodes formed 243 positive network pairs (**Figure 6**). The network displays that a single mRNA may be correlated with several lncRNAs and vice versa.

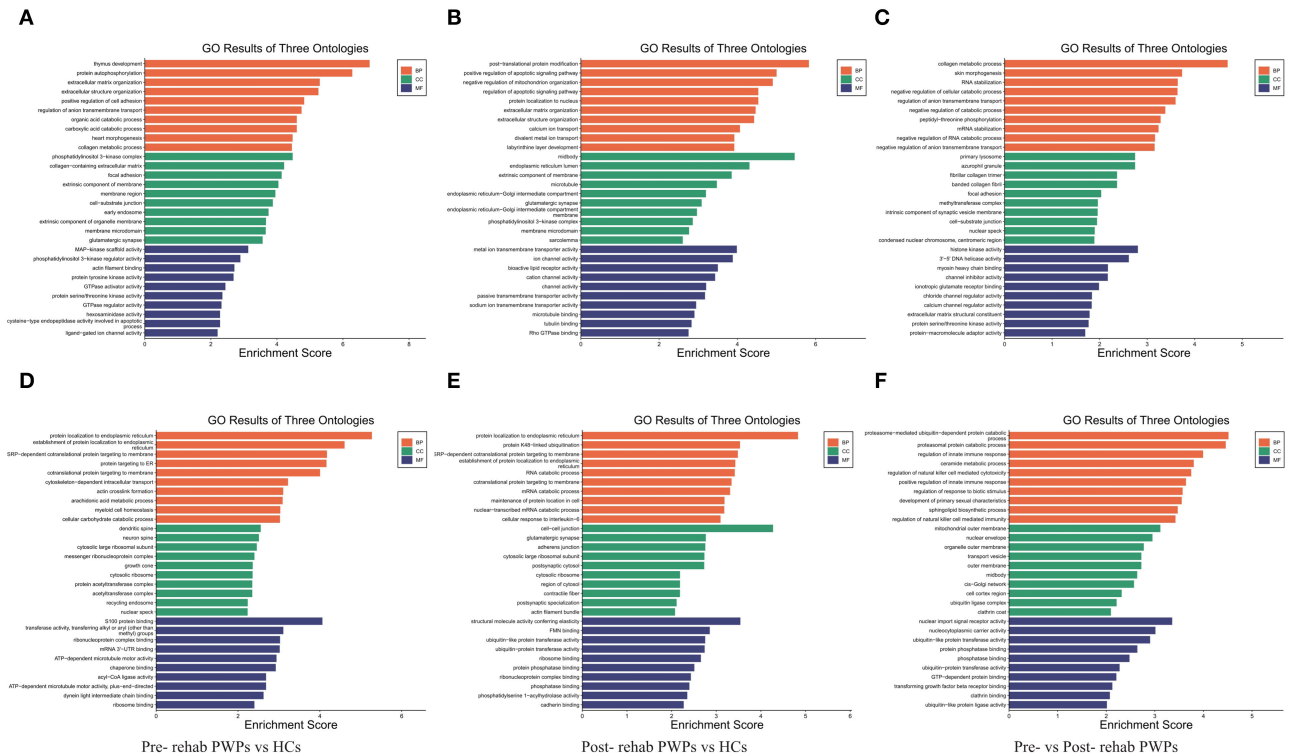

FIGURE 4 | GO analysis of differentially expressed genes. GO analysis of upregulated **(A)** and downregulated **(D)** mRNAs between Pre-rehab PWPs and HCs. GO analysis of upregulated **(B)** and downregulated **(E)** mRNAs between Post-rehab PWPs and HCs. GO analysis of upregulated **(C)** and downregulated **(F)** mRNAs between Pre- and Post-rehab PWPs. Pre-rehab, pre- rehabilitation; Post-rehab, post-rehabilitation; PWPs, patients with Parkinson's disease; GO, gene ontology; BP, biological process, MF, molecular function, CC, cellular component.

Experimental Validation of Selected lncRNAs and mRNAs

For validation purposes, we selected one DEmRNA (ENSG00000099795, NDUFB7) of interested and three related DElncRNAs (ENST00000564683, ENST00000570408, and ENST00000628340) from the co-expression pairs of DEmRNAs and DElncRNAs. The housekeeping gene β-actin was used as an internal control for normalization. NDUFB7 encodes a subunit of reduced nicotinamide adenine dinucleotide (NADH) dehydrogenase-ubiquinone oxidoreductase (complex I), which is a marker related to mitochondrial respiration. The qRT-PCR results were consistent with our sequencing results for the variation of DEmRNA (**Figure 7A**) and DElncRNAs (**Figure 7B**). According to qRT-PCR results, the expression of selected exosomal DEmRNA was significantly upregulated in pre-rehab PWPs ($P < 0.0001$) and post-rehab PWPs ($P = 0.0475$) compared with HCs, and significantly downregulated in post-rehab PWPs compared with pre-rehab PWPs ($P < 0.0001$).

Meanwhile, compared with HCs, all of the selected exosomal DElncRNAs were expressed at a significantly higher level (all $P \leq 0.0001$) in pre-rehab PWPs and two of the selected exosomal DElncRNAs, (ENST00000564683, $P = 0.0025$; ENST00000570408, $P = 0.0005$) expressed at a significantly higher level in post-rehab PWPs. All of the selected exosomal DElncRNAs were expressed at a significantly lower level in the post-rehab PWPs than in pre-rehab PWPs ($P < 0.05$).

DISCUSSION

This pilot study included 6 early-stage PWPs and 6 age- and sex-matched HCs. The PWPs responded well to rehabilitation treatment based on comprehensive clinical assessment, including motor behavior, cognition, quality of life, anxiety, and depression. Rehabilitation seems to be a promising non-pharmacological therapy for PD (Goodwin et al., 2008). Some studies have previously reported that rehabilitation measures could lead to significant improvement in motor function, including walking ability, posture, and balance control for PWPs (Ashburn et al., 2007; Chen K. K. et al., 2021). However, the underlying mechanisms for improvement of PWPs after rehabilitation is not clear.

High-quality biomarkers are important for PD diagnosis, monitoring, and treatment response evaluation (Cao et al., 2017). Exosomes are extracellular vesicles (EVs) secreted by multiple cells and contain cargos including protein, lncRNA, microRNA

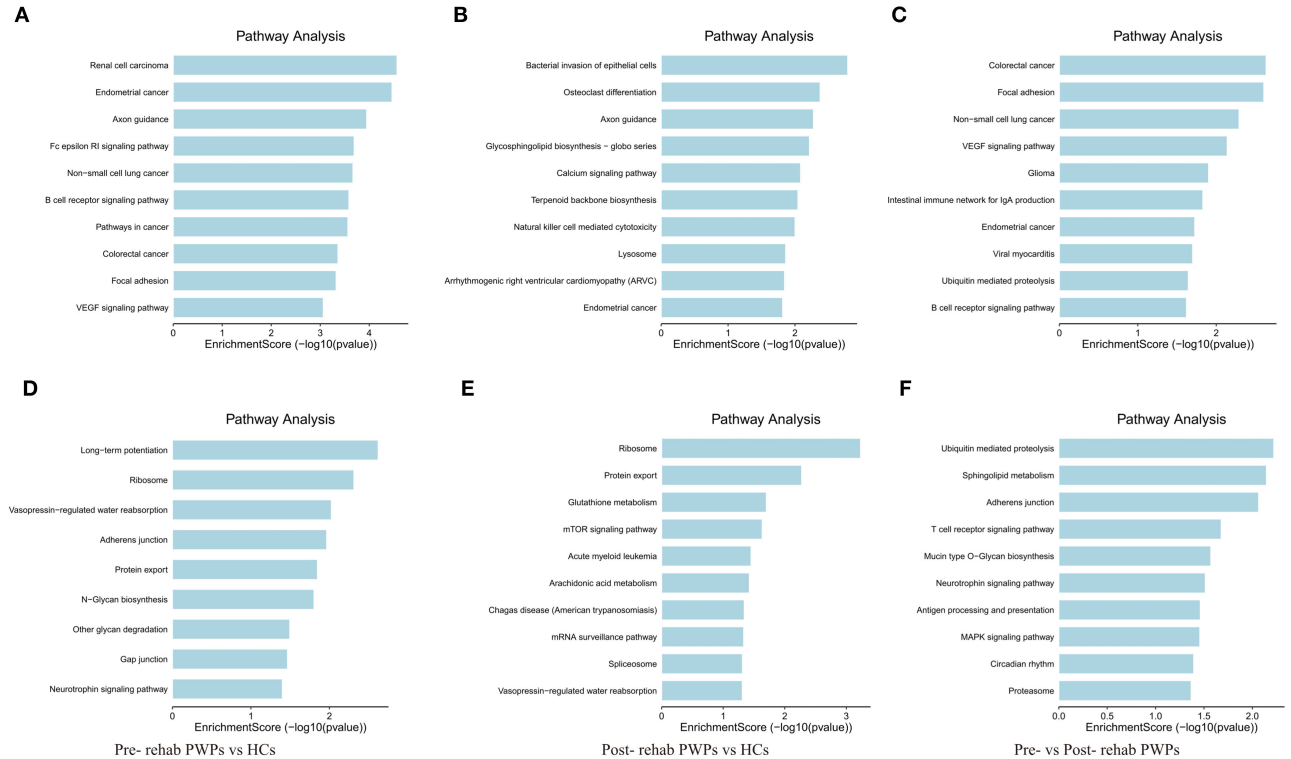

FIGURE 5 | KEGG pathway analysis of differentially expressed genes. KEGG pathway analysis of upregulated **(A)** and downregulated **(D)** mRNAs between pre-rehab PWPs and HCs. KEGG pathway analysis of upregulated **(B)** and downregulated **(E)** mRNAs between pre-rehab PWPs and HCs. KEGG pathway analysis of upregulated **(C)** and downregulated **(F)** mRNAs between pre- and post-rehab PWPs. Pre-rehab, pre-rehabilitation; post-rehab, post-rehabilitation; PWPs, patients with Parkinson's disease; KEGG, Kyoto Encyclopedia of Genes and Genomes.

(miRNA), and mRNA. Exosomes will transfer to the central nervous system (CNS) and release to exert pleiotropic effects (Deng et al., 2020). Exosomes can take part in many biological processes and contribute to intracellular communication, which makes them important in neurodegenerative diseases (Kalluri and Lebleu, 2020). Previous analysis of exosomes isolated from the blood or CSF of PWPs suggested that exosomes may be valid biomarkers of PD (Vella and Hill, 2016). As a result, we quantitatively analyzed the exosomal mRNA and lncRNA expressions in peripheral blood of PWPs and HCs using NGS and real-time quantitative PCR.

Gene ontology analysis revealed that the DEmRNAs were significantly associated with the biological processes such as regulation of mitochondrion organization, regulation of apoptotic signaling pathway, and calcium ion transport. The significantly enriched CC term included mitochondrial outer membrane, primary lysosome, and dendritic spine. The significantly enriched MF term comprised cysteine–type endopeptidase activity involved in the apoptotic process, ubiquitin–like protein ligase activity, and ribosome binding. The functional annotations demonstrated that the aberrantly expressed genes participate in mitochondrial dysfunction-related pathologic processes in PD, such as oxidative stress response, ubiquitin system, apoptosis, and calcium signaling (Zhang et al., 2010). KEGG pathway analysis revealed that DEmRNAs were involved in several biological pathways, of which protein processing in the calcium signaling pathway and the mTOR signaling pathway is related to mitochondrial metabolism in PD (Zhu et al., 2019). Thus, it is reasonable to consider that mitochondrial-related exosomal mRNA and lncRNA are implicated in the pathogenesis and rehabilitation of PD.

One DEmRNA of interest (NDUFB7) and three related DElncRNAs were selected to explore the potential role of the mRNA and lncRNAs in this process. NDUFB7 mRNA, encoding a subunit of reduced NADH dehydrogenase-ubiquinone oxidoreductase (complex I), was positively related to three DElncRNAs. Previous reports were consistent in describing a selective deficiency of respiratory chain complex I in the substantia nigra (SN) of PWPs (Janetzky et al., 1994). Adenosine triphosphate is generated through the mitochondrial electron transport chain (ETC) and the oxidative-phosphorylation system (Perier and Vila, 2012). In the process of oxidative phosphorylation, complex I works as the entry point for electrons being transmitted from mitochondrial matrix to the ETC by catalyzing the electron transfer from NADH into the ETC subunits (Subramaniam and Chesselet, 2013). A reduction in electron transfer capacity was observed in patients with PD

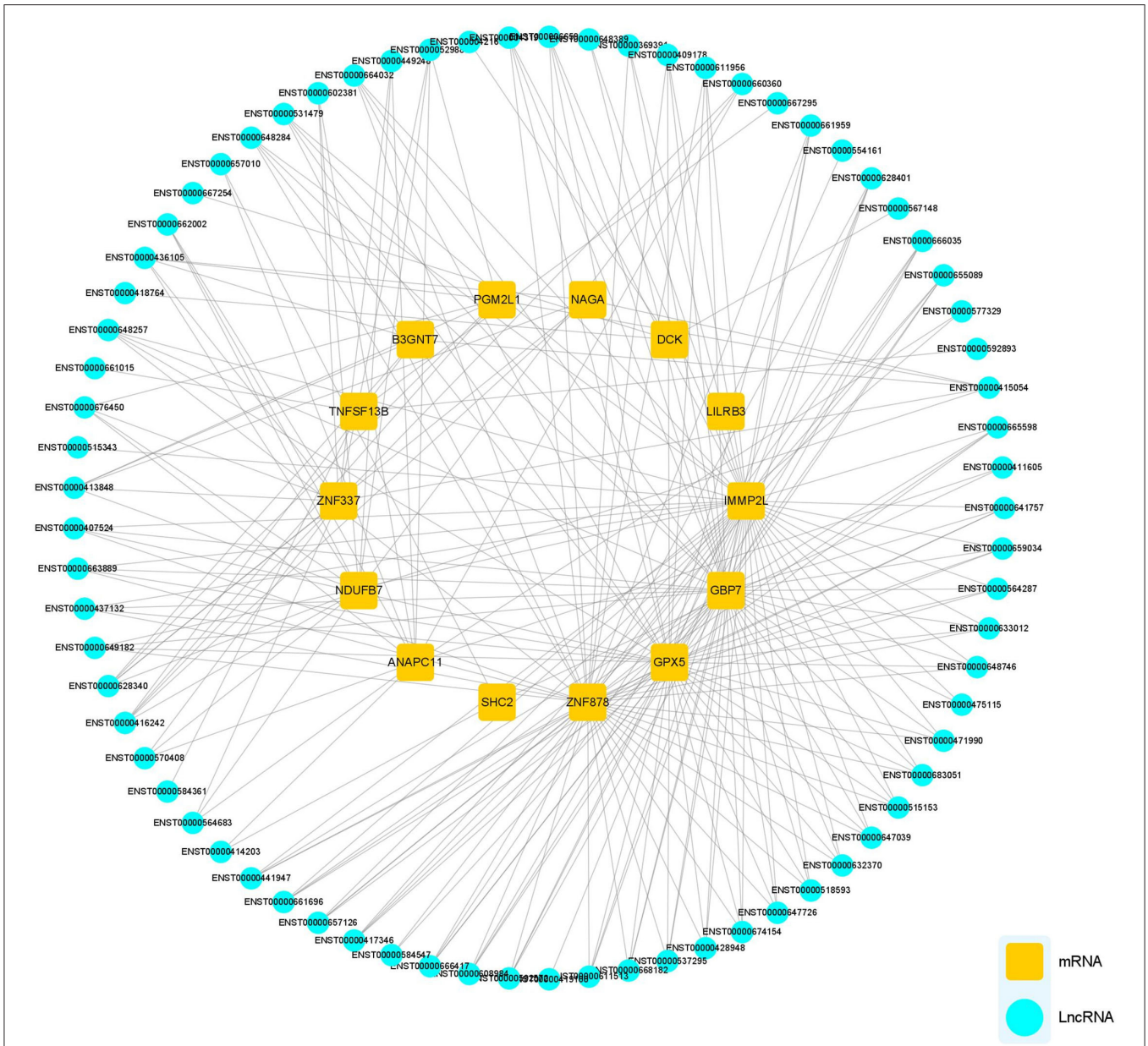

FIGURE 6 | lncRNA-mRNA Co-expression network analysis. lncRNA-mRNA co-expression networks contained 87 nodes, including 73 lncRNAs and 14 mRNA DEmRNAs which were positively related. lncRNAs, long noncoding RNAs; mRNA, messenger RNA; DElncRNAs, differentially expressed lncRNAs; DEmRNAs, differentially expressed mRNAs.

indicating that oxidative damage to mitochondria may result in complex I impairment (Keeney et al., 2006). MPTP (1-Methyl-4-phenyl-1,2,5,6-tetrahydropyridine) induced inhibition of mitochondrial CI, and subsequent DA neuronal loss has been reproduced in mammalian models such as primates and mice. Post-mortem studies have suggested a complex I deficiency in the SN of patients with PD, reflecting the mitochondrial injury of the neuronal cells (Subrahmanian and Lavoie, 2021). So, we assumed that mitochondrial pathway of NDUFB7 mRNA may be involved in the rehabilitation of PD. Some lncRNAs also play an important role in PD by promoting or inhibiting translation (Chen Y. et al., 2021). In our study, the selected lncRNAs positively regulated the selected mRNA, suggesting that the lncRNAs also play important roles in expression and regulation of the genes implicated in PD rehabilitation. However, exosomal lncRNAs have not been investigated in depth and little is known about the role of exosomal lncRNAs in the pathogenesis of PD.

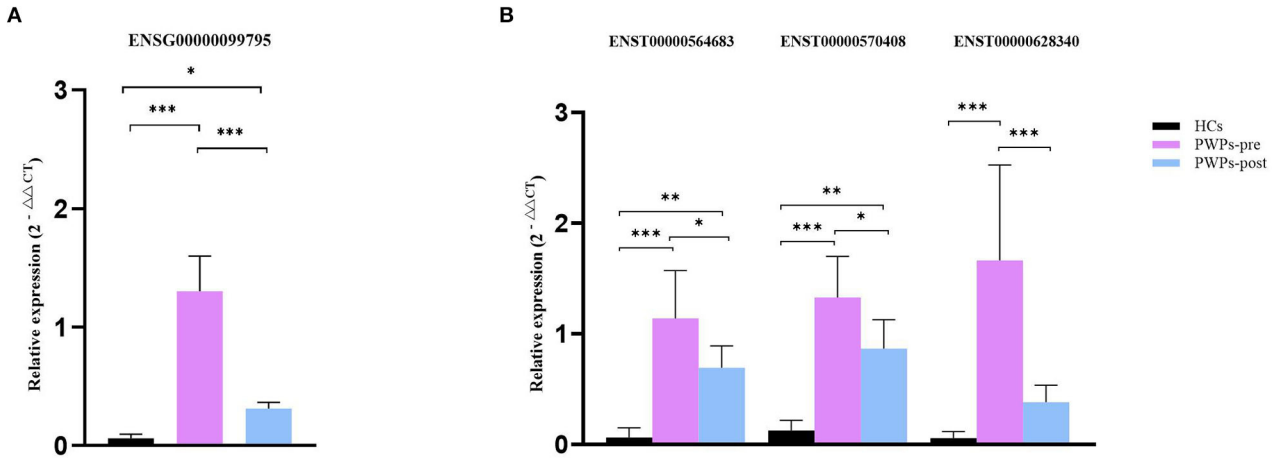

FIGURE 7 | qRT-PCR validation of differentially expressed mRNA and lncRNAs. qRT-PCR verification of the expression profiles of NDUFB7 mRNA **(A)** and 3 related lncRNAs **(B)** in HCs, pre- and post-rehab PWPs. $^{*}P < 0.05$, $^{**}P < 0.01$, $^{***}P < 0.001$. Pre-rehab, pre-rehabilitation; post-rehab, post-rehabilitation; PWPs, patients with Parkinson's disease.

The qRT-PCR validation for the DEmRNA of interest and related DElncRNAs revealed upregulated expression level of NDUFB7 in pre-rehab PWPs compared to post-rehab PWPs. The release of damage-related molecules of mitochondria is a potential mechanism connecting mitochondrial dysfunction with systemic inflammation in the setting of various diseases, such as PD (Currim et al., 2021). A previous study indicated that mildly damaged mitochondria were primed by serine/threonine-protein kinase PINK1 and Parkin and generated mitochondrial-derived vesicles (MDVs; Mclelland et al., 2014). MDVs containing mitochondrial components are secret out of the endolysosomal system and are released into the extracellular compartment as exosomes (Matheoud et al., 2016). Therefore, we suppose that the benefits of rehabilitation for PWPs may involve the restoration of mitochondrial function, and NDUFB7 is a potential biomarker for the evaluation of the effect of PD rehabilitation.

Several limitations may affect the interpretation of our findings. The insufficient sample size in our study may undermine our conclusion. More convincing evidence is required to validate the conclusion with a larger sample size. Our results suggested downregulated expression of NDUFB7 mRNA in favor of the post-rehab PWPs, but the difference between pre-rehab and post-rehab PWPs was not statistically significant. Better baseline motor function of PWPs may be partially responsible for this phenomenon. The functions of DElncRNAs were only predicted through the co-expression analyses. The precise underlying mechanisms have not been clarified yet. Additional studies are required to investigate the exact roles of exosomal lncRNAs in PD. Future research will clarify how NDUFB7 may contribute to PD pathogenesis and how rehabilitation treatment down-regulates NDUFB7 expression at cellular and animal levels.

CONCLUSION

NDUFB7 mRNA and three related lncRNAs are potentially associated with the rehabilitation of PD by restoring mitochondrial function. These findings provide valuable insight into the potential biomarkers pertinent for evaluating the treatment strategies for PD.

DATA AVAILABILITY STATEMENT

The data presented in the study can be found in online repositories. The names of the repository/repositories and accession number(s) can be found below: https://ngdc.cncb.ac.cn/gsa-human/, HRA002383.

ETHICS STATEMENT

The studies involving human participants were reviewed and approved by the Ethics Committee of Beijing Rehabilitation Hospital of Capital Medical University (2020bkky010). The patients/participants provided their written informed consent to participate in this study.

AUTHOR CONTRIBUTIONS

BF conceived and designed the study. YL and YW performed the experiments and statistical analysis. YL, ZJ, CL, XY, and KC collected patients' data. YW wrote the first draft of the manuscript. BF, AL, ZJ, and DM reviewed and edited the manuscript. All authors contributed to the manuscript revision and read and approved the submitted version.

FUNDING

This study was supported by the Science and Technology Development Fund of Beijing Rehabilitation Hospital, Capital Medical University (2019-023 to YL, 2020-069 to BF, and 2020R-001 to YW). The funding body had no role in study design, statistical analysis, and manuscript preparation.

SUPPLEMENTARY MATERIAL

The Supplementary Material for this article can be found online at: https://www.frontiersin.org/articles/10.3389/fnagi.2022.909622/full#supplementary-material

Supplementary Figure 1 | Identification of exosomes. Transmission electron microscopy. White arrow heads point to exosome **(A)**. Western blotting exosomes are positive for CD9 **(B)** and CD81 **(C)**.

REFERENCES

Ashburn, A., Fazakarley, L., Ballinger, C., Pickering, R., Mclellan, L. D., and Fitton, C. (2007). A randomised controlled trial of a home based exercise programme to reduce the risk of falling among people with Parkinson's disease. *J. Neurol. Neurosurg. Psychiatry.* 78, 678–84. doi: 10.1136/jnnp.2006.099333

Bloem, B. R., Okun, M. S., and Klein, C. (2021). Parkinson's disease. *Lancet.* 397, 2284–2303. doi: 10.1016/S0140-6736(21)00218-X

Cao, X. Y., Lu, J. M., Zhao, Z. Q., Li, M. C., Lu, T., and An, X. S. (2017). MicroRNA biomarkers of Parkinson's disease in serum exosome-like microvesicles. *Neurosci. Lett.* 644, 94–99. doi: 10.1016/j.neulet.2017.02.045

Chen, K. K., Jin, Z. H., Gao, L., Qi, L., Zhen, Q. X., and Liu, C. (2021). Efficacy of short-term multidisciplinary intensive rehabilitation in patients with different Parkinson's disease motor subtypes: a prospective pilot study with 3-month follow-up. *Neural. Regen. Res.* 16, 1336–1343. doi: 10.4103/1673-5374.301029

Chen, Y., Li, Z., Chen, X., and Zhang, S. (2021). Long non-coding RNAs: From disease code to drug role. *Acta. Pharm. Sin. B.* 11, 340–354. doi: 10.1016/j.apsb.2020.10.001

Cheng, P., Feng, F., Yang, H., Jin, S., Lai, C., and Wang, Y. (2021). Detection and significance of exosomal mRNA expression profiles in the cerebrospinal fluid of patients with meningeal carcinomatosis. *J. Mol. Neurosci.* 71, 790–803. doi: 10.1007/s12031-020-01701-w

Chung, C. L., Mak, M. K., and Hallett, M. (2020). Transcranial Magnetic Stimulation Promotes Gait Training in Parkinson Disease. *Ann. Neurol.* 88, 933–945. doi: 10.1002/ana.25881

Conradsson, D., Lofgren, N., Nero, H., Hagstromer, M., Stahle, A., and Lokk, J. (2015). The effects of highly challenging balance training in elderly with Parkinson's disease: a randomized controlled trial. *Neurorehabil. Neural. Repair.* 29, 827–36. doi: 10.1177/1545968314567150

Currim, F., Singh, J., Shinde, A., Gohel, D., Roy, M., and Singh, K. (2021). Exosome release is modulated by the mitochondrial-lysosomal crosstalk in Parkinson's disease stress conditions. *Mol. Neurobiol.* 58, 1819–1833. doi: 10.1007/s12035-020-02243-3

Deng, T., Zhang, H., Yang, H., Wang, H., Bai, M., and Sun, W. (2020). Exosome miR-155 Derived from Gastric Carcinoma Promotes Angiogenesis by Targeting the c-MYB/VEGF Axis of Endothelial Cells. *Mol. Ther. Nucleic. Acids.* 19, 1449–1459. doi: 10.1016/j.omtn.2020.01.024

Doyle, L. M., and Wang, M. Z. (2019). Overview of extracellular vesicles, their origin, composition, purpose, and methods for exosome isolation and analysis. *Cells.* 8. doi: 10.3390/cells8070727

Duncan, R. P., Leddy, A. L., and Earhart, G. M. (2011). Five times sit-to-stand test performance in Parkinson's disease. *Arch. Phys. Med. Rehabil.* 92, 1431–6. doi: 10.1016/j.apmr.2011.04.008

Folstein, M. F., Folstein, S. E., and Mchugh, P. R. (1975). "Mini-mental state". A practical method for grading the cognitive state of patients for the clinician. *J. Psychiatr. Res.* 12, 189–98. doi: 10.1016/0022-3956(75)90026-6

Giardini, M., Nardone, A., Godi, M., Guglielmetti, S., Arcolin, I., and Pisano, F. (2018). Instrumental or Physical-Exercise Rehabilitation of Balance Improves Both Balance and Gait in Parkinson's Disease. *Neural. Plast.* 2018, 5614242. doi: 10.1155/2018/5614242

Goodwin, V. A., Richards, S. H., Taylor, R. S., and Taylor, A. H.Campbell, J. L. (2008). The effectiveness of exercise interventions for people with Parkinson's disease: a systematic review and meta-analysis. *Mov. Disord.* 23, 631–40. doi: 10.1002/mds.21922

Haddad, D., and Nakamura, K. (2015). Understanding the susceptibility of dopamine neurons to mitochondrial stressors in Parkinson's disease. *FEBS. Lett.* 589, 3702–13. doi: 10.1016/j.febslet.2015.10.021

Hoehn, M. M., and Yahr, M. D. (1967). Parkinsonism: onset, progression and mortality. *Neurology.* 17, 427–42. doi: 10.1212/WNL.17.5.427

Janetzky, B., Hauck, S., Youdim, M. B., Riederer, P., Jellinger, K., and Pantucek, F. (1994). Unaltered aconitase activity, but decreased complex I activity in substantia nigra pars compacta of patients with Parkinson's disease. *Neurosci. Lett.* 169, 126–8. doi: 10.1016/0304-3940(94)90372-7

Kalluri, R., and Lebleu, V. S. (2020). The biology, function, and biomedical applications of exosomes. *Science.* 367:eaau6977. doi: 10.1126/science.aau6977

Keeney, P. M., Xie, J., and Capaldi, R. A.Bennett, J. P., Jr. (2006). Parkinson's disease brain mitochondrial complex I has oxidatively damaged subunits and is functionally impaired and misassembled. *J. Neurosci.* 26, 5256–64. doi: 10.1523/JNEUROSCI.0984-06.2006

Kim, J., Inoue, K., Ishii, J., Vanti, W. B., Voronov, S. V., and Murchison, E. (2007). A MicroRNA feedback circuit in midbrain dopamine neurons. *Science.* 317, 1220–4. doi: 10.1126/science.1140481

Koyanagi, Y., Fukushi, I., Nakamura, M., Suzuki, K., Oda, N., and Aita, T. (2021). The effect of body weight-supported overground gait training for patients with Parkinson's disease: a retrospective case-control observational study. *PLoS. One.* 16, e0254415. doi: 10.1371/journal.pone.0254415

Lee, S. W. L., Paoletti, C., Campisi, M., Osaki, T., Adriani, G., and Kamm, R. D. (2019). MicroRNA delivery through nanoparticles. *J. Control. Release.* 313, 80–95. doi: 10.1016/j.jconrel.2019.10.007

Macdonald, R., Barnes, K., Hastings, C., and Mortiboys, H. (2018). Mitochondrial abnormalities in Parkinson's disease and Alzheimer's disease: can mitochondria be targeted therapeutically? *Biochem. Soc. Trans.* 46, 891–909. doi: 10.1042/BST20170501

Matheoud, D., Sugiura, A., Bellemare-Pelletier, A., Laplante, A., Rondeau, C., and Chemali, M. (2016). Parkinson's Disease-Related Proteins PINK1 and Parkin Repress Mitochondrial Antigen Presentation. *Cell.* 166, 314–327. doi: 10.1016/j.cell.2016.05.039

Mclelland, G. L., Soubannier, V., Chen, C. X., and Mcbride, H. M.Fon, E. A. (2014). Parkin and PINK1 function in a vesicular trafficking pathway regulating mitochondrial quality control. *EMBO. J.* 33, 282–95. doi: 10.1002/embj.201385902

Meng, D., Jin, Z., Gao, L., Wang, Y., Wang, R., and Fang, J. (2022). The quality of life in patients with Parkinson's disease: Focus on gender difference. *Brain. Behav. e*2517. doi: 10.1002/brb3.2517

Ntetsika, T., and Papathoma, P. E.Markaki, I. (2021). Novel targeted therapies for Parkinson's disease. *Mol. Med.* 27, 17. doi: 10.1186/s10020-021-00279-2

Perier, C., and Vila, M. (2012). Mitochondrial biology and Parkinson's disease. *Cold. Spring. Harb. Perspect. Med.* 2, a009332. doi: 10.1101/cshperspect.a009332

Pinnell, J. R., Cui, M., and Tieu, K. (2021). Exosomes in Parkinson disease. *J. Neurochem.* 157, 413–428. doi: 10.1111/jnc.15288

Postuma, R. B., Berg, D., Stern, M., Poewe, W., Olanow, C. W., and Oertel, W. (2015). MDS clinical diagnostic criteria for Parkinson's disease. *Mov. Disord.* 30, 1591–601. doi: 10.1002/mds.26424

Puspita, L., and Chung, S. Y.Shim, J. W. (2017). Oxidative stress and cellular pathologies in Parkinson's disease. *Mol. Brain.* 10, 53. doi: 10.1186/s13041-017-0340-9

Subrahmanian, N., and Lavoie, M. J. (2021). Is there a special relationship between complex I activity and nigral neuronal loss in Parkinson's disease? A critical reappraisal. *Brain. Res.* 1767, 147434. doi: 10.1016/j.brainres.2021.147434

Subramaniam, S. R., and Chesselet, M. F. (2013). Mitochondrial dysfunction and oxidative stress in Parkinson's disease. *Prog. Neurobiol.* 106-107, 17–32. doi: 10.1016/j.pneurobio.2013.04.004

Sumec, R., Rektorova, I., Jech, R., Mensikova, K., Roth, J., and Ruzicka, E. (2017). Motion and emotion: anxiety-axial connections in Parkinson's disease. *J. Neural. Transm. (Vienna).* 124, 369–377. doi: 10.1007/s00702-016-1652-0

Tansey, M. G., and Goldberg, M. S. (2010). Neuroinflammation in Parkinson's disease: its role in neuronal death and implications for therapeutic intervention. *Neurobiol. Dis.* 37, 510–8. doi: 10.1016/j.nbd.2009.11.004

Tao, P., Shao, X., Zhuang, J., Wang, Z., Dong, Y., and Shen, X. (2021). Translation, cultural adaptation, and reliability and validity testing of a chinese version of the Freezing of Gait Questionnaire (FOGQ-CH). *Front. Neurol.* 12, 760398. doi: 10.3389/fneur.2021.760398

Van Der Pol, E., Boing, A. N., Harrison, P., Sturk, A., and Nieuwland, R. (2012). Classification, functions, and clinical relevance of extracellular vesicles. *Pharmacol. Rev.* 64, 676–705. doi: 10.1124/pr.112.005983

Van Steenoven, I., Aarsland, D., Hurtig, H., Chen-Plotkin, A., Duda, J. E., and Rick, J. (2014). Conversion between mini-mental state examination, montreal cognitive assessment, and dementia rating scale-2 scores in Parkinson's disease. *Mov. Disord.* 29, 1809–15. doi: 10.1002/mds.26062

Vella, L. J., and Hill, A. F.Cheng, L. (2016). Focus on Extracellular Vesicles: Exosomes and Their Role in Protein Trafficking and Biomarker Potential in Alzheimer's and Parkinson's Disease. *Int. J. Mol. Sci.* 17, 173. doi: 10.3390/ijms17020173

Venderova, K., and Park, D. S. (2012). Programmed cell death in Parkinson's disease. *Cold. Spring. Harb. Perspect. Med.* 2. doi: 10.1101/cshperspect.a009365

Wang, Q., Han, C. L., Wang, K. L., Sui, Y. P., Li, Z. B., and Chen, N. (2020). Integrated analysis of exosomal lncRNA and mRNA expression profiles reveals the involvement of lnc-MKRN2-42:1 in the pathogenesis of Parkinson's disease. *CNS. Neurosci. Ther.* 26, 527–537. doi: 10.1111/cns.13277

Xu, X., Fu, Z., and Le, W. (2019). Exercise and Parkinson's disease. *Int. Rev. Neurobiol.* 147, 45–74. doi: 10.1016/bs.irn.2019.06.003

Zhang, X., Zhou, J. Y., Chin, M. H., Schepmoes, A. A., Petyuk, V. A., and Weitz, K. K. (2010). Region-specific protein abundance changes in the brain of MPTP-induced Parkinson's disease mouse model. *J. Proteome. Res.* 9, 1496–509. doi: 10.1021/pr901024z

Zhao, L., Han, C., Zheng, Z., and Xiu, S. L.Chan, P. (2020). Risk of mini-mental state examination (MMSE) decline in the elderly with type 2 diabetes: a Chinese community-based cohort study. *BMC. Endocr. Disord.* 20, 129. doi: 10.1186/s12902-020-00606-4

Zhu, Z., Yang, C., Iyaswamy, A., Krishnamoorthi, S., Sreenivasmurthy, S. G., and Liu, J. (2019). Balancing mTOR Signaling and Autophagy in the Treatment of Parkinson's Disease. *Int. J. Mol. Sci.* 20:728. doi: 10.3390/ijms20030728

Conflict of Interest: The authors declare that the research was conducted in the absence of any commercial or financial relationships that could be construed as a potential conflict of interest.

Publisher's Note: All claims expressed in this article are solely those of the authors and do not necessarily represent those of their affiliated organizations, or those of the publisher, the editors and the reviewers. Any product that may be evaluated in this article, or claim that may be made by its manufacturer, is not guaranteed or endorsed by the publisher.

frontiers | Frontiers in Aging Neuroscience

ORIGINAL RESEARCH
published: 24 June 2022
doi: 10.3389/fnagi.2022.932318

Task-State Cortical Motor Network Characteristics by Functional Near-Infrared Spectroscopy in Subacute Stroke Show Hemispheric Dominance

Ziwen Yuan[1,2], Weiwei Xu[1], Jiameng Bao[1], Hui Gao[3], Wen Li[1], Yu Peng[2], Lisha Wang[1,2], Ye Zhao[1,2], Siming Song[2], Jin Qiao[2] and Gang Wang[1]**

[1] Key Laboratory of Biomedical Information Engineering of Ministry of Education, Institute of Biomedical Engineering, School of Life Sciences and Technology, Xi'an Jiaotong University, Xi'an, China, [2] Department of Rehabilitation, First Affiliated Hospital of Xi'an Jiaotong University, Xi'an, China, [3] College of Biomedical Engineering and Instrument Science, Zhejiang University, Hangzhou, China

OPEN ACCESS

Edited by:
Chuhuai Wang,
Sun Yat-sen University, China

Reviewed by:
Hongbo Xie,
Queensland University of Technology, Australia
Zhen Yuan,
University of Macau, Macao SAR, China
Xianglin Zheng,
University of South Australia, Australia

***Correspondence:**
Jin Qiao
qiaojn123@163.com
Gang Wang
ggwang@xjtu.edu.cn

Specialty section:
This article was submitted to Neurocognitive Aging and Behavior, a section of the journal Frontiers in Aging Neuroscience

Received: *29 April 2022*
Accepted: *06 June 2022*
Published: *24 June 2022*

Citation:
Yuan Z, Xu W, Bao J, Gao H, Li W, Peng Y, Wang L, Zhao Y, Song S, Qiao J and Wang G (2022) Task-State Cortical Motor Network Characteristics by Functional Near-Infrared Spectroscopy in Subacute Stroke Show Hemispheric Dominance. Front. Aging Neurosci. 14:932318. doi: 10.3389/fnagi.2022.932318

Background: There was a reorganization of the brain network after stroke. Some studies have compared the characteristics of activation or functional connectivity (FC) of cortical and subcortical regions between the dominant and non-dominant hemisphere stroke.

Objectives: To analyze hemispheric dominance differences in task-state motor network properties in subacute stroke by functional near-infrared spectroscopy (fNIRS).

Materials and Methods: Patients with first ischemic stroke in the basal ganglia within 1–3 months after onset and age- and sex-matched right-handed healthy subjects (HS) were enrolled. fNIRS with 29 channels was used to detect the oxyhemoglobin concentration changes when performing the hand grasping task. Activation patterns of motor cortex and two macroscale and two mesoscale brain network indicators based on graph theory were compared between dominant and non-dominant hemisphere stroke.

Results: We enrolled 17 subjects in each of left hemisphere stroke (LHS), right hemisphere stroke (RHS), and HS groups. Both patient groups showed bilateral activation. The average weighted clustering coefficient and global efficiency of patients were lower than those of healthy people, and the inter-density was higher than that of the HS group, but the significance was different between LHS and RHS groups. The intra-density changes in the RHS group were opposite to those in the LHS group. The correlation between mesoscale indicators and motor function differed between dominant and non-dominant hemisphere stroke.

Conclusion: The changes in macroscale cortical network indicators were similar between the two patient groups, while those of the mesoscale indicators were different. The mesoscale brain network characteristics were affected by the severity of dysfunction to varying degrees in the LHS and RHS patients.

Keywords: hemispheric dominance, fNIRS, brain network, motor, task-state, stroke

INTRODUCTION

The brain has plasticity, and makes adaptive changes after stroke, resulting in the reorganization and compensation of neural networks (Carlson et al., 2020). The mechanism of motor function rehabilitation and brain motor network remodeling after stroke has always been a research hotspot. The activation of the primary motor cortex (M1) of the affected hemisphere was weakened when the affected hand performs simple movements after stroke, while the ipsilateral premotor cortex (PMC), supplementary motor area (SMA), and the contralesional motor areas were activated to varying degrees according to the location and size of the injury (Shimizu et al., 2002; Calautti et al., 2003). Its physiological basis may be that in addition to most of the projection fibers from the M1 area, the corticospinal tract also includes projections from the PMC, SMA, parietal lobes, and other cortices, and about 10–15% of the corticospinal tract fibers do not cross (Kato et al., 2002).

Based on the abovementioned physiological mechanisms, neuromodulation techniques such as repetitive transcranial magnetic stimulation (rTMS) have been widely used to promote brain network remodeling after stroke. At present, the most commonly used strategy is the excitatory rTMS on the ipsilesional motor cortex and/or the inhibitory rTMS on the contralesional hemisphere (Harvey et al., 2018; Watanabe et al., 2018; Yang et al., 2021). However, some patients have poor treatment effects. This may be related to the heterogeneity of stroke severity, course, lesion location, and stroke type, and stroke patients with different characteristics may respond differently to stimuli. For example, the state and plasticity of the brain are different during different phases (acute, subacute, or chronic) of stroke (Miyai et al., 2003; Wang et al., 2010; Park et al., 2011). In 2015, a systematic review including 37 studies on the effect of rTMS on the upper extremity function after stroke found that low-frequency rTMS on the uninjured hemisphere had a better effect on chronic stroke, and high-frequency rTMS on the injured hemisphere had a better effect on acute stroke (Ludemann-Podubecka et al., 2015a). One study compared the effect of rTMS in patients with different infarct sites and found that facilitative rTMS on the ipsilesional M1 was more effective in patients with subcortical infarction than in patients with cortical infarction (Ameli et al., 2009). In addition, the severity of the disease is a key factor affecting the efficacy. In severely injured patients, inhibition of the contralesional motor area may not be beneficial (McCambridge et al., 2018).

In recent years, studies have found that whether the lesion is located in the dominant hemisphere also affects the effect of rTMS treatment. Ludemann-Podubecka et al. (2015b) found that low-frequency rTMS on the contralesional cortex only improved hand function in patients with lesions in the dominant hemisphere. Therefore, it is necessary to analyze the characteristics of the brain network in the dominant or non-dominant hemisphere stroke to guide rehabilitation treatment. At present, studies have used functional magnetic resonance imaging (fMRI), functional near-infrared spectroscopy (fNIRS), and electroencephalography (EEG) to compare the characteristics of activation or functional connectivity (FC) of cortical and subcortical regions between the dominant and non-dominant hemisphere stroke. For example, two fMRI-based studies analyzed cortical and subcortical activation signatures in acute and chronic stroke patients and found that they were dependent on hemisphere (Liew et al., 2018; Vidal et al., 2018). Caliandro et al. (2017) analyzed the small-world properties of resting-state brain networks by EEG in acute stroke patients, and found similar outcomes for left and right hemisphere strokes (RHSs) in delta and alpha rhythms, but in the theta rhythm, bilaterally decreased small-worldness was observed only in the left hemisphere stroke (LHS). Another two studies used fNIRS to investigate post-stroke FC changes and also found that there were differences in whether or not the dominant hemisphere stroke (Lu et al., 2019; Arun et al., 2020). However, there was no study to compare the task-state brain network characteristics between left and RHS. Considering the needs of the motor task and the advantages of fNIRS (portability, tolerance to head motion, better spatial resolution than EEG, and better temporal resolution than fMRI) (Harrivel et al., 2013; Chen et al., 2020), we used fNIRS to capture hemispheric dominance differences in task-state motor network characteristics in patients with subacute ischemic stroke.

MATERIALS AND METHODS

Participants

While brain functional compensation in the acute phase of stroke is passive or transient (Bonkhoff et al., 2020), we included stroke patients in the subacute phase to observe the actively established and relatively stable functional connections. In addition, because hemodynamic responses measured by fNIRS may be affected by brain artery occlusion and lesion location, only patients with stroke in the basal ganglia were enrolled. The main inclusion criteria were as follows: (1) Age 40–79 years; (2) First ischemic stroke in the basal ganglia within 1–3 months after onset; (3) Right-handed according to the Edinburg Handedness scale; (4) Brunnstrom stage (hand) II or above; and (5) Can cooperate with the fNIRS assessment. Exclusion criteria were as follows: (1) Be afraid of the dark; (2) Severely impaired cognition or inability to pay attention to the computer screen; and (3) Visible movements

of other limbs other than the task hand were observed during the task state collection. A total of 28 LHS and 31 RHS patients were screened from our ongoing trial "Dynamic Individualized rTMS Based on fNIRS" in our rehabilitation center (*clinicaltrials.gov*: NCT04617366), and they were divided into LHS group and RHS group. In addition, age- (difference <5 years) and sex-matched right-handed healthy subjects (HS) without motor dysfunction were recruited.

The study was approved by the Ethics Committee of the First Affiliated Hospital of Xi'an Jiaotong University on 25 March 2020 (No. 2020 G-103), and all patients or their authorized agents have signed informed consent.

Functional Near-Infrared Spectroscopy Measurement

The acquisition was performed using the NirSmart system (Danyang Huichuang Medical Equipment Co., Ltd., China) having 12 sources and eight detectors at a sampling rate of 10 Hz in a quiet and relatively darker room. The wavelengths used were 730 and 850 nm. The montage of the probes is shown in **Figure 1**. The S1 probe was placed at the Cz point (10/20 international system), and a total of 29 channels were formed with a fixed 3 cm inter-probe distance. The area covered by the probes included three regions of interest (ROI) both in the left and right hemispheres: (SMA; Left: Channel 1, 5, 6, 16; Right: Channel 1, 5, 7, 20), premotor area (PMC; Left: Channel 17, 18, 19, 24, 26, 27; Right: Channel 21, 22, 23, 25, 28, 29), and primary sensorimotor area (SM1; Left: Channel 2, 3, 8, 9, 12, 13; Right: Channel 2, 4, 10, 11, 14, 15). The Fugl-Meyer Assessment (FMA) of upper limbs (FMA-UL) was performed on the day of the fNIRS measurement. A dedicated physician was assigned to perform the FMA assessment for all patients.

Task Paradigm

All subjects were asked to remain at a resting state before performing the measurement. After communicating with the subjects about the measurement procedure, speaking was prohibited. In the resting state, the subjects remained relaxed in a sitting position, with their palms up on the legs, and the photograph of the stationary hand was observed on the computer screen for 180 s. Next was the task state, in which the patient only performed the affected hand grasping, and the HS group performed both the left (HS-L) and right hand (HS-R) tasks. The task included five trails with no gaps, and each trial included a 25 s resting block and a 20 s task block. The rules of resting-block were the same as the resting-state, and in the task-block, the subjects were taught to follow the video to perform the hand grasping task (1 Hz) while keeping the ipsilateral upper and forearm and other limbs relaxed and still.

Data Pre-processing

The NirSpark software package (Danyang Huichuang Medical Equipment Co., Ltd., China) was used to process fNIRS data. First, we converted the raw optical intensity data to optical density data. Second, we used a bandpass filter at 0.01–0.20 Hz to remove physiological noise (heart rate and respiration). Then, spline interpolation was used three times to remove motion artifacts (Scholkmann et al., 2010). Finally, the denoised optical density data were converted into hemoglobin concentration data. It has been shown that oxyhemoglobin (HbO) concentration was considered to have a better signal-to-noise ratio than deoxyhemoglobin (HbR) concentration (Strangman et al., 2002); therefore, we used HbO concentration for subsequent analysis.

Activation and Lateralization Index

The general linear model (GLM) was used to analyze hemodynamic time series in task blocks to evaluate the activations. The significantly activated channels in the task state compared with the resting state were obtained by one-sample *t*-test and FDR correction.

The lateralization index (LI) was calculated based on the mean HbO concentration in the MS1 region of both hemispheres. For example, the LI formula during the left hand task is given as follows:

$$\mathrm{LI} = \frac{\mathrm{Right} - \mathrm{Left}}{\mathrm{Right} + \mathrm{Left}} \tag{1}$$

The range of LI scores is −1 to 1, where 1 means only right hemisphere activation, and −1 means only left hemisphere activation. Besides, the activation patterns were categorized as bilateral ($|\mathrm{LI}| \leq 0.1$), hemisphere dominant ($0.1 < |\mathrm{LI}| < 0.2$), or hemisphere lateralized ($|\mathrm{LI}| \geq 0.2$) (Jansen et al., 2006).

Brain Network Analysis

We conducted brain network analysis by graph theory, treating the 29 channels as nodes in a graph. First, Pearson correlation analysis was used to calculate the correlation coefficient of time series in task blocks between 29 channels (Equation 2) (Yu et al., 2020). Then, a 29 × 29 correlation matrix (or FC matrix) was established with the averaged correlation coefficients of the five task blocks. A Fisher's z transformation was further applied to the correlation matrix to convert the sampling distribution of ρ to the normal distribution (Nguyen et al., 2018).

$$\rho_{i,j} = \frac{\sum_{n=1}^{N}\left(y_{i,n} - \overline{y_i}\right)\left(y_{j,n} - \overline{y_j}\right)}{\sqrt{\sum_{n=1}^{N}\left(y_{i,n} - \overline{y_i}\right)^2}\sqrt{\sum_{n=1}^{N}\left(y_{j,n} - \overline{y_j}\right)^2}} \tag{2}$$

where y_i represents the time series of all sampling points (N) of the channel i, $y_{i,n}$ represents the time series of a sampling point n of the channel i; $\rho_{i,j}$ represents the Pearson correlation coefficient between the channel i and j, the range is −1 to 1, where 1 means that the two channels have a perfectly positive correlation and −1 means that the two channels have a completely negative correlation.

Next, the proportional thresholding (10–50% network sparsity) was applied to exclude weak or irrelevant FC from the analysis of the graph (Duan et al., 2012), and a total of nine brain networks under corresponding sparsity thresholds were constructed. When the percentile of the correlation coefficient between two nodes among all correlation coefficients in the network was greater than the threshold, the connections between nodes were considered valid. Each

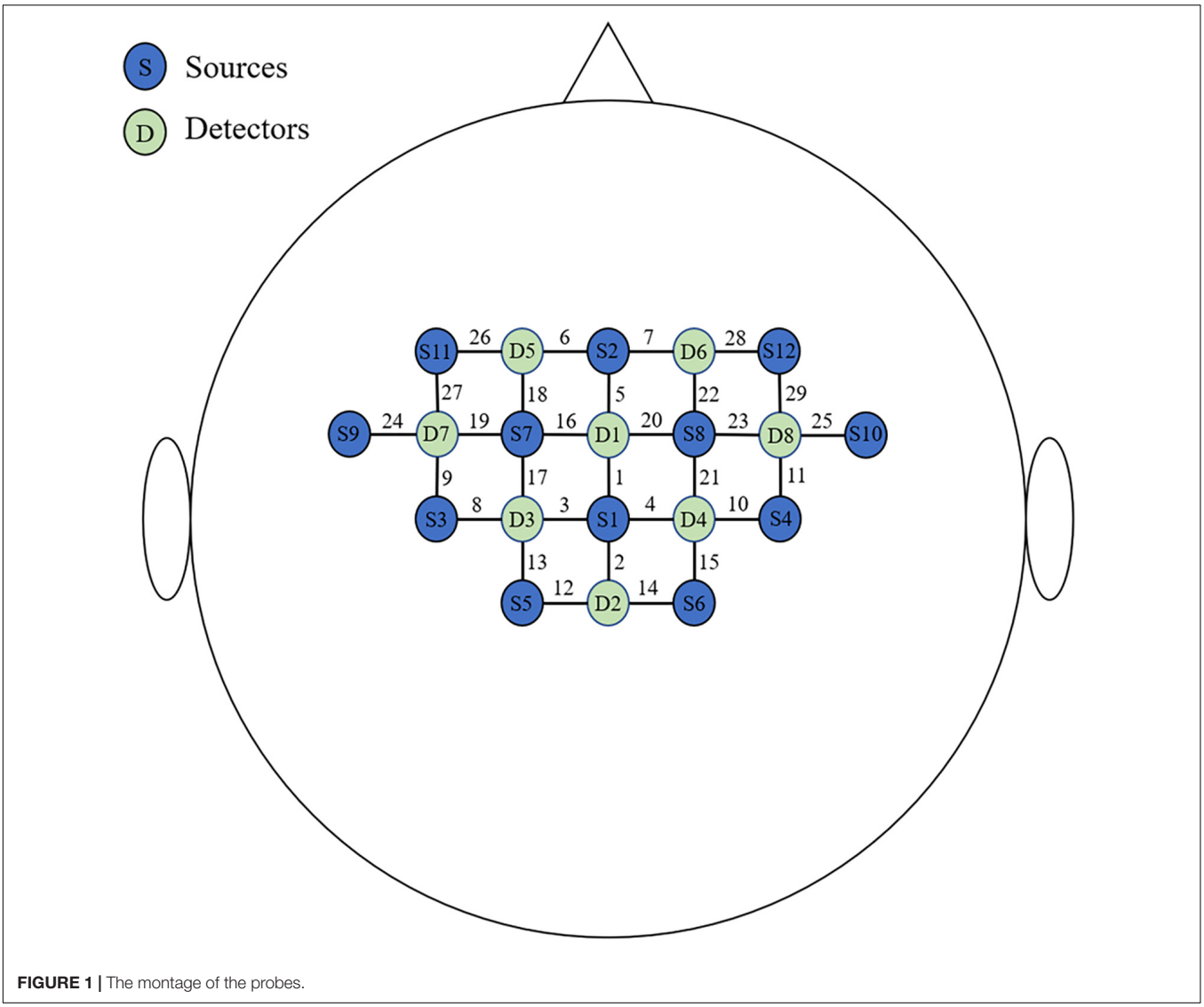

FIGURE 1 | The montage of the probes.

remaining connection was identified as an edge of the graph, and the correlation coefficient was the weight of the connection between nodes ($w_{i,j}$); thus, an undirected weighted graph was constructed. Four most commonly used graph-theoretic indicators were selected to describe the network characteristics: macroscale average weighted clustering coefficient (C) and global efficiency (E) (Mazrooyisebdani et al., 2018) and the inter-density (K-inter) and intra-density (K-intra) at the mesoscale (De Vico Fallani et al., 2013).

(1) Average weighted clustering coefficient (C)

The C represents the degree to which the nodes in the graph tend to cluster and is a measure of the local separation of the graph. The higher is the C, the higher is the degree of segregation (or specialization). The formula of weighted clustering coefficient of a node i is given as follows:

$$c_i = \frac{1}{k_i\left(k_i-1\right)}\sum_{j,k}\left(w_{i,j}w_{j,k}w_{k,i}\right)^{\frac{1}{3}} \quad (3)$$

where k_i represents the degree of a node i.

Then, the C of a network is calculated as follows:

$$C = \frac{1}{N}\sum_{i\in N} c_i \quad (4)$$

(2) Global efficiency (E)

The E is the inverse property of the shortest path length, which represents the ability of nodes to transmit information and is a measure of the level of integration of the network. The higher is the E, the stronger is the ability of the network to transmit information. The E of a network is calculated as follows:

$$E = \frac{1}{N(N-1)}\sum_{i\in N}\sum_{j\in N, j\neq i} d_{ij}^{-1} \quad (5)$$

where d_{ij} is the shortest path length from node i to j (Equation 6). The higher is the correlation coefficient between two nodes, the shorter is the path length, which is converted by reciprocal

mapping of the weights of connections ($w_{i,j}$).

$$d_{i,j} = \min\{w_{ij}^{-1}\} \quad (6)$$

(3) Inter-density (K-inter)

The K-inter is defined as the ratio of the actual number of connections among all possible connections between two sets (Equation 7). By definition, the K-inter ranges from 0 to 1, with higher K-inter reflecting more inter-hemispheric connectivity.

$$K - inter = \frac{1}{N_S^2} \sum_{i,j \in S_{Ahemi,Uhemi}} a_{i,j} \quad (7)$$

where S (or S_{Ahemi},S_{Uhemi}) represents the set of nodes within the affected hemisphere (Ahemi) and unaffected hemisphere (Uhemi), N_S represents the total number of nodes in the two sets [$N(S_{Ahemi}) = N(S_{Uhemi}) = N_S = 13$], and $a_{i,j}$ represents the connection state of the nodes i and j. The rule is given as follows:

$$a_{i,j} = \begin{cases} 0, & w_{i,j} = 0 \\ 1, & else \end{cases} \quad (8)$$

(4) Intra-density (K-intra)

The K-intra is defined as the proportion of actual connections among all possible connections within a set [$N(S_{Ahemi}) = N(S_{Uhemi}) = N_S = 16$], which also ranges from 0 to 1 (Equation 9). Higher K-intra reflects more intra-hemispheric connectivity.

$$K - intra\,(S) = \frac{2}{N_S(N_S-1)} \sum_{i \neq j \in S} a_{i,j} \quad (9)$$

(5) Area under the curve

For each brain network indicator, a curve was plotted with the ordinate as the network indicator value and the abscissa as the 10–50% sparsity stepped by 5%. Then, we calculated the area under curves (AUCs) over the whole sparsity range for the above network indicators, which may represent the average levels under different sparsity and was used for the following analysis.

Statistical Analysis

The comparison of measurement data between the two groups was performed by two independent-samples t-test or Kruskal–Wallis rank-sum test; the comparison of count data was performed by chi-square test or Fisher's exact test. After testing the normal distribution or homogeneity of variance, the comparison of the AUCs for the brain network indicators between patients and HS was performed using two independent-samples t-test. Then, Spearman correlation analysis (r) was used to analyze the correlation between the AUCs and FMA-UL (and FMA-hand). Furthermore, the generalized additive model (GAM) was used to fit the AUCs and FMA-UL (or FMA-hand) to a smooth curve to evaluate whether there is a threshold effect. Two-sided $\alpha = 0.05$ was used. The sample size was set to be larger than 15 in each group according to the previous related studies. We used Empower (R) (X&Y solutions, Inc., Boston, MA, United States),[1] R software, version 3.1.2,[2] and MATLAB version 2019b (MathWorks, Inc., Natick, MA, United States) for the statistical analyses.

[1] www.empowerstats.com

[2] http://www.r-project.org

RESULTS

Participants' Characteristics

We enrolled 17 right-handed patients with subcortical stroke both in the LHS and RHS groups and 17 HS from November 2020 to July 2021. The mean age of patients was 60.7 ± 9.6 years in both groups, and 56.1 ± 4.3 years in the HS group ($p = 0.022$). Although there was statistical difference of age between patients and HS, it was recognized that the difference of less than 5 years did not have clinical significance. There were five female patients in each group (29.4%). Most patients presented with moderate motor dysfunction in the upper limb. The mean FMA-UL score was 35.8 ± 22.2 (hand part: 7.5 ± 4.6) in the LHS group, and 35.2 ± 17.1 (hand part: 6.2 ± 4.2) in the RHS group, respectively. No significant difference was observed in time from onset to admission, the history of hypertension and diabetes, and other baseline characteristics between the two stroke groups (**Table 1**).

Activation and Lateralization Index

In the HS group, the activation of the contralateral hemisphere was dominant during the hand grasping task. The mean LI of SM1 was 0.436 (SD: 0.240) for the left-hand task, and 0.138 (SD: 0.002) for the right-hand task. Both patient groups showed activation of bilateral hemispheres (LI of SM1: RHS, −0.056 ± 0.002; LHS, 0.015 ± 0.111). We may see that absolute values of LI were both less than 0.1, so the activation pattern was thought to be bilateral (Jansen et al., 2006). In the LHS (dominant side) group, the contralesional PMC and bilateral SM1 were mainly activated in the right-hand grasping task, while the ipsilesional PMC and bilateral SMA, SM1 were mainly activated in the RHS (non-dominant side) group. The significantly activated channels are shown in **Figure 2**.

Brain Network Analysis

Under the 10–50% sparsity threshold, the average weighted clustering coefficient and global efficiency of the two groups of patients were both lower than those of healthy people (**Figures 3A,B,D,E**). The difference was significant for the LHS

TABLE 1 | Baseline characteristics of stroke patients[a].

	LHS	RHS	p
N	17	17	
Age, years	60.2 (8.3)	61.2 (11.0)	0.767[b]
Female	5 (29.4%)	5 (29.4%)	1.000[c]
Time of onset, days	38 (35–47)	34 (32–45)	0.369[d]
FMA-UL	34 (17–62)	33 (21–47)	0.959[d]
FMA-hand	6 (3–13)	4 (3–9)	0.367[d]
Hypertension	12 (70.6%)	13 (76.5%)	1.000[c]
Diabetes	3 (17.6%)	2 (11.8%)	1.000[c]

LHS, left hemisphere stroke; RHS, right hemisphere stroke; FMA, Fugl-Meyer Assessment; FMA-UL, Fugl-Meyer Assessment of upper limbs.

[a] *Values are presented as mean (SD), median (Q1–Q3), or N (%).*

[b] *Evaluated using t-test.*

[c] *Evaluated using Fisher's exact test.*

[d] *Evaluated using Kruskal-Wallis rank sum test.*

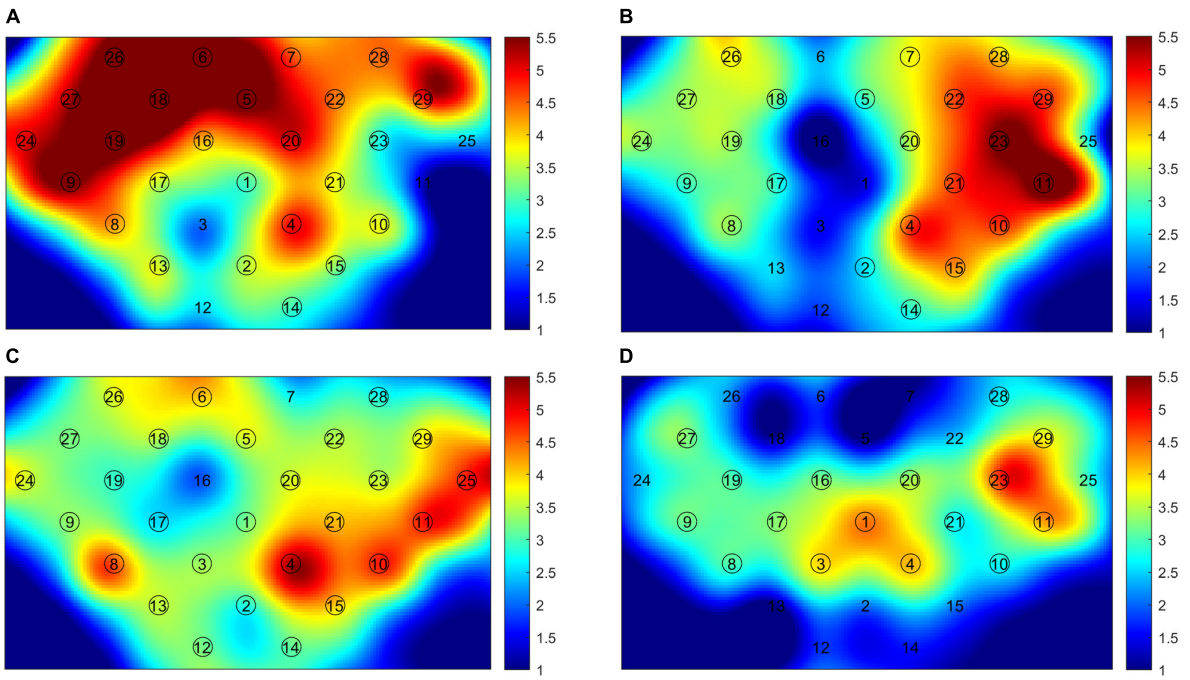

FIGURE 2 | The cerebral cortex activation map. **(A)** Right-hand task of healthy subjects (HS); **(B)** left-hand task of HS; **(C)** right-hand task of left hemisphere stroke (LHS) patients; **(D)** left-hand task of right hemisphere stroke (RHS) patients. The circled channels are significantly activated channels.

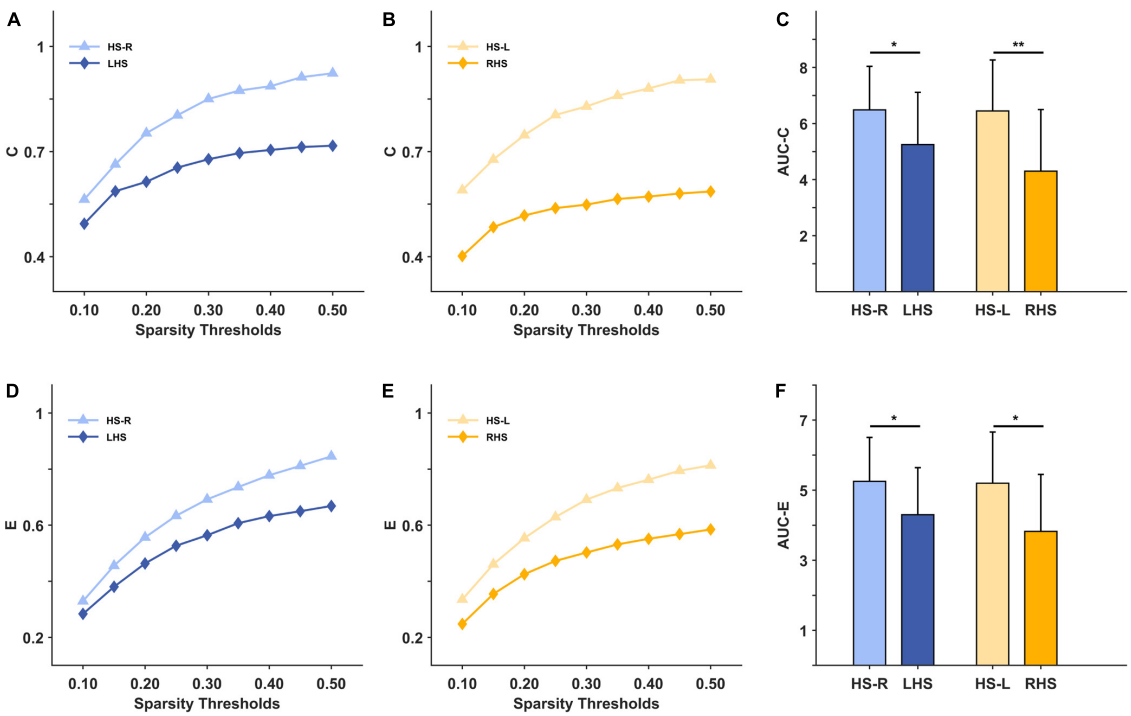

FIGURE 3 | The macroscale brain network indicators under 10–50% sparsity and their area under curves (AUCs) for patients and healthy subjects (HS). **(A)** the average weighted clustering coefficient under 10%-50% sparsity for HS group (right hand task) and LHS group; **(B)** the average weighted clustering coefficient under 10%-50% sparsity for HS group (left hand task) and RHS group; **(C)** the AUCs over the whole sparsity range for the average weighted clustering coefficient in the HS, LHS and RHS groups. **(D–F)** are for the indicator global efficiency. $^{*}p < 0.05$, $^{**}p < 0.01$.

group (C: $p = 0.044$, E: $p = 0.040$), and for the RHS group (C: $p = 0.004$, E: $p = 0.014$) (**Figures 3C,F**). The inter-density in the two groups of patients was higher than that of the HS group, and the difference was significant only in the LHS group (LHS: $p = 0.016$, RHS: $p = 0.396$) (**Figures 4A–C**). The intra-density in the left hemisphere (K-intra.L) of the LHS group was lower than that of the HS group ($p = 0.038$, **Figures 4D,F**); the intra-density in the right hemisphere (K-intra.R) was higher than that of HS group ($p = 0.427$ **Figures 4G,I**). However, the intra-density changes in the RHS group were opposite to those in the LHS group. That is, the intra-density in the affected hemisphere was higher than that of the HS group ($p = 0.639$, **Figures 4H,I**), while that in the unaffected hemisphere was lower ($p = 0.168$, **Figures 4E,F**).

Correlation With Fugl-Meyer Assessment

Correlation analysis was made between AUCs of the network indicators and FMA-UL or FMA-hand (**Table 2**). At large scales, the higher C and E values reflected greater motor function of the upper limb in both groups. But only indicator E in the LHS group was significantly correlated with FMA-UL ($r = 0.524$, $p = 0.031$). At the mesoscale, inter-density and FMA-UL were positively correlated in the LHS group ($r = 0.304$, $p = 0.235$) and slightly correlated in the RHS group ($r = -0.027$, $p = 0.918$). In the LHS

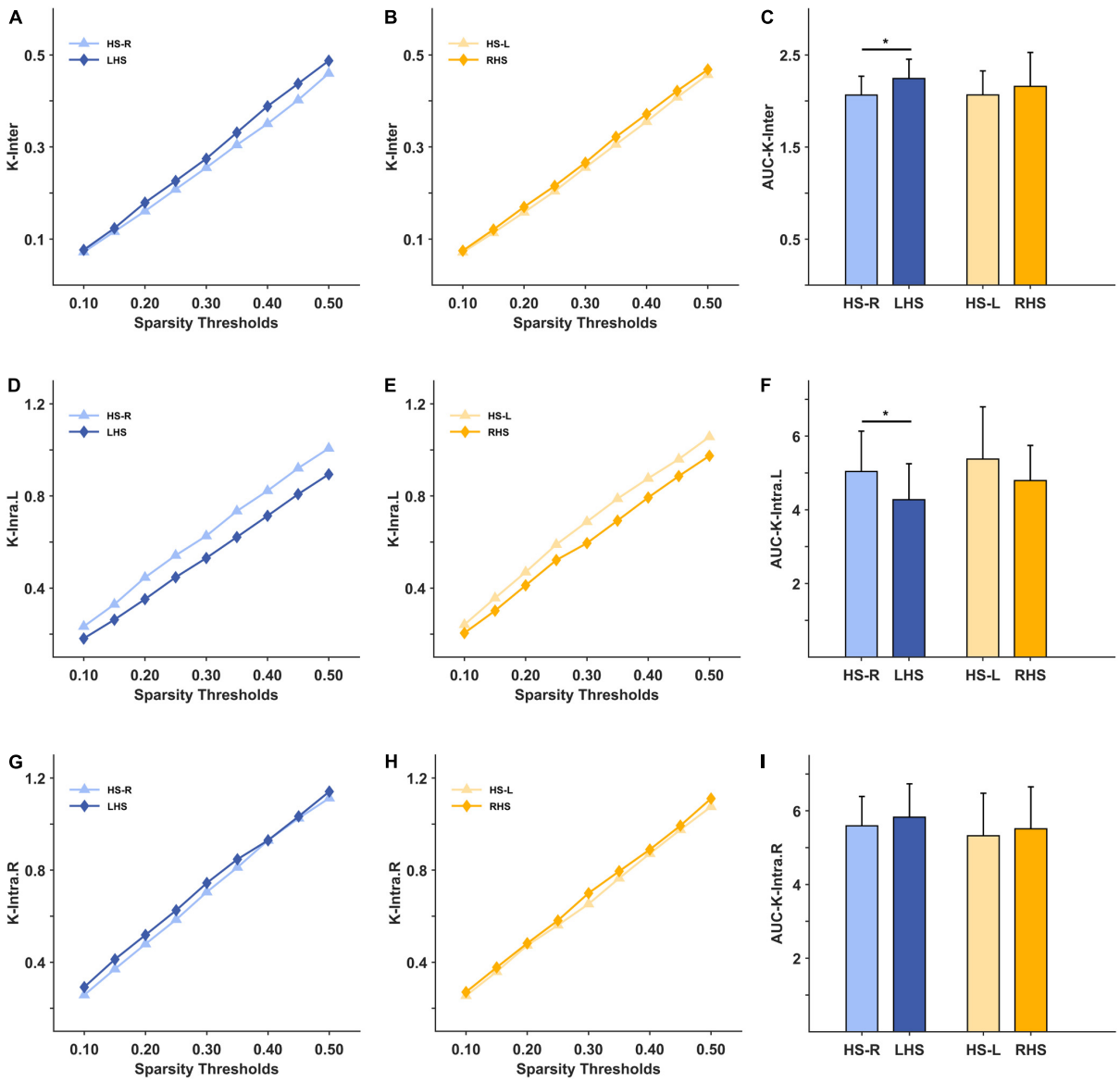

FIGURE 4 | The mesoscale brain network indicators under 10–50% sparsity and their area under curves (AUCs) for patients and healthy subjects (HS). **(A)** The inter-density under 10%–50% sparsity for HS group (right hand task) and LHS group; **(B)** the inter-density under 10%–50% sparsity for HS group (left hand task) and RHS group; **(C)** the AUCs over the whole sparsity range for the inter-density in the HS, LHS and RHS groups. **(D–F)** are for the indicator intra-density of left hemisphere; **(G–I)** are for the indicator intra-density of right hemisphere. *$p < 0.05$.

TABLE 2 | Spearman correlation coefficients (*r*) of the AUC of brain network indicators and FMA.

		FMA-UL		FMA-hand	
		r	*p*	*r*	*p*
C	LHS	0.367	0.147	0.324	0.205
	RHS	0.253	0.3288	0.319	0.212
E	LHS	0.524	0.031	0.458	0.064
	RHS	0.326	0.201	0.408	0.104
K-inter	LHS	0.304	0.235	0.266	0.303
	RHS	−0.027	0.918	0.100	0.702
K-intra.L	LHS	0.098	0.708	0.036	0.891
	RHS	−0.115	0.659	−0.345	0.175
K-intra.R	LHS	−0.262	0.311	−0.210	0.419
	RHS	0.157	0.547	0.142	0.586

AUC, area under curve; LHS, left hemisphere stroke; RHS, right hemisphere stroke; FMA, Fugl-Meyer Assessment; FMA-UL, Fugl-Meyer Assessment of upper limbs; C, average weighted clustering coefficient; E, global efficiency; K-inter, inter-density; K-intra.L, intra-density of left hemisphere; K-intra.R, intra-density of right hemisphere.

group, there was a negative correlation between the K-inter.R and FMA-UL ($r = -0.262$, $p = 0.311$). The correlation between other intra-density and FMA-UL was small. Correlation results between brain network indicators and FMA-hand were similar. Among them, the intra-density of the contralesional hemisphere was negatively correlated with the FMA-hand in the RHS group ($r = -0.345$, $p = 0.175$). It can be seen from the above results that the correlation between each network indicator and FMA in the LHS group was higher than that in the RHS group. Was that because there was a non-linear correlation?

Through smooth curve fitting, the relationship between average weighted clustering coefficient or global efficiency and FMA-UL of the two groups has the same trend as the above correlation analysis (**Figures 5A,B**). Most of the mesoscale network parameters in the LHS group remained approximately linear with the FMA-UL, except for the K-intra.L. When motor function was poor (FMA-UL < 52), a better function was associated with larger intra-density of the left hemisphere ($r = -0.196$, $p = 0.541$). But when FMA-UL ≥ 52, the relationship was the opposite ($r = -0.618$, $p = 0.191$) (**Figure 5D**). That is, only the intra-density of the left hemisphere was affected by function severity in the LHS group. However, all of the relationships between inter-density or intra-density and FMA-UL had threshold effects in the RHS group (**Figures 5C–E**). When the FMA-UL was less than 33, there was a negative correlation between inter-density and FMA-UL ($r = -0.303$, $p = 0.429$), but when FMA-UL ≥ 33, higher inter-density values reflected greater motor function of upper limb ($r = 0.571$, $p = 0.084$). The relationship between K-intra.L and FMA-UL was also affected by the severity of motor dysfunction. When motor function was poor (FMA-UL < 42), the value of K-intra.L decreases with poorer motor function was better (FMA-UL ≥ 42), the value of K-intra.L increased ($r = -0.714$, $p = 0.088$). When $33 \leq$ FMA-UL < 49, there was a significant negative correlation between ipsilesional intra-density and upper limb motor function ($r = -0.883$, $P = 0.009$), while there was a positive correlation when FMA-UL < 33 ($r = 0.555$, $p = 0.121$) and ≥ 49 ($r = 0.800$, $p = 0.333$).

DISCUSSION

Hemiplegia after stroke is especially slow in hand motor function recovery, so we tried to guide the post-stroke hand function rehabilitation by analyzing the motor-related network characteristics during the hand grasping task. Our study found that both left and RHS exhibited bilateral activation during the affected hand task, but the activation regions were different. Miyai et al. (2003) used fNIRS to dynamically observe eight stroke patients with an average onset of 3 months for 2 months and found that the activation of contralesional SM1 gradually decreased, while the activation of ipsilesional PMC gradually increased. Wang et al. (2010) observed the complete motor network topological changes from the acute phase to the chronic phase after stroke using resting-state fMRI. The connections between the ipsilesional M1 and contralesional primary sensory area (S1), ventral PMC (PMv), dorsal PMC (PMd), and M1, between the ipsilesional PMv and the contralesional dentate nucleus of the cerebellum, and between the ipsilesional PMd and the contralesional superior parietal lobule (SPL) were significantly enhanced. These studies confirmed the role of SM1 and PMC activation in neurological compensation after stroke. In our study, we also found that both groups of stroke patients had compensatory activation of contralesional SM1, but the LHS was dominated by the contralesional PMC activation, and the RHS was dominated by the ipsilesional PMC activation.

Several published studies comparing hemispheric dominance have also demonstrated whether or not the dominant hemisphere stroke differs in brain network remodeling after stroke. Vidal et al. (2018) used fMRI to analyze the motor network activation during shoulder forward flexion-maintenance-release for 10 s each in the acute phase of stroke. The brain activation for RHS occurred in bilateral motor cortex, especially in SMA; while the LHS showed the ipsilesional cortical activation during forward flexion, and bilateral activation when put down (Vidal et al., 2018). Liew et al. (2018) analyzed brain activation during motor observation by fMRI in chronic-phase stroke patients. The RHS patients showed activation of left supramarginal gyrus and bilateral M1, SPL, and occipital lobe when observing left-hand movements, while the activation of left PMC and bilateral M1, supramarginal gyrus, and occipital lobes was noted in the LHS patients during right-hand movement (Liew et al., 2018). Although the brain activation also correlated with task paradigms (Allison et al., 2000; Nirkko et al., 2001; Grefkes et al., 2008), the activation characteristics of LHS and RHS were different under the same motor task.

At the macroscale level, our study found that the clustering coefficient and global efficiency of the patients were lower than those of the HS group, but the significance at each threshold was different. Caliandro et al. (2017) analyzed the small-world characteristics of cortical connectivity in acute stroke and came to a similar conclusion: the segregation and integration abilities of both dominant and non-dominant hemisphere stroke patients were lower than healthy people in all of the δ/ θ/ α_2 rhythms, but

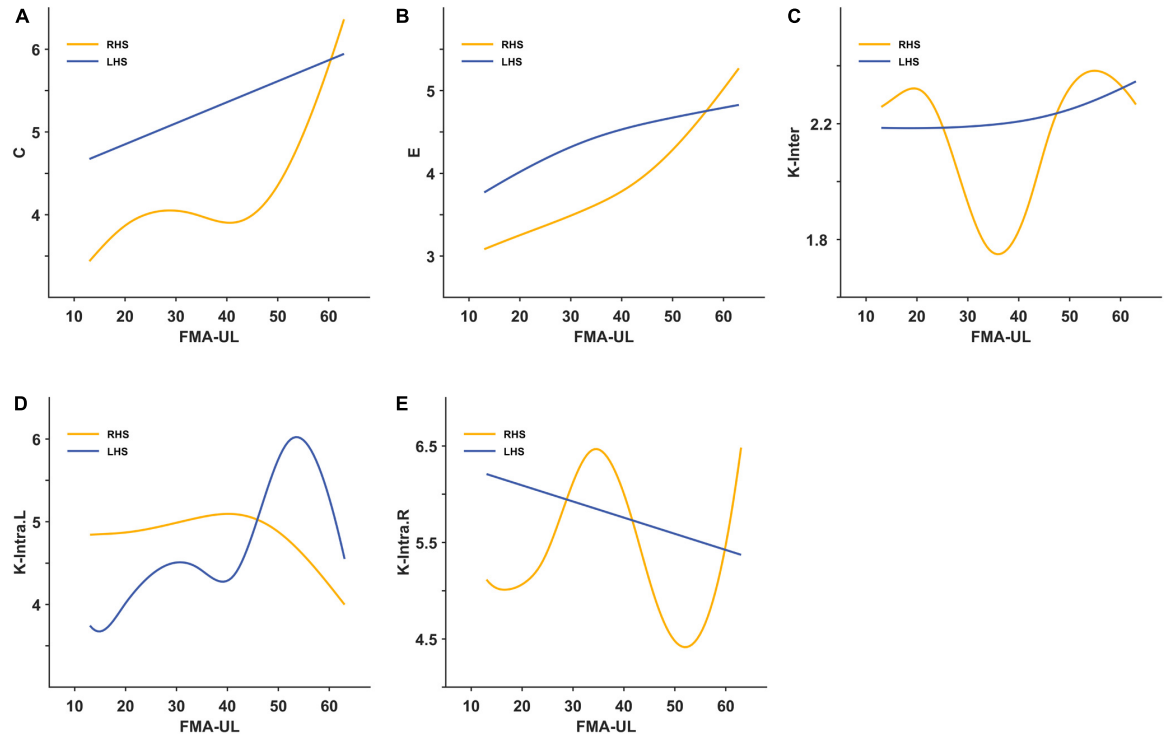

FIGURE 5 | The smooth curve fitting between area under curves (AUCs) of the brain network indicators and Fugl-Meyer Assessment of upper limbs (FMA-UL). **(A)** For the average weighted clustering coefficient; **(B)** for the global efficiency; **(C)** for the inter-density; **(D)** for the intra-density of left hemisphere; **(E)** for the intra-density of right hemisphere.

it varied in significance in different rhythms. At mesoscale, the inter-density of the patients was higher than that of HS in our study. The intra-density of the affected hemisphere was decreased and that of the unaffected hemisphere was increased in the LHS group, yet the results of the RHS group were opposite. We may infer that the motor function of the dominant hemisphere stroke was mainly compensated by the motor network of the contralesional hemisphere, while the non-dominant hemisphere stroke was compensated by the bilateral motor networks. Arun et al. (2020) compared the resting-state FC of left and RHS patients at 4–8 weeks using fNIRS; the findings of this group were similar to ours: there was decreased FC in the left hemisphere and increased FC in the right hemisphere for LHS (dominant side), and increased intrahemispheric (both sides) and interhemispheric FC for RHS.

It was considered that activation in the ipsilesional hemisphere predicted better motor recovery (Favre et al., 2014), whereas hyperactivation of the contralesional hemisphere predicted persistent neurological and motor deficits (Rehme and Grefkes, 2013; Grefkes and Fink, 2014). However, we found that brain network parameters in RHS (non-dominant side) were affected by the severity of dysfunction. When the dysfunction was higher (FMA-UL $<$ 33), the worse motor function needed greater interhemispheric connections, but less intra-density of both hemispheres. It showed that the worse is the function, the more information exchange was needed from the contralesional hemisphere to the ipsilesional side, but the information exchange was less dependent between the three motor areas in the two hemispheres, so the compensation of the contralesional hemisphere was more critical when the motor function was poor. Whereas the brain network results were reversed when the dysfunction was mild (33 $\leq$ FMA-UL $<$ 49), and smaller FMA-UL values reflected smaller inter-density and larger intra-density of the affected hemisphere. Then, the compensation in the ipsilesional hemisphere seemed to be more important. Especially when FMA-UL $\geq$ 49, the information exchange between the motor areas in the ipsilesional hemisphere increased with the further improvement of motor function, also illustrating the importance of the compensation on the lesion side for the final functional recovery. Therefore, based on the above results, we inferred that the RHS patients with more severe dysfunction may not benefit from inhibiting the unaffected hemisphere, while those with milder dysfunction may benefit more by exciting the ipsilesional hemisphere. Yet for the LHS patients, larger intra-density of the affected hemisphere reflected better function when the impairment was severe (FMA-UL $<$ 52). This phenomenon explained the importance of information exchange between the motor areas in the ipsilesional hemisphere, so these patients may benefit more by exciting the ipsilesional hemisphere. But when the left hemisphere was mildly injured (FMA-UL $\geq$ 52), there was less need for compensation from other motor areas. As demonstrated in the study by Sankarasubramanian et al. (2017),

for patients with severe injury [fraction anisotropy (FA) of DTI > 0.5, FMA of the upper extremity (max = 36) < 26–28], facilitative rTMS on the contralesional PMd yielded more benefit than inhibitory rTMS on the contralesional M1, whereas it was the opposite for mild patients. McCambridge et al. (2018) also indicated that inhibition of the motor area of the unaffected hemisphere may not be beneficial in severely injured patients. What is more, Ludemann-Podubecka et al. (2015b) found that inhibitory rTMS on the contralesional hemisphere could only improve hand function in patients with dominant hemisphere stroke, and had no significant effect on non-dominant hemisphere stroke. Therefore, it is necessary to individualize neuromodulation according to the severity of dysfunction and the location of the lesion.

There were a few limitations of this study. The first was issues about the signal pre-processing of fNIRS. We set strict collection environment and conditions: a darker and quiet room, rest for 3 min, and restricting the movement of other limbs; then, the commonly used spline interpolation method was introduced to remove motion and blinking artifacts in fNIRS. However, the effect of removing some small artifacts was relatively poor. Besides, our probe coverage was limited to the common motor networks and failed to analyze the participation of other regions. Another limitation was that the sample size was small, and some results were not statistically significant, even with large effect sizes. On the one hand, we referred to the sample size of previous related studies; on the other hand, we strictly follow the inclusion and exclusion criteria to screen suitable patients to ensure high-quality fNIRS data. This study found differences in brain network characteristics between dominant and non-dominant hemisphere strokes. Yet, whether we can benefit from individualized treatment based on these results still needs to be verified by interventional studies.

CONCLUSION

This is the first fNIRS-based study to compare the characteristics of macroscale and mesoscale brain networks between the dominant and non-dominant hemisphere stroke. Both LHS and RHS patients showed activation of bilateral hemispheres, but the activation regions were different. The average weighted clustering coefficient and global efficiency of both patient groups were lower than those of healthy people. The motor function execution of the LHS was mainly compensated by the motor network of the contralesional hemisphere, while that of the RHS was compensated by bilateral motor networks. Moreover, the mesoscale brain network characteristics were affected by the severity of dysfunction to varying degrees in the LHS and RHS patients. Our findings may help to develop an individualized neuromodulation strategy based on the patient's stroke site and severity.

DATA AVAILABILITY STATEMENT

The original contributions presented in this study are included in the article/supplementary material, further inquiries can be directed to the corresponding authors.

ETHICS STATEMENT

The studies involving human participants were reviewed and approved by the Ethics Committee of the First Affiliated Hospital of Xi'an Jiaotong University. The patients/participants provided their written informed consent to participate in this study.

AUTHOR CONTRIBUTIONS

ZY and GW conceived and designed the study. ZY, YP, LW, YZ, and SS screened participants. ZY, WX, JB, HG, and WL collected participants' data and performed the statistical analysis. ZY wrote the first draft of the manuscript. JQ and GW reviewed and edited the manuscript. All authors contributed to the manuscript revision and read and approved the submitted version.

FUNDING

This study was supported in part by the National Natural Science Foundation of China under Grant 32071372, in part by the Natural Science Basic Research Program of Shaanxi under Program 2022JQ-982 and 2022SF-379, and in part by the Science and Technology Project of Sichuan under Grant 2022YFS0030.

REFERENCES

Allison, J. D., Meador, K. J., Loring, D. W., Figueroa, R. E., and Wright, J. C. (2000). Functional MRI cerebral activation and deactivation during finger movement. *Neurology* 54, 135–142. doi: 10.1212/wnl.54.1.135

Ameli, M., Grefkes, C., Kemper, F., Riegg, F. P., Rehme, A. K., Karbe, H., et al. (2009). Differential effects of high-frequency repetitive transcranial magnetic stimulation over ipsilesional primary motor cortex in cortical and subcortical middle cerebral artery stroke. *Ann. Neurol.* 66, 298–309. doi: 10.1002/ana.21725

Arun, K. M., Smitha, K. A., Sylaja, P. N., and Kesavadas, C. (2020). Identifying Resting-State functional connectivity changes in the motor cortex using fnirs during recovery from stroke. *Brain Topogr.* 33, 710–719. doi: 10.1007/s10548-020-00785-2

Bonkhoff, A. K., Espinoza, F. A., Gazula, H., Vergara, V. M., Hensel, L., Michely, J., et al. (2020). Acute ischaemic stroke alters the brain's preference for distinct dynamic connectivity states. *Brain* 143, 1525–1540. doi: 10.1093/brain/awaa101

Calautti, C., Leroy, F., Guincestre, J. Y., and Jc, B. (2003). Displacement of primary sensorimotor cortex activation after subcortical stroke: a longitudinal PET study with clinical correlation. *Neuroimage* 19, 1650–1654. doi: 10.1016/s1053-8119(03)00205-2

Caliandro, P., Vecchio, F., Miraglia, F., Reale, G., Della Marca, G., La Torre, G., et al. (2017). Small-World characteristics of cortical connectivity changes in acute stroke. *Neurorehabil. Neural Repair* 31, 81–94. doi: 10.1177/1545968316662525

Carlson, H. L., Craig, B. T., Hilderley, A. J., Hodge, J., Rajashekar, D., Mouches, P., et al. (2020). Structural and functional connectivity of motor circuits after

perinatal stroke: a machine learning study. *Neuroimage Clin.* 28:102508. doi: 10.1016/j.nicl.2020.102508

Chen, W. L., Wagner, J., Heugel, N., Sugar, J., Lee, Y. W., Conant, L., et al. (2020). Functional near-infrared spectroscopy and its clinical application in the field of neuroscience: advances and future directions. *Front. Neurosci.* 14:724. doi: 10.3389/fnins.2020.00724

De Vico Fallani, F., Pichiorri, F., Morone, G., Molinari, M., Babiloni, F., Cincotti, F., et al. (2013). Multiscale topological properties of functional brain networks during motor imagery after stroke. *Neuroimage* 83, 438–449. doi: 10.1016/j.neuroimage.2013.06.039

Duan, L., Zhang, Y. J., and Zhu, C. Z. (2012). Quantitative comparison of resting-state functional connectivity derived from fNIRS and fMRI: a simultaneous recording study. *Neuroimage* 60, 2008–2018. doi: 10.1016/j.neuroimage.2012.02.014

Favre, I., Zeffiro, T. A., Detante, O., Krainik, A., Hommel, M., and Jaillard, A. (2014). Upper limb recovery after stroke is associated with ipsilesional primary motor cortical activity: a meta-analysis. *Stroke* 45, 1077–1083. doi: 10.1161/strokeaha.113.003168

Grefkes, C., Eickhoff, S. B., Nowak, D. A., Dafotakis, M., and Fink, G. R. (2008). Dynamic intra- and interhemispheric interactions during unilateral and bilateral hand movements assessed with fMRI and DCM. *Neuroimage* 41, 1382–1394. doi: 10.1016/j.neuroimage.2008.03.048

Grefkes, C., and Fink, G. R. (2014). Connectivity-based approaches in stroke and recovery of function. *Lancet Neurol.* 13, 206–216. doi: 10.1016/s1474-4422(13)70264-3

Harrivel, A. R., Weissman, D. H., Noll, D. C., and Peltier, S. J. (2013). Monitoring attentional state with fNIRS. *Front. Hum. Neurosci.* 7:861. doi: 10.3389/fnhum.2013.00861

Harvey, R. L., Edwards, D., Dunning, K., Fregni, F., Stein, J., Laine, J., et al. (2018). Randomized sham-controlled trial of navigated repetitive transcranial magnetic stimulation for motor recovery in stroke. *Stroke* 49, 2138–2146. doi: 10.1161/strokeaha.117.020607

Jansen, A., Menke, R., Sommer, J., Förster, A. F., Bruchmann, S., Hempleman, J., et al. (2006). The assessment of hemispheric lateralization in functional MRI–robustness and reproducibility. *Neuroimage* 33, 204–217. doi: 10.1016/j.neuroimage.2006.06.019

Kato, H., Izumiyama, M., Koizumi, H., Takahashi, A., and Itoyama, Y. (2002). Near-infrared spectroscopic topography as a tool to monitor motor reorganization after hemiparetic stroke: a comparison with functional MRI. *Stroke* 33, 2032–2036. doi: 10.1161/01.str.0000021903.52901.97

Liew, S. L., Garrison, K. A., Ito, K. L., Heydari, P., Sobhani, M., Werner, J., et al. (2018). Laterality of poststroke cortical motor activity during action observation is related to hemispheric dominance. *Neural Plast.* 2018:3524960. doi: 10.1155/2018/3524960

Lu, K., Xu, G., Li, W., Huo, C., Liu, Q., Lv, Z., et al. (2019). Frequency-specific functional connectivity related to the rehabilitation task of stroke patients. *Med. Phys.* 46, 1545–1560. doi: 10.1002/mp.13398

Ludemann-Podubecka, J., Bosl, K., and Nowak, D. A. (2015a). Repetitive transcranial magnetic stimulation for motor recovery of the upper limb after stroke. *Prog. Brain Res.* 218, 281–311. doi: 10.1016/bs.pbr.2014.12.001

Ludemann-Podubecka, J., Bosl, K., Theilig, S., Wiederer, R., and Nowak, D. A. (2015b). The effectiveness of 1 Hz rTMS over the primary motor area of the unaffected hemisphere to improve hand function after stroke depends on hemispheric dominance. *Brain Stimul.* 8, 823–830. doi: 10.1016/j.brs.2015.02.004

Mazrooyisebdani, M., Nair, V. A., Loh, P. L., Remsik, A. B., Young, B. M., Moreno, B. S., et al. (2018). Evaluation of changes in the motor network following BCI therapy based on graph theory analysis. *Front. Neurosci.* 12:861. doi: 10.3389/fnins.2018.00861

McCambridge, A. B., Stinear, J. W., and Byblow, W. D. (2018). Revisiting interhemispheric imbalance in chronic stroke: a tDCS study. *Clin. Neurophysiol.* 129, 42–50. doi: 10.1016/j.clinph.2017.10.016

Miyai, I., Yagura, H., Hatakenaka, M., Oda, I., Konishi, I., and Kubota, K. (2003). Longitudinal optical imaging study for locomotor recovery after stroke. *Stroke* 34, 2866–2870. doi: 10.1161/01.Str.0000100166.81077.8a

Nguyen, T., Babawale, O., Kim, T., Jo, H. J., Liu, H., and Kim, J. G. (2018). Exploring brain functional connectivity in rest and sleep states: a fNIRS study. *Sci. Rep.* 8:16144. doi: 10.1038/s41598-018-33439-2

Nirkko, A. C., Ozdoba, C., Redmond, S. M., Bürki, M., Schroth, G., Hess, C. W., et al. (2001). Different ipsilateral representations for distal and proximal movements in the sensorimotor cortex: activation and deactivation patterns. *Neuroimage* 13, 825–835. doi: 10.1006/nimg.2000.0739

Park, C. H., Chang, W. H., Ohn, S. H., Kim, S. T., Bang, O. Y., Pascual-Leone, A., et al. (2011). Longitudinal changes of resting-state functional connectivity during motor recovery after stroke. *Stroke* 42, 1357–1362. doi: 10.1161/strokeaha.110.596155

Rehme, A. K., and Grefkes, C. (2013). Cerebral network disorders after stroke: evidence from imaging-based connectivity analyses of active and resting brain states in humans. *J. Physiol.* 591, 17–31. doi: 10.1113/jphysiol.2012.243469

Sankarasubramanian, V., Machado, A. G., Conforto, A. B., Potter-Baker, K. A., Cunningham, D. A., Varnerin, N. M., et al. (2017). Inhibition versus facilitation of contralesional motor cortices in stroke: deriving a model to tailor brain stimulation. *Clin. Neurophysiol.* 128, 892–902. doi: 10.1016/j.clinph.2017.03.030

Scholkmann, F., Spichtig, S., Muehlemann, T., and Wolf, M. (2010). How to detect and reduce movement artifacts in near-infrared imaging using moving standard deviation and spline interpolation. *Physiol. Meas.* 31, 649–662. doi: 10.1088/0967-3334/31/5/004

Shimizu, T., Hosaki, A., Hino, T., Sato, M., Komori, T., Hirai, S., et al. (2002). Motor cortical disinhibition in the unaffected hemisphere after unilateral cortical stroke. *Brain* 125(Pt 8), 1896–1907. doi: 10.1093/brain/awf183

Strangman, G., Culver, J. P., Thompson, J. H., and Boas, D. A. (2002). A quantitative comparison of simultaneous BOLD fMRI and NIRS recordings during functional brain activation. *Neuroimage* 17, 719–731.

Vidal, A. C., Banca, P., Pascoal, A. G., Cordeiro, G., Sargento-Freitas, J., Gouveia, A., et al. (2018). Bilateral versus ipsilesional cortico-subcortical activity patterns in stroke show hemispheric dependence. *Int. J. Stroke* 12, 71–83. doi: 10.1177/1747493018767164

Wang, L., Yu, C., Chen, H., Qin, W., He, Y., Fan, F., et al. (2010). Dynamic functional reorganization of the motor execution network after stroke. *Brain* 133(Pt 4), 1224–1238. doi: 10.1093/brain/awq043

Watanabe, K., Kudo, Y., Sugawara, E., Nakamizo, T., Amari, K., Takahashi, K., et al. (2018). Comparative study of ipsilesional and contralesional repetitive transcranial magnetic stimulations for acute infarction. *J. Neurol. Sci.* 384, 10–14. doi: 10.1016/j.jns.2017.11.001

Yang, Y., Pan, H., Pan, W., Liu, Y., Song, X., Niu, C. M., et al. (2021). Repetitive transcranial magnetic stimulation on the affected hemisphere enhances hand functional recovery in subacute adult stroke patients: a randomized trial. *Front. Aging Neurosci.* 13:636184. doi: 10.3389/fnagi.2021.636184

Yu, J. W., Lim, S. H., Kim, B., Kim, E., Kim, K., Kyu Park, S., et al. (2020). Prefrontal functional connectivity analysis of cognitive decline for early diagnosis of mild cognitive impairment: a functional near-infrared spectroscopy study. *Biomed. Opt. Express* 11, 1725–1741. doi: 10.1364/boe.382197

Conflict of Interest: The authors declare that the research was conducted in the absence of any commercial or financial relationships that could be construed as a potential conflict of interest.

Publisher's Note: All claims expressed in this article are solely those of the authors and do not necessarily represent those of their affiliated organizations, or those of the publisher, the editors and the reviewers. Any product that may be evaluated in this article, or claim that may be made by its manufacturer, is not guaranteed or endorsed by the publisher.

frontiers | Frontiers in Aging Neuroscience

ORIGINAL RESEARCH
published: 13 July 2022
doi: 10.3389/fnagi.2022.909551

Sarcopenia: Body Composition and Gait Analysis

Yuxuan Fan[1†], Bo Zhang[2†], Guohao Huang[1], Guoying Zhang[1], Zhiyuan Ding[1], Zhiyu Li[3], Jonathan Sinclair[4] and Yifang Fan[1]*

[1] Foot Research Laboratory, School of Physical Education and Sport Science, Fujian Normal University, Fuzhou, China, [2] College of Sports and Health, Guangzhou Sport University, Guangzhou, China, [3] College of Foreign Studies, Jinan University, Guangzhou, China, [4] Research Centre for Applied Sport, Physical Activity and Performance, School of Sport and Health Sciences, University of Central Lancashire, Preston, United Kingdom

Background: Age-induced sarcopenia negatively affects walking stability and increases the risk of falls, which is the leading cause of accidental death in the elderly.

Objective: This study aimed to analyze and contrast body composition and gait characteristics in those with sarcopenia in relation to healthy controls to shed some light on the prevention of falls in elderly patients with sarcopenia.

Materials and Methods: In this study, 68 community dwellers were scanned by the Hologic QDR-4500A Dual-energy X-ray absorptiometry (DXA). The appendicular lean mass index (ALMI) results were used to distinguish the normal participants from those with sarcopenia: 24 in the sarcopenia group, and 44 into the normal group. The participants were asked to undergo gait analysis on a plantar pressure measurement system. Statistical analysis was conducted to contrast both groups' gait and butterfly parameters from their gait test, and then a gait forward dynamics method was performed to quantify the analysis for both groups.

Results: The ALMI of the female was not related to their age ($r = 0.06$) while that of the male was weakly related ($r = 0.17$). Body mass index (BMI) from both groups was normal, although with a statistically greater BMI from the normal group compared with sarcopenia ($p < 0.001$). Greater values and significant differences were found in step length and stride length from the normal elderly group ($p < 0.01$), and so was the length of the gait line and single support line ($p < 0.05$). Gait forward dynamics analysis results showed no motor neural or musculoskeletal disorders in their gait performance from the sarcopenia group.

Conclusion: For the elderly, age did not largely affect the ALMI, BMI, or *T*-score, but BMI and ALMI were strongly correlated. In this study, significant differences were found in certain gait parameters between the elderly with sarcopenia and the normal elderly, which were related to absolute muscle strength, suggesting that sarcopenia was a disease mainly caused by decreased muscle mass. In addition, when abnormities were identified in step length, stride length, length of gait line, or length of single support line, it is proposed to take a DXA scan to confirm whether the elderly suffer from sarcopenia.

Keywords: sarcopenia, body composition, gait parameters, butterfly parameters, gait forward dynamics method

OPEN ACCESS

Edited by:
Le Li,
Northwestern Polytechnical University, China

Reviewed by:
Mianfang Ruan,
Wenzhou University, China
He Gong,
Beihang University, China

****Correspondence:***
Yifang Fan
tfyf@fjnu.edu.cn

† These authors have contributed equally to this work

Specialty section:
This article was submitted to Neurocognitive Aging and Behavior, a section of the journal Frontiers in Aging Neuroscience

Received: *31 March 2022*
Accepted: *20 June 2022*
Published: *13 July 2022*

Citation:
Fan Y, Zhang B, Huang G, Zhang G, Ding Z, Li Z, Sinclair J and Fan Y (2022) Sarcopenia: Body Composition and Gait Analysis. Front. Aging Neurosci. 14:909551. doi: 10.3389/fnagi.2022.909551

INTRODUCTION

Over the past few decades, the decrease in fertility rate and the increase of life expectancy (Li and Lin, 2016) have caused China to be one of the fastest population aging countries in the world (Phillips and Feng, 2015). Aging is one of the major challenges for Chinese society (Han et al., 2020), leading to body structure senescence and motor function decline. The lower limb muscles in the elderly have a reduced cross-sectional area by 25–35% compared with those of the young (Lexell, 1995), explaining why the elderly are more vulnerable to sarcopenia. Sarcopenia is characterized by symptoms of age-related loss of skeletal muscle mass and poor muscle strength or physical fitness (Cruz-Jentoft et al., 2010; Kirk et al., 2021). Differences in age, gender, and race mediate different degrees of muscle loss. Among the elderly over 65 years of age, the age- and sex-adjusted prevalence of sarcopenia was 6–15%, depending on the assessment of muscle mass parameters (Baumgartner et al., 1998; Iii et al., 2000).

Sarcopenia is a complex syndrome caused by many factors (Ribeiro and Kehayias, 2014). The quality of lean principle proposes to utilize body composition assessment to indirectly assess sarcopenia. This principle connects muscle mass and metabolic function to fat-free mass (Ribeiro and Kehayias, 2014). Research findings have shown that sarcopenia presents in an impaired state of health, and is related to falls, bone fracture risk, movement disorders, reduction of daily activities, disabilities, loss of independence, and an increased risk of death (Cawthon et al., 2007; Cruz-Jentoft et al., 2010; Morley et al., 2011; Fukuoka et al., 2019; Coll et al., 2021). For instance, the decrease in walking stability and the increased risk of falling might lead to the loss of physical function independence (Dutta, 1997). Other consequences of sarcopenia included the increased risks of chronic diseases, such as diabetes and osteoporosis (Dutta, 1997; Fukuoka et al., 2019).

The clinical diagnosing standard of sarcopenia by the European Working Group on Sarcopenia in Older People (EWGSOP) included low muscle mass, low muscle strength, or poor physical performance (Cruz-Jentoft et al., 2010). The Asian Working Group for Sarcopenia (AWGS) issued regional consensus guidelines in 2014, which were mostly consistent with those from EWGSOP (Chen et al., 2014). Clinically assessment techniques included bioelectrical impedance analysis (BIA), dual energy X-ray absorptiometry (DXA), and anthropometric measures to calculate muscle mass (Falsarella et al., 2014).

To avoid suffering from sarcopenia, walking speed was one of the most frequently used measurements to assess the elderly's ability to live independently (Kang and Dingwell, 2008; Bohannon and Andrews, 2011), because muscle mass was closely associated with motor function (Rosenberg, 1997). Other syndromes or diseases might affect the accuracy of using walking speed to assess muscle function, though. In addition, the decreased hip movements in the sagittal plane and the increase in pelvic tilt in the anteroposterior plane extended the support phase and reduced the stride time (Sanchez-Rodriguez et al., 2015), which may, at the same time, affect the accuracy of using walking speed as an assessment technique. A comprehensive gait analysis served as a useful tool to assess muscle loss, whereas cameras and force plates were gold-standard tools to assess gait clinically (Kim et al., 2021). Gait analysis could be used to predict the risk of fall, or to distinguish age groups, disease types, or physical activity levels (Senden et al., 2009; Bautmans et al., 2011), to identify abnormal gait characteristics and to provide additional information about the patients' degree of functionality or their risk of fall (Senden et al., 2012; Thiede et al., 2016). To assess and identify factors that may impair gait stability was essential to design intervention programs to maintain the independence and mobility of the elderly (Leiros-Rodriguez et al., 2018).

This study aimed to explore body composition and gait characteristics in those with sarcopenia in relation to healthy controls as well as the relationship among body composition, gait parameters, and sarcopenia to shed some light on the prevention of falls among the elderly.

Abbreviations: ALM, Appendicular lean mass; ALMI, appendicular lean mass index; BMI, Body mass index; COM, Center of mass; DXA, Dual-energy X-ray absorptiometry; VGRF, vertical ground reaction force; GRF, ground reaction force.

MATERIALS AND METHODS

Participants

Community-dwelling elderly (aged 53–78 years) participants were recruited—their body composition was measured by a DXA scanner (Hologic QDR-4500A). Appendicular lean mass (ALM) was calculated by collecting the sum of arm and leg lean mass. Based on their appendicular lean mass [ALMI, height, H; ALMI = ALM/H^2 (kg/m^2)], the sarcopenia group ($n = 24$) was identified, i.e., ALMI < 7.0 kg/m^2 in men and 5.8 kg/m^2 in women (Tanimoto et al., 2014). Those without low muscle mass or strength and low physical performance were classified into the normal group ($n = 44$). Participants' basic information is shown in **Table 1**.

All participants' annual medical reports were checked to exclude patients with neural or musculoskeletal disease. The experimental procedures were explained to the participants and written informed consent forms were obtained from the participants before testing. This study was approved by the Ethics Committee of Fujian Normal University.

Equipment

A bone mineral density scanner DXA system (Hologic QDR-4500A; Hologic, Mass, USA) was utilized. The system was allowed to warm up for 10 min prior to use, and self-tests were undertaken on a daily basis in accordance with the manufacturer's requirements. The scanning parameters were as follows: 140/100 kVp, 2.5 mA; scanning mode: e whole body; software: Version 12.4:3; analysis: Auto Whole Body. **Figure 1** shows the equipment.

A Zebris FDM plantar pressure measurement system (Zebris Medical GmbH, Isny, Germany-6.08 (L) × 0.56 (W) m), with 45,056 sensors frequency of 100 Hz) was utilized. The system was calibrated prior to each testing session to ensure data integrity. **Figure 2** shows the equipment.

TABLE 1 | Basic information of the participants.

	Sarcopenia ($n = 24$)		Normal ($n = 44$)	
	Male ($n = 5$)	**Female ($n = 19$)**	**Male ($n = 26$)**	**Female ($n = 18$)**
Age, year	66.60 ± 8.17	62.68 ± 6.01	64.58 ± 5.22	63.61 ± 6.99
Height, m	161.52 ± 6.55	156.64 ± 6.14	169.10 ± 4.03	157.78 ± 4.43
Weight, kg	56.44 ± 7.27	52.68 ± 5.58	72.29 ± 7.94	59.92 ± 5.98
BMI*	21.57 ± 1.79	21.46 ± 1.77	25.26 ± 2.46	24.07 ± 2.27
ALM#, g	16193.22 ± 2534.52	13369.89 ± 1553.64	23226.45 ± 2008.18	15731.66 ± 1392.78
ALMI@ kg/m^2	6.18 ± 0.58	5.43 ± 0.31	8.12 ± 0.62	6.32 ± 0.44
T-score	−1.74 ± 1.59	−1.72 ± 1.30	−0.21 ± 1.04	−0.83 ± 1.12

*BMI, body mass index; #ALM, appendicular lean mass index; @ALMI [H, height, ALMI=ALM/H^2(kg/m^2)].

FIGURE 1 | A dual-energy X-ray absorptiometry (DXA) scanner (Hologic QDR-4500A).

Gait Test and Calculation

Participants were asked to walk at a self-selected velocity on the Zebris FDM System. Data were collected at a sampling rate of 100 Hz. For each participant, data that included 10 complete successive foot contacts were accepted and then analyzed. Gait parameters were processed by the Win FDM (V1.18.40).

Gait Forward Dynamics Method

For bipedal walking, the ground reaction force (GRF) satisfies the following conditions:

$$\int_o^T \left(F_1(t) + F_2(t) - mg\right) dt = 0 \quad (1)$$

where, $F_1(t)$ and $F_2(t)$ refer to the GRF of the left and right foot at a certain time, respectively; T the stride time, t a certain moment in a stride cycle, m the body mass, and g the acceleration of gravity.

Introduce the foot's ground contact moment $t_{initial}$, $F(t + t_{initial})$ GRF. Since $F_1(t) + F_2(t) = F(t + t_{initial})$, the component form of GRF is as follows:

$$F(t + t_{initial}) = F_x(t + t_{initial}) + F_y(t + t_{initial}) + F_z(t + t_{initial}) \quad (2)$$

where, $F_x\,(t + t_{initial})$, $F_y\,(t + t_{initial})$, *and* $F_z(t + t_{initial})$ refer to the components of GRF in x, y, z directions of the Cartesian

FIGURE 2 | A Zebris FDM plantar pressure measurement system.

coordinate system respectively, and t a certain moment in a stride cycle.

By Equations (1) and (2), restraint conditions of $\int_0^T F_x(t)dt = 0$ in x direction will be

$$\int_0^T F_x(t)dt = \int_0^T F_x(t + t_{initial})dt = 0 \tag{3}$$

By Equations (1) and (2), restraint conditions of $\int_0^T F_y(t)dt = 0$ in y direction will be

$$\int_0^T F_y(t)dt = -\int_0^T F_y(t + t_{initial})dt \tag{4}$$

By Equations (1) and (2), restraint conditions of $\int_0^T F_z(t)dt = \int_0^T mgdt$ in z direction, and since $\int_0^T F_z(t)dt = \int_0^T F_z(t + t_o)dt$, we will get

$$\int_0^T F_z(t)dt + \int_0^T F_z(t + t_{initial})dt = \int_0^T mgdt \tag{5}$$

By Equation (5), and by Newton's second law, the acceleration equation of the body's center of mass (COM) at a certain moment in a stride cycle in z direction will be

$$a_z\,(t + t_{initial}) = F_z\,(t) + F_z\,(t + t_{initial}) - mg \tag{6}$$

where, a_z stands for acceleration, F_z GRF, t a certain moment in a stride cycle, $t_{initial}$ initial ground contact moment, m body weight, and g the acceleration of gravity.

Take the body coordinates of COM as a non-inertial reference frame, and set the initial velocity of COM at the beginning of the stride cycle to be $v_0(t_{initial})$. By Equation (6), when the ground contact moment is $t_{initial}$, the relationship between the centroid velocity at any time t in a stride cycle and the acceleration and initial velocity will be

$$v(t, t_{initial}) = \int_0^t a(t, t_{initial})dt + v_0(t_{initial}) \tag{7}$$

v_x, v_y and v_z stand for the velocities in the three directions of COM, respectively. So, $v_x\,(t, t_{initial}) = \int_0^t a_x\,(t, t_{initial})\,dt + v_{x0}\,(t_{initial})$, $v_y\,(t, t_{initial}) = \int_0^t a_y\,(t, t_{initial})\,dt + v_{y0}\,(t_{initial})$, *and* $v_z(t, t_{initial}) = \int_0^t a_z(t, t_{initial})dt + v_{z0}(t_{initial})$. It seems impossible to determine the magnitude of $v_0(t_{initial})$ in Equation (7) by means of dynamics method, but based on the least-action principle in gait (Fan et al., 2009), $v_0(t_{initial})$ has a unique value. Equation (7) shows that $v_0(t_{initial})$ is a function of $t_{initial}$ for the ground contact moment. The relationship between the initial velocity of relative motion and acceleration is

as follows:

$$v_0(t_{initial}) = -\sum_{\lambda=1}^{T}\int_0^{\lambda} a(t, t_{initial})dt \quad (8)$$

For any ground contact moment, $\int_0^T a(t, t_{initial})dt = 0$. By Equation (7), $v(T, t_{initial}) = v_0(t_{initial})$. It should be noted that the initial velocity calculated by Equation (8) refers to the stable stepping speed of body at the beginning of the stride cycle, and it is the initial velocity of the COM relative to the dynamic reference frame, not the absolute velocity of the COM relative to the static reference frame. By Equations (6) and (8), the foot's ground contact moment determines the initial speed of relative motion, but it has nothing to do with the implicated velocity, which is quite intriguing. When running on a linear path, the commonly used gait parameter of "step velocity" is the implicated speed, and the step velocity is related to stride frequency and stride length. Relative velocity, therefore, is independent of stride frequency and stride length.

When the body coordinate of COM is used as a non-inertial reference frame, the sum of the potential energy of COM is $\sum_1^T E_p(t) = 0$, and the mean potential energy is $\overline{E}_p = 0$; the kinetic energy of COM t at any time of relative motion is $E_k(t) \geq 0$. In a stride cycle, the sum of kinetic energy is $\sum_1^T E_k(t) > 0$, and the mean kinetic energy is $\overline{E}_k > 0$. Therefore, we use the relative motion centroid energy to simplify the description of mechanical energy consumption in gait as follows:

$$E(t, t_{initial}) = \frac{1}{2}v^2(t, t_{initial}) \quad (9)$$

Vertical ground reaction force (VGRF) and gravity from Zebris FDM System gait analysis report were normalized by self-weight, and stride cycle normalized by percentage. Equations (1)–(9) were established to calculate both groups' VGRF, acceleration, velocity, displacement, and dynamic energy of COM, respectively. An application of these equations is shown in **Supplementary Tables 1–3**.

Statistical Analyses

Data from the sarcopenia and normal groups were expressed in the format of means ± standard deviation (SD). Gait parameters from the two groups were compared using an independent sample t-test analysis (two-tailed distribution). In addition, linear associations between the experimental measurements were explored using correlation analyses. Correlation analyses were interpreted as follows: 0–0.2 = very weak, 0.21–0.4 = weak, 0.41–0.6 = moderate, 0.61–0.8 = strong, and 0.81–1.0 = very strong. The statistical significance level throughout was determined at the $p \leq 0.05$ level.

RESULTS

Correlations

Scanning reports derived from Hologic QDR-4500A were presented in six scatter plot figures—participants' age and ALMI, age and BMI, age and T-score, BMI and ALMI, BMI and T-score, and ALMI and T-score, as shown in **Figures 3–8**. In addition, linear regression equations were given.

The relationship between gender, age, and ALMI is shown in **Figure 3**, where y (*female*) $= -0.0068x + 6.3098$ ($p < 0.01$), a linear equation of scatter plot of the female's age and ALMI, with the correlation coefficient of 0.06, suggesting a very weak correlation between conditions. Furthermore, y (*male*) $= -0.0323x + 9.9173$ ($p < 0.01$) was the linear equation of scatter plot of the male's age and ALMI, with the correlation coefficient of 0.17, suggesting a weak correlation.

The relationship among gender, age, and ALMI is shown in **Figure 4**, where y (*female*) $= -0.0084x + 23.318$ ($p < 0.01$) was a linear equation of scatter plot of the female's age and BMI, with the correlation coefficient of 0.05, suggesting a very weak association. *In addition*, y (*male*) $= -0.0096x + 24.045$ ($p < 0.01$) was a linear equation of scatter plot of the male's age and BMI, with the correlation coefficient of 0.5, also suggesting a moderate correlation.

The relationship between among gender, age, and T-score is shown in **Figure 5**, where y (*female*) $= 0.0073x$ 1.759 ($p < 0.01$) was a linear equation of scatter plot of the female's age and T-score, with the correlation coefficient of 0.03, showing a very weak association. Whereas, y (*male*) $= 0.0308x$ 2.4408 ($p < 0.01$) was a linear equation of scatter plot of male age and T-score, with the correlation coefficient of 0.13, suggesting a very weak correlation.

The relationship between BMI and ALMI in female and male is shown in **Figure 6**, where y (*female*) $= 2.5775x + 7.6501$ ($p < 0.001$) was a linear equation of scatter plot of the female's BMI and ALMI, with the correlation coefficient of 0.62, suggesting a strong correlation. Whereas, y (*male*) $= 1.9554x + 9.4156$ ($p < 0.001$) was a linear equation of scatter plot of the male's BMI and ALMI, with the correlation coefficient of 0.69, also suggesting a strong correlation.

The relationship between BMI and T-score in female and male is shown in Figure 7, where y (*female*) $= 0.0218x + 22.797$ ($p < 0.01$) was a linear equation of scatter plot of the female's BMI and T-score, with the correlation coefficient of 0.01, suggesting a very weak association; y (*male*) $= 0.7615x + 24.997$ ($p < 0.01$) was a linear equation of scatter plot of the male's BMI and T-score, with the correlation coefficient of 0.35, suggesting a weak correlation.

The relationship between ALMI and T-score in female and male is shown in **Figure 8**. In **Figure 8**, where y (*female*) $= 0.1735x + 6.0839$ ($p < 0.01$) was a linear equation of scatter plot of the female's ALMI and T-score, with the correlation coefficient of 0.38, suggesting a weak correlation; y (*male*) $= 0.4529x + 8.0133$ ($p < 0.001$) was a linear equation of scatter plot of the male's ALMI and T-score, with the correlation coefficient of 0.60, suggesting a moderate correlation.

Comparisons Between Groups

Comparisons between the sarcopenia and normal groups are presented below and more details are shown in **Tables 2**, **3**.

Table 2 demonstrates extremely significant differences in both sides' step length and stride length between the sarcopenia group and the normal group ($p < 0.01$). The mean cadence of the

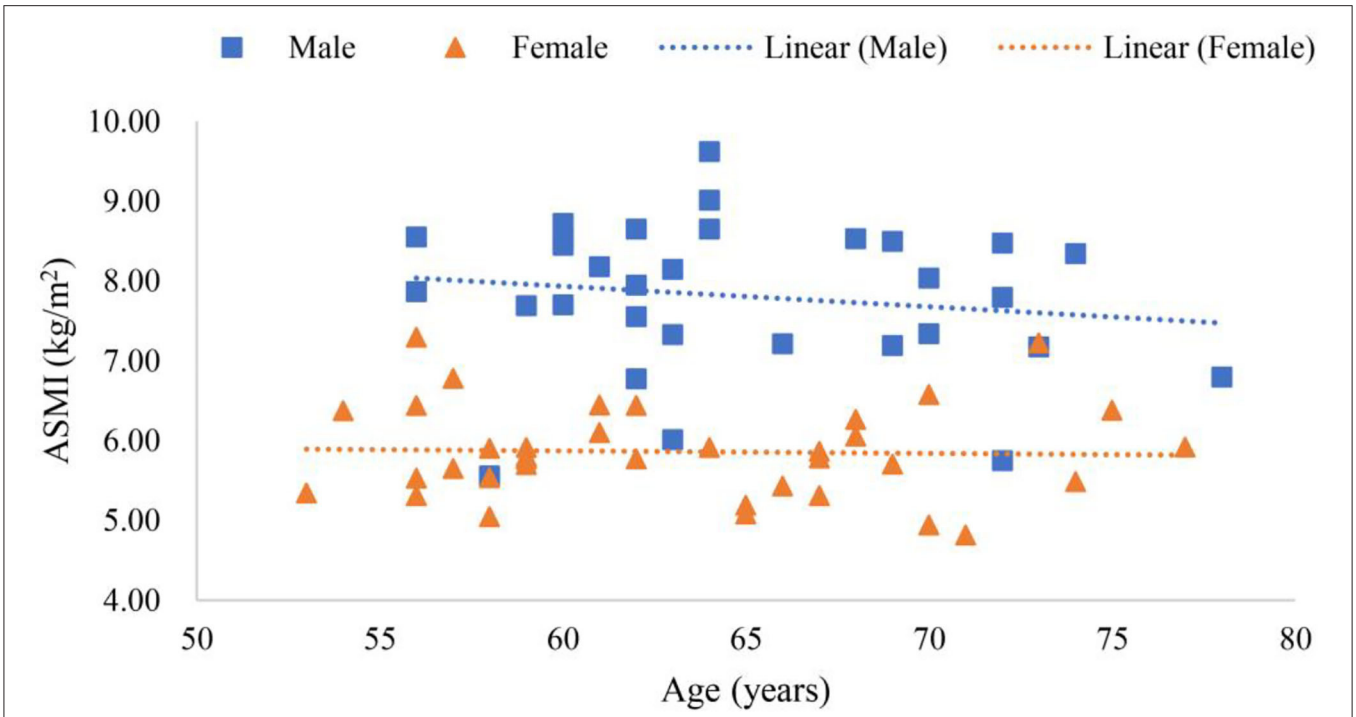

FIGURE 3 | Scatter plots of participants' age and appendicular lean mass index (ALMI).

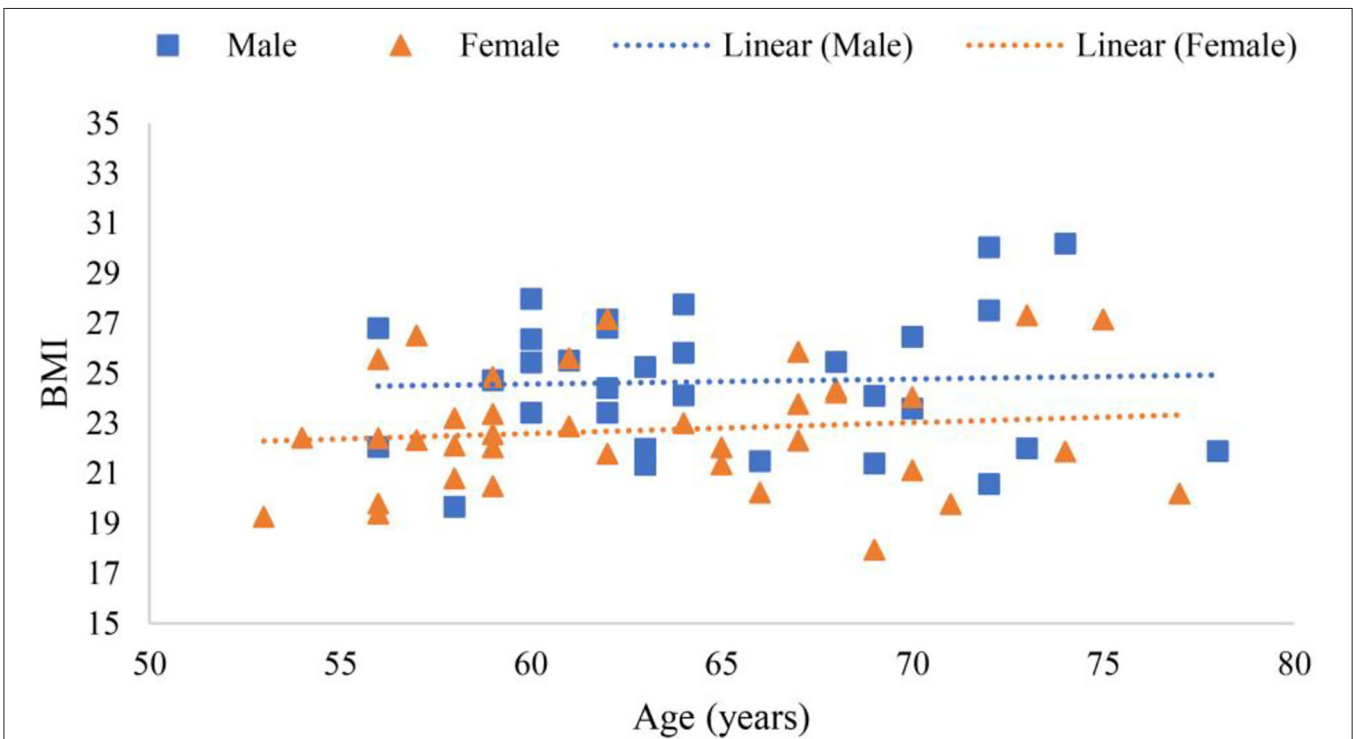

FIGURE 4 | Scatter plots of participants' age and body mass index (BMI).

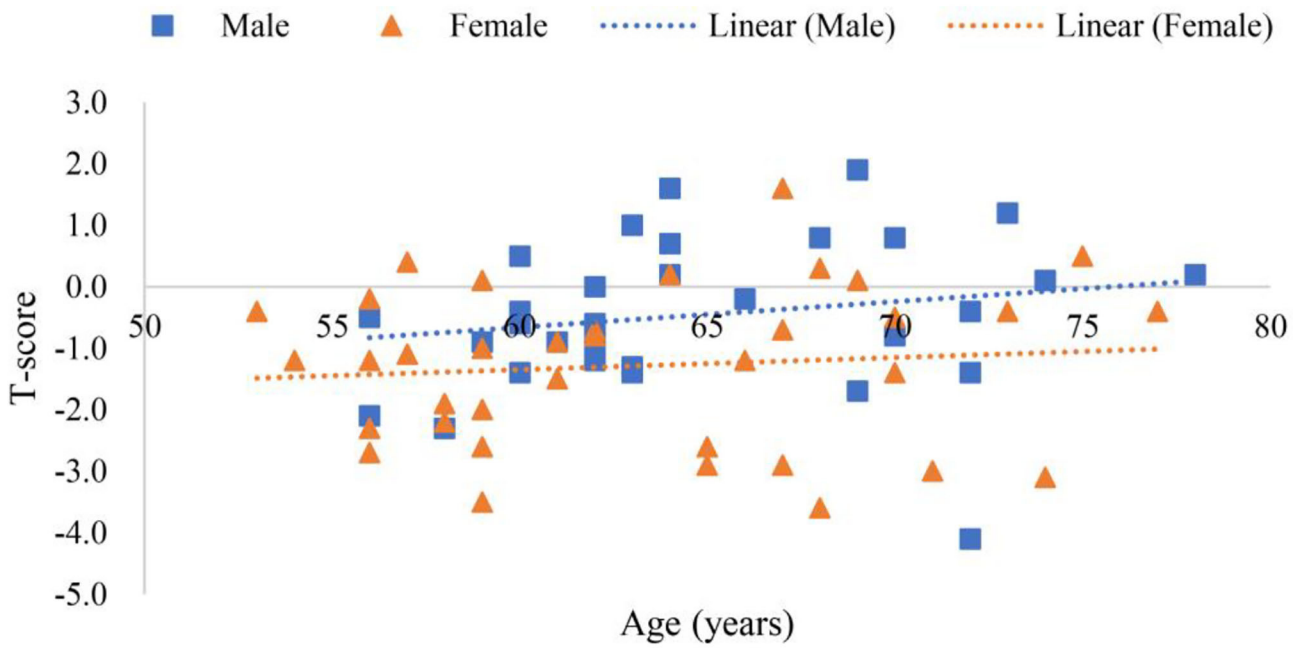

FIGURE 5 | Scatter plots of participants' age and *T*-score.

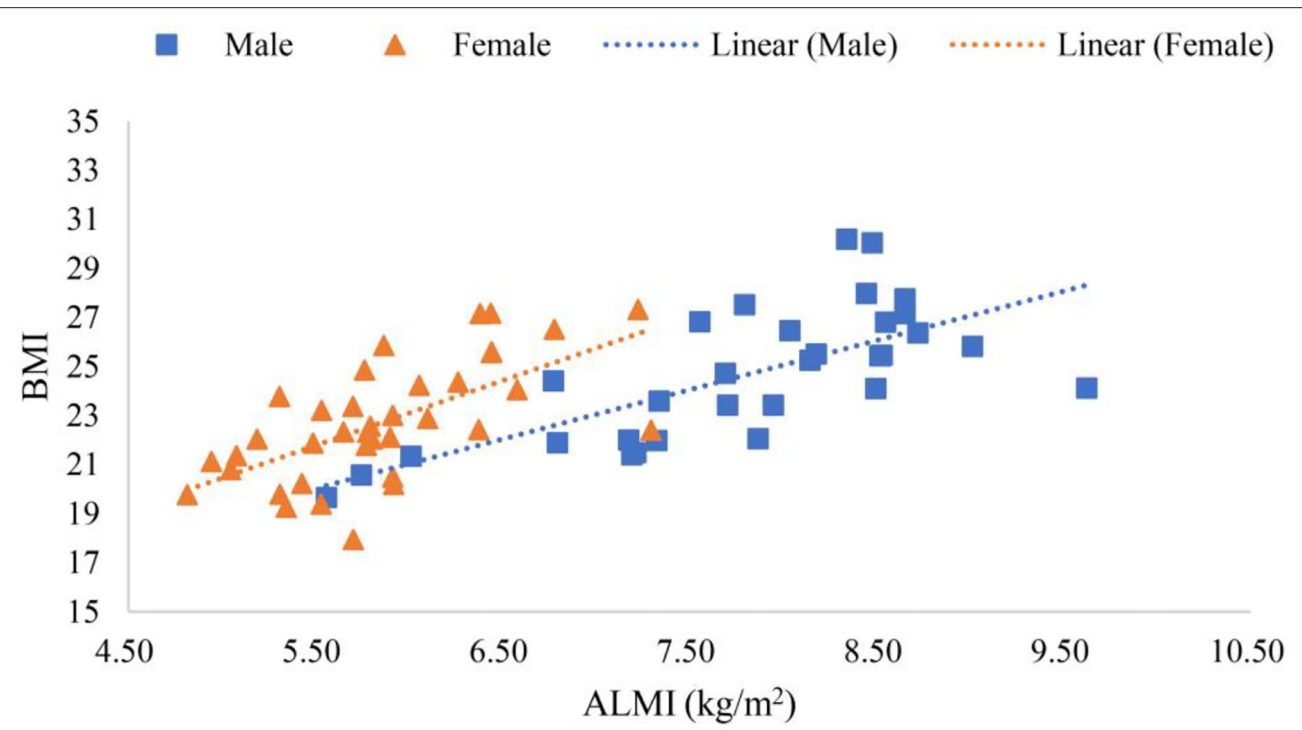

FIGURE 6 | Scatter plots of participants' BMI and ALMI.

sarcopenia group was higher than that of the normal group, and the mean step speed is smaller than that of the normal group, but there were no significant differences between them.

Table 3 demonstrates extremely significant differences in the length of right gait line and left single support line between the two groups ($p < 0.01$). Significant differences were found in

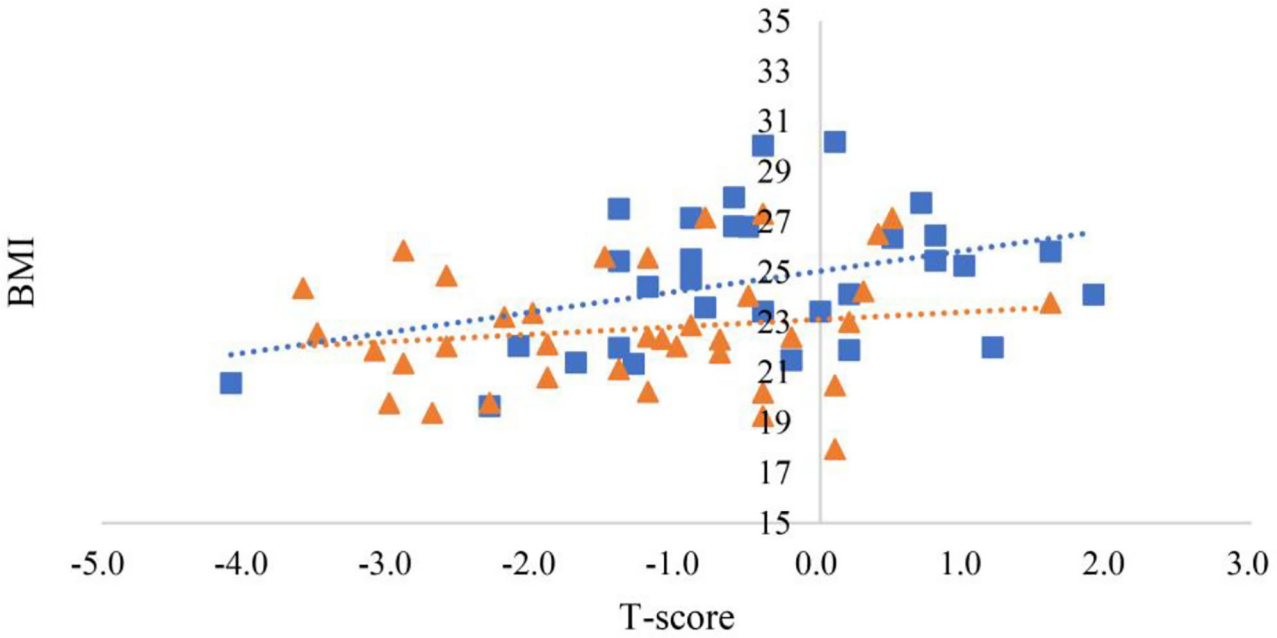

FIGURE 7 | Scatter plots of participants' BMI and *T*-score.

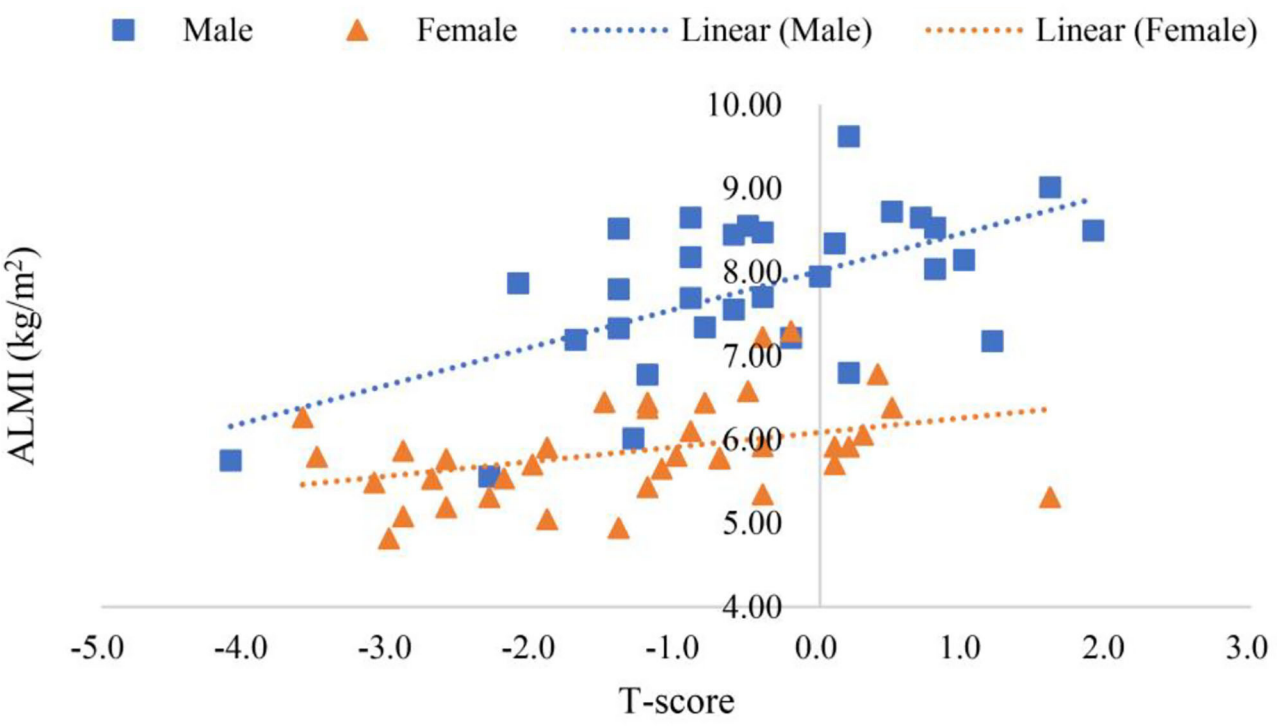

FIGURE 8 | Scatter plots of participants' ALMI and *T*-score.

TABLE 2 | Basic gait parameters of the participants.

		Sarcopenia ($n = 24$)	Normal ($n = 44$)
Step length, cm	Left	59.6 ± 4.96♦	64.04 ± 7.52♦
	Right	59.78 ± 4.36♦	63.96 ± 7.15♦
Step time, sec	Left	0.52 ± 0.03	0.53 ± 0.05
	Right	0.52 ± 0.04	0.53 ± 0.05
Stance phase, %	Left	62.74 ± 1.43	62.44 ± 1.70
	Right	63.03 ± 1.62	62.98 ± 1.72
Swing phase, %	Left	37.26 ± 1.43	37.56 ± 1.70
	Right	36.97 ± 1.62	37.02 ± 1.72
Double stance phase, %		25.61 ± 2.83	25.13 ± 3.07
Stride length, cm		119.39 ± 9.15♦	128.01 ± 14.46♦
Stride time, sec		1.05 ± 0.08	1.06 ± 0.09
Cadence, steps/min		115.10 ± 7.81	113.11 ± 9.66
Velocity, km/h		1.14 ± 0.14	1.21 ± 0.18

♦$p < 0.01$; *Paired samples t-test (two-tailed distribution) is used for the gait parameters of participants in both groups.*

TABLE 3 | Butterfly parameters of the participants.

		Sarcopenia ($n = 24$)	Normal ($n = 44$)
Length of gait line, mm	Left	195.17 ± 15.10◇	205.28 ± 17.29◇
	Right	193.53 ± 15.60♦	205.31 ± 18.15♦
Single support line. mm	Left	111.08 ± 7.12♦	117.21 ± 11.45♦
	Right	110.11 ± 12.19◇	117.21 ± 11.24◇
Anterior/posterior position, mm		74.24 ± 63.68	97.64 ± 64.24
Anterior/posterior position variability, mm		2.98 ± 2.98	2.43 ± 1.41
Lateral symmetry, mm		0.03 ± 4.71	−0.71 ± 3.83
Lateral variability, mm		3.59 ± 2.84	2.6 ± 1.33
Max gait line velocity, cm/sec		153.64 ± 93.07	143.87±114.64

♦$p < 0.01$, ◇$p < 0.05$; *Paired samples t-test (two-tailed distribution) is used for the gait parameters of participants in both groups.*

the length of left gait line and right single support line ($p < 0.05$). The mean values of anterior/posterior position variability, lateral variability, and max gait line velocity of the sarcopenia group were greater than those of the normal group, but without significant difference in all of them.

Equations (1)–(9) were established to calculate both groups' VGRF, acceleration, velocity, displacement, and dynamic energy of COM, respectively, and the results are shown in **Figure 9**, where the variation trend of VGRF with standardized weight of both groups was similar in a stride cycle. However, the peak value of the left resultant VGRF in the sarcopenia group was greater than that of the normal group, while the peak value of the right resultant VGRF was smaller than that of the normal group. In both groups, the resultant VGRF peaked at 1.4 times of their body weight. The other dynamic quantities of the COM conformed to these characteristics.

DISCUSSION

This study aimed to explore body composition and gait characteristics in those with sarcopenia in relation to healthy controls as well as the relationship among body composition, gait parameters, and sarcopenia to shed some light on the prevention of falls among the elderly. Importantly, in this study, we calculated gait parameters and COM dynamics between the two groups by providing correlations between body composition and gender and age. We found that the elderly with sarcopenia have abnormal gait parameters, which may be useful to predict and assess the risk of sarcopenia using a simple gait test.

Research has shown that the limb muscles of the elderly are reduced in the cross-sectional area by 25–35% compared with those of the young (Lexell, 1995; Jeon et al., 2021). Sarcopenia occurs with aging, and it is a major factor for frailty (Rolland et al., 2008), mainly due to age-related declines in muscle strength and function, that affects postural reflexes (Landi et al., 2012). **Figure 3** shows that ALMI of the female was not correlated with age, while that in men, it was weakly correlated. What was notable was the weak correlation among elderly men. For example, **Supplementary Table 4** shows 13 participants with sarcopenia before the age of 65 years, including 10 women and 3 men. Among participants over 65 years old, 11 suffered from sarcopenia. Lifestyle habits, exercise, diet (Fiatarone et al., 1994), and sleep may reduce the incidence of sarcopenia (Piovezan et al., 2015). For instance, resistance exercise was reported to increase muscle mass and strength even in the very elderly (Fiatarone et al., 1994; Hurst et al., 2022).

Body mass index is the gold standard for diagnosing obesity (Romero-Corral et al., 2008; Liu et al., 2022), which is considered a metabolic disease (Pedersen and Saltin, 2015; Korac et al., 2021), and associated with many other comorbidities (Afolabi et al., 2020). For example, obese patients often have hypertension or symptomatic ischemic cardiovascular disease (Johns et al., 2014; Valensi et al., 2021). However, a U-shaped association has been reported between BMI and mortality rate (Allison et al., 2008; Childers and Allison, 2010). **Figure 4** showed that age in the elderly was not correlated with BMI, which may be explained by the "obesity paradox" (Childers and Allison, 2010). In **Table 1**, the BMI of the sarcopenia group was 21.48 ± 1.73 and that of the normal group was 24.77 ± 2.43, and significant difference ($p < 0.001$) was found. It may provide evidence to the fact that people with moderate BMI tend to live longer than those with a higher or lower BMI (Childers and Allison, 2010).

Figure 5 shows that the age of the female was not correlated to *T*-score while that of the male was weakly correlated. Using only a certain part of bone mineral density (g/cm^2) to diagnose osteoporosis may lead to misdiagnose (Binkley et al., 2005). In this study, "e Whole Body" scanning mode and "Auto Whole Body" analysis were used to avoid measurement errors when selecting measuring body part (Bazzocchi et al., 2016). Results from **Figure 5** revealed that the decreasing trend of bone mineral

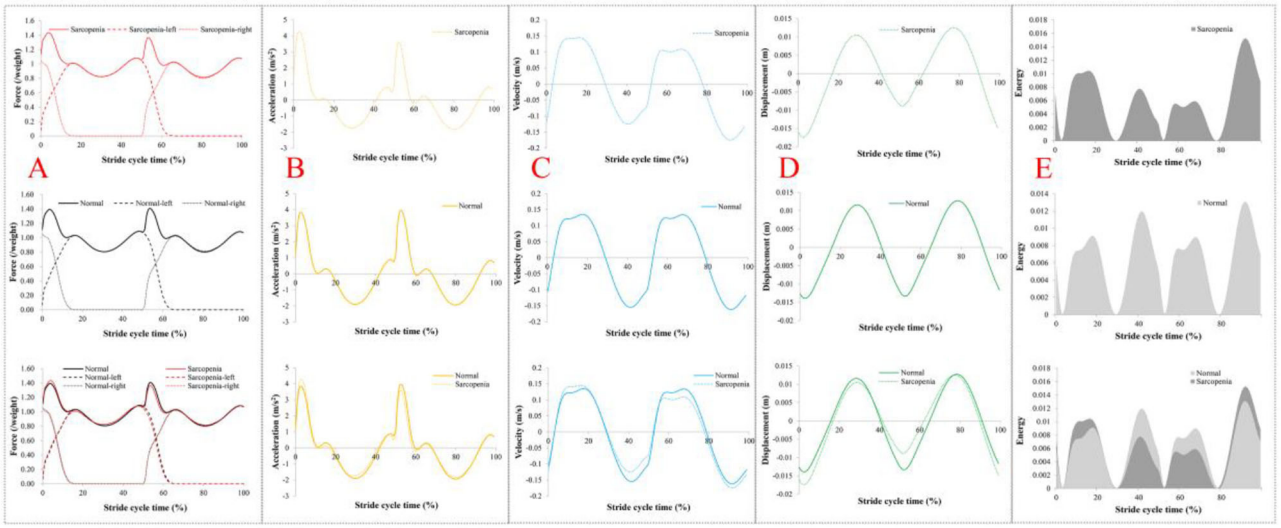

FIGURE 9 | Dynamics results of center of mass (COM). **(A)** The vertical ground reaction force (VGRF) on COM in a stride cycle. **(B)** Vertical acceleration of COM in a stride cycle. **(C)** Vertical velocity of the COM in the stride cycle. **(D)** Vertical displacement of COM in a stride cycle. **(E)** The vertical dynamic energy of COM in a stride cycle. In **(A)**, the dashed line is VGRF on both sides, and the solid line is the resultant force. In **(B–D)**, dashed lines represent the sarcopenia group and solid lines the normal group. In **(E)**, the dark color is sarcopenia and the light color is normal.

density with age was indisputable (Pocock et al., 1989; O'Gorman et al., 2022). However, lifestyle and other factors may slow down the possibility of suffering from osteoporosis due to aging (Zhu and Prince, 2015). However, in **Supplementary Tables 4, 5**, among the 41 participants younger than 65 years old, the number of people with low *T*-score (*T*-score < -1) reached 18 (Kanis et al., 1994), which should be attended. This confirms the relationship between "functional vs. chronological age" and disease again (Soto-Perez-de-Celis et al., 2018).

Figure 6 shows that BMI was positively correlated with the ALMI in all participants, though moderately correlated, with correlation coefficients greater than 0.6 for both women and men. The U-shaped association between BMI and mortality rate (Allison et al., 2008; Childers and Allison, 2010) highlighted the importance of moderate BMI for the elderly. **Table 1** shows that, within the range of normal BMI values, it was wise to choose the Highest Normal, because **Figure 6** reflected the positive correlation between BMI and ALMI, indicating that maintaining a BMI of Highest Normal was significantly correlated with the absence of sarcopenia ($p < 0.001$).

Figure 7 shows that BMI of the female was not correlated with *T*-score while that of the male was moderately correlated. **Figure 5** shows that the female's *T*-score was not correlated with age nor BMI, while that of the male was positively correlated with age and BMI. Though the correlation coefficient was low, the gender difference was significant. The reason remains to be further investigated (Greco et al., 2010; Kim et al., 2017; Wung et al., 2021).

Sarcopenia and osteoporosis are two diseases that require further exploration for evidence of biochemical and molecular interactions between the two (Reginster et al., 2016). Diagnostic standards for sarcopenia were controversial (Edwards et al., 2015; Landi et al., 2018), but the ALMI was an indicator for diagnosing sarcopenia, and *T*-score an indicator for diagnosing osteoporosis. According to the diagnostic standard of *T*-score (Kanis et al., 1994; El Maghraoui and Roux, 2008), in the morbidity rate of osteopenia and osteoporosis in sarcopenia was 75.00%, while the morbidity rate in the normal group was 25.00% as shown in **Supplementary Tables 4, 5**. The morbidity rate of osteoporosis in sarcopenia was 33.33%, while that in the normal group was 4.55%. The moderate positive correlation between ALMI and *T*-score of all participants in **Figure 8** was consistent with the connotation of the difference in the incidence of osteoporosis between both groups presented in **Supplementary Tables 4, 5**.

Table 2 shows that no statistical difference was found in parameters, such as stride frequency and stride time between both groups ($p > 0.05$), and there were significant differences in bilateral stride length and step lengths ($p < 0.01$). Though considerable debate about the value of step velocity was ongoing (Kim et al., 2012; Liu et al., 2013; Tanimoto et al., 2014), consensus had been reached, i.e., slow step velocity was associated with the incidence of sarcopenia. **Table 2** confirms the differences in step velocity in patients with sarcopenia—the incidence of sarcopenia was significantly increased when bilateral stride length reduced, which was the main cause of the decreased step velocity (Kim et al., 2021).

The butterfly parameter assessment has been used in the assessment of the patients with acute stroke (Jin, 2010). Butterfly parameters in **Table 3** shows significant differences between the sarcopenic group and the normal group in both the bilateral length of the gait line and the single support line. The length of the gait line represented the trajectory of center of pressure during the interaction between the foot and the supporting surface (Lugade and Kaufman, 2014). While walking, the support phase includes single support and double support phase. The ratio of the support phase was correlated to the walking speed,

so the faster the walking speed, the smaller the support phase ratio (Fan et al., 2016). No statistical difference between the support phase and the swing phase was found between both the groups in **Table 2**, and the shorter the single support line in **Table 3** the longer the double support phase, which was normal for sarcopenia. In addition, aging is accompanied by the decline of the function of the first metatarsophalangeal joint (Fan et al., 2016), and the shorter length of gait line in sarcopenia in **Table 3** offered evidence for the decline of the first metatarsophalangeal joint during the propulsive phase.

The COM dynamics method is used to diagnose diseases of the musculoskeletal system of the lower limb by the changing law of force, acceleration, velocity, and displacement of the COM during walking (Fan et al., 2009, 2016). **Figure 7** shows that sarcopenia is neither an asymmetric musculoskeletal disease caused by sports injury or a motor nerve-induced musculoskeletal condition (Fan et al., 2009), but a disease of decreased appendicular muscle mass (Ribeiro and Kehayias, 2014). It can be concluded that the method of assessing sarcopenia by ALMI from a DXA scanner for the assessment of sarcopenia is reliable. Furthermore, considering the radiation of X-ray and the cost of the DXA, a simple gait test for screening sarcopenia offers an attractive new method.

From **Tables 2**, **3**, significant differences were found in step length, stride length, length of gait line, and single support line between the sarcopenia group and the normal group, but no significant difference was found in velocity or cadence, suggesting that sarcopenia was related to the reduction of muscle mass. In addition, **Figure 9** shows that in the load response phase, the VGRF peak values from the left and right side of the sarcopenia group were 1.43 and 1.36 times of their body weight, respectively, while those of the normal group were 1.39 and 1.40 times, respectively, suggesting that no significant difference was found in relative muscle strength between these two groups. In **Table 1**, however, significant difference was found in BMI between these two groups, and BMI of the normal group (115.33%) was greater than that of the sarcopenia group, suggesting that significant difference was found in the absolute muscle strength. Observations of gait parameters and mechanical parameters showed that sarcopenia was a disease mainly caused by decreased muscle mass.

The reduced muscle mass led to the shorter step length, length of gait line, and single support line, which means a change in the gait pattern of the sarcopenia elderly. An increase in cadence and decrease in stride length in the elderly would not cause instability (Fan et al., 2016). However, the cadence of the sarcopenia group was very similar to that of the normal group, and the absolute muscle strength of the sarcopenia group decreased, suggesting decreased stability of body control and increased risk of falling. This study offers a preliminary screening for sarcopenia by a gait test and BMI calculation, speeding up screening and greatly reducing the cost of testing. In addition, the mortality rate of the elderly with slow walking speed was higher than that of the elderly with fast walking speed. The general manifestation of the elderly with slow walking speed included: the older the age, the higher their BMI, depressive mood, and less daily exercise (Harwood and Conroy, 2009; Studenski et al., 2011), consistent with the results of this study.

The study's limitations included the following: (1) elderly male generally reported faster velocity and longer stride length and lower cadence than those of the female, suggesting that there may be gender differences in gait in elderly men and women (Winter et al., 1990; Román et al., 2014). Due to the limited number of community dwellers' screening, both male and female participants were included in the comparative analysis of this study, so future analyses should be conducted with a larger sample size with separated gender; (2) participants were differentiated only by ALMI, calculated from ALM obtained from DXA scans, and no other functional tests were performed to functionally diagnose sarcopenia. A longitudinal study to correlate changes in body composition with gait stability during aging can be an important future research topic.

CONCLUSION

This study examined the correlations between body composition and gender and age in the elderly with sarcopenia by ALMI screening as well as differences in gait parameters between healthy controls and patients with sarcopenia. For the elderly, age did not largely affect ALMI, BMI, or *T*-score, but BMI and ALMI were strongly correlated. Significant differences were found in certain gait parameters between the elderly with sarcopenia and normal elderly. The dynamics of COM based on the gait forward dynamics method showed that sarcopenia is a disease mainly caused by decreased muscle mass. When abnormities were found in step length, stride length, length of gait line, or single support line, a DXA scan can then be performed. This may shed some light on the prevention of falls among the elderly.

DATA AVAILABILITY STATEMENT

The raw data supporting the conclusions of this article will be made available by the authors, without undue reservation.

ETHICS STATEMENT

The studies involving human participants were reviewed and approved by Ethics Committee of Fujian Normal University. The patients/participants provided their written informed consent to participate in this study.

AUTHOR CONTRIBUTIONS

YiF conceived and designed the study. YuF, BZ, and GH performed the experiments and collected patients' data. YuF, BZ, GH, GZ, and ZD performed the statistical analysis. YiF and YuF wrote the first draft of the manuscript. ZL and JS reviewed and edited the manuscript. All authors contributed to the manuscript revision and read and approved the submitted version.

FUNDING

This study was supported by the National Natural Science Foundation of China (Grant No. 11972119) and the Natural

Science Foundation of Fujian Province (Grant No. 2019J01429). The funders played no role in the study design, data collection, analyses, interpretation, manuscript writing, or submission.

ACKNOWLEDGMENTS

The authors would like to thank all of the participants for their contribution to this study. They also would like to thank the editor and the reviewers for their comments and suggestions to improve the quality of this manuscript.

SUPPLEMENTARY MATERIAL

The Supplementary Material for this article can be found online at: https://www.frontiersin.org/articles/10.3389/fnagi.2022.909551/full#supplementary-material

REFERENCES

Afolabi, H. A., Zakariya, Z., Ahmed Shokri, A. B., Mohammad Hasim, M. N. B., Vinayak, R., Afolabi-Owolabi, O. T., et al. (2020). The relationship between obesity and other medical comorbidities. *Obes. Med* 0.17, 100164. doi: 10.1016/j.obmed.2019.100164

Allison, D. B., Downey, M., Atkinson, R. L., Billington, C. J., Bray, G. A., Eckel, R. H., et al. (2008). Obesity as a disease: a white paper on evidence and arguments commissioned by the council of the obesity society. *Obesity* 16, 1161–1177. doi: 10.1038/oby.2008.231

Baumgartner, R. N., Koehler, K. M., Gallagher, D., Romero, L., Heymsfield, S. B., Ross, R. R., et al. (1998). Epidemiology of sarcopenia among the elderly in New Mexico. *Am. J. Epidemiol.* 147, 755–763. doi: 10.1093/oxfordjournals.aje.a009520

Bautmans, I., Jansen, B., Van Keymolen, B., and Mets, T. (2011). Reliability and clinical correlates of 3D-accelerometry based gait analysis outcomes according to age and fall-risk. *Gait Posture* 33, 366–372. doi: 10.1016/j.gaitpost.2010.12.003

Bazzocchi, A., Ponti, F., Albisinni, U., Battista, G., and Guglielmi, G. (2016). DXA: technical aspects and application. *Eur. J. Radiol.* 85, 1481–1492. doi: 10.1016/j.ejrad.2016.04.004

Binkley, N., Kiebzak, G. M., Lewiecki, E. M., Krueger, D., Gangnon, R. E., Miller, P. D., et al. (2005). Recalculation of the NHANES database SD improves T-score agreement and reduces osteoporosis prevalence. *J. Bone Miner. Res.* 20, 195–201. doi: 10.1359/JBMR.041115

Bohannon, R. W., and Andrews, A. W. (2011). Normal walking speed: a descriptive meta-analysis. *Physiotherapy* 97, 182–189. doi: 10.1016/j.physio.2010.12.004

Cawthon, P. M., Marshall, L. M., Michael, Y., Dam, T.-T., Ensrud, K. E., Barrett-Connor, E., et al. (2007). Frailty in older men: prevalence, progression, and relationship with mortality. *J. Am. Geriatr. Soc.* 55, 1216–1223. doi: 10.1111/j.1532-5415.2007.01259.x

Chen, L.-K., Liu, L.-K., Woo, J., Assantachai, P., Auyeung, T.-W., Bahyah, K. S., et al. (2014). Sarcopenia in Asia: consensus report of the Asian working group for sarcopenia. *J. Am. Med. Dir. Assoc.* 15, 95–101. doi: 10.1016/j.jamda.2013.11.025

Childers, D. K., and Allison, D. B. (2010). The "obesity paradox": a parsimonious explanation for relations among obesity, mortality rate and aging? *Int. J. Obes.* 34, 1231–1238. doi: 10.1038/ijo.2010.71

Coll, P. P., Phu, S., Hajjar, S. H., Kirk, B., Duque, G., and Taxel, P. (2021). The prevention of osteoporosis and sarcopenia in older adults. *J. Am. Geriatr. Soc.* 69, 1388–1398. doi: 10.1111/jgs.17043

Cruz-Jentoft, A. J., Baeyens, J. P., Bauer, J. M., Boirie, Y., Cederholm, T., Landi, F., et al. (2010). Sarcopenia: european consensus on definition and diagnosis: report of the european working group on sarcopenia in older people. *Age Ageing* 39, 412–423. doi: 10.1093/ageing/afq034

Dutta, C. (1997). Significance of sarcopenia in the elderly. *J. Nutr.* 127, 992S−993S.

Edwards, M. H., Dennison, E. M., Aihie Sayer, A., Fielding, R., and Cooper, C. (2015). Osteoporosis and sarcopenia in older age. *Bone* 80, 126–130. doi: 10.1016/j.bone.2015.04.016

El Maghraoui, A., and Roux, C. (2008). DXA scanning in clinical practice. *QJM* 101, 605–617. doi: 10.1093/qjmed/hcn022

Falsarella, G. R., Coimbra, I. B., Barcelos, C. C., Iartelli, I., Montedori, K. T., Santos, M. N. J., et al. (2014). Influence of muscle mass and bone mass on the mobility of elderly women: an observational study. *BMC Geriatr.* 14, 13. doi: 10.1186/1471-2318-14-13

Fan, Y., Li, Z., Han, S., Lv, C., and Zhang, B. (2016). The influence of gait speed on the stability of walking among the elderly. *Gait Posture* 47, 31–36. doi: 10.1016/j.gaitpost.2016.02.018

Fan, Y. F., Loan, M., Fan, Y. B., Li, Z. Y., and Luo, D. L. (2009). Least-action principle in gait. *EPL* 87, 58003. doi: 10.1209/0295-5075/87/58003

Fiatarone, M. A., O'Neill, E. F., Ryan, N. D., Clements, K. M., Solares, G. R., Nelson, M. E., et al. (1994). Exercise training and nutritional supplementation for physical frailty in very elderly people. *New Engl. J. Med.* 330, 1769–1775. doi: 10.1056/NEJM199406233302501

Fukuoka, Y., Narita, T., Fujita, H., Morii, T., Sato, T., Sassa, M. H., et al. (2019). Importance of physical evaluation using skeletal muscle mass index and body fat percentage to prevent sarcopenia in elderly Japanese diabetes patients. *J. Diabetes Invest.* 10, 322–330. doi: 10.1111/jdi.12908

Greco, E. A., Fornari, R., Rossi, F., Santiemma, V., Prossomariti, G., Annoscia, C., et al. (2010). Is obesity protective for osteoporosis? Evaluation of bone mineral density in individuals with high body mass index. *Int. J. Clin. Pract* 0.64, 817–820. doi: 10.1111/j.1742-1241.2009.02301.x

Han, Y., He, Y., Lyu, J., Yu, C., Bian, M., and Lee, L. (2020). Aging in China: perspectives on public health. *J. Glob. Health* 4, 11–17. doi: 10.1016/j.glohj.2020.01.002

Harwood, R. H., and Conroy, S. P. (2009). Slow walking speed in elderly people. *BMJ Br. Med. J.* 339, b4236. doi: 10.1136/bmj.b4236

Hurst, C., Robinson, S. M., Witham, M. D., Dodds, R. M., Granic, A., Buckland, C., et al. (2022). Resistance exercise as a treatment for sarcopenia: prescription and delivery. *Age Ageing* 51, afac003. doi: 10.1093/ageing/afac003

Iii, L. J. M., Khosla, S., Crowson, C. S., O'Connor, M. K., O'Fallon, W. M., and Riggs, B. L. (2000). Epidemiology of sarcopenia. *J. Am. Geriatr. Soc.* 48, 625–630. doi: 10.1111/j.1532-5415.2000.tb04719.x

Jeon, W., Hsiao, H.-Y., and Griffin, L. (2021). Effects of different initial foot positions on kinematics, muscle activation patterns, and postural control during a sit-to-stand in younger and older adults. *J. Biomech.* 117, 110251. doi: 10.1016/j.jbiomech.2021.110251

Jin, Y.-W. (2010). The scientific research of rehabilitation training program participants in stroke patients. *Life Sci. J.* 20, 1704–1710. doi: 10.5352/JLS.2010.20.11.1704

Johns, D. J., Hartmann-Boyce, J., Jebb, S. A., Aveyard, P., and Behavioural Weight Management Review Group (2014). Diet or exercise interventions vs combined behavioral weight management programs: a systematic review and meta-analysis of direct comparisons. *J. Acad. Nutr. Diet.* 114, 1557–1568. doi: 10.1016/j.jand.2014.07.005

Kang, H. G., and Dingwell, J. B. (2008). Effects of walking speed, strength and range of motion on gait stability in healthy older adults. *J. Biomech.* 41, 2899–2905. doi: 10.1016/j.jbiomech.2008.08.002

Kanis, J. A., Melton, III, L. J., Christiansen, C., Johnston, C. C., and Khaltaev, N. (1994). The diagnosis of osteoporosis. *J. Bone Miner. Res.* 9, 1137–1141. doi: 10.1002/jbmr.5650090802

Kim, H.-S., Kim, T., Ahn, J.-Y., Hwang, K.-Y., Park, J.-Y., Lim, T.-T., et al. (2012). Aging characteristics and reactivity of two types of nanoscale zero-valent iron particles (FeBH and FeH_2) in nitrate reduction. *Chem. Eng. J.* 197, 16–23. doi: 10.1016/j.cej.2012.05.018

Kim, J.-K., Bae, M.-N., Lee, K. B., and Hong, S. G. (2021). Identification of patients with sarcopenia using gait parameters based on inertial sensors. *Sens. Basel* 21, 1786. doi: 10.3390/s21051786

Kim, Y.-S., Han, J.-J., Lee, J., Choi, H. S., Kim, J. H., and Lee, T. (2017). The correlation between bone mineral density/trabecular bone score and

body mass index, height, and weight. *Osteoporos Sarcopenia* 3, 98–103. doi: 10.1016/j.afos.2017.02.001

Kirk, B., Zanker, J., Bani Hassan, E., Bird, S., Brennan-Olsen, S., and Duque, G. (2021). Sarcopenia definitions and outcomes consortium (sdoc) criteria are strongly associated with malnutrition, depression, falls, and fractures in high-risk older persons. *J. Am. Med. Dir. Assoc.* 22, 741–745. doi: 10.1016/j.jamda.2020.06.050

Korac, B., Kalezic, A., Pekovic-Vaughan, V., Korac, A., and Jankovic, A. (2021). Redox changes in obesity, metabolic syndrome, and diabetes. *Redox Biol.* 42, 101887. doi: 10.1016/j.redox.2021.101887

Landi, F., Calvani, R., Cesari, M., Tosato, M., Martone, A. M., Ortolani, E., et al. (2018). Sarcopenia: an overview on current definitions, diagnosis and treatment. *Curr. Protein Pept. Sci.* 19, 633–638. doi: 10.2174/1389203718666170607113459

Landi, F., Liperoti, R., Russo, A., Giovannini, S., Tosato, M., Capoluongo, E., et al. (2012). Sarcopenia as a risk factor for falls in elderly individuals: results from the ilSIRENTE study. *Clin. Nutr.* 31, 652–658. doi: 10.1016/j.clnu.2012.02.007

Leiros-Rodriguez, R., Romo-Perez, V., Arce-Farina, M. E., and Garcia-Soidan, J. L. (2018). Associations between body composition and movements during gait in women. *Rev. Int. Med. Cienc. Act* 18, 693–707. doi: 10.15366/rimcafd2018.72.006

Lexell, J. (1995). Human aging, muscle mass, and fiber type composition. *J. Gerontol. Biol. Sci. Med. Sci.* 50A, 11–16. doi: 10.1093/gerona/50A.Special_Issue.11

Li, S., and Lin, S. (2016). Population aging and China's social security reforms. *J. Policy Model* 38, 65–95. doi: 10.1016/j.jpolmod.2015.10.001

Liu, J., Ayada, I., Zhang, X., Wang, L., Li, Y., Wen, T., et al. (2022). Estimating global prevalence of metabolic dysfunction-associated fatty liver disease in overweight or obese adults. *Clin. Gastroenterol. Hepatol.* 20, e573–e582. doi: 10.1016/j.cgh.2021.02.030

Liu, L.-K., Lee, W.-J., Liu, C.-L., Chen, L.-Y., Lin, M.-H., Peng, L.-N., et al. (2013). Age-related skeletal muscle mass loss and physical performance in Taiwan: implications to diagnostic strategy of sarcopenia in Asia. *Geriatr. Gerontol. Int.* 13, 964–971. doi: 10.1111/ggi.12040

Lugade, V., and Kaufman, K. (2014). Center of pressure trajectory during gait: a comparison of four foot positions. *Gait Posture* 40, 719–722. doi: 10.1016/j.gaitpost.2014.07.001

Morley, J. E., Abbatecola, A. M., Argiles, J. M., Baracos, V., Bauer, J., Bhasin, S., et al. (2011). Sarcopenia with limited mobility: an international consensus. *J. Am. Med. Dir. Assoc.* 12, 403–409. doi: 10.1016/j.jamda.2011.04.014

O'Gorman, C. A., Minnock, S., Mulhall, J., and Gleeson, N. (2022). Attention to bone health in follow-up of gynaecological cancers in tertiary care. *Womens Health* 18, 17455065211070748. doi: 10.1177/17455065211070747

Pedersen, B. K., and Saltin, B. (2015). Exercise as medicine - evidence for prescribing exercise as therapy in 26 different chronic diseases. *Scand. J. Med. Sci. Spor.* 25(Suppl. 3), 1–72. doi: 10.1111/sms.12581

Phillips, D. R., and Feng, Z. (2015). Challenges for the aging family in the people's republic of China. *Can. J. Aging* 34, 290–304. doi: 10.1017/S0714980815000203

Piovezan, R. D., Abucham, J., dos Santos, R. V. T., Mello, M. T., Tufik, S., and Poyares, D. (2015). The impact of sleep on age-related sarcopenia: possible connections and clinical implications. *Ageing Res. Rev.* 23, 210–220. doi: 10.1016/j.arr.2015.07.003

Pocock, N., Eisman, J., Gwinn, T., Sambrook, P., Kelly, P., Freund, J., et al. (1989). Muscle strength, physical fitness, and weight but not age predict femoral neck bone mass. *J. Bone Miner. Res.* 4, 441–448. doi: 10.1002/jbmr.5650040320

Reginster, J.-Y., Beaudart, C., Buckinx, F., and Bruyère, O. (2016). Osteoporosis and sarcopenia: two diseases or one? *Curr. Opin. Clin. Nutr.* 19, 31–36. doi: 10.1097/MCO.0000000000000230

Ribeiro, S. M. L., and Kehayias, J. J. (2014). Sarcopenia and the analysis of body composition. *Adv. Nutr.* 5, 260–267. doi: 10.3945/an.113.005256

Rolland, Y., Czerwinski, S., van Kan, G. A., Morley, J. E., Cesari, M., Onder, G., et al. (2008). Sarcopenia: its assessment, etiology, pathogenesis, consequences and future perspectives. *J. Nutr. Health Aging* 12, 433–450. doi: 10.1007/BF02982704

Román, P. L., García-Pinillos, F., Herrador, J. H., Barba, M. C., and Jiménez, M. M. (2014). Relationship between sex, body composition, gait speed and body satisfaction in elderly people. *Nutr. Hosp.* 30, 851–857. doi: 10.3305/nh.2014.30.4.7669

Romero-Corral, A., Somers, V. K., Sierra-Johnson, J., Thomas, R. J., Collazo-Clavell, M. L., Korinek, J., et al. (2008). Accuracy of body mass index in diagnosing obesity in the adult general population. *Int. J. Obesity* 32, 959–966. doi: 10.1038/ijo.2008.11

Rosenberg, I. H. (1997). Sarcopenia: origins and clinical relevance. *J. Nutr.* 127, 990S—991S. doi: 10.1093/jn/127.5.990S

Sanchez-Rodriguez, D., Marco, E., Miralles, R., Guillen-Sola, A., Vazquez-Ibara, O., Escalada, F., et al. (2015). Does gait speed contribute to sarcopenia case-finding in a postacute rehabilitation setting? *Arch. Gerontol. Geriat* 61, 176–181. doi: 10.1016/j.archger.2015.05.008

Senden, R., Grimm, B., Heyligers, I. C., Savelberg, H. H. C. M., and Meijer, K. (2009). Acceleration-based gait test for healthy subjects: reliability and reference data. *Gait Posture* 30, 192–196. doi: 10.1016/j.gaitpost.2009.04.008

Senden, R., Savelberg, H. H. C. M., Grimm, B., Heyligers, I. C., and Meijer, K. (2012). Accelerometry-based gait analysis, an additional objective approach to screen subjects at risk for falling. *Gait Posture* 36, 296–300. doi: 10.1016/j.gaitpost.2012.03.015

Soto-Perez-de-Celis, E., Li, D., Yuan, Y., Lau, Y. M., and Hurria, A. (2018). Functional versus chronological age: geriatric assessments to guide decision making in older patients with cancer. *Lancet Oncol.* 19, e305–e316. doi: 10.1016/S1470-2045(18)30348-6

Studenski, S., Perera, S., Patel, K., Rosano, C., Faulkner, K., Inzitari, M., et al. (2011). Gait speed and survival in older adults. *JAMA* 305, 50–58. doi: 10.1001/jama.2010.1923

Tanimoto, Y., Watanabe, M., Sun, W., Sugiura, Y., Hayashida, I., Kusabiraki, T., et al. (2014). Sarcopenia and falls in community-dwelling elderly subjects in Japan: defining sarcopenia according to criteria of the european working group on sarcopenia in older people. *Arch. Gerontol. Geriat* 59, 295–299. doi: 10.1016/j.archger.2014.04.016

Thiede, R., Toosizadeh, N., Mills, J. L., Zaky, M., Mohler, J., and Najafi, B. (2016). Gait and balance assessments as early indicators of frailty in patients with known peripheral artery disease. *Clin. Biomech.* 32, 1–7. doi: 10.1016/j.clinbiomech.2015.12.002

Valensi, P., Henry, P., Boccara, F., Cosson, E., Prevost, G., Emmerich, J., et al. (2021). Risk stratification and screening for coronary artery disease in asymptomatic patients with diabetes mellitus: position paper of the French Society of Cardiology and the French-speaking Society of Diabetology. *Diabetes Metab.* 47, 101185. doi: 10.1016/j.diabet.2020.08.002

Winter, D. A., Patla, A. E., Frank, J. S., and Walt, S. E. (1990). Biomechanical walking pattern changes in the fit and healthy elderly. *Phys. Ther.* 70, 340–347. doi: 10.1093/ptj/70.6.340

Wung, C.-H., Chung, C.-Y., Wu, P.-Y., Huang, J.-C., Tsai, Y.-C., Chen, S.-C., et al. (2021). Associations between metabolic syndrome and obesity-related indices and bone mineral density t-score in hemodialysis patients. *J. Pers. Med.* 11, 775. doi: 10.3390/jpm11080775

Zhu, K., and Prince, R. L. (2015). Lifestyle and osteoporosis. *Curr. Osteoporos. Rep.* 13, 52–59. doi: 10.1007/s11914-014-0248-6

Conflict of Interest: The authors declare that the research was conducted in the absence of any commercial or financial relationships that could be construed as a potential conflict of interest.

Publisher's Note: All claims expressed in this article are solely those of the authors and do not necessarily represent those of their affiliated organizations, or those of the publisher, the editors and the reviewers. Any product that may be evaluated in this article, or claim that may be made by its manufacturer, is not guaranteed or endorsed by the publisher.

frontiers | Frontiers in Aging Neuroscience

ORIGINAL RESEARCH
published: 14 July 2022
doi: 10.3389/fnagi.2022.909571

Analysis of the Relationship Between Motor Imagery and Age-Related Fatigue for CNN Classification of the EEG Data

Xiangyun Li[1,2], *Peng Chen*[3]*, *Xi Yu*[4,5] *and Ning Jiang*[2,6]

[1] West China Biomedical Big Data Center, West China Hospital, Sichuan University, Chengdu, China, [2] Med-X Center for Manufacturing, West China Hospital, Sichuan University, Chengdu, China, [3] School of Mechanical Engineering, Southwest Jiaotong University, Chengdu, China, [4] Department of Orthopedic Surgery and Orthopedic Research Institute, West China Hospital, Sichuan University, Chengdu, China, [5] Rehabilitation Medicine Center, West China Hospital, Sichuan University, Chengdu, China, [6] National Clinical Research Center for Geriatrics, West China Hospital, Sichuan University, Chengdu, China

OPEN ACCESS

Edited by:
Chuhuai Wang,
Sun Yat-sen University, China

Reviewed by:
Peng Xu,
University of Electronic Science and Technology of China, China
Ren Xu,
g.tec Medical Engineering GmbH, Austria
Mevan Ekanayake,
Monash University, Australia

***Correspondence:**
Peng Chen
chenpeng@swjtu.edu.cn

Specialty section:
This article was submitted to Neurocognitive Aging and Behavior, a section of the journal Frontiers in Aging Neuroscience

Received: *31 March 2022*
Accepted: *14 June 2022*
Published: *14 July 2022*

Citation:
Li X, Chen P, Yu X and Jiang N (2022) Analysis of the Relationship Between Motor Imagery and Age-Related Fatigue for CNN Classification of the EEG Data. Front. Aging Neurosci. 14:909571. doi: 10.3389/fnagi.2022.909571

Background: The aging of the world population poses a major health challenge, and brain–computer interface (BCI) technology has the potential to provide assistance and rehabilitation for the elderly.

Objectives: This study aimed to investigate the electroencephalogram (EEG) characteristics during motor imagery by comparing young and elderly, and study Convolutional Neural Networks (CNNs) classification for the elderly population in terms of fatigue analysis in both frontal and parietal regions.

Methods: A total of 20 healthy individuals participated in the study, including 10 young and 10 older adults. All participants completed the left- and right-hand motor imagery experiment. The energy changes in the motor imagery process were analyzed using time–frequency graphs and quantified event-related desynchronization (ERD) values. The fatigue level of the motor imagery was assessed by two indicators: $(\theta + \alpha)/\beta$ and θ/β, and fatigue-sensitive channels were distinguished from the parietal region of the brain. Then, rhythm entropy was introduced to analyze the complexity of the cognitive activity. The phase-lock values related to the parietal and frontal lobes were calculated, and their temporal synchronization was discussed. Finally, the motor imagery EEG data was classified by CNNs, and the accuracy was discussed based on the analysis results.

Result: For the young and elderly, ERD was observed in C3 and C4 channels, and their fatigue-sensitive channels in the parietal region were slightly different. During the experiment, the rhythm entropy of the frontal lobe showed a decreasing trend with time for most of the young subjects, while there was an increasing trend for most of the older ones. Using the CNN classification method, the elderly achieved around 70% of the average classification accuracy, which is almost the same for the young adults.

Conclusion: Compared with the young adults, the elderly are less affected by the level of cognitive fatigue during motor imagery, but the classification accuracy of motor imagery data in the elderly may be slightly lower than that in young persons. At the

same time, the deep learning method also provides a potentially feasible option for the application of motor-imagery BCI (MI-BCI) in the elderly by considering the ERD and fatigue phenomenon together.

Keywords: aging, brain–computer interfaces, motor imagery, fatigue, CNN

INTRODUCTION

Population aging is one of the severe challenges faced by all countries in the world nowadays and in the next few decades. According to the report of the Global Health and Aging published by WHO, by the middle of this century, the proportion of people over 65 years will increase from 11 to 22%, and the 85 years-and-over population is projected to increase by 351% between 2010 and 2050 (Mary et al., 2007). It also indicates that there will be a larger number of older people aged 60 years or over than adolescents aged 10–24 years by the middle of this century (Rudnicka et al., 2020). With the increase of age, the elderly generally have a decline in self-care ability and suffer from the risks of various diseases, which affect both their physical and mental health, leading to the degradation of the life quality in this group. Therefore, promoting the health level of the elderly is a critical factor in solving the aging problem.

As part of the aging process, a great number of changes occur in the central nervous system (CNS), and the brain function of the elderly is inevitably changed with the increase of age. Aging may also cause chronic neurological diseases which affect the motor system (Nikhil et al., 2014), and even healthy aging is accompanied by a decline in cognitive function (Gard et al., 2014). These kinds of cognitive or motor problems are reflected in the electrical activity of the brain and could be studied from electroencephalogram (EEG) signals. EEG analysis reveals the features of brain activities during the motor and cognitive tasks by various signal processing approaches (Pavlov et al., 2020). Many studies use EEG to explain the changes in the CNS due to the appearance of some aging-related diseases (Paiva et al., 2012). Brain–computer interface (BCI) establishes the direct interaction path between the brain and the external world by decoding the information from the brain during the mental tasks (Wolpaw et al., 2000). To help the elderly maintain a healthy, good quality of life, and sense of wellbeing, a number of BCI applications have been developed in recent years (Belkacem et al., 2020).

EEG could provide a non-invasive way to BCI with the characteristics of simple structure, high safety, and good real-time performance (Castermans et al., 2013). With the features extracted from the EEG signals, the classification based on the machine learning algorithms can convert them into the control commands for assistive or rehabilitation devices (Li et al., 2016). Several common paradigms are proposed to make the brain generate proper EEG signals. Generally, the EEG could be categorized as self-paced or non-self-paced ones. The self-paced ones only need the inner brain activities of the users (Müller-Putz et al., 2016), so these users can make their own decisions for control aims. In self-paced EEG, motor imagery (MI) is a dynamic cognitive process during which the movement is mentally simulated without actually being executed (Jeannerod, 2011). In the cerebral cortex, MI and motor execution of the same action have similar activity patterns. The goal of motor-imagery BCIs (MI-BCIs) is to control an external object by inducing and modulating the brainwaves of interest during the training sessions so that the BCI system can determine the user's intention in real-time in testing sessions (Jiang et al., 2022). Several studies have explored the influences of aging on different aspects of MI, such as vividness (Malouin et al., 2010), working memory (Schotta, 2012), and the temporal performance of the MI (Personnier et al., 2010). However, these studies are based on scales and statistics analysis, and the EEG indicators have not been introduced to evaluate the difference in MI ability across different age groups.

EEG sensorimotor rhythm changes from the resting state to the MI or motor execution state. This phenomenon reflects a decrease in the power of EEG over the primary sensorimotor area in the alpha (7–4 Hz) and beta (15–35 Hz) bands indicating underlying cortical cells to be desynchronized, which is named as event-related desynchronization (ERD) (Hisato et al., 2018). A comparative study of the ERD of EEG signals during MI tasks in different age groups would be helpful to understand the changes in cerebral cortex activity and the influence of aging on improving the MI training in neurological rehabilitation and BCI system design for the elderly.

In the MI-BCI, it is significant to make a cognitive effort to focus on MI tasks, but the EEG signal quality heavily depends on the mental state, level of attention, and fatigue of BCI users. Loss of attention due to mental fatigue significantly decreases signal characteristics, and thus reduces the performance of BCI systems (Cao et al., 2014). Some studies (Talukdar et al., 2018) also have confirmed that long-term MI can cause mental fatigue, and the level of mental fatigue corresponds to the EEG data separability of MI, which relates to the further application of MI-BCI. However, most of the current studies were only conducted on young adults. Aging increases the complexity of human brains (Anokhin et al., 1996), and this effect is demonstrated in the frontal inferior and sensorimotor areas (Scheel et al., 2018). In addition, entropy-based tools are widely used to quantify complexity, and approaches related to time–frequency analysis in separate frequency bands provide a clear physiological interpretation of the changes in EEG signals (Pavlov et al., 2020). Thus, it is necessary to investigate the fatigue caused by MI from the aspects of EEG power on both frontal inferior and sensorimotor regions.

With the different fatigue characteristics of EEG in the young and elderly population, a suitable MI data classification method is crucial for generating the control commands for the assistive and rehabilitation device application in aging groups. In the MI data classification stage, the extracted features are interpreted as the BCI user intentions, and machine learning is the most frequently used classification method. Deep learning belongs to

representation learning, which aims to better represent input data using multiple layers of processing blocks such as neural networks (e.g., CNN and RNN). CNN (Lecun et al., 1989), proposed for the first time in the 1980s, was used to classify handwritten digits. CNN is of vital importance for EEG decoding using deep learning methods. To introduce CNN algorithms to EEG data classification, two measures are generally taken. First, in the aspect of the good performance of CNN for image classification, many researchers firstly convert the EEG signal into image information and then input it into CNN for classification. It uses the time–frequency maps of C3, Cz, and C4 channels at 6∼13 Hz and 17∼30 Hz for splicing as the feature of EEG data input to the convolutional neural network (CNN) for classification (Tabar and Halici, 2017). Another idea is to utilize the "end-to-end" characteristics of deep learning by importing the preprocessed EEG data as the input of the neural network and directly extracting the deep abstract features in the EEG data through the neural network. EEGNet (Lawhern et al., 2018) builds a deep learning model based on a CNN to directly classify EEG data samples, and the core idea is to convolve the channel dimension and the time dimension, respectively, and directly extract and classify features from these two dimensions. In the previous studies, the classification of EEG signals by CNN is usually applied to younger subjects, while the comparative study of young adults and the elderly has not been thoroughly carried out. If this effectiveness of the tool is also verified on MI data from older groups, it will promote the development of rehabilitation and assistive BCI more suitable for the elderly population and facilitate their everyday lives.

This study investigates the ERD of EEG signals in MI tasks in different age groups to clarify the differences in MI ability in both groups. The changes in fatigue level during MI will be studied. Fatigue analysis includes three aspects: the first is to distinguish fatigue-sensitive channels in the parietal region; another is to calculate rhythm entropy (RE) in the frontal region; the third is to analyze whether the fatigue in the parietal region and the EEG complexity in the frontal lobe are synchronized through phase-locked values (PLVs). Based on such analysis, it investigates the differences in the classification performance of deep learning methods (CNN) on young and the elderly, which will provide a reference for designing BCIs for rehabilitation and daily living aids used by the elderly.

METHODS

Participants

Ten young adults (S1–S10, 8 males and 2 females, mean age 23) and 10 older adults (T1–T10, 3 males and 7 females, mean age 66) participated in this study. All participants were right-handed and had a normal or corrected vision, without known neurological or psychological disorders, use of psychiatric drugs, or any drugs affecting the CNS. The participants were asked to have a good sleep before the experiment. Each participant was informed about the experimental protocol and included after receiving verbal consent for the experimental trials. The protocol studied was approved by the local ethical committee and performed in accordance with the Declaration of Helsinki.

EEG Recording

EEG data were acquired with a 64-channel EEG cap (Waveguard Original, ANT Neuro b.v., Enschede, Netherlands) and a mobile EEG amplifier (eego sports, ANT Neuro b.v., Enschede, Netherlands) at a sampling rate of 1,024 Hz. The 64-electrode configuration was set according to the international 10–20 system. The reference and ground electrodes were placed on CPz and AFz, respectively. Most electrodes (about 65%) had impedances <5 KΩ.

Experiment Setup and Paradigm

Participants are asked to sit in a comfortable chair and look at the computer screen, which displays the experimental paradigm. Participants are asked to avoid blinking and body movements during EEG recording. The two different MI tasks (left-hand movement vs. right-hand movement) are performed by the participants. The experimental session consists of four runs of continuous EEG signal recording. Each participant performs 40 trials in each run, with a total of 160 trials. During each trial, the computer screen first displays a black screen for 3 s, then a video of the left or right-hand movement of the fist for 3 s, and finally a 5-s up-left or up-right arrow together with 30 s rest for every 10 trials. Participants keep relaxed when the screen is black, concentrate when the video is playing, and begin to imagine the corresponding movement when the arrow appears. The sequence of events in the trial is illustrated in **Figure 1**, and a 5-min rest is given between runs. It should be noted that S8 collected two more runs for some reasons, reaching 240 samples.

EEG Data Pre-processing

The EEG signals were processed using the EEGLAB toolbox. A 50 Hz industrial frequency interference has been removed and the band-pass was filtered from 1 to 35 Hz using a finite impulse response (FIR) filter. The filtered data is resampled to 512 Hz. Then, the resample data was segmented to extract epochs and removed baseline. This resulted in a total of 160 epochs for each participant, except for S8. All artifacts were removed in each epoch (such as eyeblinks and body movement) by independent component analysis (ICA). The attributes of components were observed by the ICLabel function, and the components which belong to EOG, EMG, noises, and other artifacts were discarded, and only those with more than 60% probability of being estimated as EEG were retained. The run with more artifacts in the four runs of experiments was eliminated in young adults when ERD and fatigue were analyzed, but all runs were retained in older adults.

Event-Related Desynchronization/Synchronization (ERD/S)

To analyze the fatigue levels in the process of MI, it needs to verify the ERD/ERS phenomenon in the process of MI through time–frequency analysis and the results are used for time–frequency analysis to carry out the subsequent related calculation of fatigue. The time–frequency analysis implemented by Letswave7.ERD/ERS is calculated in a defined frequency band about a baseline reference interval. The baseline reference

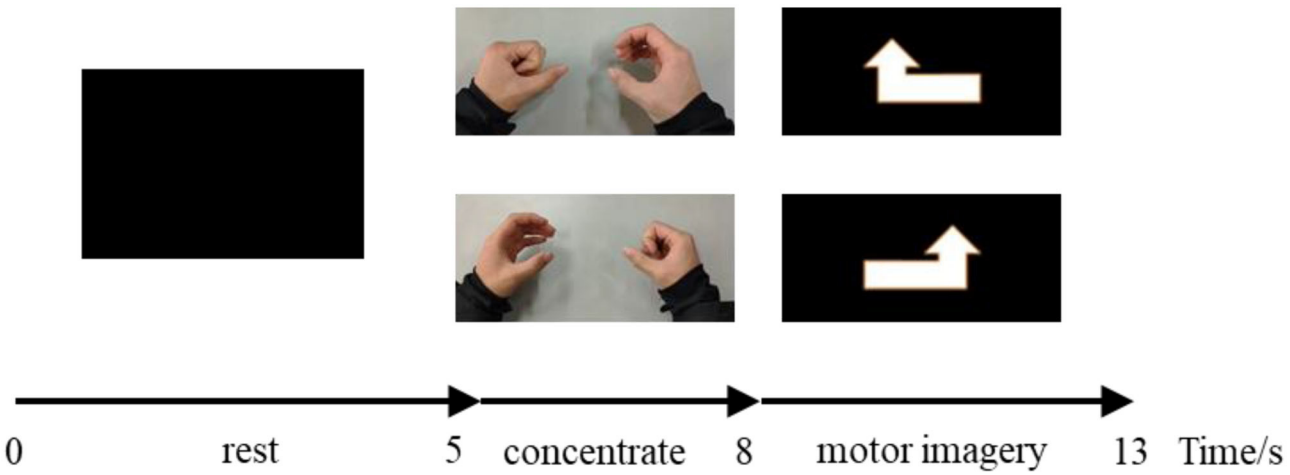

FIGURE 1 | Experimental protocol for a single trial.

interval for the ERD/ERS calculation was taken from 0 to 1 s for each epoch. After performing the artifact removal mentioned above, wavelet transformation was applied to analyze the law of EEG signal energy changing with frequency and time. The single time–frequency map under the same task is superimposed and averaged to obtain the final time–frequency map.

Fatigue Analysis in Motor Imagery

The α and β EEG signals increase and θ EEG signal decrease during fatigue, and the (θ + α)/β has the strongest positive correlation with fatigue (Jap et al., 2009). This paper fuses (θ + α)/β and θ/β into a comprehensive fatigue index to analyze and evaluate the fatigue level in real-time. The preprocessed EEG signal is decomposed and reconstructed by wavelet transform, and the EEG signal of different characteristic frequency bands (θ, α, and β frequency bands) is extracted. The EEG signal has strong individual differences, and the EEG channels sensitive to fatigue differ among subjects. It calculates the correlation between the fatigue index and the experimental time of each channel, selects the channel whose correlation value is larger than the threshold, and then sets it as the sensitive channel. According to experience, the threshold is set to 0.75 in this paper. Fatigue-sensitive channels in the parietal lobe are extracted, which are located in the center of the human brain that processes sensory. After that, the power spectral density of each sensitive channel is calculated separately, and the fatigue level is finally obtained.

Entropy is robust in assessing the regularity and predictability of complex systems and has been used to analyze EEG signals (Arunkumar et al., 2018). RE extracts each rhythm of the EEG signal and then calculates its entropy value. For the six channels (F3, F4, F5, F1, F2, and F6) located in the frontal cortex of each subject, their RE is calculated.

First, calculate the energy for each trial of different rhythmic cortical activity:

$$Power = \sum_{i=1}^{m} S(x)^2$$

where $S(x)$ represents estimated cortical activity and m is the number of sample points.

Then, the energy normalized by the jth frequency band rhythm cortical activity is calculated, and the value is obtained by dividing the sum of the energies of the three frequency bands according to the following equation:

$$P_j = \frac{Power_j}{\sum_{j=1}^{k} Power_j}$$

where $Power_j$ represents the energy of the jth frequency band rhythm cortical activity and k is the number of the frequency band.

The formula of RE calculation is:

$$En = -\sum_{j=1}^{k} P_j log_2 P_j$$

To verify the selection of parietal lobe fatigue channels and the rationality of prefrontal lobe RE fatigue analysis, the synchronization of the channels was verified by calculating the PLVs of fatigue-sensitive channels and prefrontal lobe channels. For two univariate continuous-time signals, x(t) and y(t), the phase synchronization relationship can be expressed by the PLV.

$$PLV = \left|\left\langle e^{i\Phi_{xy}(t)}\right\rangle_t\right| = \sqrt{\langle cos\Phi_{xy}(t)\rangle_t^2 + \langle sin\Phi_{xy}(t)\rangle_t^2}$$

$$\Phi_{xy}(t) = \Phi_x(t) - \Phi_y(t)$$

where, <> represents the average value of time and $\Phi_x(t)$ and $\Phi_y(t)$ represent the instantaneous phases $x(t)$ and $y(t)$, respectively. According to the above formula, the PLVs of any two time-signals x(t) and y(t) can be obtained. If PLV = 0, it means that x(t) and y(t) have no phase synchronization. If PLV = 1, then x(t) and y(t) synchronize in their phases. The range of PLVs is [0,1].

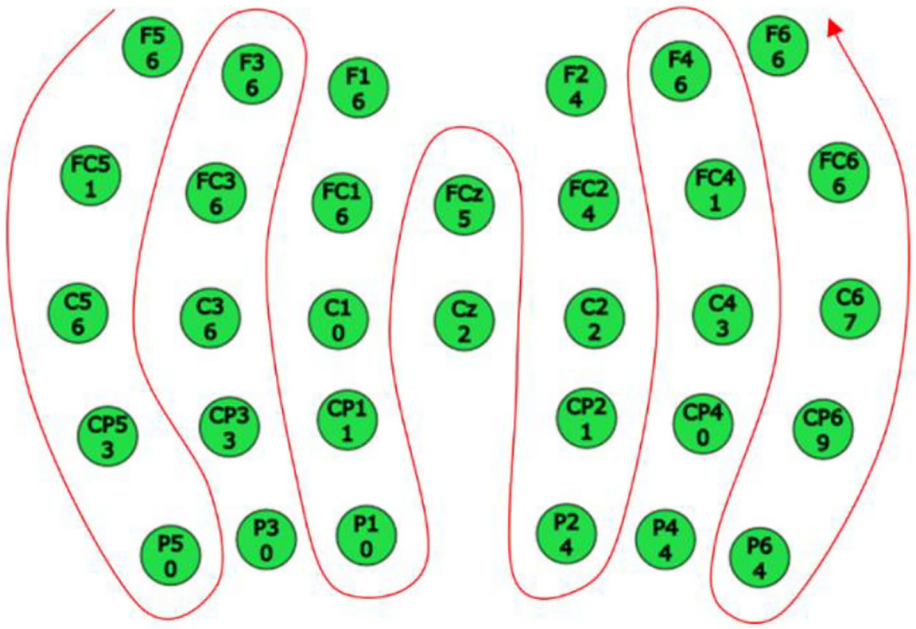

FIGURE 2 | The rearranged order of the selected 32 channels.

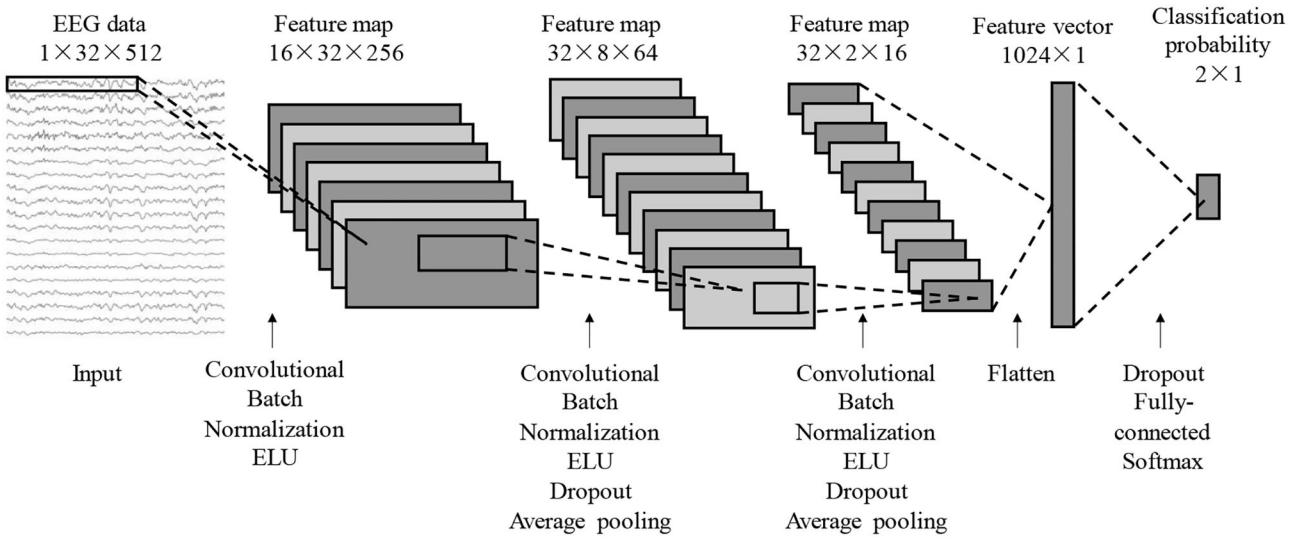

FIGURE 3 | CNN structure diagram that fuses spatial information.

Proposed CNN Architecture

Referring to the network structure of EEGNet, combined with the MI characteristics of the young and elderly, a CNN algorithm that integrates spatial information to classify and identify MI-EEG signals is proposed. It is of great help to improve the classification accuracy and enhance the generalization ability of the CNN model by extracting time, frequency, and space information from the EEG signals (Yimin et al., 2020). To preserve the spatial information on the ipsilateral side and distinguish that on the opposite side, the rearranged order of the selected 32 channels, as shown in **Figure 2**, was as follows: F5, FC5, C5, CP5, P5, P3, CP3, C3, FC3, F3, F1, FC1, C1, CP1, P1, Cz, FCz, F2, FC2, C2, CP2, P2, P4, CP4, C4, FC4, F4, F6, FC6, C6, CP6, and P6. In addition, it normalized the samples as a whole. The standardization method was to subtract the mean value of all the data in the sample and divide it by the standard deviation. After normalization, all data points of each sample fit a distribution with mean 0 and standard deviation 1, which helped to speed up the rate of

TABLE 1 | Implementation details for proposed CNN architecture.

Type	Maps	Size	Kernel size	Stride	Padding	Parameter
Input	1	32 × 512	–	–	–	0
Convolutional 1	16	32 × 256	1 × 24 × 16	1 × 2	0 × 11	400
Batch normalization 1	16	32 × 256	–	–	–	0
Activation 1	16	32 × 256	–	–	–	0
Convolutional 2	32	16 × 256	2 × 11 × 32	2 × 1	0 × 5	11,296
Batch normalization 2	32	16 × 256	–	–	–	0
Activation 2	32	16 × 256	–	–	–	0
Average pooling 1	32	8 × 64	2 × 4	2 × 4	0	0
Spatial dropout 1	32	8 × 64	–	0.25	–	0
Convolutional 3	32	4 × 64	2 × 5 × 32	2 × 1	0 × 2	10,272
Batch normalization 3	32	4 × 64	–	–	–	0
Activation 3	32	4 × 64	–	–	–	0
Average pooling 2	32	2 × 16	2 × 4	2 × 4	0	0
Spatial dropout 2	32	2 × 16	–	0.25	–	0
Flatten	–	1,024	–	–	–	0
Fully-connected	–	2	–	–		2,050
Softmax	–	2	–	–		4
Total						24,022

gradient descent in CNN. The MI-EEG classification problem in this paper belongs to a small sample set classification problem. To avoid the overfitting phenomenon caused by the overcomplicated model, the CNN structure designed in this paper only contains three convolutional layers, with two pooling layers and one fully connected layer, as shown in **Figure 3**. Based on the classic EEGNet, the structure modifies the size of the convolution kernel and the convolution stride.

As shown in **Figure 3** and **Table 1**, the dimension of a single sample input to CNN is 1 × 32 × 512. The size of the convolution kernel of the first layer of convolution is 1 × 24, the stride of the convolution kernel is 1 × 2, and the mode of partial filling is adopted. The first layer of convolution is mainly to perform time-domain convolution of one-dimensional signals. Its function is to refine the characteristics of each channel in the time domain signal. The main purpose is to reduce the length of the signal in the time dimension. The number of feature map channels output by the first layer of convolution is 16. The second layer of convolution uses a 2 × 11 convolution kernel, and the convolution stride is 2 × 1. This convolution operation can integrate the information of adjacent channels while keeping the signals of the left and right brain channels from mixing. After the second layer of convolution, the pruning operation is performed at a ratio of 0.25. The pruning randomly makes some neurons inactive, thereby avoiding overfitting in the neural network. This is followed by the first pooling layer with a pooling kernel size of 2 × 4. The pooling layer can extract important information from the feature map computed by the convolutional layer. As the feature map is much longer than the width, a 2 × 4 pooling kernel is used. The third layer of convolution uses a 2 × 5 convolution kernel, and the stride of the convolution is still 2 × 1. After that, pruning is performed at a ratio of 0.25, and a 2 × 4 pooling operation is also performed. The padding parameter of all convolution operations is set to 0, i.e., no padding mode. In addition, batch normalization is performed after each convolution operation, and the activation is performed using the exponential linear unit (ELU) activation function. The batch normalization operation can speed up the learning of the neural network and reduce the dependence on the initial weights. The ELU activation function is an improved version of the ReLu activation function. Compared with the ReLu activation function, the average value of its output is close to 0, which will not add additional bias to the next layer of neurons, thereby speeding up the convergence of the model. In the negative case, it has soft saturation characteristics and is more robust to noise.

RESULTS

Time–Frequency Diagram of the ERD/ERS

To analyze the fatigue of young and elderly subjects and find out the difference between them, it needs to prove that the subjects have obvious ERD/ERS phenomenon in the process of MI and then carry out fatigue calculation on this theoretical basis. For this purpose, the most representative C3 and C4 channels in the sensorimotor area of the cerebral cortex were selected for analysis, and the time–frequency diagram of the channels of the S1 subject is shown in **Figure 4**. The desynchronization at channels C3 and C4 is visually more pronounced in the alpha–beta (8–30 Hz) frequency band. The same subject had different levels of desynchronization in different periods and showed a trend of decreasing ERD significance with the increase of experimental time.

Table 2 gives the quantified average value of ERD of C3 and C4 channels within 0∼1 s and 1∼2.5 s in the alpha frequency band, and *t*-tests were performed, respectively. In both channels, the desynchronization phenomenon in the 1∼2.5 s time period is more significant than that in the 0∼1 s time period (C3: $P < 0.05$; C4: $P < 0.05$). It is regarded that 0∼1 s is the preparation period of MI, and 1∼2.5 s is the execution period of MI. Through the above process, other subjects were also verified, and the conclusion could prove that these subjects showed obvious ERD/ERS phenomenon in the MI process.

Results of the Fatigue Analysis During Motor Imagery

Based on verifying the ERD/ERS phenomenon, it can conduct fatigue analysis on the parietal lobe channels of the subjects according to the fatigue calculation method mentioned above for selecting the fatigue-sensitive channels. The fatigue-sensitive channels of young and older participants in the parietal lobe areas are shown in **Table 3**. In this group of young participants, the P6 channels were more sensitive to fatigue, and the P5 channels were relatively less sensitive to fatigue. The P2 channels were more sensitive to fatigue in elderly subjects, and the P6 channels were relatively less sensitive to fatigue. The relationship between fatigue and test time is shown in **Figures 5**, **6**. For most of the young subjects, the increase in the experimental time did not have a strong effect on the fatigue level, and the general trend was that the fatigue level increased with the duration of the

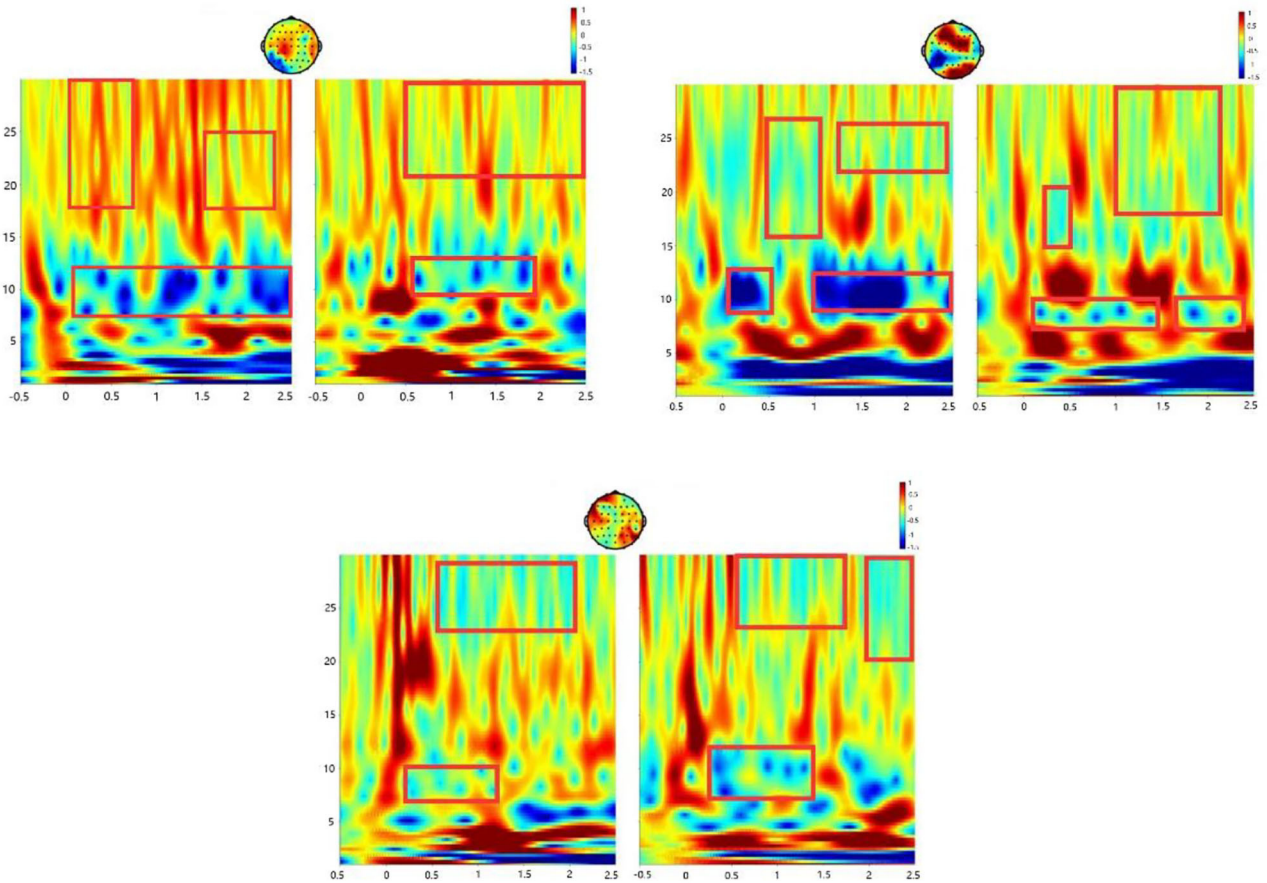

FIGURE 4 | ERD/ERS time–frequency analysis of three groups in S1.

TABLE 2 | *T*-test of ERD phenomena for C3 and C4.

	Channel	Band	ERD quantitative values	
			0∼1 s	1∼2.5 s
S1-1	C3	α (8∼13Hz)	−0.45044	−0.94739
S1-2	C3	α (8∼12Hz)	−0.31794	−1.0896
S1-3	C3	α (9∼12Hz)	−0.56522	−1.6016
Significant		0.021975815		
S1-1	C4	α (8∼12Hz)	0.026749	−0.51328
S1-2	C4	α (8∼13Hz)	−0.047736	−0.34357
S1-3	C4	α (9∼12Hz)	0.20375	−0.15104
Significant		0.036622313		

TABLE 3 | The fatigue-sensitive channels of the young and elderly subjects on the parietal lobe.

	Subject	Fatigue-sensitive channels	Subject	Fatigue-sensitive channels
The young subjects	S1	P1 P6	S6	P7 P3 P4 P2 P6
	S2	P4 P8 P2 P6	S7	P7 P3 P4 P1 P6
	S3	P3 P8 P1 P2 P6	S8	P7 P4 P8 P2 P6
	S4	P7 P3 P4 P1 P6	S9	P4 P8 P2 P6
	S5	P7 P4 P1 P8 P6	S10	P7 P3 P4 P8 P2
The elderly subjects	T1	P3 P4 P1 P2	T6	P3 P4 P8 P1
	T2	P4 P5 P1 P2 P6	T7	P7 P3 P8 P5 P1 P6
	T3	P7 P3 P5 P1 P2	T8	P7 P3 P4 P5 P1 P2
	T4	P7 P4 P8 P2 P6	T9	P7 P3 P4 P5 P2
	T5	P7 P4 P8 P5 P2 P6	T10	P4 P8 P1 P2

experimental time. For most older subjects, the fatigue showed a general increasing trend with the experimental time. Moreover, the increase in experimental time had less effect on fatigue for them than for the young ones.

Fatigue is a set of events produced by labor or prolonged exercise and can influence the performance of most tasks, since it contributes to the reduction of perceptual, cognitive, and motor skills (Tello et al., 2014). The parietal lobes are responsible for spatial reasoning and motor information processing, while the frontal lobes are involved in planning and higher cognitive abilities (Rao, 2013). Entropy-based feature analysis can obtain

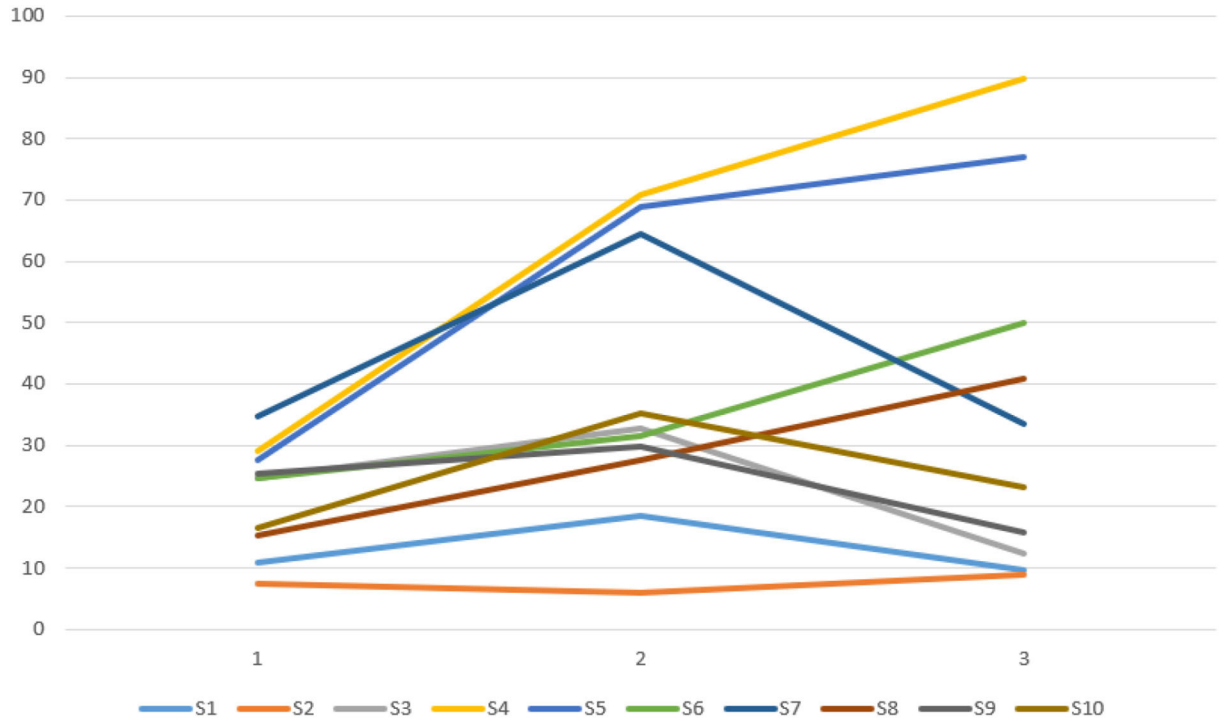

FIGURE 5 | Relationship between fatigue changes over time in 10 young subjects.

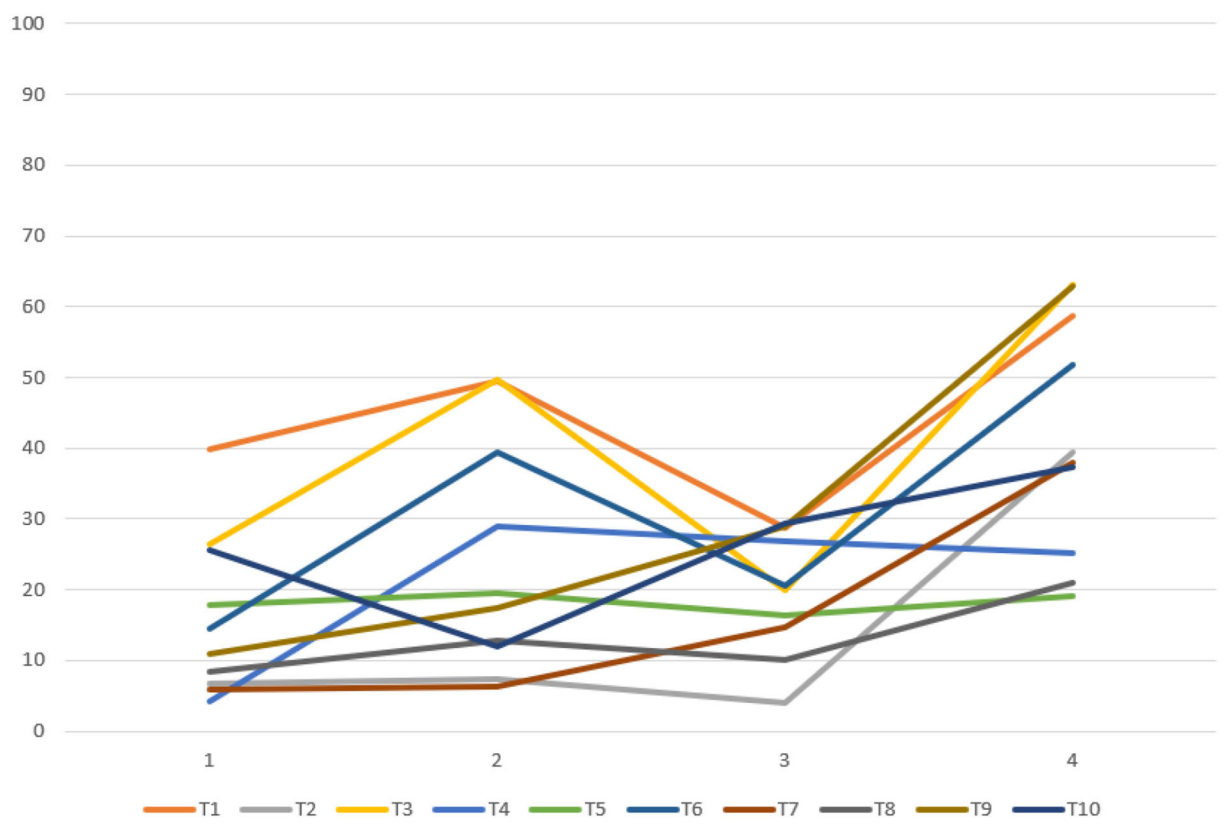

FIGURE 6 | Relationship between fatigue changes over time in 10 elderly subjects.

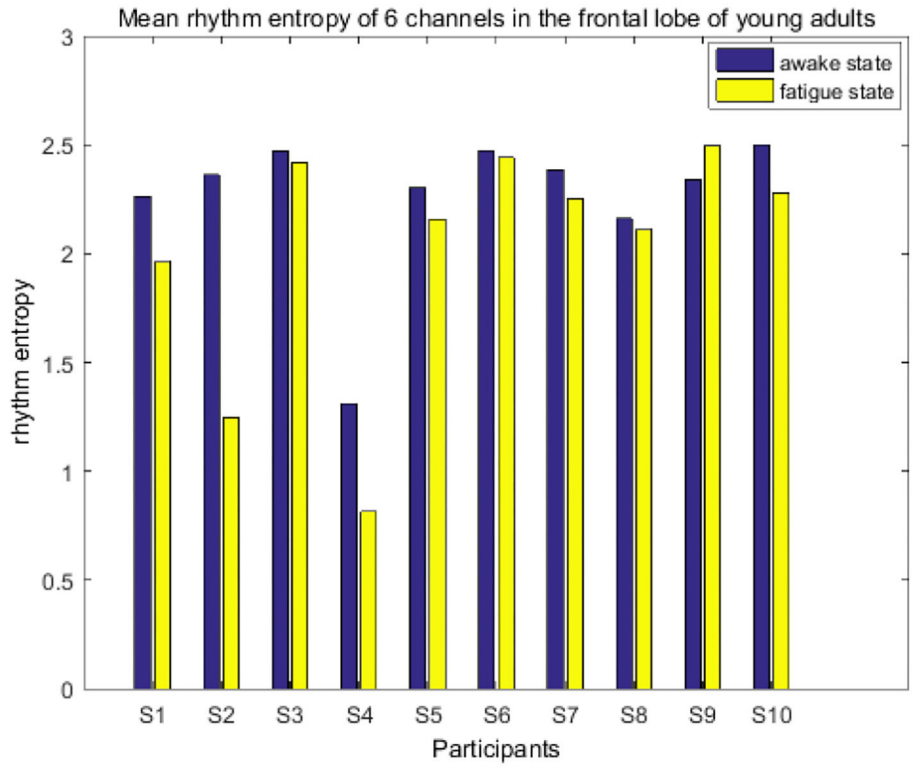

FIGURE 7 | Mean rhythm entropy of six channels on the frontal lobe of young adults.

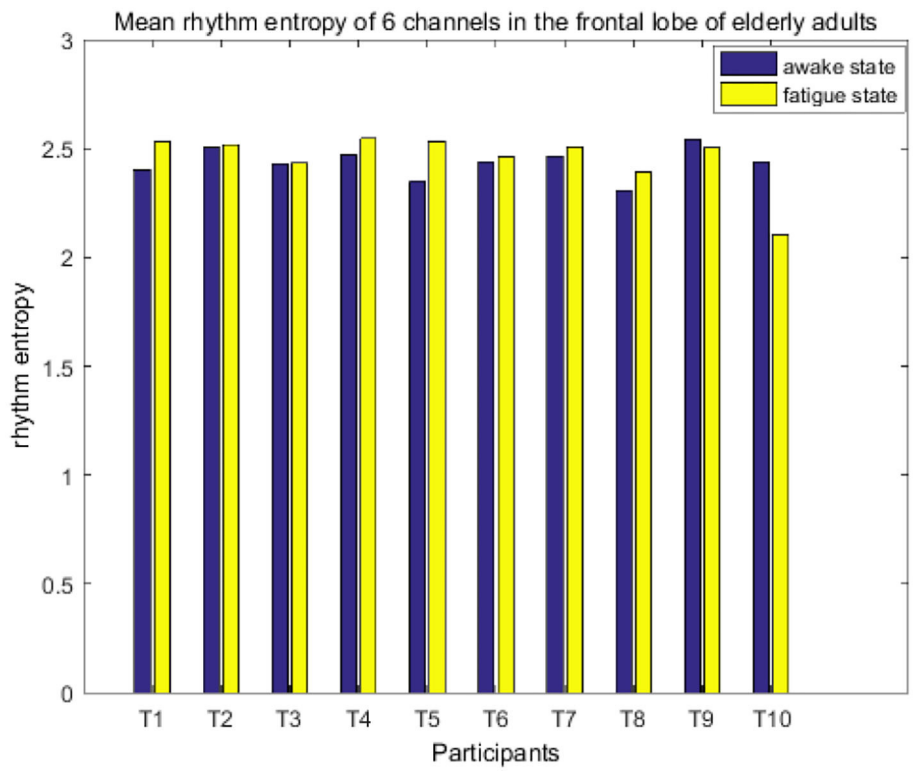

FIGURE 8 | Mean rhythm entropy of six channels on the frontal lobe of elderly adults.

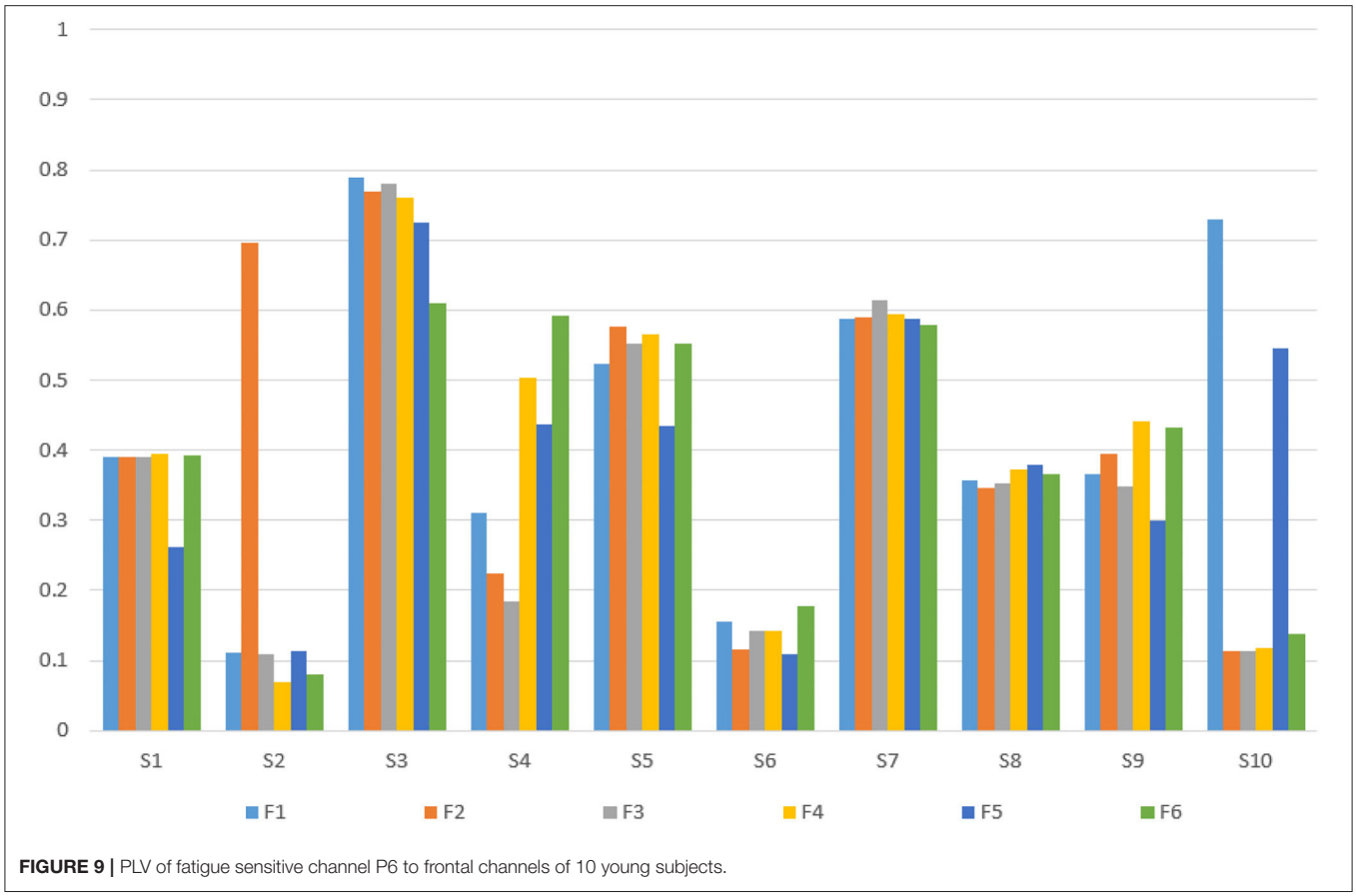

FIGURE 9 | PLV of fatigue sensitive channel P6 to frontal channels of 10 young subjects.

the relationship between the complexity of the EEG signal and the fatigue state of the subjects (Hu and Min, 2018). Lehmann et al. (2022) observed that prefrontal activity was generally a more important predictor of balance performance in older adults than in younger ones. The above analysis of fatigue is only done in the parietal lobe area. Here, RE is used to detect fatigue changes in the frontal lobe area.

It treated the first 20 MI trials as awake state and the last 20 trials as fatigue state, and then calculated the average of the RE of the six channels of the frontal cortex (F3, F4, F5, F1, F2, and F6) in the awake state and the fatigue state of the 20 participants. As shown in **Figures 7**, **8**, RE is roughly equal in young and elderly in the awake state, while such value in the fatigued state is lower than that in the awake state in the youngest subjects (9 participants) but higher in the most elderly ones (8 participants). The RE changes of subjects S9 and T9 differed from others in their own groups, with the changes not obvious between the two states, which may be due to individual differences, especially for subject T10. Human brain activity is complex in the awake state, so the RE is high. When the brain activity becomes orderly and complexity is reduced in the fatigued state, it results in a decrease in RE. From the RE variations, it can infer that for the young adults, the fatigue occurred accompanied by the execution of the MI, while older adults remain alert during the experiment in that they might require greater cognitive effort to complete MI tasks.

Combining with the above conclusion, it selected the 10 groups of young subjects fatigue sensitive channels (P6) and 10 groups of elderly subjects fatigue sensitive channels (P2), and the PLV of P6 and P2 to 6 frontal channels (F3, F4, F5, F1, F2, and F6) were calculated, respectively. **Figure 9** shows the calculation results of PLVs for 10 young subjects, and **Figure 10** shows the results of PLVs for 10 older subjects. It can be found that there is a high synchronization between the fatigue-sensitive pathway and the frontal cortex pathway for both young and old subjects.

Results of the Classification by CNN

For validating the classification method, the dataset was separated into 80% as the training set and the remaining 20% as the test set. At first, all the original samples of each subject were preprocessed, and then they were divided. At the same time, considering that the original sample size is too small and the neural network training model performance is insufficient, the sliding window method is introduced to expand the sample size of the data. The expansion steps are as follows: a 32 × 2,048 EEG fragment is obtained by taking the first 2 s as a time window, and a 32 × 512 sample is generated by taking the data with the 4-point interval from the fist point. The starting position moves to the second, the third, and the fourth point for further sampling. In this way, a 2 s time window is divided into four samples. Meanwhile, to avoid a high repetition rate between samples, the next 2 s time window started from 1 s, and the following 2 s time

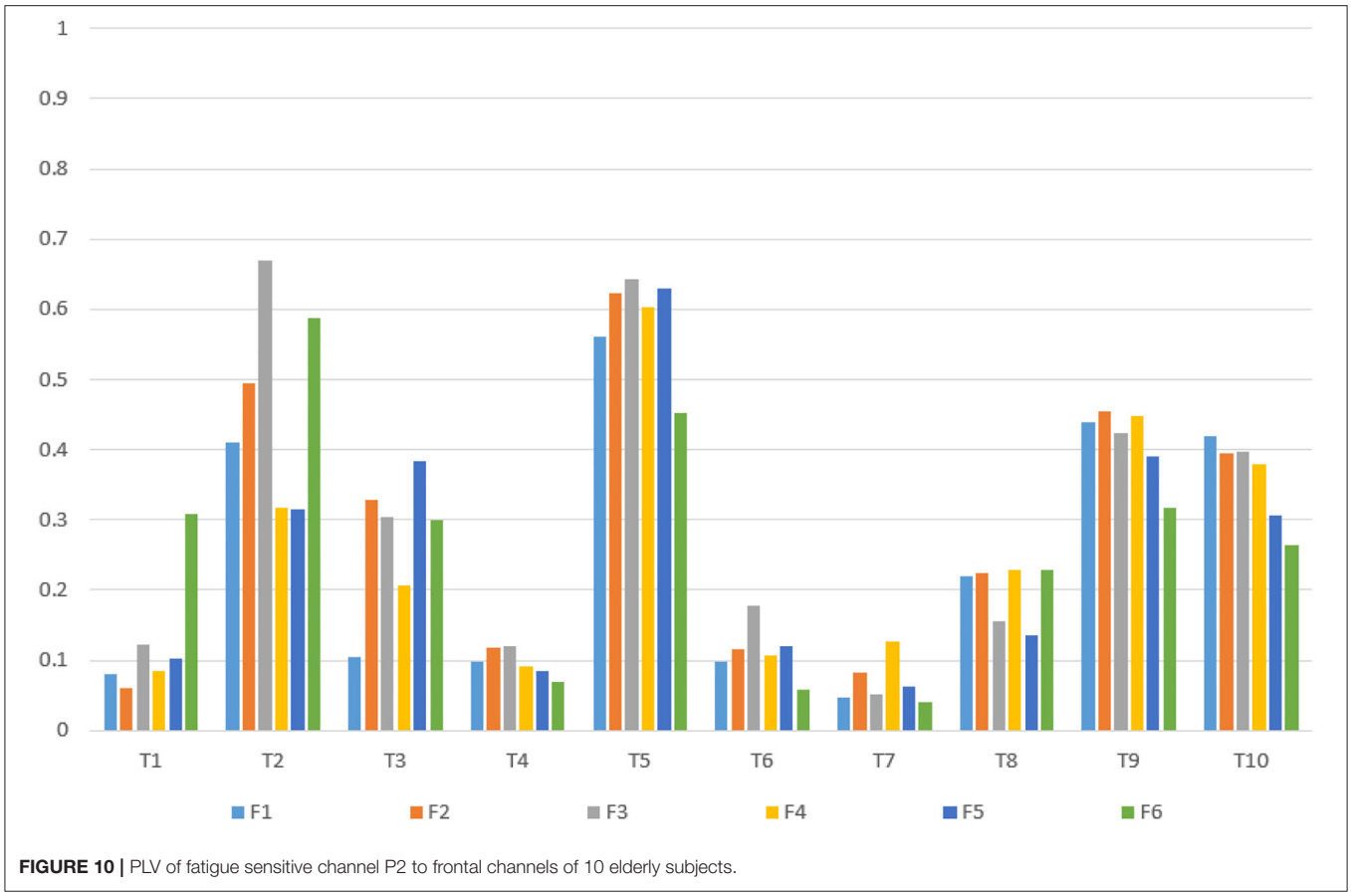

FIGURE 10 | PLV of fatigue sensitive channel P2 to frontal channels of 10 elderly subjects.

window began on 2 s. With the data enhancement, each original sample was converted into 12 32 × 512 samples, and the total data dimension of the experiment became 1,920 × 32 × 512. Then, it divided the training set and test set according to the ratio of 8:2 mentioned above, and the training set with about 1,536 samples and the test set with about 384 samples would be produced (except for S8), and compared the elderly and young people separately, as shown in **Figure 11**.

From **Figures 11A,B**, it can be seen that the global average accuracy rate of young people is higher than that of the elderly group, with a peak value of 82.81%, while the average and maximum accuracy rates of the elderly are lower than those of young people. In addition, the overall accuracy rate for most of the young subjects was above 0.7, while the older ones were a little lower, around 0.7. During the training stage, the epochs of young subjects gradually tended to stabilize around 240 iterations, while most older ones stabilized after 350 iterations, and the data quality of young persons is slightly better than that of the elderly. In addition, from **Figures 11B,D**, it also can be seen that the difference in the loss function of different young people is significantly larger than that of different elderly people, and the difference in data quality between young persons may be slightly larger than that between elderly individuals.

In addition, it also attempted classification tests on the cross-sample dataset for each age group. Here the data of two subjects S6 and S8 were selected as the mixed dataset of young adults, and the data of two subjects of T2 and T3 as the mixed dataset of old ones. It can be clearly seen from **Figure 12A** that the average accuracy of the youth mixed sample set is higher than the two data sets of the elderly mixed sample, and the highest accuracy rate of the mixed sample of young people can reach 0.725, indicating that the quality of mixed data between young individuals is still better than that of older individuals. The loss function on the training set is different. From **Figure 12B**, it can be seen that the decline rate of the mixed sample of young adults is lower than that of the mixed sample data of the elderly, probably because the mixed sample of S6 and S8 has 80 more trials than that of T2 and T3, and this result is also consistent with the highest loss function for S8 in **Figure 11B**. At the same time, due to the differences among subjects, the classification accuracy on the mixed dataset is lower than the classification accuracy on each separate dataset.

DISCUSSION

The analysis of the trend of decreasing ERD significance with the increase of experimental time is conducted, and the average of the RE of the six channels on the prefrontal lobe region is calculated. From the function activity aspect, the work on synchronization between the signal amplitudes and the phase has

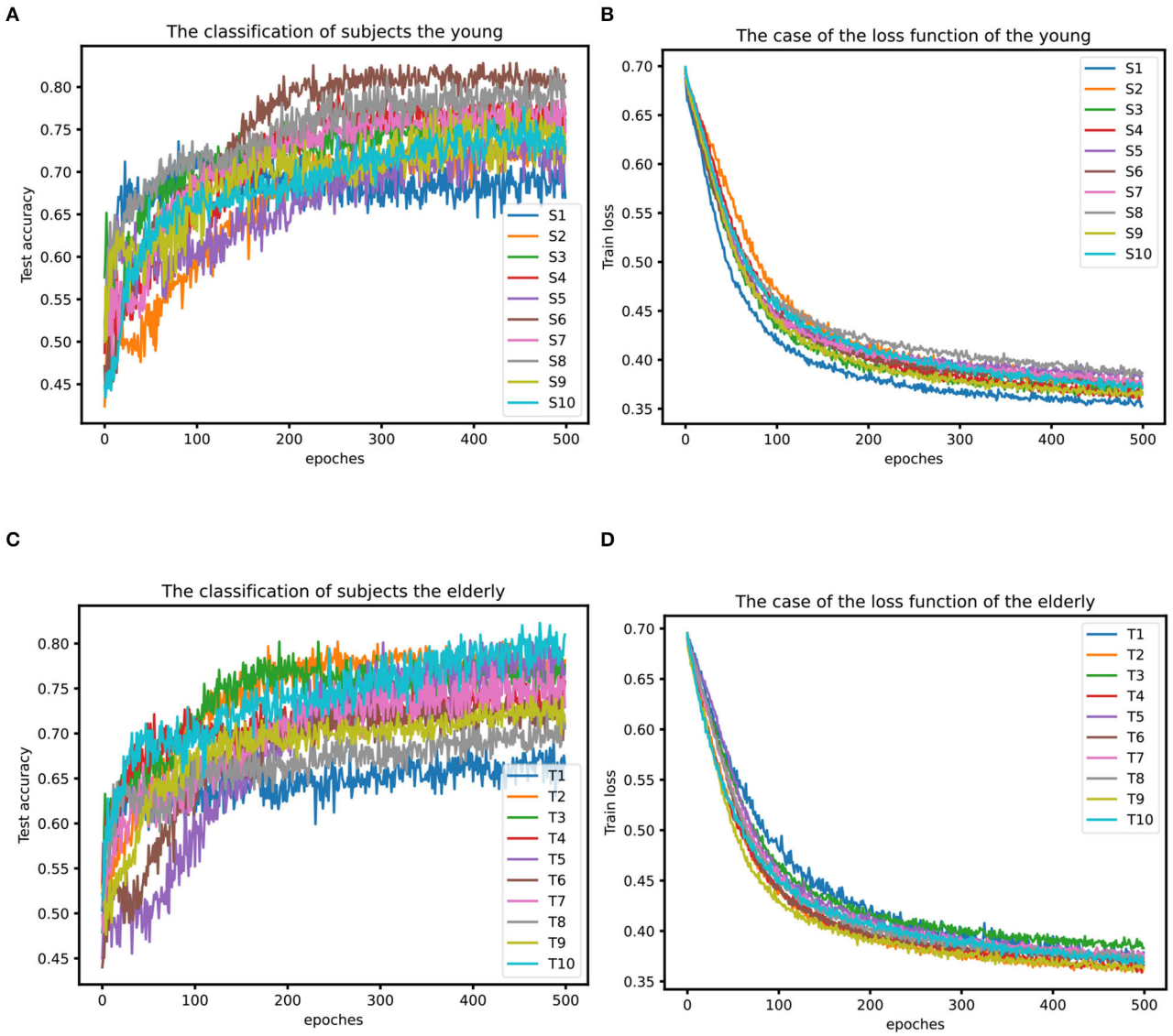

FIGURE 11 | (A) Classification results of the young. **(B)** Loss function situation of the young. **(C)** Classification results of the elderly. **(D)** Loss function situation of the elderly.

been discussed (Rosenblum et al., 1996; Nolte et al., 2004). It hypothesizes that integrating these complementary features will allow a better characterization of the BCI-related mental states and that including them in the feature extraction block, which is helpful to increase the BCI accuracy compared to standard approaches solely based on power spectra (Cattai et al., 2019). In this way, the phase relationship between EEG signals on the prefrontal and parietal lobes will be characterized by PLV. Aiming at the calculation and analysis of classification accuracy of 10 young subjects and 10 older ones in the previous sections, it analyzed the correlation between classification accuracy and the PLV, which is between the fatigue-sensitive channels on the parietal lobe and the specified channels in the frontal lobe for RE calculation.

Combined with the above conclusions, the average fatigue value of 10 young subjects was 32.086, and that of 10 older subjects is 25.796. The average fatigue value of young persons is higher than that of the elderly, indicating that young adults are more prone to fatigue during MI, which might be caused by their more concentrated attention during the MI. At the same time, the results of the PLV obtained above are statistically analyzed, with the channels whose PLV is significantly higher than the mean value of the corresponding test group removed. The average PLV of the young is 0.398, and that of the elderly is 0.270. The average PLV of young persons is higher than that of the elderly, indicating that compared with the elderly, the parietal lobe fatigue sensitive channels and specified prefrontal lobe channels have higher synchronization. From the perspective of fatigue, RE, and PLV,

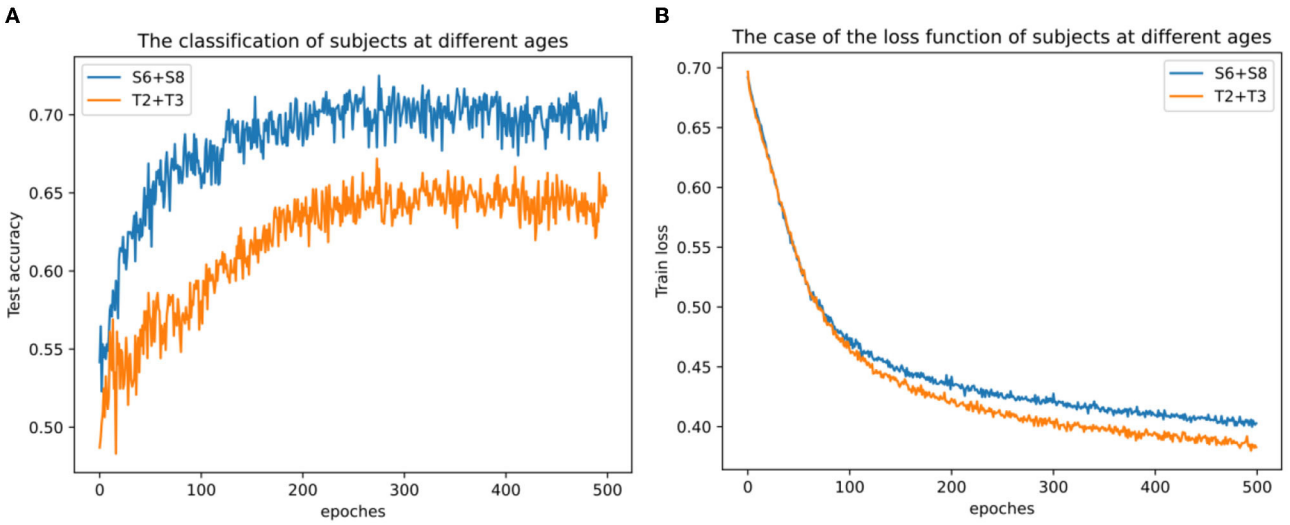

FIGURE 12 | Classification results across subjects with mixed datasets. **(A)** Classification results across subjects with mixed datasets at different ages and **(B)** loss function across subjects with mixed datasets at different ages.

young persons are more likely to concentrate on MI tasks and thus fatigue is caused. The elderly subjects make more cognitive efforts to complete the task, but the MI classification accuracy is slightly lower than that of young adults, and it could hereby be inferred that age may affect the ability of MI.

According to the classification accuracy results mentioned above, the correlation between the PLV of young subjects and the elderly subjects to each classification accuracy is calculated here. For 10 young subjects, the correlation coefficient between the average PLV from the fatigue-sensitive channel P6 and the classification accuracy was 0.760, while for 10 elderly subjects, the correlation coefficient between the average PLV from the fatigue sensitive channel P2 and the classification accuracy was 0.731. The results show that there is a strong positive correlation between the classification accuracy and the average PLV of the fatigue-sensitive channel to the specified prefrontal lobe channel in both young and older subjects.

As a deep learning method, a CNN model is established for detecting left and right hands MI using a Muse headband that has potential use on older adults, but the experiment is performed on four healthy users aging from 33 to 55 years (Garcia-Moreno et al., 2020). More than 90% accuracy is achieved, however, the classification method beyond the EEG headset still requires further evaluation on aging people. For cognitive tasks, it indicates that robust plasticity of the prefrontal cognitive control system was found in the aging brain, and it also provides a custom-designed video game environment to assess cognitive abilities across the lifespan of human subjects (Anguera et al., 2013). Therefore, it is necessary to apply a CNN method by introducing the EEG data from channels on both frontal and parietal lobes for the MI-EEG classification by considering the ERD and fatigue phenomenon together in the aging group.

It also mentions that change in the location of activation in the brain is be more bilateral throughout the aging process. In that case, the application of sensorimotor rhythm (SMR) for BCI based on spatial information such as common spatial pattern (CSP) and Laplacian filtering becomes not so effective (Bashashati et al., 2007). The study also showed that age-related electrophysiological changes in healthy older adults significantly affected SMR characteristics in EEG, and found that the classification accuracy in the elderly is significantly lower than in the younger population by 15.9% (Chen et al., 2019). It means that the traditional classification methods depend more on the input features from the CSP enhancement. Compared with this pipeline mode, as an end-to-end method, CNN does not require these intermediate results of feature extraction, which can make full use of the features from the EEG signals. Therefore, the CNN classification accuracy keeps around 70% on the 10 older subjects by selecting 32 channels in the frontal and parietal regions, which have a close performance to young subjects. However, the number of young and older subjects is limited in the current study, and all the subjects are healthy ones. The classification strategies of the MI-BCI system for those who suffer neurological diseases such as stroke rehabilitation will be investigated in the future.

CONCLUSION

The primary finding of our study is that the elderly are less affected by the level of fatigue during MI, even though the MI energy of the elderly is lower than that of the young. However, the deep learning method by extracting frontal and parietal channel data can be still suitable for the elderly, and the classification accuracy on MI tasks is at the acceptable levels of around 70% by CNN. It could be inferred that future BCI

for the elderly population on MI will not merely depend on the SMR, and appropriate algorithms can be applied without obvious lateralization of ERD. However, the CNN model based on fused spatial information greatly improves the accuracy of the classification and leads to a longer training time. Supported by the rehabilitation robot previously developed, more participants will attend the EEG data collection, and an improved CNN classification method for real-time BCI based on MI would be attempted in the future.

DATA AVAILABILITY STATEMENT

The raw data supporting the conclusions of this article will be made available by the authors, without undue reservation.

ETHICS STATEMENT

The studies involving human participants were reviewed and approved by Ethics Committee of West China Hospital of Sichuan University. The patients/participants provided their written informed consent to participate in this study.

AUTHOR CONTRIBUTIONS

XL and PC wrote the manuscript. NJ provided the suggestion of experiment design. PC and XY analyzed the EEG data and implemented the CNN classification method. All authors contributed to the article and approved the submitted version.

FUNDING

The work has been financially supported by the National Natural Science Foundation of China (Grant Nos. 51805449 and 62103291), the Sichuan Science and Technology Program (Grant Nos. 2021ZHYZ0019 and 2022YFS0021), and the 1 · 3 · 5 project for disciplines of excellence, West China Hospital, Sichuan University (Grant Nos. ZYYC21004 and ZYJC21081). All findings and results presented in this paper are those of the authors and do not represent the funding agencies.

ACKNOWLEDGMENTS

We thank all volunteers who participated in this study.

REFERENCES

Anguera, J., Boccanfuso, J., Rintoul, J., Al-Hashimi, O., Faraji, F., Janowich, J., et al. (2013). Video game training enhances cognitive control in older adults. *Nature* 501, 97–101. doi: 10.1038/nature12486

Anokhin, A. P., Birbaumer, N., Lutzenberger, W., Nikolaev, A., and Vogel, F. (1996). Age increases brain complexity. *Electroencephalogr. Clin. Neurophysiol.* 99, 63–68. doi: 10.1016/0921-884X(96)95573-3

Arunkumar, N., Kumar, K. R., and Venkataraman, V. (2018). Entropy features for focal eeg and non focaleeg. *J. Comput. Sci.* 27, 440–444. doi: 10.1016/j.jocs.2018.02.002

Bashashati, A., Fatourechi, M., Ward, R. K., and Birch, G. E. (2007). A survey of signal processing algorithms in brain-computer interfaces based on electrical brain signals. *J. Neural Eng.* 4, R32. doi: 10.1088/1741-2560/4/2/R03

Belkacem, A. N., Jamil, N., Palmer, J. A., Ouhbi, S., and Chen, C. (2020). Brain computer interfaces for improving the quality of life of older adults and elderly patients. *Front. Neurosci.* 14, 692. doi: 10.3389/fnins.2020.00692

Cao, T., F., Wan, Wong, C., Da Cruz, J., and Hu, Y. (2014). Objective evaluation of fatigue by eeg spectral analysis in steady-state visual evoked potential-based brain-computer interfaces. *Biomed. Eng. Online* 13, 1–13. doi: 10.1186/1475-925X-13-28

Castermans, T., Duvinage, M., Cheron, G., and Dutoit, T. (2013). Towards effective non-invasive brain-computer interfaces dedicated to gait rehabilitation systems. *Brain Sci.* 4, 1–48. doi: 10.3390/brainsci4010001

Cattai, T., Colonese, S., Corsi, M. C., Bassett, D. S., Scarano, G., and Fallani, F. (2019). Phase/amplitude synchronization of brain signals during motor imagery bci tasks. *IEEE Trans. Neural Syst. Rehabilit. Eng.* 29, 1168–1177. doi: 10.1109/TNSRE.2021.3088637

Chen, M. L., Fu, D., Boger, J., and Jiang, N. (2019). Age-related changes in vibro-tactile eeg response and its implications in bci applications: a comparison between older and younger populations. *IEEE Trans. Neural Syst. Rehabil. Eng.* 27, 603–610. doi: 10.1109/TNSRE.2019.2890968

Garcia-Moreno, F. M., Bermudez-Edo, M., Fórtiz, M. J. R., and Garrido, J. L. (2020). "A CNN-LSTM deep learning classifier for motor imagery EEG detection using a low-invasive and low-cost BCI headband," in *2020 16th International Conference on Intelligent Environments (IEEE)*. doi: 10.1109/IE49459.2020.9155016

Gard, T., Hölzel, B. K., and Lazar, S. W. (2014). The potential effects of meditation on age-related cognitive decline: a systematic review. *Ann. N. Y. Acad. Sci.* 1307, 89–103. doi: 10.1111/nyas.12348

Hisato, T., Junichi, U., and Junichi, U. (2018). Subjective vividness of kinesthetic motor imagery is associated with the similarity in magnitude of sensorimotor event-related desynchronization between motor execution and motor imagery. *Front. Hum. Neurosci.* 12, 295. doi: 10.3389/fnhum.2018.00295

Hu, J., and Min, J. (2018). Automated detection of driver fatigue based on eeg signals using gradient boosting decision tree model. *Cogn. Neurodyn.* 12, 431–440. doi: 10.1007/s11571-018-9485-1

Jap, B. T., Lai, S., Fischer, P., and Bekiaris, E. (2009). Using eeg spectral components to assess algorithms for detecting fatigue. *Expert Syst. Applic. Int. J.* 36, 2352–2359. doi: 10.1016/j.eswa.2007.12.043

Jeannerod, M. (2011). Mental imagery in the motor context. *Neuropsychologia* 33, 1419. doi: 10.1016/0028-3932(95)00073-C

Jiang, Y., Jessee, W., Hoyng, S., Borhani, S., Liu, Z., Zhao, X., et al. (2022). Sharpening working memory with real-time electrophysiological brain signals: which neurofeedback paradigms work? *Front. Aging Neurosci.* 14, 780817. doi: 10.3389/fnagi.2022.780817

Lawhern, V. J., Solon, A. J., Waytowich, N. R., Gordon, S. M., Hung, C. P., and Lance, B. (2018). EEGNet: a compact convolutional network for EEG-based brain-computer interfaces. *J. Neural Eng.* 15, 056013. doi: 10.1088/1741-2552/aace8c

Lecun, Y., Boser, B., Denker, J., Henderson, D., Howard, R., and Hubbard, W., et al. (1989). Backpropagation applied to handwritten zip code recognition. *Neural Comput.* 1, 541–551. doi: 10.1162/neco.1989.1.4.541

Lehmann, N., Kuhn, Y.-A., Keller, M., Aye, N., Herold, F., Draganski, B., et al. (2022). Brain activation during active balancing and its behavioral relevance in younger and older adults: a Functional Near-Infrared Spectroscopy (fNIRS) study. *Front. Aging Neurosci.* 14, 828474. doi: 10.3389/fnagi.2022.828474

Li, J., Chen, G., Thangavel, P., Yu, H., Thakor, N., Bezerianos, A., et al. (2016). "A robotic knee exoskeleton for walking assistance and connectivity topology exploration in EEG signal," in *2016 6th IEEE International Conference on Biomedical Robotics and Biomechatronics (IEEE)*, 1068–1073. doi: 10.1109/BIOROB.2016.7523773

Malouin, F., Richards, C. L., and Durand, A. (2010). Normal aging and motor imagery vividness: implications for mental practice training in rehabilitation. *Arch. Phys. Med. Rehabil.* 91, 1122–1127. doi: 10.1016/j.apmr.2010.03.007

Mary, K. M., Jouni, P., and Anthony, S. (2007). *Global Health and Global Aging*. San Francisco, CA: Wiley.

Müller-Putz, G. R., Schwarz, A., Pereira, J., and Ofner, P. (2016). From classic motor imagery to complex movement intention decoding: the noninvasive Graz-BCI approach. *Prog. Brain Res.* 228, 39–70. doi: 10.1016/bs.pbr.2016.04.017

Nikhil, S., Jean-Claude, B., and Xi-Nian, Z. (2014). Effects of healthy ageing on activation pattern within the primary motor cortex during movement and motor imagery: an fmri study. *PLoS ONE* 9, e88443. doi: 10.1371/journal.pone.0088443

Nolte, G., Bai, O., Wheaton, L., Mari, Z., and Hallett, M. (2004). Identifying true brain interaction from eeg data using the imaginary part of coherency. *Clin. Neurophysiol.* 115, 2292–2307. doi: 10.1016/j.clinph.2004.04.029

Paiva, L. R. M. D., Pereira, A. A., Almeida, M. F. S. D., Cavalheiro, G. L., and Andrade, A. D. O. (2012). Analysis of the relationship between eeg signal and aging through linear discriminant analysis (lda). *Rev. Brasil. Engenharia Biomed.* 28, 155–168. doi: 10.4322/rbeb.2012.023

Pavlov, A. N., Pitsik, E. N., Frolov, N. S., Badarin, A., and Hramov, A. E. (2020). Age-related distinctions in eeg signals during execution of motor tasks characterized in terms of long-range correlations. *Sensors* 20, 5843. doi: 10.3390/s20205843

Personnier, P., Kubicki, A., Laroche, D., and Papaxanthis, C. (2010). Temporal features of imagined locomotion in normal aging. *Neurosci. Lett.* 476, 146–149. doi: 10.1016/j.neulet.2010.04.017

Rao, R. (2013). *Brain-Computer Interfacing: An Introduction*. Cambridge University Press. doi: 10.1017/CBO9781139032803

Rosenblum, M. G., Pikovsky, A. S., and Kurths, J. (1996). Phase synchronization of chaotic oscillators. *Phys. Rev. Lett.* 76, 1804. doi: 10.1103/PhysRevLett.76.1804

Rudnicka, E., Napieraa, P., Podfigurna, A., Mczekalski, B., and Grymowicz, M. (2020). The world health organization (who) approach to healthy ageing. *Maturitas* 139, 6–11. doi: 10.1016/j.maturitas.2020.05.018

Scheel, N., Franke, E., Münte, T. F., and Mamlouk, A. M. (2018). Dimensional complexity of the resting brain in healthy aging, using a normalized mpse. *Front. Hum. Neurosci.* 12, 451. doi: 10.3389/fnhum.2018.00451

Schotta, N. (2012). Age-related differences in motor imagery: working memory as a mediator. *Exp. Aging Res.* 38, 559–583. doi: 10.1080/0361073X.2012.726045

Tabar, Y. R., and Halici, U. (2017). A novel deep learning approach for classification of eeg motor imagery signals. *J. Neural Eng.* 14, 016003. doi: 10.1088/1741-2560/14/1/016003

Talukdar, U., Hazarika, S. M., and Gan, J. Q. (2018). Motor imagery and mental fatigue: inter-relationship and eeg based estimation. *J. Comput. Neurosci.* 46, 55–76. doi: 10.1007/s10827-018-0701-0

Tello, R. G., Pomer-Escher, A., and Bastos, T. F. (2014). "Analysis of mental fatigue in motor imagery and emotional stimulation based on EEG," in *XXIV CongressoBrasileiro de EngenhariaBiomédica* (Sociedade Brasileira de Engenharia Biomédica).

Wolpaw, J. R., Birbaumer, N., Heetderks, W. J., Mcfarland, D. J., Peckham, P. H., and Schalk, G., et al. (2000). Brain-computer interface technology: a review of the first international meeting. *IEEE Trans. Rehabil. Eng.* 8, 164–173. doi: 10.1109/TRE.2000.847807

Yimin, H., Lu, Z., Shuyue, J., and Xiangmin, L. (2020). A novel approach of decoding EEG four-class motor imagery tasks via scout ESI and CNN. *J. Neural Eng.* 17, 16–48. doi: 10.1088/1741-2552/ab4af6

Conflict of Interest: The authors declare that the research was conducted in the absence of any commercial or financial relationships that could be construed as a potential conflict of interest.

Publisher's Note: All claims expressed in this article are solely those of the authors and do not necessarily represent those of their affiliated organizations, or those of the publisher, the editors and the reviewers. Any product that may be evaluated in this article, or claim that may be made by its manufacturer, is not guaranteed or endorsed by the publisher.

frontiers | Frontiers in Aging Neuroscience

TYPE Systematic Review
PUBLISHED 08 August 2022
DOI 10.3389/fnagi.2022.975711

OPEN ACCESS

EDITED BY
Chuhuai Wang,
Sun Yat-sen University, China

REVIEWED BY
Samantha M. Loi,
Royal Melbourne Hospital, Australia
Ying Shen,
The First Affiliated Hospital of Nanjing Medical University, China

*CORRESPONDENCE
Jie-Jiao Zheng
zjjcss@163.com
Xue-Qiang Wang
wangxueqiang@sus.edu.cn

SPECIALTY SECTION
This article was submitted to Neurocognitive Aging and Behavior, a section of the journal Frontiers in Aging Neuroscience

RECEIVED 22 June 2022
ACCEPTED 18 July 2022
PUBLISHED 08 August 2022

CITATION
Wu C-C, Xiong H-Y, Zheng J-J and Wang X-Q (2022) Dance movement therapy for neurodegenerative diseases: A systematic review. *Front. Aging Neurosci.* 14:975711. doi: 10.3389/fnagi.2022.975711

Dance movement therapy for neurodegenerative diseases: A systematic review

Cheng-Cheng Wu[1], Huan-Yu Xiong[1], Jie-Jiao Zheng[2]* and Xue-Qiang Wang[1,3]*

[1]Department of Sport Rehabilitation, Shanghai University of Sport, Shanghai, China, [2]Huadong Hospital, Shanghai, China, [3]Department of Rehabilitation Medicine, Shanghai Shangti Orthopaedic Hospital, Shanghai, China

Background: The proportion of the world's elderly population continues to rise, and the treatment and improvement of neurodegenerative diseases have become issue of public health importance as people live longer and many countries have aging populations. This systematic review aims to discuss the effects of dance movement therapy (DMT) on motor function, cognitive deficit, mood, and quality of life in people with neurodegenerative diseases, such as Parkinson's disease (PD), mild cognitive impairment (MCI), Alzheimer's disease (AD).

Methods: Two reviewers independently conducted systematic search on the Cochrane library, PubMed database, Web of Science Core Collection database, and Physiotherapy Evidence database until February 1, 2022. Only systematic analyses and randomized controlled trials were included and further analyzed.

Results: Thirty-three studies on PD, 16 studies on MCI, 4 studies on AD were obtained. This systematic review found that DMT substantially improved the global cognitive function, memory, and executive function on the population with MCI. Compared with the non-dance group, DMT remarkably improved general disease condition, balance, and gait for individuals with PD. The evidence of the efficacy of DMT on AD is insufficient, and further research is needed.

Conclusion: DMT can effectively improve the motor function and cognitive deficits in neurodegenerative diseases. Positive effects of DMT on the mood and quality of life in ND patients are controversial and require further evidence. Future research on the effects of DMT on AD requires scientific design, large sample size, long-term comprehensive intervention, and clear reporting standards.

Systematic Review Registration: www.osf.io/wktez, identifier: 10.17605/OSF.IO/UYBKT.

KEYWORDS

dance movement, aging, neurodegenerative disease, Parkinson's disease, mild cognitive impairment, Alzheimer's disease, neurorehabilitation

Introduction

Eurostat forecasts show that the proportion of the population over 60 years old will reach 35%, and the number of people aged 65 and over with Alzheimer's disease (AD) in the United States may increase to 13.8 million by the middle of this century (2020 Alzheimer's disease facts and figures, 2020). Aging is the primary risk factor for

most neurodegenerative diseases (NDs), which include Parkinson's disease (PD), mild cognitive impairment (MCI) and AD. One in 10 individuals aged ≥65 suffering from NDs will increase with the proportion of the elderly population, which will cause a great burden on individuals, families, and society (Hou et al., 2019). Therefore, the treatment and improvement of NDs with aging as a major risk factor have become the issue of public health that needs to be solved urgently in the medical and health field. Previous studies suggested that the functional recovery of patients with NDs depends on the ability of spare neurons to rebuild and reshape the damaged network to compensate for the lost function by growing neurites and forming new synapses (Reetz et al., 2010; Tomassini et al., 2012; Nudo, 2013). This traditional strategy of function is considered to achieve rehabilitation through targeted training of weakened functions (Herholz et al., 2013; Zeiler and Krakauer, 2013; Agosta et al., 2017). Another method is to increase the overall level of brain activity through sensory and cognitive stimulation (Baroncelli et al., 2010).

Dance is a rhythmic movement that has been choreographed or improvised in advance and usually performed with music. The American Dance Therapy Association (ADTA) defines dance movement therapy (DMT) as "the psychotherapeutic use of movement as a process that promotes the emotional, social, cognitive, and physical integration of the individual." Formal DMT can be defined as active interventions (such as performing tango, waltz, dances) or receptive interventions (such as watching stage plays) by qualified dance therapists (groups). The meta-analysis results of Fong Yan et al. (2018) confirmed that the therapeutic effect of performing any type of DMT is better than other types of structured exercise in improving a series of health outcomes, such as body composition and musculoskeletal function (Fong Yan et al., 2018). Many studies have reported the positive effects of DMT in various conditions, such as cancer (Aktas and Ogce, 2005; Bradt et al., 2015), brain health (Rios Romenets et al., 2015; Karkou and Meekums, 2017; Poier et al., 2019; Ruiz-Muelle and López-Rodríguez, 2019), cardiovascular disease (Conceição et al., 2016; Fong Yan et al., 2018; Gronek et al., 2021), and fall (Fernández-Argüelles et al., 2015; Veronese et al., 2017). Studies examining the effects of DMT have mostly focused on the population with NDs, particularly PD. Various neuroimaging studies of dance observation showed that DMT can improve the neuronal connectivity in specific brain regions of older participants' brain, promote neuroplasticity, and induce changes in gray and white matter in multiple brain regions, especially the frontotemporal region. Previous studies suggested DMT as a rehabilitation tool of disease management and clinical improvement for patients with AD (Mabire et al., 2019; Ruiz-Muelle and López-Rodríguez, 2019), MCI (Liu et al., 2021; Wang et al., 2021; Wu et al., 2021), and PD (Barnish and Barran, 2020; Berti et al., 2020; Carapellotti et al., 2020; de Almeida et al., 2020; Emmanouilidis et al., 2021; Ismail et al., 2021). The pooled results of the latest meta-analysis of the efficacy of DMT in PD patients showed that DMT can improve motor function and reduce the burden on caregivers (Emmanouilidis et al., 2021; Ismail et al., 2021). The meta-analysis findings of randomized controlled trials (RCTs) and non-RCTs reported the positive effects of DMT in improving the motor, cognitive, and psychological functions in patients with AD (Ruiz-Muelle and López-Rodríguez, 2019). Among the studies on the dance treatment of MCI, many systematic reviews and meta-analyses confirmed that DMT can improves memory and other cognitive function, psychological function, and quality of life (Zhu et al., 2020; Liu et al., 2021; Wu et al., 2021).

At present, there are various types of dance-movement therapy and widely accepted by groups of all ages. For example, the Videogame-Based Dance Exercise Program attracts many young people, and Chinese-style square dance is also recognized by middle-aged and elderly groups. In the foreseeable future, there will be a variety of ways for people to access dance movement therapy, no longer limited to one-on-one or one-to-many treatment modes between dance therapists and patients. This also provides one of the treatment options for at-home rehabilitation for the elderly population who have limited cognition, activity and social skills due to aging. However, extant studies only summarized some aspects of the effectiveness of DMT for a certain NDs. A comprehensive overview and interpretation of the benefits and potential mechanisms of DMT in the rehabilitation of major neurodegenerative diseases with aging as a major risk factor are needed. We conducted an integrated review of systematic analyses and RCTs of DMT in patients with PD, MCI, AD and discussed the underlying mechanisms of the efficacy of DMT.

Materials and methods

This protocol of this systematic review has been registered in the Open Science Framework (OSF) systematic review database, international prospective register for systematic review under the registration doi: 10.17605/OSF.IO/UYBKT.

Search strategy and selection criteria

We searched the literature *via* the PubMed database, Web of Science Collection database, Cochrane library, and Physiotherapy Evidence Database (PEDro). No limit was set on data search. The key words of search strategies were as follows: "dance," "Alzheimer's disease," "cognitive impairment," "Parkinson's disease," (Supplementary material).

Studies were chosen on the basis of four criteria: 1. Studies must be written in English language; 2. The types of studies were limited to systematic analysis and RCT; 3. Only dance was used as a patient-specific intervention; 4. Studies should include patients with MCI, PD and AD. 5. Studies must be published

before February 1, 2022. All articles were screened by title and abstract. When the article may be a systematic analysis or RCT, the full text was queried for quality assessment, and a list analysis was performed.

Data collection, extraction, and quality assessment

Two reviewers independently conducted the literature search, data extraction, and quality assessment. For each eligible systematic analysis or RCT, we extracted and developed the characteristics for the included study, the size of participants and conditions, professional dance therapists involved, blind method setting, primary outcome, main results, and overall duration of intervention (Tables 1–4). Periodic study group meetings were held to review the process, and disagreements were resolved by consensus or referral to a third reviewer.

PEDro scores (Collins et al., 2018) (total score/10) were used to grade the quality assessment of the included clinical trials and to compare the scientificity of the experimental design of the included studies. The Assessment of Multiple Systematic Reviews (AMSTAR) tool (total score/11) (Shea et al., 2007) was used to assess the methodological quality of included systematic reviews and meta-analysis. Two reviewers independently assessed the methodological quality of included studies. On the basis of the Consensus Statements (Crossley et al., 2016; Collins et al., 2018), the included studies were graded as low quality, moderate quality or high quality. On the basis of PEDro and AMSTAR scores, low quality was $\leq$3, moderate quality was between 4 and 6, and high quality was $\geq$7.

Data analysis

We reviewed the effects of exercise interventions on motor function, cognitive limitation, psychology, and quality of life in accordance with disease type (i.e., MCI, AD, or PD classification). This process was performed because of differences in disease type, intervention group, and primary outcome assessment in the included studies. The effects of DMT were compared with other exercises, usual care, and treatment involved in the meta-analyses and RCTs in accordance with the clinical features of each disease.

Results

A total of 262 papers overlapped (i.e., the same papers were extracted from different search source) out of the 721 papers extracted in the preliminary search. A total of 295 reports were excluded because of the following reasons: (1) the experimental design was not a systematic analysis or RCT; (2) the type of participants included in the study was complex (e.g., included MCI, stroke, etc.); (3) no control group; (4) no comparison or missing results were provided; (5) study was not completed. A total of 130 articles were retained for further research, and 73 articles were excluded for reasons similar to those described above. Thirty-three RCTs and 24 systematic analyses were included. As shown in Figure 1, thirty-three RCTs and 24 systematic analyses were included.

Dance-movement therapy for mild cognitive impairment

Description of mild cognitive impairment

MCI was introduced as the intermediate stage between healthy aging with mild cognitive changes and dementia (Petersen et al., 2014). In accordance with the main symptoms, MCI was divided into amnestic MCI (aMCI) with memory dysfunction predominates and non-amnestic MCI with other cognitive deficit syndrome predominates (e.g., language, visuospatial, executive) (Petersen et al., 2018). Higher prevalence of MCI is related to increased age and lower educational level. Among the 65-year-old population, 16–20% had MCI, with a 5-year cumulative incidence ranging from 22.9 to 30.1%. MCI had a tendency to convert to dementia, with an annual conversion rate of 10% (Zhu et al., 2018). Although the neuropathogenesis of MCI and dementia is still being further explored and without definitive treatment. The population with MCI retains neuroplasticity. Existing studies have found that rTMS (Chou et al., 2020), cognitive therapy (Kirova et al., 2015), aerobic exercise, psychological and social activities (Langa and Levine, 2014; Jongsiriyanyong and Limpawattana, 2018), supplementing nutrition (Eshkoor et al., 2015) and maintaining adequate sleep (Blackman et al., 2021) can prevent the deterioration of the disease to a certain extent. In accordance with the recommendations for the management of MCI, regular physical activity for twice a week was more effective than cognitive impairment drugs. Recent studies demonstrated that dance movement intervention has a positive effect on cognitive function in MCI patients.

Effect on global cognitive function

The Mini-Mental State Examination (MMSE), Montreal Cognitive Assessment (MoCA), and Function and Cognitive Assessment Test (FUCAS) were used to assess the global cognitive level of MCI patients. Three high-quality systemic and meta-analysis studies (Chan et al., 2020; Liu et al., 2021; Wu et al., 2021) reported that global cognitive function remarkably increased when older adults with MCI practiced dance compared with the control group [Wu et al. (2021), SMD = 0.54, Z = 3.55, $p < 0.001$; Liu et al. (2021), SMD = 0.73, 95%CI = 0.47 to 0.99, $p < 0.001$; Chan et al. (2020), SMD =

TABLE 1 Randomized controlled trials assessing various dance-based movement interventions in patients with mild cognitive impairment or Alzheimer's disease.

Experimental group vs. control group; (Participants: n)	Primary outcome	Overall duration of intervention	Main results
Mild cognitive impairment			
Aerobic dance routine vs. usual care; (60) (Zhu et al., 2018)	(1) MoCA; (2) WMS-R; (3) DST; (4) SDMT; (5) TMT; (6) FAQ; (7) SF-36; (8) GDS-15; (9) ERP; (10) Adverse events;	21 h in 12 weeks; No reported.	(2) DG vs. CG: mean change = 4.6; 95% CI = 2.2 to 7.0; $p = 0.001$ (at 3 months); (1); (3); (4); (5); (6); (7); (8); (9); (10) NS (between-group difference);
Aerobic dance vs. health education; (68) (Zhu et al., 2022)	(1) WMS-RLM; (2) Unilateral hippocampal volume;	21 h in 12 weeks; 88.6%.	(1) DG vs. CG: β = 0.326, 95%CI = 1.005 to 6.773, $p = 0.009$; (2) DG vs. CG: β = 0.379, 95% CI = 0.117 to 0.488, $p = 0.002$ (right); β = 0.344, 95% CI = 0.082, 0.446, $p = 0.005$ (total);
Dance vs. a life as usual; (62) (Rektorova et al., 2020)	(1) MoCA; (2) TFT; (3) Logical memory; (4) FPT; (5) ToH; (6) JLO; (7) MAST; (8) BADLS;	60 h in 24 weeks; No reported.	(1); (2); (3) DG vs. CG: NS (between-group difference); (4) DG vs. CG: F = 4.07, $p = 0.05$; (5); (6); (7); (8); (9) DG vs. CG: NS (between-group difference);
Specially designed moderate-intensity aerobic dance vs. usual care; (32) (Qi et al., 2019)	(1) MMSE; (2) MoCA; (3) WMS-R LM; (4) DST-F; DST-B; (5) SDMT; (6) BBS;	21 h in 12 weeks; No reported.	(1); (2) DG vs. CG: NS (between-group difference); (3) $p < 0.05$; (4); (5); (6) DG vs. CG: NS (between-group difference);
Participants familiarized dance vs. usual care; (129) (Lazarou et al., 2017)	(1) MMSE; (2) MoCA; (3) FUCAS; (4) TEA-4; (5) RAVLT; (6) RBMT; (7) FAS; (8) ROCFT; (9) GDS; (10) NPI;	80 h in 40 weeks; No reported.	(1) DG vs. CG: $p < 0.001$; (2) DG vs. CG: $p = 0.03$; (3) NS (between-group difference); (4) DG vs. CG: $p = 0.002$; (5) DG vs. CG: $p = 0.003$; (6) DG vs. CG: RBMT-1, $p = 0.004$; RBMT-2, $p = 0.001$; (7) DG vs. CG: $p = 0.005$; (8) DG vs. CG: $p < 0.001$; (9) DG vs. CG: $p = 0.022$; (10) DG vs. CG: $p = 0.02$;
Dance vs. life-as-usual; (99) (Kropacova et al., 2019)	(1) TCF 1; (2) TCF 2; (3) WMS III: LogPam; (4) LogPam2; (5) DigitSpan; (6) WAIS III: Symbols; (7) ToH 3; (8) ToH 4; (9) FPT; (10) JLO;	72 h in 24 weeks; 78.1%.	(1) (2); (3); (4); (5); (6); (7); (8); (10): DG vs. CG: NS (between-group difference); (9) DG vs. CG: $p = 0.008$;
Dance, music, and health education; (201) (Doi et al., 2017)	(1) Story memory; (2) Word memory;	40 h in 40 weeks; 93%.	(1) DG vs. CG: $p = 0.011$; (2) NS (between-group difference);
Dance vs. music; (100) (Cross et al., 2012)	(1) BDI; (2) RMT-F;	0.5 h; No reported.	(1) DG vs. MG: $p < 0.001$ (at after-intervention 3 days); $p = 0.008$ (at after-intervention 10 days); (2) DG vs. MG: $p = 0.002$ (at after-intervention 3 days);
Chinese square dance vs. usual care; (109) (Chang et al., 2021)	(1) MoCA; (2) SF-12; (3) GDS-15; (4) BBS;	27h in 18 weeks; 19.9%.	(1) DG vs. CG: NS (group*time effect, at 9 weeks); $p = 0.004$ (group*time effect, at 18 weeks); (2) DG vs. CG: MCS, $p = 0.004$ (group*time effect, at 9 weeks); $p = 0.001$ (group*time effect, at 18 weeks); PCS, NS (group*time effect, at 9 weeks and 18 weeks); (3) DG vs. CG: NS (group*time effect, at 9 weeks); $p = 0.009$ (group*time effect, at 18 weeks); (4) DG vs. CG: NS (group*time effect, at 9 weeks); NS (group*time effect, at 18 weeks);
Fitness-dance vs. life as usual; (12) (Ammar et al., 2021)	(1) CERAD-Plus; (2) PAR-Q; (3) Physical performance and heart rate;	24 h in 8 weeks; No reported.	(1); (2); (3) DG vs. CG: NS (between-group difference);
BAILAMOS vs. waitlist control; (21) (Aguiñaga and Marquez, 2017)	Focus groups;	32h in 16 weeks. 100%	The focus group data revealed that participants were energized by the dance program, and they enjoyed learning new dance styles and techniques.

(Continued)

TABLE 1 Continued

Experimental group vs. control group; (Participants: n)	Primary outcome	Overall duration of intervention	Main results
Alzheimer's disease			
Dance groups vs. music appreciation and socialization groups; (18) (Low et al., 2016)	(1) The number of falling; (2) Neuropsychological tests; (3) Standing balance, walking speed and sit to stand speed: (4) Global functioning	36h in 12 weeks; 67%.	There were no significant differences between the groups.

MCI, Mild cognitive impairment; MoCA, The Montreal Cognitive Assessment; WMS-R, Wechsler Memory Scale-revised logical memory test; SDMT, Symbol Digit Modalities Test; TMT, Trail Making Test; DST, Forward and backward Digit Span Task; FAQ, Functional Activities Questionnaire; SF-36, The 36-item Short Form Health Survey; GDS-15, The 15-item Geriatric Depression Scale (GDS-15); ERP, event-related potential; DG, dance group; CG, control group; NS, none significant; TFT, Taylor Figure Test; FPT, Five-Point Test; ToH, Tower of Hanoi; JLO, Judgment of Line Orientation; MAST, Mississippi Aphasia Screening Test; BADLS, Bristol Activities of Daily Living Scale; WMS-R LM, Wechsler Memory Scale-Revised Logical Memory; DST-forward, Digit Span Test-F; DST-backward, DST-B; SDMT, Symbol Digit Modalities Test; BBS, Berg Balance Scale; FUCAS, Functional and Cognitive Assessment Test; TEA-4, Test of Everyday Attention; RAVLT, Rey Osterrieth Complex Figure Test copy and delay recall; RBMT, Rivermead Behavioral Memory Test; FAS, The Verbal Fluency F-A-S Test; ROCFT, Rey Osterrieth Complex Figure Test; GDS, Global Deterioration Scale; NPI, Neuropsychiatric Inventory; BDI, Beck Depression Inventory; RMT-F, Recognition Memory Test–Faces; MG, music group; SF-12, The Short-Form 12 Health Survey; GDS-15, The Geriatric Depression Scale; CERAD-Plus, Consortium to Establish a Registry for Alzheimer's Disease.

0.48, 95%CI = 0.21 to 0.74]. The meta-analysis results of Wu et al. (2021) showed that the efficacy of DMT on the MMSE is related to the overall duration of intervention. The longer the intervention duration (≥3 months), the better the clinical benefit (Wu et al., 2021). Of the five RCTs that examined the efficacy of DMT in patients with MCI using global cognitive function as the primary outcome, two RCTs reported the positive effect of DMT (Lazarou et al., 2017; Chang et al., 2021). Lazarou et al. (2017) reported that MCI patients who performed dancing for 10 months have improved MMSE ($p < 0.001$) and MoCA ($p = 0.03$) scores compared with usual care. Chang et al. (2021) compared the effects of Chinese square dancing and usual care in MCI patients and reported that the group*time effect of MoCA scores is only seen at week 18. Rektorova et al. (2020) showed no remarkable difference in MoCA score between dance practice and life as usual for 24 weeks in MCI patients. Two 12-week RCTs of aerobic dance versus usual care reported no significant between-group differences in MoCA scores in MCI patients (Zhu et al., 2018; Qi et al., 2019). Performing DMT for at least 3 months has positive effects on the global cognitive function of MCI patients.

Effect on memory and other cognitive functions

Comprehensive cognitive function assessment includes memory, working memory, attention, executive function, and language. Immediate and delayed recall was commonly used to assess participant's memory ability. Five systematic reviews and meta-analyses confirmed that DMT significantly improved memory ability in MCI patients (Chan et al., 2020; Zhu et al., 2020; Liu et al., 2021; Wu et al., 2021). Among the seven (Cross et al., 2012; Doi et al., 2017; Lazarou et al., 2017; Zhu et al., 2018; Kropacova et al., 2019; Qi et al., 2019; Rektorova et al., 2020) included RCTs, two employed Digit Span Task (DST) (Zhu et al., 2018; Qi et al., 2019), one (Lazarou et al., 2017) used Rey Osterrieth Complex Figure Test copy and delay recall (RAVLT) and Rivermead Behavioral Memory Test-1 (RBMT-1), and others used word memory (Doi et al., 2017) to assess the immediate memory recall. Two studies comparing usual care found that 12 weeks of moderate aerobic dance did not produce a significant positive effect on the DST score in MCI patients (Zhu et al., 2018; Qi et al., 2019). Wechsler Memory Scale (WMS), RAVLT, RBMT-2, and story memory test were used to evaluate the delayed recall. Four RCTs (Zhu et al., 2018, 2022; Kropacova et al., 2019; Qi et al., 2019) with WMS as the primary outcome reported that 12 weeks of aerobic dance had positive effects on delayed recall ability in MCI patients compared with usual care or health education. The RCT of Lazarou et al. (2017) showed that better immediate and delayed recall performance is detected in 10 months of international ballroom dancing compared with the control group (RAVLT: $p = 0.003$; RBMT-1, $p = 0.004$; RBMT-2, $p = 0.001$). The results of Doi et al. (2017) reported that one dance intervention for 0.5 h can improve story memory recall in patients with MCI compared with health education or music. And the finding of Zhu et al. (2022) showed that 12 weeks of aerobic dance could improve episodic memory ($\beta = 0.326$, 95%CI = 1.005 to 6.773, $p = 0.009$) and increase the right ($\beta = 0.379$, 95% CI = 0.117 to 0.488, $p = 0.002$) and total ($\beta = 0.344$, 95% CI = 0.082 to 0.446, $p = 0.005$) hippocampal volumes in the individual with MCI. Remarkable cortical thickening was observed in the right inferior temporal, fusiform, and lateral occipital regions of MCI participants undergoing a 6-month dance intervention (Rektorova et al., 2020). Overall, DMT had significant positive effects in improving the memory ability in MCI patients regardless of the intervention type and duration.

TABLE 2 Randomized controlled trials assessing various dance-based movement interventions in patients with Parkinson's disease.

Experimental group vs. control group	Primary outcome	Overall duration of intervention; participant rate (%)	Main results
Irish set dancing classes vs. physiotherapy; (24) (Volpe et al., 2013)	(1) MDS-UPDRS-III; (2) TUG; (3) BBS; (4) FOG-Q;	36h (mean: 32.745h) in 24 weeks; 90.9%.	(1) DG vs. CG: F = 6.35, $p = 0.019$; (2) DG vs. CG: F = 8.938, $p = 0.007$; (3) DG vs. CG: NS (between-group difference, F = 4.254, $p = 0.051$); (4) DG vs. CG: t = 16.296, $p < 0.001$;
Irish set dancing classes vs. exercises or usual care; (41) (Shanahan et al., 2017)	(1) UPDRS-III; (2) 6 MWT; (3) Mini-BESTest; (4) PDQ-39;	25h in 10 weeks; 93.5%.	(1) Postintervention, the dance group had greater nonsignificant gains in quality of life than the usual care group; (2) (3) (4) (5) DG vs. CG: NS (between-group difference)
Sardinian folk dance vs. usual care; (20) (Solla et al., 2019)	(1) UPDRS-III; (2) 6MWT; (3) FTSST; (4) TUG test; (5) BBS; (6) MIMUs; (6) MoCA; (7) BDI-II; (8) SAS;	36h in 12 weeks; 92.9%.	(1) DG vs. CG: F = 22.191, $p < 0.001$; (2) DG vs. CG: F = 41.124, $p < 0.001$; (3) DG vs. CG: F = 95.685; $p < 0.001$; (4) DG vs. CG: F = 26.014; $p < 0.001$; (5) DG vs. CG: F = 49.834; $p < 0.001$; (5) Stride length: DG vs. CG, F = 5.608; $p = 0.03$; Walking speed: DG vs. CG, F = 4.524; $p = 0.049$; Walking cadence: DG vs. CG, F = 4.572; $p = 0.048$; GFI revealed: DG vs. CG, F = 10.797; $p = 0.005$; (6) DG vs. CG: F = 7.913; $p = 0.012$; (7) DG vs. CG: F = 47.957; $p < 0.001$; (8) DG vs. CG: F = 7.106; $p = 0.016$
Tango, parted vs. usual care; (33) (Rios Romenets et al., 2015)	(1) the MDS-UPRDS-3; (2) Mini-BESTest; (3) TUG; (4) Dual-task TUG; (5) Fall; (6) FOG-Q; (7) FSS; (8) Upper extremity function; (9) MoCA; (10) BDI; (11) AS;	24h in 12 weeks; 61%.	(1) (5) (6) (7) (10): DG vs. CG: NS (between-group difference); (2) DG vs. CG: $p = 0.032$; (3) DG vs. CG: $p = 0.042$; (4) DG vs. CG: $p = 0.012$; (8) DG vs. CG: $p = 0.038$ (After multivariate adjustment for baseline average time on exercise/dance); (9) DG vs. CG: $p = 0.01$ (after exclusion of the 9 protocol violations);
Tango single vs. usual care; (13) (Michels et al., 2018)	(1) MDS-UPRDS-3; (2) Hoehn and Yahr scale;	10h in 10 weeks; Not reported.	The study was not powered to assess whether any of these differences were statistically significant.
Tango vs. Tai Chi; (29) (Poier et al., 2019)	(1) the MDS-UPRDS-3; (2) The MoCA; (3) PDQ-39; (4) BMLSS; (5) BDI; (6) FSS; (7) VAFS;	10h in 10 weeks; Not reported.	(1) (2) (3) (4) (5) (6) (7): NS (between-group difference)
Group/Partnered vs. group structured strength/flexibility exercise; (19) (Hackney et al., 2007)	(1). The MDS-UPRDS; (2) BBS; (3) TUG and Dual-Task TUG; (5) Freezing of Gait; (6) Walking and Dual-Task Walking;	21h in 13 weeks; 100%.	(1) (2) (3) (4) (5) (6): NS (between-group difference)
Partnered vs. Nonpartnered tango; (39) (Hackney and Earhart, 2010)	(1) The MDS-UPRDS-3;	20h in 10 weeks; 80%.	No group comparisons were made in this RCT.
Tango vs. waltz/foxtrot or no intervention (control) groups; (58) (Hackney and Earhart, 2009)	(1) The MDS-UPRDS-3; (2) BBS; (3) TUG; (4) 6 MWT; (5) FOG; (6) TUG; (7) Gait speed, stride length, and single support time;	20h in 13 weeks; Not reported.	(1) (3) (5) (6) Tang vs. CG: NS (between-group difference); Waltz/foxtrot vs. CG: NS (between-group difference); (2) Tang vs. CG: $p < 0.05$; Waltz/foxtrot vs. CG: $p < 0.05$; (4) Tang vs. CG: $p < 0.05$; Waltz/foxtrot vs. CG: $p < 0.05$; (7) Tang vs. CG: backward stride length, $p < 0.05$; Waltz/foxtrot vs. CG: backward stride length, $p < 0.05$;
Partnered community-based tango vs. no intervention control group; (52) (Foster et al., 2013)	(1) UPRDS-1 and 3; (2) BDI; (3) ACS;	96h in 48 weeks; Not reported. 90%	These patterns were similar in the separate activity domains. The tango group gained a significant number of new social activities ($p = 0.003$), but the control group did not ($p = 0.71$).

(Continued)

TABLE 2 Continued

Experimental group vs. control group	Primary outcome	Overall duration of intervention; participant rate (%)	Main results
Partnered community-based tango vs. no intervention control group; (62) (Duncan and Earhart, 2012)	(1) MDS-UPRDS-3; (2) Mini-BESTest; (3) FOG-Q; (4) 6 MWT; (5) Walking velocity during comfortable forward, fast as possible forward, dual task, and backward walking; (6) 9HPT;	96h in 48 weeks; 78.5 ± 3%.	(1) DG vs. CG: total scores, F = 9.82, $p < 0.001$; tremor scores, NS (between-group difference); rigidity, F = 11.72, $p < 0.001$ (time*group effect, at 6 and 12 months); Bradykinesia, F = 8.35, $p < 0.001$ (time*group effect, at 6 and 12 months); (2) DG vs. CG: F = 11.73, $p < 0.001$ (time*group effect, at 3, 6 and 12 months); (3) DG vs. CG: NS (between-group difference); (4) DG vs. CG: distance of walking, $p < 0.05$; (5) DG vs. CG: forward walking velocity, $p < 0.05$ (between-group difference, at 6 and 12 months); dual-task walking, F = 3.57, $p = 0.02$; (6) DG vs. CG: F = 3.83, $p = 0.01$;
Partnered community-based tango vs. no prescribed exercise control group; (10) (Duncan and Earhart, 2014)	(1) MDS-UPRDS-1, 2, and 3; (2) Mini-BESTest; (3) gait velocity (forward and backward); (4) TUG and dual-task TUG; (5) 6MWT; (6) FOG-Q;	192 h in 96 weeks; Not reported.	(1) DG vs. CG: MDS-UPRDS-3, F= 17.59; $p < 0.001$ (time*group effect, at 12 and 24 months); UPRDS-2, F = 3.53; $p = 0.05$ (time*group effect, at 12 and 24 months); UPRDS-1, F = 5.10; $p = 0.02$ (time*group effect, at 12 and 24 months); (2) DG vs. CG: F = 11.33; $p < 0.001$ (time*group effect, at 12 and 24 months); (3) (6) DG vs. CG: NS (between-group difference); (4) DG vs. CG: TUG, NS (between-group difference); Dual-Task TUG, F = 3.7; $p = 0.048$ (time*group effect, at 12 and 24 months); (5) DG vs. CG: F = 5.67; $p = 0.013$ (time*group effect, at 12 and 24 months);
Turo (mixed Qigong dance); (20) (Lee et al., 2018)	(1) UPDRS; (2) ADL; (3) PDQ-39; (3) BDI-21; (4) BBS;	8 weeks; Not reported.	(1) DG vs. CG: $p = 0.001$; (2) DG vs. CG: $p = 0.002$; (3) DG vs. CG: $p = 0.049$; (4) DG vs. CG: NS (between-group difference, $p = 0.051$);
Double ballroom and Latin American dance vs. usual care; (27) (Hulbert et al., 2017)	Twelve, 180° on-the-spot turns	20h in 10 weeks; Not reported.	Significant 4-way interactions between the groups, over time and turn style, with longer latency of the head ($p = 0.008$) and greater rotation in the pelvis ($p = 0.036$), alongside a trend of slower movement of the first ($p = 0.063$) and second ($p = 0.081$) foot in controls were shown, with minimal change in dancers.
Incorporated strategies-based dance vs. PD exercise; (46) (Hashimoto et al., 2015)	(1) UPDRS; (2) TUG; (3) BBS; (4) FAB; (5) MRT; (6) AS; (7) SDS;	12h in 12 weeks; Not reported.	(1) DG vs. CG: $p < 0.001$; (2) DG vs. CG: TUG time, $p = 0.006$, TUG step number, $p = 0.005$; (3) DG vs. CG: $p = 0.001$; (4) DG vs. CG: $p = 0.001$; (5) DG vs. CG: MRT response time, $p < 0.001$; (6) DG vs. CG: $p < 0.001$; (7) DG vs. CG: $p = 0.006$;
Dance-physiotherapy combined intervention vs. conventional physiotherapy; (38) (Frisaldi et al., 2021)	(1) MDS-UPDRS-III; (2) 6 MWT; (3) TUG; (4) Mini BESTest; (5) New FOG-Q; (6) MoCA;(7) TUG-DTT; (8) PDQ-39; (9) BDI;	15h in 5 weeks; 100%	(1) DG vs. CG: MD = −2.72, 95% CI = −5.28 to −0.16, $p = 0.038$; (2) (3) (4) DG vs. CG: NS (between-group difference); (5) Significant improvements were only found in the control group; (6) Significant improvement was only found in the dance group ($p = 0.03$); (7) Significant improvement was only found in the dance group ($p = 0.02$); (8) DG vs. CG: NS (between-group difference); (9) Significant improvement was only found in the control group;

(Continued)

TABLE 2 Continued

Experimental group vs. control group	Primary outcome	Overall duration of intervention; participant rate (%)	Main results
Binary vs. quaternary dance rhythm; (31) (Moratelli et al., 2021)	(1) Hoehn and Yahr scale; (2) UPDRS-1, and 2; (3) MMSE; (4) MoCA; (5) PDQ-39; (6) mental activity;	18h in 12 weeks; 84.3%	Both intervention groups improved cognition (MoCA: $p < 0.001$, d = 0.05), mental activity (UPDRS-1: $p < 0.001$). UPDRS-1 items, the QG was highlighted in intellectual impairment ($p = 0.005$) and motivation ($p = 0.021$).
Virtual reality dance exercise vs. usual care; (20) (Lee et al., 2015)	(1) BBS; (2) MBI; (3) BDI;	15h in 6 weeks; Not reported.	(1) DG vs. CG: $p < 0.05$; (2) DG vs. CG: $p < 0.05$; (3) DG vs. CG: $p < 0.05$;

PD, Parkinson's disease; UPDRS-III, Unified Parkinson's Disease Rating Scale Part-III; TUG, Timed Up-and-Go; BBS, Berg Balance Scale; FOG, Freezing of Go Questionnair; MD, Mean Difference; 6 MWT, 6-minute walk test; Mini-BESTest, Mini-Balance Evaluation Systems Test; PDQ-39, Parkinson's disease questionnaire-39; FTSST, the Five Times Sit-to-Stand Test; SRT, Sit-and-Reach Test; BST, Back Scratch Test; MIMUs, MagnetoInertial Measurement Units; PFS-16, Fatigue Scale; BDI-II, The Beck Depression Inventory; SAS, Starkstein Apathy Scale; FSS, Fatigue Severity Scale; AS, Apathy Scale; VAFS, Visual Analog Fatigue Scale; BMLSS, Brief Multidimensional Life Satisfaction Scale; ACS, the Activity Card Sort; 9HPT, the Nine-Hole Peg Test; MRT, Mental Rotation Task; SDS, Self-rating Depression Scale; MBI, the Modified Barthel Index; STAIL, State-Trait Anxiety Inventory; FES-1, Falls Efficacy ScaleInternational; TRAIL, Trail Making Test; MCS, the mental component summary; PCS, the physical component summary; PAR-Q, The Modified German version of the Physical Activity Readiness Questionnaire; yr, year.

Tables 1–4 show the effects of DMT on executive function, which is assessed by using Trail Making Test, Five-Point Test, Tower of Hanoi, and Rey Osterrieth Complex Figure Test. Two meta-analyses showed (Zhu et al., 2020; Wu et al., 2021) that DMT has remarkable effects on executive function compared with non-dance intervention. Among the five included RCTs with executive function as the primary outcome, three trials supported that DMT can significantly increase the response time and accuracy in MCI patients (Zhu et al., 2018; Kropacova et al., 2019; Qi et al., 2019). The Verbal Fluency F-A-S Test (FAS) and Mississippi Aphasia Screening Test (MAST) are the commonly used language-cognition assessment tools. The results of three meta-analyses demonstrated that DMT positively enhances the verbal fluency in MCI patients (Liu et al., 2021; Wu et al., 2021). Two meta-analyses confirmed that DMT can improve in the visuospatial function of patients with MCI (Chan et al., 2020; Wu et al., 2021).

Effect on physical and psychological function

Balance and depression contribute to reduced quality of life in individuals with MCI. The efficacy of DMT is associated with the intervention time to some extent. Aerobic dancing for 12 weeks did not improve the balance in MCI patients compared with usual care (Qi et al., 2019). Participants in the intervention group showed remarkable time*group effect in improving balance, depression, and quality of life compared with usual care after 18 weeks of Chinese square dancing (Chang et al., 2021). Compared with music, 0.5 h dance intervention showed significant improvement in depressive symptoms in MCI patients over the first 3 days (Cross et al., 2012). Two RCTs reported that more than 8 weeks of dance training provided cardioprotective benefits in patients with MCI (Aguiñaga and Marquez, 2017; Ammar et al., 2021). Therefore, DMT is an efficient rehabilitation strategy to promote the wellbeing of patients with MCI.

Dance-movement therapy for Parkinson's disease

Description of Parkinson's disease

PD is a chronic, progressive, and disabling ND. As the second most common ND, PD affects more than 6 million older adults worldwide. The gold standard for its diagnosis is the pathological changes in Lewy bodies and the degeneration of substantia nigra pars compacta (SNpc) at autopsy (Dickson et al., 2009). In the misfolded state, α-synuclein becomes insoluble and aggregates within the cell bodies (Lewy bodies) and processes (Lewy neurites) of neurons to form intracellular inclusions (Polymeropoulos et al., 1997; Wong and Krainc, 2017). This condition is due to the death of the dopaminergic neurons of SNpc in the early stage, resulting in dopamine deficiency in the basal ganglia and typical Parkinson's motor dysfunction (Dickson et al., 2009). The symptoms of PD include slow movements, muscle stiffness, rest tremor, postural instability, and gait disturbances. PD involves non-motor features, including psychiatric disturbances, cognitive impairments, olfactory disturbances, sleep disturbances, autonomic dysfunction, pain, and fatigue. It affects physical, mental, emotional, and social functioning, which can have a profound effect on the quality of life (Sharp and Hewitt, 2014). Despite the recent advances in gene and drug therapy, no disease treatments that can improve PD. Current research suggests that exercise

TABLE 3 Systemic reviews assessing various dance-based movement interventions in patients with mild cognitive impairment or Alzheimer's disease.

Author (Year; Studies; Participants)	Primary outcome	Main results
Mile cognition impairment		
Zhu et al. (2020; 5 RCTs; 644; 8)	(1) FAS;(2) TMT; (3) Immediate recall ability; (4) Delayed recall;	Compared to control: (1) MD = 1.73, 95%CI = 0.58 to 2.88, $p = 0.003$; (2) TMT-A, MD= −2.37, 95%CI= −4.16 to 0.58; $p = 0.010$; TMT-B, MD= −16.07, 95%CI= −30.03 to 0.01, $p = 0.020$; (3) SMD = 0.24, 95%CI = 0.01 to 0.46, $p = 0.04$; (4) SMD = 0.46, 95%CI = 0.30 to 0.62, $p < 0.001$;
Wu et al. (2021; 8 RCTs; 548; 11)	(1) Global cognition; (2) Memory; (3) Visuospatial function; (4) Language; (5) Motor function;	Compared to control: (1) SMD = 0.54, Z = 3.55, $p < 0.001$; (2) SMD = 0.33, Z = 3.97, $p < 0.001$; (3) SMD = 0.42, Z = 2.41, $p = 0.02$; (4) SMD = 0.39, Z = 2.69, $p = 0.007$; (5) SMD = 0.93, Z = 5.04, $p < 0.001$;
Wang et al. (2021; 5; 579; 9)	(1) Depression; (2) Anxiety;	Compared to control: (1) SMD = −0.42, 95%CI = −0.60 to −0.23, $p < 0.05$; (2) NS (between-group difference)
Liu et al. (2021; 12 RCTs; 896; 9)	(1) Global cognition; (2) Executive function; (3) Immediate Recall; (4) Delayed Recall; (5) Language;	Compared to control: (1) SMD = 0.73, 95%CI = 0.47 to 0.99, $p < 0.001$; (2) NS (MD = −3.16, 95%CI = −7.16 to −0.85, $p = 0.12$); (3) SMD = 0.54, 95%CI = 0.30 to 0.78, $p < 0.0001$; (4) SMD = 0.56, 95%CI = 0.26 to 0.86, $p = 0.0002$; (5) $p < 0.05$;
Chan et al. (2020; 5 RCTs; 358; 9)	(1) Global cognition; (2) Attention; (3) Immediate Recall; (4) Delayed Recall; (5) Visuospatial ability;	Compared to control: (1) SMD = 0.48, 95%CI = 0.21 to 0.74, $p < 0.05$; (2) SMD = 0.33, 95%CI = 0.12 to 0.54, $p < 0.05$; (3) SMD = 0.54, 95%CI = 0.38 to 0.71, $p < 0.05$; (4) SMD = 0.33, 95%CI = 0.01 to 0.64, $p < 0.05$; (5) SMD = 0.16, 95%CI = 0.01 to 0.32, $p < 0.05$;
Alzheimer's disease		
Karkou and Meekums (2017; 0; 0; 8)	(1) Challenging behaviors; (2) Cognitive function; (3) Depression; (4) Quality of life;	None of which met the inclusion criteria.
Mabire et al. (2019; 14 studies; 967; 5)	(1) Motor function; (2) Psychological function; (3) Cognitive function; (4) Quality of life; (5) Self-esteem; (6) Social interactions; (7) Behavioral outcomes;	This review found that nine practice recommendations for implementing dance interventions were identified according to primary intentions of the intervention (therapeutic or recreational): indications; contra-indications; participant profile; dosage; session sequencing; setting of intervention; observance/attendance; contributors and facilitators; and assessments.
Ruiz-Muelle and López-Rodríguez (2019; 12 studies; 349; 8)	(1) Physical function; (2) Cognitive function; (3) Psychological function; (4) Quality of life; (5) Burden of Care;	This mini-review confirmed the positive effect of dance therapy on physical and cognitive function, functionality, psychological outcomes, and quality of life in cognitive dysfunction people

RCT, randomized control trial; AD, Alzheimer's disease; Quality of Life; MCI, mild cognition impairment; FAS, The Verbal Fluency F-A-S Test; TMT, Trail Making Test; MD, Mean Difference; CI, Confidence Interval; SMD, Standardized Mean Difference; NS, No significant; High quality: total score ≥7; moderate quality: total score 4–6; low quality: total score ≤3.

increases brain volume, promotes the activation of a wide range of brain regions, and produces neuroprotective effects that allow the brain to repair itself. Exercise-induced behavioral recovery and increased dopamine synthesis and release in PD rats have been reported in several animal studies. A number of studies have confirmed that active intervention for dance therapy may be the most suitable exercise intervention for PD patients due to the musical rhythm background and high patient compliance.

Effects on motor symptoms

Sixteen systematic analyses (Mandelbaum and Lo, 2014; Sharp and Hewitt, 2014; Lötzke et al., 2015; Shanahan et al., 2015; Aguiar et al., 2016; Dos Santos Delabary et al., 2018; Kalyani et al., 2019; Tang et al., 2019; Zhang Q. et al., 2019; Barnish and Barran, 2020; Berti et al., 2020; Carapellotti et al., 2020; Hidalgo-Agudo et al., 2020; Emmanouilidis et al., 2021; Ismail et al., 2021; Hasan et al., 2022), 18 RCTs (Hackney et al., 2007; Hackney and Earhart, 2009, 2010; Hashimoto et al., 2015; Rios Romenets et al., 2015; Hulbert et al., 2017; Shanahan et al., 2017; Lee et al., 2018; Michels et al., 2018; Poier et al., 2019; Solla et al., 2019; Frisaldi et al., 2021), and 62 clinical trials investigated the effects of dance on Parkinson's symptoms (Tables 1–4, Supplementary Tables 1, 2). Most studies (11/13 systematic analyses and all RCTs) examined the effects of dance exercise therapy in PD patients using exercise parameters as the primary outcome measure. Movement

TABLE 4 Systemic reviews assessing various dance-based movement interventions in patients with Parkinson's disease.

Author (Year; Studies; Participants; Quality)	Primary outcome	Main results
Zhang Q. et al., (2019; 7 RCTs; 185; 7)	(1) MoCA; (2) FAB; (3) SDS; (4) BDI; (5) AS;	Compared to control: (1) WMD = 2.02, 95%CI:0.65 to 3.38, $p = 0.004$; (2) WMD = 1.17, 95%CI:0.39 to 1.95, $p = 0.003$; (3) (4) (5) NS;
Sharp and Hewitt (2014; 5 RCTs; 143; 10)	(1) UPDRS−3 motor scores; (2) Gait speed; (3) Balance; (4) PDQ−39;	Compared to no treatment: (1) MD = −10.73, 95%CI = −15.01 to −6.16, $p = 0.004$; (2) MD = 0.14m/s, 95%CI = 0.02 to 0.26, $p = 0.02$; (3) MD = 0.72, 95%CI = 0.31 to 1.44, $p < 0.001$; compared with other exercise: MD = 3.98, 95%CI = 1.52 to 6.44, $p = 0.002$; (4) Compared with other exercise: MD = −4.00, 95%CI = −7.13 to −0.87, $p = 0.01$.
Shanahan et al. (2015; 12 studies; 359; 6)	(1) UPDRS−3; (2) BBS; (3) TUG; (4) 6–MWT; (5) PDQ−39; (6) PAS;	In this review, dance was found to be more effective than a control intervention for improving balance, motor impairment. Two 1–hour dance classes per week, for at least 10 weeks, can have positive effects. Greater benefit might also be seen with longer duration interventions
Lötzke et al. (2015; 12 sudies; 433; 6)	(1) UPDRS−3; (2) The Mini–BESTest; (3) BBS; (4) TUG; (5) 6 MWT; (6) FOG–Q;	Compared to control: (1) 95%CI = −1.04 to −0.21, $p < 0.05$; (2) 95%CI = 0.60 to 1.31, $p < 0.05$; (3) 95%CI = 0.01 to 0.90, $p < 0.05$ (4) 95%CI = −0.72 to −0.2, $p < 0.05$; (5) (6) NS, p> 0.05
Kalyani et al. (2019; 12 studies; 589; 10)	(1) UPDRS−3; (2) Gait speed; (3) TUG; (4) FOG–Q; (5) 6 MWT; (6) Dual–task TUG; (7) MoCA	Compared to control: (1) SMD = −1.04, 95%CI = −1.69 to −0.39, $p < 0.05$; (2) NS (SMD = 0.37, 95%CI = −0.13 to 0.86); (3) SMD = −0.54, 95%CI = −0.91 to −0.16, $p < 0.05$; (4) NS (SMD = −0.38, 95%CI = −0.09 to 0.34); (5) SMD = 0.75, 95%CI = 0.15 to 1.35, $p < 0.05$; (6) SMD = −0.85, 95%CI = −1.50 to −0.21, $p < 0.05$; (7) SMD = 0.52, 95%CI= −0.00 to 1.04, $p < 0.05$;
Ismail et al. (2021; 20 RCTs; 723; 6)	(1) MDS–UPDRS−1; (2) MDS–UPDRS−2; (3) MDS–UPDRS−3; (4) MDS–UPDRS−4; (5) The Mini–BEST Test; (6) BBS; (7) FOG–Q; (8) TUG; (10) 6 MWT; (11) BST;	Compared to no treatment: (1) MD= −3.50, 95%CI = −18.68 to 11.67, $p < 0.05$; (2) MD = −2.09, 95%CI=-7.57 to 3.40, $p < 0.05$; (3) MD = −6.91, 95%CI = −9.97 to −3.84, $p < 0.05$ (at 3 months); (4) NS (MD= −0.10, 95%CI= −0.79 to 0.59) (5) MD= 4.47, 95%CI = 2.29 to 6.66, $p < 0.05$; (6) MD = 8.42, 95%CI = 3.68 to 13.17, $p < 0.05$ (at 3 months);; (7) MD = −0.39, 95%CI= −2.99 to 2.24, $p < 0.05$; (8) MD = −1.16, 95%CI = −2.17 to −0.15, $p < 0.05$; (9) MD = 238.80, 95%CI = 157.99 to 319.61, $p < 0.05$; (10) NS (MD = 5.30, 95%CI= −2.94 to 13.54); (11) NS (RR = 0.56, 95%CI = 0.11 to 2.90);
Emmanouilidis et al. (2021; 39 studies; 1198; 7)	(1) Gait; (2) Balance; (3) Movement; (4) Mobility; (5) Movement disorders; (6) Participation;	This review found that there are positive associations between therapeutic dancing and improvements in gait, balance, movement disorders, and disability.
Dos Santos Delabary et al. (2018; 5 RCTs; 159; 8)	(1) UPDRS−3; (2) TUG; (3) 6 MWT; (4) FOG–Q; (5) Velocity of forward and backward walking; (6) PDQ−39;	Compared to control: (1) CI= −13.79 to 2.91, $p = 0.003$; (3) NS (CI= −6.72 to 79.19, $p = 0.10$); (4) NS (CI= −4.95 to 0.29, $p = 0.08$); (5) Forward waling, Cl = 0.33 to 0.20, $p = 0.15$; Backward Walking, CI = −0.09 to 0.24, $p = 0.38$; (6) NS (CI = −8.33 to 4.26, $p = 0.53$); (2) Compared to other exercise: CI = −2.03 to −0.27, $p = 0.01$;
Carapellotti et al. (2020; 16 RCTs; 636; 9)	(1) Motor outcome; (2) Cognitive function; (3) Mental health related outcomes; (4) Quality of life;	The reviewed evidence demonstrated that dance can improve motor impairments, specifically balance and motor symptom severity in individuals with mild to moderate PD, and that more research is needed to determine its effects on non–motor symptoms and quality of life.
Berti et al. (2020; 21 studies; 383; 7)	The Template for Intervention Description and Replication guidelines and checklist were used to assess quality and quantity of the content of Argentine tango interventions' description.	This review found that the included RCT interventions were well described, such as details of intervention procedures and doses. In addition, participants in the dance intervention showed strong adaptability and compliance.
Hidalgo-Agudo et al. (2020; 11 RCTs; 982; 8)	(1) UPDRS–III; (2) TUG; (3) BBS; (4) ABC; (5) FES; (6) PDQ−39;	Compared to no treatment: (1) NS ($p = 0.14$); (2) MD = −1.16, 95%CI = −2.30 to −0.03, $p = 0.04$; (3) MD = 4.05, 95%CI = 1.34 to 6.75, $p = 0.003$; (4) No relevant research;

(Continued)

TABLE 4 Continued

Author (Year; Studies; Participants; Quality)	Primary outcome	Main results
Barnish and Barran (2020; 56 studies; 1531; 6)	(1) UPDRS−3 motor; (2) TUG; (3) PDQ−39 total score (4) MMSE; (5) MoCA; (6) FAB;	Compared to other exercise: (1) NS ($p = 0.96$); (2) Compared to usually care: NS ($p = 0.33$); (3) Compared to usually care: $p = 0.0002$; (4) (5) (6) No comparable studies for meta–analysis;
Tang et al. (2019; 19 studies; 920; 8)	(1) UPDRS–III; (2) Gait velocity; (3) TUG; (4) BBS; (5) PDQ−39;	Tango vs. control: (1) MD = −9.30, 95%CI = −15.11 to −3.48, $p < 0.05$; (2) MD = 0.13, 95%CI= 0.0748 to 0.1852, $p < 0.05$; (3) MD = 3.15, 95%CI = −5.60 to −0.70, $p < 0.05$; (4) MD = 5.00, 95%CI = 3.74 to 6.26, $p < 0.05$; (5) NS (MD = 2.40, 95%CI = 0.78 to 4.02);
Aguiar et al. (2016; 10 studies; 532; 3)	(1) Walking performance; (2) FOG–Q; (3) Mobility; (4) Balance; (5) Quality of life; (6) Disease severity	This review found weight of the evidence suggests that therapeutic dancing can be beneficial for improving motor performance and balance in people with PD.
Hasan et al. (2022; 14 RCTs; 372; 7)	(1) MDS–UPDRS−1, (2) MDS–UPDRS−2, (3) MDS–UPDRS−3; (4) TUG; (5) BBS; (6) FOG; (7) 6–MWT; (8) Forward velocity (m/s) and Backward velocity (m/s); (9) Mini–BESTest; (10) BDI; (11) AS; (12) PDQ−39; (13) MoCA;	Compared to control: (1) NS ($p = 0.20$); (2) NS ($p = 0.26$); (3) MD = −4.49, 95%CI = −6.78 to −2.21, p = 0.0001 (at 3 months) (4) MD = −1.28, 95%CI = −1.99 to −0.57, $p < 0.004$ (at 3 months); (5) MD = 5.25, 95%CI = 3.8 to 6.7, $p < 0.00001$ (at 3 months); (6) NS (at 3 months); (7) NS (at 3 months, $p = 0.42$) (8) NS (forward velocity: at 3 months); (9) MD= 2.68, 95%CI = 0.82 to 4.54, $p = 0.005$ (at 3 months); (10) NS (at 3 months, $p = 0.33$); (11) MD = −3.37, 95%CI = −5.86 to −0.88, $p = 0.008$ (at 3 months); (12) NS (at 10 weeks, $p = 0.68$; at 3 months, $p = 0.81$); (13) MD= 1.1, 95%CI = 0.36 to 1.85, $p = 0.004$ (at 3 months);
Mandelbaum and Lo (2014; 9 RCTs; 295; 4)	(1) Gait; (2) Balance; (3) Upper Extremity Function; (4) Disability Rating; (5) Falls; (6) Quality of life; (7) Drop-out/Exit Survey; (8) Safety and Tolerability;	This review concluded that studies of dance intervention for PD patients should include an active randomized controlled group, a blinded evaluator, power analysis, minimally important difference, and intention-to-treat analysis.

PD, Parkinson's disease; MoCA, The Montreal Cognitive Assessment; FAB, Frontal Assessment Battery; SDS, Self-rating Depression Scale; BDI, Beck Depression Inventory; AS, Apathy Scale; WMD, Weighted Mean Difference; UPDRS-3, Unified Parkinson's Disease Rating Scale Part-3; HandY, Hoehn-Yahr Score; BBS, Berg Balance Scale; TUG, Timed Up-and-Go; 6MWT,6-minute walking test; PDQ-39, Parkinson's Disease Quality of Life Scale; PAS, Physical Activity Scale; Mini-BESTest, Mini-Balance Evaluation Systems Test; FOG-Q, The Freezing of Gait Questionnaire; FTSST, the Five Times Sit-to-Stand Test; SRT, Sit-and-Reach Test; BST, Back Scratch Test; ABC, Activities-Specific Balance Confidence; FES, Fall-Related Self-Efficacy; FSS, Fatigue Severity Scale; High quality: total score ≥7; moderate quality: total score 4–6; low quality: total score ≤3.

Disorder Society Unified Parkinson's Disease Rating Scale (MDS-UPDRS) Section Introduction–Result was applied to evaluate the global disease severity condition of patients with PD. Cognitive and psychological symptoms were measured by MDS-UPDRS-1. MDS-UPDRS-2 covered the activities of activity daily living. MDS-UPDRS-3 evaluated motor functions, such as tremor, bradykinesia, postural instability, rigidity, and gait. Six meta-analyses (Sharp and Hewitt, 2014; Lötzke et al., 2015; Dos Santos Delabary et al., 2018; Kalyani et al., 2019; Ismail et al., 2021; Hasan et al., 2022) reported higher MDS-UPDRS-3 scores on PD patients who had DMT compared with the non-dance group. The DMT group obtained significantly better MDS-UPDRS-3 scores compared with the no treatment or other exercise groups (SMD = −10.73, 95%CI = −15.05 to −6.16, $p = 0.004$), and standard or other physical therapy (MD= −6.91, 95%CI = −9.97 to −3.84, $p < 0.05$) (Sharp and Hewitt, 2014; Ismail et al., 2021). More than half of trials with MDS-UPDRS-3 as the primary outcome measure demonstrated that dance intervention improved the overall motor performance in PD patients (Duncan and Earhart, 2012, 2014; Volpe et al., 2013; Hashimoto et al., 2015; Lee et al., 2018; Solla et al., 2019; Frisaldi et al., 2021). In a 2-year RCT of dance intervention, a significant time-group interaction effect was found on MDS-UPDRS-3 in PD patients ($F_{[2,8]} = 17.59$; $p < 0.001$) (Duncan and Earhart, 2014). DMT can be a long-term intervention for the management and rehabilitation of patients with PD.

Timed Up and Go test (TUG) (Hackney et al., 2007; Hackney and Earhart, 2009, 2010; Volpe et al., 2013; Duncan and Earhart, 2014; Hashimoto et al., 2015; Rios Romenets et al., 2015; Michels et al., 2018; Solla et al., 2019; Tang et al., 2019; Frisaldi et al., 2021), the mini-BESTest (Lötzke et al., 2015), and BBS (Hackney et al., 2007; Hackney and Earhart, 2009, 2010; Volpe et al., 2013; Hashimoto et al., 2015; Lee et al., 2015, 2018; Michels et al., 2018; Solla et al., 2019; Tang et al., 2019) were used to assess the participant's balance. Six-minute walk test (6 MWT) (Hackney and Earhart, 2009, 2010; Duncan and Earhart, 2012; Volpe et al., 2013; Shanahan et al., 2017; Solla et al., 2019; Frisaldi et al., 2021) and the Freezing of Gait Questionnaire (FOG-Q)

(Hackney et al., 2007; Hackney and Earhart, 2009; Duncan and Earhart, 2012, 2014; Volpe et al., 2013; Rios Romenets et al., 2015) were the commonly used gait evaluation methods. Eight meta-analyses showed that DMT had positive effects in the balance and gait of PD patients compared with the non-dance treatment group (Sharp and Hewitt, 2014; Lötzke et al., 2015; Dos Santos Delabary et al., 2018; Kalyani et al., 2019; Tang et al., 2019; Hidalgo-Agudo et al., 2020; Ismail et al., 2021; Hasan et al., 2022). The meta-analysis results of Ismail et al. (2021) reported that DMT is significantly more effective than usual care or other physical therapies in terms of balance and gait (BBS, MD = 8.42, 95%CI = 3.68 to 13.17, $p < 0.05$, at 3 months; TUG, MD= −1.16, 95%CI = −2.17 to −0.15, $p < 0.05$; FOG-Q, MD = −0.39, 95%CI = −2.99 to 2.24, $p < 0.05$; 6 MWT, MD = 238.80, 95%CI = 157.99 to 319.61, $p < 0.05$). The meta-analysis results showed that Tango is more advantageous in improving balance and gait speed in individuals with PD by comparing the effects of Tai chi, Qigong, yoga, and resistance training on PD in terms of gait velocity, TUG, and BBS (Tang et al., 2019). The meta-analysis finding of Shanahan et al. (2015) reported that two 1 h DMTs per week for 10 to 13 weeks can provide potential positive effects on endurance, balance, and disease management. However, the effect of DMT on BBS is controversial. More than half (5/9) of RCTs using BBS as the primary outcome did not observe significant difference between the DMT group and no-treatment, usual care or other exercise groups (Hackney et al., 2007; Volpe et al., 2013; Lee et al., 2018; Qi et al., 2019; Chang et al., 2021). The RCT results of Hulbert et al. (2017) of DMT for 27 mild to moderate PD patients, 3D motion analysis, and clinical measurements found that head, pelvis, and foot movements during turning were affected by dancing with tighter coupling of body segments. Compared with conventional treatment, 20 dance sessions resulted in longer head latency ($p = 0.008$) and increased pelvic rotation ($p = 0.036$) in PD patients when turning around (Hulbert et al., 2017). As of June 2020, the finding of Emmanouilidis et al. (2021) supported that DMT can remarkably improve the disease condition, mobility, balance, and gait in PD patients in the short term.

Of the 18 RCTs, 9 studied Tango, and the rest included Irish dance, Sardinian dance, double ballroom, Latin American dance, and Turo. Tango is more suitable for PD patients than other dance styles due to its characteristic of "frequent movement starts and stops, a series of changes in speed and rhythm." However, none of the trials had a dance therapist assisting during the intervention. The total intervention duration ranged from 15 h in 5 weeks to 192 h in 96 weeks. Taking 12 weeks as the dividing line, 8 short-term (Hackney and Earhart, 2010; Lee et al., 2015, 2018; Hulbert et al., 2017; Shanahan et al., 2017; Michels et al., 2018; Poier et al., 2019; Frisaldi et al., 2021) interventions (total intervention duration <12 weeks) and 11 long-term (Hackney et al., 2007; Hackney and Earhart, 2009; Duncan and Earhart, 2012, 2014; Foster et al., 2013; Volpe et al., 2013; Hashimoto et al., 2015; Rios Romenets et al., 2015; Solla et al., 2019; Young et al., 2019; Moratelli et al., 2021) interventions (total intervention duration ≥12 weeks) were found. The attendance of participants in DMT group was not reported in 9 of the 18 RCTs assessing various DMT in the population with PD. In RCTs studies that have reported attendance rates, participants in the DMT group had an average attendance rate of greater than 70% and greater compliance than the traditional exercise or usual care control group (Hackney et al., 2007; Hackney and Earhart, 2010; Duncan and Earhart, 2012; Volpe et al., 2013; Rios Romenets et al., 2015; Shanahan et al., 2017; Michels et al., 2018; Solla et al., 2019; Moratelli et al., 2021). Two RCTs reported that participants in the dance group continued to take dance lessons after completing the entire experiment (Hackney et al., 2007; Rios Romenets et al., 2015). In accordance with the criteria of ASMART and PEDro, all RCTs were of moderate or above quality (>4 score).

Effects on cognitive deficit

Four systematic reviews and meta-analyses explored the efficacy of DMT on the overall cognitive level of PD patients, where three of them confirmed that the DMT group is better than the control group (Kalyani et al., 2019; Zhang Q. et al., 2019; Hasan et al., 2022). The meta-analysis of Zhang Q. et al. (2019) reported that DMT had remarkable difference in executive function compared with the non-dance group (WMD = 1.17, 95%CI = 0.39 to 1.95, $p = 0.003$). Cognitive dual-task evaluation by dual-task TUG showed that PD patients in the dance groups had better improvement (SMD = −0.85, 95% CI = −1.50 to −0.21, $p < 0.05$) (Kalyani et al., 2019). In four (Rios Romenets et al., 2015; Solla et al., 2019; Frisaldi et al., 2021; Moratelli et al., 2021) RCTs, DMT improved the overall cognitive function in PD patients compared with usual care, which were measured by MoCA. Two RCTs (Hashimoto et al., 2015; Solla et al., 2019) reported that 12-week dance program showed significant differences in PD patients in terms of task switching and mental flexibility (measured by the Frontal Assessment Battery at bedside ($p = 0.001$), and the Mental Rotation Task (response time: $p < 0.001$).

Effects on mood and quality of life

The clinical evaluation tools commonly used for depression and apathy include the Beck Depression Inventory and the Apathy Scale. As of April 2020, no meta-analysis showed that dance can improve the depression in PD patients. More than half (Rios Romenets et al., 2015; Poier et al., 2019; Frisaldi et al., 2021) of the RCTs examining the effects of dance on depression showed the same results. The results of two meta-analysis considering the effect of DMT on apathy in PD patients were controversial. Compared with non-dance intervention, the meta-analysis results of Zhang Q. et al. (2019) reported no

positive effects in the depression and apathy of PD patients in the dance group. The meta-analysis result of Hasan et al. (2022) showed that the reduction in apathy scores was greater in the DMT group than in the no-treatment group at 3 months (MD $= -3.37$, 95%CI $= -5.86$ to -0.88, $p = 0.008$). In a 12-week Sardinian dance RCT, the significant time*group interactions for depression ($p < 0.001$) and apathy ($p = 0.016$) were observed in the dance group (Solla et al., 2019).

Whether DMT can improve the Quality of Life Scale-39 item (PDQ-39) in PD patients remains controversial. Compared with the non-dance group, more than half of the meta-analyses (Dos Santos Delabary et al., 2018; Tang et al., 2019; Hasan et al., 2022) and RCTs (Shanahan et al., 2017; Poier et al., 2019; Frisaldi et al., 2021; Moratelli et al., 2021) reported no remarkable differences in the DMT group. The meta-analysis result of Sharp and Hewitt (2014) reported that DMT can have short-term clinically meaningful benefits in PD patients (PDQ-39, MD$= -4.00$, 95%CI$= -7.13$ to -0.87, $p = 0.01$). Compared with usual care, DMT provided PD patients with a large number of new social activities ($p = 0.003$) (Foster et al., 2013) and better emotional wellbeing ($p = 0.039$) (Poier et al., 2019).

Dance-movement therapy for Alzheimer's disease

AD is a collective term for a variety of progressive degenerative brain syndromes that affect cognition, behavior, mood, and social function. As the seventh leading cause of death, AD affects more than 50 million people worldwide (Hodson, 2018; Estimates, 2022). In accordance with the estimation of the Alzheimer's Association, individuals with AD will reach 115.4 million by 2050 due to the increasing population of older adults. AD has become an increasing issue of public health importance as people live longer and many countries have aging populations.

Three above-moderate quality systematic analyses (Karkou and Meekums, 2017; Mabire et al., 2019; Ruiz-Muelle and López-Rodríguez, 2019), 1 low RCT (Low et al., 2016), and 1 review (Bennett et al., 2021) reported the role of dance in patients with AD. All three systematic analyses looked at motor symptoms, cognitive impairment, mood, and quality of life in AD patients, but their focus varied. The analyses of Karkou and Meekums (2017) found that no professional dance therapists are involved in the RCTs of AD patients. The finding of (Ruiz-Muelle and López-Rodríguez, 2019) supported that DMT has potential positive effects on the recovery of cognitive function and the improvement of the quality of life in patients with AD. The results of Mabire et al. (2019) confirmed the positive effect of dance in improving the symptoms of AD patients and provided nine practical recommendations for implementing dance intervention, including intervention dosage, precautions. This review suggests that dance has the potential to influence motor symptoms, cognitive deficits, mood, and quality of life of AD patients. However, the evidence is weak, and further research is warranted. The therapeutic waltz for 10 weeks can significantly improve the concentration and communication with others in patients with AD (Hamill et al., 2012). Physical exercise, including dancing, lowered the MMSE score for AD patients (Hernandez et al., 2010). In two studies, a 10-min elderly clown intervention for twice a week in 12 weeks was provided for moderate to severe elderly patients with AD by using improvisation, humor, empathy and expressions of song, instrument or dance) Neuropsychiatric Inventory-Nursing Home version. The score of these patients decreased significantly ($t = -2.58$, $p = 0.02$) compared with the conventional treatment group, thereby improving the quality of life of AD patients and reduced the burden on nursing staff (Kontos et al., 2016).

Discussion

Benefits of dance-movement therapy on neurodegenerative diseases

Combining the results of Karkou and Meekums (2017), this review summarized the characteristics of dance as (a) repetitive body movement exercise; (b) musical and rhythmic auditory stimulant; (c) creativity and "motor mirroring." DMT is widely recommended for the brain health. Currently, studies on the efficacy of DMT in the intervention of ND mainly focus on the population with MCI, PD or AD. Our systematic review suggested that DMT had positive effects on cognitive function in MCI and motor function in PD. Controversy remains on the effect of dance interventions in improving the mood and quality of life in ND patients. This condition may be related to the stage of a specific ND, intervention method, and the duration of the intervention. These findings were based on 25 comprehensive systematic reviews and 33 RCTs. Future research on the effects of DMT on AD requires scientific design, large sample size, long-term comprehensive intervention, and clear reporting standards. Overall, DMT can be a safe, beneficial, and easily accessible adjunctive treatment for individuals with MCI, PD, or AD.

Mechanisms of dance therapy for neurodegenerative diseases

No appropriate animal experimental model is available, and animal experiments related to dance are lacking due to the artistic creativity of dance. Clinical trials involving dance still focus on behavioral outcomes. This review uses the mechanistic framework of Sihvonen et al. (2017) on the intervention of music in NDs and attempts to combine the characteristics of dance to

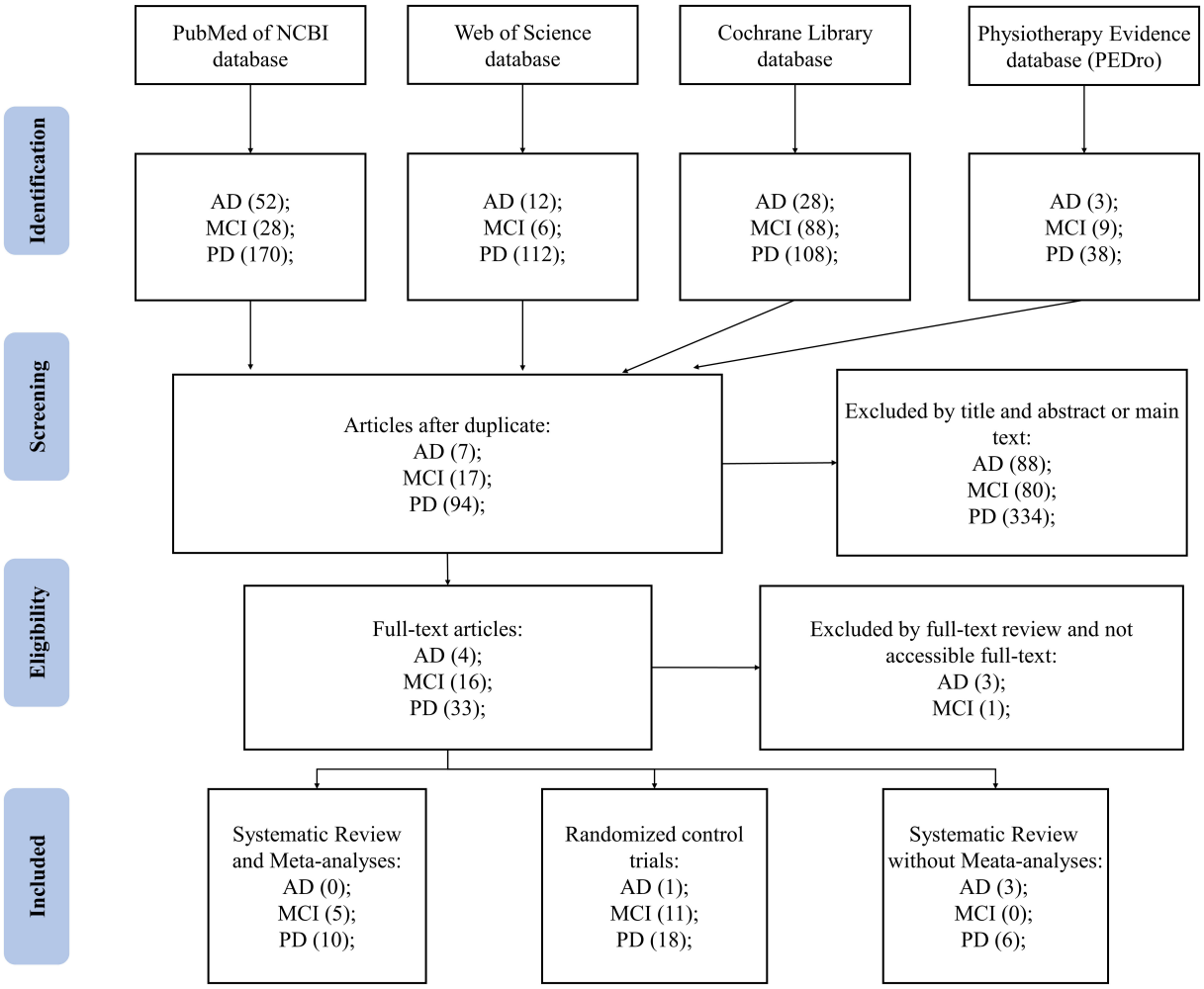

FIGURE 1
Flowchart of article search, exclusion, and analyses. AD, Alzheimer's disease; MCI, Mild cognition impairment; PD, Parkinson's disease.

explain the mechanisms behind behavioral outcomes in clinical trials (Figure 2).

Neural activation, neuroplasticity, and nerve recovery

The atrophy of brain function and structure in NDs precedes the typical symptoms. On the basis of the result of structural magnetic resonance imaging, typical Alzheimer's brain atrophy begins in the medial temporal lobe to the lateral temporal lobe and then to the parietal cortex. Neuroimaging studies reported that a network of brain regions, including the superior temporal gyrus, superior parietal lobule, frontopolar cortex, and middle temporal gyrus, is involved in dancing (Brown et al., 2006; Cruz-Garza et al., 2014). The activation of corresponding brain regions may be related to DMT involving repetitive body movement exercise coupled with auditory feedback and extensive cognitive processing. Concomitant with angiogenesis and endothelial cell proliferation induced by exercise, blood flow in the middle cerebral artery increases and maintains these effects over time (van Praag et al., 2005; van Praag, 2009). This autoregulation induced by dance has protective benefits against the progression of symptoms in ND. The effect of functional improvement in the population with PD depends on the subjective motivation of dance participation and the duration of the intervention.

Studies have reported that patients with mild to moderate AD still retain motor learning function, which can be due to the potential for neuroplasticity (Sabe et al., 1995; Rösler et al., 2002). The research of Sihvonen et al. (2017) supported dance as active music-based neurological rehabilitation inducing similar structural and functional neuroplastic changes reported in ND patients who received DMT. Existing animal studies confirmed that physical activity can induce hippocampal plasticity, which

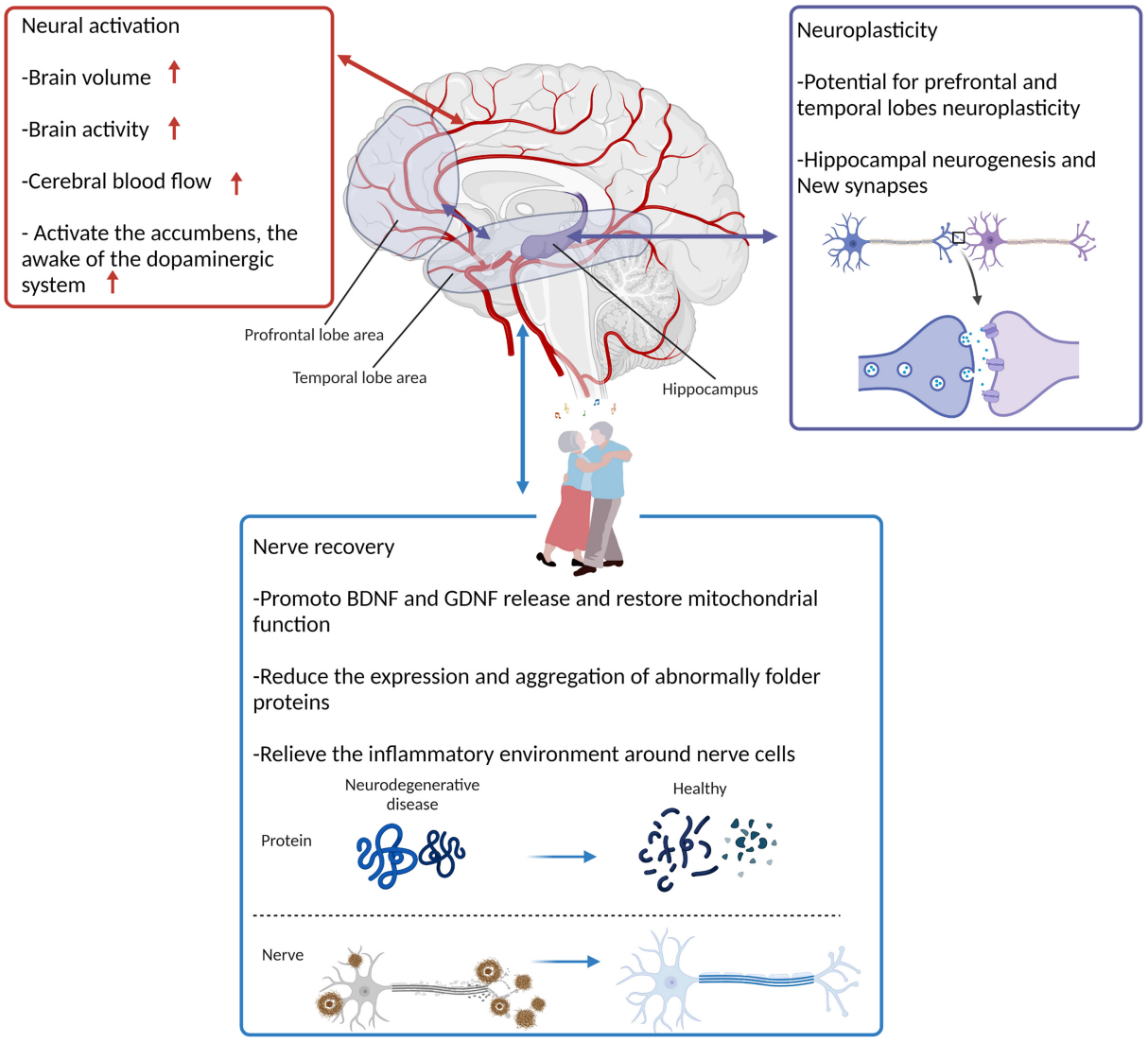

FIGURE 2
Possible neurobiological mechanisms for the rehabilitative effect of DMT. BDNF, Brain-derived neurotrophic factor; GDNF, Glial derived neurotrophic factor. Created with BioRender.com.

is associated with hippocampal neurogenesis (van Praag et al., 1999b; van Praag, 2008), form new synapses (van Praag et al., 1999a, 2005; Stranahan et al., 2006), and modulate the release and utilization of neurotransmitters (Vaynman et al., 2004; Vaynman and Gomez-Pinilla, 2005) to rebuild and remodel damaged neural networks. Compared with the control group, 8-week treadmill training in PD rats increased the potential of dopamine D2 receptor binding, suggesting that the efficacy of exercise in improving PD symptoms is associated with neuroplasticity in the dopaminergic pathway (Fisher et al., 2013). When participants performed a dance exercise, a "mirror neuron system" was activated to learn and correct dance movements by observed and imagined performing either familiar or novel movement sequences. Premotor and parietal cortices are considered the key cortices for the "mirror neuron system." Prefrontal lobe and temporal lobe activity increases, and its regional neuroplasticity is enhanced by receiving a steady stream of dance movement image stimuli, action commands, and musical awakening. Some RCTs reported improvement in the overall cognitive function level after dance training in PD patients. Others studies have provided further evidence for auditory- and motor-related neuroplasticity following community dance therapy and rhythm-movement therapy in PD patients.

Animal research results have shown that physical activity has neurorestorative and neuroprotective effects, and supports synapse formation and angiogenesis by modulating brain-derived neurotrophic factor and glial-derived neurotrophic factor, inhibiting oxidative stress, and improving mitochondrial function (Tajiri et al., 2010; Correale et al., 2017). Treadmill exercise can increase the sirtuin-1 expression, which results in increased mitochondrial biogenesis and decreased oxidative stress (Koo and Cho, 2017). The result of Wu et al. (2018) reported that exercise can inhibit apoptosis-like cell death of neurons in hippocampal area, significant loss of presynaptic/postsynaptic markers, release of proinflammatory cytokines, and oxidative damage in AD rats caused by streptozotocin. Exercise can reduce hippocampal volume atrophy (Tarumi et al., 2019), the expression of α-synuclein in PD rats, and deposition of β-amyloid in the hippocampus of AD rats (Zhang X. et al., 2019; Pena et al., 2020; Wu et al., 2020). Co-stimulation of music and physical activity can provide participants an effect similar to the enriched environment used in animal studies, contributing to the recovery of patients with NDs at the behavioral and neurobiological levels (Baroncelli et al., 2010; Sihvonen et al., 2017).

Activation of reward, arousal, and emotion networks

Music and exercise can activate the dopaminergic mesolimbic system, which is involved in the regulation of movement, reward mechanisms, emotion, and cognition. The nucleus accumbens, a key part of the brain's reward system, can be activated by strong emotional responses to music, regulating the dopaminergic mesolimbic system and promoting increased dopamine secretion (Salimpoor et al., 2011). Music-induced increases in parasympathetic activity, lower serum cortisol levels, and inhibition of cardiovascular stress responses have been suggested as the possible underlying mechanisms to explain the cognitive-emotional gains induced by music stimulations in patients with NDs (Salimpoor et al., 2011; Karkou and Meekums, 2017). Physical activity can modulate an intensive increase in dopamine concentration (Kami et al., 2018; Di Liegro et al., 2019). The therapeutic efficacy of physical activity in ND patients includes increasing endorphin levels (Remy et al., 2005; Politis et al., 2010) and attenuation of the hypothalamic pituitary-adrenal axis response to stress (Mayberg et al., 1990; Feldmann et al., 2008). Increased levels of extracellular dopamine secretion may partially explain the cognitive-emotional gains caused by elevated levels of physical activity in patients with ND. A regular, moderate level of physical activity corresponds to a good mental state (Wen et al., 2016). Several clinical studies have reported that physical activity leads to positive emotions associated with mastery and self-efficacy (Leentjens, 2004; Sheng et al., 2014; Lou et al., 2015).

Dancers engage in social interaction and emotional expression through choreographed or improvised body language in specific linguistic and cultural contexts, which may be what differentiates DMT from most physical activities. For example, people perform circle dances around a bonfire to express the joy of a good harvest. And DMT challenges the ability of cognition and balance beyond traditional exercise mode. During the dance programme, participants were required to engage in working memory, attentional control, and multitasking to integrate newly learned and previously learned dance moves, stay in rhythm with the music, and bypass others on the dance floor (Foster et al., 2013). Age-related changes associated with diminished emotional perception may contribute to states of depression or apathy (Alexopoulos, 2005). The results of (Hashimoto et al., 2015) reported 12-week incorporated strategies-based dance can significantly improve the overall disease status, balance, gait, cognitive function, and negative emotions of apathy and depression in PD patients compared with PD exercise (Hashimoto et al., 2015). In addition, participants were able to engage in a certain degree of emotional interaction and catharsis regardless of whether they were actively or passively watching the dance performance. When people watch or perform sad art performances, the emotional resonance it evokes promotes the release of prolactin, which leads to a sense of belonging, comfort, and joy (Christensen et al., 2017).

Social cognition is defined as the ability to interpret and predict the behavior of others based on their beliefs and intentions, and to interact in complex social environments and relationships (Baron-Cohen, 2000). Memory, decision-making, attention, motivation, and mood all increase significantly when socially relevant stimuli trigger behavior (Adolphs, 2009). The findings suggest that even during normal cognitive aging, social cognition declines with age, in part independent of more general cognitive functions. The decline in social cognition in the elderly may be related to the decline observed in neurodegeneration of age-related diseases (Kemp et al., 2012). The study of Foster et al. (2013) reported that PD participants in the dance group had significantly increased social engagement, leisure and social activities compared to the usual living control group, returning most of their activities since the onset of the disease. Compared to traditional exercise, dance classes have additional features that are beneficial to participation. For example, in a pair or multi-person dance, the leader needs to initiate movements and movement plans, while the follower needs to understand and appropriately respond to the leader's instructions. These challenges may further enhance the ability to perform on a daily basis and lead to an increase or maintenance of engagement. The social interaction, social support, and emotional exchange generated by dance class may be beneficial for older people with social cognitive decline. On a personal level, dancing interactions with others may help participants challenge themselves more freely in the complexity and difficulty

of dance moves, thereby increasing self-efficacy, which translates into motivation for social activity and social engagement. This may also be one of the reasons why the participants resumed most of their pre-onset activities (Foster et al., 2013).

A distinctive feature of dance therapy is its creativity. Participants immerse themselves in the stimulation of music and rhythm, and engage their emotions in the physical activity that ensues rather than simply learning dance steps. Due to neurocognitive demands, the more complex the motor task, the greater its impact on neuroplasticity. Dance therapists encourage participants to choose or create their own preferred dance moves. This creative and improvised movement engages participants in the non-verbal expression of hard-to-express thoughts and emotions, not only providing opportunities to interact with others, but also helping to promote healthy communication and restore mental balance, which may lead to better emotional and social life (Quinones and Kaddurah-Daouk, 2009). Research has shown that individuals receiving creative activity interventions show significant increases in overall health, quality of life, and physical wellbeing, which in turn have an impact on overall wellbeing (Archer et al., 2015).

Activation of alternative or spared neural networks

Therapists often utilize a musical metronome to assist PD patients in the gait starting and walking stages. Sihvonen et al. (2017) speculated that rhythmic entrainment can activate alternative networks in patients with motor system dysfunction. Rhythmic entrainment timed the movement to regular musical beats, enhancing the connectivity between the auditory and motor systems. Bypassing motor system dysfunction and the rhythmic auditory system are used to cue movement execution.

In daily life, a familiar musical melody can recall the memories and emotionally respond. The caudal anterior cingulate gyrus and the ventral pre-supplementary motor area are the key regions for the encoding of musical memory. A neuroimaging study of AD patients found that regions associated with musical memory showed essentially minimal cortical atrophy and less disturbance of glucose metabolism compared with other regions of the brain. This finding provides a potential explanation for the improvement of apathy, depression, and other affective disorders in patients with NDs by musical activity.

Limitations and future directions

The viewpoints of this review remain limited because of the following reasons. The sample sizes of included RCTs are small, thereby restricting the generalizability of results to the population in the early stages of ND. Most studies included patients with mild to moderate disease, and the findings cannot be generalized to end-stage disease patients. The efficacy of DMT may vary because of different disease stages. Many studies did not control the effects of levodopa or other PD drugs. Furthermore, the different types of DMT and how these make differentially affect mood, physical and cognitive function in various NDs require further exploration. Only studies written in English were included, which may lead to publication bias. Few clinical studies were reported on DMT in the treatment of AD (3 systematic analyses and 1 RCT). These studies had small sample sizes and insufficient follow-up with hidden allocation and blinding. Current studies do not provide sufficient evidence to explain the whole therapeutic mechanisms of DMT. Additional high-quality, large-scale intervention studies and multimodal studies combining behavioral outcome measures with neuroimaging and neuroendocrine markers are needed to elucidate the effects and mechanisms of dance exercise therapy on NDs.

Conclusions

The proportion of the elderly population in the world continues to increase, and the loss of independence of the elderly due to NDs leads to an increased social burden. Thirty-three RCTs and 24 systematic analyses reported the effects of DMT in NDs. DMT had remarkable effects on the condition, balance, and gait in PD patients worldwide. DMT significantly improved the cognitive function, memory, and executive function for patients with MCI. However, data are insufficient to fully demonstrate that DMT has a positive effect in patients with AD. Future research on the effects of DMT on AD requires scientific design, large sample size, long-term comprehensive intervention, and clear reporting standards.

Data availability statement

The original contributions presented in the study are included in the article/Supplementary material, further inquiries can be directed to the corresponding author/s.

Author contributions

X-QW had substantial contributions to the conception of the study. X-QW and J-JZ designed this systematic review. C-CW and H-YX conduct the research. C-CW wrote the original draft of the manuscript. X-QW, J-JZ, H-YX, and C-CW participated in the revision of the draft. All authors read and approved the final submitted version.

Funding

This study was supported by the National Natural Science Foundation of China (81871844), Shuguang Program supported by Shanghai Education Development Foundation and Shanghai Municipal Education Commission (18SG48), the Science and Technology Commission of Shanghai Municipality (grant numbers 19080503100 and 21S31902400), the Fok Ying-Tong Education Foundation of China (grant number 161092), the Talent Development Fund of Shanghai Municipal (grant number 2021081), the Shanghai Clinical Research Center for Rehabilitation Medicine (grant number 21MC1930200), and the Shanghai Key Lab of Human Performance (Shanghai University of Sport) (grant number 11DZ2261100), as well as by the Shanghai Frontiers Science Research Base of Exercise and Metabolic Health.

Acknowledgments

We thank the authors of the primary studies for providing their data and other critical information. Additionally, the authors would like to thank the researchers and participants for their valuable contributions to this article.

Conflict of interest

The authors declare that the research was conducted in the absence of any commercial or financial relationships that could be construed as a potential conflict of interest.

Publisher's note

All claims expressed in this article are solely those of the authors and do not necessarily represent those of their affiliated organizations, or those of the publisher, the editors and the reviewers. Any product that may be evaluated in this article, or claim that may be made by its manufacturer, is not guaranteed or endorsed by the publisher.

Supplementary material

The Supplementary Material for this article can be found online at: https://www.frontiersin.org/articles/10.3389/fnagi.2022.975711/full#supplementary-material

References

2020 Alzheimer's disease facts and figures (2020). *Alzheimers Dement*. Available online at: https://doi.org/10.1002/alz.12068 (accessed March, 2022).

Adolphs, R. (2009). The social brain: neural basis of social knowledge. *Annu. Rev. Psychol.* 60, 693–716. doi: 10.1146/annurev.psych.60.110707.163514

Agosta, F., Gatti, R., Sarasso, E., Volonté, M. A., Canu, E., Meani, A., et al. (2017). Brain plasticity in Parkinson's disease with freezing of gait induced by action observation training. *J. Neurol.* 264, 88–101. doi: 10.1007/s00415-016-8309-7

Aguiar, L. P. C., da Rocha, P. A., and Morris, M. (2016). Therapeutic dancing for Parkinson's disease. *Int. J. Gerontol.* 10, 64–70. doi: 10.1016/j.ijge.2016.02.002

Aguiñaga, S., and Marquez, D. X. (2017). Feasibility of a latin dance program for older latinos with mild cognitive impairment. *Am. J. Alzheimers. Dis. Other Demen.* 32, 479–488. doi: 10.1177/1533317517719500

Aktas, G., and Ogce, F. (2005). Dance as a therapy for cancer prevention. *Asian Pac. J. Cancer Prev.* 6, 408–411.

Alexopoulos, G. S. (2005). Depression in the elderly. *Lancet* 365, 1961–1970. doi: 10.1016/S0140-6736(05)66665-2

Ammar, A., Boukhris, O., Halfpaap, N., Labott, B. K., Langhans, C., Herold, F., et al. (2021). Four weeks of detraining induced by COVID-19 reverse cardiac improvements from eight weeks of fitness-dance training in older adults with mild cognitive impairment. *Int. J. Environ. Res. Public Health* 18, 5930. doi: 10.3390/ijerph18115930

Archer, S., Buxton, S., and Sheffield, D. (2015). The effect of creative psychological interventions on psychological outcomes for adult cancer patients: a systematic review of randomised controlled trials. *Psychooncology* 24, 1–10. doi: 10.1002/pon.3607

Barnish, M. S., and Barran, S. M. (2020). A systematic review of active group-based dance, singing, music therapy and theatrical interventions for quality of life, functional communication, speech, motor function and cognitive status in people with Parkinson's disease. *BMC Neurol.* 20, 371. doi: 10.1186/s12883-020-01938-3

Baroncelli, L., Braschi, C., Spolidoro, M., Begenisic, T., Sale, A., and Maffei, L. (2010). Nurturing brain plasticity: impact of environmental enrichment. *Cell Death Differ.* 17, 1092–1103. doi: 10.1038/cdd.2009.193

Baron-Cohen, S. (2000). Is asperger syndrome/high-functioning autism necessarily a disability? *Dev. Psychopathol.* 12, 489–500. doi: 10.1017/S0954579400003126

Bennett, C. G., Fox, H., McLain, M., and Medina-Pacheco, C. (2021). Impacts of dance on agitation and anxiety among persons living with dementia: an integrative review. *Geriatr Nurs.* 42, 181–187. doi: 10.1016/j.gerinurse.2020.07.016

Berti, A., Pini, M., and Ferrarello, F. (2020). Argentine tango in the care of Parkinson's disease: a systematic review and analysis of the intervention. *Complement Ther. Med.* 52, 102474. doi: 10.1016/j.ctim.2020.102474

Blackman, J., Swirski, M., Clynes, J., Harding, S., Leng, Y., and Coulthard, E. (2021). Pharmacological and non-pharmacological interventions to enhance sleep in mild cognitive impairment and mild Alzheimer's disease: a systematic review. *J. Sleep Res.* 30, e13229. doi: 10.1111/jsr.13229

Bradt, J., Shim, M., and Goodill, S. W. (2015). Dance/movement therapy for improving psychological and physical outcomes in cancer patients. *Cochrane Database Syst. Rev.* 1, Cd007103. doi: 10.1002/14651858.CD007103.pub3

Brown, S., Martinez, M. J., and Parsons, L. M. (2006). The neural basis of human dance. *Cereb. Cortex* 16, 1157–1167. doi: 10.1093/cercor/bhj057

Carapellotti, A. M., Stevenson, R., and Doumas, M. (2020). The efficacy of dance for improving motor impairments, non-motor symptoms, and quality of life in Parkinson's disease: a systematic review and meta-analysis. *PLoS ONE* 15, e0236820. doi: 10.1371/journal.pone.0236820

Chan, J. S. Y., Wu, J., Deng, K., and Yan, J. H. (2020). The effectiveness of dance interventions on cognition in patients with mild cognitive impairment: a meta-analysis of randomized controlled trials. *Neurosci. Biobehav. Rev.* 118, 80–88. doi: 10.1016/j.neubiorev.2020.07.017

Chang, J., Chen, Y., Liu, C., Yong, L., Yang, M., et al. (2021). Effect of square dance exercise on older women with mild mental disorders. *Front. Psychiatry* 12, 699778. doi: 10.3389/fpsyt.2021.699778

Chou, Y. H., Ton That, V., and Sundman, M. (2020). A systematic review and meta-analysis of rTMS effects on cognitive enhancement in mild cognitive impairment and Alzheimer's disease. *Neurobiol. Aging* 86, 1–10. doi: 10.1016/j.neurobiolaging.2019.08.020

Christensen, J. F., Cela-Conde, C. J., and Gomila, A. (2017). Not all about sex: neural and biobehavioral functions of human dance. *Ann. N Y Acad. Sci.* 1400, 8–32. doi: 10.1111/nyas.13420

Collins, N. J., Barton, C. J., van Middelkoop, M., Callaghan, M. J., Rathleff, M. S., Vicenzino, B. T., et al. (2018). Consensus statement on exercise therapy and physical interventions (orthoses, taping and manual therapy) to treat patellofemoral pain: recommendations from the 5th International Patellofemoral Pain Research Retreat, Gold Coast, Australia, 2017. *Br. J. Sports Med.* 52, 1170–1178. doi: 10.1136/bjsports-2018-099397

Conceição, L. S., Neto, M. G., do Amaral, M. A., Martins-Filho, P. R., and Oliveira Carvalho, V. (2016). Effect of dance therapy on blood pressure and exercise capacity of individuals with hypertension: a systematic review and meta-analysis. *Int. J. Cardiol.* 220, 553–557. doi: 10.1016/j.ijcard.2016.06.182

Correale, J., Gaitán, M. I., Ysrraelit, M. C., and Fiol, M. P. (2017). Progressive multiple sclerosis: from pathogenic mechanisms to treatment. Brain. 140, 527–546. doi: 10.1093/brain/aww258

Cross, K., Flores, R., Butterfield, J., Blackman, M., and Lee, S. (2012). The effect of passive listening versus active observation of music and dance performances on memory recognition and mild to moderate depression in cognitively impaired older adults. *Psychol. Rep.* 111, 413–423. doi: 10.2466/10.02.13.PR0.111.5.413-423

Crossley, K. M., van Middelkoop, M., Callaghan, M. J., Collins, N. J., Rathleff, M. S., and Barton, C. J. (2016). Patellofemoral pain consensus statement from the 4th International Patellofemoral Pain Research Retreat, Manchester. Part 2: recommended physical interventions (exercise, taping, bracing, foot orthoses and combined interventions). *Br. J. Sports Med.* 50, 844–852. doi: 10.1136/bjsports-2016-096268

Cruz-Garza, J. G., Hernandez, Z. R., Nepaul, S., Bradley, K. K., and Contreras-Vidal, J. L. (2014). Neural decoding of expressive human movement from scalp electroencephalography (EEG). *Front Hum. Neurosci.* 8, 188. doi: 10.3389/fnhum.2014.00188

de Almeida, H. S., Porto, F., Porretti, M., Lopes, G., Fiorot, D., et al. (2020). Effect of dance on postural control in people with parkinson's disease: a meta-analysis review. *J. Aging Phys. Act.* 29, 130–141. doi: 10.1123/japa.2019-0255

Di Liegro, C. M., Schiera, G., Proia, P., and Di Liegro, I. (2019). Physical activity and brain health. *Genes* 10, 720. doi: 10.3390/genes10090720

Dickson, D. W., Braak, H., Duda, J. E., Duyckaerts, C., Gasser, T., Halliday, G. M., et al. (2009). Neuropathological assessment of Parkinson's disease: refining the diagnostic criteria. *Lancet Neurol.* 8, 1150–1157. doi: 10.1016/S1474-4422(09)70238-8

Doi, T., Verghese, J., Makizako, H., Tsutsumimoto, K., Hotta, R., Nakakubo, S., et al. (2017). Effects of cognitive leisure activity on cognition in mild cognitive impairment: results of a randomized controlled trial. *J. Am. Med. Dir. Assoc.* 18, 686–691. doi: 10.1016/j.jamda.2017.02.013

Dos Santos Delabary, M., Komeroski, I. G., Monteiro, E. P., Costa, R. R., and Haas, A. N. (2018). Effects of dance practice on functional mobility, motor symptoms and quality of life in people with Parkinson's disease: a systematic review with meta-analysis. *Aging Clin. Exp. Res.* 30, 727–735. doi: 10.1007/s40520-017-0836-2

Duncan, R. P., and Earhart, G. M. (2012). Randomized controlled trial of community-based dancing to modify disease progression in Parkinson disease. *Neurorehabil. Neural. Repair* 26, 132–143. doi: 10.1177/1545968311421614

Duncan, R. P., and Earhart, G. M. (2014). Are the effects of community-based dance on Parkinson disease severity, balance, and functional mobility reduced with time? A 2-year prospective pilot study. *J. Altern. Complement Med.* 20, 757–763. doi: 10.1089/acm.2012.0774

Emmanouilidis, S., Hackney, M. E., Slade, S. C., Heng, H., Jazayeri, D., and Morris, M. E. (2021). Dance is an accessible physical activity for people with parkinson's disease. *Parkinsons Dis.* 2021, 7516504. doi: 10.1155/2021/7516504

Eshkoor, S. A., Hamid, T. A., Mun, C. Y., and Ng, C. K. (2015). Mild cognitive impairment and its management in older people. *Clin. Interv. Aging* 10, 687–693. doi: 10.2147/CIA.S73922

Estimates, T. W. G. H. (2022). WHO's Global Health Estimates provide the latest available data on causes of death and disability globally, by WHO region and country, by age, sex and by income group. Available online at: https://www.who.int/data/gho/data/themes/mortality-and-global-health-estimates (accessed March 2021).

Feldmann, A., Illes, Z., Kosztolanyi, P., Illes, E., Mike, A., Kover, F., et al. (2008). Morphometric changes of gray matter in Parkinson's disease with depression: a voxel-based morphometry study. *Mov. Disord.* 23, 42–46. doi: 10.1002/mds.21765

Fernández-Argüelles, E. L., Rodríguez-Mansilla, J., Antunez, L. E., Garrido-Ardila, E. M., and Muñoz, R. P. (2015). Effects of dancing on the risk of falling related factors of healthy older adults: a systematic review. *Arch Gerontol. Geriatr.* 60, 1–8. doi: 10.1016/j.archger.2014.10.003

Fisher, B. E., Li, Q., Nacca, A., Salem, G. J., Song, J., Yip, J., et al. (2013). Treadmill exercise elevates striatal dopamine D2 receptor binding potential in patients with early Parkinson's disease. *Neuroreport* 24, 509–514. doi: 10.1097/WNR.0b013e328361dc13

Fong Yan, A., Cobley, S., Chan, C., Pappas, E., Nicholson, L. L., Ward, R. E., et al. (2018). The effectiveness of dance interventions on physical health outcomes compared to other forms of physical activity: a systematic review and meta-analysis. *Sports Med.* 48, 933–951. doi: 10.1007/s40279-017-0853-5

Foster, E. R., Golden, L., Duncan, R. P., and Earhart, G. M. (2013). Community-based Argentine tango dance program is associated with increased activity participation among individuals with Parkinson's disease. *Arch. Phys. Med. Rehabil.* 94, 240–249. doi: 10.1016/j.apmr.2012.07.028

Frisaldi, E., Bottino, P., Fabbri, M., Trucco, M., De Ceglia, A., Esposito, N., et al. (2021). Effectiveness of a dance-physiotherapy combined intervention in Parkinson's disease: a randomized controlled pilot trial. *Neurol. Sci.* 42, 5045–5053. doi: 10.1007/s10072-021-05171-9

Gronek, P., Boraczyński, M., Haas, A. N., Adamczyk, J., Pawlaczyk, M., Czarny, W., et al. (2021). Body adaptation to dance: a gerontological perspective. *Aging Dis.* 12, 902–913. doi: 10.14336/AD.2020.1107

Hackney, M. E., and Earhart, G. M. (2009). Effects of dance on movement control in Parkinson's disease: a comparison of Argentine tango and American ballroom. *J. Rehabil. Med.* 41, 475–481. doi: 10.2340/16501977-0362

Hackney, M. E., and Earhart, G. M. (2010). Effects of dance on gait and balance in Parkinson's disease: a comparison of partnered and nonpartnered dance movement. *Neurorehabil Neural Repair* 24, 384–392. doi: 10.1177/1545968309353329

Hackney, M. E., Kantorovich, S., Levin, R., and Earhart, G. M. (2007). Effects of tango on functional mobility in Parkinson's disease: a preliminary study. *J. Neurol. Phys. Ther.* 31, 173–179. doi: 10.1097/NPT.0b013e31815ce78b

Hamill, M., Smith, L., and Röhricht, F. (2012). Dancing down memory lane: circle dancing as a psychotherapeutic intervention in dementia-A pilot study. *Dementia* 11, 709–724. doi: 10.1177/1471301211420509

Hasan, S. M., Alshafie, S., Hasabo, E. A., Saleh, M., Elnaiem, W., Qasem, A., et al. (2022). Efficacy of dance for Parkinson's disease: a pooled analysis of 372 patients. *J. Neurol.* 269, 1195–1208. doi: 10.1007/s00415-021-10589-4

Hashimoto, H., Takabatake, S., Miyaguchi, H., Nakanishi, H., and Naitou, Y. (2015). Effects of dance on motor functions, cognitive functions, and mental symptoms of Parkinson's disease: a quasi-randomized pilot trial. *Complement Ther. Med.* 23, 210–219. doi: 10.1016/j.ctim.2015.01.010

Herholz, S. C., Herholz, R. S., and Herholz, K. (2013). Non-pharmacological interventions and neuroplasticity in early stage Alzheimer's disease. *Expert Rev. Neurother.* 13, 1235–1245. doi: 10.1586/14737175.2013.845086

Hernandez, S. S., Coelho, F. G., Gobbi, S., and Stella, F. (2010). Effects of physical activity on cognitive functions, balance and risk of falls in elderly patients with Alzheimer's dementia. *Rev. Bras. Fisioter.* 14, 68–74. doi: 10.1590/S1413-35552010000100011

Hidalgo-Agudo, R. D., Lucena-Anton, D., Luque-Moreno, C., Heredia-Rizo, A. M., and Moral-Munoz, J. A. (2020). Additional physical interventions to conventional physical therapy in Parkinson's disease: a systematic review and meta-analysis of randomized clinical trials. *J. Clin. Med.* 9, 1038. doi: 10.3390/jcm9041038

Hodson, R. (2018). Alzheimer's disease. *Nature* 559, S1. doi: 10.1038/d41586-018-05717-6

Hou, Y., Dan, X., Babbar, M., Wei, Y., Hasselbalch, S. G., Croteau, D. L., and Bohr, V. A. (2019). Ageing as a risk factor for neurodegenerative disease. *Nat. Rev. Neurol.* 15, 565–581. doi: 10.1038/s41582-019-0244-7

Hulbert, S., Ashburn, A., Roberts, L., and Verheyden, G. (2017). Dance for Parkinson's-The effects on whole body co-ordination during turning around. *Complement Ther. Med.* 32, 91–97. doi: 10.1016/j.ctim.2017.03.012

Ismail, S. R., Lee, S. W. H., Merom, D., Megat Kamaruddin, P. S. N., Chong, M. S., Ong, T., et al. (2021). Evidence of disease severity, cognitive and physical outcomes of dance interventions for persons with Parkinson's disease: a systematic review and meta-analysis. *BMC Geriatr.* 21, 503. doi: 10.1186/s12877-021-02446-w

Jongsiriyanyong, S., and Limpawattana, P. (2018). Mild cognitive impairment in clinical practice: a review article. *Am. J. Alzheimers Dis. Other Demen.* 33, 500–507. doi: 10.1177/1533317518791401

Kalyani, H. H. N., Sullivan, K., Moyle, G., Brauer, S., Jeffrey, E. R., Roeder, L., et al. (2019). Effects of dance on gait, cognition, and dual-tasking in Parkinson's disease: a systematic review and meta-analysis. *J. Parkinsons Dis.* 9, 335–349. doi: 10.3233/JPD-181516

Kami, K., Tajima, F., and Senba, E. (2018). Activation of mesolimbic reward system via laterodorsal tegmental nucleus and hypothalamus in exercise-induced hypoalgesia. *Sci. Rep*. 8, 11540. doi: 10.1038/s41598-018-29915-4

Karkou, V., and Meekums, B. (2017). Dance movement therapy for dementia. *Cochrane Database Syst. Rev.* 2, Cd011022. doi: 10.1002/14651858.CD011022.pub2

Kemp, J., Després, O., Sellal, F., and Dufour, A. (2012). Theory of Mind in normal ageing and neurodegenerative pathologies. *Ageing Res. Rev*. 11, 199–219. doi: 10.1016/j.arr.2011.12.001

Kirova, A. M., Bays, R. B., and Lagalwar, S. (2015). Working memory and executive function decline across normal aging, mild cognitive impairment, and Alzheimer's disease. *Biomed. Res. Int*. 2015, 748212. doi: 10.1155/2015/748212

Kontos, P., Miller, K. L., Colobong, R., Palma Lazgare, L. I., Binns, M., Low, L. F., et al. (2016). Elder-clowning in long-term dementia care: results of a pilot study. *J. Am. Geriatr. Soc*. 64, 347–353. doi: 10.1111/jgs.13941

Koo, J. H., and Cho, J. Y. (2017). Treadmill exercise attenuates α-synuclein levels by promoting mitochondrial function and autophagy possibly via SIRT1 in the chronic MPTP/P-induced mouse model of Parkinson's disease. *Neurotox Res*. 32, 473–486. doi: 10.1007/s12640-017-9770-5

Kropacova, S., Mitterova, K., Klobusiakova, P., Brabenec, L., Anderkova, L., Nemcova-Elfmarkova, N., et al. (2019). Cognitive effects of dance-movement intervention in a mixed group of seniors are not dependent on hippocampal atrophy-6/11. *J. Neural. Transm*. 126, 1455–1463. doi: 10.1007/s00702-019-02068-y

Langa, K. M., and Levine, D. A. (2014). The diagnosis and management of mild cognitive impairment: a clinical review. *JAMA* 312, 2551–2561. doi: 10.1001/jama.2014.13806

Lazarou, I., Parastatidis, T., Tsolaki, A., Gkioka, M., Karakostas, A., Douka, S., et al. (2017). International ballroom dancing against neurodegeneration: a randomized controlled trial in greek community-dwelling elders with mild cognitive impairment-6. *Am. J. Alzheimers Dis. Other Demen.* 32, 489–499. doi: 10.1177/1533317517725813

Lee, H. J., Kim, S. Y., Chae, Y., Kim, M. Y., Yin, C., Jung, W. S., et al. (2018). Turo (Qi Dance) program for Parkinson's disease patients: randomized, assessor blind, waiting-list control, partial crossover study. *Explore* 14, 216–223. doi: 10.1016/j.explore.2017.11.002

Lee, N. Y., Lee, D. K., and Song, H. S. (2015). Effect of virtual reality dance exercise on the balance, activities of daily living, and depressive disorder status of Parkinson's disease patients. *J. Phys. Ther. Sci.* 27, 145–147. doi: 10.1589/jpts.27.145

Leentjens, A. F. (2004). Depression in Parkinson's disease: conceptual issues and clinical challenges. *J. Geriatr. Psychiatry Neurol.* 17, 120–126. doi: 10.1177/0891988704267456

Liu, C., Su, M., Jiao, Y., Ji, Y., and Zhu, S. (2021). Effects of dance interventions on cognition, psycho-behavioral symptoms, motor functions, and quality of life in older adult patients with mild cognitive impairment: a meta-analysis and systematic review. *Front. Aging Neurosci*. 13, 706609. doi: 10.3389/fnagi.2021.706609

Lötzke, D., Ostermann, T., and Büssing, A. (2015). Argentine tango in Parkinson disease–a systematic review and meta-analysis. *BMC Neurol*. 15, 226. doi: 10.1186/s12883-015-0484-0

Lou, Y., Huang, P., Li, D., Cen, Z., Wang, B., Gao, J., et al. (2015). Altered brain network centrality in depressed Parkinson's disease patients. *Mov. Disord*. 30, 1777–1784. doi: 10.1002/mds.26321

Low, L. F., Carroll, S., Merom, D., Baker, J. R., Kochan, N., Moran, F., et al. (2016). We think you can dance! *A pilot randomised controlled trial of dance for nursing home residents with moderate to severe dementia. Complement Ther. Med*. 29, 42–44. doi: 10.1016/j.ctim.2016.09.005

Mabire, J. B., Aquino, J. P., and Charras, K. (2019). Dance interventions for people with dementia: systematic review and practice recommendations. *Int. Psychogeriatr*. 31, 977–987. doi: 10.1017/S1041610218001552

Mandelbaum, R., and Lo, A. C. (2014). Examining dance as an intervention in Parkinson's disease: a systematic review. *Am. J. Dance Ther*. 36, 160–175. doi: 10.1007/s10465-014-9181-6

Mayberg, H. S., Starkstein, S. E., Sadzot, B., Preziosi, T., Andrezejewski, P. L., Dannals, R. F., et al. (1990). Selective hypometabolism in the inferior frontal lobe in depressed patients with Parkinson's disease. *Ann. Neurol*. 28, 57–64. doi: 10.1002/ana.410280111

Michels, K., Dubaz, O., Hornthal, E., and Bega, D. (2018). "Dance Therapy" as a psychotherapeutic movement intervention in Parkinson's disease. *Complement Ther. Med*. 40, 248–252. doi: 10.1016/j.ctim.2018.07.005

Moratelli, J., Alexandre, K. H., Boing, L., Swarowsky, A., Corrêa, C. L., and Guimarães, A. C. A. (2021). Binary dance rhythm or Quaternary dance rhythm which has the greatest effect on non-motor symptoms of individuals with Parkinson's disease? *Complement Ther. Clin. Pract.* 43, 101348. doi: 10.1016/j.ctcp.2021.101348

Nudo, R. J. (2013). Recovery after brain injury: mechanisms and principles. *Front Hum. Neurosci*. 7, 887. doi: 10.3389/fnhum.2013.00887

Pena, G. S., Paez, H. G., Johnson, T. K., Halle, J. L., Carzoli, J. P., Visavadiya, N. P., et al. (2020). Hippocampal Growth Factor and Myokine Cathepsin B Expression following Aerobic and Resistance Training in 3xTg-AD Mice. *Int. J. Chronic Dis.* 2020, 5919501. doi: 10.1155/2020/5919501

Petersen, R. C., Caracciolo, B., Brayne, C., Gauthier, S., Jelic, V., and Fratiglioni, L. (2014). Mild cognitive impairment: a concept in evolution. *J. Int. Med*. 275, 214–228. doi: 10.1111/joim.12190

Petersen, R. C., Lopez, O., Armstrong, M. J., Getchius, T. S. D., Ganguli, M., Gloss, D., et al. (2018). Practice guideline update summary: mild cognitive impairment: report of the guideline development, dissemination, and implementation subcommittee of the American academy of neurology. *Neurology* 90, 126–135. doi: 10.1212/WNL.0000000000004826

Poier, D., Rodrigues Recchia, D., Ostermann, T., and Büssing, A. (2019). A randomized controlled trial to investigate the impact of tango Argentino versus Tai Chi on quality of life in patients with Parkinson disease: a short report. *Complement Med. Res*. 26, 398–403. doi: 10.1159/000500070

Politis, M., Wu, K., Loane, C., Turkheimer, F. E., Molloy, S., Brooks, D. J., et al. (2010). Depressive symptoms in PD correlate with higher 5-HTT binding in raphe and limbic structures. *Neurology* 75, 1920–1927. doi: 10.1212/WNL.0b013e3181feb2ab

Polymeropoulos, M., Lavedan, C., Leroy, E., Ide, S. E., Dehejia, A., and Dutra, A. (1997). Mutation in the alpha-synuclein gene identified in families with Parkinson's disease. *Science* 276, 2045–2047. doi: 10.1126/science.276.5321.2045

Qi, M., Zhu, Y., Zhang, L., Wu, T., and Wang, J. (2019). The effect of aerobic dance intervention on brain spontaneous activity in older adults with mild cognitive impairment: a resting-state functional MRI study. *Exp. Ther. Med*. 17, 715–722. doi: 10.3892/etm.2018.7006

Quinones, M. P., and Kaddurah-Daouk, R. (2009). Metabolomics tools for identifying biomarkers for neuropsychiatric diseases. *Neurobiol. Dis*. 35, 165–176. doi: 10.1016/j.nbd.2009.02.019

Reetz, K., Tadic, V., Kasten, M., Brüggemann, N., Schmidt, A., Hagenah, J., et al. (2010). Structural imaging in the presymptomatic stage of genetically determined parkinsonism. *Neurobiol. Dis*. 39, 402–408. doi: 10.1016/j.nbd.2010.05.006

Rektorova, I., Klobusiakova, P., Balazova, Z., Kropacova, S., Sejnoha Minsterova, A., Grmela, R., et al. (2020). Brain structure changes in nondemented seniors after six-month dance-exercise intervention-4. *Acta Neurol. Scand*. 141, 90–97. doi: 10.1111/ane.13181

Remy, P., Doder, M., Lees, A., Turjanski, N., and Brooks, D. (2005). Depression in Parkinson's disease: loss of dopamine and noradrenaline innervation in the limbic system. *Brain* 128, 1314–1322. doi: 10.1093/brain/awh445

Rios Romenets, S., Anang, J., Fereshtehnejad, S. M., Pelletier, A., and Postuma, R. (2015). Tango for treatment of motor and non-motor manifestations in Parkinson's disease: a randomized control study. *Complement Ther. Med*. 23, 175–184. doi: 10.1016/j.ctim.2015.01.015

Rösler, A., Seifritz, E., Kräuchi, K., Spoerl, D., Brokuslaus, I., Proserpi, S. M., et al. (2002). Skill learning in patients with moderate Alzheimer's disease: a prospective pilot-study of waltz-lessons. *Int. J. Geriatr. Psychiatry* 17, 1155–1156. doi: 10.1002/gps.705

Ruiz-Muelle, A., and López-Rodríguez, M. M. (2019). Dance for people with Alzheimer's disease: a systematic review. *Curr. Alzheimer Res*. 16, 919–933. doi: 10.2174/1567205016666190725151614

Sabe, L., Jason, L., Juejati, M., Leiguarda, R., and Starkstein, S. E. (1995). Dissociation between declarative and procedural learning in dementia and depression. *J. Clin. Exp. Neuropsychol*. 17, 841–848. doi: 10.1080/01688639508402433

Salimpoor, V. N., Benovoy, M., Larcher, K., Dagher, A., and Zatorre, R. J. (2011). Anatomically distinct dopamine release during anticipation and experience of peak emotion to music. *Nat Neurosci*. 14, 257–262. doi: 10.1038/nn.2726

Shanahan, J., Morris, M. E., Bhriain, O. N., Saunders, J., and Clifford, A. M. (2015). Dance for people with Parkinson disease: what is the evidence telling us? *Arch. Phys. Med. Rehabil*. 96, 141–153. doi: 10.1016/j.apmr.2014.08.017

Shanahan, J., Morris, M. E., Bhriain, O. N., Volpe, D., Lynch, T., and Clifford, A. M. (2017). Dancing for Parkinson disease: a randomized trial of irish set dancing compared with usual care. *Arch. Phys. Med. Rehabil*. 98, 1744–1751. doi: 10.1016/j.apmr.2017.02.017

Sharp, K., and Hewitt, J. (2014). Dance as an intervention for people with Parkinson's disease: a systematic review and meta-analysis. *Neurosci. Biobehav. Rev*. 47, 445–456. doi: 10.1016/j.neubiorev.2014.09.009

Shea, B. J., Grimshaw, J. M., Wells, G. A., Boers, M., Andersson, N., Hamel, C., et al. (2007). Development of AMSTAR: a measurement tool to assess the methodological quality of systematic reviews. *BMC Med. Res. Methodol.* 7, 10. doi: 10.1186/1471-2288-7-10

Sheng, K., Fang, W., Su, M., Li, R., Zou, D., Han, Y., Wang, X., and Cheng, O. (2014). Altered spontaneous brain activity in patients with Parkinson's disease accompanied by depressive symptoms, as revealed by regional homogeneity and functional connectivity in the prefrontal-limbic system. *PLoS ONE* 9, e84705. doi: 10.1371/journal.pone.0084705

Sihvonen, A. J., Särkäm,ö, T., Leo, V., Tervaniemi, M., Altenmüller, E., and Soinila, S. (2017). Music-based interventions in neurological rehabilitation. *Lancet Neurol.* 16, 648–660. doi: 10.1016/S1474-4422(17)30168-0

Solla, P., Cugusi, L., Bertoli, M., Cereatti, A., Della Croce, U., Pani, D., et al. (2019). Sardinian folk dance for individuals with parkinson's disease: a randomized controlled pilot trial. *J. Altern. Complement Med.* 25, 305–316. doi: 10.1089/acm.2018.0413

Stranahan, A. M., Khalil, D., and Gould, E. (2006). Social isolation delays the positive effects of running on adult neurogenesis. *Nat. Neurosci.* 9, 526–533. doi: 10.1038/nn1668

Tajiri, N., Yasuhara, T., Shingo, T., Kondo, A., Yuan, W., Kadota, T., et al. (2010). Exercise exerts neuroprotective effects on Parkinson's disease model of rats. *Brain Res.* 1310, 200–207. doi: 10.1016/j.brainres.2009.10.075

Tang, L., Fang, Y., and Yin, J. (2019). The effects of exercise interventions on Parkinson's disease: a Bayesian network meta-analysis. *J. Clin. Neurosci.* 70, 47–54. doi: 10.1016/j.jocn.2019.08.092

Tarumi, T., Rossetti, H., Thomas, B. P., Harris, T., Tseng, B. Y., Turner, M., et al. (2019). Exercise training in amnestic mild cognitive impairment: a one-year randomized controlled trial. *J. Alzheimers Dis.* 71, 421–433. doi: 10.3233/JAD-181175

Tomassini, V., Matthews, P. M., Thompson, A. J., Fuglø, D., Geurts, J. J., Johansen-Berg, H., et al., (2012). Neuroplasticity and functional recovery in multiple sclerosis. *Nat. Rev. Neurol.* 8, 635–46. doi: 10.1038/nrneurol.2012.179

van Praag, H. (2008). Neurogenesis and exercise: past and future directions. *Neuromolecular Med.* 10, 128–140. doi: 10.1007/s12017-008-8028-z

van Praag, H. (2009). Exercise and the brain: something to chew on. *Trends Neurosci.* 32, 283–290. doi: 10.1016/j.tins.2008.12.007

van Praag, H., Christie, B. R., Sejnowski, T. J., and Gage, F. H. (1999a). Running enhances neurogenesis, learning, and long-term potentiation in mice. *Proc. Natl. Acad. Sci. U.S.A.* 96, 13427–13431. doi: 10.1073/pnas.96.23.13427

van Praag, H., Kempermann, G., and Gage, F. H. (1999b). Running increases cell proliferation and neurogenesis in the adult mouse dentate gyrus. *Nat. Neurosci.* 2, 266–270. doi: 10.1038/6368

van Praag, H., Shubert, T., Zhao, C., and Gage, F. H. (2005). Exercise enhances learning and hippocampal neurogenesis in aged mice. *J. Neurosci.* 25, 8680–8685. doi: 10.1523/JNEUROSCI.1731-05.2005

Vaynman, S., and Gomez-Pinilla, F. (2005). License to run: exercise impacts functional plasticity in the intact and injured central nervous system by using neurotrophins. *Neurorehabil Neural Repair* 19, 283–295. doi: 10.1177/1545968305280753

Vaynman, S., Ying, Z., and Gómez-Pinilla, F. (2004). Exercise induces BDNF and synapsin I to specific hippocampal subfields. *J. Neurosci. Res.* 76, 356–362. doi: 10.1002/jnr.20077

Veronese, N., Maggi, S., Schofield, P., and Stubbs, B. (2017). Dance movement therapy and falls prevention. *Maturitas* 102, 1–5. doi: 10.1016/j.maturitas.2017.05.004

Volpe, D., Signorini, M., Marchetto, A., Lynch, T., and Morris, M. E. (2013). A comparison of Irish set dancing and exercises for people with Parkinson's disease: a phase II feasibility study. *BMC Geriatr.* 13, 54. doi: 10.1186/1471-2318-13-54

Wang, Y., Liu, M., Tan, Y., Dong, Z., Wu, J., Cui, H., Shen, D., and Chi, I. (2021). Effectiveness of dance-based interventions on depression for persons with mci and dementia: a systematic review and meta-analysis. *Front Psychol.* 12, 709208. doi: 10.3389/fpsyg.2021.709208

Wen, M. C., Chan, L. L., Tan, L. C., and Tan, E. K. (2016). Depression, anxiety, and apathy in Parkinson's disease: insights from neuroimaging studies. *Eur. J. Neurol.* 23, 1001–1019. doi: 10.1111/ene.13002

Wong, Y. C., and Krainc, D. (2017). α-synuclein toxicity in neurodegeneration: mechanism and therapeutic strategies. *Nat. Med.* 23, 1–13. doi: 10.1038/nm.4269

Wu, C., Yang, L., Li, Y., Dong, Y., Yang, B., Tucker, L. D., Zong, X., and Zhang, Q. (2020). Effects of exercise training on anxious-depressive-like behavior in Alzheimer rat. *Med. Sci. Sports Exerc* 52, 1456–1469. doi: 10.1249/MSS.0000000000002294

Wu, C., Yang, L., Tucker, D., Dong, Y., Zhu, L., Duan, R., et al. (2018). Beneficial effects of exercise pretreatment in a sporadic Alzheimer's rat model. *Med. Sci. Sports Exerc.* 50, 945–956. doi: 10.1249/MSS.0000000000001519

Wu, V. X., Chi, Y., Lee, J. K., Goh, H. S., Chen, D. Y. M., Haugan, G., et al. (2021). The effect of dance interventions on cognition, neuroplasticity, physical function, depression, and quality of life for older adults with mild cognitive impairment: a systematic review and meta-analysis. *Int. J. Nurs. Stud.* 122, 104025. doi: 10.1016/j.ijnurstu.2021.104025

Young, H. J., Mehta, T. S., Herman, C., Wang, F., and Rimmer, J. H. (2019). The effects of M2M and adapted yoga on physical and psychosocial outcomes in people with multiple sclerosis. *Arch. Phys. Med. Rehabil.* 100, 391–400. doi: 10.1016/j.apmr.2018.06.032

Zeiler, S. R., and Krakauer, J. W. (2013). The interaction between training and plasticity in the poststroke brain. *Curr. Opin. Neurol.* 26, 609–616. doi: 10.1097/WCO.0000000000000025

Zhang, Q., Hu, J., Wei, L., Jia, Y., and Jin, Y. (2019). Effects of dance therapy on cognitive and mood symptoms in people with Parkinson's disease: a systematic review and meta-analysis. *Complement Ther. Clin. Pract.* 36, 12–17. doi: 10.1016/j.ctcp.2019.04.005

Zhang, X., He, Q., Huang, T., Zhao, N., Liang, F., Xu, B., et al. (2019). Treadmill exercise decreases Aβ deposition and counteracts cognitive decline in APP/PS1 mice, possibly via hippocampal microglia modifications. *Front. Aging Neurosci.* 11, 78. doi: 10.3389/fnagi.2019.00078

Zhu, Y., Gao, Y., Guo, C., Qi, M., Xiao, M., Wu, H., et al. (2022). Effect of 3-month aerobic dance on hippocampal volume and cognition in elderly people with amnestic mild cognitive impairment: a randomized controlled trial. *Front. Aging Neurosci.* 14, 771413. doi: 10.3389/fnagi.2022.771413

Zhu, Y., Wu, H., Qi, M., Wang, S., Zhang, Q., Zhou, L., et al. (2018). Effects of a specially designed aerobic dance routine on mild cognitive impairment. *Clin. Interv. Aging* 13, 1691–1700. doi: 10.2147/CIA.S163067

Zhu, Y., Zhong, Q., Ji, J., Ma, J., Wu, H., Gao, Y., et al. (2020). Effects of aerobic dance on cognition in older adults with mild cognitive impairment: a systematic review and meta-analysis. *J. Alzheimers Dis.* 74, 679–690. doi: 10.3233/JAD-190681

frontiers | Frontiers in Aging Neuroscience

TYPE Brief Research Report
PUBLISHED 22 August 2022
DOI 10.3389/fnagi.2022.976164

OPEN ACCESS

EDITED BY
Wenxin Niu,
Tongji University, China

REVIEWED BY
Fumig Zheng,
Sun Yat-sen University, China
Ying Shen,
The First Affiliated Hospital of Nanjing Medical University, China

*CORRESPONDENCE
Xue-Qiang Wang
wangxueqiang@sus.edu.cn

†These authors have contributed equally to this work and share first authorship

SPECIALTY SECTION
This article was submitted to Neurocognitive Aging and Behavior, a section of the journal Frontiers in Aging Neuroscience

RECEIVED 23 June 2022
ACCEPTED 03 August 2022
PUBLISHED 22 August 2022

CITATION
Weng L-M, Wang R, Yang Q-H, Chang T-T, Wu C-C, Li W-L, Du S-H, Wang Y-C and Wang X-Q (2022) Effect of exercise intervention on social distance in middle-aged and elderly patients with chronic low back pain. *Front. Aging Neurosci.* 14:976164. doi: 10.3389/fnagi.2022.976164

Effect of exercise intervention on social distance in middle-aged and elderly patients with chronic low back pain

Lin-Man Weng[1†], Rui Wang[1†], Qi-Hao Yang[1], Tian-Tian Chang[1], Cheng-Cheng Wu[1], Wen-Long Li[2], Shu-Hao Du[1], Yu-Chen Wang[1] and Xue-Qiang Wang[1,3,4*]

[1]Department of Sport Rehabilitation, Shanghai University of Sport, Shanghai, China, [2]College of Chinese Wushu, Shanghai University of Sport, Shanghai, China, [3]Department of Rehabilitation Medicine, Shanghai Shangti Orthopedic Hospital, Shanghai, China, [4]Shanghai Key Lab of Human Performance, Shanghai University of Sport, Shanghai, China

Background: Increased social distance is one of the manifestations of social impairment. Chronic low back pain (CLBP) is one of factors associated with increased social distance and social withdrawal. Exercise therapy is an effective means to social impairment. However, whether exercise could reduce social distance in patients with CLBP remains unknown. This study aimed to investigate the effect of exercise on social distance in middle-aged and elderly patients with CLBP.

Methods: The longitudinal intervention recruited 29 middle-aged and elderly patients with CLBP from various communities in Yangpu District, Shanghai, China. The participants received exercise intervention for 8 weeks. The assessments were conducted before and after the intervention, including social distance, pain intensity, unpleasantness of pain, Roland-Morris Questionnaire (RMDQ), Self-Rating Anxiety Scale (SAS), and Self-Rating Depression Scale (SDS). Intention to treat analysis was performed.

Results: After the 8-week exercise intervention, the social distance of patients with CLBP was shorter than that before intervention and showed significant difference ($p < 0.05$). The scores of pain intensity, unpleasantness of pain, RMDQ, SAS, and SDS also decreased and were significantly different between pre- and post-intervention ($p < 0.05$). In addition, the social distance, pain intensity, unpleasantness of pain, RMDQ, SAS, and SDS scores of the moderate CLBP group decreased more after the intervention compared with those of the mild CLBP group.

Conclusion: The 8-week exercise intervention cannot only shorten the social distance in middle-aged and elderly patients with CLBP but also relieve pain, disability, and negative emotions.

KEYWORDS

social distance, chronic low back pain, exercise therapy, stop-distance, personal space

Introduction

Low back pain (LBP) is a common symptom experienced by people of almost all ages, and it is one of the main reasons for seeking medical health care (Hartvigsen et al., 2018). The lifetime prevalence of LBP is approximately 84%, and the prevalence of chronic LBP (CLBP) is approximately 23% (Balagué et al., 2012). CLBP can lead to physical, psychological, and social dysfunction. Along with pain and disability, patients with CLBP often experience depression and anxiety and have a negative impact on social, entertainment, and work life. Our previous study has also found that patients with CLBP exhibit social withdrawal and great social distance (Weng et al., 2021). In addition, CLBP causes a huge economic burden to families and society. In the United States, the total cost of LBP is more than $100 billion a year, two-thirds of which is the indirect cost of lost work or reduced productivity (Katz, 2006; Deyo et al., 2014).

Social distance is mediated by comfort or discomfort resulting from the distance between individuals and others. Appropriate social distance is the basis for establishing effective communication and good interpersonal relationships, while too short social distance will cause discomfort and anxiety (Gessaroli et al., 2013; Perry et al., 2016). The increase of social distance is one of the manifestations of social withdrawal, which is caused by poor mental health (Simon and Walker, 2018; Achterbergh et al., 2020).

Most guidelines recommend exercise therapy as an intervention for CLBP (Chou et al., 2017; Qaseem et al., 2017). Exercise is more effective than no-exercise intervention for CLBP (Hayden et al., 2005; van Middelkoop et al., 2010; Searle et al., 2015). Passive therapy alone (such as ultrasound, cold therapy, heat therapy, massage) offers limited improvement of the pain and physical function in patients with CLBP (Furlan et al., 2002; French et al., 2006; Ebadi et al., 2020; Owen et al., 2020). Numerous studies suggested that exercise therapy can relieve pain, improve back muscle strength, enhance physical function, and prompt mental health (Searle et al., 2015; Owen et al., 2020; Peng et al., 2022; Wu et al., 2022). Furthermore, exercise can improve social withdrawal but is mainly concentrated in diseases involving severely impaired social function (such as mental illness) (Richardson et al., 2005; Firth et al., 2015; Kimhy et al., 2016; van der Stouwe et al., 2018).

To our knowledge, a limited number of studies explored the benefits of exercise on social psychology in patients with CLBP. Whether exercise can improve social withdrawal and reduce social distance in patients with CLBP remains unknown. Thus, we conducted a longitudinal intervention study to investigate the effect of exercise on social distance in patients with CLBP over an 8-week intervention period.

Materials and methods

Study design

We conducted an 8-week exercise intervention to explore the effect of exercise on social distance in patients with CLBP. Two rounds of assessments, including those for social distance task, pain intensity, unpleasantness of pain, Roland-Morris Questionnaire (RMDQ), Self-Rating Anxiety Scale (SAS), and Self-Rating Depression Scale (SDS) were completed pre- and post- intervention.

Participants

The effect size was calculated to be 0.67 in accordance with the study by Cho (2014). After G*Power calculation (two tails, $\alpha = 0.05$, power $= 0.80$), the sample size was 20. Considering that the turnover rate of 20%, 25 subjects were required for this study. Finally, 29 middle-aged and elderly patients with CLBP were recruited from various communities in Yangpu District, Shanghai, China. The inclusion criteria were as follows: (1) aged 50–75 years old; (2) with LBP lasting for at least 12 weeks; (3) with maximum pain intensity of at least 3 on the Numerical Rating Scale (NRS); (4) no pain in other parts of the body except LBP; (5) no cognitive impairment and can understand the experimental content. The exclusion criteria were as follows:

Abbreviations: CLBP, chronic low back pain; RMDQ, Roland-Morris Questionnaire; SAS, Self-Rating Anxiety Scale; SDS, Self-Rating Depression Scale; LBP, Low back pain; MCID, minimal clinically important difference; TOM, theory of mind (TOM).

(1) Specific LBP caused by definite tissue structure or pathology, such as intervertebral disc (or spinal canal) disease, tumor, visceral disease, spinal disease, or injury. All subjects met the inclusion and exclusion criteria, voluntarily attended to the study, and signed an informed consent. The study was approved by the Ethics Committee of Shanghai University of Sport.

Outcome measures

Assessments were performed at baseline and after the 8-week exercise intervention, including social distance, pain intensity, disability, unpleasantness of pain, anxiety, and depression.

Social distance under various experimental conditions was measured by a stop-distance paradigm with high reliability and validity (Kennedy et al., 2009; Lough et al., 2016). It includes comfortable distance and uncomfortable distance when the subject actively approaches an experimenter (consistent or inconsistent with the subject's gender) or when is approached. A digital laser measurer (Bosch GLM 30C) was used to measure the true distance under different experimental conditions. The NRS was applied to measure the maximum pain intensity (NRS_{max}), average pain intensity (NRS_{avg}), pain intensity at rest (NRS_{rest}), and pain intensity at the moment (NRS_{now}) during the last 3 days. The NRS is an 11-grade rating scale: 0, "no pain at all"; 1–3, "mild pain"; 4–6, "moderate pain"; 7–9, "severe pain"; 10, "maximum pain." This scale has good validity and reliability (Bendinger and Plunkett, 2016; Yao et al., 2020). Following international consensus, a 2-point decrease for NRS was considered a minimal clinically important difference (MCID) (Ostelo et al., 2008). LBP-related disability was assessed with the 24-item RMDQ, which yields scores ranging from 0 to 24. A high score indicates a serious disability. Following international consensus, a 2-point decrease for RMDQ was considered a MCID (Ostelo et al., 2008). The NRS also measures the unpleasantness of pain ("0" means "no pain-induced unpleasantness at all," and "10" means "maximum pain-induced unpleasantness"), including the average unpleasantness of pain (NRS_{unavg}) and unpleasantness of pain at the moment (NRS_{unnow}) during the last 3 days. The levels of anxiety and depression were evaluated by the 20-item SAS and the 20-item SDS, respectively. The total scores of both scales are 20–80. A high score means serious anxiety or depression (Yu et al., 2012).

Social distance task

A stop-distance paradigm has been widely applied in the studies of detecting individual social distance (Kennedy et al., 2009; Lough et al., 2016). The starting distance of the task was 3 m, and the subjects and experimenters were unfamiliar with each other. Task 1: The experimenter (same gender as the subject) walked toward the subject who was standing still at a natural pace. They looked into each other's eyes. The experimenter stopped walking when he reached a distance that the subject normally keeps from strangers. This distance was the comfortable distance (CD1, **Figure 1A**). Thereafter, the experimenter continued walking and stopped when he reached a distance at which the subject felt uncomfortable. This distance was the uncomfortable distance (UD1, **Figure 1A**). Task 2 (like Task 1): The subject walked toward the experimenter and stopped at a comfortable distance (CD3, UD3; **Figure 1C**). After the bidirectional tests, the process was repeated, but with the experimenter of the opposite gender (Task 3 and 4, **Figures 1B,D**). The distance was measured with a digital laser measurer (Bosch GLM 30C). Each task was performed thrice, and the average was considered the outcome.

Intervention

Tai Chi was selected as the intervention method of the study. The clinical practice guideline from the American College of Physicians strongly recommends Tai Chi as a non-invasive treatment for CLBP (Qaseem et al., 2017). Tai Chi moves slowly, gently, and rhythmically, with smooth circular motion of the upper limbs and continuous weight shifting of the low limbs (Peng, 2012). Previous studies have confirmed that Tai Chi is a safe and effective exercise. It cannot only improve physical functions, such as by alleviating LBP, enhancing muscle strength and endurance, and promoting core stability, but also improve mental health, including through alleviating depression and anxiety and helping a person to relax (Hall et al., 2009; Cho, 2014).

The intervention consisted of 8 Yang-Style Tai Chi movements: (1) Part the Wild Horse's Mane; (2) Fair Lady Works at Shuttles; (3) Brush Knee and Twist Step; (4) Pull, Block and Pound; (5) Grasp the Peacock's Tail; (6) Step Back and Whirl Arms on Both Sides; (7) Golden Rooster Stands on One leg; (8) Cloudy Hands (Wang et al., 2022). It adopted group training. Tai Chi was carried out by a trained professional Tai Chi coach to give instruction and correct the wrong actions in time. The program lasted for 8 weeks, with a session lasting for 60 min and being conducted twice a week. An intervention session included 10 min warm-up exercise, 40 min Tai Chi, and 10 min relaxation training. The exercise intensity of the subjects was controlled at 3–5 in the Borg Scale, accounting for 40–60% of their maximum heart rate. In the study, the first to third weeks were allotted for learning and mastery of the single movements of Tai Chi, whereas the fourth to eighth weeks involved repetitive practicing and consolidation of the integrated movements.

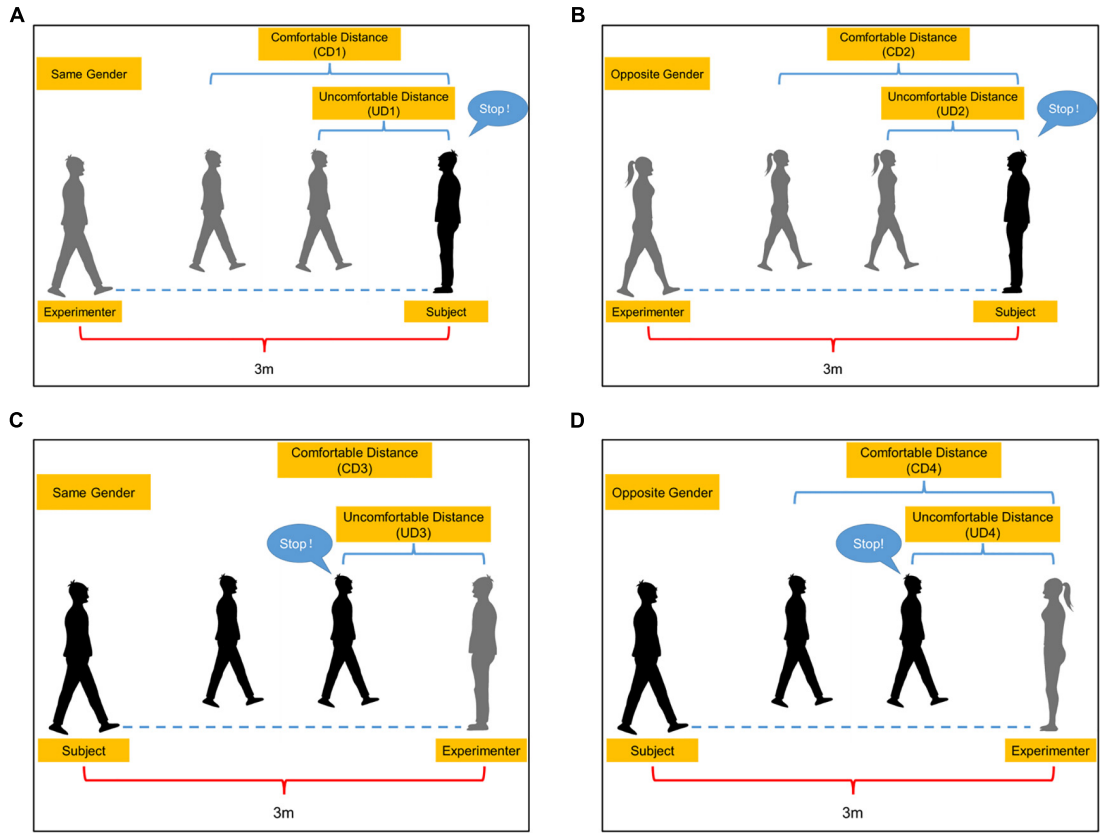

FIGURE 1
Social distance task. **(A)** The subject (black) is approached by the experimenter (gray) of the same gender. **(B)** The subject (black) is approached by the experimenter (gray) of the opposite gender. **(C)** The subject (black) walks toward the experimenter (gray) of the same gender. **(D)** The subject (black) walks toward the experimenter (gray) of the opposite gender. CD1, The comfortable distance when the subject is approached by the experimenter of the same gender; CD2, The comfortable distance when the subject is approached by the experimenter of the opposite gender; CD3, The comfortable distance when the subject walks toward the experimenter of the same gender; CD4, The comfortable distance when the subject walks toward the experimenter of the opposite gender; UD1, The uncomfortable distance when the subject is approached by the experimenter of the same gender; UD2, The uncomfortable distance when the subject is approached by the experimenter of the opposite gender; UD3, The uncomfortable distance when the subject walks toward the experimenter of the same gender; UD4, The uncomfortable distance when the subject walks toward the experimenter of the opposite gender.

Statistical analysis

All results were analyzed by the IBM SPSS Statistics 26. Quantitative variables were presented as mean ± standard deviation ($\bar{x} \pm s$). All data were tested for normality by Shapiro-Wilk test and normal transformation when necessary. The parameter test was used for the data conformation to normal distribution, and non-parametric test was used for data with severely skewed distribution and cannot be converted to a normal one. $p < 0.05$ was considered statistically significant.

Based on the average pain intensity, we divided the data into three groups, namely, overall, moderate ($NRS_{avg} > 3$), and mild ($NRS_{avg} \leq 3$) CLBP group. The inter-group comparison of baseline data, the result of pre-intervention, and post-intervention—pre-intervention were compared by the independent sample *t*-test, Mann-Whitney *U*-test and Chi-Square test. Paired sample *t*-test or Wilcoxon signed-rank test was selected to detect the intra-group differences pre- and post-intervention. All the results were analyzed by intention-to-treat, and the method of regression estimation was performed to fill in the missing values. Subjects who had an attendance rate of less than 75% or failed to attend the assessment were considered to have been dropped out.

Results

Of the 49 middle-aged and elderly subjected recruited, 12 did not meet the inclusion criteria, 5 declined to participate, 3 had other reasons for inability to participate, and finally 29 met the inclusion criteria and received 8-week exercise intervention. The flow of subjects through the study was shown in **Supplementary Figure 1**. Three subjects participated in Tai Chi courses less than 12 times across the study period

(Supplementary Figure 1). Overall, the mean age was 65.90 (4.97) years, 9 subjects were men (31.03%), and 20 were women (68.97%). A total of 13 subjects were included in the moderate CLBP group, with an average age of 67.31 (4.35) years. Exactly 16 subjects were included in the mild CLBP group, with an average age of 64.75 (5.29) years. No significant difference was observed in baseline the information between the moderate and mild CLBP groups ($p > 0.05$, Table 1).

Social distance outcomes

All data on social distance are presented in Figure 2 and Table 2. Before the intervention, no significant difference was recorded in each distance between the moderate and mild CLBP groups ($p > 0.05$, Table 2). Figures 2A–C shows that the distances of each group in post-intervention were shorter than those in pre-intervention. A significant difference was observed in CD1, CD2, UD1, UD2, CD4, UD3, and UD4 of the overall CLBP group, all distances of the moderate CLBP group, and CD1, CD2, UD1, and UD2 of the mild CLBP group between pre- and post-intervention ($p < 0.05$). Compared with the mild CLBP group, the moderate CLBP group had more marked changes, and the inter-group differences of post-pre CD1 (difference, −6.91; 95% confidence interval (CI): −31.28 to 17.47), CD3 (difference, −17.53; 95% CI: −34.62 to −0.43), and UD3 (difference, −10.77; 95% CI: −21.11 to −0.44) were statistically significant ($p < 0.05$) (Table 2).

Pain intensity and unpleasantness outcomes

All data on pain intensity and the unpleasantness of pain are presented in Figure 2 and Table 2. Before the intervention, the scores of pain intensity and unpleasantness in the moderate CLBP group were higher than those in the mild CLBP group, with significant differences in the NRS_{max}, NRS_{avg}, and NRS_{rest} between the two groups ($p < 0.05$, Table 2). Figures 2D–F shows that the pain intensity and unpleasantness of pain scores of each group in post-intervention were lower than those in pre-intervention. A significant difference was observed in all pain intensity and the unpleasantness of pain in the overall and moderate CLBP groups and NRS_{max}, NRS_{avg}, NRS_{now}, NRS_{unavg}, and NRS_{unnow} of the mild CLBP group between pre- and post- intervention ($p < 0.05$). Compared with the mild CLBP group, the moderate CLBP group had a greater improvement, and the inter-group difference of post-pre NRS_{rest} (difference, −1.44; 95% CI: −2.69 to −0.19) was statistically significant ($p < 0.05$, Table 2). In terms of MCID, the decrease in NRS_{max} in the overall and mild CLBP groups reached MCID but not those of NRS_{avg}, NRS_{rest}, and NRS_{now}. The decrease in NRS_{max}, NRS_{avg}, and NRS_{rest} in the moderate CLBP group reached MCID but not NRS_{now}.

Disability outcomes

All disability data are presented in Figure 2 and Table 2. Before the intervention, no significant difference was observed in the disability between the moderate and mild CLBP groups ($p > 0.05$, Table 2). Figures 2G–I shows that the disability of each group improved post-intervention. A significant difference was observed in the disability of the overall, moderate, and mild CLBP groups between pre- and post-intervention ($p < 0.05$). Compared with the mild CLBP group, the moderate CLBP group had more marked changes, but the inter-group difference of post-pre disability was not statistically significant ($p > 0.05$, Table 2). In addition, the decrease in RMDQ in the overall, moderate, and mild CLBP groups reached MCID.

Negative emotion outcomes

All data of negative emotions are presented in Figure 2 and Table 2. Before the intervention, no significant difference was observed in the anxiety and depression between the moderate and mild CLBP groups ($p > 0.05$, Table 2). Figure 2J–L shows that the anxiety and depression of each group in post-intervention were alleviated. A significant difference was noticed in the negative emotions of the overall, moderate, and mild CLBP groups between pre- and post-intervention ($p < 0.05$). Compared with the mild CLBP group, the moderate CLBP group had more marked changes, but the inter-group difference of post-pre disability was not statistically significant ($p > 0.05$, Table 2).

Discussion

This study explored the effect of an 8-week exercise intervention on social distance and CLBP symptoms in subjects with CLBP. We observed that the social distance of subjects with CLBP was shorter than that in pre-intervention. In addition, the pain intensity, unpleasantness of pain, disability, anxiety, and depression were reduced compared with those before the intervention.

Social distance

The study showed that the subjects with CLBP shorten social distance after receiving exercise intervention. The decrease in interpersonal distance reflects the alleviation of social withdrawal and the improvement of social interaction and

TABLE 1 Baseline demographic and clinical characteristics.

	Group, mean (*SD*)			*p*
	Overall (*n* = 29)	**Moderate (*n* = 13)**	**Mild (*n* = 16)**	
Male, *n* (%)	9 (31.03%)	4 (30.77%)	5 (31.25%)	0.978
Age, years	65.90 (4.97)	67.31 (4.35)	64.75 (5.29)	0.186
Height, cm	161.63 (7.62)	163.12 (7.91)	160.43 (7.42)	0.353
Weight, kg	64.62 (11.43)	64.02 (7.32)	65.12 (14.15)	0.801
BMI (kg/m^2)	24.62 (3.18)	24.03 (1.86)	25.10 (3.94)	0.380
Smoking, *n* (%)	4 (13.79%)	1 (7.69%)	3 (18.75%)	0.390
Drinking, *n* (%)	3 (10.34%)	1 (7.69%)	2 (12.50%)	0.672
Education, *n* (%)				0.214
Primary school or below	1 (3.45%)	/	1 (6.25%)	NA
Junior high school	10 (34.48%)	7 (53.85%)	3 (18.75%)	NA
Senior high school	14 (48.28%)	5 (38.46%)	9 (56.25%)	NA
College or above	4 (13.79%)	1 (7.69%)	3 (18.75%)	NA
Course of CLBP, years	11.88 (11.14)	12.73 (13.29)	11.20 (9.45)	0.982
Types of pain				0.422
Continuous	3 (10.34%)	2 (15.38%)	1 (6.25%)	NA
Intermittent	26 (89.66%)	13 (84.62%)	15 (93.75%)	NA
Nature of pain				0.352
Aching pain	14 (48.28%)	4 (30.77%)	10 (65.50%)	NA
Bursting pain	2 (6.90%)	2 (15.38%)	/	NA
Prickling pain	2 (6.90%)	1 (7.69%)	1 (6.25%)	NA
Radiant pain	2 (6.90%)	1 (7.69%)	1 (6.25%)	NA
Mixed pain	9 (31.03%)	5 (38.46%)	4 (25.00%)	NA
SAD	7.38 (5.18)	6.38 (4.61)	8.19 (5.61)	0.361
IPAQ				NA
Total physical activity per week (MET-min/w)	4415.10 (2796.05)	4120.39 (2991.87)	4654.54 (2701.10)	0.599
Physical activity level				0.730
Low	/	/	/	NA
Medium	8 (27.59%)	4 (30.77%)	4 (25.00%)	NA
High	21 (72.41%)	9 (69.23%)	12 (75.00%)	NA

BMI, body mass index; CLBP, chronic low back pain; SAD, Social Avoidance and Distress Scale; IPAQ, International Physical Activity Questionnaire.

function. Similar findings have also been reported in other papers. A systematic review conducted by Koren et al. (2021) pointed out that Tai Chi can promote social interaction and participation and increase social support. Likewise, other exercise interventions have similar effects. Nishida et al. (2016) observed that a youth with severe social withdrawal was relieved of anxiety and depression after the treatment with sertraline alone, but social withdrawal still existed. When combined with exercise therapy, the symptoms of social withdrawal significantly improved. In addition, a high level of physical activity had been associated with a low degree of social isolation among the elderly (Robins et al., 2018). The explanation that exercise improves social withdrawal can be multifactorial. The social interaction hypothesis holds that a stable social relationship exists in sports activities. Individuals participating in sports provide support to each other, which make exercise beneficial on mental health (Peluso and Guerra de Andrade, 2005). The intervention of this study adopted the way of team training rather than one-to-one guidance, which provided subjects with more opportunities for social contact and promoted social interaction and support. Furthermore, sports activities with more social connections are more conductive to reducing social isolation and loneliness, and improving health than individual sports (Brady et al., 2020). On the other hand, the bilateral temporal hemodynamics increased significantly in the youth with social withdrawal after a 3-month jogging intervention (Nishida et al., 2016). The temporal-parietal junction belongs to the theory of mind (TOM) network which is related to prosocial actions. When the network activity increases, the shortening of social distance is one of its manifestations (Simon and Walker, 2018). Moreover, numerous studies stated that exercise can enhance the functional connection of temporal and parietal lobe and the activation of precuneus lobe, which all belongs to the

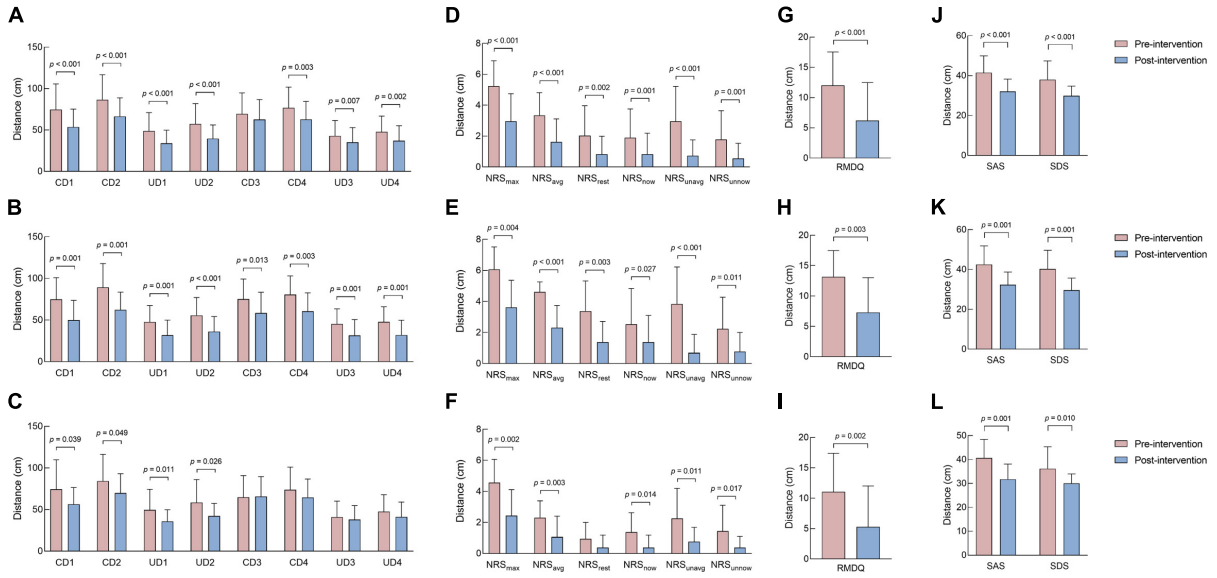

FIGURE 2
Difference in social distance, pain intensity and unpleasantness, disability, and negative emotion outcomes before and after intervention. **(A)** Difference in social distance outcomes in the overall CLBP group before and after intervention. **(B)** Difference in social distance outcomes in the moderate CLBP group before and after intervention. **(C)** Difference in social distance outcomes in the mild CLBP group before and after intervention. **(D)** Difference in pain intensity and unpleasantness outcomes in the overall CLBP group before and after intervention. **(E)** Difference in pain intensity and unpleasantness outcomes in the moderate CLBP group before and after intervention. **(F)** Difference in pain intensity and unpleasantness outcomes in the mild CLBP group before and after intervention. **(G)** Difference in disability outcomes in the overall CLBP group before and after intervention. **(H)** Difference in disability outcomes in the moderate CLBP group before and after intervention. **(I)** Difference in disability outcomes in the mild CLBP group before and after intervention. **(J)** Difference in negative emotion outcomes in the overall CLBP group before and after intervention. **(K)** Difference in negative emotion outcomes in the moderate CLBP group before and after intervention. **(L)** Difference in negative emotion outcomes in the mild CLBP group before and after intervention. CD1, The comfortable distance when the subject is approached by the experimenter of the same gender; CD2, The comfortable distance when the subject is approached by the experimenter of the opposite gender; CD3, The comfortable distance when the subject walks toward the experimenter of the same gender; CD4, The comfortable distance when the subject walks toward the experimenter of the opposite gender; UD1, The uncomfortable distance when the subject is approached by the experimenter of the same gender; UD2, The uncomfortable distance when the subject is approached by the experimenter of the opposite gender; UD3, The uncomfortable distance when the subject walks toward the experimenter of the same gender; UD4, The uncomfortable distance when the subject walks toward the experimenter of the opposite gender. NRS_{max}, the maximum pain intensity during the last 3 days; NRS_{avg}, the average pain intensity during the last 3 days; NRS_{rest}, the pain intensity at rest during the last 3 days; NRS_{now}, the pain intensity at the moment during the last 3 days; NRS_{unavg}, the average unpleasantness of pain during the last 3 days; NRS_{unnow}, the unpleasantness of pain at the moment during the last 3 days; RMDQ, Roland-Morris Questionnaire; SAS, Self-Rating Anxiety Scale; SDS, Self-Rating Depression Scale.

TOM network. Therefore, exercise reduces social withdrawal by activating the TOM network. This series of evidence supports that exercise improves psychosocial health through neurophysiological regulation.

Pain, disability, and negative emotions

After 8 weeks of Tai Chi intervention, the pain, disability, and negative emotions of subjects with CLBP decreased. The effect of Tai Chi on CLBP has also been confirmed in different studies. A meta-analysis of Tai Chi for LBP showed that Tai Chi can relieve pain and improve physical function (Qin et al., 2019). Hall et al. (2009) divided patients with non-specific CLBP into the Tai Chi and waitlist control groups. The Tai Chi group received Tai Chi for 10 weeks, with each session lasting for 40 min, and being conducted 1–2 times a week. The results revealed that the Tai Chi group was better than the waitlist control group in reducing the bothersomeness of back symptoms, pain intensity, and pain-related disability (Hall et al., 2011). Wang et al. (2010) conducted a meta-analysis that included 40 studies of Tai Chi on psychological health. The results suggested that Tai Chi can reduce depression, anxiety, mood disturbance, and mental pressure. Traditional Chinese medicine believes that Tai Chi improves LBP based on the interaction of "yin," "yang," and "qi." It can promote the balance of "yin" and "yang" and the free flow of "qi," which is conductive to physical and mental health (Peng, 2012). Physical activities related to LBP (such as sitting, standing, walking) are bound up with lower limb function. In Tai Chi training, the movements of continuous squatting and weight shift can improve the muscle strength and flexibility of lower limbs (Zou et al., 2019). Tai Chi can also enhance the lower limb muscle strength and posture control, maintain dynamic and

TABLE 2 Social distance outcomes after 8-week exercise intervention.

	Group, mean (*SD*)				*p*
	Overall (*n* = 29)	**Moderate (*n* = 13)**	**Mild (*n* = 16)**	**Between-group difference (95% CI)**	
CD1 (cm)					
Pre-intervention	74.63 (31.02)	74.83 (26.13)	74.46 (35.35)	0.38 (−23.82, 24.58)	0.770
Post-pre intervention	−21.08 (31.43)	−24.89 (19.19)	−17.98 (39.08)	−6.91 (−31.28, 17.47)	0.020*
CD2 (cm)					
Pre-intervention	86.56 (30.14)	89.34 (28.64)	82.29 (32.05)	5.05 (−18.38, 28.48)	0.560
Post-pre intervention	−20.15 (27.18)	−27.08 (21.30)	−14.52 (30.65)	−12.55 (−33.17, 8.06)	0.054
UD1 (cm)					
Pre-intervention	48.83 (22.28)	47.87 (19.58)	49.62 (24.87)	−1.75 (−19.12, 15.63)	0.838
Post-pre intervention	−14.84 (18.89)	−16.07 (14.26)	−13.85 (22.38)	−2.23 (−16.93, 12.48)	0.161
UD2 (cm)					
Pre-intervention	57.22 (24.62)	55.64 (21.45)	58.50 (27.55)	−2.86 (−22.03, 16.31)	0.762
Post-pre intervention	−17.69 (21.16)	−19.47 (14.18)	−16.25 (25.88)	−3.23 (−19.69, 13.23)	0.125
CD3 (cm)					
Pre-intervention	69.49 (25.26)	75.21 (24.06)	64.84 (26.02)	10.36 (−8.92, 29.65)	0.220
Post-pre intervention	−6.96 (23.64)	−16.63 (20.67)	0.90 (23.55)	−17.53 (−34.62, −0.43)	0.045*
CD4 (cm)					
Pre-intervention	76.85 (24.95)	80.50 (22.50)	73.87 (27.14)	6.63 (−12.66, 25.92)	0.487
Post-pre intervention	−14.10 (23.61)	−19.97 (19.81)	−9.33 (25.93)	−10.64 (−28.58, 7.29)	0.066
UD3 (cm)					
Pre-intervention	42.92 (18.53)	45.32 (18.10)	40.98 (19.24)	4.34 (−10.02, 18.70)	0.540
Post-pre intervention	−7.80 (14.32)	−13.74 (10.80)	−2.97 (15.31)	−10.77 (−21.11, 0.44)	0.042*
UD4 (cm)					
Pre-intervention	47.75 (19.01)	48.00 (17.98)	47.55 (20.39)	0.45 (−14.38, 15.27)	0.951
Post-pre intervention	−10.63 (16.55)	−15.90 (12.80)	−6.34 (18.34)	−9.56 (−21.90, 2.79)	0.124
NRS_{max}					
Pre-intervention	5.24 (1.64)	6.08 (1.44)	4.56 (1.50)	1.51 (0.38, 2.65)	0.011*
Post-pre intervention	−2.28 (2.09)	−2.46 (1.94)	−2.12 (2.25)	−0.34 (−1.96, 1.29)	0.372
NRS_{avg}					
Pre-intervention	3.34 (1.47)	4.62 (0.65)	2.31 (1.08)	2.30 (1.60, 3.00)	<0.001**
Post-pre intervention	−1.72 (1.44)	−2.31 (1.44)	−1.25 (1.29)	−1.06 (−2.10, −0.02)	0.051
NRS_{rest}					
Pre-intervention	2.03 (1.94)	3.38 (1.94)	0.94 (1.06)	2.45 (1.29, 3.61)	0.001**
Post-pre intervention	−1.21 (1.76)	−2.00 (1.96)	−0.56 (1.32)	−1.44 (−2.69, −0.19)	0.047*
NRS_{now}					
Pre-intervention	1.90 (1.86)	2.54 (2.30)	1.38 (1.26)	1.16 (−0.21, 2.54)	0.160
Post-pre intervention	−1.07 (1.31)	−1.15 (1.46)	−1.00 (1.21)	−0.15 (−1.17, 0.86)	0.789
NRS_{unavg}					
Pre-intervention	2.97 (2.26)	3.85 (2.38)	2.25 (1.95)	1.60 (−0.05, 3.24)	0.057
Post-pre intervention	−2.24 (2.29)	−3.15 (2.34)	−1.50 (2.03)	−1.65 (−3.32, 0.01)	0.052
NRS_{unnow}					
Pre-intervention	1.79 (1.86)	2.23 (2.05)	1.44 (1.67)	0.79 (−0.62, 2.21)	0.326
Post-pre intervention	−1.24 (1.57)	−1.46 (1.51)	−1.06 (1.65)	−0.40 (−1.61, 0.81)	0.418
RMDQ					
Pre-intervention	12.00 (5.54)	13.15 (4.34)	11.06 (6.34)	2.09 (−2.15, 6.34)	0.291
Post-pre intervention	−5.79 (5.92)	−5.85 (5.73)	−5.75 (6.27)	−0.10 (−4.72, 4.53)	0.966
SAS					
Pre-intervention	41.48 (8.44)	42.54 (9.36)	40.63 (7.82)	1.91 (−4.63, 8.46)	0.553
Post-pre intervention	−9.48 (8.47)	−10.23 (8.19)	−8.87 (8.91)	−1.36 (−7.94, 5.23)	0.676

(Continued)

TABLE 2 (Continued)

	Group, mean (*SD*)				*p*
	Overall ($n = 29$)	Moderate ($n = 13$)	Mild ($n = 16$)	Between-group difference (95% CI)	
SDS					
Pre-intervention	38.03 (9.32)	40.31 (9.37)	36.19 (9.16)	4.12 (−2.97, 11.21)	0.186
Post-pre intervention	−8.17 (9.18)	−10.69 (8.42)	−6.12 (9.52)	−4.57 (−11.50, 2.37)	0.091

CD1, The comfortable distance when the subject is approached by the experimenter of the same gender; CD2, The comfortable distance when the subject is approached by the experimenter of the opposite gender; CD3, The comfortable distance when the subject walks toward the experimenter of the same gender; CD4, The comfortable distance when the subject walks toward the experimenter of the opposite gender; UD1, The uncomfortable distance when the subject is approached by the experimenter of the same gender; UD2, The uncomfortable distance when the subject is approached by the experimenter of the opposite gender; UD3, The uncomfortable distance when the subject walks toward the experimenter of the same gender; UD4, The uncomfortable distance when the subject walks toward the experimenter of the opposite gender. NRS_{max}, the maximum pain intensity during the last 3 days; NRS_{avg}, the average pain intensity during the last 3 days; NRS_{rest}, the pain intensity at rest during the last 3 days; NRS_{now}, the pain intensity at the moment during the last 3 days; NRS_{unavg}, the average unpleasantness of pain during the last 3 days; NRS_{unnow}, the unpleasantness of pain at the moment during the last 3 days. RMDQ, Roland-Morris Questionnaire; SAS, Self-Rating Anxiety Scale; SDS, Self-Rating Depression Scale. $^{*}p < 0.05$; $^{**}p < 0.01$.

static balance (Hong and Li, 2007; Hall et al., 2011). Moreover, combining Tai Chi with breathing, the movement is gentle and slow, which can reduce muscle tension and physical pain (Huston and McFarlane, 2016). Furthermore, Tai Chi can alleviate pain and disability by improving the cognition of LBP or reducing psychological pressure (Wayne and Kaptchuk, 2008; Sherman et al., 2010). Hall et al. (2011) also reported that pain-catastrophization plays the role of a mediator between Tai Chi and symptoms related to CLBP.

On the other hand, compared with the mild CLBP group, the moderate CLBP group showed more improvement in all aspects, and such result may be due to the more severe pain, disability, and negative emotions. Our previous study on CLBP and social distance revealed that pain, disability, anxiety, and depression were positively correlated with social distance (Weng et al., 2021). The improvement of CLBP was associated with a high likelihood of subsequent decrease in social distance. The amygdala is not only related to emotional processing but also a key brain region regulating social distance (Kennedy et al., 2009; Martinsen et al., 2018; Kami et al., 2020; Weng et al., 2021). Kami et al. (2020) explored the effect of voluntary running on amygdala using partial sciatic-nerve ligation model mice. They observed that voluntary running cannot only inhibit the negative emotions, such as anxiety and fear, that are closely related to the chronicity of pain, but also promote pleasure and alleviate pain: this finding might have been caused by the plasticity of the amygdala. It also provided evidence indicating that exercise can improve CLBP symptoms and adjust social distance directly or indirectly by regulating the amygdala.

Limitations

This study had several limitations. First, only one experimental group was included. Therefore, waitlist or other intervention control groups should be considered in future research. Second, we did not perform follow-up after 8 weeks of exercise intervention. Thus, we should continue to explore the maintenance effect of exercise on the social distance of CLBP patients. Third, a narrow age range of the recruited subjects was used and there were imbalances in the gender sample size. Thus, future research designed for a stratified age and gender is needed.

Practical implications and future prospects for research

CLBP is one of the most common chronic diseases, and causes serious harm to physiological, psychological, and social functions. However, its damage to psychosocial health is usually ignored. Patients with CLBP show increased social distance and withdrawal, reflecting the impairment of individual psychosocial health. This outcome is one of the hazards of CLBP that cannot be ignored. Through a longitudinal intervention experiment, we observed that exercise not only alleviated the symptoms related to CLBP but also improved psychosocial health. Therefore, for the management of this disease in the future, we should also pay attention to the psychological problems and consider exercise therapy as a complementary means of psychological and physiological rehabilitation. In addition, future research can be combined with neuroimaging technology to detect changes in brain activity to explain the underlying neural mechanism of exercise in improving abnormal social distance regulation behavior. It can provide a basis for CLBP to formulate more targeted intervention methods.

Conclusion

The 8-week exercise intervention cannot only shorten the social distance and improve the abnormal behavior of social distance regulation of middle-aged and elderly patients with CLBP, but also relieve pain, disability, and negative emotions. In addition, follow-up will be conducted in the future to explore the

long-term effects of exercise intervention, and further work is required to determine whether this new finding applies equally to other types of exercise.

Data availability statement

The original contributions presented in this study are included in the article/**Supplementary material**, further inquiries can be directed to the corresponding author.

Ethics statement

The studies involving human participants were reviewed and approved by the Ethics Committee of Shanghai University of Sport. The patients/participants provided their written informed consent to participate in this study.

Author contributions

L-MW and X-QW conceived and designed the study. L-MW, RW, Q-HY, T-TC, C-CW, W-LL, S-HD, and Y-CW collected the data. L-MW and RW analyzed and interpreted the data and revised the manuscript for important intellectual content. L-MW drafted the manuscript. All authors discussed the results, commented on the manuscript, and approved the final manuscript.

Funding

This work was supported by the Scientific and Technological Research Program of the Shanghai Science and Technology Committee (19080503100 and 21S31902400), the Shanghai Key Lab of Human Performance (Shanghai University of Sport) (11DZ2261100), the Talent Development Fund of Shanghai Municipal (2021081), and the Shanghai Clinical Research Center for Rehabilitation Medicine (21MC1930200).

Conflict of interest

The authors declare that the research was conducted in the absence of any commercial or financial relationships that could be construed as a potential conflict of interest.

Publisher's note

All claims expressed in this article are solely those of the authors and do not necessarily represent those of their affiliated organizations, or those of the publisher, the editors and the reviewers. Any product that may be evaluated in this article, or claim that may be made by its manufacturer, is not guaranteed or endorsed by the publisher.

Supplementary material

The Supplementary Material for this article can be found online at: https://www.frontiersin.org/articles/10.3389/fnagi.2022.976164/full#supplementary-material

SUPPLEMENTARY FIGURE 1
Flow diagram of the subjects. NRSavg, the average pain intensity during the last 3 days; CLBP, chronic low back pain.

References

Achterbergh, L., Pitman, A., Birken, M., Pearce, E., Sno, H., and Johnson, S. (2020). The experience of loneliness among young people with depression: A qualitative meta-synthesis of the literature. *BMC Psychiatry* 20:415. doi: 10.1186/s12888-020-02818-3

Balagué, F., Mannion, A. F., Pellisé, F., and Cedraschi, C. (2012). Non-specific low back pain. *Lancet* 379, 482–491. doi: 10.1016/s0140-6736(11)60610-7

Bendinger, T., and Plunkett, N. (2016). Measurement in pain medicine. *BJA Educ.* 16, 310–315. doi: 10.1093/bjaed/mkw014

Brady, S., D'Ambrosio, L. A., Felts, A., Rula, E. Y., Kell, K. P., and Coughlin, J. F. (2020). Reducing isolation and loneliness through membership in a fitness program for older adults: Implications for health. *J. Appl. Gerontol.* 39, 301–310. doi: 10.1177/0733464818807820

Cho, Y. (2014). Effects of tai chi on pain and muscle activity in young males with acute low back pain. *J. Physical Ther. Sci.* 26, 679–681. doi: 10.1589/jpts.26.679

Chou, R., Deyo, R., Friedly, J., Skelly, A., Hashimoto, R., Weimer, M., et al. (2017). Nonpharmacologic therapies for low back pain: A systematic review for an american college of physicians clinical practice guideline. *Anna. Intern. Med.* 166, 493–505. doi: 10.7326/m16-2459

Deyo, R. A., Dworkin, S. F., Amtmann, D., Andersson, G., Borenstein, D., Carragee, E., et al. (2014). Report of the NIH task force on research standards for chronic low back pain. *J. Pain* 15, 569–585. doi: 10.1016/j.jpain.2014.03.005

Ebadi, S., Henschke, N., Forogh, B., Ansari, N. N., van Tulder, M. W., Babaei-Ghazani, A., et al. (2020). Therapeutic ultrasound for chronic low back pain. *Cochrane Database Syst. Rev.* 7, CD009169. doi: 10.1002/14651858.CD009169.pub3

Firth, J., Cotter, J., Elliott, R., French, P., and Yung, A. R. (2015). A systematic review and meta-analysis of exercise interventions in schizophrenia patients. *Psychol. Med.* 45, 1343–1361. doi: 10.1017/s0033291714003110

French, S. D., Cameron, M., Walker, B. F., Reggars, J. W., and Esterman, A. J. (2006). Superficial heat or cold for low back pain. *Cochrane Database Syst. Rev.* 2006, CD004750. doi: 10.1002/14651858.CD004750.pub2

Furlan, A. D., Brosseau, L., Imamura, M., and Irvin, E. (2002). Massage for low-back pain: A systematic review within the framework of the cochrane collaboration back review group. *Spine* 27, 1896–1910. doi: 10.1097/00007632-200209010-00017

Gessaroli, E., Santelli, E., di Pellegrino, G., and Frassinetti, F. (2013). Personal space regulation in childhood autism spectrum disorders. *PLoS One* 8:8. doi: 10.1371/journal.pone.0074959

Hall, A. M., Maher, C. G., Lam, P., Ferreira, M., and Latimer, J. (2011). Tai chi exercise for treatment of pain and disability in people with persistent low back pain: A randomized controlled trial. *Arthritis Care Res.* 63, 1576–1583. doi: 10.1002/acr.20594

Hall, A. M., Maher, C. G., Latimer, J., Ferreira, M. L., and Lam, P. (2009). A randomized controlled trial of tai chi for long-term low back pain (TAI CHI): Study rationale, design, and methods. *BMC Musculoskelet. Disorder.* 10:55. doi: 10.1186/1471-2474-10-55

Hartvigsen, J., Hancock, M. J., Kongsted, A., Louw, Q., Ferreira, M. L., Genevay, S., et al. (2018). What low back pain is and why we need to pay attention. *Lancet* 391, 2356–2367. doi: 10.1016/s0140-6736(18)30480-x

Hayden, J. A., van Tulder, M. W., and Tomlinson, G. (2005). Systematic review: Strategies for using exercise therapy to improve outcomes in chronic low back pain. *Anna. Intern. Med.* 142, 776–785. doi: 10.7326/0003-4819-142-9-200505030-00014

Hong, Y., and Li, J. X. (2007). Biomechanics of tai chi: A review. *Sports Biomech.* 6, 453–464. doi: 10.1080/14763140701491674

Huston, P., and McFarlane, B. (2016). Health benefits of tai chi: What is the evidence? *Can. Fam. Physician* 62, 881–890.

Kami, K., Tajima, F., and Senba, E. (2020). Plastic changes in amygdala subregions by voluntary running contribute to exercise-induced hypoalgesia in neuropathic pain model mice. *Mol. Pain* 16:12. doi: 10.1177/1744806920971377

Katz, J. N. (2006). Lumbar disc disorders and low-back pain: Socioeconomic factors and consequences. *J. Bone Joint Surg. Am. Volume* 88A, 21–24. doi: 10.2106/jbjs.E.01273

Kennedy, D. P., Glascher, J., Tyszka, J. M., and Adolphs, R. (2009). Personal space regulation by the human amygdala. *Nat. Neurosci.* 12, 1226–1227. doi: 10.1038/nn.2381

Kimhy, D., Lauriola, V., Bartels, M. N., Armstrong, H. F., Vakhrusheva, J., Ballon, J. S., et al. (2016). Aerobic exercise for cognitive deficits in schizophrenia – The impact of frequency, duration, and fidelity with target training intensity. *Schizophr. Res.* 172, 213–215. doi: 10.1016/j.schres.2016.01.055

Koren, Y., Leveille, S., and You, T. (2021). Tai Chi interventions promoting social support and interaction among older adults: A systematic review. *Res. Gerontol. Nurs.* 14, 126–137. doi: 10.3928/19404921-20210325-02

Lough, E., Flynn, E., and Riby, D. M. (2016). Personal space regulation in williams syndrome: The effect of familiarity. *J. Autism Dev. Disorder.* 46, 3207–3215. doi: 10.1007/s10803-016-2864-8

Martinsen, S., Flodin, P., Berrebi, J., Lofgren, M., Bileviciute-Ljungar, I., Mannerkorpi, K., et al. (2018). The role of long-term physical exercise on performance and brain activation during the stroop colour word task in fibromyalgia patients. *Clin. Physiol. Funct. Imaging* 38, 508–516. doi: 10.1111/cpf.12449

Nishida, M., Kikuchi, S., Fukuda, K., and Kato, S. (2016). Jogging therapy for hikikomori social withdrawal and increased cerebral hemodynamics: A case report. *Clin. Pract. Epidemiol. Ment. Health* 12, 38–42. doi: 10.2174/1745017901612010038

Ostelo, R. W., Deyo, R. A., Stratford, P., Waddell, G., Croft, P., Von Korff, M., et al. (2008). Interpreting change scores for pain and functional status in low back pain: Towards international consensus regarding minimal important change. *Spine* 33, 90–94. doi: 10.1097/BRS.0b013e31815e3a10

Owen, P. J., Miller, C. T., Mundell, N. L., Verswijveren, S., Tagliaferri, S. D., Brisby, H., et al. (2020). Which specific modes of exercise training are most effective for treating low back pain? Network meta-analysis. *Br. J. Sports Med.* 54, 1279–1287. doi: 10.1136/bjsports-2019-100886

Peluso, M. A., and Guerra de Andrade, L. H. (2005). Physical activity and mental health: The association between exercise and mood. *Clinics* 60, 61–70. doi: 10.1590/s1807-59322005000100012

Peng, M. S., Wang, R., Wang, Y. Z., Chen, C. C., Wang, J., Liu, X. C., et al. (2022). Efficacy of therapeutic aquatic exercise vs physical therapy modalities for patients with chronic low back pain: A randomized clinical trial. *JAMA Netw. Open* 5, e2142069. doi: 10.1001/jamanetworkopen.2021.42069

Peng, P. W. (2012). Tai chi and chronic pain. *Reg. Anesth. Pain Med.* 37, 372–382. doi: 10.1097/AAP.0b013e31824f6629

Perry, A., Nichiporuk, N., and Knight, R. T. (2016). Where does one stand: A biological account of preferred interpersonal distance. *Soc. Cogn. Affect. Neurosci.* 11, 317–326. doi: 10.1093/scan/nsv115

Qaseem, A., Wilt, T. J., McLean, R. M., Forciea, M. A., and Amer Coll, P. (2017). Noninvasive treatments for acute, subacute, and chronic low back pain: A clinical practice guideline from the american college of physicians. *Anna. Intern. Med.* 166, 514–530. doi: 10.7326/m16-2367

Qin, J. W., Zhang, Y., Wu, L. J., He, Z. X., Huang, J., Tao, J., et al. (2019). Effect of tai chi alone or as additional therapy on low back pain systematic review and meta-analysis of randomized controlled trials. *Medicine* 98:10. doi: 10.1097/md.0000000000017099

Richardson, C. R., Faulkner, G., McDevitt, J., Skrinar, G. S., Hutchinson, D. S., and Piette, J. D. (2005). Integrating physical activity into mental health services for persons with serious mental illness. *Psychiatr. Serv.* 56, 324–331. doi: 10.1176/appi.ps.56.3.324

Robins, L. M., Hill, K. D., Finch, C. F., Clemson, L., and Haines, T. (2018). The association between physical activity and social isolation in community-dwelling older adults. *Aging Ment. Health* 22, 175–182. doi: 10.1080/13607863.2016.1242116

Searle, A., Spink, M., Ho, A., and Chuter, V. (2015). Exercise interventions for the treatment of chronic low back pain: A systematic review and meta-analysis of randomised controlled trials. *Clin. Rehab.* 29, 1155–1167. doi: 10.1177/0269215515570379

Sherman, K. J., Cherkin, D. C., Cook, A. J., Hawkes, R. J., Deyo, R. A., Wellman, R., et al. (2010). Comparison of yoga versus stretching for chronic low back pain: Protocol for the Yoga Exercise Self-care (YES) trial. *Trials* 11:36. doi: 10.1186/1745-6215-11-36

Simon, E. B., and Walker, M. P. (2018). Sleep loss causes social withdrawal and loneliness. *Nat. Commun.* 9:9. doi: 10.1038/s41467-018-05377-0

van der Stouwe, E. C. D., van Busschbach, J. T., de Vries, B., Cahn, W., Aleman, A., and Pijnenborg, G. H. M. (2018). Neural correlates of exercise training in individuals with schizophrenia and in healthy individuals: A systematic review. *Neuroimage Clin.* 19, 287–301. doi: 10.1016/j.nicl.2018.04.018

van Middelkoop, M., Rubinstein, S. M., Verhagen, A. P., Ostelo, R. W., Koes, B. W., and van Tulder, M. W. (2010). Exercise therapy for chronic nonspecific low-back pain. *Best Pract. Res. Clin. Rheumatol.* 24, 193–204. doi: 10.1016/j.berh.2010.01.002

Wang, C., Bannuru, R., Ramel, J., Kupelnick, B., Scott, T., and Schmid, C. H. (2010). Tai Chi on psychological well-being: Systematic review and meta-analysis. *BMC Complement. Altern. Med.* 10:23. doi: 10.1186/1472-6882-10-23

Wang, R., Chang, X. L., Kiartivich, S., and Wang, X. Q. (2022). Effect of tai chi quan on the pressure pain thresholds of lower back muscles in healthy women. *J. Pain Res.* 15, 403–412. doi: 10.2147/jpr.S353465

Wayne, P. M., and Kaptchuk, T. J. (2008). Challenges inherent to t'ai chi research: Part I–t'ai chi as a complex multicomponent intervention. *J. Altern. Complement. Med.* 14, 95–102. doi: 10.1089/acm.2007.7170a

Weng, L. M., Wu, B., Chen, C. C., Wang, J., Peng, M. S., Zhang, Z. J., et al. (2021). Association of chronic low back pain with personal space regulation. *Front. Psychiatry* 12:719271. doi: 10.3389/fpsyt.2021.719271

Wu, B., Zhou, L., Chen, C., Wang, J., Hu, L. I., and Wang, X. (2022). Effects of exercise-induced hypoalgesia and its neural mechanisms. *Med. Sci. Sports Exerc.* 54, 220–231. doi: 10.1249/mss.0000000000002781

Yao, M., Xu, B.-P., Li, Z.-J., Zhu, S., Tian, Z.-R., Li, D.-H., et al. (2020). A comparison between the low back pain scales for patients with lumbar disc herniation: Validity, reliability, and responsiveness. *Health. Qual. Life Outcomes* 18, 175–175. doi: 10.1186/s12955-020-01403-2

Yu, S., Zhao, Q., Wu, P., Qin, M., Huang, H., Cui, H., et al. (2012). Effect of anxiety and depression on the recurrence of paroxysmal atrial fibrillation after circumferential pulmonary vein ablation. *J. Cardiovasc. Electrophysiol.* 23(Suppl. 1), S17–S23. doi: 10.1111/j.1540-8167.2012.02436.x

Zou, L., Zhang, Y., Liu, Y., Tian, X., Xiao, T., Liu, X., et al. (2019). The effects of tai chi chuan versus core stability training on lower-limb neuromuscular function in aging individuals with non-specific chronic lower back pain. *Medicina* 55:10. doi: 10.3390/medicina55030060

frontiers | Frontiers in Aging Neuroscience

TYPE Systematic Review
PUBLISHED 08 September 2022
DOI 10.3389/fnagi.2022.984708

OPEN ACCESS

EDITED BY
Sheng Li,
University of Texas Health Science Center at Houston, United States

REVIEWED BY
Francesco Iodice,
San Raffaele Pisana (IRCCS), Italy
Zude Zhu,
Jiangsu Normal University, China

*CORRESPONDENCE
Tong Wang
wangtong60621@163.com
Ying Shen
shenying@njmu.edu.cn

†These authors have contributed equally to this work and share first authorship

SPECIALTY SECTION
This article was submitted to Alzheimer's Disease and Related Dementias, a section of the journal Frontiers in Aging Neuroscience

RECEIVED 02 July 2022
ACCEPTED 22 August 2022
PUBLISHED 08 September 2022

CITATION
Zhang T, Sui Y, Lu Q, Xu X, Zhu Y, Dai W, Shen Y and Wang T (2022) Effects of rTMS treatment on global cognitive function in Alzheimer's disease: A systematic review and meta-analysis.
Front. Aging Neurosci. 14:984708.
doi: 10.3389/fnagi.2022.984708

Effects of rTMS treatment on global cognitive function in Alzheimer's disease: A systematic review and meta-analysis

Tianjiao Zhang[1†], Youxin Sui[1†], Qian Lu[2†], Xingjun Xu[1], Yi Zhu[1], Wenjun Dai[1], Ying Shen[1*] and Tong Wang[1*]

[1]Rehabilitation Medicine Center, The First Affiliated Hospital of Nanjing Medical University, Nanjing, China, [2]Department of Rehabilitation Medicine, The Affiliated Jiangsu Shengze Hospital of Nanjing Medical University, Suzhou, China

Background: Although repetitive transcranial magnetic stimulation (rTMS) has been extensively studied in patients with Alzheimer's disease (AD), the clinical evidence remains inconsistent. The purpose of this meta-analysis was to evaluate the effects of rTMS on global cognitive function in patients with AD.

Methods: An integrated literature search using 4 databases (PubMed, Web of Science, Embase, and Cochrane Library) was performed to identify English language articles published up to October 6, 2021. We pooled Mini-Mental State Examination (MMSE) and Alzheimer's Disease Assessment Scale-cognitive subscale (ADAS-Cog) scores using a random-effects model *via* RevMan 5.4 software. We calculated estimates of mean differences (MD) with 95% confidence intervals (CI). The primary outcomes were pre-post treatment changes in global cognition as measured using MMSE and ADAS-Cog immediately after rTMS treatment, and the secondary outcome was duration of cognitive improvement (1–1.5 and ≥3 months).

Results: Nine studies with 361 patients were included in this meta-analysis. The results showed that rTMS significantly improved global cognitive function immediately following rTMS treatment [(MD) 1.82, 95% confidence interval (CI) 1.41–2.22, $p < 0.00001$, MMSE; 2.72, 95% CI, 1.77–3.67, $p < 0.00001$, ADAS-Cog], and the therapeutic effects persisted for an extended duration (2.20, 95% CI, 0.93–3.47, $p = 0.0007$, MMSE; 1.96, 95% CI, 0.96–2.95, $p = 0.0001$, ADAS-Cog). Subgroup analyses showed that high frequency rTMS targeted to the left dorsolateral prefrontal cortex (DLPFC) for over 20 sessions induced the greatest cognitive improvement, with effects lasting for more than 1 month after the final treatment. There were no significant differences in dropout rate ($p > 0.05$) or adverse effect rate ($p > 0.05$) between the rTMS and control groups.

Conclusions: Repetitive TMS is a potentially effective treatment for cognitive impairment in AD that is safe and can induce long-lasting effects. Our results

also showed that ADAS-cog and MMSE differed in determination of global cognitive impairment.

Systematic review registration: http://www.crd.york.ac.uk/PROSPERO, PROSPERO CRD42022315545.

KEYWORDS

Alzheimer's disease, repetitive transcranial magnetic stimulation (rTMS), cognitive function, MMSE, ADAS-cog, systematic review, meta-analysis

Introduction

Alzheimer's disease (AD)-associated dementia accounts for 60–80% of dementia cases, and is a significant health concern in the elderly (Alzheimer's, 2018). Cognitive impairments are the main clinical manifestations of AD, and affect patients and caregivers, and increase societal burden (Yin et al., 2021). Drugs such as donepezil, rivastigmine, and galantamine commonly used for treatment if AD do not impact long-term prognosis (Liao et al., 2015). As a result, non-pharmacological interventions have received increased attention.

Repetitive transcranial magnetic stimulation (rTMS) is a non-invasive brain stimulation technique that affects brain metabolism and neurological function by regulating cortical excitability (Kobayashi and Pascual-Leone, 2003). Stimulation parameters of rTMS are critical to treatment effects. Low frequency rTMS ($\leq$1 Hz) inhibits cortical excitability, high frequency rTMS ($\geq$5 Hz) induces cortical excitability (Dong et al., 2018). Repetitive TMS can also enhance cognition through stimulation of specific cortical areas (such as DLPFC) (Alvarez-Salvado et al., 2014). Many *in vivo* and *in vitro* studies have shown that rTMS cognition in AD, and may be a promising therapy (Vlachos et al., 2012; Lenz et al., 2015; Zhao et al., 2017; Chen et al., 2019; Jia et al., 2021).

Four meta-analyses have been performed on the beneficial effects of rTMS on cognitive function in AD (Liao et al., 2015; Dong et al., 2018; Lin et al., 2019; Wang et al., 2020). However, these articles varied in rTMS parameters (i.e., treatment sessions, stimulation site, etc.) and the therapeutic outcomes. Furthermore, none have evaluated the effects of rTMS on cognitive function during follow-up. Although rTMS has shown promise as a treatment for AD, rTMS parameters and treatment schemes that produce favorable therapeutic value require further development. This meta-analysis summarized studies of global cognitive function in patients with AD.

Methods and materials

Our work adhered to the preferred reporting items for systematic reviews and meta-analyses (PRISMA) guidelines (Moher et al., 2010) and was registered in the PROSPERO database for systematic reviews (CRD 42022315545).

Search strategy

PubMed, Web of Science, Embase, and Cochrane Library were searched for relevant studies published before October 6, 2021. We used the following key words: ("Alzheimer disease" OR "Alzheimer's disease" OR "Alzheimer dementia" OR "Alzheimer's dementia" OR "Alzheimer syndrome" OR "Alzheimer type dementia" OR "AD") AND ("transcranial magnetic stimulation" OR "repetitive transcranial magnetic stimulation" OR "brain stimulation" OR "TMS" OR "rTMS"). We also searched for additional unpublished and in-progress trials from ClinicalTrials.gov, and searched the reference lists of identified articles for additional studies.

Eligibility criteria and quality assessment

The inclusion criteria for the study were as follows: (1) rTMS was performed on patients with Alzheimer's disease; (2) global cognition was quantitatively determined using the Alzheimer's Disease Assessment Scale-cognitive subscale (ADAS-cog) or Mini-Mental State Examination (MMSE); (3) rTMS was conducted alone or in combination with cognitive training; (4) the active rTMS control group received sham rTMS, cognitive training, or other treatments; (5) mean cognition outcome score changes and standard deviation (SD) were accessible, or absolute original scale scores were available to calculate mean $\pm$ SD; and (6) randomized controlled studies. The exclusion criteria were as follows: (1) animal studies; (2) included patients with neurological disorders other than Alzheimer's disease; (3) reviews, letters, comments, unpublished reports, or meeting minutes; (4) duplicate articles; and (5) non-English articles.

Cochrane Collaboration was used by two statisticians independently to determine study quality. The evaluation criteria were: (a) sequence generation; (b) allocation concealment; (c) blinding; (d) approach for handling incomplete

outcome data; (e) selective reporting; and (f) other potential bias. The risk of bias was rated as low, high, or uncertain.

Data extraction

Data from the included studies were extracted and examined by two researchers (TZ, YXS, and QL). During screening and comparison, disagreements were resolved by consensus between the researchers or by a third specialized researcher. For each included article, we recorded the following information: basic characteristics of the included studies (author, year of publication, and study design), sample size, disease type, rTMS parameters (number of sessions, frequency, intensity, stimulation targets), global cognitive performance (ADAS-cog or MMSE) score, follow-up time, and adverse effects.

Data analysis

We used Rev-Man 5.4 software (Review Manger of Cochrane Collaboration) for all data synthesis and analysis. Effect size was computed by mean differences (MD) with 95% confidence intervals (CIs). The degree of heterogeneity was considered significant if the I^2 statistic was >50%. Based on the inherent clinical heterogeneity in our pooled studies, a random-effects models was used for more conservative outcomes. Planned subgroup analyses were used for rTMS frequency, target sites, treatment sessions, and concomitant cognitive training. For all statistical analyses, $P < 0.05$ was considered significant. When heterogeneity between studies was significant, sensitivity analyses were performed using the leave-one-out technique. Due to the low number of included studies, Egger's tests were used instead of funnel plots, and $p < 0.05$ indicated publication bias (Egger et al., 1997).

Search and selection of studies

The search identified 986 studies from four English databases (PubMed, Web of Science, Embase, and Cochrane Library), and 401 duplicates were removed. After assessing titles and abstracts, 54 articles were include in the full-text reading phase, and nine studies were included in the meta-analysis. The study selection process is shown in Figure 1.

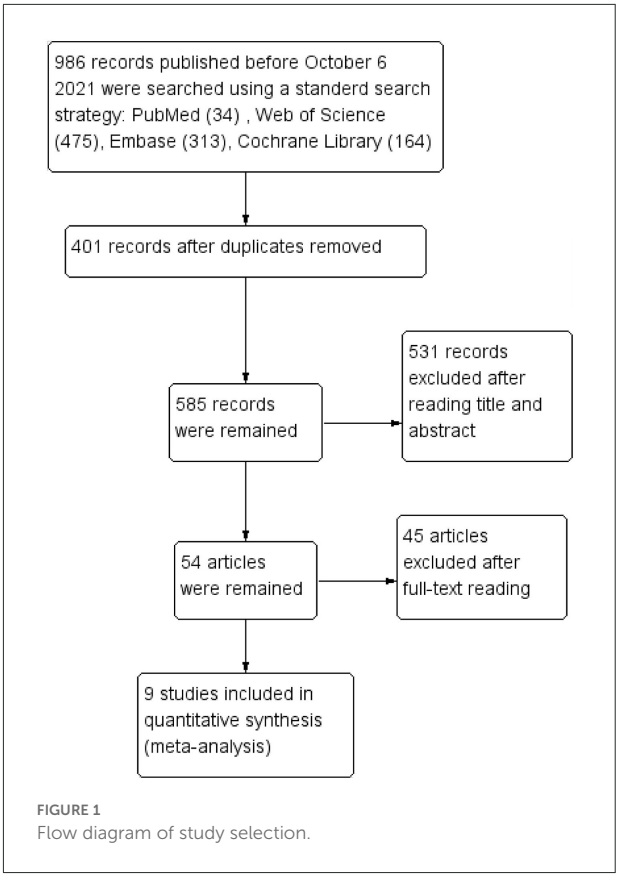

FIGURE 1
Flow diagram of study selection.

Identifications and descriptions of the included studies

Supplementary Table 1 shows the characteristics of the nine trials included in this meta-analysis. The meta-analysis included 361 participants (192 in the rTMS group and 169 in the control group (Ahmed et al., 2012; Rabey et al., 2013; Wu et al., 2015; Lee et al., 2016; Zhao et al., 2017; Zhang et al., 2019; Brem et al., 2020; Jia et al., 2021; Li et al., 2021). Participants were diagnosed with AD based on different diagnostic criteria. However, one study reported the outcomes for mild to moderate AD and severe AD. Therefore, we chose the mild to moderate AD subgroup for the meta-analysis (Ahmed et al., 2012). For the interventions, four studies combined rTMS with cognitive training (Rabey et al., 2013; Lee et al., 2016; Zhang et al., 2019; Brem et al., 2020). Global cognitive function assessments included MMSE (six studies) (Ahmed et al., 2012; Lee et al., 2016; Zhao et al., 2017; Zhang et al., 2019; Jia et al., 2021; Li et al., 2021) and ADAS-Cog (seven studies) (Rabey et al., 2013; Wu et al., 2015; Lee et al., 2016; Zhao et al., 2017; Zhang et al., 2019; Brem et al., 2020; Li et al., 2021). Six studies assessed cognitive function at various follow-up times from 1 to 3 months after the final session (Ahmed et al., 2012; Lee et al., 2016; Zhao et al., 2017; Zhang et al., 2019; Brem et al., 2020; Li et al., 2021). Five trials reported adverse effects with diverse causes (Wu et al., 2015; Lee et al., 2016; Zhao et al., 2017; Zhang et al., 2019; Jia et al., 2021).

Supplementary Table 2 presents the characteristics of the rTMS protocols from the included studies. Only one study used low-frequency rTMS (Ahmed et al., 2012), and the other eight studies only used high-frequency rTMS. Five studies used a

frequency of 10 Hz (Rabey et al., 2013; Lee et al., 2016; Zhang et al., 2019; Brem et al., 2020; Jia et al., 2021), and four studies used a frequency of 20 Hz (Ahmed et al., 2012; Wu et al., 2015; Zhao et al., 2017; Li et al., 2021). Repetitive TMS stimulation sites included DLPFC (Wu et al., 2015; Li et al., 2021), left lateral parietal cortex (Jia et al., 2021), bilateral DLPFC (Ahmed et al., 2012), left DLPFC, left lateral temporal lobe (LTL) (Zhang et al., 2019), parietal lobe, and posterior temporal lobe (Zhao et al., 2017). Three studies performed rTMS stimulation on the following six brain areas: (a) Broca's area, Wernicke's area, bilateral DLPFC and bilateral parietal somatosensory association (pSAC) (Rabey et al., 2013; Lee et al., 2016), (b) Broca's area, Wernicke's area, bilateral DLPFC, and bilateral inferior parietal lobule (Brem et al., 2020). The intensity of rTMS was 80–120% of resting motor threshold (rMT), and the number of interventions was 5–54 sessions.

Research quality

Figure 2 summarizes the risk of bias for the included studies. Each of the nine trials stated random allocation, but only four described how to generate the random sequence in detail and were rated as "low risk" (Wu et al., 2015; Zhang et al., 2019; Jia et al., 2021; Li et al., 2021). Only two studies described the allocation concealment procedure adequately (Brem et al., 2020; Jia et al., 2021). Seven trials reported that participants and researchers were double-blinded, and the remaining two trials did not mention blinding (Ahmed et al., 2012; Zhang et al., 2019). Outcome assessors were blind to group allocation in all studies except for one study; which did not indicate whether blinding occurred (Brem et al., 2020). The risk of attrition bias in three studies was rated as "high risk" because the research data were incomplete (Ahmed et al., 2012; Rabey et al., 2013; Brem et al., 2020). The reporting bias of two studies were rated as "high risk" owing to selectively reporting of pre-specified outcome indicators (Lee et al., 2016; Brem et al., 2020). Most studies with unclear information were rated as "unclear risk" in other potential sources of bias. However, center bias in one study resulted in "high risk" (Brem et al., 2020).

Results

Global cognitive function (immediately after the intervention)

Nine studies involving 361 participants with AD assessed the immediate post-treatment effect of rTMS on global cognitive ability. Six of the nine studies used MMSE (Ahmed et al., 2012; Lee et al., 2016; Zhao et al., 2017; Zhang et al., 2019; Jia et al., 2021; Li et al., 2021), and seven studies used ADAS-Cog (Rabey et al., 2013; Wu et al., 2015; Lee et al., 2016; Zhao et al., 2017; Zhang et al., 2019; Brem et al., 2020; Li et al., 2021). All global cognitive function results from MMSE and ADAS-Cog indicated that active rTMS treatment was superior to control treatment with a mean effect size of 1.82 (95% CI, 1.41–2.22, $p < 0.00001$, $I^2 = 5\%$, Figure 3) and 2.72 (95% CI, 1.77–3.67, $p < 0.00001$, $I^2 = 0\%$, Figure 4), respectively. Egger's regression showed no publication bias across studies that used ADAS-Cog (intercept = 0.16, df = 6, $t = 0.08$, two-tailed $p = 0.94$) or studies that used MMSE (intercept = −0.44, df = 5, $t = 0.92$, two-tailed $p = 0.40$). Sensitivity analysis was also performed, and omitting studies one by one did not alter the significance of the pooled MD.

Subgroup analysis of global cognitive function (immediately after the intervention) by MMSE

Several subgroups were evaluated to identify variables that might influence the heterogeneity and cognitive outcomes by MMSE. Subgroup analysis was performed according to stimulation site. The efficacy of "Other areas" stimulation was 0.91 (95% CI −0.46 to 2.29), and a significant rTMS effect was found among those targeted to the DLPFC (MD = 1.78 95% CI 0.83– 2.73) (Figure 5). The excluded study by Zhang et al. included the left DLPFC and left lateral temporal lobe as the stimulus targets, so it could not be divided into either of the two subgroups.

We also analyzed the effects of rTMS treatment in combination with cognitive training ("CT = Yes" vs. "CT = No"). A significant rTMS effect was found among studies that excluded cognitive training (1.84; 95% CI 1.56–2.12), but not in the studies involving cognitive training (1.43; 95% CI −1.23 to 4.08) (Figure 6).

Subgroup analysis for session number generated significant results for MMSE scores in the "20" and "30" subgroups (MD = 2.52 95% CI 1.06–3.98; MD = 1.73 95% CI 1.13–2.34), but not in the "≤10" subgroup (MD = 1.35 95% CI −0.39 to 3.08), which suggested that long-term rTMS treatment produced cognitive enhancement (Figure 7).

Treatment with high frequency stimulation result in a significant effect size of 1.87 (95% CI 1.59–2.15), whereas treatment with low frequency stimulation showed no positive effect 0.00 (95% CI −2.50 to 2.50) (Figure 8).

Global cognitive function (follow-up)

Six trials assessed the effects of rTMS on global cognitive function at follow-up. The results showed low heterogeneity in the five studies that used ADAS-Cog ($I^2 = 0\%$, $p =$

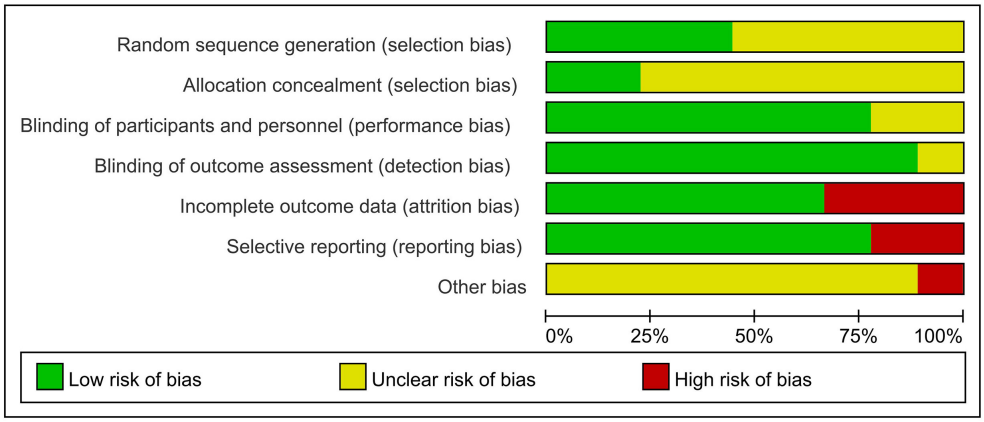

FIGURE 2
Risks of bias.

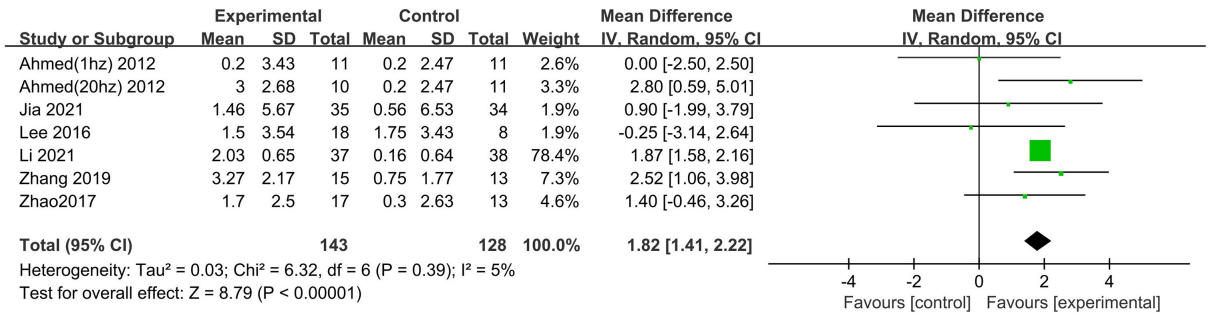

FIGURE 3
Forest plot of repetitive transcranial magnetic stimulation vs. the control group by MMSE immediately after the intervention.

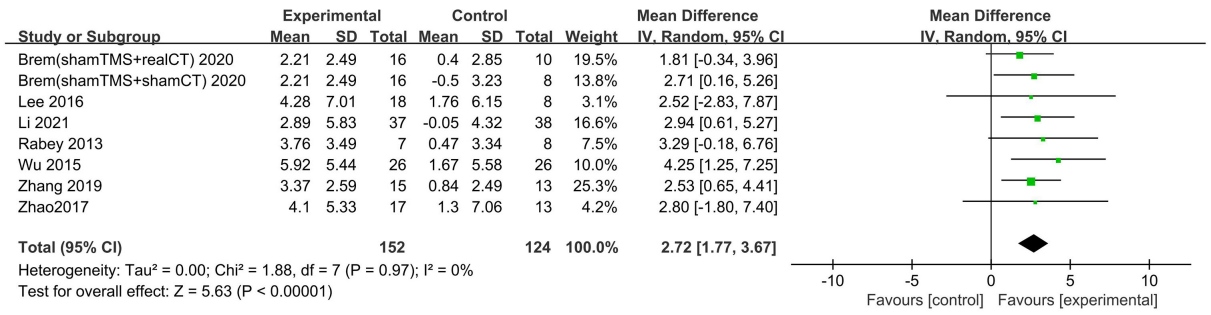

FIGURE 4
Forest plot of repetitive transcranial magnetic stimulation vs. the control group by ADAS-Cog immediately after the intervention.

0.55) (Lee et al., 2016; Zhao et al., 2017; Zhang et al., 2019; Brem et al., 2020; Li et al., 2021), The five studies that used MMSE had high heterogeneity (I^2 = 76%, p = 0.0001) (Ahmed et al., 2012; Lee et al., 2016; Zhao et al., 2017; Zhang et al., 2019; Li et al., 2021). No significant asymmetry was found using Egger's regression test in studies that used ADAS-Cog (intercept = 0.37, df = 4, t = 0.32, two-tailed p = 0.76), and in MMSE (intercept = 1.59, df = 6, t = 2.28, two-tailed p = 0.06). The mean effect size was 1.96 for ADAS-Cog (95% CI, 0.96–2.95, p =0.0001, Figure 9) and 2.20 for MMSE (95% CI, 0.93–3.47, p = 0.0007, Figure 10). Both results showed that rTMS provided superior cognitive effects at follow-up compared with those in the control group.

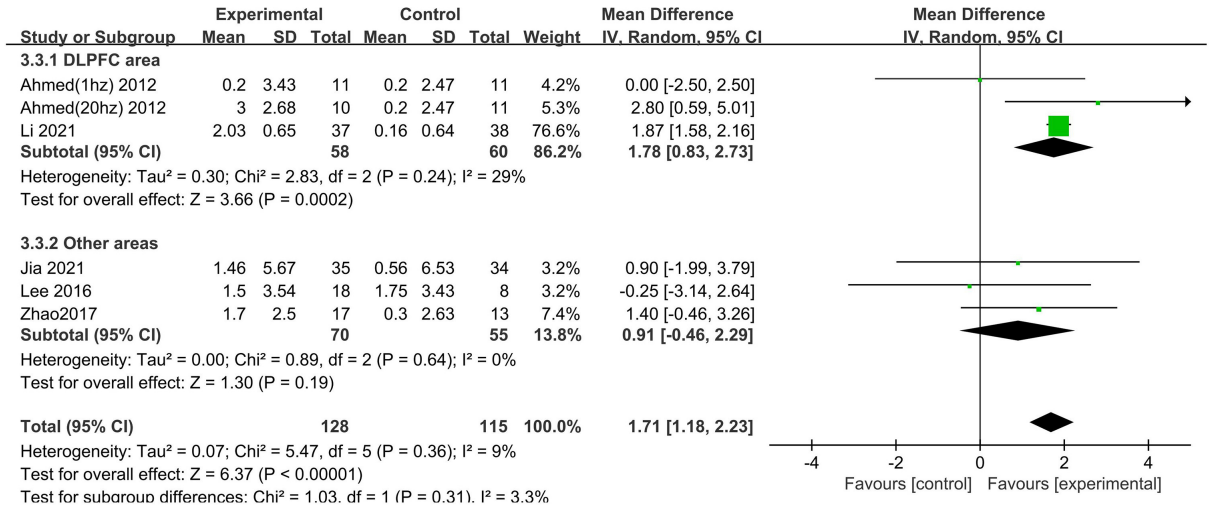

FIGURE 5
Subgroup analyses of repetitive transcranial magnetic stimulation vs. the control group by MMSE: DLPFC area vs. other areas.

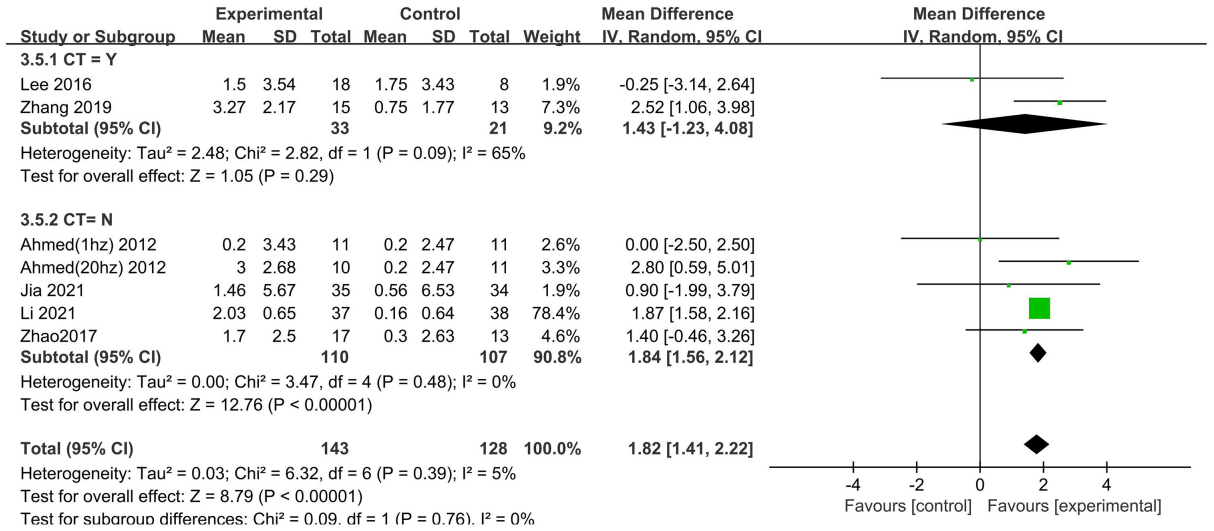

FIGURE 6
Subgroup analyses of repetitive transcranial magnetic stimulation vs. the control group by MMSE: CT = Yes vs. CT = No.

Subgroup analysis of global cognitive function (follow-up)

The follow-up times of the included studies ranged from 1 to 3 months. We divided the long-term effects into short-lasting effects (≤1.5 months) and longer-duration effects (3 months). The subgroup analysis of follow-up times revealed a mean effect size of 0.19 (95% CI −2.13 to 2.51) for ADAS-Cog with longer-duration effects. The mean effect size for short-lasting effects was 2.36 (95% CI 1.26–3.46). A significant rTMS effect was found at the shorter follow-up period (Figure 11). However, the results in two subgroup analyses (≤1.5 and 3 months) for MMSE were identical, with effect sizes of 1.90 (95% CI 0.29–3.51) and 2.75 (95% CI 0.02–5.48), respectively (Figure 12).

Adverse effects and dropout

Of the 9 studies, 4 reported no adverse events during the study period and 3 reported adverse effects in both the active and sham groups (Wu et al., 2015; Zhao et al., 2017; Jia et al., 2021). Lee et al. described one patient in the

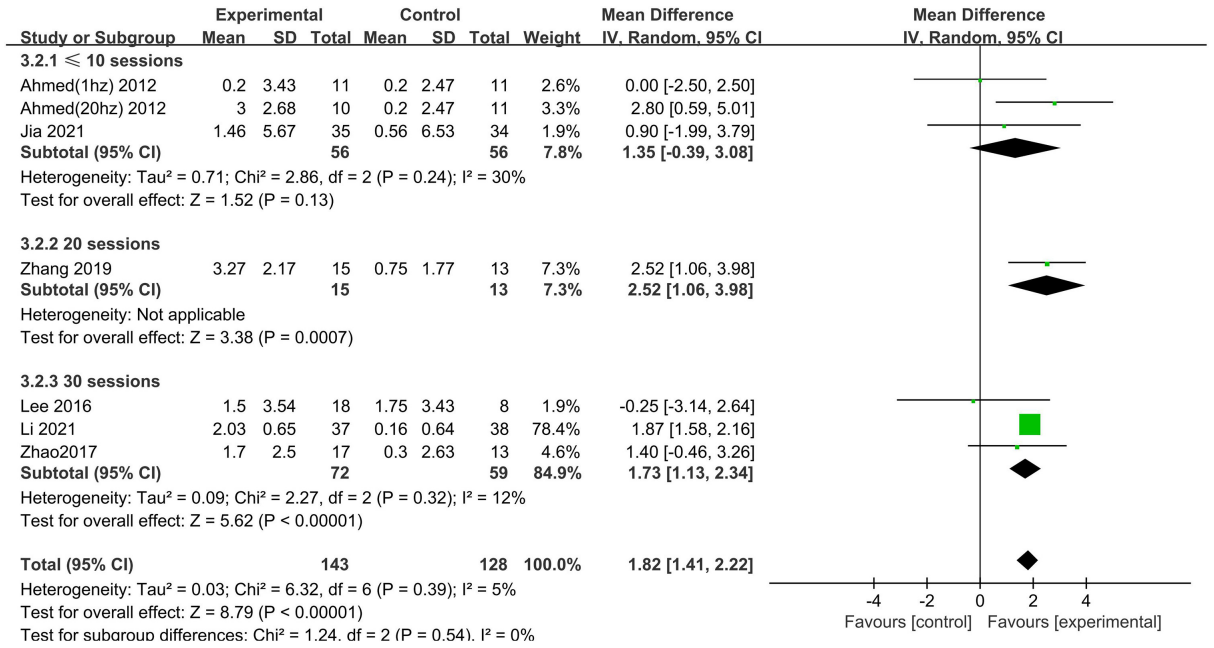

FIGURE 7
Subgroup analyses of repetitive transcranial magnetic stimulation vs. the control group by MMSE: ≤10 sessions vs. 20 sessions vs. 30 sessions.

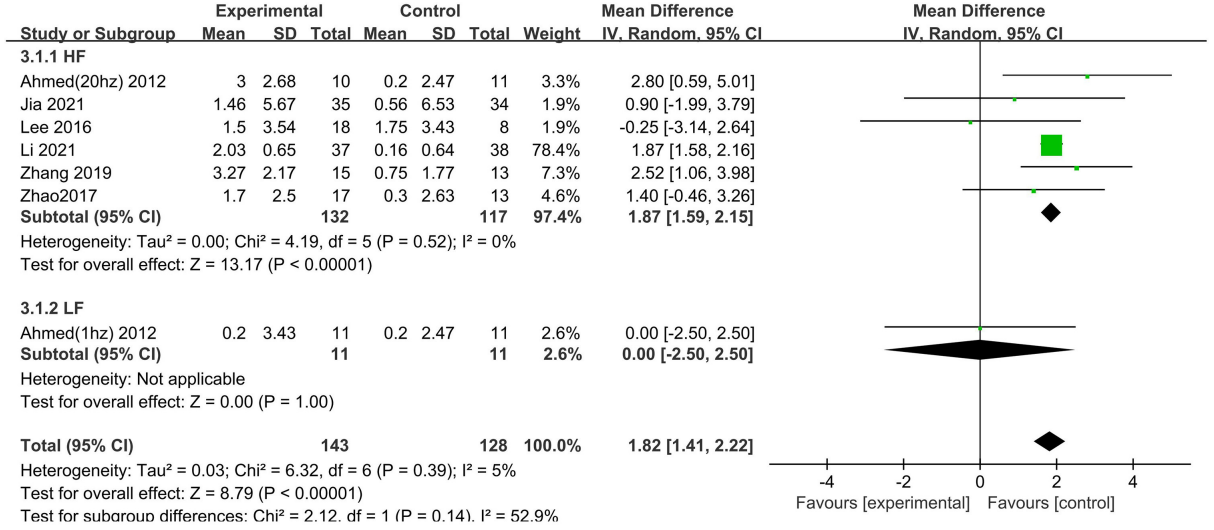

FIGURE 8
Subgroup analyses of repetitive transcranial magnetic stimulation vs. the control group by MMSE: HF vs. LF.

sham arm who complained of mild headache and fatigue at the first follow-up visit (Lee et al., 2016). Seven participants who received rTMS in Zhang et al.'s (2019) study felt mild discomfort of the head, which eased after 3 days. Headaches, fatigue, and scalp discomfort were the most-reported adverse effects. The adverse effect rates were 12.6% (14/111) and 9.4% (10/94) in the active and sham groups, respectively, and the difference between the groups was not significant ($\chi^2 = 0.192$, $p = 0.661$).

Two studies did not report any dropout (Ahmed et al., 2012; Zhao et al., 2017). The drop-out rate was 10.5% (18/172) of the experimental group, with no significant difference compared with 14.1% (24/170) of the control group ($\chi^2 = 1.059$, $p = 0.303$).

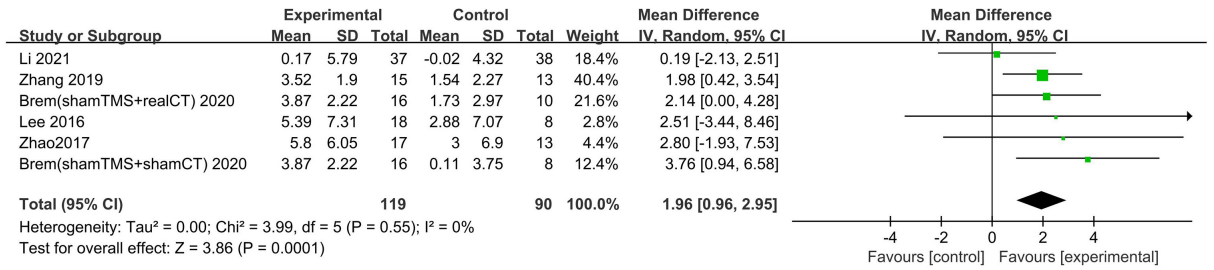

FIGURE 9
Forest plot of repetitive transcranial magnetic stimulation vs. the control group by ADAS-Cog at follow-up period.

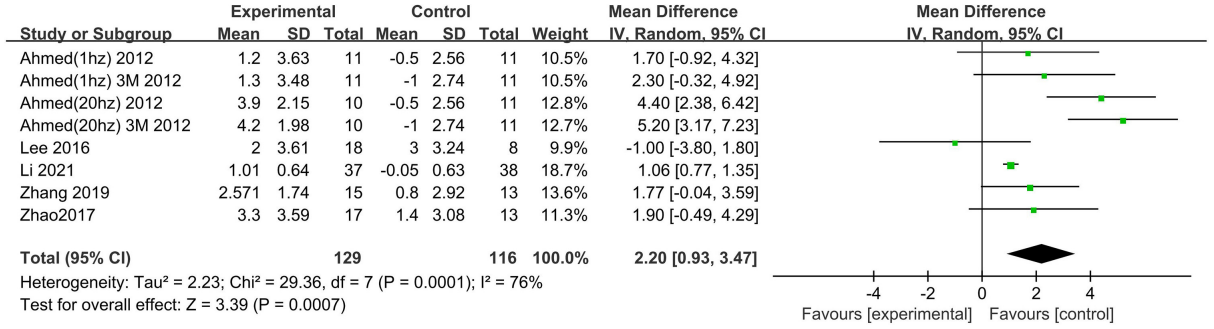

FIGURE 10
Forest plot of repetitive transcranial magnetic stimulation vs. the control group by MMSE at follow-up period.

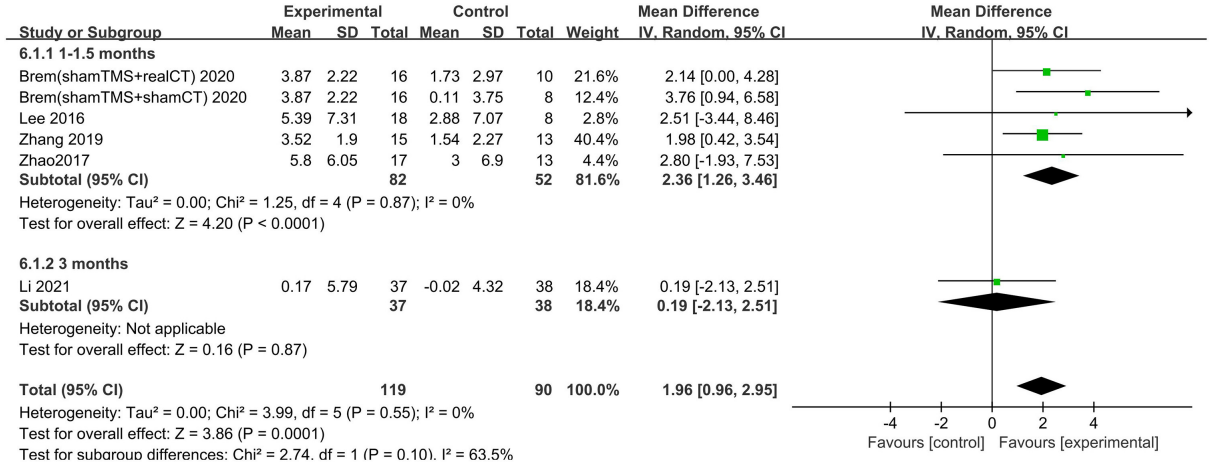

FIGURE 11
Subgroup analyses of repetitive transcranial magnetic stimulation vs. the control group by ADAS-Cog: 1–1.5 months vs. 3 months.

Discussion

Our review involved nine randomized sham controlled studies, and provided the most recent and detailed data regarding immediate and long-lasting treatment of global cognitive function in patients with AD following rTMS treatment. Subgroup analyses showed that rTMS protocols with high frequency and performed over the DLPFC for more than 20 sessions induced the best improvements in global cognitive function. In addition, we also showed that rTMS stimulation

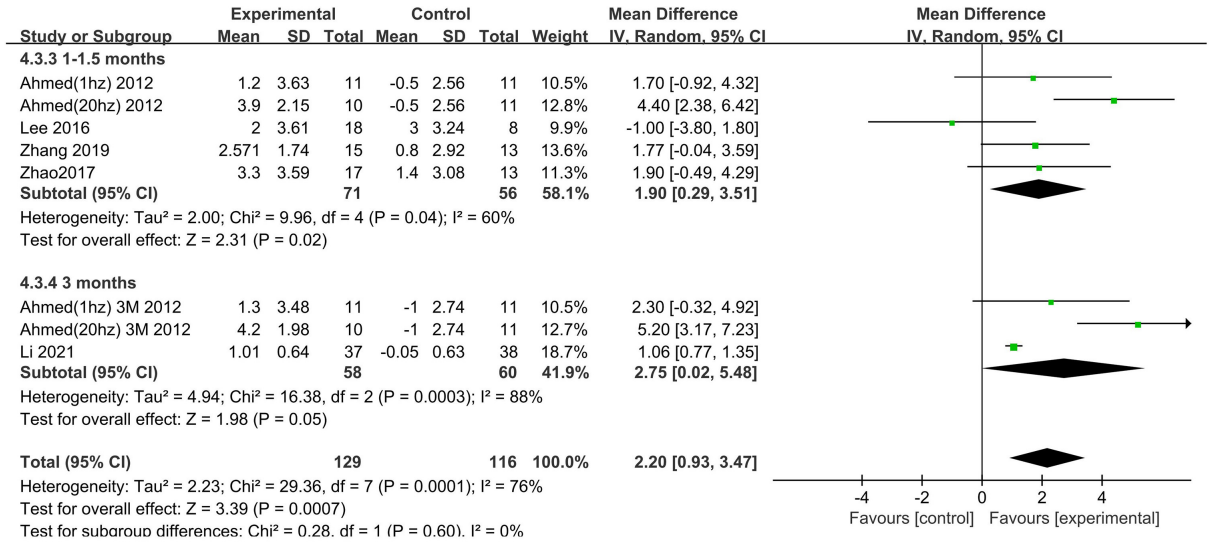

FIGURE 12
Subgroup analyses of repetitive transcranial magnetic stimulation vs. the control group by MMSE: 1–1.5 months vs. 3 months.

yielded cognitive benefits for 3 month in patients with AD assessed using MMSE, but not ADAS-Cog. Moreover, rTMS was safe and well-tolerated and did not induce severe adverse effects.

Consistent with a previous meta-analysis, high-frequency rTMS resulted in better therapeutic results than low-frequency rTMS for treatment of cognitive function. High-frequency rTMS altered synaptic plasticity and the level of brain-derived neurotrophic factor (BDNF). Studies showed a 55% reduction in synapses in early AD compared with mild cognitive impairment (MCI) and healthy subjects, as determined using electron microscopy, and the degree of synaptic loss correlated with cognitive deficits (DeKosky et al., 1996; Coleman and Yao, 2003). High-frequency rTMS attenuated synaptic damage in AD by inducing long-term potentiation (LTP) to increase synaptic activity, which is beneficial to learning and memory (Bliss and Collingridge, 1993). Memory formation is associated with BDNF, which is an important neurotrophic factor that promotes dendrite development and neuronal tolerance (Bekinschtein et al., 2008; Banerjee and Shenoy, 2021). A study showed that BDNF levels decreased with increased clinical severity of AD, and was most closely associated with memory decline in preclinical AD (Lim et al., 2021). One study reported that both high-frequency (20 Hz) and low-frequency (1 Hz) rTMS increased dopamine concentration and up-regulated the expression of dopamine receptor 4 in AD mice. However, only high-frequency rTMS intervention increased BDNF levels and enhanced the expression of Nestin and NeuN in brain tissue (Choung et al., 2021). In a review by Cheng et al., only two studies with relatively small sample sizes included low-frequency rTMS for treatment of patients with AD. Each of these studies showed superior efficacy of high-frequency rTMS on cognition (Ahmed et al., 2012; Ash et al., 2012; Cheng et al., 2018). These results should be treated with caution because few studies evaluated low-frequency rTMS.

Our meta-analysis found that stimulation of the DLPFC, the most common stimulation target for improving cognitive function in patients with AD, was most effective (Cotelli et al., 2011; Wu et al., 2015). Use of rTMS on the DLPFC improved cognition by directly stimulating this cortical region and activating connective circuits in distal structures (Dong et al., 2018). Our data differed from that of Alcalá-Lozano et al. (2018), which reported that rTMS over the left DLPFC and the six brain regions (Broca's area, Wernicke's area, bilateral DLPFC and bilateral pSAC) were similarly effective for improvement of cognitive function. Further studies are needed to determine the optimal targets for rTMS. In addition, our subgroup analysis of number of treatment sessions showed that long-term treatment (≥20 sessions) may have resulted in better cognitive improvement in patients with AD. Our findings agree with those of Lin et al. (2019), Jiang et al. (2020), Wang et al. (2020), and Xie et al. (2021).

Previous meta-analyses have reported significant effects (Sitzer et al., 2006; Cheng et al., 2018; Xie et al., 2021) and no effects (Lin et al., 2019; Chu et al., 2021) of combined CT with rTMS. In our study, the combination of rTMS and CT did not result in additional improvement. These results indicated that rTMS and CT may not have induced additive effects, and the combination may be counterproductive. Little is known about the underlying mechanisms by which rTMS and CT improve cognition. De Marco et al. suggested that cognitive

training increased default mode network (DMN) connectivity in individuals with MCI, and a recent study noted that rTMS could induce deactivation of functional connectivity within the DMN to reduce cognitive deficits in patients with amnestic mild cognitive impairment (De Marco et al., 2018; Cui et al., 2019). Further studies are needed to explore the complexity of brain functional networks in patients with AD. However, Chu et al. indicated that CT may have been more effective for treatment of early AD than rTMS (Chu et al., 2021). Our results should be interpreted with caution since the subgroups had different sample sizes, and the CT designs were not consistent across the included studies.

The effective duration of rTMS in patients was also evaluated. In our meta-analysis, the effects of rTMS treatment lasted for 1–1.5 months, as determined using ADAS-Cog. Furthermore, outcomes were poorer with increased follow-up time. However, few studies have evaluated the duration of the effects of rTMS on cognition. Cotelli et al. (2011) showed persistent effects on sentence comprehension for 2 months with either 2 or 4 weeks of rTMS treatment applied over the left DLPFC. This finding agreed with the findings of another study that showed cognitive function improvement for 3 months after 5 days 20 Hz rTMS over the bilateral DLPFC (Ahmed et al., 2012). More data are needed to characterize the duration of the effects of rTMS treatment. Long-term effects may be related to modifications in functional connectivity of brain networks and synaptic plasticity in patients with AD patients through rTMS, because memory and learning activity can be regulated by synaptic neuronal activities (Demirtas-Tatlidede et al., 2013; Zhang et al., 2019). Furthermore, studies mainly reported off-line general cognitive improvement in early AD with less gray matter atrophy, which supported the role of network and synaptic impairment in patients with AD (Ahmed et al., 2012; Anderkova et al., 2015; Lee et al., 2016; Zhao et al., 2017). To determine the duration of rTMS efficacy and to determine the mechanisms underlying the effects of rTMS, future RCTs should include data on cortical excitability and functional magnetic resonance imaging.

Limitations

This study was subject to the following limitations. First, we only focused on global cognitive ability of patients with AD, and it is possible we missed some Chinese literature due to the limited database searches we performed. Second, the optimal rTMS parameters are unclear because of small sample sizes and heterogeneous stimulation parameters of the included studies. Finally, because of the small number of included articles using both ADAS-cog and MMSE, consistent criteria for subgroup divisions for the two scales were difficult to determine. We only compared the efficacy of rTMS using ADAS-cog and MMSE at follow-up, which might have limited the ability to explore the differences between MMSE and ADAS-cog for evaluation of cognitive function. The results in the follow-up subgroup analysis showed that ADAS-Cog and MMSE differed in global cognitive function results in patients with AD, which led to the clinical evaluators having to choose the appropriate measure based on the intrinsic characteristics of the scales and the requirements for assessments.

Conclusion

In conclusion, our meta-analysis showed that rTMS is a safe add-on therapy that induces cognitive enhancements in patients with AD. Patients with AD benefitted most from multiple high frequency rTMS sessions over the DLPFC, and post-treatment improvements persisted for at least 1 month. However, the optimal parameters of rTMS therapy could not be determined due to the limitations of the included studies. Additional investigations with large sample sizes and long-term follow-up are required to determine optimal rTMS parameters and to evaluate the long-term efficacy of rTMS for treatment of AD. Differences in ADAS-cog and MMSE scores also suggested that the clinical evaluator should choose the appropriate instrument based on the intrinsic characteristics of the scales and the requirements for assessments.

Data availability statement

The original contributions presented in the study are included in the article/Supplementary material, further inquiries can be directed to the corresponding author/s.

Author contributions

YS and TW conceived and propelled the study. TZ, YS, and QL screened literature and finished data extraction. XX and WD were in charge of risk of bias assessment and statistical analyses. TZ wrote and edited the manuscript. YZ offered guidance on meta methodology. All authors contributed to the article and approved the submitted version.

Funding

This study was funded by the National Key R&D Program of China (Nos. 2018YFC2001600 and 2018YFC2001603) and the Nanjing Municipal Science and Technology Bureau (No. 2019060002).

Acknowledgments

We appreciated all the authors of included original studies sincerely.

Conflict of interest

The authors declare that the research was conducted in the absence of any commercial or financial relationships that could be construed as a potential conflict of interest.

Publisher's note

All claims expressed in this article are solely those of the authors and do not necessarily represent those of their affiliated organizations, or those of the publisher, the editors and the reviewers. Any product that may be evaluated in this article, or claim that may be made by its manufacturer, is not guaranteed or endorsed by the publisher.

Supplementary material

The Supplementary Material for this article can be found online at: https://www.frontiersin.org/articles/10.3389/fnagi.2022.984708/full#supplementary-material

References

Ahmed, M. A., Darwish, E. S., Khedr, E. M., El Serogy, Y. M., and Ali, A. M. (2012). Effects of low versus high frequencies of repetitive transcranial magnetic stimulation on cognitive function and cortical excitability in Alzheimer's dementia. *J. Neurol.* 259, 83–92. doi: 10.1007/s00415-011-6128-4

Alcalá-Lozano, R., Morelos-Santana, E., Cortés-Sotres, J. F., Garza-Villarreal, E. A., Sosa-Ortiz, A. L., and González-Olvera, J. J. (2018). Similar clinical improvement and maintenance after rTMS at 5 Hz using a simple vs. complex protocol in Alzheimer's disease. *Brain Stimul.* 11, 625–627. doi: 10.1016/j.brs.2017.12.011

Alvarez-Salvado, E., Pallarés, V., Moreno, A., and Canals, S. (2014). Functional MRI of long-term potentiation: imaging network plasticity. *Philos. Trans. R. Soc. Lond. B. Biol. Sci.* 369, 20130152. doi: 10.1098/rstb.2013.0152

Alzheimer's, A. (2018). 2018 Alzheimer's disease facts and figures. *Alzheimers Dementia* 14, 367–425. doi: 10.1016/j.jalz.2018.02.001

Anderkova, L., Eliasova, I., Marecek, R., Janousova, E., and Rektorova, I. (2015). Distinct pattern of gray matter atrophy in mild Alzheimer's disease impacts on cognitive outcomes of noninvasive brain stimulation. *J. Alzheimers Dis.* 48, 251–260. doi: 10.3233/JAD-150067

Ash, E. L., Vakhapova, V., Bova, I., Simon, E., Korem, M., Eldad, M., et al. (2012). Transcranial magnetic stimulation of deep brain regions in Alzheimer's disease: a pilot study. *Ann. Neurol.* 72, S126–S126. doi: 10.1016/j.jalz.2014.05.611

Banerjee, M., and Shenoy, R. R. (2021). Emphasizing roles of BDNF promoters and inducers in Alzheimer's disease for improving impaired cognition and memory. *J. Basic Clin. Physiol. Pharmacol.* 000010151520210182. doi: 10.1515/jbcpp-2021-0182

Bekinschtein, P., Cammarota, M., Izquierdo, I., and Medina, J. H. (2008). BDNF and memory formation and storage. *Neuroscientist* 14, 147–156. doi: 10.1177/1073858407305850

Bliss, T. V., and Collingridge, G. L. (1993). A synaptic model of memory: long-term potentiation in the hippocampus. *Nature* 361, 31–39. doi: 10.1038/361031a0

Brem, A. K., Di Iorio, R., Fried, P. J., Oliveira-Maia, A. J., Marra, C., Profice, P., et al. (2020). Corticomotor plasticity predicts clinical efficacy of combined neuromodulation and cognitive training in Alzheimer's disease. *Front. Aging Neurosci.* 12, 200. doi: 10.3389/fnagi.2020.00200

Chen, X., Chen, S., Liang, W., and Ba, F. (2019). Administration of repetitive transcranial magnetic stimulation attenuates Aβ (1-42)-induced Alzheimer's disease in mice by activating β-catenin signaling. *Biomed. Res. Int.* 2019, 1431760. doi: 10.1155/2019/1431760

Cheng, C. P. W., Wong, C. S. M., Lee, K. K., Chan, A. P. K., Yeung, J. W. F., and Chan, W. C. (2018). Effects of repetitive transcranial magnetic stimulation on improvement of cognition in elderly patients with cognitive impairment: a systematic review and meta-analysis. *Int. J. Geriatr. Psychiatry* 33, e1–e13. doi: 10.1002/gps.4726

Choung, J. S., Kim, J. M., Ko, M. H., Cho, D. S., and Kim, M. (2021). Therapeutic efficacy of repetitive transcranial magnetic stimulation in an animal model of Alzheimer's disease. *Sci. Rep.* 11, 437. doi: 10.1038/s41598-020-80147-x

Chu, C. S., Li, C. T., Brunoni, A. R., Yang, F. C., Tseng, P. T., Tu, Y. K., et al. (2021). Cognitive effects and acceptability of non-invasive brain stimulation on Alzheimer's disease and mild cognitive impairment: a component network meta-analysis. *J. Neurol. Neurosurg. Psychiatry* 92, 195–203. doi: 10.1136/jnnp-2020-323870

Coleman, P. D., and Yao, P. J. (2003). Synaptic slaughter in Alzheimer's disease. *Neurobiol. Aging* 24, 1023–1027. doi: 10.1016/j.neurobiolaging.2003.09.001

Cotelli, M., Calabria, M., Manenti, R., Rosini, S., Zanetti, O., Cappa, S. F., et al. (2011). Improved language performance in Alzheimer disease following brain stimulation. *J. Neurol. Neurosurg. Psychiatry* 82, 794–797. doi: 10.1136/jnnp.2009.197848

Cui, H., Ren, R., Lin, G., Zou, Y., Jiang, L., Wei, Z., et al. (2019). Repetitive transcranial magnetic stimulation induced hypoconnectivity within the default mode network yields cognitive improvements in amnestic mild cognitive impairment: a randomized controlled study. *J. Alzheimers. Dis.* 69, 1137–1151. doi: 10.3233/JAD-181296

De Marco, M., Meneghello, F., Pilosio, C., Rigon, J., and Venneri, A. (2018). Up-regulation of DMN connectivity in mild cognitive impairment via network-based cognitive training. *Curr. Alzheimer Res.* 15, 578–589. doi: 10.2174/1567205015666171212103323

DeKosky, S. T., Scheff, S. W., and Styren, S. D. (1996). Structural correlates of cognition in dementia: quantification and assessment of synapse change. *Neurodegeneration* 5, 417–421. doi: 10.1006/neur.1996.0056

Demirtas-Tatlidede, A., Vahabzadeh-Hagh, A. M., and Pascual-Leone, A. (2013). Can noninvasive brain stimulation enhance cognition in neuropsychiatric disorders? *Neuropharmacology* 64, 566–578. doi: 10.1016/j.neuropharm.2012.06.020

Dong, X., Yan, L., Huang, L., Guan, X., Dong, C., Tao, H., et al. (2018). Repetitive transcranial magnetic stimulation for the treatment of Alzheimer's disease: A systematic review and meta-analysis of randomized controlled trials. *PLoS ONE* 13, e0205704. doi: 10.1371/journal.pone.0205704

Egger, M., Davey Smith, G., Schneider, M., and Minder, C. (1997). Bias in meta-analysis detected by a simple, graphical test. *BMJ* 315, 629–634. doi: 10.1136/bmj.315.7109.629

Jia, Y., Xu, L., Yang, K., Zhang, Y., Lv, X., Zhu, Z., et al. (2021). Precision repetitive transcranial magnetic stimulation over the left parietal cortex improves memory in Alzheimer's disease: a randomized, double-blind, sham-controlled study. *Front. Aging Neurosci.* 13, 693611. doi: 10.3389/fnagi.2021.693611

Jiang, L., Cui, H., Zhang, C., Cao, X., Gu, N., Zhu, Y., et al. (2020). Repetitive transcranial magnetic stimulation for improving cognitive function in patients with mild cognitive impairment: a systematic review. *Front. Aging Neurosci.* 12, 593000. doi: 10.3389/fnagi.2020.593000

Kobayashi, M., and Pascual-Leone, A. (2003). Transcranial magnetic stimulation in neurology. *Lancet Neurol.* 2, 145–156. doi: 10.1016/S1474-4422(03)00321-1

Lee, J., Choi, B. H., Oh, E., Sohn, E. H., and Lee, A. Y. (2016). Treatment of Alzheimer's disease with repetitive transcranial magnetic stimulation combined with cognitive training: a prospective, randomized, double-blind, placebo-controlled study. *J. Clin. Neurol.* 12, 57–64. doi: 10.3988/jcn.2016.12.1.57

Lenz, M., Platschek, S., Priesemann, V., Becker, D., Willems, L. M., Ziemann, U., et al. (2015). Repetitive magnetic stimulation induces plasticity of excitatory postsynapses on proximal dendrites of cultured mouse CA1 pyramidal neurons. *Brain Struct. Funct.* 220, 3323–3337. doi: 10.1007/s00429-014-0859-9

Li, X., Qi, G., Yu, C., Lian, G., Zheng, H., Wu, S., et al. (2021). Cortical plasticity is correlated with cognitive improvement in Alzheimer's disease patients after rTMS treatment. *Brain Stimul.* 14, 503–510. doi: 10.1016/j.brs.2021.01.012

Liao, X., Li, G., Wang, A., Liu, T., Feng, S., Guo, Z., et al. (2015). Repetitive transcranial magnetic stimulation as an alternative therapy for cognitive impairment in Alzheimer's disease: a meta-analysis. *J. Alzheimers. Dis.* 48, 463–472. doi: 10.3233/JAD-150346

Lim, Y. Y., Laws, S. M., Perin, S., Pietrzak, R. H., Fowler, C., Masters, C. L., et al. (2021). BDNF VAL66MET polymorphism and memory decline across the spectrum of Alzheimer's disease. *Genes Brain Behav.* 20, e12724. doi: 10.1111/gbb.12724

Lin, Y., Jiang, W. J., Shan, P. Y., Lu, M., Wang, T., Li, R. H., et al. (2019). The role of repetitive transcranial magnetic stimulation (rTMS) in the treatment of cognitive impairment in patients with Alzheimer's disease: a systematic review and meta-analysis. *J. Neurol. Sci.* 398, 184–191. doi: 10.1016/j.jns.2019.01.038

Moher, D., Liberati, A., Tetzlaff, J., and Altman, D. G. (2010). Preferred reporting items for systematic reviews and meta-analyses: the PRISMA statement. *Int. J. Surg.* 8, 336–341. doi: 10.1016/j.ijsu.2010.02.007

Rabey, J. M., Dobronevsky, E., Aichenbaum, S., Gonen, O., Marton, R. G., and Khaigrekht, M. (2013). Repetitive transcranial magnetic stimulation combined with cognitive training is a safe and effective modality for the treatment of Alzheimer's disease: a randomized, double-blind study. *J. Neural Transm.* 120, 813–819. doi: 10.1007/s00702-012-0902-z

Sitzer, D. I., Twamley, E. W., and Jeste, D. V. (2006). Cognitive training in Alzheimer's disease: a meta-analysis of the literature. *Acta Psychiatr. Scand.* 114, 75–90. doi: 10.1111/j.1600-0447.2006.00789.x

Vlachos, A., Müller-Dahlhaus, F., Rosskopp, J., Lenz, M., Ziemann, U., and Deller, T. (2012). Repetitive magnetic stimulation induces functional and structural plasticity of excitatory postsynapses in mouse organotypic hippocampal slice cultures. *J. Neurosci.* 32, 17514–17523. doi: 10.1523/JNEUROSCI.0409-12.2012

Wang, X., Mao, Z., Ling, Z., and Yu, X. (2020). Repetitive transcranial magnetic stimulation for cognitive impairment in Alzheimer's disease: a meta-analysis of randomized controlled trials. *J. Neurol.* 267, 791–801. doi: 10.1007/s00415-019-09644-y

Wu, Y., Xu, W., Liu, X., Xu, Q., Tang, L., and Wu, S. (2015). Adjunctive treatment with high frequency repetitive transcranial magnetic stimulation for the behavioral and psychological symptoms of patients with Alzheimer's disease: a randomized, double-blind, sham-controlled study. *Shanghai Arch Psychiatry* 27, 280–288.

Xie, Y., Li, Y., Nie, L., Zhang, W., Ke, Z., and Ku, Y. (2021). Cognitive enhancement of repetitive transcranial magnetic stimulation in patients with mild cognitive impairment and early Alzheimer's disease: a systematic review and meta-analysis. *Front. Cell Dev. Biol.* 9, 734046. doi: 10.3389/fcell.2021.734046

Yin, X., Xie, Q., Huang, L., Liu, L., Armstrong, E., Zhen, M., et al. (2021). Assessment of the psychological burden among family caregivers of people living with Alzheimer's disease using the Zarit burden interview. *J. Alzheimers Dis.* 82, 285–291. doi: 10.3233/JAD-210025

Zhang, F., Qin, Y., Xie, L., Zheng, C., Huang, X., and Zhang, M. (2019). High-frequency repetitive transcranial magnetic stimulation combined with cognitive training improves cognitive function and cortical metabolic ratios in Alzheimer's disease. *J. Neural Transm.* 126, 1081–1094. doi: 10.1007/s00702-019-02022-y

Zhao, J., Li, Z., Cong, Y., Zhang, J., Tan, M., Zhang, H., et al. (2017). Repetitive transcranial magnetic stimulation improves cognitive function of Alzheimer's disease patients. *Oncotarget* 8, 33864–33871. doi: 10.18632/oncotarget.13060

frontiers | Frontiers in Aging Neuroscience

TYPE Original Research
PUBLISHED 08 September 2022
DOI 10.3389/fnagi.2022.1004188

OPEN ACCESS

EDITED BY
Le Li,
Northwestern Polytechnical University, China

REVIEWED BY
Jing Jin,
East China University of Science and Technology, China
Zafer Iscan,
Bahçeşehir University, Turkey

*CORRESPONDENCE
Xin Zhang
zx2929108zx@cqu.edu.cn
Ning Jiang
jiangning21@wchscu.cn

SPECIALTY SECTION
This article was submitted to Neurocognitive Aging and Behavior, a section of the journal Frontiers in Aging Neuroscience

RECEIVED 27 July 2022
ACCEPTED 22 August 2022
PUBLISHED 08 September 2022

CITATION
Zhang X, Jiang Y, Hou W and Jiang N (2022) Age-related differences in the transient and steady state responses to different visual stimuli. *Front. Aging Neurosci.* 14:1004188. doi: 10.3389/fnagi.2022.1004188

Age-related differences in the transient and steady state responses to different visual stimuli

Xin Zhang[1]*, Yi Jiang[2,3], Wensheng Hou[1] and Ning Jiang[2,3]*

[1]Bioengineering College, Chongqing University, Chongqing, China, [2]National Clinical Research Center for Geriatrics, West China Hospital, Sichuan University, Chengdu, China, [3]The Med-X Center for Manufacturing, Sichuan University, Chengdu, China

Objective: Brain-computer interface (BCI) has great potential in geriatric applications. However, most BCI studies in the literature used data from young population, and dedicated studies investigating the feasibility of BCIs among senior population are scarce. The current study, we analyzed the age-related differences in the transient electroencephalogram (EEG) response used in visual BCIs, i.e., visual evoked potential (VEP)/motion onset VEP (mVEP), and steady state-response, SSVEP/SSMVEP, between the younger group (age ranges from 22 to 30) and senior group (age ranges from 60 to 75).

Methods: The visual stimulations, including flicker, checkerboard, and action observation (AO), were designed with a periodic frequency. Videos of several hand movement, including grasping, dorsiflexion, the thumb opposition, and pinch were utilized to generate the AO stimuli. Eighteen senior and eighteen younger participants were enrolled in the experiments. Spectral-temporal characteristics of induced EEG were compared. Three EEG algorithms, canonical correlation analysis (CCA), task-related component analysis (TRCA), and extended CCA, were utilized to test the performance of the respective BCI systems.

Results: In the transient response analysis, the motion checkerboard and AO stimuli were able to elicit prominent mVEP with a specific P1 peak and N2 valley, and the amplitudes of P1 elicited in the senior group were significantly higher than those in the younger group. In the steady-state analysis, SSVEP/SSMVEP could be clearly elicited in both groups. The CCA accuracies of SSVEPs/SSMVEPs in the senior group were slightly lower than those in the younger group in most cases. With extended CCA, the performance of both groups improved significantly. However, for AO targets, the improvement of the senior group (from 63.1 to 71.9%) was lower than that of the younger group (from 63.6 to 83.6%).

Conclusion: Compared with younger subjects, the amplitudes of P1 elicited by motion onset is significantly higher in the senior group, which might be

a potential advantage for seniors if mVEP-based BCIs is used. This study also shows for the first time that AO-based BCI is feasible for the senior population. However, new algorithms for senior subjects, especially in identifying AO targets, are needed.

KEYWORDS

age, brain computer interface, steady state motion visual evoked potential, motion onset visual evoked potential, action observation

Introduction

Brain-computer interface (BCI) is a direct communication pathway between the brain and an external device, receiving increasing attention in aging research and geriatrics. A BCI acquires and analyses brain signals in real time and provides a non-muscular channel of communications and control for individuals with disabilities, majority of which are seniors (Wolpaw et al., 2002). In the BCI research, various independent electroencephalogram (EEG) signals or stimuli-dependent EEG signals have been investigated as the source signal for non-invasive BCI paradigms. Among these, event-related desynchronization/synchronization (ERD/ERS) (Wang et al., 2019) and movement related cortical potentials (MRCP) (Niu and Jiang, 2022) are spontaneous and independent modalities, while P300 (Hoffmann et al., 2008), transient visual evoked potential (VEP) (Liparas et al., 2014), and steady-state visual evoked potential (SSVEP) (Vialatte et al., 2010) are stimuli-dependent. In particular, transient VEPs are elicited by light flashing or patterned stimuli at low rates. SSVEPs are evoked by periodic flickers with a stationary distinct spectrum in EEG recordings mainly at the occipital cortical area. Among the various BCI paradigms, the SSVEP-based BCI has the advantage of a high information transfer rate (ITR) and no or little need for subject training to achieve high decoding accuracy. These advantages make it popular in spelling (Chen et al., 2021) and brain-controlled robots (Chen et al., 2020).

To date, BCI applications have mainly focused on assisting people with disability in participating in daily life activities. Senior individuals accounts for a large proportion of individuals disability. The average age of stroke patients admitted was 66 years old reported in China stroke statistics 2019 (Wang et al., 2020). While there are well-documented age-related changes in EEG signals, few studies in the current BCIs literature investigated the feasibility of various EEG modalities in senior population. For example, researchers have shown that there are changes in the brain with age in processing speed, working memory, inhibitory functions, brain structure size, and white matter integrity (Park and Reuter-Lorenz, 2009). A model which is called hemispheric asymmetry reduction in older adults (HAROLD) stated that older adults tended to be less lateralized than younger adults when performing the same task (Cabeza, 2002). A reduced lateralization of ERD was also reported in the elderly when the participants were performing covert hand movements (Zich et al., 2015). In particular, the algorithms in BCI research are almost exclusively developed with data from young population under the age of 30. The above age-related change has been shown to have a dramatic change on algorithms developed from young subjects' data when used in senior population (Chen et al., 2019). For example, the reduced lateralization in older subjects caused the accuracy dropping from 82.3 to 66.4% in sensory-motor rhythm (SMR)-based BCI. As such, careful investigations should be conducted before these BCIs algorithms can be applied in geriatric applications.

Steady-state visual evoked potential is one of the most popular non-invasive BCI modalities, and its age-related effect has been investigated. For example, a BCI spelling performance from young adults (between the ages of 19 and 27) and older adults (between the ages of 54 and 76) was compared. The results showed a significant difference in the ITR between these two groups (Volosyak et al., 2017). Another study reported SSVEP-based BCI performance using the medium frequency range (approximately 15 Hz) and the high-frequency range (above 30 Hz) in 86 subjects aged 18–55 (Volosyak et al., 2011). But that study may not be reflective of the general population. The subjects tended to be young men (25.83 $\pm$ 7.84 years). And a controlled survey has to be carried in the future to examine the effect of age. In addition, a two-class SSVEP-based BCI was tested in young adults, older adults, and ALS patients. The average accuracy reached 96.1% in young adults, 91.8% in older adults, and 81.2% in ALS patients (Hsu et al., 2016). Thus, age seems to have some influence on the performance of the SSVEP-based BCI.

The flickering stimuli used in SSVEP-based BCI can easily cause visual fatigue and has the risk of eliciting seizures, a potential risk increasing with age. Recently, motion stimuli without flickers have been proposed and attracted more attention. For example, periodic motions, such as rotation,

spiral, and radial motion, have been shown to elicit steady-state motion visual evoked potentials (SSMVEPs) (Yan et al., 2018). The SSMVEP-based BCI maintains the low- or no-subject training characteristics of SSVEP-based BCIs, but with the benefit of less visual discomfort (Xie et al., 2012), and higher robustness to competing stimuli (Ravi et al., 2022), among others. Moreover, the perception of motion is one of the fundamental tasks of higher visual systems. The dorsal pathway in the visual system mainly deals with motion, which is a different pathway from that dealing with flicker. Thus, the EEG responses to the motion stimulus is different from that to flicker stimuli. However, to the best knowledge of the authors, no comparison of EEG responses to motion stimuli among different age groups has been reported in the literature.

Steady-state visual evoked potential/steady-state motion visual evoked potential-based BCIs mainly apply to spelling (Chen et al., 2015) and might not directly apply to stroke rehabilitation, which is one of the key sub-group in seniors with disability that BCIs might help. The flicker and the motion stimuli mentioned above can activate the occipital area but have little effect on the sensorimotor area, which is important for stroke rehabilitation purposes (Biasiucci et al., 2018).

The novel action observation (AO)-based BCI shows great potential for promoting motor cortical activation in neural rehabilitation applications. Our recent study showed that observing the carefully designed gaiting stimulus could simultaneously elicit SSMVEPs in the occipital area and induce SMR in the primary sensorimotor area (Zhang et al., 2021b). We have further shown that designed action video of fine hand movements could also simultaneously elicit SSMVEP in the occipital area and SMR in the sensorimotor area (Zhang et al., 2021a). The induced SMR in both cases could be beneficial for motor cortical activation, consequently with great potential in rehabilitation applications. However, the AO-based BCI was only tested in younger subjects, not in senior population.

To evaluate the ability of visual stimuli in BCI, especially the motion stimulus, inducing EEG characteristics in senior subjects, the transient response and the steady state response to three typical paradigms were explored in the current study for the first time. The flicker, motion checkerboard, and AO were selected as the visual stimuli, which were designed with periodic frequency. Not only the steady state response, i.e., SSVEP/SSMVEP, but also the transient response, i.e., VEP/motion onset VEP (mVEP) (Heinrich, 2007), were illustrated in two age groups (young and senior). The amplitudes of the transient components were compared between these two age groups. The feasibility of AO stimuli, such as grasping, the opposition movement, and pinching, eliciting the SSMVEP in senior subjects was also investigated. Furthermore, three typic algorithms, which were widely utilized to identify the target stimulus in the multi-stimuli scenario based on the induced SSVEP/SSMVEP in younger subjects, were investigated to the applicability of dealing with senior EEG signals.

Materials and methods

Participants

Two different age groups of healthy volunteer participants, i.e., a senior group and a young group, participated in this study. Each group contained eighteen subjects. The senior group consisted of four males and 14 females, aged 60–75 years old (mean ± SD: 67.50 ± 4.20), and the younger group consisted of nine males and nine females, aged 22 to 30 years old (mean ± SD: 26.17 ± 2.68). All 36 volunteer participants were naïve to BCI.

Stimulation design

Three different kinds of visual stimulation, i.e., flicker, checkerboard, and AO, as shown in **Figure 1**, were designed to induce the visual evoked potential (transient and steady state) in brain. The stimulations were presented on a liquid crystal display monitor. The screen refresh rate was 60 Hz, i.e., 60 frames per second.

The sampled sinusoidal stimulation method (Chen et al., 2014) was utilized to present visual flickers. The period flicker was intended to elicit SSMVEP. Checkerboard stimulation consists of multiple concentric rings (Zhang et al., 2017, 2019). Each ring was divided into white and black lattices with equal sizes and numbers. Thus, the total areas of the bright and dark regions in each ring were always identical. The multiple rings in the checkerboard contracted as the phase of the sinusoid signal of the targeted frequency changed from 0° to 180° and expanded as the phase changed from 180° to 0°. The period movement was intended to elicit SSMVEPs.

In addition, videos of several hand movements, including grasping, dorsiflexion, the thumb opposition, and pinch, were recorded. A frame rate reduction method (Zhang et al., 2021a) was utilized to generate the AO stimulus. Taking the stimulus of pinch as an example, as shown in **Figure 1D**, each frame was extracted from a video. The same image would last for N/60 s, followed by the next different image. Consequently, the frame rate of the designed stimulus decreased to 60/N Hz. In one cycle of the action movement, there were a total of M_AO captured images. Thus, the frequency of the action movement was 60/($M\_AO \times N$). The background of the stimuli was unchanged so that the subject intuitive perception was that the finger was moving instead of flicker. If the optical frequency of the stimulus was lower than 4 Hz, the SSVEP cannot be induced. Thus, we designed the AO stimulus containing two frequencies, i.e., the frame rate and the frequency of the action movement. The frame rates were higher than 4 Hz to ensure the effective induction of the SSMVEP. The frequencies of the action movement were approximately 1 Hz, within the normal speed of human movement. In addition to the SSVEP/SSMVEP, the onset

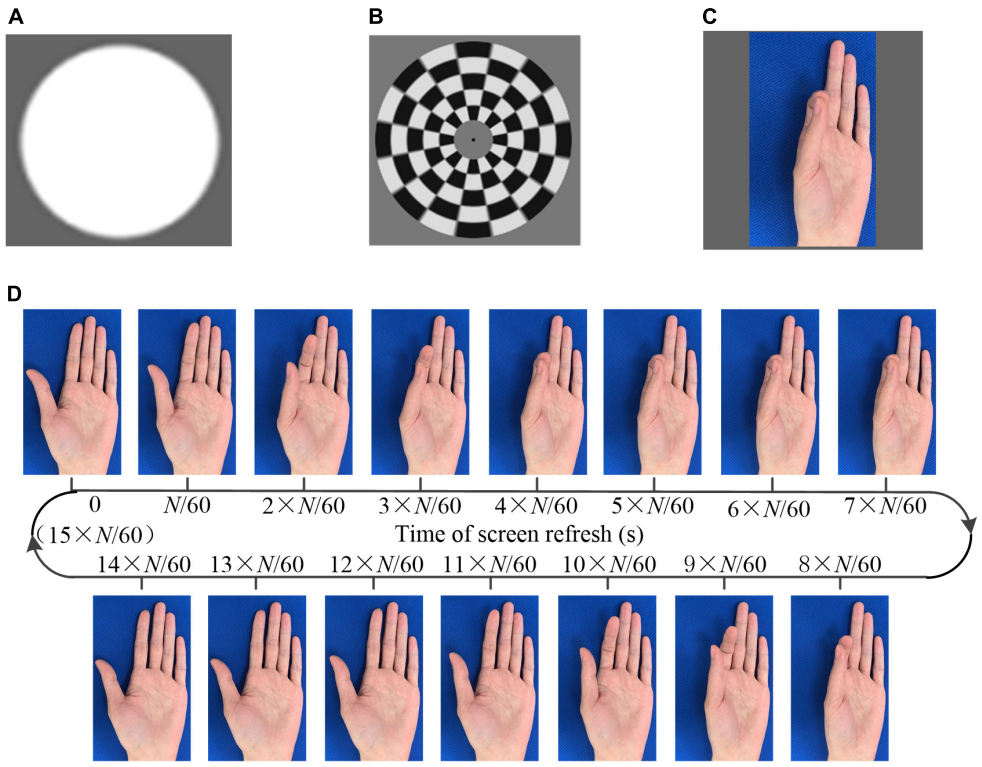

FIGURE 1
The visual stimulation. **(A)** Flicker **(B)** checkerboard **(C)** action observation **(D)** generation of the action observation (AO) stimulus (pinch).

of the visual stimulus was anticipated to elicit VEP/mVEP. The program presenting the stimulus was developed with MATLAB using the Psychophysics Toolbox (Brainard, 1997).

Experimental design

During the experiment, the participant was seated in a comfortable chair and was briefed on the tasks to be performed. In total, four tasks were designed, as shown in Figure 2. Multiple visual stimuli were presented simultaneously in task 1–3. The inter-stimulus distance (ISD) was measured as the visual angles between two individual stimuli. The minimal ISD was 9.46° in the first three tasks. And that ISD had little influence on the decoding performance of SSVEP/SSMVEP-based BCI (Gao et al., 2021). To avoid the unknown effect of competing stimuli which may be a confounding factor for the novel AO stimulus, we further designed task 4 that only one stimulus was presented. Task 1: the subject engaged his or her gaze at the flicker stimulus according to the cues displayed on the screen (Flicker). Task 2: the subject engaged his or her gaze at the checkerboard stimulus (Checkerboard). Task 3: the subject engaged his or her gaze at the AO stimulus and imagined the same movement simultaneously (AO+MI). Task 4: the subject engaged his or her gaze at the AO stimulus and performed the same movement simultaneously (AO+ME). The experimental tasks were designed based on the requirements of the target application, i.e., BCI-based rehabilitation training. In addition to gazing, the participants were instructed to imagine the movement or performance the movement, which will be benefit for rehabilitation training. Thus, the mental tasks were added in the AO stimulus.

Figure 2A illustrates the trial sequence in the experiment. Each trial consisted of three phases: the cue phase, stimulus phase and relaxation phase. For the first three tasks, each trial started with the cue phase (from −2 to 0 s), where one of the four cue letters ("1," "2," "3," and "4") would appear at the screen, at one corner of the screen. It indicated the target stimulus for the current trial, at which participant would then engage his or her gaze during the stimulus phase. The stimulus phase started at 0 s and lasted 5 s. In this phase, the four stimuli (Task 1: Four flicker stimuli. Task 2: Four cherkerbaord stimuli. Task 3: The left-hand opposition movement stimulus, the left-hand pinch stimulus, the right-hand opposition movement stimulus, and the right-hand pinch stimulus) appeared on the four corners of the screen for 5 s. The flicker frequencies of the four flicker stimuli, the motion frequencies of the four checkerboard stimuli, and the frame rates of the four AO stimuli were all 6, 5, 4.615, and 6.667 Hz. For the AO stimulus, the frequencies of the action movement were 0.6, 0.83, 0.58, and

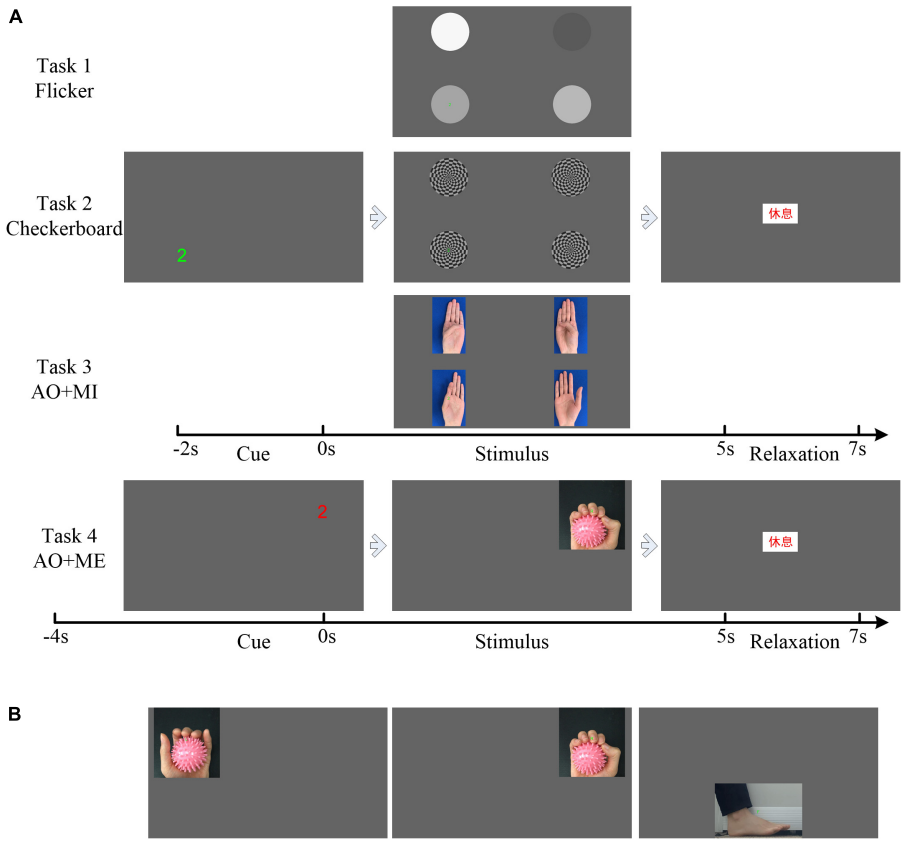

FIGURE 2
Illustration of the experimental protocol. **(A)** The trial sequence of the four tasks. **(B)** The action observation (AO) stimulus in the stimulus phase used in task 4.

1.11 Hz, respectively (M_AO = 10, 6, 8, and 6, respectively). The participants were asked to gaze at the target appearing in the same position as the letter shown in the cue phase or to imagine the movement based on the task requirement mentioned above. This was followed by the 2 s long relaxation phase, during which the participant could relax the gaze. The text "rest" in Chinese appeared on the screen. The videos of the single trial in each task could be found in the **Supplementary material**.

The trial sequence in task 4 was similar to that in task 3. The main differences were the cue phase and the stimulus phase. The duration of the cue phase in task 4 was 4 s, and a countdown in 1 s intervals appeared at the screen in the cue phase. In the stimulus phase, only one stimulus would appear in the same position as the countdown shown in the cue phase. **Figure 2B** shows all possibile AO stimuli (including left-hand grasping, right-hand grasping, and dorsiflexion in the stimulus phase) that could appear in this phase. The frame rates of these three AO stimuli were 10, 6, and 4.615 Hz. The frequencies of the action movement were 1, 1, and 0.77 Hz, respectively (M_AO = 10, 6, and 6, respectively).

For the first three tasks, the experiment consisted of four runs in each task. In each run, each of the four targets was repeated five times in a randomized order resulted in a total of 20 experimental trials. Thus, there were a total of 80 experimental trials for each task. For task 4, the experiment consisted of five runs, and each of the three targets was repeated seven times in a randomized order in each run.

Electroencephalogram data recording

Electroencephalogram signals were recorded using a 32-channel wireless g.Nautilus EEG system (g.tec, Austria). Electrodes were placed at Fp1, Fp2, AF3, AF4, F7, F3, Fz, F4, F8, FC5, FC1, FC2, FC4, T7, C3, Cz, C4, T8, CP5, CP1, CP2, CP6, P7, P3, Pz, P4, P8, PO7, PO3, PO4, PO8, and Oz according to the extended 10/20 system. The reference electrode was located on the right earlobe, and the ground electrode was located on the forehead. A hardware notch filter at 50 Hz was used, and signals were digitally sampled at 500 Hz. All EEG data, event timestamps (the beginning and the end of each trial) and true labels were recorded for subsequent processing.

Target detection

In this study, canonical correlation analysis (CCA), task-related component analysis (TRCA), and extended CCA-based method (extended CCA) were investigated for target stimulus detection and classification based on SSVEPs/SSMVEPs. The classification accuracy was computed to evaluate the target identification performance in different age groups. The classification accuracy is defined as the percentage of the correct predictions out of all predictions. EEG data from electrodes P3, Pz, P4, PO7, PO3, PO4, PO8, and Oz were selected for analysis. EEG data in the stimulus phase were bandpass filtered from 3 to 40 Hz with the Butterworth filter. Then, the three abovementioned methods were utilized to perform classification. The details of the target identification methods are described below.

Canonical correlation analysis-based target identification

Canonical correlation analysis is a statistical way to measure the underlying correlation between two multidimensional variables and has been widely used to detect the frequency of SSVEPs (Lin et al., 2006). It is a training free method. Single trial test data are denoted as $X \in \mathbb{R}^{N_c \times N_s}$. Here, N_c is the number of channels, and N_s is the number of sampling points in each trial. In the current study, multichannel EEG data in the occipital region and sine-cosine reference signals were calculated by the following formula.

$$\rho(x, y) = \frac{E[w_x^T X Y_f{}^T w_y]}{\sqrt{E[w_x^T X X^T w_y E[w_x^T Y_f Y_f{}^T w_y]]}}$$

where ρ is the CCA correlation coefficient and Y_f is the reference signal.

The sine-cosine reference signals are as follows:

$$Y_f = \begin{Bmatrix} \sin \times (2 \times \pi \times f \times t) \\ \cos \times (2 \times \pi \times f \times t) \\ \sin \times (4 \times \pi \times f \times t) \\ \cos \times (4 \times \pi \times f \times t) \end{Bmatrix}$$

where f is the motion frequency.

The target on which the participant focused could be identified by taking the maximum CCA coefficient.

Task-related component analysis-based target identification

Task-related component analysis is an approach to extract task-related components from a linear weighted sum of multiple time series. TRCA was first proposed to maximize the reproducibility during task periods from near-infrared spectroscopy data (Tanaka et al., 2013). As it had the ability to maximize inter-block covariance and to remove task-unrelated artifacts, TRCA was successfully used as a spatial filter to remove background EEG activities in SSVEP-based BCIs (Nakanishi et al., 2018). The spatial filter can be achieved as follows:

$$\omega = \arg\max_{\omega} \frac{\omega^T S \omega}{\omega^T Q \omega}$$

The normalization matrix Q is defined as:

$$Q = \sum_{j_1, j_2 = 1}^{N_c} Cov(x_{j_1}(t), x_{j_2}(t))$$

where $x_{j_1}(t)$ is the EEG data in the j_1-th channel and $x_{j_2}(t)$ is the EEG data in the j_2-th channel. $Cov(.,.)$ represents the cross covariance.

The symmetric matrix $S = (S_{j_1 j_2})_{1 \le j_1, j_2 \le N_c}$ is defined as:

$$S_{j_1 j_2} = \sum_{\substack{h_1, h_2 = 1 \\ h_1 \neq h_2}}^{N_t} Cov(x_{j_1}^{(h_1)}(t), x_{j_2}^{(h_2)}(t))$$

where $x_{j_1}^{(h_1)}(t)$ is the EEG signal in the h_1-th trial in the j_1-th channel. $x_{j_2}^{(h_2)}(t)$ is the EEG signal in the h_2-th trial in the j_2-th channel.

With the help of the Rayleigh-Ritz theorem, the eigenvector of the matrix $Q^{-1}S$ provides the optimal coefficient vector.

If there were four individual training data corresponding to four stimuli in one task, four different spatial filters could be obtained. Then, an ensemble spatial filter $W = [\omega_1\ \omega_2\ \omega_3\ \omega_4]$ was obtained. Through spatial filtering $X^T W$, the test data X were expected to be optimized to achieve maximum performance.

The correlation coefficient was selected as the feature. Pearson's correlation analysis between the single-trial test signal X and averaging multiple training trials as $\overline{\chi}_i = \frac{1}{N_t} \sum_{h=1}^{N_t} \chi_{ih}$ across trials for the i-th stimulus was calculated as $r_i = \rho\left(X^T W, \left(\overline{\chi}_i\right)^T W\right)$. Here, ρ is Pearson's correlation, i indicates the stimulus index, h indicates the index of training trials, and N_t is the number of training trials.

The target on which the participant focused could also be identified by taking the maximum coefficient as $Target = \max(r_i),\ i = 1, 2, 3, 4$.

Extended canonical correlation analysis-based target identification

The extended CCA-based method incorporated individual template signals obtained by averaging multiple training trials as $\overline{\chi}_i$ (Chen et al., 2015). The following three weight vectors are

utilized as spatial filters to enhance the SNR of SSMVEPs: (1) $W_X(X, \overline{\chi}_i)$ between test signal X and individual template $\overline{\chi}_i$, (2) $W_X(X, Y_f)$ between test signal X and the sine-cosine reference signals Y_f, and (3) $W_{\overline{\chi}_i}(\overline{\chi}_i, Y_f)$ between the individual template $\overline{\chi}_i$ and the sine-cosine reference signals Y_f. Then a correlation vector $\hat{r}_i$ is defined as follows.

$$\hat{r}_i = \begin{bmatrix} \rho_{i,1} \\ \rho_{i,2} \\ \rho_{i,3} \\ \rho_{i,4} \end{bmatrix} = \begin{bmatrix} \rho(X, Y_f) \\ \rho(X^T W_X (X, \overline{\chi}_i), \overline{\chi}_i{}^T W_X(X, \overline{\chi}_i)) \\ \rho(X^T W_X (X, Y_f), \overline{\chi}_i{}^T W_X(X, Y_f)) \\ \rho(X^T W_{\overline{\chi}_i}(\overline{\chi}_i, Y_f), \overline{\chi}_i{}^T W_{\overline{\chi}_i}(\overline{\chi}_i, Y_f)) \end{bmatrix}$$

Finally, the following weighted correlation coefficient is used as the feature in target identification.

$$r_i = \sum_{l=1}^{4} sign(\rho_{i,l}) \cdot \rho_{i,l}{}^2$$

where *sign*() is used to retain discriminative information from negative correlation coefficients between the test signals and individual templates.

The target on which the participant focused could also be identified by taking the maximum coefficient.

In addition, a fourfold cross-validation scheme was performed for the first three tasks. One run's data were retained as the validation data for testing, and the other three runs' data were used as training data. There was no overlapping part in either the training or test subsets. The cross-validation process was then repeated four times, with each of the four runs' data used exactly once as the validation data. Similarly, a fivefold cross-validation scheme was performed for the fourth task.

Statistical analysis

A mixed-effect model of ANOVA was used to quantify the differences in the amplitudes of P1 and N2 in each task. The group with two levels (1: senior, 2: young) was one fixed factor. The subject nested within the group and target were two random factors. The mixed-effect model of ANOVA was also used to quantify the differences in the classification accuracies. The method with three levels (1: CCA, 2: TRCA, and 3: extended CCA), data length with three levels (1: 1 s, 2: 3 s, and 3: 5 s), and group with two levels (1: senior and 2: young) were three fixed factors, and subject was a random factor nested within groups.

Results

Temporal characteristics of the induced transient response

High contrast and bright luminance of a visual object was able to evoke VEP, and the motion behavior of visual objects could evoke mVEP. Thus, the transient EEG components immediately following the onset of the visual stimuli were first analyzed. EEG data epochs during the beginning of the stimulus phase (0–0.5 s) were averaged over all trials registered from each of the subjects. **Figure 3** illustrates the grand average waveforms for all senior subjects (blue line) and all younger subjects (red line) at electrode PO8 response to different kinds of stimuli. 0 s referred to the moment when the stimulus occurred on the screen. Overall, the grand average visually evoked potentials in response to target stimuli had a positive deflection (P1) with a latency of 100–160 ms, followed by a negative deflection (N2) with a latency of 160–230 ms post-flicker or postmotion onset. The transient response to the motion stimulus was clearer than that to the flicker. Furthermore, the amplitudes of the P1 and N2 repsonses to the flicker stimulus were similar in these two age groups. But the amplitudes of the P1 and N2 repsonses to the motion stimulus in the senior group were larger than those in the younger group. For example, in the AO+MI task, the amplitudes (mean ± SD) of those two components were 7.70 ± 4.03 μV and −7.01 ± 3.34 μV in senior group, whereas the amplitudes (mean ± sd) of P1 and N2 were 4.69 ± 1.85 μV and −6.01 ± 2.35 μV in younger group.

A mixed-effect model of ANOVA was used to quantify the differences in the amplitudes of P1 and N2 in different tasks. In task 1 (Flicker), the fix factor Group had no significant influences on the amplitudes of P1 [$F_{(1,\ 34)} = 3.71$, $p = 0.063$] and N2 [$F_{(1,\ 34)} = 0.71$, $p = 0.405$]. The random factor Target also had no significant influence on the amplitude of the P1 ($p = 0.126$) and N2 ($p = 0.127$). In task 2 (Checkerboard), the mixed-effect model of ANOVA revealed that the fix factor Group had a significant influence on the amplitudes of the P1 [$F_{(1,\ 32.18)} = 12.12$, $p = 0.001$]. But the Group had no significant influence on the amplitude of N2 [$F_{(1,\ 34)} = 3.78$, $p = 0.06$]. The random factor Target had no significant influence on the amplitude of P1 and N2 responses to the checkerboard stimulus ($p = 0.205$ and 0.132, respectively). For the AO stimulus in task 3 and 4, the mixed-effect model of ANOVA revealed that the fix factor Group had a significant influence on the amplitudes of the P1 in task 3 [$F_{(1,\ 34)} = 10.1$, $p = 0.003$] and in task 4 [$F_{(1,6.98)} = 11.82$, $p = 0.011$]. But the Group had no significant influence on the amplitude of N2 in task 3 [$F_{(1,31.97)} = 1.31$, $p = 0.216$] and in task 4 [$F_{(1,7.81)} = 1.7$, $p = 0.229$]. The random factor Target had no significant influence on the amplitude of P1 and N2 in task 3 ($p = 0.161$ and 0.137, respectively) and in task 4 ($p = 0.276$ and 0.19, respectively).

In addition, the type of motion (translation, contraction, expansion, and rotation) might differentially affect the spatial and temporal characteristics of mVEP (Delon-Martin et al., 2006). For example, the N2 component response to the moving line (moving leftward) had an asymmetrical activation in occipito-temporal area (Wang et al., 2006). The P1 and N2 components that respond to expansion and contraction, such as Newton's ring stimulus or the checkerboard stimulus, exhibited

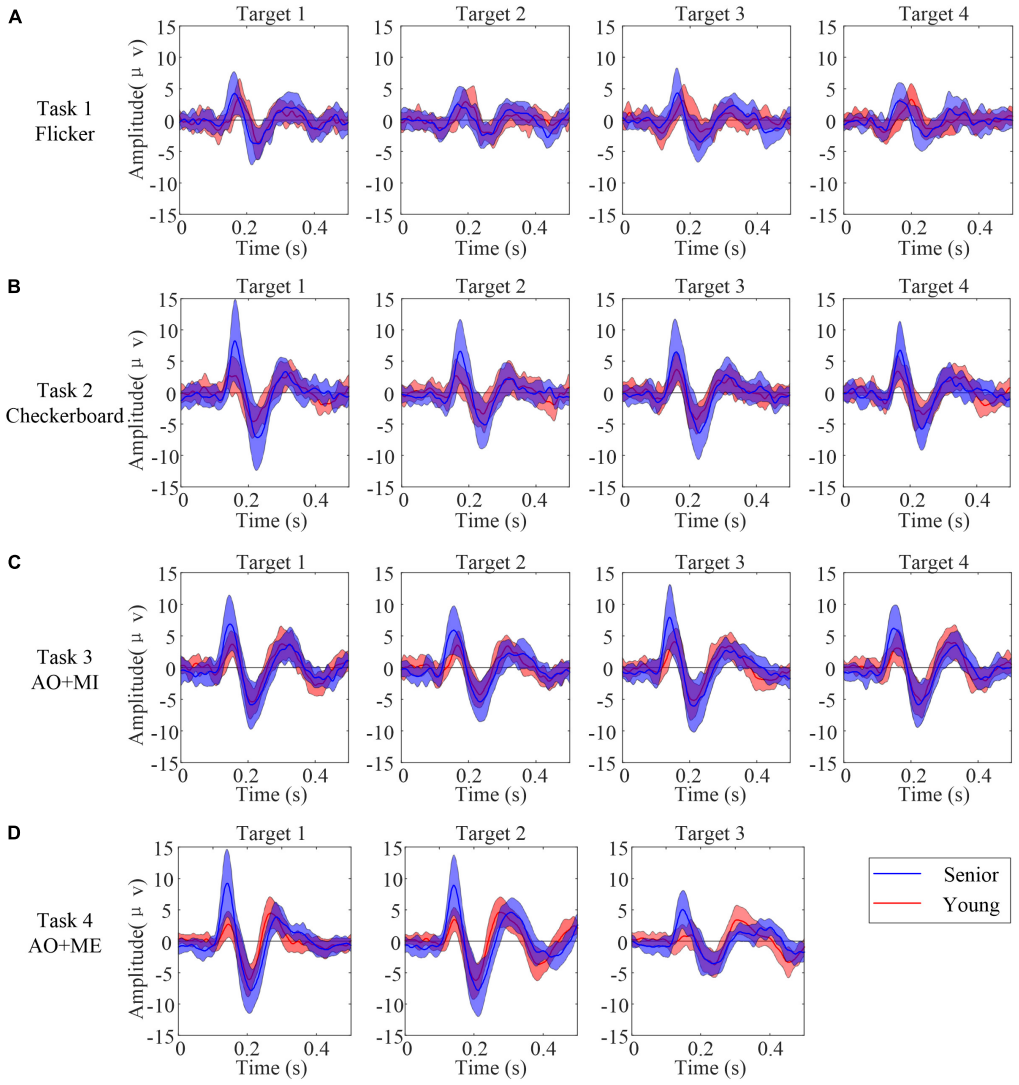

FIGURE 3
The grand average waveforms for all senior subjects (blue line) and all younger subjects (red line) at electrode PO8 response to different kinds of stimuli. 0 indicate the onset of the stimulus. The center dashed line shows the averaged amplitudes while the shading around the dash line indicates averaged amplitudes ± SD. **(A)** Task 1 **(B)** task 2 **(C)** task 3 **(D)** task 4.

symmetrical activations in the occipital lobe (Xie et al., 2012). Thus, as the AO stimulus was a new paradigm, the topographies for P1 and N2 in task 3 were further analyzed. **Figure 4** illustrates the grand average amplitude topographic maps of target 1 among all the senior subjects and all the younger subjects at 140 ms and 210 ms. In both age groups, the topographies for P1 and N2 were all nearly symmetric.

Spectral characteristics of the induced steady state response

In addition to the above induced transient response, the steady-state rhythmic EEG components in different age groups were explored. The steady-state response is mainly reflected in frequency domain. Thus, the spectral characteristics of SSVEP/SSMVEP induced by the stimuli in different age groups were analyzed. The spectra of the EEG data in the stimulus phase (0–5 s) were calculated. **Figure 5** illustrates the spectra of EEG data averaged from all trials and all subjects in the same age group (blue line: senior and red line: young) from Oz in different tasks. Overall, for all stimulus frequencies, a clean peak at the stimulus frequency in each spectrum was clearly situated at the corresponding frequency when subjects in both age groups stared at each target. The second harmonic of the stimulus frequencies were either unexpectedly weak or completely absent in SSMVEPs induced by the checkerboard, which was different from the

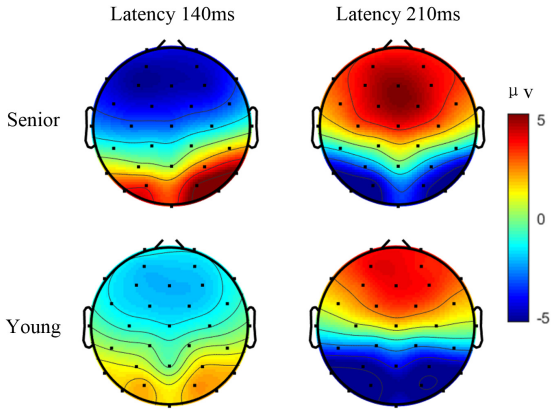

FIGURE 4
The grand average amplitude topographic maps of target 1 in task 3 among all the senior subjects and all the younger subjects at 140 and 210 ms.

SSVEPs induced by the flicker. For the AO stimulus, the second harmonic of the stimulus frequencies occurred in some targets.

Furthermore, for the SSVEPs induced by the flicker, the averaged amplitudes of the peak at the flicker frequencies in senior subjects were slightly lower than those in younger subjects. For the SSMVEP induced by the checkerboard, the averaged amplitudes of the peak at the motion frequencies between senior subjects and younger subjects were highly similar. For the SSMVEP induced by the AO stimulus, the averaged amplitudes of the peak at the frame rates in these two age groups were different among different targets.

Classification accuracies

To compare the BCI system performance between senior subjects and younger subjects, three algorithms were utilized to detect SSVEPs/SSMVEPs and classify the target stimulus. Figure 6 illustrates the classification accuracies with different data lengths in different age groups (green line: senior and red line: young). As expected, with the increase in the EEG epoch length, the classification accuracies increased monotonically in both groups, regardless of the algorithm used. The average accuracies in the senior group were lower than those in the younger group utilizing the CCA-based method, TRCA-based method and extended CCA-based method in most cases.

A mixed-effect model of ANOVA was used to quantify the differences in the accuracies in each task. The analysis results showed that the fix factors method and data length both had a significant effect on the accuracies (all $p < 0.001$) in all tasks, as expected. However, the fix factor group had no significant effect on the accuracies in all tasks [task 1: $F_{(1,\ 34)} = 0.34$, $p = 0.564$, task 2: $F_{(1,\ 34)} = 1.6$, $p = 0.214$, task 3: $F_{(1,\ 34)} = 1.73$, $p = 0.198$, and task 4: $F_{(1,\ 34)} = 2.58$, $p = 0.117$].

In addition, compared with the CCA-based method, the TRCA-based method mainly achieved superior performance with a 1 s data length in both groups. The extended CCA-based method achieved the best identification performance in all data lengths in both groups compared with the other two methods. Moreover, the accuracy of identifying the traditional flicker stimulus was highest compared with other stimuli in both groups. The average accuracy achieved 93.75 ± 10.33% within 5 s data length in the senior group. And the average accuracy achieved 97.85 ± 2.93% within 5 s data length in the younger group. The accuracy of identifying the motion checkerboard stimulus was slightly lower. The average accuracies achieved were 86.39 ± 16.37% in the senior group and 93.96 ± 5.68% in the younger group. The accuracy of identifying the AO stimulus in task 3 was lowest compared with other stimuli. The average accuracies were 71.88 ± 18.68% in the senior group and 83.61 ± 14.08% in the younger group. While the average accuracies of identifying the AO stimulus in task 4 (three targets) achieved 87.09 ± 12.87% in the senior group and 92.65 ± 8.47% in the younger group.

Furthermore, the difference in the accuracies utilizing the CCA-based method between these two age groups was similar. However, differences in the accuracies utilizing the TRCA-based method or extended CCA-based method were great, especially when identifying AO stimuli. For example, in task 3, the average accuracy utilizing the extended CCA-based method increased 20% compared with the CCA-based method with 5 s data length in the younger group. However, in the senior group, the accuracies utilizing the extended CCA-based method only increased 8.8% compared with those utilizing the CCA-based method. A pairwise t-test revealed that the senior group had a significantly larger difference in the accuracies, utilizing the extended CCA-based method and the accuracies utilizing the CCA-based method with 5 s data length, than the younger group ($t = -3.35$, $p = 0.004$) in task 3.

To further compare the relative identification performance of the stimulus targets based on the multichannel classification methods in different age groups, the confusion matrices of the identification accuracy utilizing the extended CCA-based method with 5 s data length for all participants in the same age group were calculated, as shown in Figure 7. The color scale revealed the average classification accuracies and the diagonals labeled the correct classification accuracies among all the participants. We observed that the influence of the four stimulus frequencies on the accuracies was not too great. We also observed that the identification accuracy of the target 4 was lower than other targets in task 3, which might be caused of the unexpected peak in the spectrum and inducing the low amplitude at the stimulus frequency in target 4 as shown in Figure 5C.

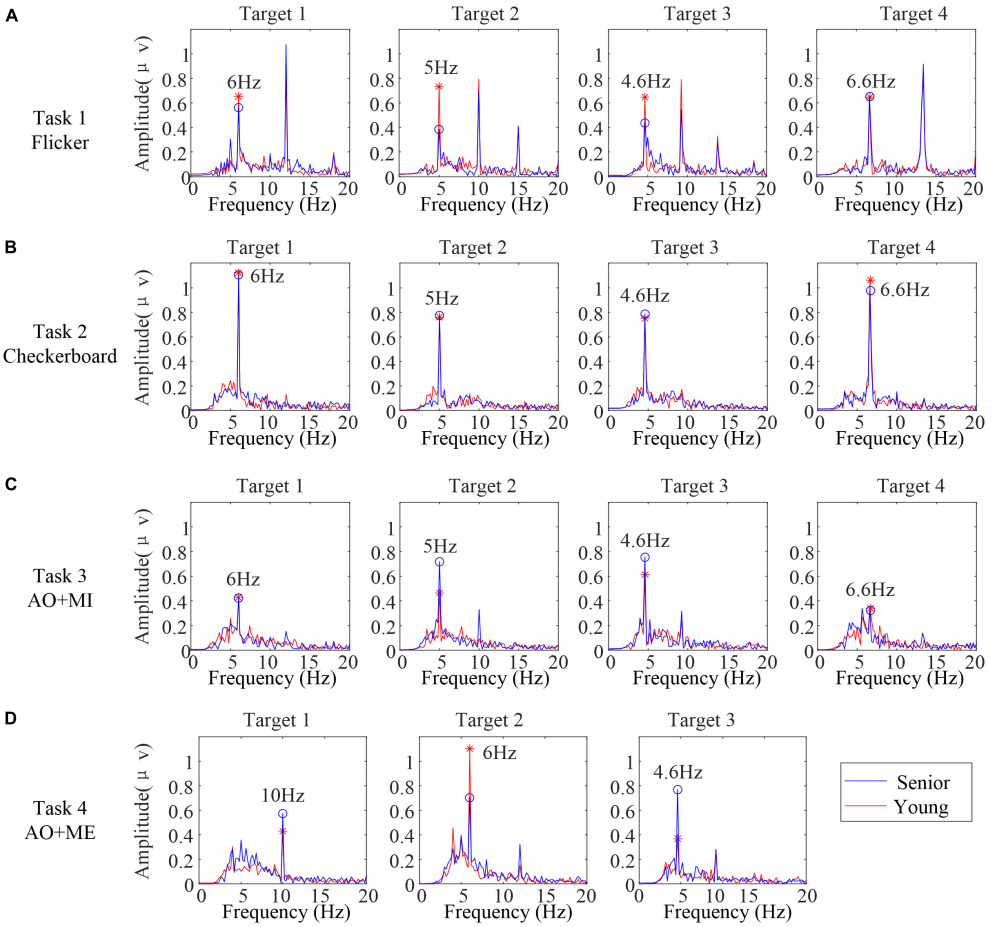

FIGURE 5
The spectra of electroencephalogram (EEG) data averaged from all the trials and all the subjects in the same age group from Oz in different tasks. **(A)** Task 1 **(B)** task 2 **(C)** task 3 **(D)** task 4.

Discussion and conclusion

The results of the current study indicate that (1) the motion checkerboard and AO stimuli are able to elicit prominent mVEP with specific P1 peak and N2 valley. The amplitude of the P1 peak in the senior group was significantly higher than that in the younger group, which might be a potential advantage for seniors in leveraging mVEP detection to identify when the user engages with a visual stimulus. (2) Except for the traditional flicker and the checkerboard stimulus with periodic frequency, the newly designed AO stimulus can also elicit clearly SSMVEPs at the stimulus frequency in the senior group. As such, the SSVEP/SSMVEP-based BCI is feasible for the senior population. And with the AO stimuli, it has great potential for rehabilitation applications, common in senior population.

To the best of our knowledge, this is the first study to report the differences in both transient response and steady-state response to different kinds of visual stimuli between younger subjects and senior subjects. In the literature, one study utilized the approach of capturing the EEG segment occurring at the onset of the SSVEP stimulus to analyze the transient VEP (Xie et al., 2012). And the spectral-temporal characteristics of the EEG induced by the checkerboard are similar to the results in that study, which utilized the oscillating Newton's rings as the motion stimuli with young subjects.

In general, low stimulus frequencies (lower than 4 to 6 Hz) could evoke a transient VEP. As the stimulus frequencies increase, the EEG responses overlap one another and merge into the steady state. Thus, transient VEP only occurs at the stimulus onset, and then the EEG response changes into SSVEPs/SSMVEPs in each trial in the current study. In contrast with flash VEP, mVEP has a much lower amplitude decrease with increasing retinal eccentricity (Schlykowa et al., 1993). mVEP displays the largest amplitudes and the lowest inter- and intra-subject variabilities (Guo et al., 2008). This might be the reason that the motion stimulus elicits strong mVEP, while the transient VEP elicited by the flicker was weak in the current study.

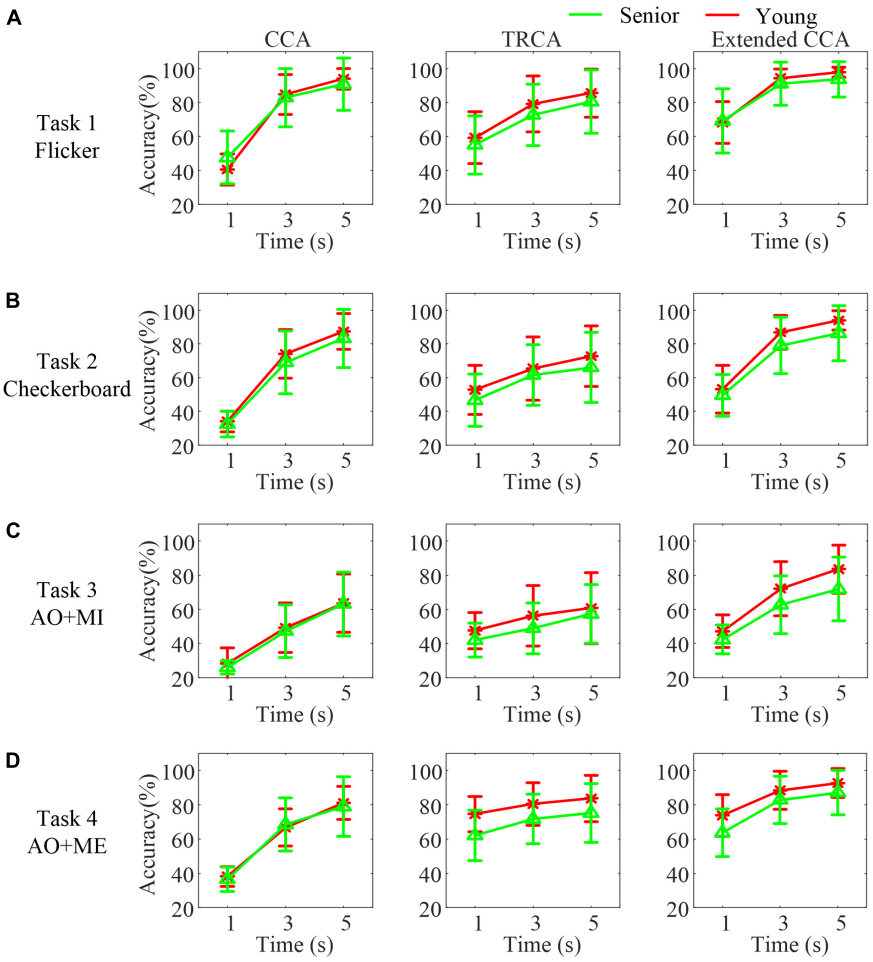

FIGURE 6
The classification accuracies with different data lengths in different age groups in different tasks. **(A)** Task 1 **(B)** task 2 **(C)** task 3 **(D)** task 4.

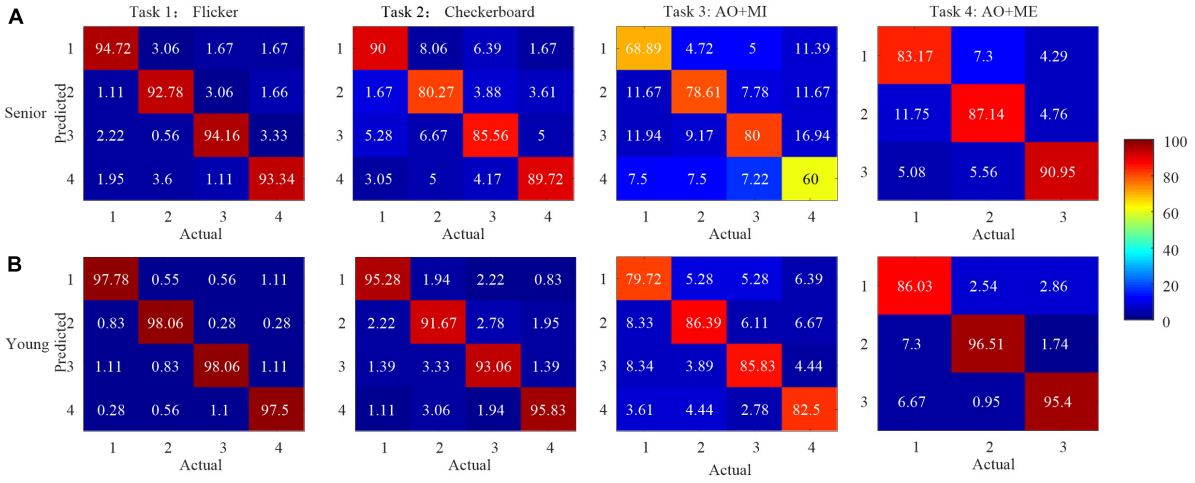

FIGURE 7
The confusion matrices of the identification accuracy (%) utilizing extended canonical correlation analysis (CCA)-based method with 5 s data length for all participants in the same age group in different tasks. **(A)** Senior group **(B)** younger group.

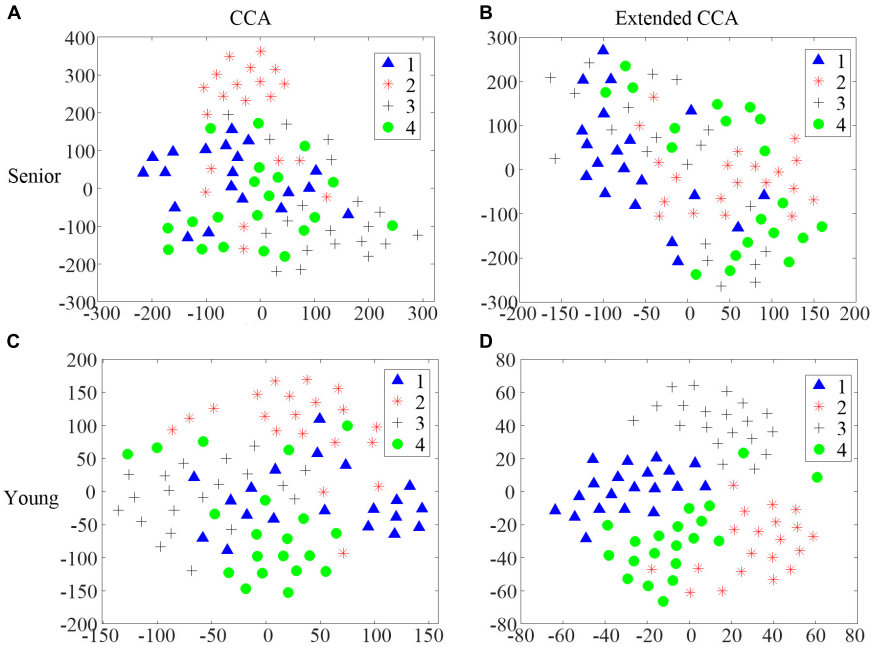

FIGURE 8
The t-distributed stochastic neighbor embedding (t-SNE) of the correlation coefficients in different age groups. **(A)** The distribution of the CCA correlation coefficient ρ in S9 in the senior group. **(B)** The distribution of the weighted correlation coefficient *r* in S9 in the senior group. **(C)** The distribution of the CCA correlation coefficient ρ in S9 in the younger group. **(D)** The distribution of the weighted correlation coefficient *r* in S9 in the younger group.

Interestingly, the significantly larger amplitude in P1 in mVEP in the senior group was unexpected. One possible reason is that the senior subjects paid more attention than younger subjects, when either checkerboard or AO stimulus was presented. Many senior subjects reported, post-experiment, that they were involuntarily counting the times of the movement in the stimulus during the experiments, while no participants in the younger group reported doing so. Previous studies found that the amplitudes of mVEP components can be modulated by attention (Torriente et al., 1999). "Counting" may help subjects to be more engaged and concentrate more on the target stimulus. In the literature, larger amplitudes of VEP in older females, compared with younger females, were reported, in which the authors suggested that this was due to a heightened sensitivity of the older female visual system to patterned stimuli (La Marche et al., 1986). Furthermore, the characteristics of mVEP are influenced by the type of visual stimuli. The reason for the larger amplitude in mVEP still needs further investigation. The characteristics of the mVEP in senior subjects may provide a valuable signal modality in designing more appropriate BCIs for targeting the senior population. This will be the focus of our future studies. Moreover, the HAROLD model is mainly supported by evidence in the domains of episodic memory, semantic memory, working memory, perception, and inhibitory control. For the EEG response to the visual stimulus, it exhibited symmetrical activations in the occipital lobe as shown in **Figure 4**. The HAROLD model seems to be not applicable.

On the other hand, the steady-state response, i.e., SSVEP/SSMVEP, provides an even more robust way of determining the subject's choice of visual target. While no significant difference was found, the average accuracy of identifying the flicker stimulus achieved 93.75% in senior subjects, which was lower than the accuracy in younger subjects (97.85%), with no statistical significance. A similar level of difference in accuracies in these two age groups was also reported a prior study (Volosyak et al., 2017). The current study also reported that no significant difference was found in the accuracies of identifying the checkerboard stimulus or the AO stimulus in the two age groups despite no previous reports. Consistent with this lack of difference, the BCI performance between the two groups were not significant. This might be because the EEG data from channels O1, O2, and POz were not utilized in the classification. Limited by the EEG device, where the positions of the electrodes are fixed and no electrodes were located at O1, O2, and POz.

In the current study, three popular SSVEP algorithms were investigated. In recent literature, many studies have utilized TRCA-based methods to process SSVEPs with short durations (<1 s) and have reported enhanced performance (Nakanishi et al., 2018). The current study also achieved improved accuracy with 1 s data length compared with the

more traditional CCA-based method. However, for longer data lengths, the current study found no difference in performance between CCA-based and TRCA-based methods. Furthermore, the extended CCA-based method achieved the highest accuracy in three data lengths.

It is worth noting that the improvement in accuracy, utilizing the extended CCA-based method compared with the CCA-based method, in the senior group was significantly lower than that in the younger group for the AO stimulus in task 3. Even though the accuracies utilizing the CCA-based method were similar between these two age groups, the distributions of the CCA correlation coefficient were quite different. T-distributed stochastic neighbor embedding (t-SNE) (Van Der Maaten and Hinton, 2008) was utilized to visualize the distribution of the CCA correlation coefficient ρ and the weighted correlation coefficient r in different groups. **Figure 8** illustrates the t-SNE of S9 in the senior group and S9 in the younger group. The classification accuracy was 70% utilizing the CCA-based method in S9 in the senior group. S9 in the younger group achieved slightly lower accuracy, i.e., 68.75%. The target on which the participant focused was identified by taking the maximum CCA coefficient. However, the boundaries among the four categories are clearer for the younger group (**Figure 8C**), than in the senior group (**Figure 8A**). This implies that the quality of the individual training data to build the CCA-based spatial filter, as distributed in the extended CCA-based method, is better in the younger group. Thus, the extended CCA-based method achieved better performance improvement in the younger group, which could also be reflected in **Figures 8B,D**. Thus, detecting SSMVEPs induced by AO stimuli for seniors calls for better more complex algorithms, which is another research direction.

Furthermore, the current study shows for the first time that the AO-based BCI is feasible for the senior population. The average accuracies of identifying the target stimulus on which the senior participant focused among four AO stimuli (i.e., the left-hand opposition movement, the left-hand pinch, the right-hand opposition movement, and the right-hand pinch) and three AO stimuli (i.e., left-hand grasping, right-hand grasping, and dorsiflexion) reached 71.88 ± 18.68% and 87.09 ± 12.87%, respectively. It is observed that the accuracies in these two tasks are quite different. Even though the stimulations are both AO stimuli in task 3 and task 4, several differences exist. First, it is the four-target classification in task 3, while it is the three-target classification in task 4. In addition, the parameters of the AO stimulus, such as different frame rates and different actions, are different. This finding is in line with our recent study, which showed that the parameters of the AO stimulus influence the classification accuracy (Zhang et al., 2021a).

Overall, the current study reports the differences in spectral-temporal characteristics of the EEG induced by the three types of visual stimuli: flicker, checkerboard, and AO, in both senior and younger groups. The characteristics of the mVEP in senior subjects may provide a valuable signal modality in designing more appropriate BCIs for targeting the senior population. Not only the traditional flicker and the checkerboard stimulus with periodic frequency but also the newly designed AO stimulus, including various actions, could clearly elicit SSMVEP at the stimulus frequency in both age groups. The accuracies of identifying SSVEP/SSMVEP in the senior group were slightly lower than those in the younger group. These findings may be helpful for researchers designing algorithms to achieve high classification performance, specifically for senior subjects. In addition, current study focused on the transient and steady state responses in occipital cortex to different visual stimuli in senior and younger subjects and investigating the applicability of typical algorithms in dealing with senior EEG signals. Analysis of the SMR and the brain network in task 3 and 4 will be our next study.

Data availability statement

The raw data supporting the conclusions of this article will be made available by the authors, without undue reservation.

Ethics statement

The studies involving human participants were reviewed and approved by the Ethical Committee of West China Hospital of Sichuan University. The patients/participants provided their written informed consent to participate in this study.

Author contributions

XZ drafted the manuscript and analyzed the EEG data. NJ and WH provided the suggestion of experiment design. XZ and YJ collected the EEG data. NJ revised the manuscript. All authors contributed to the article and approved the submitted version.

Funding

This work was supported by the National Key R&D Program of China under Grant 2020YFC2004200, China Postdoctoral Science Foundation under Grant 2021M700605, and Postdoctoral Research Program of Chongqing under Grant 2021XM3060.

Acknowledgments

We would like to thank the participants for participating in these experiments and reviewers for their helpful comments.

Conflict of interest

The authors declare that the research was conducted in the absence of any commercial or financial relationships that could be construed as a potential conflict of interest.

Publisher's note

All claims expressed in this article are solely those of the authors and do not necessarily represent those of their affiliated organizations, or those of the publisher, the editors and the reviewers. Any product that may be evaluated in this article, or claim that may be made by its manufacturer, is not guaranteed or endorsed by the publisher.

Supplementary material

The Supplementary Material for this article can be found online at: https://www.frontiersin.org/articles/10.3389/fnagi.2022.1004188/full#supplementary-material

References

Biasiucci, A., Leeb, R., Iturrate, I., Perdikis, S., Al-Khodairy, A., Corbet, T., et al. (2018). Brain-actuated functional electrical stimulation elicits lasting arm motor recovery after stroke. *Nat. Commun.* 9:2421. doi: 10.1038/s41467-018-04673-z

Brainard, D. H. (1997). The psychophysics toolbox. *Spat. Vis.* 10, 433–436. doi: 10.1163/156856897X00357

Cabeza, R. (2002). Hemispheric asymmetry reduction in older adults: The HAROLD model. *Psychol. Aging* 17, 85–100. doi: 10.1037/0882-7974.17.1.85

Chen, M. L., Fu, D., Boger, J., and Jiang, N. (2019). Age-related changes in vibro-tactile EEG response and its implications in BCI Applications: A comparison between older and younger populations. *IEEE Trans. Neural Syst. Rehabil. Eng.* 27, 603–610. doi: 10.1109/TNSRE.2019.2890968

Chen, X., Chen, Z., Gao, S., and Gao, X. (2014). A high-ITR SSVEP-based BCI speller. *Brain Comput. Interfaces* 1, 181–191. doi: 10.1080/2326263X.2014.944469

Chen, X., Huang, X., Wang, Y., and Gao, X. (2020). Combination of augmented reality based brain- computer interface and computer vision for high-level control of a robotic arm. *IEEE Trans. Neural Syst. Rehabil. Eng.* 28, 3140–3147. doi: 10.1109/TNSRE.2020.3038209

Chen, X., Wang, Y., Nakanishi, M., Gao, X., Jung, T. P., and Gao, S. (2015). High-speed spelling with a noninvasive brain-computer interface. *Proc. Natl. Acad. Sci. U.S.A.* 112, E6058–E6067. doi: 10.1073/pnas.1508080112

Chen, Y., Yang, C., Ye, X., Chen, X., Wang, Y., and Gao, X. (2021). Implementing a calibration-free SSVEP-based BCI system with 160 targets. *J. Neural Eng.* 15:046094. doi: 10.1088/1741-2552/ac0bfa

Delon-Martin, C., Gobbelé, R., Buchner, H., Haug, B. A., Antal, A., Darvas, F., et al. (2006). Temporal pattern of source activities evoked by different types of motion onset stimuli. *Neuroimage* 31, 1567–1579. doi: 10.1016/j.neuroimage.2006.02.013

Gao, Y., Ravi, A., and Jiang, N. (2021). "Does inter-stimulus distance influence the decoding performance of SSVEP and SSMVEP BCI?," in *Proceedings of the 10th International IEEE/EMBS Conference on Neural Engineering (NER) 2021*, (Manhattan, NY: IEEE), 507–510. doi: 10.1109/NER49283.2021.9441069

Guo, F., Hong, B., Gao, X., and Gao, S. (2008). A brain-computer interface using motion-onset visual evoked potential. *J. Neural Eng.* 5, 477–485. doi: 10.1088/1741-2560/5/4/011

Heinrich, S. P. (2007). A primer on motion visual evoked potentials. *Doc. Ophthalmol.* 114, 83–105. doi: 10.1007/s10633-006-9043-8

Hoffmann, U., Vesin, J. M., Ebrahimi, T., and Diserens, K. (2008). An efficient P300-based brain-computer interface for disabled subjects. *J. Neurosci. Methods* 167, 115–125. doi: 10.1016/j.jneumeth.2007.03.005

Hsu, H. T., Lee, I. H., Tsai, H. T., Chang, H. C., Shyu, K. K., Hsu, C. C., et al. (2016). Evaluate the feasibility of using frontal SSVEP to implement an SSVEP-Based BCI in young, elderly and ALS groups. *IEEE Trans. Neural Syst. Rehabil. Eng.* 24, 603–615. doi: 10.1109/TNSRE.2015.2496184

La Marche, J. A., Dobson, W. R., Cohn, N. B., and Dustman, R. E. (1986). Amplitudes of visually evoked potentials to patterned stimuli: Age and sex comparisons. *Electroencephalogr. Clin. Neurophysiol.* 65, 81–85. doi: 10.1016/0168-5597(86)90039-0

Lin, Z., Zhang, C., Wu, W., and Gao, X. (2006). Frequency recognition based on canonical correlation analysis for SSVEP-based BCIs. *IEEE Trans. Biomed. Eng.* 53, 2610–2614. doi: 10.1109/TBME.2006.886577

Liparas, D., Dimitriadis, S. I., Laskaris, N. A., Tzelepi, A., Charalambous, K., and Angelis, L. (2014). Exploiting the temporal patterning of transient VEP signals: A statistical single-trial methodology with implications to brain-computer interfaces (BCIs). *J. Neurosci. Methods* 232, 189–198. doi: 10.1016/j.jneumeth.2014.04.032

Nakanishi, M., Wang, Y., Chen, X., Wang, Y. T., Gao, X., and Jung, T. P. (2018). Enhancing detection of SSVEPs for a high-speed brain speller using task-related component analysis. *IEEE Trans. Biomed. Eng.* 65, 104–112. doi: 10.1109/TBME.2017.2694818

Niu, J., and Jiang, N. (2022). Pseudo-online detection and classification for upper-limb movements. *J. Neural Eng.* 19:036042. doi: 10.1088/1741-2552/ac77be

Park, D. C., and Reuter-Lorenz, P. (2009). The adaptive brain: Aging and neurocognitive scaffolding. *Annu. Rev. Psychol.* 60, 173–196. doi: 10.1146/annurev.psych.59.103006.093656

Ravi, A., Lu, J., Pearce, S., and Jiang, N. (2022). Enhanced system robustness of asynchronous BCI in augmented reality using steady-state motion visual evoked potential. *IEEE Trans. Neural Syst. Rehabil. Eng.* 30, 85–95. doi: 10.1109/TNSRE.2022.3140772

Schlykowa, L., van Dijk, B. W., and Ehrenstein, W. H. (1993). Motion-onset visual-evoked potentials as a function of retinal eccentricity in man. *Cogn. Brain Res.* 1, 169–174. doi: 10.1016/0926-6410(93)90024-Y

Tanaka, H., Katura, T., and Sato, H. (2013). Task-related component analysis for functional neuroimaging and application to near-infrared spectroscopy data. *Neuroimage* 64, 308–327. doi: 10.1016/j.neuroimage.2012.08.044

Torriente, I., Valdes-Sosa, M., Ramirez, D., and Bobes, M. A. (1999). Visual evoked potentials related to motion-onset are modulated by attention. *Vision Res.* 39, 4122–4139. doi: 10.1016/S0042-6989(99)00113-3

Van Der Maaten, L., and Hinton, G. (2008). Visualizing data using t-SNE. *J. Mach. Learn. Res.* 9, 2579–2625.

Vialatte, F.-B., Maurice, M., Dauwels, J., and Cichocki, A. (2010). Steady-state visually evoked potentials: Focus on essential paradigms and future perspectives. *Prog. Neurobiol.* 90, 418–438. doi: 10.1016/j.pneurobio.2009.11.005

Volosyak, I., Gembler, F., and Stawicki, P. (2017). Age-related differences in SSVEP-based BCI performance. *Neurocomputing* 250, 57–64. doi: 10.1016/j.neucom.2016.08.121

Volosyak, I., Valbuena, D., Lüth, T., Malechka, T., and Gräser, A. (2011). BCI demographics II: How many (and What Kinds of) people can use a high-frequency SSVEP BCI? *IEEE Trans. Neural Syst. Rehabil. Eng.* 19, 232–239. doi: 10.1109/TNSRE.2011.2121919

Wang, Y. J., Li, Z. X., Gu, H. Q., Zhai, Y., Jiang, Y., Zhao, X. Q., et al. (2020). China stroke statistics 2019: A report from the National center for healthcare quality management in neurological diseases, China National clinical research center for neurological diseases, the Chinese stroke association, National center for chronic and non-communicable disease control and prevention, Chinese center for disease control and prevention and institute for global neuroscience and stroke collaborations. *Stroke Vasc. Neurol.* 5, 211–239. doi: 10.1136/svn-2020-000457

Wang, Y., Wang, R., Gao, X., Hong, B., and Gao, S. (2006). A practical VEP-based brain-computer interface. *IEEE Trans. Neural Syst. Rehabil. Eng.* 14, 234–239. doi: 10.1109/TNSRE.2006.875576

Wang, Z., Zhou, Y., Chen, L., Gu, B., Yi, W., Liu, S., et al. (2019). BCI monitor enhances electroencephalographic and cerebral hemodynamic activations during motor training. *IEEE Trans. Neural Syst. Rehabil. Eng.* 27, 780–787. doi: 10.1109/TNSRE.2019.2903685

Wolpaw, J. R., Birbaumer, N., McFarland, D. J., Pfurtscheller, G., and Vaughan, T. M. (2002). Brain-computer interfaces for communication and control. *Clin. Neurophysiol.* 113, 767–791. doi: 10.1016/S1388-2457(02)00057-3

Xie, J., Xu, G., Wang, J., Zhang, F., and Zhang, Y. (2012). Steady-state motion visual evoked potentials produced by oscillating Newton's rings: Implications for brain-computer interfaces. *PLoS One* 7:e39707. doi: 10.1371/journal.pone.0039707

Yan, W., Xu, G., Xie, J., Li, M., and Dan, Z. (2018). Four novel motion paradigms based on steady-state motion visual evoked potential. *IEEE Trans. Biomed. Eng.* 65, 1696–1704. doi: 10.1109/TBME.2017.2762690

Zhang, X., Xu, G., Mou, X., Ravi, A., Li, M., Wang, Y., et al. (2019). A convolutional neural network for the detection of asynchronous steady state motion visual evoked potential. *IEEE Trans. Neural Syst. Rehabil. Eng.* 27, 1303–1311. doi: 10.1109/TNSRE.2019.2914904

Zhang, X., Xu, G., Ravi, A., Pearce, S., and Jiang, N. (2021b). Can a highly accurate multi-class SSMVEP BCI induce sensory-motor rhythm in the sensorimotor area? *J. Neural Eng.* 18:35001. doi: 10.1088/1741-2552/ab85b2

Zhang, X., Hou, W., Wu, X., Feng, S., and Chen, L. (2021a). A novel online action observation-based brain-computer interface that enhances event-related desynchronization. *IEEE Trans. Neural Syst. Rehabil. Eng.* 29, 2605–2614. doi: 10.1109/TNSRE.2021.3133853

Zhang, X., Xu, G., Xie, J., and Zhang, X. (2017). Brain response to luminance-based and motion-based stimulation using inter-modulation frequencies. *PLoS One* 12:e0188073. doi: 10.1371/journal.pone.0188073

Zich, C., Debener, S., De Vos, M., Frerichs, S., Maurer, S., and Kranczioch, C. (2015). Lateralization patterns of covert but not overt movements change with age: An EEG neurofeedback study. *Neuroimage* 116, 80–91. doi: 10.1016/j.neuroimage.2015.05.009

frontiers | Frontiers in Aging Neuroscience

TYPE Original Research
PUBLISHED 23 September 2022
DOI 10.3389/fnagi.2022.1006696

OPEN ACCESS

EDITED BY
Howe Liu,
Allen College, United States

REVIEWED BY
Ying Shen,
The First Affiliated Hospital of Nanjing Medical University, China
Qiang Wang,
The Affiliated Hospital of Qingdao University, China

*CORRESPONDENCE
Jie Bao
baojie@suda.edu.cn
Huang Yulun
huangyulun@suda.edu.cn
Min Su
sumin@suda.edu.cn

†These authors have contributed equally to this work and share first authorship

SPECIALTY SECTION
This article was submitted to Neuroinflammation and Neuropathy, a section of the journal Frontiers in Aging Neuroscience

RECEIVED 29 July 2022
ACCEPTED 06 September 2022
PUBLISHED 23 September 2022

CITATION
Cao H, Chen X, Ren X, Chen Z, Liu C, Ni J, Liu H, Fan Y, Xu D, Jin H, Bao J, Yulun H and Su M (2022) Repetitive transcranial magnetic stimulation combined with respiratory muscle training for pulmonary rehabilitation after ischemic stroke—A randomized, case-control study. *Front. Aging Neurosci.* 14:1006696. doi: 10.3389/fnagi.2022.1006696

Repetitive transcranial magnetic stimulation combined with respiratory muscle training for pulmonary rehabilitation after ischemic stroke—A randomized, case-control study

Haiyan Cao[1,2,3†], Xiaoming Chen[1,2†], Xuyan Ren[1,3], Zhiguo Chen[4], Chuandao Liu[4], Jianqiang Ni[4], Haoyu Liu[1,4], Yingjie Fan[1,3], Dandan Xu[1,4], Huaping Jin[4], Jie Bao[5*], Huang Yulun[1,2*] and Min Su[1,2,3*]

[1]Department of Physical Medicine and Rehabilitation, Dushu Lake Hospital of Soochow University, Suzhou, China, [2]Kunshan Rehabilitation Hospital, Suzhou, China, [3]Institute of Rehabilitation, Soochow University, Suzhou, China, [4]The First Affiliated Hospital of Soochow University, Suzhou, Jiangsu, China, [5]School of Physical Education and Sports Science, Soochow University, Suzhou, China

Respiratory muscle weakness often occurs after stroke, which can lead to pulmonary dysfunction (PD). Pulmonary dysfunction prolongs the length of hospital stay and increases the risk of death. In a prospective, randomized, case-control study, we used musculoskeletal ultrasonography (MSUS), and pulmonary function tester to objectively evaluate the efficacy of repetitive transcranial magnetic stimulation (rTMS) combined with respiratory muscle training (RMT) in the treatment of PD in patients with acute ischemic stroke. Sixty-two stroke patients with PD were recruited and eventually 60 patients participated in this study. The control group was treated with RMT, and the treatment group was treated with rTMS on the basis of RMT. Treatment occurred five times a week for 8 weeks. Before and after treatment, diaphragmatic thickness (DT), diaphragmatic thickening fraction (DTF) and diaphragmatic mobility (DM) in patients, bilateral chest wall were measured by MSUS. Meanwhile, FVC, FEV1, FEV1/FVC, PEF, and MVV tested by pulmonary function tester was used to evaluate the improvement of lung functional. activities of daily living (ADL) was used as an objective criterion to evaluate the overall functional recovery of patients before and after treatment. After treatment, DT, DTF, and DM values improved significantly in both the affected and unaffected sides. The FVC, FEV1, FEV1/FVC, PEF, MVV, and ADL were all increased after the treatment. Combined treatment showed a stronger increase than that by RMT treatment alone. The study preliminarily shows that rTMS and RMT could improve lung functional after acute ischemic stroke.

KEYWORDS

respiratory muscle weakness, pulmonary dysfunction, transcranial magnetic stimulation, respiratory muscle training, ischemic stroke

Introduction

Stroke can cause severe dysfunction (Hreha et al., 2020). Up to 50% of stroke patients experiencing long-term disability, and up to 30% of people are still unable to take care of themselves 6 months after a stroke (Writing Group Members et al., 2012). The research on functional recovery after stroke mainly focused on motor recovery of the hemiplegic limb, language, cognitive and dysphagia recovery. Too little attention was paid to the lung function recovery (Miryutova et al., 2019; Li et al., 2022). Studies have proved that the respiratory muscle strength of the affected side also decreases after stroke (Ramos et al., 2020). The weakness of respiratory muscle shows low endurance during exercise and independent walking ability (Morisawa et al., 2021). Respiratory muscle weakness in stroke patients is usually manifested as pulmonary infection, respiratory failure, atelectasis or sleep disorders (Jung et al., 2014; Liaw et al., 2020; Bruce et al., 2022). If not intervened early, it will progress to restrictive respiratory disease (Lima et al., 2014). They may be due to the intervention of the respiratory control center or respiratory mechanical changes caused by respiratory muscle weakness (Rochester and Mohsenin, 2002 Diaphragmatic dysfunction after stroke is another important factor leading to lung dysfunction, with an incidence of 51.7% (Fabero-Garrido et al., 2022). About 70% of these patients will develop severe respiratory disease (Catalá-Ripoll et al., 2020). It has been reported that the healthy side diaphragm deviation in stroke patients is greater than that of the affected side (Liaw et al., 2020; Yoon et al., 2020). Meanwhile, Lanini et al. (2003) studied the spontaneous breathing of 8 stroke patients. The results showed that the affected hemithorax respiratory movement reduced during voluntary hyperventilation.

Respiratory muscle training (RMT) can improve the lung function of stroke survivors (Yoo and Pyun, 2018). A review study suggests that inspiratory muscle training is more helpful to improve the quality of life and cardiopulmonary fitness of stroke patients (Xiao et al., 2012). In addition, studies have shown that lower respiratory intensity increases the risk of stroke (Yoon et al., 2020).

As a non-invasive *in vitro* neuromodulation technique, rTMS has received much attention from researchers since its birth in 1985 (Matsuda et al., 2021). Research shows that magnetic stimulation can be applied to human respiratory motor cortex (Nierat et al., 2015; Cember et al., 2022). The cortex of rTMS induced unilateral diaphragmatic response is located in the contralateral brain region, 3 cm outside the midline and 2–3 cm before the ear plane (Maskill et al., 1991). Studies have been shown to increase regional blood flow in the bilateral primary motor cortex as defined by rTMS during volitional breathing (Colebatch et al., 1991). So we hypothesize that rTMS may improve the lung function and promote the activities of daily living (ADL) in hemiplegic patients.

We aimed at exploring the effects of rTMS combined with RMT on the lung function in patients with cardiopulmonary dysfunction after acute ischemic stroke. The lesions in the stroke patients we selected were located in the anterior circulation of the brain. Compared with single RMT, rTMS combined with RMT may obtain better therapeutic effect from central and peripheral pathways.

Materials and methods

Participants

Patients hospitalized in the rehabilitation department of the Dushu Lake Hospital of Soochow University from June 2019 to June 2020 were screened. The inclusion criteria were described as follows: (1) The first incidence of ischemic stroke with the lesion at the anterior cerebral circulation confirmed by the head MRI scan. (2) Presence of pulmonary dysfunction (less than 80% of the predicted value) assessed by spirometry. (3) Without aphasia or cognitive dysfunction. (4) Vital signs stable. Exclusion criteria: (1) History of lung, chest and abdominal disease. (2) History of smoking. (3) Combined with myasthenia gravis or phrenic nerve palsy. (4) Combined with severe heart disease, liver cirrhosis, renal failure, severe systemic illness and history of malignant disease. (5) Metallic implants in the body.

Study design

The study is a prospective, randomized, case-control study. The subjects were numbered in the order of inclusion and divided into control and treatment groups by random number tables. Patients voluntarily participated in the experiment and signed informed consent. The study was approved by the ethics committee of the Dushu Lake Hospital of Soochow University. Collect basic information of patients, including age, gender, stroke duration and affected side. Assess the patient's ADL score. The above work is collected and analyzed by the same person.

Treatment

Both groups received conventional rehabilitation and treated by one therapist. Conventional rehabilitation training includes respiratory training and limb function training. Each time, for 40 min. Breathing training is to blow balloons and blow bubbles. Limb function training, such as muscle strength training, body position transfer, walking training, activities of daily life training, etc. The control group received threshold RMT (POWERbreathe®, International Ltd., Warwickshire, UK) twice a day, 10 min each time in the morning and afternoon, with an interval of 3 h. The initial intensity was 30% of the

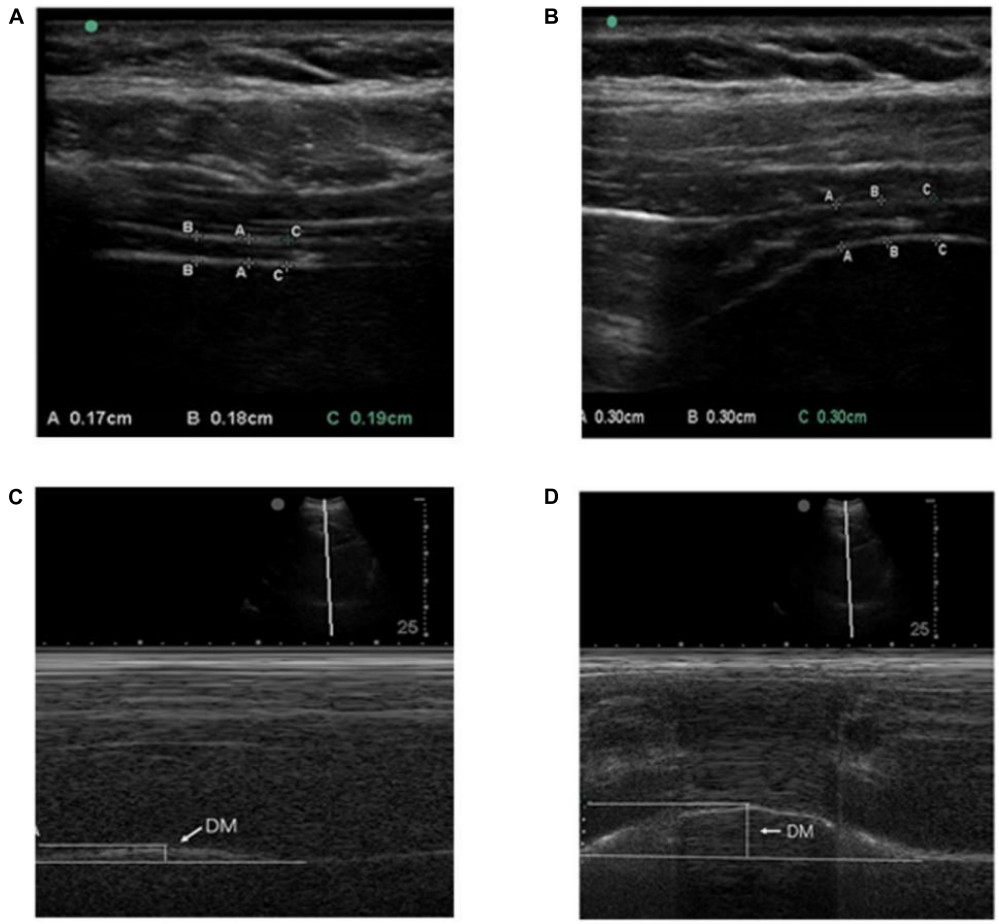

FIGURE 1
(A,B) Respectively indicate the method of measuring the diaphragm thickness of calm end-expiratory and maximum end-inspiratory with the linear array probe. The diaphragm was identified as a three-layered structure, namely the hyperechoic area on both sides (pleural layer and peritoneum) and the middle mixed echo area (composed of anechoic diaphragmatic muscle tissue and hyperechoic fascia). DT is represented by the vertical line between the pleural layer and peritoneum; **(C,D)** respectively, indicates diaphragm mobility during quiet and deep breathing on the M-mode screen. DM is represented by the vertical axis between the line passing through the end of the normal expiration and inspiratory peaks.

maximum inspiratory pressure (MIP) and increased by 5% every week until the training intensity reached 60% MIP. Continue to practice with 60% MIP for 2 weeks.

The treatment group used a magnetic stimulator (MagPro R30, Medtronic A/S, Denmark) connected with a 75 mm figure-of-eight water-cooled coil (MCF-B65) for stimulation. The patient wore an International 10–20 system positioning cap. The stimulation site was located 3 cm lateral to the midline and 2–3 cm anterior to the auricular plane. The frequency of 5 Hz with the stimulus intensity was set at 30% above the unaffected side diaphragmatic motor threshold applied (Urban et al., 2002). Patients received 4,200 rTMS pulses per day for 10 min. The RMT was performed after 3 h. Five times a week for 8 weeks. During the treatment the participants were seated in their own wheelchairs. The rTMS, in general, has no special side effects. However, if not used properly, it can cause seizures or syncope, so the treatments were performed by two senior physiotherapists, who observed the patient closely during the treatment process to avoid accidents. One patient in the control group failed to adhere to training due to a new cerebral infarction. With no patient withdrew from the treatment group.

Clinical evaluations

A portable diagnostic ultrasound system (M-Turbo, ICTx, SonoSite, America) connected with a 6–13 MHz linear array transducer was used to assess DT, DTF and with a 3.0–5.5 MHz transducer was used to assess DM in patients, bilateral chest wall.

Diaphragm thickness

The participants in a supine position with spontaneous breathing. Take the linear array probe and place it on the

TABLE 1 Anthropometric data, ADL, and pulmonary function test results.

	Control group	Treatment group
	$n = 30$	$n = 30$
Age (yr)	59.13 ± 11.55	62.27 ± 13.17
Gender (female/male)	1.43 ± 0.50	1.40 ± 0.50
Duration	29.30 ± 24.00	32.10 ± 19.46
Hemiplegia	1.53 ± 0.51	1.40 ± 0.50
ADL	28.50 ± 9.21	27.83 ± 8.17
FVC (L)	2.05 ± 0.57	2.04 ± 0.44
FEV1 (L)	1.16 ± 0.34	1.21 ± 0.27
FEV1/FVC (%)	56.69 ± 3.00	59.52 ± 6.47
PEF (L)	2.69 ± 1.03	2.39 ± 0.70
MVV (L)	53.81 ± 12.60	54.94 ± 12.22

Values are presented as mean ± standard deviation. ADL, activities of daily living; FVC, forced vital capacity; FEV1, forced expiratory volume in 1 s; FEV1/FVC, ratio of FEV1 to FVC; PEF, peak expiratory flow; MVV, maximal voluntary ventilation.

right anterior axillary line. The probe is perpendicular to the 8th–9th intercostal space. If the diaphragm cannot be seen at this position, the probe can be moved up to the 7th–8th intercostal space. The diaphragm is a 3-layer structure under diagnostic sonography. The three-layer structure includes the hyperechoic area of the upper and lower layer (pleural layer and peritoneal layer), and the hypochoechoic middle muscular layer (composed of anechoic diaphragmatic muscle tissue and hyperechoic fascia). Move the cursor to measure the calm end-expiratory diaphragm thickness and the maximum end-inspiratory diaphragm thickness. Values were measured for 3 breathing cycles and averaged (Figures 1A,B). The change in diaphragm thickness from calm end-expiratory to maximum end-inhalation can be calculated, that is, diaphragm thickening rate = (maximum end-inspiratory diaphragm thickness-end-expiratory thickness)/maximum end-expiratory thickness. The measurement method is the same on the left and right sides.

Diaphragm mobility

The participants in a supine position with spontaneous breathing. A 2D mode was used to find the best exploration line for each hemidiaphragm. The right used liver as a window, while the spleen was used on the left hemidiaphragm. For right hemidiaphragm, the ultrasound probe was placed at the lower costal margin between the midclavicular and anterior axillary lines. Diaphragm movements were recorded in M-mode and the sampling line should be perpendicular to the diaphragm. Diaphragm movements were recorded during quiet breathing (QB) and deep breathing (DB) (Figures 1C,D). The measurement method is the same on the left and right sides.

Pulmonary function tests by standard spirometry. The Participants take seats. The main indicators of observation including FVC, FEV1, FEV1/FVC, PEF, and MVV using an Master-Screen spirometer (Leibinzstrasse7, 97204 Hoechberg, Germany).

Statistical analysis

Used Spss20.0 for statistical analysis of all experimental data, values are presented as mean ± standard deviation (X ± SD). For the comparison of data before and after treatment within the group, the paired sample *t*-test was used for those that conformed to the normal distribution, and the non-parametric Wilcoxon rank-sum test was used for the data that did not conform to the normal distribution. The data before and after treatment in the two groups were compared, and the independent samples *t*-test was used for those that conformed to the normal distribution, and the non-parametric Wilcoxon rank-sum test was used for those that did not conform to the normal distribution. $P < 0.05$ representatives have significant differences.

Results

General information

Sixty-two patients participated in the experiment, excluding one patient with new cerebral infarction who did not complete the experiment, and 61 patients completed the

TABLE 2 DT, DTF, and DM in patients, bilateral chest wall before treatment.

		Control group		Treatment group	
		Affected side	Unaffected side	Affected side	Unaffected side
DT (cm)	CEE	0.20 ± 0.12	0.23 ± 0.17	0.19 ± 0.13	0.23 ± 0.17
	MEI	0.27 ± 0.20	0.34 ± 0.31	0.26 ± 0.19	0.35 ± 0.30
DM (cm)	QB	1.27 ± 0.11	1.46 ± 0.13	1.25 ± 0.10	1.41 ± 0.13
	DB	2.75 ± 0.40	5.08 ± 0.68	2.77 ± 0.41	4.96 ± 0.62
DTF (%)		34.19 ± 6.32	48.99 ± 6.39	34.29 ± 3.89	50.10 ± 7.12

Values are presented as mean ± standard deviation. DT, diaphragmatic thickness; DM, diaphragmatic mobility; DTF, diaphragmatic thickening fraction; CEE, calm end-expiratory; MEI, maximum end-inspiratory; QB, quiet breathing.

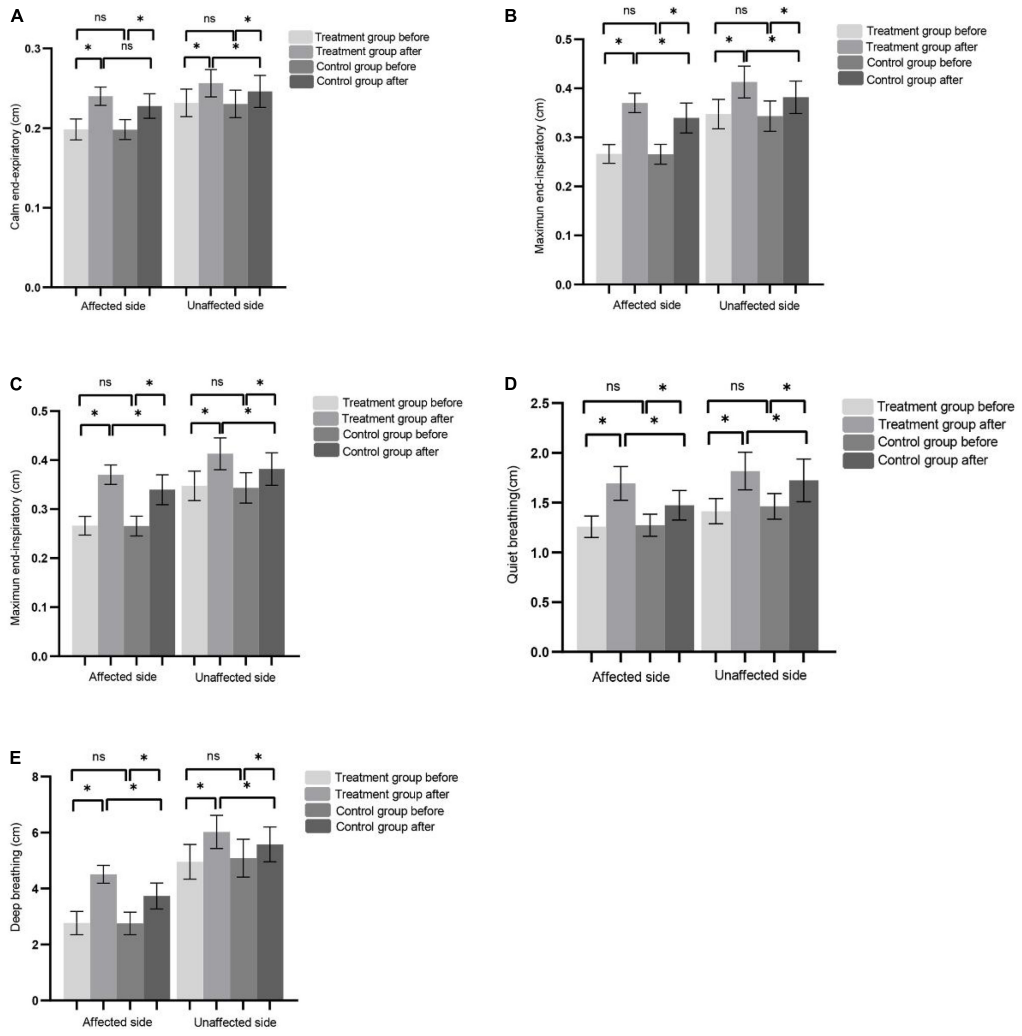

FIGURE 2
(A–C) Represents CEE, MEI, and DTF of the affected side and non-affected side before and after treatment in the control group and the treatment group, respectively. **(D)** The DM of affected side and unaffected side during QB before and after treatment in control and treatment group. **(E)** The DM of affected side and unaffected side during DB before and after treatment in control and treatment group. (*$P < 0.05$), ns ($P > 0.05$).

experiment. Finally, 60 patients aged 26–80, with an average age of 60.7 years, a duration of 4–90 days and an average duration of 30.7 days were eligible for the study. Before treatment, there was no difference in gender (female/male), age, duration, affected side, ADL score, FVC, FEV1, FEV1 \/FVC, PEF, and MVV between the two groups ($P > 0.05$) (see Table 1).

The results of musculoskeletal ultrasonography measurement

Before treatments, the DT, DTF, and DM were not significantly different between the two groups (Table 2, $P > 0.05$).

After 8 weeks of treatment, the values of DT, DTF, and DM in the affected and unaffected sides in the two groups were significantly improved compared with those before treatment. After treatment, the improvement of DT, DTF, and DM in the affected side and unaffected side in the treatment group was significantly better than that in the control group (Figures 2A–E).

The results of lung function assessment

We used pulmonary function tester to assess the FVC, FEV1, FEV1/FVC, PEF, and MVV before and after the treatments, respectively. There was no significant difference

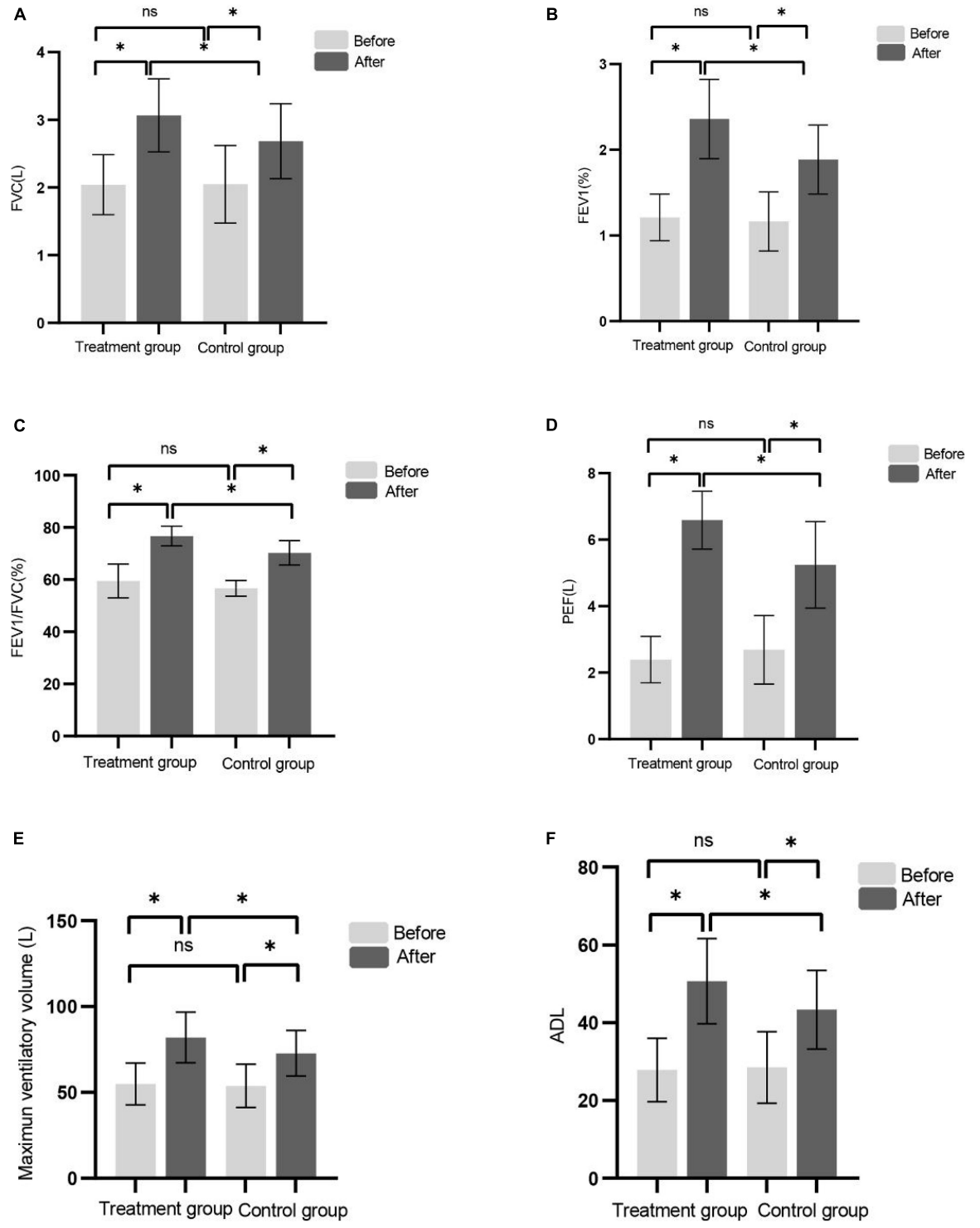

FIGURE 3
(A–F) Shows FVC, FEV1, FEV1/FVC, PEF, MVV, and ADL before and after treatment in the control group and the treatment group, respectively. (*$P < 0.05$), ns ($P > 0.05$).

in the lung function index between the two groups before treatment ($P > 0.05$). Lung function was improved in both groups after treatment. After 8-week treatment, compared with the control group, the pulmonary function test indicators increased more significantly in the treatment group (Figures 3A–E).

The results of activities of daily living assessments

There was no significant difference in ADL score between the two groups before treatment. After 8 weeks of treatment, the ADL score in the two groups were higher than that before treatment and the effect of the treatment group were better than that of the control group (**Figure 3F**). Consistent with recent studies (Britto et al., 2011; Ramos et al., 2020).

Discussion

In our study, both the affected and unaffected sides of DT, DTF, and DM were significantly increased after treatment, and the lung function detection indexes FVC, FEV1, FEV1/FVC, PEF, and MVV all improved significantly. These results indicate that a short time of rTMS combined with RMT training (8 weeks) can improve the lung function in hemiplegic patients with acute ischemic stroke. Cohen found that diaphragm deviation was significantly positively associated with inspiratory volume in hemiplegic patients (Cohen et al., 1994). In our study, the changes in multiple indicators, including DT, DTF, and DM, were consistent with the lung function in hemiplegic patients.

Volitional breathing is controlled by the brain center and located on both sides of the primary motor cortex (Gandevia and Rothwell, 1987). Studies have shown that each hemi-diaphragm is mainly controlled by a unilateral contralateral center. The rTMS also showed that the diaphragmatic response to the stimulation of a single cerebral hemisphere was mainly contralateral, while the ipsilateral response was lower (Maskill et al., 1991). Therefore, in order to better improve the lung function, we stimulated both hemispheres of the brain.

Pulmonary rehabilitation is a central part of the treatment of patients with chronic respiratory diseases (Nici et al., 2012). Stroke patients are often accompanied by respiratory dysfunction, which increases the probability of respiratory tract infection, extends the hospital stay, and brings serious pain to the patients. Therefore, it is vital to promote pulmonary function rehabilitation in stroke. The diaphragm has atrophy after stroke, and it is significantly thinner on the affected side than on the non-affected side at end expiration and TLC (total vital capacity) (Kim et al., 2017; Fabero-Garrido et al., 2022). Which resonates with our findings. Jung et al. (2014) Suggest that diaphragmatic movement is associated with the lung function in stroke patients. Therefore, our aim is to promote the activity of diaphragm, enhance thickness and mobility of diaphragm, promote the recovery of respiratory function, and further promote the functional recovery of stroke patients by using a simple and effective rehabilitation program.

RMT mainly improves the lung function by strengthening peripheral respiratory muscle strength. Transcranial magnetic stimulation can act on the central nervous system and has been widely used. In our paper, we adopted the central plus peripheral mode of respiratory function training to treat stroke patients. The results showed that RMT combined with rTMS could obtain better therapeutic effect.

Ultrasonography can dynamically observe the respiratory muscle function in real time. Ultrasonic probes with different shapes and resolutions can be used to observe the shape and contraction of diaphragm and auxiliary respiratory muscles during calm and deep breathing, including the position, shape, motion amplitude, motion time, acceleration of diaphragm and the thickness changes before and after contraction of diaphragm. Therefore, Ultrasonography was used for evaluation and measurement in this study.

Study has shown that the critical time to begin recovery after stroke is in the first 30 days after stroke (Krakauer et al., 2012), with the majority of patients reached or near to their maximum recovery by 3 months after stroke (Verstraeten et al., 2020). Therefore, we limited the included patients to a stroke course of less than 3 months.

This study also has some limitations. On the one hand, the sample size is not large enough and the research cycle is not long enough. On the other hand, whether rTMS is effective for PD in patients with chronic hemiplegia has not been verified. In the future, we can further study the therapeutic effect of rTMS on patients with chronic hemiplegia. However, this study confirms the therapeutic role of rTMS, which can be used for the rehabilitation of lung function.

Conclusion

The rTMS combined with RMT can effectively improve the lung function in early hemiplegia patients, which is more effective than RMT alone. Improvement of lung function may be attributed to increased local blood flow during stimulation. Meanwhile, the changes both before and after treatment in DT, DTF, and DM measured by musculoskeletal ultrasonography (MSUS) are consistent with the lung function and can be used as objective indicators in response to lung function. At the same time, the changes of ultrasound index, such as DT, DTF, and DM, as well as lung function index FVC, FEV1, FEV1/FVC, and PEF were consistent with the improvement of patients, activity of daily living. Therefore, we believe that the improvement of pulmonary function can further improve the activity of daily living of stroke patients.

Data availability statement

The original contributions presented in this study are included in the article/supplementary material, further inquiries can be directed to the corresponding author/s.

Ethics statement

The studies involving human participants were reviewed and approved by the Department of Physical Medicine and Rehabilitation Dushu Lake Hospital of Soochow University. The patients/participants provided their written informed consent to participate in this study. Written informed consent was obtained from the individual(s) for the publication of any potentially identifiable images or data included in this article.

Author contributions

All authors listed have made a substantial, direct, and intellectual contribution to the work, and approved it for publication.

Funding

This work was supported by the National Natural Science Foundation of China (grant no. 81672244), the Suzhou Minsheng Science and Technology Key Technology Application Research Project in 2019 (Project No. SS2019051), and Horizontal Project of Soochow University in 2020 (Project No. H201173).

Conflict of interest

The authors declare that the research was conducted in the absence of any commercial or financial relationships that could be construed as a potential conflict of interest.

Publisher's note

All claims expressed in this article are solely those of the authors and do not necessarily represent those of their affiliated organizations, or those of the publisher, the editors and the reviewers. Any product that may be evaluated in this article, or claim that may be made by its manufacturer, is not guaranteed or endorsed by the publisher.

References

Britto, R. R., Rezende, N. R., Marinho, K. C., Torres, J. L., Parreira, V. F., and Teixeira-Salmela, L. F. (2011). Inspiratory muscular training in chronic stroke survivors: A randomized controlled trial. *Arch. Phys. Med. Rehabil.* 92, 184–190. doi: 10.1016/j.apmr.2010.09.029

Bruce, S. S., Navi, B. B., Zhang, C., Kim, J., Devereux, R. B., and Schenck, E. J. (2022). Transesophageal echocardiography and risk of respiratory failure in patients who had ischemic stroke or transient ischemic attack: An IDEAL phase 4 study. *BMJ Surg. Interv. Health Technol.* 4:e000116. doi: 10.1136/bmjsit-2021-000116

Catalá-Ripoll, J. V., Monsalve-Naharro, J. Á, and Hernández-Fernández, F. (2020). Incidence and predictive factors of diaphragmatic dysfunction in acute stroke. *BMC Neurol.* 20:79. doi: 10.1186/s12883-020-01664-w

Cember, A. T., Deck, B. L., Kelkar, A., Faseyitan, O., Zimmerman, J. P., and Erickson, B. (2022). Glutamate-Weighted Magnetic Resonance Imaging (GluCEST) Detects Effects of Transcranial Magnetic Stimulation to the Motor Cortex. *Neuroimage* 256:119191. doi: 10.1016/J.NEUROIMAGE.2022.119191

Cohen, E., Mier, A., Heywood, P., Murphy, K., Boultbee, J., and Guz, A. (1994). Diaphragmatic movement in hemiplegic patients measured by ultrasonography. *Thorax* 49, 890–895. doi: 10.1136/thx.49.9.890

Colebatch, J. G., Adams, L., Murphy, K., Martin, A. J., Lammertsma, A. A., Tochon-Danguy, H. J., et al. (1991). Regional cerebral blood flow during volitional breathing in man. *J. Physiol.* 443, 91–103. doi: 10.1113/jphysiol.1991.sp018824

Fabero-Garrido, R., Del Corral, T., Angulo-Díaz-Parreño, S., Plaza-Manzano, G., Martín-Casas, P., and Cleland, J. A. (2022). Respiratory muscle training improves exercise tolerance and respiratory muscle function/structure post-stroke at short term: A systematic review and meta-analysis. *Ann. Phys. Rehabil. Med.* 65:101596. doi: 10.1016/j.rehab.2021.101596

Gandevia, S. C., and Rothwell, J. C. (1987). Activation of the human diaphragm from the motor cortex. *J. Physiol.* 384, 109–118. doi: 10.1113/jphysiol.1987.sp016445

Hreha, K., Wong, J., Molton, I., Nelson, I. K., and Lee, D. (2020). The impact of stroke on psychological and physical function outcomes in people with long-term physical disability. *Disabil. Health J.* 13:100919. doi: 10.1016/j.dhjo.2020.100919

Jung, K. J., Park, J. Y., Hwang, D. W., Kim, J. H., and Kim, J. H. (2014). Ultrasonographic diaphragmatic motion analysis and its correlation with pulmonary function in hemiplegic stroke patients. *Ann. Rehabil. Med.* 38, 29–37. doi: 10.5535/arm.2014.38.1.29

Kim, M., Lee, K., Cho, J., and Lee, W. (2017). Diaphragm thickness and inspiratory muscle functions in chronic stroke patients. *Med. Sci. Monit.* 23:1247. doi: 10.12659/msm.900529

Krakauer, J. W., Carmichael, S. T., Corbett, D., and Wittenberg, G. F. (2012). Getting neurorehabilitation right: What can be learned from animal models? *Neurorehabil. Neural Repair* 26, 923–931. doi: 10.1177/1545968312440745

Lanini, B., Bianchi, R., Romagnoli, I., Coli, C., Binazzi, B., and Gigliotti, F. (2003). Chest wall kinematics in patients with hemiplegia. *Am. J. Respir. Crit. Care Med.* 168, 109–113. doi: 10.1164/rccm.200207-745OC

Li, R., Li, L., and Chen, Q. (2022). Effect of Respiratory Training Combined with Core Muscle Training on the Overall Motor Function and Activities of Daily Living of Patients with Early and Midterm Stroke. *J. Healthc. Eng.* 2022:2830711. doi: 10.1155/2022/2830711

Liaw, M. Y., Hsu, C. H., Leong, C. P., Liao, C. Y., Wang, L. Y., Lu, C. H., et al. (2020). Respiratory muscle training in stroke patients with respiratory muscle weakness, dysphagia, and dysarthria–a prospective randomized trial. *Medicine* 99:e19337. doi: 10.1097/MD.0000000000019337

Lima, ÍN., Fregonezi, G. A., Melo, R., Cabral, E. E., Aliverti, A., Campos, T. F., et al. (2014). Acute effects of volume-oriented incentive spirometry on chest wall volumes in patients after a stroke. *Respir. Care* 59, 1101–1107. doi: 10.4187/respcare.02651

Maskill, D., Murphy, K., Mier, A., Owen, M., and Guz, A. (1991). Motor cortical representation of the diaphragm in man. *J. Physiol.* 443, 105–121. doi: 10.1113/jphysiol.1991.sp018825

Matsuda, Y., Yamazaki, R., Shigeta, M., and Kito, S. (2021). Transcranial magnetic stimulation modalities for psychiatric disorders: Publication trends from 1985 to 2019. *Neuropsychopharmacol. Rep.* 41, 538–543. doi: 10.1002/npr2.12212

Miryutova, N. F., Vorobyev, V. A., Minchenko, N. N., Samoilova, I. M., Zaitsev, A. A., and Mareeva, L. V. (2019). The integral estimation of health problems and effectiveness of stage rehabilitation in patients after ischemic stroke. *Vopr. Kurortol. Fizioter. Lech. Fiz. Kult.* 96, 5–16. doi: 10.17116/kurort2019960615

Morisawa, T., Kunieda, Y., Koyama, S., Suzuki, M., Takahashi, Y., Takakura, T., et al. (2021). The Relationship between Sarcopenia and Respiratory Muscle

Weakness in Community-Dwelling Older Adults. *Int. J. Environ. Res. Public Health* 18:13257. doi: 10.3390/ijerph182413257

Nici, L., ZuWallack, R., and American Thoracic Society Subcommittee on Integrated Care of the COPD Patient. (2012). An official American Thoracic Society workshop report: The integrated care of the COPD patient. *Proc. Am. Thorac. Soc.* 9, 9–18. doi: 10.1513/pats.201201-014ST

Nierat, M. C., Hudson, A. L., Chaskalovic, J., Similowski, T., and Laviolette, L. (2015). Repetitive transcranial magnetic stimulation over the supplementary motor area modifies breathing pattern in response to inspiratory loading in normal humans. *Front. Physiol.* 6:273. doi: 10.3389/fphys.2015.00273

Ramos, S. M., Silva, D. M. D., Buchaim, D. V., Buchaim, R. L., and Audi, M. (2020). Evaluation of respiratory muscular strength compared to predicted values in patients with stroke. *Int. J. Environ. Res. Public Health* 17:1091. doi: 10.3390/ijerph17031091

Rochester, C. L., and Mohsenin, V. (2002). Respiratory complications of stroke. *Semin. Respir. Crit. Care Med.* 23, 248–260. doi: 10.1055/s-2002-33033

Urban, P. P., Morgenstern, M., Brause, K., Wicht, S., Vukurevic, G., Kessler, S., et al. (2002). Distribution and course of cortico-respiratory projections for voluntary activation in man. *J. Neurol.* 249, 735–744. doi: 10.1007/s00415-002-0702-8

Verstraeten, S., Mark, R. E., Dieleman, J., van Rijsbergen, M., de Kort, P., and Sitskoorn, M. M. (2020). Motor impairment three months post stroke implies a corresponding cognitive deficit. *J. Stroke Cerebrovasc. Dis.* 29:105119. doi: 10.1016/j.jstrokecerebrovasdis.2020.105119

Writing Group Members„ V. L., Go, A. S., Lloyd-Jones, D. M., Benjamin, E. J., and Berry, J. D. (2012). Heart disease and stroke statistics—2012 update: A report from the American Heart Association. *Circulation* 125:e2–e220. doi: 10.1161/CIR.0b013e31823ac046

Xiao, Y., Luo, M., Wang, J., and Luo, H. (2012). Inspiratory muscle training for the recovery of function after stroke. *Cochrane Database Syst. Rev.* 2012:CD009360. doi: 10.1002/14651858.CD009360.pub2

Yoo, H. J., and Pyun, S. B. (2018). Efficacy of bedside respiratory muscle training in patients with stroke: A randomized controlled trial. *Am. J. Phys. Med. Rehabil.* 97, 691–697. doi: 10.1097/PHM.0000000000000933

Yoon, H. S., Cha, Y. J., and You, J. S. H. (2020). Effects of dynamic core-postural chain stabilization on diaphragm movement, abdominal muscle thickness, and postural control in patients with subacute stroke: A randomized control trial. *Neurorehabilitation* 46, 381–389. doi: 10.3233/NRE-192983

frontiers | Frontiers in Aging Neuroscience

TYPE Review
PUBLISHED 29 September 2022
DOI 10.3389/fnagi.2022.987732

OPEN ACCESS

EDITED BY
Chuhuai Wang,
Sun Yat-sen University, China

REVIEWED BY
Ying Shen,
The First Affiliated Hospital of Nanjing Medical University, China
Min Su,
Soochow University, Taiwan
Xiao Bao,
Yuebei People's Hospital, China

*CORRESPONDENCE
Xin-An Zhang
zhangxa2725@163.com
Xue-Qiang Wang
wangxueqiang@sus.edu.cn

SPECIALTY SECTION
This article was submitted to Neurocognitive Aging and Behavior, a section of the journal Frontiers in Aging Neuroscience

RECEIVED 06 July 2022
ACCEPTED 26 August 2022
PUBLISHED 29 September 2022

CITATION
Zhu H-Q, Luo J, Wang X-Q and Zhang X-A (2022) Non-invasive brain stimulation for osteoarthritis. *Front. Aging Neurosci.* 14:987732. doi: 10.3389/fnagi.2022.987732

Non-invasive brain stimulation for osteoarthritis

Hui-Qi Zhu[1,3], Jing Luo[2], Xue-Qiang Wang[3,4]* and Xin-An Zhang[1]*

[1]College of Kinesiology, Shenyang Sport University, Shenyang, China, [2]Department of Sport Rehabilitation, Xi'an University of Sport, Xi'an, China, [3]Department of Sport Rehabilitation, Shanghai University of Sport, Shanghai, China, [4]Department of Rehabilitation Medicine, Shanghai Shangti Orthopaedic Hospital, Shanghai, China

Osteoarthritis (OA) is a degenerative joint disease, the prevalence of OA is increasing, and the elderly are the most common in patients with OA. OA has a severe impact on the daily life of patients, this increases the demand for treatment of OA. In recent years, the application of non-invasive brain stimulation (NIBS) has attracted extensive attention. It has been confirmed that NIBS plays an important role in regulating cortical excitability and oscillatory rhythm in specific brain regions. In this review, we summarized the therapeutic effects and mechanisms of different NIBS techniques in OA, clarified the potential of NIBS as a treatment choice for OA, and provided prospects for further research in the future.

KEYWORDS

osteoarthritis, NIBS, rTMS, single-pulse TMS, tDCS, tRNS, tACS, tFUS

Introduction

As a general degenerative disease and the most common form of arthritis, osteoarthritis (OA) is pathologically characterized by cartilage degeneration, subchondral bone sclerosis, and osteophyte formation (Pereira et al., 2015). Cartilage degeneration is also a hallmark of OA (Egloff et al., 2012). The major clinical symptoms of OA are joint pain and activity disorders. The new subchondral bone tissue that results from subchondral bone sclerosis and osteophyte formation contains new blood vessels and nerve fibers, which may be related to OA pathogenesis and pain perception (Walsh et al., 2010). These in turn cause the patient's dysfunction, poor sleep, and low mood; these conditions seriously affect the quality of life (QOL) of patients. In accordance with statistics, the prevalence rate of OA in people over 60 years old can reach 50%, it in people over 75 years old is as high as 80%, the prevalence in women is higher than that in men, and the disability rate of the disease can reach 53% (Zhang et al., 2020). Patients with OA worldwide are expected to exhibit an increasing trend in the next few decades (Mantovani et al., 2016) partly due to increasing risk factors for OA, such as genetics, obesity, lack of exercise, or exercise injury (Hawker, 2019; Kakouris et al., 2021). The disease not only exerts a huge influence on the QOL of

patients but also considerably increases the economic burden of society. At present, however, the complex pathological mechanism of OA is not yet fully known; it mostly involves increased inflammatory components, mechanical overload, altered metabolic changes, and cellular aging (Jeon et al., 2017). In contrast with other inflammatory joint diseases, varying responses to different parts of OA further complicate treatment, and thus, treatment for OA remains a challenge (Hermann et al., 2018).

OA is currently mainly treated with drugs (Guo et al., 2022), mainly non-steroidal anti-infective drugs, which have anti-inflammatory and analgesic effects, but these drugs have many adverse reactions, and long-term use can lead to different degrees of cardiovascular complications (da Costa et al., 2017). Intra-articular injections such as glucocorticoids can reduce joint adhesion and promote cartilage repair, but they only have short-term effects, and long-term injections may cause infection (Kavanaugh et al., 2016). Cartilage protective drugs such as glucosamine can reduce joint edema, maintain synovial fluid viscosity, and inhibit inflammation, but long-term use has serious adverse reactions to gastrointestinal function and is expensive (Arden et al., 2021). Joint-targeted drug therapy only works in the diseased part and has no effect on other normal parts, which is conducive to cartilage repair and pain relief (Zhang et al., 2022). However, the current targeted therapy is still in the clinical trial stage, and the potential adverse reactions are not yet clear. Therefore, it is considered to explore a non-drug-safe treatment method for OA.

OA is also mostly treated with physical therapy, mainly exercise therapy, hydrotherapy, and extracorporeal shock wave therapy (Griffin et al., 2020). Anti-blocking exercise combined with hydrotherapy is prone to adverse events such as worsening pain (Waller et al., 2017) and other symptoms in patients with moderate to severe OA, and hydrotherapy has had only a small short-term clinical effect in patients with OA (Bartels et al., 2016) and does not appear to have a significant effect on the patient's drug dose or quality of life (Forestier et al., 2016). Extracorporeal shock wave therapy (ESWT) is important for the protection of articular cartilage in patients with early OA, but it can only slow down the course of OA. Moreover, the experimental subjects are mostly mice, and the doses for humans have not been standardized (Chou et al., 2019). Whole-body vibration therapy also does not improve joint stiffness in patients with OA (Qiu et al., 2022).

Bioelectronic medicine uses the body's electrical signals to improve the diagnosis and treatment of disease. As an emerging bioelectronic medical technology, Non-invasive brain stimulation (NIBS) has been widely used in clinical treatment, particularly for pain (Xiong et al., 2022), neuronal function regulation, brain function cognition, behavior, and other aspects of the evident treatment effect (Miniussi and Ruzzoli, 2013). NIBS not only brings hope for treating diseases that cannot be solved by common drugs and medical means, but also provides drug alternatives with rapid and precise targeting. This paper describes the therapeutic effects and possible mechanisms of six commonly used NIBS methods in OA, namely single pulse transcranial magnetic stimulation (TMS), repetitive transcranial magnetic stimulation (rTMS), transcranial direct current stimulation (tDCS), transcranial alternating current stimulation (tACS), transcranial random noise stimulation (tRNS), transcranial focused ultrasound stimulation (tFUS), to provide directions for future research.

Methods

A comprehensive literature search was conducted in PubMed and Web of Science databases using [Osteoarthritis(Title/Abstract)] OR [OA(Title/Abstract)], [Osteoarthritides(Title/Abstract)] OR [Osteoarthrosis(Title/Abstract)] OR [Osteoarthroses(Title/Abstract)] OR [Arthritis, Degenerative(Title/Abstract)] OR [Arthritides, Degenerative(Title/Abstract)] OR [Degenerative Arthritides(Title/Abstract)] OR [Degenerative Arthritis(Title/Abstract)] OR [Arthrosis(Title/Abstract)] OR [Arthroses(Title/Abstract)] OR [Osteoarthrosis Deformans(Title/Abstract)], [Non-invasive brain stimulation(Title/Abstract)] OR [NIBS(Title/Abstract)], rTMS[Title/Abstract] and Osteoarthritis, Single-pulse TMS[Title/Abstract] and Osteoarthritis, tDCS[Title/Abstract] and Osteoarthritis, tFUS[Title/Abstract] and Osteoarthritis, tACS[Title/Abstract] and Osteoarthritis, tRNS[Title/Abstract] and Osteoarthritis. From the date initially provided until November 2021, it is not limited to randomized controlled trials (RCT). Firstly, irrelevant articles were excluded according to the article titles or abstracts, and after reading and summarizing the remaining articles, the articles with high relevance, in-depth research, or lack of research were selected for inclusion.

Non-invasive brain stimulation

NIBS has become an effective and multi-field treatment technology in recent years. It is used to study the behavioral correlation of specific brain regions; neuronal regulatory function and its related perceptual, cognitive, and behavioral characteristics play a huge role (Plewnia et al., 2015), significantly deepening researchers' understanding of NIBS. However, NIBS is more dependent on brain state and task content, and some variability can be observed even among or within individuals. And the long-term effects of NIBS have not been explored (Polanía et al., 2018). Recent research trends on NIBS are presented in **Figures 1A,B**.

Clinically, common NIBS technologies include TMS (Ansari et al., 2021) and transcranial electrical stimulation (tES)

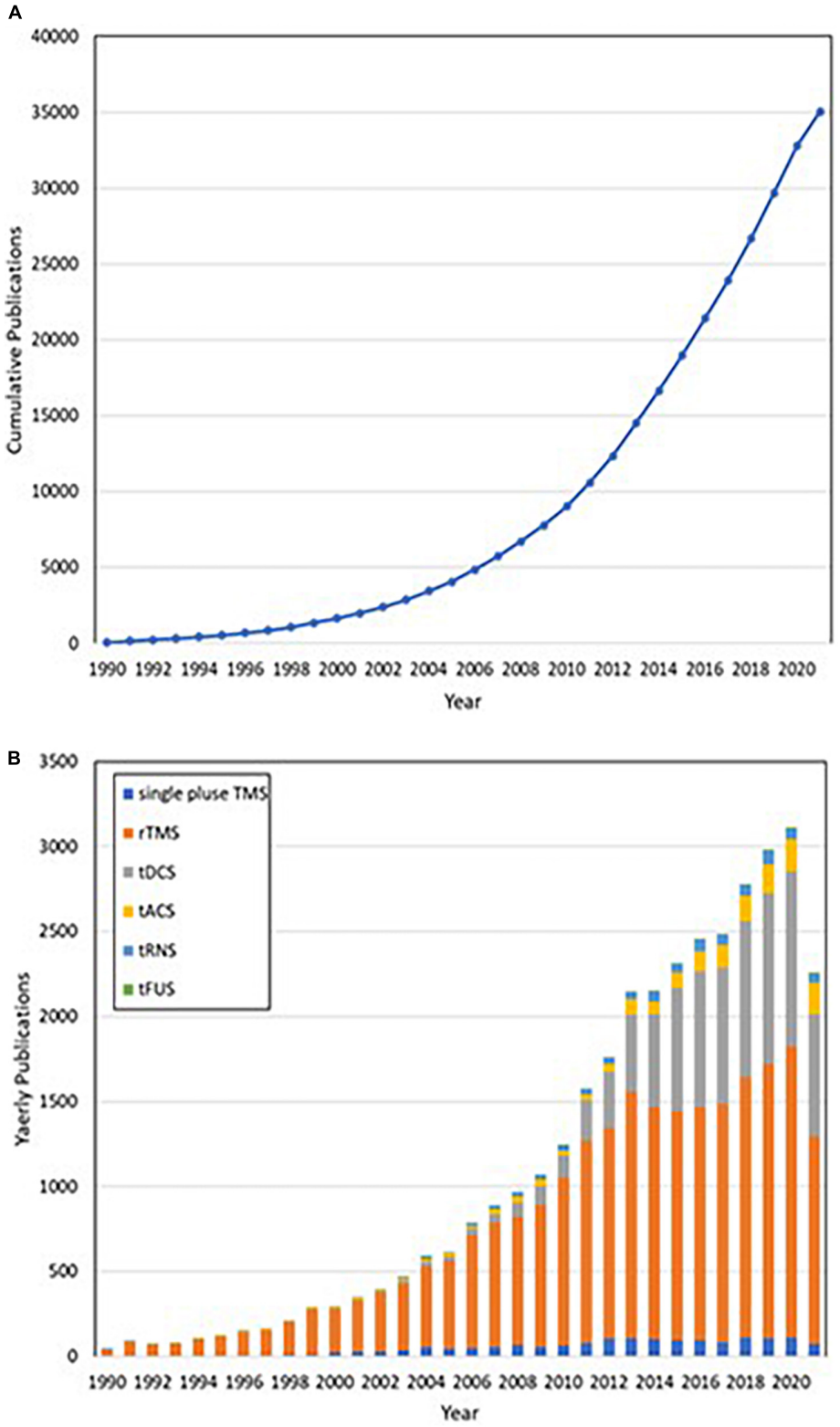

FIGURE 1
(A) Publications accumulated by year. **(B)** From 1990 to 2020, publications were classified annually in accordance with different non-invasive brain stimuli in categories that included repetitive transcranial magnetic stimulation (rTMS, orange), single-pulse transcranial magnetic stimulation (single-pulse TMS, blue), transcranial direct current stimulation (tDCS, gray), transcranial alternating current stimulation (tACS, yellow), transcranial random noise stimulation (tRNS, light blue), and transcranial focused ultrasound stimulation (tFUS, green).

(Abhishek and Doherty, 2013; Terranova et al., 2018). Among TMS techniques, single-pulse and rTMS are more commonly used. Meanwhile, tES can be divided into tACS and tDCS. In addition, tFUS (Badran et al., 2020) and tRNS (Battaglini et al., 2020) are also commonly used methods of NIBS (O'Connell et al., 2018).

TMS is a late-model neurophysiological technique based on the theory of the principle of electromagnetic induction (Barker et al., 1985; Hallett, 2007). Its principle is to use the rapidly changing magnetic field that emerges when a high-voltage current passes through a coil, acting on a certain region of the cerebral cortex, or the corresponding skull surface; hence, the magnetic field produces an induction current, which, in turn, changes the neural cell excitability in that region (Klomjai et al., 2015). Such changes can be recorded on effectors through the neural pathway. TMS is divided into three categories: single pulse TMS, double pulse TMS, and rTMS (Auvichayapat and Auvichayapat, 2009; Ansari et al., 2021). There is also an emerging TMS model called Theta Burst Stimulation (TBS). rTMS is a new neuroelectrophysiological technology. rTMS not only affects the local function of the cerebral cortex, but relatively distant cortical function can also achieve cortical function reconstruction. High-frequency TMS can enhance the metabolism of nerve cells, while low-frequency TMS can inhibit nerve cell metabolism (Du et al., 2019). Thus rTMS can produce lasting changes in cortical excitability (Pell et al., 2011) and has become a new treatment for neurological disorders. However, rTMS remains in the preliminary exploration stage. Its treatment effect and optimal treatment parameters have not been scientifically confirmed, and its treatment mechanism also requires further research and discussion (D'Agati et al., 2010). Single-pulse TMS emits only one stimulation pulse at a time; such pulse can depolarize neurons and cause a measurable response (Mathew and Danion, 2018), primarily for the detection of neural pathways, i.e., motion-evoked potential or measurement of a motor threshold. Single-pulse magnetic stimulation can also be used to detect central conduction time, and resting time, accurately map the motor cortex, and measure the motor evoked potential amplitude related to motor cortical conduction (Zorn et al., 2012). However, the aforementioned studies, have no targeted disease or standardized parameters. Dual-pulse magnetic stimulation refers to the emission of two consecutive pulses or one pulse pair after each issued instruction; it can be used in the research on cortical excitability (de Goede et al., 2020). TBS is similar to the frequency of theta waves in the hippocampus of the brain and is a special type of rTMS. It uses short pulses in clumps, with an intra-frequency of 50 Hz and an inter-frequency of 5 Hz (Ferrarelli and Phillips, 2021), which has the advantages of short stimulation time, long duration of therapeutic effect, and closer to the physiological state of neurophysiological activity. Different TBS models have different effects on neuronal excitability. Intermittent TBS (iTBS) acts by continuous stimulation for 2 s with 8 s intervals, which can increase neuronal excitability. On the other hand, continuous TBS (cTBS) provides continuous stimulation at a frequency of 5 Hz, which reduces neuronal excitability (Bai et al., 2022). This article mainly describes two ways of treating OA, rTMS and Single-pulse TMS.

tDCS (Ahn et al., 2019a) is a pair of electrodes that use constant, low-intensity current (1–2 mA) on specific brain regions to regulate cortical neural activity (Cucca et al., 2019). It is widely used in the clinical treatment of Parkinsonism and other neurological diseases; it can also be used to improve motor, language, cognitive, and swallowing functions (Santos Ferreira et al., 2019). However, the exact mechanism of tDCS is not yet completely clear. Its clinical application remains in the incremental research phase, and a single mechanism cannot explain the multiple effects of tDCS; moreover, no unified scheme is available for the choice of stimulation intensity, time, and location of tDCS (Palm et al., 2016a). Currently, for tDCS, the widely recognized mechanism of action is the effect on membrane potential and ion channels, synaptic plasticity, cortical excitability (Nitsche and Paulus, 2000), bilateral hemispheric excitability, and regulation of local cortical and brain network connections (Lapenta et al., 2018).

tACS (Antal et al., 2008) is a special mode of NIBS that transmits sinusoidal alternating current electricity to the scalp, mostly affecting the excitability of cortical neurons (Bland and Sale, 2019). The currently recognized action mechanism of tACS is to regulate brain function by guiding brain oscillations (Antal et al., 2008) and inducing synaptic plasticity over a long period to regulate cognitive processes (Elyamany et al., 2021); it can also link cellular neuronal activity to brain network mechanisms to recover disturbed brain oscillations and perfect behavioral outcomes (Del Felice et al., 2019). tACS can be used as a practical means to judge the diagnosis, classification, and prognosis of mental diseases. tACS is relatively safe and non-invasive (Matsumoto and Ugawa, 2017); hence, it exhibits considerable potential in basic research and as a tool for clinical care. However, information on how tACS ultimately affects neural activity (Vieira et al., 2020) is minimal, and the two practical factors of tACS and electric field are difficult to focus on accurately, which is a common problem in tACS; thus, this technique should be further optimized and studied (Wu et al., 2021).

tRNS is a type of TMS, which exhibits the potential to induce improvements with a lasting perception when combined with assignments such as a contrast detection test (Terney et al., 2008). Nevertheless, the mechanism of these long-range improvements is not yet fully determined. tRNS can strengthen contrast sensitivity after one training cycle; however, this early onset also depends on the characteristics of the stimulus (Battaglini et al., 2020). tRNS can sense the effect of duration (Mioni et al., 2018). Interference with persistent neuronal oscillations can ultimately generate neuroplasticity effects if suitable parameters are applied (Paulus, 2011).

tFUS has a higher spatial resolution and can reach deeper organizations compared with other NIBS methods (di Biase et al., 2019). tFUS acting on the brain can modulate human cortical function (Legon et al., 2014). For example, two 10-min tFUS in the front of the thalamus will induce analgesic effects in healthy individuals (Badran et al., 2020). tFUS can also be used to regulate emotion regulatory networks in the prefrontal cortex (Goh et al., 2020; Sanguinetti et al., 2020). Low-intensity tFUS enhances the neuromodulatory effect of human autonomous motor-related cortical activity (Yu et al., 2021). Through an in-depth study, tFUS was found to be safe, and adverse reactions rarely occur. However, under high stimulation intensity or rate, tFUS may lead to bleeding, cell death or injury, and accidental opening of the blood–brain barrier. Thus, the study of tFUS is necessary to set up a good and secure framework for the application and promotion of clinical treatment of tFUS (Pasquinelli et al., 2019).

The six methods of NIBS are commonly used in clinical treatment, and they exhibit unique characteristics, including their respective sites of action, as indicated in **Figure 2**.

Therapeutic effects of non-invasive brain stimulation on osteoarthritis

Relieve pain

Pain is a common symptom in patients with OA (Perrot, 2015), and with an increase in incidence in OA and the risk factors that affect OA, pain places heavy burdens on the daily life of patients with OA and society. The treatment of pain of patients with OA is particularly important. NIBS has been shown to exhibit a therapeutic function on the pain brought by OA in many studies. For example, Jean-Paul Nguyen et al. (2019) performed a monthly rTMS treatment of 10 Hz in the right motor cortex of an elderly female patient suffering from left knee OA. One week after the third treatment, the pain was significantly reduced, and after 1 year of follow-up, the effect of pain reduction continued. Ahn et al. (2017) performed a tDCS intervention of 2 mA per day in middle-aged and elderly patients with knee OA, placing the anode on the primary motor cortex (M1) and the cathode on the contralateral supraorbital (SO). After five interventions, the patient's NRS scores decreased significantly and the Short-Form McGill Pain Questionnaire (SF-MPQ-2) scores also improved. The therapeutic effect of pain relief was found to be maintained after the 3-week follow-up. Ahn et al. (2018) also evaluated the pain sensitivity of 400 elderly patients with knee OA and conducted five tDCS interventions. Their results showed that the experimental pain sensitivity of the patients was reduced, and tDCS exerted a beneficial effect on the improvement of clinical pain. tFUS is frequently used in chronic neuropathic pain. However, targeted studies on the pain of OA are few. Research on tACS, Trns, and single-pulse TMS with regard to the pain of OA remains in its infancy and requires further exploration.

Alleviate symptoms of depression

Depression and other bad moods are closely related to OA. The occurrence of OA may aggravate depressive symptoms

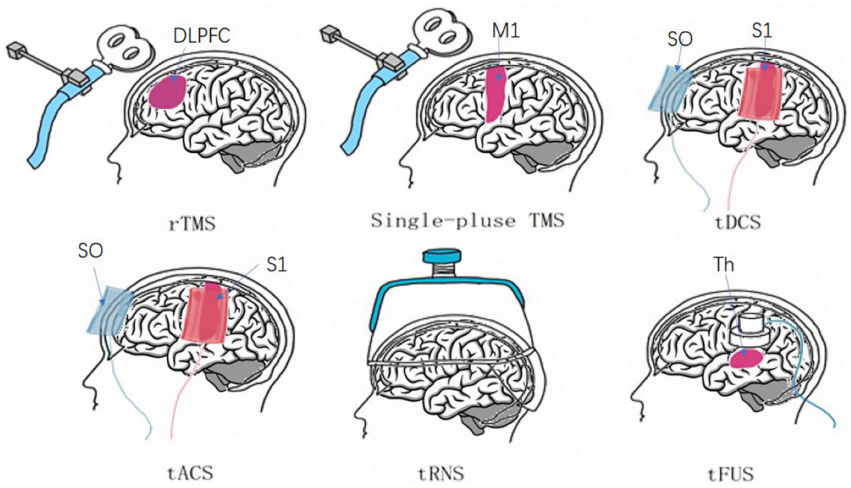

FIGURE 2
Six major non-invasive brain stimuli and their site of action. rTMS generally functions in the dorsolateral PFC (DLPFC) (Lefaucheur et al., 2020). Single-pulse TMS uses frequent sites of action, such as the primary motor cortex (M1) (Savoie et al., 2020). tDCS and tACS cathode and anode positions: contralateral orbit (SO), primary sensory cortex (S1) (Marlow et al., 2013; May et al., 2021). tRNS: cerebral cortex. tFUS: thalamus (Th) (Palm et al., 2016b; Badran et al., 2020).

(Zheng et al., 2021), and the long-term accumulation of these symptoms may aggravate the pain grade and joint dysfunction of patients with OA (Rathbun et al., 2018, 2020). NIBS has been widely used in research related to depressive symptoms. Depression assessment, such as the Hamilton Depression Rating Scale, was used as a secondary evaluation index in the research of Nguyen et al. (2019) on the program of rTMS intervention in the treatment of OA. Patients with 20 years of OA showed a significant increase in their HAD scores after ten rTMS interventions. This suggests that rTMS is effective in treating depression in patients with OA. Ahn et al. (2019b) evaluated the efficacy of remotely supervised tDCS for the treatment of OA patients, elderly KOA patients did not experience significant improvement in anxiety and depression scores after 10 consecutive tDCS interventions. This may be the result of various factors, such as autonomously improper use of tDCS. Luz-Santos et al. (2017) and Tavares et al. (2018) also studied tDCS for depression in OA patients, although the results were not available. This requires further research by researchers. The other basic NIBS methods have minimal research on the depressive symptoms of OA, and more studies are still required to confirm their result.

Improve joint motor function

The articular cartilage, as an important basic structure of joints, is the major structure affected by OA, which can cause joint deformities, joint swelling, and a decrease in the range of motion (Abhishek and Doherty, 2013), resulting in limited motor function in patients with OA. In severe cases, joint replacement surgery should be considered. Drug therapy is mostly used in the early treatment of OA, but the efficacy of drug therapy is limited (Cao et al., 2022). The safety and non-invasive characteristics of NIBS make it indispensable in the auxiliary treatment of OA. In a randomized controlled trial of tDCS combined with conventional physical therapy on the functional ability of patients with OA, Fatemeh Rahimi et al. (2021) used the anode of tDCS to intervene in the left primary motor cortex (Ahn et al., 2017), primary sensory cortex (Ahn et al., 2018), and dorsolateral PFC. The subjects were evaluated functionally with the Keen Injury and OA Outcome Score rating scale, the range of motion of the knee joint, 30-s chair standing, and 4 × 10-m walking training before and after treatment. The results show that various functional indicators were significantly improved after tDCS intervention. The strength of the muscles around the joints is also an important factor affecting joint function. Quadriceps weakness is a typical symptom of KOA. Kittelson et al. (2014) performed TMS stimulation on subjects with this symptom. After stimulation, quadriceps torque was reduced, resting motion threshold was also decreased, and the Western Ontario and McMaster Universities OA Index (Luz-Santos et al., 2017) scores increased. All these findings suggested the improvement of the motor function of subjects. The effects of tACS, tRNS and other methods on joint motor function have not yet been confirmed.

Quality of life

As a common degenerative disease of the elderly, OA is becoming increasingly in many young individuals at present, and it is one of the major factors that affect the daily activities and QOL of patients (Sabashi et al., 2021). Studies have shown that (Paget et al., 2021) the QOL of young people is more affected by OA than that of older patients in ankle OA. In the research protocol of Tavares et al. (2018) on elderly KOA patients with defective endogenous pain-inhibitory systems, health-related QOL (HRQOL) was included in the evaluation indicators of OA subjects after tDCS intervention. In the subsequent trial (Tavares et al., 2021), 2 mA tDCS intervention at the stimulation site of M1 and SO for 20 min at 15 times in 3 weeks did not significantly improve the HRQOL and WOMAC scores, and did not exert an evident effect on the QOL of patients with OA. However, in patients with OA after total knee replacement surgery, the SF-36 score was significantly improved, and the QOL of the patients was also improved after 6 weeks of treatment with electroacupuncture and exercise therapy combined with tDCS (Li et al., 2021). The curative effect of NIBS in the QOL of OA patients remains uncertain, and other factors should be excluded for further research. The detailed process and results of other research are provided in **Table 1**.

Mechanisms of non-invasive brain stimulation for osteoarthritis

Controlling central sensitization

OA has a complicated physiological mechanism. Studies have shown that (Fingleton et al., 2015; Perrot, 2015; Vincent, 2020) nerve mediators such as the nerve growth factor (NGF) and central sensitization are closely related to the severity of OA pain. An excitatory–inhibitory mechanism has been proven in the corticospinal system that is related to the degree of pain and the disorder of pain downward control (Passard et al., 2007). rTMS can inhibit the corticospinal system's excitability by stimulating it, modifying the central pain regulation system (Tarragó et al., 2016), and activating a large number of structures involved in pain processing bilaterally, leading to the long-term relief of chronic extensive pain. The high-frequency rTMS of the motor cortex can also restore the endoscopic suppression control associated with pain relief, and further reduce the pain of OA. tDCS interrupts mechanical pain processing, regulates high-order neuronal circuits that are altered by central sensitization, and weakens the mechanical stimulation response

TABLE 1 Characteristics of the research literature of the six NIBS methods for the treatment of OA.

Authors/ Publication time	Journal	*N*	Stimulation				Evaluation indicators	Experimental results
			Treatment methods	Duration	Intensity	Rate		
rTMS								
Ansari et al. (2021) 2021-4	ACS Chem Neurosci							rTMS can improve muscle fibrous pain.
Nguyen et al. (2019) 2019-4	Front Neurosci	1 (71 years old, female, KOA)	rTMS	10 months	10 Hz	Once a month	HAD, LISO, NRS	rTMS is particularly appealing to treat pain associated with KOA
Single-pulse TMS								
tDCS								
Sajadi et al. (2020) 2020-10	Neurophysiol Clin	40 (Adult, KOA)	Knee strengthening exercises + tDCS, knee strengthening exercises + TENS	2 weeks	1–2 mA	Six times	VAS?WOMAC	Effects of tDCS and TENS were not significantly different on the pain and function of patients with KOA
Fillingim et al. (2020) 2020-11	Contemp Clin Trials	60 (NHBs and NHWs with KOA)	Four groups of BAT (real vs. sham) + tDCS (real vs. sham)	1 week	1–2 mA	Five times a week	QST, WOMAC, SPPB	–
Pollonini et al. (2020b) 2020-11	J Neuroimaging	19 (The elderly with KOA)	MBM + tDCS, sham MBM + tDCS	2 weeks	2 mA	Five times a week	fNIRS, NRS, WOMAC	Combining tDCS and MBM reduced experimentally induced pain and pain perception on KOA.
Ahn et al. (2017) 2017-9	Brain Stimul	40 (50–70-year-old, KOA)	tDCS, sham tDCS	5 days	2 mA	Once a day	NRS, WOMAC, SF-MPQ-2, 6 MWT, SPPB	tDCS was efficacious in reducing of clinical pain perception in patients with KOA.
Ahn et al. (2019a) 2019-8	J Clin Neurosci	20 (50–85-year-old, KOA)	tDCS	10 Days	2 mA	Once a day	PROMIS, VAS, WOMAC, SF-MPQ	tDCS was feasible and beneficial in alleviating pain in older adults with KOA
Pollonini et al. (2020a) 2020-4	Neurophotonics	10 (9 females, 1 male, 62.4 ± 6.9 years, OA-related pain suffering 37.7 ± 31.5months, affected by right KOA from the greater Houston community)	tDCS	2 weeks	2 mA	Five times a week	VAS, WOMAC, fNIRS	tDCS can increase cortical excitability and alleviate pain in patients with KOA.
Teixeira et al. (2020) 2020-4	Princ Pract Clin Res	Adult, KOA > 3 months	tDCS + PTM, PTM alone, PTM + sham tDCS				VAS	Potential analgesic effect of tDCS in combination with PTM for fibromyalgia and KOA.
Ahn et al. (2018) 2018-9	J Pain Res	40 (50–70 years with KOA pain)	tDCS, sham tDCS	5 days	2 mA	Once a day	NRS, WOMAC, QST	tDCS can reduce experimental pain sensitivity and facilitate pain inhibition in older patients with KOA.
Ahn et al. (2019b) 2019-12	J Clin Neurosci	30 (50–85 years old with symptomatic KOA)	MBM + tDCS, sham MBM + sham tDCS	10 days	2 mA	Once a day	NRS, WOMAC, QST	Promising clinical efficacy of home-based tDCS paired with MBM for older adults with KOA

(*Continued*)

TABLE 1 (Continued)

Authors/ Publication time	Journal	*N*	Stimulation				Evaluation indicators	Experimental results
			Treatment methods	Duration	Intensity	Rate		
Rahimi et al. (2021) 2021-9	Neurophysiol Clin	80 (KOA)	PT + tDCS in M1, PT + tDCS in S1, PT + tDCS in DLPFC, sham PT + sham tDCS	1 month	2 mA	Once every 3 days	VAS, KOOS	tDCS can be a beneficial additional treatment for pain relief, disability reduction, and functional improvement in patients with KOA.
Luz-Santos et al. (2017) 2017-12	Trials	80 (KOA)	Active anodal tDCS + sham PES, sham tDCS + active PES, sham tDCS + PES, active tDCS + PES	5 days	2 mA	Once a day	SF-36, VAS, WOMAC, HAD	–
da Graca-Tarragó et al. (2019) 2019-1	J Pain Res	60 (women with KOA, aged 50–75 years old)	a-tDCS/a-EIMS, s-tDCS/s-EIMS, a-tDCS/s-EIMS, s-tDCS/a-EIMS	5 days	2 mA	Once a day	VAS, WOMAC, PPT	tDCS combing with EIMS can improve pain measures and descending pain inhibitory controls in KOA.
Suchting et al. (2020a) 2020-1	Biol Res Nurs	40 (50–70 years with KOA)	Sham tDCS, tDCS	5 days	2 mA	Once a day	IL-1β, IL-6, IL-10 TNF-α, CPR, cortisol, β-endorphin	Active Tdcs can reduce inflammation in patients with KOA.
Chang et al. (2015) 2015-8	BMJ Open	20 (age over 50 years, morning stiffness lasting less than 30 min, a minimum pain score of 40 on a 100 VAS, KOA)	Active tDCS + exercise, sham tDCS + exercise	8 Weeks	2 mA	Two times a week	VAS, WOMAC	–
Laste et al. (2012) 2012-8	Exp Brain Res	18 (rats)	Sham tDCS, tDCS	8 days	500 μA	Once a day	Von Frey test	tDCS induced significant, long-lasting, neuroplastic effects of OA
Suchting et al. (2020b) 2020-11	Pain Med	60 (aged 50–85 years, with self-reported unilateral or bilateral KOA pain)	tDCS	2 weeks	2 mA	Five times a week	VAS, WOMAC, QST	tDCS improved pain in older adults with KOA
Li et al. (2021) 2021-6	Med Sci Monit	80 (KOA who underwent TKA)	tDCS + electroacupuncture	6 weeks	1.5 mA	Five times a week	SF-36, VAS, FOOS, HSS	tDCS plus electroacupuncture effectively reduces pain following TKA
Chang et al. (2017) 2017-6	PLoS One	57 (age over 50 years, morning stiffness lasting less than 30 min, a minimum pain score of 40 on a 100 VAS, KOA)	Sham tDCS + exercise, active tDCS + exercise	8 weeks	1 mA	Two times a week	VAS, WOMAC	AT + EX may improve pain, function and pain mechanisms in KOA
Tavares et al. (2021) 2018-10	JMIR Res Protoc	94 (KOA, pain in the knee for a minimum of 6 months)	tDCS, sham tDCS	3 weeks	2 mA	Five times a week	NRS, BPI, PPT	–
Tavares et al. (2018) 2021-5	Brain Stimul	104 (age over 60 years with KOA pain and a dysfunctional DPIS)	tDCS, sham tDCS	15 days	2 mA	Once a day	BPI, the 12-item short form health survey questionnaire, MMSE, 0–100 VAS	–
tACS								
tRNS								
tFUS								

(*Continued*)

TABLE 1 (Continued)

Authors/ Publication time	Journal	*N*	Stimulation				Evaluation indicators	Experimental results
			Treatment methods	Duration	Intensity	Rate		
di Biase et al. (2021) 2021-6	Neurol Res Int		_____				VAS	tFUS has huge research potential in the field of pain management.

NRS, numeric rating scale; BPI, the Brief Pain Inventory; MMSE, the Mini-Mental State Examination; VAS, 0–100 visual analog scale; WOMAC, the Western Ontario and McMaster Universities Osteoarthritis Index; PPT, pressure pain threshold; QST, quantitative sensory testing; TKA, total knee arthroplasty; KOOS, Knee Injury and Osteoarthritis Outcome Score; SF-36, The Short Form-36 Health Survey; HSS, the Hospital for Special Surgery; TNF-α, tumor necrosis factor-α; IL, interleukin; CRP, C-reactive protein; MBM, mindfulness-based meditation; HAD, the hospital anxiety and depression scale; LISO, The lequesne index of severity for osteoarthritis; BAT, Breathing and Attention Training; SPPB, Short Physical Performance Battery; fNIRS, functional near-infrared spectroscopy; SF-MPQ-2, Short-Form McGill Pain Questionnaire; PROMIS, the Patient-Reported Outcomes Measurement Information System; PTM, physical therapy modality; EIMS, intramuscular electrical stimulation.

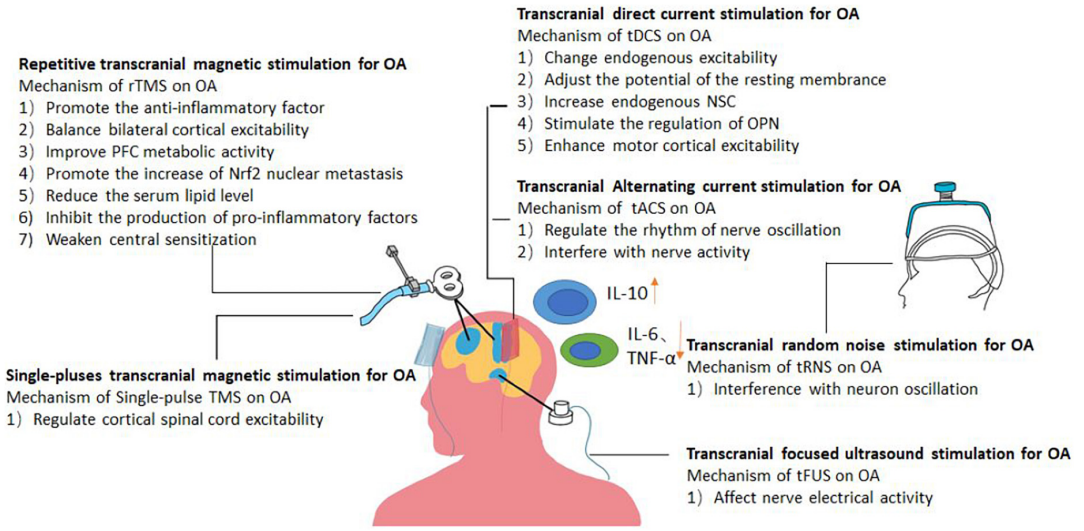

FIGURE 3
Picture showing the likely mechanism of action of different forms of NIBS in the treatment of osteoarthritis.

of spinal dorsal horn neurons (Meeker et al., 2019), controlling central sensitization and alleviating pain. Single-pulse TMS can also act on the motor cortex of the brain to increase the overall excitability of the corticospinal cord and the inner periphery of the patient (Woods et al., 2016), reducing quadriceps torque and improving motor function.

Reducing inflammatory factors

Inflammation has been proven to play an important role in OA (Sokolove and Lepus, 2013). Compared with healthy people, OA patients have higher levels of inflammatory factors, such as the tumor necrosis factor-α (Hong et al., 2020), interleukin-1β (Cao et al., 2022), and IL-6 (Wang and He, 2018). The increase of these inflammatory factors may damage the articular cartilage, synovium, and other structures (Mathiessen and Conaghan, 2017); it can also cause the release of adipokines such as leptin, which indirectly causes OA. rTMS can act on microglia, induce the capability of synaptic plasticity, promote the secretion of the anti-inflammatory factor IL-10, and inhibit the production of pro-inflammatory factors, reducing inflammatory response (Lenz et al., 2021). Under the stimulation of cathodic tDCS, endogenous neural stem cells (NSCs) exhibit a tendency to increase (Ryu et al., 2009), inducing a strong regenerative response and reducing the inflammatory response. Neuritis has beneficial and harmful effects on the prevention of secondary tissue damage (Stoll et al., 2002), regeneration, and recovery. Therefore, the parameters of NIBS should be controlled to promote the beneficial aspects of inducing the recruitment of endogenous NSCs and minimizing inflammation as much as possible (Mabuchi et al., 2000). Promoting the production of factors is conducive to

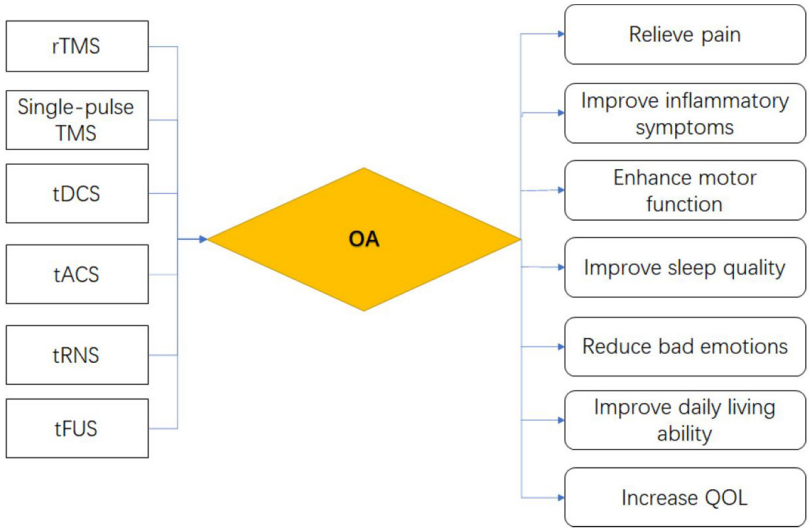

FIGURE 4
Effects of six major NIBS on OA.

the normal growth of chondrocytes and slows down the development of OA.

Influencing gene expression

Mitochondria are the cell organelles where genetic genes are replicated and transcribed; they also have their gene-mitochondrial (Blanco et al., 2018), and the variation of mtDNA directly affects OA phenotypes (Blanco et al., 2018). Therefore, different gene expressions exert varying effects on the OA process. Among them, rTMS can effectively affect the regulation of astrocytes related to the expression of pro-inflammatory or anti-inflammatory genes (Hong et al., 2020) and may change the cell membrane potential and cell function of astrocytes (Ruohonen and Karhu, 2012) to produce anti-inflammatory mediators for the neuroprotection effect, further reducing inflammation response (Liddelow et al., 2017). rTMS can promote the increase of Nrf2 nuclear metastasis (Tian et al., 2020), and Nrf2 can activate genes via antioxidant response, which can effectively protect cells under inflammatory conditions and can also inhibit the expression of signal channels that induce inflammation, effectively reducing the inflammatory response. In addition, tDCS can stimulate the regulation of osteopontin (Rabenstein et al., 2015, 2019). OPN can increase the survival, proliferation, migration, and neuronal differentiation of endogenous NSC (Rabenstein et al., 2015); enhance the proliferation and migration of neuronal precursors after cerebral ischemia (Denhardt et al., 2001), and play an important role in organizational balance, wound healing, immune regulation, and other aspects. These conditions can alleviate secondary damage in patients with OA, promote cartilage repair, and accelerate functional recovery in patients with OA. Although tACS, tFUS, and other methods still lack research on OA gene expression, NIBS plays a role in the pathological mechanism of OA gene expression.

Improving cortex excitability

Studies suggest that higher cortical excitability may be a mechanism of OA and is closely linked to chronic pain and motor capacity in OA patients (Kittelson et al., 2014; Simis et al., 2021). OA patients with lower cortical inhibition had higher degrees of pain and a more obvious decrease in quadriceps motor function. As one of the NIBS methods for stimulating nerve cells in the superficial brain area (Fan et al., 2021), rTMS can regulate cortical excitability and recovery through different frequency stimulations (Barker, 1991). Among the rehabilitation studies based on the hypothesis of cross-hemisphere competition (Chen and Seitz, 2001), low-frequency rTMS may cause a short-term decline in the excitability of the unaffected hemisphere cortex (Wang et al., 2019), balance the excitability of the cerebellum, improve patients' learning ability, and increase walking ability. By contrast, high-frequency rTMS can enhance the cortical excitability of the affected hemisphere during exercise (Goh et al., 2020), reducing competition and gradually improving the exercise capacity of patients. The improvement of specific motor functions by tDCS is also related to changes in the excitability of the motor cortex. The tDCS acting on M1 can increase the activity of the cerebral cortex, reduce the body's response time, and better activate a

patient's motor function (Stagg et al., 2012). Therefore, NIBS might alleviate the symptoms of OA by improving cortical hyperexcitability.

Adjusting endocrine

Obesity is an important risk factor for OA, and obesity is driven by complex endocrine mechanisms (Steidle-Kloc et al., 2018). Under the intervention of rTMS, the serum lipid level is significantly reduced (Ren et al., 2017), while the contents of thyroid-stimulating hormone and thyroxine are increased simultaneously. This finding indicates that rTMS can regulate serum lipid metabolism by changing the hypothalamic–pituitary–thyroid axis (George et al., 1996). Therefore, rTMS has the functions of regulating endocrine, improving PFC metabolic activity (Trojak et al., 2011), and regulating serum metabolic activity of lipid levels, thereby stabilizing blood lipid levels, reducing the incidence of obesity, and ultimately decreasing the effect of obesity on OA. tDCS is also extremely important in the control of obesity, but its specific mechanism remains unclear (Araujo et al., 2018), and the endocrine regulation mechanism that affects OA should be further explored.

In summary, on the basis of its role in complex pathophysiological mechanisms, NIBS can be further applied to OA to test its therapeutic mechanism and efficacy of OA. We summarize the mechanism and effects of six commonly used NIBS methods on OA, as shown in **Figures 3**, **4**.

Future perspectives

Although NIBS has been proven to be effective and feasible in the treatment of OA, there are still some limitations that need to be improved. First, existing research has focused on the tDCS and rTMS methods. Studies on OA treatment of single-pulse TMS, tACS, tRNS, and tFUS are few. Second, although NIBS, as a mature treatment technique, has been extensively applied to the treatment of clinical diseases in many fields in recent years, the treatment of OA is still in its infancy. No uniform treatment standard for regulating the treatment of OA by NIBS is available. Moreover, when OA occurs in different joints, it will exhibit different symptoms and require more targeted treatment. In addition, current NIBS studies have mostly focused on the pain symptoms of OA, and the treatment of other symptoms lacks evidence to confirm. In summary, the understanding of NIBS in the treatment of OA is limited, and more in-depth exploration can be performed from the aforementioned aspects, such that OA can be treated with more standardized NIBS, enabling OA patients to participate better in family and social life, and reduce social burdens.

Conclusion

With the continuous research on NIBS, the feasibility and effectiveness of NIBS in the treatment of OA have been confirmed by research. This paper summarizes the current research progress of NIBS for OA, describes the main clinical effects and possible mechanisms of NIBS in treating OA, and provides a basis for further research on NIBS in the therapy of OA in the future. However, the treatment protocol of NIBS for the treatment of OA is not unified, which provides a research direction for future research.

Author contributions

X-QW and X-AZ: draft conception, project administration, and funding acquisition. H-QZ, X-QW, X-AZ, and JL: writing – review and editing. All authors contributed to the article and approved the submitted version.

Funding

This research was supported by the Innovative Talents Support Program for Universities of Liaoning Province (No. WR2019024), the Shanghai Frontiers Science Research Base of Exercise and Metabolic Health, and the Shanghai Key Lab of Human Performance (Shanghai University of Sport) (No. 11DZ2261100).

Conflict of interest

The authors declare that the research was conducted in the absence of any commercial or financial relationships that could be construed as a potential conflict of interest.

Publisher's note

References

Abhishek, A., and Doherty, M. (2013). Diagnosis and clinical presentation of osteoarthritis. *Rheum. Dis. Clin. North Am.* 39, 45–66.

Ahn, H., Sorkpor, S., Miao, H., Zhong, C., Jorge, R., Park, L., et al. (2019a). Home-based self-administered transcranial direct current stimulation in older adults with knee osteoarthritis pain: An open-label study. *J. Clin. Neurosci.* 66, 61–65. doi: 10.1016/j.jocn.2019.05.023

Ahn, H., Suchting, R., Woods, A. J., Miao, H., Green, C., Cho, R. Y., et al. (2018). Bayesian analysis of the effect of transcranial direct current stimulation on experimental pain sensitivity in older adults with knee osteoarthritis: Randomized sham-controlled pilot clinical study. *J. Pain Res.* 11, 2071–2082. doi: 10.2147/JPR.S173080

Ahn, H., Woods, A. J., Kunik, M. E., Bhattacharjee, A., Chen, Z., Choi, E., et al. (2017). Efficacy of transcranial direct current stimulation over primary motor cortex (anode) and contralateral supraorbital area (cathode) on clinical pain severity and mobility performance in persons with knee osteoarthritis: An experimenter- and participant-blinded, randomized, sham-controlled pilot clinical study. *Brain Stimul.* 10, 902–909. doi: 10.1016/j.brs.2017.05.007

Ahn, H., Zhong, C., Miao, H., Chaoul, A., Park, L., Yen, I. H., et al. (2019b). Efficacy of combining home-based transcranial direct current stimulation with mindfulness-based meditation for pain in older adults with knee osteoarthritis: A randomized controlled pilot study. *J. Clin. Neurosci.* 70, 140–145. doi: 10.1016/j.jocn.2019.08.047

Ansari, A. H., Pal, A., Ramamurthy, A., Kabat, M., Jain, S., and Kumar, S. (2021). Fibromyalgia pain and depression: An update on the role of repetitive transcranial magnetic stimulation. *ACS Chem. Neurosci.* 12, 256–270. doi: 10.1021/acschemneuro.0c00785

Antal, A., Boros, K., Poreisz, C., Chaieb, L., Terney, D., and Paulus, W. (2008). Comparatively weak after-effects of transcranial alternating current stimulation (tACS) on cortical excitability in humans. *Brain Stimul.* 1, 97–105. doi: 10.1016/j.brs.2007.10.001

Araujo, C., Fitz, R. C., Nogara, D. A., Schestatsky, P., and Gerchman, F. (2018). Effect of transcranial direct current stimulation associated with hypocaloric diet on weight loss and metabolic profile in overweight or obesity: study protocol for a double-blind, randomized controlled clinical trial. *Trials* 19:386.

Arden, N. K., Perry, T. A., Bannuru, R. R., Bruyère, O., Cooper, C., Haugen, I. K., et al. (2021). Non-surgical management of knee osteoarthritis: Comparison of ESCEO and OARSI 2019 guidelines. *Nat. Rev. Rheumatol.* 17, 59–66. doi: 10.1038/s41584-020-00523-9

Auvichayapat, P., and Auvichayapat, N. (2009). Basic principle of transcranial magnetic stimulation. *J. Med. Assoc. Thail.* 92, 1560–1566.

Badran, B. W., Caulfield, K. A., Stomberg-Firestein, S., Summers, P. M., Dowdle, L. T., Savoca, M., et al. (2020). Sonication of the anterior thalamus with MRI-Guided transcranial focused ultrasound (tFUS) alters pain thresholds in healthy adults: A double-blind, sham-controlled study. *Brain Stimul.* 13, 1805–1812.

Bai, Z., Zhang, J., and Fong, K. N. K. (2022). Effects of transcranial magnetic stimulation in modulating cortical excitability in patients with stroke: A systematic review and meta-analysis. *J. Neuroeng. Rehabil.* 19:24. doi: 10.1186/s12984-022-00999-4

Barker, A. T. (1991). An introduction to the basic principles of magnetic nerve stimulation. *J. Clin. Neurophysiol.* 8, 26–37. doi: 10.1097/00004691-199101000-00005

Barker, A. T., Jalinous, R., and Freeston, I. L. (1985). Non-invasive magnetic stimulation of human motor cortex. *Lancet* 1, 1106–1107.

Bartels, E. M., Juhl, C. B., Christensen, R., Hagen, K. B., Danneskiold-Samsøe, B., Dagfinrud, H., et al. (2016). Aquatic exercise for the treatment of knee and hip osteoarthritis. *Cochrane Database Syst. Rev.* 3:Cd005523.

Battaglini, L., Contemori, G., Penzo, S., and Maniglia, M. (2020). tRNS effects on visual contrast detection. *Neurosci. Lett.* 717:134696. doi: 10.1016/j.neulet.2019.134696

Blanco, F. J., Valdes, A. M., and Rego-Pérez, I. (2018). Mitochondrial DNA variation and the pathogenesis of osteoarthritis phenotypes. *Nat. Rev. Rheumatol.* 14, 327–340.

Bland, N. S., and Sale, M. V. (2019). Current challenges: The ups and downs of tACS. *Expe. Brain Res.*. 237, 3071–3088. doi: 10.1007/s00221-019-05666-0

Cao, R., Yu, H., Long, H., Zhang, H., Hao, C., Shi, L., et al. (2022). Low deacetylation degree chitosan oligosaccharide protects against IL-1β induced inflammation and enhances autophagy activity in human chondrocytes. *J. Biomater. Sci. Polym. Ed.* 33, 517–531. doi: 10.1080/09205063.2021.1996962

Chang, W. J., Bennell, K. L., Hodges, P. W., Hinman, R. S., Liston, M. B., and Schabrun, S. M. (2015). Combined exercise and transcranial direct current stimulation intervention for knee osteoarthritis: Protocol for a pilot randomised controlled trial. *BMJ Open.* 5:e008482. doi: 10.1136/bmjopen-2015-008482

Chang, W. J., Bennell, K. L., Hodges, P. W., Hinman, R. S., Young, C. L., Buscemi, V., et al. (2017). Addition of transcranial direct current stimulation to quadriceps strengthening exercise in knee osteoarthritis: A pilot randomised controlled trial. *PLoS One* 12:e0180328. doi: 10.1371/journal.pone.0180328

Chen, R., and Seitz, R. J. (2001). Changing cortical excitability with low-frequency magnetic stimulation. *Neurology* 57, 379–380.

Chou, W. Y., Cheng, J. H., Wang, C. J., Hsu, S. L., Chen, J. H., and Huang, C. Y. (2019). Shockwave targeting on subchondral bone is more suitable than articular cartilage for knee osteoarthritis. *Int. J. Med. Sci.* 16, 156–166. doi: 10.7150/ijms.26659

Cucca, A., Sharma, K., Agarwal, S., Feigin, A. S., and Biagioni, M. C. (2019). Tele-monitored tDCS rehabilitation: Feasibility, challenges and future perspectives in Parkinson's disease. *J. Neuroeng. Rehabil.* 16:20. doi: 10.1186/s12984-019-0481-4

D'Agati, D., Bloch, Y., Levkovitz, Y., and Reti, I. (2010). rTMS for adolescents: Safety and efficacy considerations. *Psychiatry Res.* 177, 280–285.

da Costa, B. R., Reichenbach, S., Keller, N., Nartey, L., Wandel, S., Jüni, P., et al. (2017). Effectiveness of non-steroidal anti-inflammatory drugs for the treatment of pain in knee and hip osteoarthritis: A network meta-analysis. *Lancet.* 390, e21–e33.

da Graca-Tarragó, M., Lech, M., Angoleri, L. D. M., Santos, D. S., Deitos, A., Brietzke, A. P., et al. (2019). Intramuscular electrical stimulus potentiates motor cortex modulation effects on pain and descending inhibitory systems in knee osteoarthritis: A randomized, factorial, sham-controlled study. *J. Pain Res.* 12, 209–221. doi: 10.2147/JPR.S181019

de Goede, A. A., Cumplido-Mayoral, I., and van Putten, M. (2020). Spatiotemporal dynamics of single and paired pulse TMS-EEG responses. *Brain Topogr.* 33, 425–437. doi: 10.1007/s10548-020-00773-6

Del Felice, A., Castiglia, L., Formaggio, E., Cattelan, M., Scarpa, B., Manganotti, P., et al. (2019). Personalized transcranial alternating current stimulation (tACS) and physical therapy to treat motor and cognitive symptoms in Parkinson's disease: A randomized cross-over trial. *Neuroimage Clin.* 22:101768. doi: 10.1016/j.nicl.2019.101768

Denhardt, D. T., Noda, M., O'Regan, A. W., Pavlin, D., and Berman, J. S. (2001). Osteopontin as a means to cope with environmental insults: Regulation of inflammation, tissue remodeling, and cell survival. *J. Clin. Invest.* 107, 1055–1061. doi: 10.1172/JCI12980

di Biase, L., Falato, E., and Di Lazzaro, V. (2019). Transcranial Focused Ultrasound (tFUS) and Transcranial Unfocused Ultrasound (tUS) Neuromodulation: From theoretical principles to stimulation practices. *Front. Neurol.* 10:549. doi: 10.3389/fneur.2019.00549

di Biase, L., Falato, E., Caminiti, M. L., Pecoraro, P. M., Narducci, F., and Di Lazzaro, V. (2021). Focused Ultrasound (FUS) for chronic pain management: Approved and potential applications. *Neurol. Res. Int.* 2021:8438498. doi: 10.1155/2021/8438498

Du, J., Yang, F., Hu, J., Hu, J., Xu, Q., Cong, N., et al. (2019). Effects of high- and low-frequency repetitive transcranial magnetic stimulation on motor recovery in early stroke patients: Evidence from a randomized controlled trial with clinical, neurophysiological and functional imaging assessments. *Neuroimage Clin.* 21:101620. doi: 10.1016/j.nicl.2018.101620

Egloff, C., Hügle, T., and Valderrabano, V. (2012). Biomechanics and pathomechanisms of osteoarthritis. *Swiss Med. Wkly.* 142:w13583.

Elyamany, O., Leicht, G., Herrmann, C. S., and Mulert, C. (2021). Transcranial alternating current stimulation (tACS): From basic mechanisms towards first applications in psychiatry. *Eur. Arch. Psychiatry Clin. Neurosci.* 271, 135–156. doi: 10.1007/s00406-020-01209-9

Fan, H., Song, Y., Cen, X., Yu, P., Bíró, I., and Gu, Y. (2021). The effect of repetitive transcranial magnetic stimulation on lower-limb motor ability in stroke patients: A systematic review. *Front. Hum. Neurosci.* 15:620573. doi: 10.3389/fnhum.2021.620573

Ferrarelli, F., and Phillips, M. L. (2021). Examining and modulating neural circuits in psychiatric disorders with transcranial magnetic stimulation and electroencephalography: Present practices and future developments. *Am. J. Psychiatry* 178, 400–413. doi: 10.1176/appi.ajp.2020.20071050

Fillingim, R. B., Woods, A. J., Ahn, H., Wu, S. S., Redden, D. T., Lai, S., et al. (2020). Pain relief for osteoarthritis through combined treatment (PROACT): Protocol for a randomized controlled trial of mindfulness meditation combined

with transcranial direct current stimulation in non-Hispanic black and white adults with knee osteoarthritis. *Contemp. Clin. Trials* 98:106159. doi: 10.1016/j.cct.2020.106159

Fingleton, C., Smart, K., Moloney, N., Fullen, B. M., and Doody, C. (2015). Pain sensitization in people with knee osteoarthritis: A systematic review and meta-analysis. *Osteoarthritis Cartilage* 23, 1043–1056.

Forestier, R., Erol Forestier, F. B., and Francon, A. (2016). Spa therapy and knee osteoarthritis: A systematic review. *Ann. Phys. Rehabil. Med.* 59, 216–226.

George, M. S., Wassermann, E. M., Williams, W. A., Steppel, J., Pascual-Leone, A., Basser, P., et al. (1996). Changes in mood and hormone levels after rapid-rate transcranial magnetic stimulation (rTMS) of the prefrontal cortex. *J. Neuropsychiatry Clin. Neurosci.* 8, 172–180. doi: 10.1176/jnp.8.2.172

Goh, H. T., Connolly, K., Hardy, J., McCain, K., and Walker-Batson, D. (2020). Single session of repetitive transcranial magnetic stimulation to left dorsolateral prefrontal cortex increased dual-task gait speed in chronic stroke: A pilot study. *Gait Posture.* 78, 1–5. doi: 10.1016/j.gaitpost.2020.02.020

Griffin, T. M., Batushansky, A., Hudson, J., and Lopes, E. B. P. (2020). Correlation network analysis shows divergent effects of a long-term, high-fat diet and exercise on early stage osteoarthritis phenotypes in mice. *J. Sport Health Sci.* 9, 119–131. doi: 10.1016/j.jshs.2019.05.008

Guo, X., Lou, J., Wang, F., Fan, D., and Qin, Z. (2022). Recent advances in nano-therapeutic strategies for osteoarthritis. *Front. Pharmacol.* 13:924387. doi: 10.3389/fphar.2022.924387

Hallett, M. (2007). Transcranial magnetic stimulation: A primer. *Neuron* 55, 187–199.

Hawker, G. A. (2019). Osteoarthritis is a serious disease. *Clin. Exp. Rheumatol.* 37 Suppl 120, 3–6.

Hermann, W., Lambova, S., and Muller-Ladner, U. (2018). Current treatment options for osteoarthritis. *Curr. Rheumatol. Rev.* 14, 108–116.

Hong, Y., Liu, Q., Peng, M., Bai, M., Li, J., Sun, R., et al. (2020). High-frequency repetitive transcranial magnetic stimulation improves functional recovery by inhibiting neurotoxic polarization of astrocytes in ischemic rats. *J. Neuroinflammation* 17:150. doi: 10.1186/s12974-020-01747-y

Jeon, O. H., Kim, C., Laberge, R. M., Demaria, M., Rathod, S., Vasserot, A. P., et al. (2017). Local clearance of senescent cells attenuates the development of post-traumatic osteoarthritis and creates a pro-regenerative environment. *Nat. Med.* 23, 775–781. doi: 10.1038/nm.4324

Kakouris, N., Yener, N., and Fong, D. T. P. (2021). A systematic review of running-related musculoskeletal injuries in runners. *J. Sport Health Sci.* 10, 513–522.

Kavanaugh, T. E., Werfel, T. A., Cho, H., Hasty, K. A., and Duvall, C. L. (2016). Particle-based technologies for osteoarthritis detection and therapy. *Drug Deliv. Transl. Res.* 6, 132–147. doi: 10.1007/s13346-015-0234-2

Kittelson, A. J., Thomas, A. C., Kluger, B. M., and Stevens-Lapsley, J. E. (2014). Corticospinal and intracortical excitability of the quadriceps in patients with knee osteoarthritis. *Expe. Brain Res.* 232, 3991–3999. doi: 10.1007/s00221-014-4079-6

Klomjai, W., Katz, R., and Lackmy-Vallée, A. (2015). Basic principles of transcranial magnetic stimulation (TMS) and repetitive TMS (rTMS). *Ann. Phys. Rehabil. Med.* 58, 208–213.

Lapenta, O. M., Marques, L. M., Rego, G. G., Comfort, W. E., and Boggio, P. S. (2018). tDCS in Addiction and impulse control disorders. *J. ECT.* 34, 182–192.

Laste, G., Caumo, W., Adachi, L. N., Rozisky, J. R., de Macedo, I. C., Filho, P. R., et al. (2012). After-effects of consecutive sessions of transcranial direct current stimulation (tDCS) in a rat model of chronic inflammation. *Exp. Brain Res.* 221, 75–83. doi: 10.1007/s00221-012-3149-x

Lefaucheur, J. P., Aleman, A., Baeken, C., Benninger, D. H., Brunelin, J., Di Lazzaro, V., et al. (2020). Evidence-based guidelines on the therapeutic use of repetitive transcranial magnetic stimulation (rTMS): An update (2014-2018). *Clin. Neurophysiol.* 131, 474–528.

Legon, W., Sato, T. F., Opitz, A., Mueller, J., Barbour, A., Williams, A., et al. (2014). Transcranial focused ultrasound modulates the activity of primary somatosensory cortex in humans. *Nat. Neurosci.* 17, 322–329.

Lenz, M., Eichler, A., and Vlachos, A. (2021). Monitoring and modulating inflammation-associated alterations in synaptic plasticity: Role of brain stimulation and the blood-brain interface. *Biomolecules* 11:359. doi: 10.3390/biom11030359

Li, X., Yu, W., Li, H., Wang, B., and Xu, J. (2021). Prospective, single-center comparison of transcranial direct current stimulation plus electroacupuncture and standard analgesia in patients after total knee arthroplasty: Effect on rehabilitation and functional recovery. *Med. Sci. Monitor* 27:e930363. doi: 10.12659/MSM.930363

Liddelow, S. A., Guttenplan, K. A., Clarke, L. E., Bennett, F. C., Bohlen, C. J., Schirmer, L., et al. (2017). Neurotoxic reactive astrocytes are induced by activated microglia. *Nature* 541, 481–487.

Luz-Santos, C., Ribeiro Camatti, J., Barbosa Paixão, A., Nunes Sá, K., Montoya, P., Lee, M., et al. (2017). Additive effect of tDCS combined with Peripheral Electrical Stimulation to an exercise program in pain control in knee osteoarthritis: Study protocol for a randomized controlled trial. *Trials* 18:609. doi: 10.1186/s13063-017-2332-6

Mabuchi, T., Kitagawa, K., Ohtsuki, T., Kuwabara, K., Yagita, Y., Yanagihara, T., et al. (2000). Contribution of microglia/macrophages to expansion of infarction and response of oligodendrocytes after focal cerebral ischemia in rats. *Stroke* 31, 1735–1743. doi: 10.1161/01.str.31.7.1735

Mantovani, V., Maccari, F., and Volpi, N. (2016). Chondroitin Sulfate and glucosamine as disease modifying Anti- Osteoarthritis Dru gs (DMOADs). *Curr. Med. Chem.* 23, 1139–1151. doi: 10.2174/0929867323666160316123749

Marlow, N. M., Bonilha, H. S., and Short, E. B. (2013). Efficacy of transcranial direct current stimulation and repetitive transcranial magnetic stimulation for treating fibromyalgia syndrome: A systematic review. *Pain Pract.* 13, 131–145.

Mathew, J., and Danion, F. R. (2018). Ups and downs in catch-up saccades following single-pulse TMS-methodological considerations. *PLoS One* 13:e0205208. doi: 10.1371/journal.pone.0205208

Mathiessen, A., and Conaghan, P. G. (2017). Synovitis in osteoarthritis: Current understanding with therapeutic implications. *Arthritis Res. Ther.* 19:18.

Matsumoto, H., and Ugawa, Y. (2017). Adverse events of tDCS and tACS: A review. *Clin. Neurophysiol. Pract.* 2, 19–25.

May, E. S., Hohn, V. D., Nickel, M. M., Tiemann, L., Gil Ávila, C., Heitmann, H., et al. (2021). Modulating brain rhythms of pain using transcranial alternating current stimulation (tACS) - A sham-controlled study in healthy human participants. *J. Pain* 22, 1256–1272. doi: 10.1016/j.jpain.2021.03.150

Meeker, T. J., Keaser, M. L., Khan, S. A., Gullapalli, R. P., Seminowicz, D. A., and Greenspan, J. D. (2019). Non-invasive motor cortex neuromodulation reduces secondary hyperalgesia and enhances activation of the descending pain modulatory network. *Front. Neurosci.* 13:467. doi: 10.3389/fnins.2019.00467

Miniussi, C., and Ruzzoli, M. (2013). Transcranial stimulation and cognition. *Handb. Clin. Neurol.* 116, 739–750.

Mioni, G., Grondin, S., Mapelli, D., and Stablum, F. A. (2018). tRNS investigation of the sensory representation of time. *Sci. Rep.* 8:10364. doi: 10.1038/s41598-018-28673-7

Nguyen, J. P., Dixneuf, V., Esnaut, J., Moreno, A. S., Malineau, C., Nizard, J., et al. (2019). The value of high-frequency repetitive transcranial magnetic stimulation of the motor cortex to treat central pain sensitization associated with knee osteoarthritis. *Front. Neurosci.* 13:388. doi: 10.3389/fnins.2019.00388

Nitsche, M. A., and Paulus, W. (2000). Excitability changes induced in the human motor cortex by weak transcranial direct current stimulation. *J. Physiol.* 527 Pt 3, 633–639.

O'Connell, N. E., Marston, L., Spencer, S., DeSouza, L. H., and Wand, B. M. (2018). Non-invasive brain stimulation techniques for chronic pain. *Cochrane Database Syst. Rev.* 4:Cd008208.

Paget, L. D. A., Tol, J. L., Kerkhoffs, G., and Reurink, G. (2021). Health-related quality of life in ankle osteoarthritis: A case-control study. *Cartilage* 13(1_suppl), 1438S–1444S.

Palm, U., Ayache, S. S., Padberg, F., and Lefaucheur, J. P. (2016a). [Transcranial direct current stimulation (tDCS) for depression: Results of nearly a decade of clinical research]. *Encephale* 42, 39–47.

Palm, U., Chalah, M. A., Padberg, F., Al-Ani, T., Abdellaoui, M., Sorel, M., et al. (2016b). Effects of transcranial random noise stimulation (tRNS) on affect, pain and attention in multiple sclerosis. *Restor. Neurol. Neurosci.* 34, 189–199. doi: 10.3233/RNN-150557

Pasquinelli, C., Hanson, L. G., Siebner, H. R., Lee, H. J., and Thielscher, A. (2019). Safety of transcranial focused ultrasound stimulation: A systematic review of the state of knowledge from both human and animal studies. *Brain Stimul.* 12, 1367–1380. doi: 10.1016/j.brs.2019.07.024

Passard, A., Attal, N., Benadhira, R., Brasseur, L., Saba, G., Sichere, P., et al. (2007). Effects of unilateral repetitive transcranial magnetic stimulation of the motor cortex on chronic widespread pain in fibromyalgia. *Brain* 130(Pt 10), 2661–2670.

Paulus, W. (2011). Transcranial electrical stimulation (tES - tDCS; tRNS, tACS) methods. *Neuropsychol. Rehabil.*. 21, 602–617.

Pell, G. S., Roth, Y., and Zangen, A. (2011). Modulation of cortical excitability induced by repetitive transcranial magnetic stimulation: Influence of timing and geometrical parameters and underlying mechanisms. *Prog. Neurobiol.* 93, 59–98. doi: 10.1016/j.pneurobio.2010.10.003

Pereira, D., Ramos, E., and Branco, J. (2015). Osteoarthritis. *Acta Med. Port.* 28, 99–106.

Perrot, S. (2015). Osteoarthritis pain. *Best pract. Res. Clin. Rheumatol.* 29, 90–97.

Plewnia, C., Schroeder, P. A., and Wolkenstein, L. (2015). Targeting the biased brain: Non-invasive brain stimulation to ameliorate cognitive control. *Lancet Psychiatry* 2, 351–356.

Polanía, R., Nitsche, M. A., and Ruff, C. C. (2018). Studying and modifying brain function with non-invasive brain stimulation. *Nat. Neurosci.* 21, 174–187.

Pollonini, L., Miao, H., and Ahn, H. (2020a). Longitudinal effect of transcranial direct current stimulation on knee osteoarthritis patients measured by functional infrared spectroscopy: A pilot study. *Neurophotonics* 7:025004. doi: 10.1117/1.NPh.7.2.025004

Pollonini, L., Montero-Hernandez, S., Park, L., Miao, H., Mathis, K., and Ahn, H. (2020b). Functional Near-Infrared Spectroscopy to Assess Central Pain Responses in a Nonpharmacologic Treatment Trial of Osteoarthritis. *J. Neuroimaging* 30, 808–814. doi: 10.1111/jon.12782

Qiu, C. G., Chui, C. S., Chow, S. K. H., Cheung, W. H., and Wong, R. M. Y. (2022). Effects of whole-body vibration therapy on knee Osteoarthritis: A systematic review and meta-analysis of randomized controlled trials. *J. Rehabil. Med.* 54:jrm00266. doi: 10.2340/jrm.v54.2032

Rabenstein, M., Hucklenbroich, J., Willuweit, A., Ladwig, A., Fink, G. R., Schroeter, M., et al. (2015). Osteopontin mediates survival, proliferation and migration of neural stem cells through the chemokine receptor CXCR4. *Stem Cell Res. Ther.* 6:99. doi: 10.1186/s13287-015-0098-x

Rabenstein, M., Unverricht-Yeboah, M., Keuters, M. H., Pikhovych, A., Hucklenbroich, J., Vay, S. U., et al. (2019). Transcranial current stimulation alters the expression of immune-mediating genes. *Front. Cell. Neurosci.* 13:461. doi: 10.3389/fncel.2019.00461

Rahimi, F., Nejati, V., Nassadj, G., Ziaei, B., and Mohammadi, H. K. (2021). The effect of transcranial direct stimulation as an add-on treatment to conventional physical therapy on pain intensity and functional ability in individuals with knee osteoarthritis: A randomized controlled trial. *Neurophysiol. Clin.* 51, 507–516. doi: 10.1016/j.neucli.2021.06.002

Rathbun, A. M., Shardell, M. D., Ryan, A. S., Yau, M. S., Gallo, J. J., Schuler, M. S., et al. (2020). Association between disease progression and depression onset in persons with radiographic knee osteoarthritis. *Rheumatology* 59, 3390–3399.

Rathbun, A. M., Stuart, E. A., Shardell, M., Yau, M. S., Baumgarten, M., and Hochberg, M. C. (2018). Dynamic effects of depressive symptoms on osteoarthritis knee pain. *Arthritis Care Res.* 70, 80–88.

Ren, W., Ma, J., Li, J., Zhang, Z., and Wang, M. (2017). Repetitive Transcranial Magnetic Stimulation (rTMS) modulates lipid metabolism in aging adults. *Front. Aging Neurosci.* 9:334. doi: 10.3389/fnagi.2017.00334

Ruohonen, J., and Karhu, J. (2012). tDCS possibly stimulates glial cells. *Clin. Neurophysiol.* 123, 2006–2009.

Ryu, J. K., Cho, T., Wang, Y. T., and McLarnon, J. G. (2009). Neural progenitor cells attenuate inflammatory reactivity and neuronal loss in an animal model of inflamed AD brain. *J. Neuroinflammation* 6:39. doi: 10.1186/1742-2094-6-39

Sabashi, K., Ishida, T., Matsumoto, H., Mikami, K., Chiba, T., Yamanaka, M., et al. (2021). Dynamic postural control correlates with activities of daily living and quality of life in patients with knee osteoarthritis. *BMC Musculoskelet. Disord.* 22:287. doi: 10.1186/s12891-021-04164-1

Sajadi, S., Karimi, M., Forogh, B., Raissi, G. R., Zarnegar, F., and Ahadi, T. (2020). Randomized clinical trial comparing of transcranial direct current stimulation (tDCS) and transcutaneous electrical nerve stimulation (TENS) in knee osteoarthritis. *Neurophysiol. Clin.* 50, 367–374. doi: 10.1016/j.neucli.2020.08.005

Sanguinetti, J. L., Hameroff, S., Smith, E. E., Sato, T., Daft, C. M. W., Tyler, W. J., et al. (2020). Transcranial focused ultrasound to the right prefrontal cortex improves mood and alters functional connectivity in humans. *Front. Hum. Neurosci.* 14:52. doi: 10.3389/fnhum.2020.00052

Santos Ferreira, I., Teixeira Costa, B., Lima Ramos, C., Lucena, P., Thibaut, A., and Fregni, F. (2019). Searching for the optimal tDCS target for motor rehabilitation. *J. Neuroeng. Rehabil.* 16:90.

Savoie, F. A., Dallaire-Jean, L., Thénault, F., Whittingstall, K., and Bernier, P. M. (2020). Single-Pulse TMS over the parietal cortex does not impair sensorimotor perturbation-induced changes in motor commands. *eNeuro* 7, ENEURO.209–ENEURO.219.

Simis, M., Imamura, M., de Melo, P. S., Marduy, A., Pacheco-Barrios, K., Teixeira, P. E. P., et al. (2021). Increased motor cortex inhibition as a marker of compensation to chronic pain in knee osteoarthritis. *Sci. Rep.* 11:24011. doi: 10.1038/s41598-021-03281-0

Sokolove, J., and Lepus, C. M. (2013). Role of inflammation in the pathogenesis of osteoarthritis: Latest findings and interpretations. *Ther. Adv. Musculoskelet. Dis.* 5, 77–94. doi: 10.1177/1759720X12467868

Stagg, C. J., Bachtiar, V., O'Shea, J., Allman, C., Bosnell, R. A., Kischka, U., et al. (2012). Cortical activation changes underlying stimulation-induced behavioural gains in chronic stroke. *Brain J. Neurol.* 135(Pt 1), 276–284.

Steidle-Kloc, E., Dannhauer, T., Wirth, W., and Eckstein, F. (2018). Responsiveness of infrapatellar fat pad volume change to body weight loss or gain: Data from the osteoarthritis initiative. *Cells Tissues Organs.* 205, 53–62.

Stoll, G., Jander, S., and Schroeter, M. (2002). Detrimental and beneficial effects of injury-induced inflammation and cytokine expression in the nervous system. *Adv. Exp. Med. Biol.* 513, 87–113.

Suchting, R., Colpo, G. D., Rocha, N. P., and Ahn, H. (2020a). The effect of transcranial direct current stimulation on inflammation in older adults with knee osteoarthritis: A bayesian residual change analysis. *Biol. Res. Nurs.* 22, 57–63. doi: 10.1177/1099800419869845

Suchting, R., Kapoor, S., Mathis, K. B., and Ahn, H. (2020b). Changes in experimental pain sensitivity from using home-based remotely supervised transcranial direct current stimulation in older adults with knee osteoarthritis. *Pain Med.* 21, 2676–2683. doi: 10.1093/pm/pnaa268

Tarragó, M., Deitos, A., Brietzke, A. P., Vercelino, R., Torres, I. L. S., Fregni, F., et al. (2016). Descending control of nociceptive processing in knee osteoarthritis is associated with intracortical disinhibition: An exploratory study. *Medicine* 95:e3353. doi: 10.1097/MD.0000000000003353

Tavares, D. R. B., Okazaki, J. E. F., Rocha, A. P., Santana, M. V. A., Pinto, A., Civile, V. T., et al. (2018). Effects of transcranial direct current stimulation on knee osteoarthritis pain in elderly subjects with defective endogenous pain-inhibitory systems: Protocol for a randomized controlled trial. *JMIR Res. Protoc.* 7:e11660. doi: 10.2196/11660

Tavares, D. R. B., Okazaki, J. E. F., Santana, M. V. A., Pinto, A., Tutiya, K. K., Gazoni, F. M., et al. (2021). Motor cortex transcranial direct current stimulation effects on knee osteoarthritis pain in elderly subjects with dysfunctional descending pain inhibitory system: A randomized controlled trial. *Brain Stimul.* 14, 477–487. doi: 10.1016/j.brs.2021.02.018

Teixeira, P. E. P., Alawdah, L., Alhassan, H. A. A., Guidetti, M., Priori, A., Papatheodorou, S., et al. (2020). The Analgesic Effect of Transcranial Direct Current Stimulation (tDCS) combined with Physical Therapy on Common Musculoskeletal Conditions: A Systematic Review and Meta-Analysis. *Princ. Pract. Clin. Res. (2015).* 6, 23–26. doi: 10.21801/ppcrj.2020.61.5

Terney, D., Chaieb, L., Moliadze, V., Antal, A., and Paulus, W. (2008). Increasing human brain excitability by transcranial high-frequency random noise stimulation. *J. Neurosci.* 28, 14147–14155.

Terranova, C., Rizzo, V., Cacciola, A., Chillemi, G., Calamuneri, A., Milardi, D., et al. (2018). Is there a future for Non-invasive brain stimulation as a therapeutic tool? *Front. Neurol.* 9:1146. doi: 10.3389/fneur.2018.01146

Tian, L., Sun, S. S., Cui, L. B., Wang, S. Q., Peng, Z. W., Tan, Q. R., et al. (2020). Repetitive transcranial magnetic stimulation elicits antidepressant- and anxiolytic-like effect via nuclear factor-E2-related Factor 2-mediated anti-inflammation mechanism in rats. *Neuroscience* 429, 119–133. doi: 10.1016/j.neuroscience.2019.12.025

Trojak, B., Chauvet-Gelinier, J. C., Vergès, B., and Bonin, B. (2011). Significant increase in plasma thyroid-stimulating hormone during low-frequency repetitive transcranial magnetic stimulation. *J. Neuropsychiatry Clin. Neurosci.* 23:E12. doi: 10.1176/jnp.23.1.jnpe12

Vieira, P. G., Krause, M. R., and Pack, C. C. (2020). tACS entrains neural activity while somatosensory input is blocked. *PLoS Biol.* 18:e3000834. doi: 10.1371/journal.pbio.3000834

Vincent, T. L. (2020). Peripheral pain mechanisms in osteoarthritis. *Pain* 161 Suppl 1, S138–S146.

Waller, B., Munukka, M., Rantalainen, T., Lammentausta, E., Nieminen, M. T., Kiviranta, I., et al. (2017). Effects of high intensity resistance aquatic training on body composition and walking speed in women with mild knee osteoarthritis: A 4-month RCT with 12-month follow-up. *Osteoarthr. Cartil.* 25, 1238–1246.

Walsh, D. A., McWilliams, D. F., Turley, M. J., Dixon, M. R., Fransès, R. E., Mapp, P. I., et al. (2010). Angiogenesis and nerve growth factor at the osteochondral junction in rheumatoid arthritis and osteoarthritis. *Rheumatology* 49, 1852–1861. doi: 10.1093/rheumatology/keq188

Wang, R. Y., Wang, F. Y., Huang, S. F., and Yang, Y. R. (2019). High-frequency repetitive transcranial magnetic stimulation enhanced treadmill training effects on gait performance in individuals with chronic stroke: A double-blinded randomized controlled pilot trial. *Gait Posture* 68, 382–387. doi: 10.1016/j.gaitpost.2018.12.023

Wang, T., and He, C. (2018). Pro-inflammatory cytokines: The link between obesity and osteoarthritis. *Cytokine Growth Factor Rev.* 44, 38–50.

Woods, A. J., Antal, A., Bikson, M., Boggio, P. S., Brunoni, A. R., Celnik, P., et al. (2016). A technical guide to tDCS, and related non-invasive brain stimulation tools. *Clin. neurophysiol.* 127, 1031–1048. doi: 10.1016/j.clinph.2015.11.012

Wu, L., Liu, T., and Wang, J. (2021). Improving the effect of transcranial alternating current stimulation (tACS): A systematic review. *Front. Hum. Neurosci.* 15:652393. doi: 10.3389/fnhum.2021.652393

Xiong, H. Y., Zheng, J. J., and Wang, X. Q. (2022). Non-invasive brain stimulation for chronic pain: State of the art and future directions. *Front. Mol. Neurosci.* 15:888716. doi: 10.3389/fnmol.2022.888716

Yu, K., Liu, C., Niu, X., and He, B. (2021). Transcranial focused ultrasound neuromodulation of voluntary movement-related cortical activity in humans. *IEEE Trans. Biomed. Eng.* 68, 1923–1931. doi: 10.1109/TBME.2020.3030892

Zhang, M., Hu, W., Cai, C., Wu, Y., Li, J., and Dong, S. (2022). Advanced application of stimuli-responsive drug delivery system for inflammatory arthritis treatment. *Mater. Today Bio.* 14:100223. doi: 10.1016/j.mtbio.2022.100223

Zhang, Z., Huang, C., Jiang, Q., Zheng, Y., Liu, Y., Liu, S., et al. (2020). Guidelines for the diagnosis and treatment of osteoarthritis in China (2019 edition). *Ann. Transl. Med.* 8:1213. doi: 10.21037/atm-20-4665

Zheng, S., Tu, L., Cicuttini, F., Zhu, Z., Han, W., Antony, B., et al. (2021). Depression in patients with knee osteoarthritis: Risk factors and associations with joint symptoms. *BMC Musculoskelet. Disord.* 22:40. doi: 10.1186/s12891-020-03875-1

Zorn, L., Renaud, P., Bayle, B., Goffin, L., Lebossé, C., de Mathelin, M., et al. (2012). Design and evaluation of a robotic system for transcranial magnetic stimulation. *IEEE Trans. Biomed. Eng.* 59, 805–815.

frontiers | Frontiers in Aging Neuroscience

TYPE Original Research
PUBLISHED 04 October 2022
DOI 10.3389/fnagi.2022.969822

OPEN ACCESS

EDITED BY
Le Li,
Northwestern Polytechnical University, China

REVIEWED BY
Lejun Wang,
Tongji University, China
Areerat Suputtitada,
Chulalongkorn University, Thailand

*CORRESPONDENCE
Qiang Lin
qianglin0925@gzhmu.edu.cn
Haining Ou
ouhaining@gzhmu.edu.cn

†These authors share first authorship

SPECIALTY SECTION
This article was submitted to Neurocognitive Aging and Behavior, a section of the journal Frontiers in Aging Neuroscience

RECEIVED 15 June 2022
ACCEPTED 15 August 2022
PUBLISHED 04 October 2022

CITATION
Zheng Y, Lang S, Liang J, Jiang Y, Zhao B, Chen H, Huang D, Li Q, Liu H, Chen S, Yilifate A, Xu F, Ou H and Lin Q (2022) Effects of motor-cognitive interaction based on dual-task gait analysis recognition in middle age to aging people with normal cognition and mild cognitive impairment. *Front. Aging Neurosci.* 14:969822. doi: 10.3389/fnagi.2022.969822

Effects of motor-cognitive interaction based on dual-task gait analysis recognition in middle age to aging people with normal cognition and mild cognitive impairment

Yuxin Zheng[1,2†], Shijuan Lang[1,2†], Junjie Liang[1,2], Yongchun Jiang[1,2], Biyi Zhao[1,2], Hongxin Chen[1,2], Dongqing Huang[3], Qinyi Li[2,4], Huijin Liu[2,5], Shudi Chen[1,2], Anniwaer Yilifate[1,2], Fangqiu Xu[6], Haining Ou[1,2,7*] and Qiang Lin[1,2,7*]

[1]Department of Rehabilitation, The Fifth Affiliated Hospital of Guangzhou Medical University, Guangzhou, China, [2]Department of Rehabilitation, Fifth Clinical College, Guangzhou Medical University, Guangzhou, China, [3]Health Science Center, Shenzhen University, Shenzhen, China, [4]Department of Rehabilitation, Zhanjiang Central Hospital, Guangdong Medical University, Zhanjiang, China, [5]Department of Physiology and Pathophysiology, School of Basic Medical Sciences, Capital Medical University, Beijing, China, [6]Department of Clinical Medicine, Guangzhou Medical University, Guangzhou, China, [7]Key Laboratory of Biological Targeting Diagnosis, Therapy and Rehabilitation of Guangdong Higher Education Institutes, The Fifth Affiliated Hospital of Guangzhou Medical University, Guangzhou, China

Background: Mild cognitive impairment (MCI) is considered a transitional stage between cognitive normality and dementia among the elderly, and its associated risk of developing Alzheimer's disease (AD) is 10–15 times higher than that of the general population. MCI is an important threshold for the prevention and control of AD, and intervention in the MCI stage may be the most effective strategy to delay the occurrence of AD.

Materials and methods: In this study, 68 subjects who met the inclusion criteria were divided into an MCI group (38 subjects) and normal elderly (NE) group (30 subjects). Both groups underwent clinical function assessments (cognitive function, walking function, and activities of daily living) and dual-task three-dimensional gait analysis (walking motor task and walking calculation task). Spatial-temporal parameters were obtained and reduced by principal component analysis, and the key biomechanical indexes were selected. The dual-task cost (DTC) was calculated for intra-group (task factor) and inter-group (group factor) comparisons.

Results: The results of the principal component analysis showed that the cadence parameter had the highest weight in all three walking tasks. In addition, there were significant differences in the cadence both walking motor task (WMT) vs. walking task (WT) and walking calculation task (WCT) vs. WT

in the MCI group. The cadence in the NE group only showed a significant difference between WMT and WT. The only differences between the MCI group and NE group was DTC cadence in WCT, and no differences were found for cadence in any of the three walking tasks.

Conclusion: The results show that dual tasks based on cognitive-motor gait analysis of $DTC_{cadence}$ in MCI have potential value for application in early identification and provide theoretical support to improve the clinical diagnosis of MCI.

KEYWORDS

gait analysis, MCI, dual-task, dual-task cost, rehabilitation

Introduction

Mild cognitive impairment (MCI) is considered as the transitional stage from a normal cognitive state to dementia in the elderly and is a typical clinical manifestation of pre-dementia (Petersen, 2004). A cross-sectional survey of Chinese communities showed that the prevalence of MCI in those over 55 years old is 14.5%, which increases with age. The risk of Alzheimer's disease (AD) in MCI patients is 10–15 times higher than that in the general population (Liu-Ambrose et al., 2008). Therefore, MCI is an important gateway for interventions and the prevention of AD. Interventions in the MCI stage may be the most effective strategy to delay the occurrence of AD.

However, MCI is still symptomatically diagnosed in clinic, and neuropsychological assessment is still important in diagnosis and research on MCI (Chipi et al., 2019). Therefore, the evaluation results are semi-quantitative data, which are greatly affected by subjective factors and have poor consistency and low sensitivity. It is challenging to evaluate and diagnose MCI patients accurately. Studies have shown that the motor ability of MCI patients is reduced to a certain extent, and the risk of falls is higher than that of normal elderly people (Schwenk et al., 2016; Tyrovolas et al., 2016).

As an A-level recommendation, the 2018 Chinese Guidelines for the Diagnosis and Treatment of Dementia and Cognitive Impairment in China pointed out that gait performance can help with early identification and prediction of the progress of MCI (Classification Types and Causes of Diseases, 2018). Gait analysis with a single task shows a decline in gait performance in patients with MCI, especially in walking velocity (Grande et al., 2019). However, slow walking velocity may also be associated with aging (Noce Kirkwood et al., 2018). Therefore, gait velocity may be a non-specific variable, and assessing walking performance with a single task may be unsatisfactory for accurately identifying MCI. Thus, dual-task gait analysis was developed and provides a new perspective for the identification of early MCI.

Dual-task walking is walking while performing another task that occupies cognitive resources, such as using mobile phones or talking. Compared with single-task walking, dual-task walking is more challenging, more common in daily life, and more conducive to the discovery of potential gait abnormalities in activities of daily living (ADL) (Liang et al., 2019; Oh, 2021). Imaging studies have also shown that gait and cognitive control share a brain network, especially in the cognitive and motor zones of the frontal cortex (Rosano et al., 2006; Annweiler et al., 2012; Montero-Odasso et al., 2017). Manuel Montero-Odasso et al. confirmed the reliability of dual-task quantitative gait analysis for MCI recognition by analyzing the changes of gait parameters in single-task and dual-task walking (Montero-Odasso et al., 2009; Bishnoi and Hernandez, 2021). In addition, the dual-task cost (DTC) introduced in dual-task gait analysis can be used to calculate the dual-task consumption of cognitive resources. Compared with the original data, it reduces the influence of specific factors of patients, such as height, weight, physical health status, and physical activity level. Thus, it can more accurately quantify the dual-task performance and shows great potential in identifying MCI.

Nevertheless, locating and identifying important biomechanical indicators of MCI among many parameters is an urgent problem to solve and has great significance for guiding the clinical evaluation and diagnosis of MCI. In recent years, principal component analysis (PCA) has been widely used in biomechanics research. PCA is a dimensionality reduction algorithm that can convert multiple indicators into a few unrelated principal components. Thus, fewer unrelated variables can be used to reflect the information conveyed by a large number of relevant raw data. Wakako et al. extracted 26 principal component vectors from many gait parameters by the PCA method and found that knee-angle variability and ankle-angle variability are important gait indicators for distinguishing between frail and non-frail older women (Tsuchida et al., 2022). Therefore, the goal of this study is to increase the understanding of

spatio-temporal parameters of MCI and normal elderly participants by using PCA.

In addition, the following key problems still need to be solved in clinical and mechanism research on dual-task gait analysis for early diagnosis of MCI. First, the key to diagnosis is distinguishing MCI from middle age to elderly population. MCI is mainly manifested as a decline in the function of single or multiple cognitive fields, but normal middle-aged and elderly population also shows a decline in cognitive ability due to factors such as reduced hippocampal volume and adverse changes in cerebrovascular structure (Sun et al., 2022). Therefore, distinguishing MCI from normal aging-induced cognitive decline is a key issue in the clinical diagnosis of MCI (Naidu et al., 2019).

Another problem is that further clarification is needed in regard to the difference in MCI recognition effect between different types of dual tasks needs. There are many types of dual tasks, and the sensitivity of different cognitive tasks to MCI recognition is not clear (Hunter et al., 2018; Bishnoi and Hernandez, 2021). Therefore, selecting different types of dual tasks may affect the accurate recognition of MCI. Therefore, in this study, three-dimensional gait analysis was used to compare the biomechanical characteristics of MCI patients and middle-aged and elderly population during conventional walking and different dual tasks. PCA was then used to explore the sensitive indicators for the objective evaluation of MCI patients, which could provide an important basis for clinical applications.

Materials and methods

Participants

This study recruited MCI elderly subjects and healthy elderly subjects in the Huangpu District of Guangzhou City. The inclusion criteria for MCI subjects were an age of 55–85 years, the DSM-5 diagnostic criteria for MCI, Montreal cognitive assessment (MoCA) score < 24 (Julayanont et al., 2014), and ability to walk independently without gait aids (such as a walking stick or walker). The inclusion criteria of healthy subjects were an age of 55–85 years, MoCA score ≥ 24 (consistent with a normal cognitive level), no aphasia, no history of psychosis, and walking independently without gait aids (such as crutches or walkers). The exclusion criteria for both groups were language dysfunction, history of Parkinson's disease, or any neurological disorder (such as stroke or epilepsy), musculoskeletal diseases, a history of knee or hip arthroplasty that affects gait performance, consumption of psychotropic drugs that affect sports performance, history of mental illness, congestive heart failure, deep venous thrombosis of the lower extremities, malignant progressive hypertension, respiratory failure, active liver disease, and liver or kidney dysfunction.

This study was approved by the Ethics Committee of the Fifth Affiliated Hospital of Guangzhou Medical University (No. KY01-2019-03-01) and has been registered in an international clinical trials registry (ChiCTR1800018832[1]). All participants signed informed consent forms.

Study design

This study is a cross-sectional control study. The subjects with MCI were included in the experimental group (MCI group), and the healthy subjects were included in the normal elderly group (NE group) as control. Both groups received the same assessment, including standardized questionnaire collection of basic information, clinical function assessment (including cognitive function, gait, and ADL assessment), and three-dimensional gait analysis (single task and dual task). Clinical function assessment was conducted by two experienced therapists, and three-dimensional gait analysis was conducted by a professional gait analysis technician in the Gait Analysis Laboratory of the Fifth Affiliated Hospital of Guangzhou Medical University.

Clinical function evaluation

Cognitive function assessment

MoCA was used to evaluate cognitive function. The scale consists of 11 items in eight cognitive fields, including attention and concentration, executive function, memory, language, visual-spatial skills, abstract thinking, calculation, and orientation. The total score was 30, and scores ≥ 26 are regarded as normal cognitive function (Nasreddine et al., 2005).

Gait assessment

A 10-meter walking test (10WMT) was used to evaluate the functional walking ability of subjects. The subjects were asked to walk three times on a 10-m footpath at their own comfortable speed. A therapist used a stopwatch to measure the completion time and calculated the average speed of the middle 6 m of the three tests (m/s).

The Timed Up and Go test (TUGT) (Liang et al., 2019) is commonly used to screen the risk of fall for hospitalized patients and elderly people and can also be used as a monitoring tool for cognitive ability. The subject stood up from an armchair, which was about 46 cm high, crossed marked line 3 m away at a comfortable speed, turned back to the chair, and sat down while being protected and guided by an experienced therapist throughout the test. The therapist used a stopwatch to record the completion time and calculated the average time of the three

1 https://www.chictr.org.cn

tests. Times over 13.5 s were considered to indicate increased risk of falls (Barry et al., 2014).

Activity of daily living assessment

The Modified Barthel Index (MBI) was used to evaluate the ADL of subjects and includes 10 items: eating, dressing, toilet use, bathing, personal hygiene, bed/chair transfer, walking up and down stairs, defecation, and bladder control. Each activity can be divided into grades 1–5 (5 points) (Kaambwa et al., 2021). A higher grade indicates greater independence. A score of 21–60 means high dependence and a great need for help, 61–90 indicates moderate dependence and a need for help, 91–99 indicates mild dependence and basic self-care capability, and100 indicates complete independence and self-care capability. The total scores of the subjects were included in the data statistics.

Three-dimensional gait analysis

A three-dimensional gait analysis system (Italy BTS SMART DX infrared motion capture and analysis system) was used to collect the motion trajectory of fluorescent markers on the subjects. Twenty-two markers were placed on the subjects, and three-dimensional spatial and temporal data were obtained through six high-precision infrared cameras while the subjects walked.

Subject preparation

The subjects wore tight underwear and with the neck, shoulder, waist, and lower limbs fully exposed. The height, weight, bilateral ankle width, bilateral knee-joint diameters, pelvic width, bilateral pelvic depth, and bilateral leg lengths were measured and recorded. According to the Davis Heel Protocol, 22 fluorescent markers were attached to the subject. Three markers were located on the trunk (seventh cervical vertebra, shoulders on both sides), 3 markers were located on the pelvis (bilateral anterior superior iliac spine and ankle joints), 6 markers were located on the thigh (bilateral femoral trochanter, femoral condyle and midpoint of femoral trochanter and ipsilateral femoral condyle), 6 markers were located on the calf (bilateral fibula head, lateral ankle joint and midpoint of ipsilateral fibula head and lateral ankle joint), and 4 markers were located on the foot (fifth metatarsal head and bilateral heels) (Ou et al., 2021).

Walking data acquisition

Standing task

Subjects were asked to remain upright for at least 3–5 s, and their feet were aligned to obtain baseline data.

Walking tasks

Subjects were asked to perform three different walking tasks at a preferred speed on an 8-m footpath: (1) single-task walking (WT): subjects walked at a preferred speed (2) walking + holding a water bottle (WMT) (walking + exercise load as a dual-motion task) (3) walking + computation (WCT): subjects completed consecutive computation tasks of subtracting 7 starting from 100 while walking.

The task sequence was as follows. Subjects completed the baseline gait assessment (WT), and then the order of WMT and WCT dual-task walking was determined by a single-blind random lottery. Each task was performed five times in a row, and the first two to four data were selected as experimental data. If data were missing when processing the data, data from the subsequent experiment were selected to replace them to ensure the integrity of the experimental data.

Gait analysis data processing

The BTSFreeEMG300 acquisition system (BTS Engineering, version 2.9.37.0, Italy) was used to analyze the three-dimensional gait data. Firstly, all the gait data collected by the subjects were selected, and at least two heel-strike events and one toe-off event calibrated in the gait cycle were automatically identified by the system. Four gait events were manually checked for accuracy (eRHS: right heel-to-ground, eRTO: right toe-to-ground, eLHS: left heel-to-ground, eLTO: left toe-to-ground). By selecting the "Rep_Gait_Standing" module, we checked whether the label positions of the 22 markers were symmetrical, and by selecting the "Rep_Gait_Consistency" module, we tested the consistency and repeatability of the data. Finally, we generated a module by clicking on "report."

The spatiotemporal motion parameters for different tasks were obtained, including time parameters (stance phase, swing phase, first double support phase, average velocity, and cadence) and spatial parameters (stride length, step length, and step width). DTC was introduced to calculate the gait-performance difference between single-task gait and dual-task gait and to eliminate the differences in experimental data caused by subjects' own heterogeneity. The DTC was calculated according to the following: ([single-task gait parameter-dual-task gait parameter]/single-task gait parameter) × 100 (Montero-Odasso et al., 2017).

Principal component analysis

Considering the potential correlation between gait variables, PCA method was used to extract the principal features of the 22 spatial-temporal gait variables in order to remove redundancy and locate target parameters. The spatial-temporal data from recruited subjects were imported into SPSS software. For each task paradigm, PCA was performed to identify the potential contribution of spatial-temporal variables, which took into account the changes observed in each task paradigm. For each task paradigm, subjects and variables were arranged in a matrix with gait variables as columns and subjects as rows. A principal component (PC) is represented by varimax rotation to minimize the number of variables with high load on each component factor. PC is retained according to the gravel map

describing the individual contribution of each PC to explain the overall variance. The goal was for all retained PCs together to explain ≥ 80% of the total variance. Then Pearson correlation (r) and explicitness value were used to cross-validate the factor load (correlation between original spatial-temporal variables and each PC) and component score coefficient (contribution or weight of spatial-temporal variables to each PC). The contributions of the first two PCs were reported.

Statistical analysis

After all the data were collected, IBM SPSS statistical software (version 25.0, IBM, Armonk, NY, United States) and GraphPad Prism (La Jolla, CA, United States) were used for statistical analysis and plotting. The data are represented by the mean and standard deviation (SD). In terms of the basic information and spatial-temporal parameters between MCI and NE groups, two independent-sample t-tests were used to compare the differences between the two groups. The repeated-measures analysis of variance was used to analyze the effect of multiple factors (group factors: MCI group and NE group; task factors: WT, WMT, and WCT).

Results

In this study, 156 subjects were recruited. Of the subjects who met the research conditions, 36 subjects withdrew from the experiment due to low motivation, 13 subjects withdrew because their families did not agree to the experiment, 9 subjects had severe knee osteoarthritis, 16 subjects were beyond the age requirement, and 14 subjects were unable to complete the experiment due to schedule conflicts. During the experiment, no subjects reported any adverse events or results. Finally, 68 subjects completed all the evaluations, including 38 subjects in the MCI group and 30 subjects in the NE group (Figure 1).

The basic information of the subjects can be found in Table 1. There was no significant difference in age, height, weight, BMI, years of education, 10WMT, and TUGT between the two groups ($P > 0.05$). The MoCA score of the MCI group was lower than that of the NE group, and the difference was statistically significant (MCI group: 21.0 ± 1.9; NE group: 26.4 ± 1.4; $p < 0.001$) (Table 1).

All spatial-temporal data for both groups are detailed in the Supplementary Table 1. The PCA results of 22 spatial-temporal parameters of different tasks are shown in Table 2 (WT), Table 3 (WMT), and Table 4 (WCT). Six PCs (PC1–PC6) accounted for

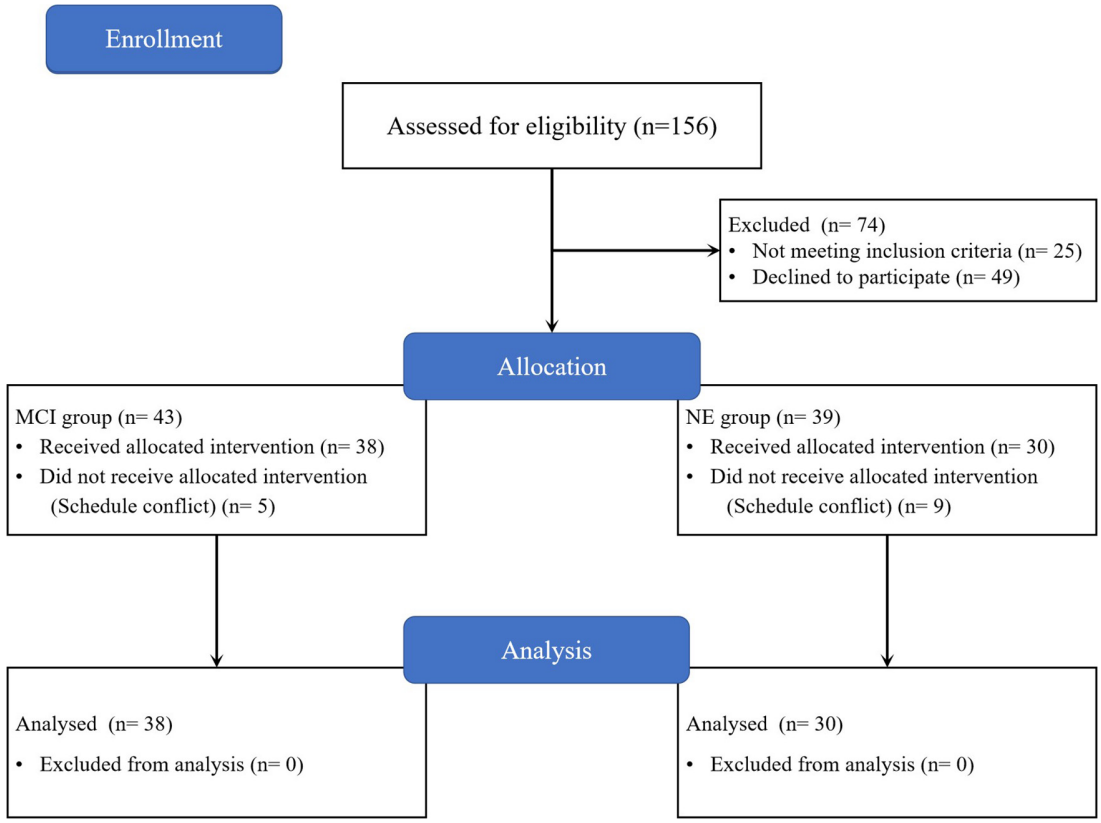

FIGURE 1
Study flow diagram. NE, normal elder; MCI, mild cognitive impairment.

80% of the spatial-temporal changes. Among the three tasks, the parameters with the highest weight proportion of PC1 were cadence (fqCADENCE, fqRCADENCE, fqLCADENCE) (Tables 2–4). At the same time, PC2 of WT and WMT had the highest proportion weight for gait substage parameters (swing and stance), and PC2 of WCT had the highest proportion weight for spatial parameters (LSTRIDE% height, RSTRIDE% height). Figure 2 shows the data points of the three walking tasks (68 * 22 * 3 * 1496 measurements in the three tasks from 68 subjects) projected onto a two-dimensional plane based on two spatiotemporal variations.

Table 5 shows results of the repeated-measures analysis of variance on group factor (MCI group and NE group) and task factors (WT, WMT, and WCT) for fqRCADENCE, fqLCADENCE, fqCADENCE. The raw data of fqCADENCE and the DTC of the three CADENCE parameters were significantly different among tasks and groups (group factor: Raw $Data_{fqCADENCE}$: $F = 6.310$, $P = 0.013$; $DTC_{fqRCADENCE}$: $F = 22.021$, $P < 0.001$; $DTC_{fqLCADENCE}$: $F = 9.121$, $P = 0.003$; $DTC_{fqCADENCE}$: $F = 17.054$, $P < 0.001$; task factor: Raw $Data_{fqCADENCE}$: $F = 6.226$, $P = 0.002$; $DTC_{fqRCADENCE}$: $F = 23.616$, $P < 0.001$; $DTC_{fqLCADENCE}$: $F = 8.957$, $P = 0.003$; $DTC_{fqCADENCE}$: $F = 19.537$, $P < 0.001$). The raw data of fqRCADENCE and fqLCADENCE just presented significant difference among three walking tasks (Raw $Data_{fqRCADENCE}$: $F = 4.220$, $P = 0.016$; Raw $Data_{fqLCADENCE}$: $F = 4.256$, $P = 0.015$).

Table 6 shows the differences in fqCADENCE among single and dual walking tasks in the MCI group and NE group respectively. In the MCI group, the fqCADENCE in WCT was significantly smaller than that in WT (Mean difference = 4.442 ± 1.144 steps/min, $P = 0.001$). Whereas, in the NE group, the fqCADENCE in WMT was significantly smaller than that in WT (Mean difference = −6.924 ± 1.147 steps/min, $P < 0.001$). Moreover, the fqCADENCE between MCI group and NE group in WMT were significantly larger than those in WCT (MCI group: Mean difference = 6.537 ± 1.153 steps/min, $P < 0.001$; NE group: Mean difference = 5.790 ± 1.298 steps/min, $P < 0.001$). The $DTC_{fqRCADENCE}$ in WMT in both groups were significantly smaller than those in WCT (MCI group: Mean difference = −5.970 ± 0.868%, $P < 0.001$; NE group: Mean difference = −3.718 ± 0.977%, $P < 0.001$).

Table 7 shows the difference in fqCADENCE between the MCI group and the NE group in different single and dual walking tasks respectively. The fqCADENCE of the MCI group in WMT and WCT were both significantly smaller than those of the NE group (WMT: Mean

TABLE 1 Baseline demographic characteristics of the MCI group and NE group.

Characteristics	MCI group	NE group	*P*-value
Age (year)	60.9 ± 7.3	60.1 ± 6.7	0.705
55–64	52.7 ± 2.6 (30)	57.4 ± 2.9 (24)	–
65–74	67.8 ± 3.4 (5)	68.8 ± 2.2 (5)	–
75–85	80.3 ± 4.1 (3)	83.0 ± 0.0 (1)	–
Gender (female/male)	38 (male 7/female 31)	30 (male 2/female 28)	–
Height (cm)	159.7 ± 6.8	159.8 ± 5.4	0.143
Weight (kg)	61.1 ± 9.5	58.2 ± 6.3	0.943
BMI (kg/m^2)	23.9 ± 3.1	22.8 ± 2.3	0.104
Education (years)	11.0 ± 2.8	11.8 ± 2.6	0.232
MoCA (score)	21.0 ± 1.9	26.4 ± 1.4	**<0.001**
10WMT (s)	5.5 ± 0.7	5.5 ± 0.8	0.91
TUGT (s)	10.9 ± 1.6	10.7 ± 1.7	0.549
MBI (score)	100	100	–

The data are presented as the means ± SD or numbers. *P*-value less than 0.05 indicate statistically significant differences and are marked in bold.
BMI, body mass index; MoCA, montreal cognitive assessment; TUGT, time up and go test; 10WMT, 10–meter walk test; MBI, modified barthel index.

TABLE 2 Results of principal component analysis of WT.

Parameters	Component					
	PC 1	PC 2	PC 3	PC 4	PC 5	PC 6
velseqRHSTRIDE	0.473	0.744	0.199	0.075	−0.021	0.224
velseqLHSTRIDE	0.656	0.501	0.43	0.066	0.035	−0.097
velseqRHSWING	0.759	0.107	0.544	0.021	0.002	0.235
velseqLHSWING	0.732	0.196	0.533	0.113	−0.058	0
fqRCADENCE	**0.922**[a]	−0.029	0.216	0.002	−0.018	0.088
fqLCADENCE	**0.868**[a]	0.032	0.294	−0.01	−0.003	−0.233
fqCADENCE	**0.906**[a]	0.357	0.039	−0.008	−0.014	−0.051
sRSTANCE	−0.029	**−0.919**[a]	0.186	−0.121	0.027	0.143
sRSWING	0.178	**0.812a**	0.154	0.205	−0.055	−0.081
sLDBLSTANCE	−0.506	−0.185	0.142	−0.03	0.108	0.459
sLSTANCE	−0.043	**−0.854**[a]	0.019	0.166	−0.244	−0.062
sLSWING	0.186	0.731	0.389	0.011	0.113	0.153
sRDBLSTANCE	−0.289	−0.551	−0.517	0.077	0.043	0.163
RGDI	−0.068	−0.177	−0.029	**−0.892**[a]	−0.2	−0.059
sRGPS	−0.023	−0.045	0.002	**0.933**[a]	0.091	−0.087
LGDI	0.041	−0.138	0.085	−0.169	**−0.915**[a]	−0.059
sLGPS	−0.02	−0.002	0.135	0.114	**0.916**[a]	0.035
sRSINGSTANCE	0.122	0.507	0.293	0.028	0.107	**0.731**[a]
sLSINGSTANCE	0.222	0.521	0.37	0.12	−0.008	**−0.637**[a]
velMEAN%height/s	0.71	0.37	0.506	−0.014	0.02	−0.07
LSTRIDE%height	0.299	0.082	**0.91**[a]	0.026	0.051	0.129
RSTRIDE%height	0.337	0.047	**0.911**[a]	0.011	0.039	0.017

The parameters that obtained membership to each component (>0.500) are in bold and with the superscript symbol "a".
velseqRHSTRIDE, right heel stride velocity; velseqLHSTRIDE, left heel stride velocity; velseqRHSWING, right heel swing velocity; velseqLHSWING, left heel swing velocity; fqRCADENCE, the cadence of right foot; fqLCADENCE, the cadence of left foot; fqCADENCE, the cadence of double feet; sRSTANCE, right stance phase; sRSWING, right swing phase; sRDBLSTANCE, right double support phase; sLSTANCE, left stance phase; sLSWING, left swing phase; sLDBLSTANCE, left double support phase; RGDI, right gait deviation index; LGDI, left gait deviation index; sRGPS, right gait profile score; sLGPS, left gait profile score; velMEAN%height/s, mean velocity in relation to the height of the subject; RSTRIDE%height, length of the right stride in relation to the height of the subject; LSTRIDE%height, length of the left stride in relation to the height of the subject.

TABLE 3 Results of principal component analysis of WMT.

Parameters	Component					
	PC 1	PC 2	PC 3	PC 4	PC 5	PC 6
velseqRHSTRIDE	0.473	0.744	0.199	0.075	−0.021	0.224
velseqLHSTRIDE	0.656	0.501	0.43	0.066	0.035	−0.097
velseqRHSWING	0.759	0.107	0.544	0.021	0.002	0.235
velseqLHSWING	0.732	0.196	0.533	0.113	−0.058	0
fqRCADENCE	**0.922**[a]	−0.029	0.216	0.002	−0.018	0.088
fqLCADENCE	**0.868**[a]	0.032	0.294	−0.01	−0.003	−0.233
fqCADENCE	**0.906**[a]	0.357	0.039	−0.008	−0.014	−0.051
sRSTANCE	−0.029	**−0.919**[a]	0.186	−0.121	0.027	0.143
sRSWING	0.178	**0.812**[a]	0.154	0.205	−0.055	−0.081
sLDBLSTANCE	−0.506	−0.185	0.142	−0.03	0.108	0.459
sLSTANCE	−0.043	**−0.854**[a]	0.019	0.166	−0.244	−0.062
sLSWING	0.186	0.731	0.389	0.011	0.113	0.153
sRDBLSTANCE	−0.289	−0.551	−0.517	0.077	0.043	0.163
RGDI	−0.068	−0.177	−0.029	**−0.892**[a]	−0.2	−0.059
sRGPS	−0.023	−0.045	0.002	**0.933**[a]	0.091	−0.087
LGDI	0.041	−0.138	0.085	−0.169	**−0.915**[a]	−0.059
sLGPS	−0.02	−0.002	0.135	0.114	**0.916**[a]	0.035
sRSINGSTANCE	0.122	0.507	0.293	0.028	0.107	**0.731**[a]
sLSINGSTANCE	0.222	0.521	0.37	0.12	−0.008	**−0.637**[a]
velMEAN%height/s	0.71	0.37	0.506	−0.014	0.02	−0.07
LSTRIDE%height	0.299	0.082	**0.91**[a]	0.026	0.051	0.129
RSTRIDE%height	0.337	0.047	**0.911**[a]	0.011	0.039	0.017

The parameters that obtained membership to each component (>0.500) are in bold and with the superscript symbol "a".
velseqRHSTRIDE, right heel stride velocity; velseqLHSTRIDE, left heel stride velocity; velseqRHSWING, right heel swing velocity; velseqLHSWING, left heel swing velocity; fqRCADENCE, the cadence of right foot; fqLCADENCE, the cadence of left foot; fqCADENCE, the cadence of double feet; sRSTANCE, right stance phase; sRSWING, right swing phase; sRDBLSTANCE, right double support phase; sLSTANCE, left stance phase; sLSWING, left swing phase; sLDBLSTANCE, left double support phase; RGDI, right gait deviation index; LGDI, left gait deviation index; sRGPS, right gait profile score; sLGPS, left gait profile score; velMEAN%height/s, mean velocity in relation to the height of the subject; RSTRIDE%height, length of the right stride in relation to the height of the subject; LSTRIDE%height, length of the left stride in relation to the height of the subject.

difference = −5.069 ± 2.326 steps/min, P = 0.033; WCT: Mean difference = −5.816 ± 2.684 steps/min, P = 0.034). Moreover, the $DTC_{fqRCDENCE}$ of the MCI group both in WMT and WCT were significantly smaller than those of the NE group (WMT: Mean difference = 3.400 ± 1.390%, P = 0.017; WCT: Mean difference = 5.652 ± 1.694%, P = 0.001).

Discussion

In this study, the difference of gait parameters between MCI patients and healthy elderly people in single and dual tasks was explored by using dual-task three-dimensional gait analysis. The aim was to explore the biomechanical targets of MCI patients and optimize the clinical quantitative evaluation and identification methods for MCI patients. The results of principal component analysis showed that the cadence parameters (fqRCADENCE, fqLCADENCE, and fqCADENCE) presented the highest weight in distinguishing MCI group and NE group. Furthermore, the repeated-measures analysis of variance results showed that the significant advantages of three DTCcadence parameters in distinguishing MCI group and NE group, while only raw date of the fqCADENCE parameter presented significant differences between groups. At the same time, the significant differences between the two groups under different dual tasks were found in both in raw date and DTC, indicating that dual task paradigm of gait analysis could be used to distinguish MCI group and NE group. The more significant difference between two groups were under the DTC than raw data, Moreover, the more significant difference was found in WCT than in WMT.

TABLE 4 Results of principal component analysis of WCT.

Parameters	Component					
	PC 1	PC 2	PC 3	PC 4	PC 5	PC 6
velseqRHSTRIDE	0.413	0.32	0.613	0.481	0.016	−0.036
velseqLHSTRIDE	0.388	0.365	0.639	0.433	−0.024	−0.023
velseqRHSWING	0.718	0.592	−0.028	0.287	0.026	−0.024
velseqLHSWING	0.659	0.667	0.107	0.188	−0.015	0.015
fqRCADENCE	**0.95**[a]	0.143	0.03	0.224	−0.02	−0.046
fqLCADENCE	**0.966**[a]	0.169	0.066	0.035	−0.05	−0.024
fqCADENCE	**0.97**[a]	0.071	0.151	−0.008	−0.042	−0.036
sRSTANCE	0.035	0.166	**−0.948**[a]	−0.023	0.011	0.036
sRSWING	0.054	0.358	0.638	0.481	0.024	−0.051
sLDBLSTANCE	−0.062	−0.33	−0.236	0.392	0.533	0.173
sLSTANCE	−0.036	0.192	−0.86	−0.225	0.007	0.063
sLSWING	0.16	0.265	0.494	**0.747**[a]	0.025	−0.094
sRDBLSTANCE	−0.112	−0.199	−0.07	−0.363	0.094	0.256
RGDI	0.067	−0.149	−0.245	0.067	**−0.838**[a]	0.285
sRGPS	−0.008	−0.036	−0.122	−0.01	**0.933**[a]	−0.113
LGDI	0.038	−0.003	−0.191	−0.083	−0.112	**0.93**[a]
sLGPS	0.095	−0.037	−0.106	0.125	0.179	**−0.892**[a]
sRSINGSTANCE	0.183	0.247	0.199	**0.861**[a]	0.081	−0.121
sLSINGSTANCE	0.129	0.404	0.707	−0.02	−0.038	0
velMEAN%height/s	0.67	0.664	0.161	0.217	−0.036	−0.023
LSTRIDE%height	0.178	**0.928**[a]	0.01	0.239	−0.008	−0.008
RSTRIDE%height	0.221	**0.917**[a]	0.055	0.203	0.002	0.007

The parameters that obtained membership to each component (>0.500) are in bold and with the superscript symbol "a"
velseqRHSTRIDE, right heel stride velocity; velseqLHSTRIDE, left heel stride velocity; velseqRHSWING, right heel swing velocity; velseqLHSWING, left heel swing velocity; fqRCADENCE, the cadence of right foot; fqLCADENCE, the cadence of left foot; fqCADENCE, the cadence of double feet; sRSTANCE, right stance phase; sRSWING, right swing phase; sRDBLSTANCE, right double support phase; sLSTANCE, left stance phase; sLSWING, left swing phase; sLDBLSTANCE, left double support phase; RGDI, right gait deviation index; LGDI, left gait deviation index; sRGPS, right gait profile score; sLGPS, left gait profile score; velMEAN%height/s, mean velocity in relation to the height of the subject; RSTRIDE%height, length of the right stride in relation to the height of the subject; LSTRIDE%height, length of the left stride in relation to the height of the subject.

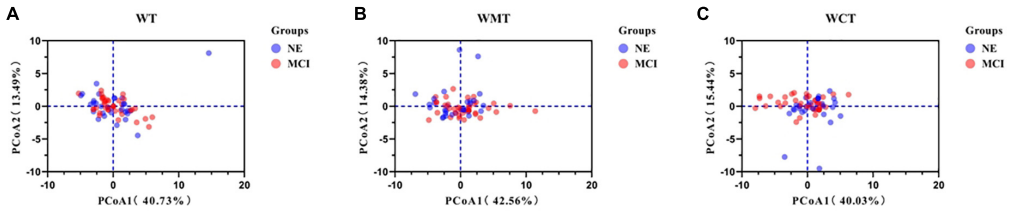

FIGURE 2
Principal component analysis of spatial-temporal parameters. Component loading plot of spatial-temporal parameters for all 68 patients in three different tasks. **(A)** Walking task; **(B)** walking motor task; **(C)** walking calculate task. WT, walking task; WMT, walking motor task; WCT, walking calculate task; NE, normal elder; MCI, mild cognitive impairment.

The effectiveness of dual-task gait analysis in identifying MCI has been confirmed in previous studies. Doi et al. (2014) compared the gait velocity of MCI patients between a single task and dual task (walking while counting backward from 100) and found that the working memory ability of MCI patients in the dual task significantly affected their gait velocity. There was no significant difference in the single task. Furthermore, Montero-Odasso et al. found that the DTC parameters of walking speed in the reciprocal (counting backward) dual-task walking test could be used to predict the progress of dementia in MCI patients by constructing a prediction model. They confirmed the potential of a dual-task gait test for clinical cognitive function assessment (Montero-Odasso et al., 2017). This study also found that the DTC value of step frequency of MCI patients in dual tasks (walking while counting down from 100 by 7) was greater than that of the normal elderly subjects, which was similar to the result of other studies. The DTC value of cadence can be used as an important biomechanical indicator to identify MCI, which once again verifies the positive role of dual-task gait analysis in clinical evaluation and diagnosis of MCI.

There are many biomechanical indicators available from gait analysis, but accurate determination of target indicators is of great significance for the clinical application and promotion of MCI diagnosis based on this method. Therefore, we used PCA to reduce the dimensions of the spatial-temporal parameters in three walking tasks and selected cadence as the index with the largest proportion weight for in-depth intra-group comparison. Cadence refers to the frequency of legs switching support points when running or walking. The results of PCA showed that cadence had the largest weight in distinguishing the MCI group and the NE group. The possible reasons are as follows. First, when walking at a preferred velocity, factors such as height and leg length may lead to inconsistent individual strides, resulting in inconsistent paces. Therefore, when comparing the two groups, simply considering the pace may be biased. When studying the cognitive function training effect of MCI patients, Liao et al. (2019) found that $DTC_{cadence}$ results were statistically significant, while $DTC_{velocity}$ was not, which was similar to the results of this study. Second, steps/min is the unit of step cadence, and m/s is the unit of gait velocity. Cadence is measured per minute, and the gait velocity is measured per second. Thus, in the statistical analysis, the cadence parameter makes the differences accumulate compared with the gait velocity, which is more conducive to identifying the cognitive-function difference between MCI and NE groups. Therefore, cadence may be more likely to be an important biomechanical marker to identify MCI gait decline. Third, in previous studies, velocity was often used as an important result indicator in the analysis of dual-task gait. This may be due to the fact that the gait velocity parameters are more easily obtained in clinical evaluation, such as the commonly used 10-meter walking test and TUGT test. The gait velocity parameters can be obtained with only timing tools, while the cadence parameters are difficult to obtain in non-instrumental evaluation. In this study, a three-dimensional gait analysis system was used for the dual-task gait analysis, and the gait parameters such as cadence and gait velocity can be obtained easily. The results showed that the cadence of the MCI group and the NE group decreased in the dual task, and the decrease of the MCI group was more obvious than that of the NE group. This result can be used to confirm that MCI can lead to a decrease of dual-task gait performance, which can be used to identify MCI patients and new ideas for MCI gait research. The results indicated that DTC parameters might be more sensitive than raw data in distinguishing MCI group and NE group. DTC parameters can be used for quantification of dual tasks and comparison between different dual-task paradigms. At the same time, DTC can remove gait physiological differences between different individuals by calculating the difference between single and dual tasks, as well as reduce the impact of heterogeneity on experimental design (Bayot et al., 2018). Due to these advantages of DTC, $DTC_{cadence}$ is more effective than raw cadence in distinguishing MCI and healthy subjects. Ying et al. also studied the effect of VR-based physical and cognitive training on the performance of dual-task gait in MCI patients. They found that $DTC_{cadence}$ was improved, while the original data of step frequency had no statistical difference. Thus, promptly obtained DTC parameters have advantages for clinical assessment and diagnosis of MCI. The significant differences between the two groups under different dual tasks

TABLE 5 Results of the repeated-measures analysis of variance on group and task for fqRCADENCE, fqLCADENCE, fqCADENCE.

	Main effect (Group)		Main effect (Task)		Interaction effect	
	F-value	*P*-value	*F*-value	*P*-value	*F*-value	*P*-value
Raw data (steps/min)						
fqRCADENCE	3.044	0.083	4.220	**0.016**	1.220	0.297
fqLCADENCE	3.842	0.051	4.256	**0.015**	0.839	0.434
fqCADENCE	6.310	**0.013**	6.226	**0.002**	1.401	0.249
DTC (%)						
fqRCADENCE	22.021	<**0.001**	23.616	<**0.001**	1.117	0.292
fqLCADENCE	9.121	**0.003**	8.957	**0.003**	0.603	0.439
fqCADENCE	17.054	<**0.001**	19.537	<**0.001**	1.055	0.306

DTC = 100 * (single-task gait parameters − dual-task gait parameters)/single-task gait parameters; *P*-value less than 0.05 indicate statistically significant differences and are marked in bold.
fqRCADENCE, the cadence of right foot; fqLCADENCE, the cadence of left foot; fqCADENCE, the cadence of double feet.

TABLE 6 Paired comparison of fqCADENCE parameters (raw date and DTC) in different tasks respectively.

	MCI group		NE group	
	Mean difference (Mean ± SE)	*P*-value	Mean difference (Mean ± SE)	*P*-value
Raw data (steps/min)				
WT vs. WMT	−2.095 ± 1.019	0.132	−6.924 ± 1.147	<**0.001**
WT vs. WCT	4.442 ± 1.144	**0.001**	−1.134 ± 1.288	1.000
WMT vs. WCT	6.537 ± 1.153	<**0.001**	5.790 ± 1.298	<**0.001**
DTC (%)				
WMT vs. WCT	−5.970 ± 0.868	<**0.001**	−3.718 ± 0.977	<**0.001**

DTC = 100 * (single-task gait parameters − dual-task gait parameters)/single-task gait parameters; *P*-value less than 0.05 indicate statistically significant differences and are marked in bold.
SE, standard error; WT, walking task; WMT, walking motor task; WCT, walking calculate task; DTC, Dual task cost.

were found both in raw date and DTC. Moreover, the more significant difference was found in WCT than in WMT under the DTC. Our results suggested that both the motor-cognitive dual task and dual motor task in this study could be used to distinguish MCI patients from healthy elderly, however, the motor-cognitive dual task presented more advantageous in the diagnosis of MCI population. The results are also consistent with the pathological characteristics of MCI—that is the ADL of MCI patients is partially retained, while the cognitive function is impaired.

Furthermore, the dual-motor task WMT designed in this study involves holding a water bottle and walking, which can be regarded as a single motor task whether (holding a water bottle or walking) (McIsaac et al., 2015). The demand for cognitive brain function resources of the subjects is not large, and it is not easy to occupy significant cognitive resources compared to the single walking task. However, the subjects in WCT with continuous subtraction by 7 needed more cognitive brain function resources, which is more challenging for MCI patients (Tsang et al., 2022). Therefore, WCT is more likely to identify MCI patients than WMT. Thus, there are many types of dual tasks in clinical evaluation, and it is possible to choose motor-cognitive tasks with higher sensitivity for MCI recognition than dual motor tasks.

TABLE 7 Paired comparison of fqCADENCE parameters (raw date and DTC) between MCI group and NE group.

	Mean difference (Mean ± SE)	*P*-value
Raw data (steps/min)		
WT	−0.240 ± 2.645	0.928
WMT	−5.069 ± 2.326	**0.033**
WCT	−5.816 ± 2.684	**0.034**
DTC (%)		
WMT	3.400 ± 1.390	**0.017**
WCT	5.652 ± 1.694	**0.001**

DTC = 100 * (single-task gait parameters − dual-task gait parameters)/single-task gait parameters; *P*-value less than 0.05 indicate statistically significant differences and are marked in bold.
SE, standard error; WT, walking task; WMT, walking motor task; WCT, walking calculate task; DTC, Dual task cost.

Limitations

This study has the following limitations. Most of the subjects were female, and few were male. However, due to the high prevalence of women among MCI patients, the gender ratio of subjects was in line with epidemiological characteristics (Jia et al., 2020; Shi et al., 2022). In subsequent studies, we will include more male subjects to reduce the impact of gender on the experimental results. The key spatial-temporal parameters for MCI recognition under dual-task gait were discussed, and future research should further explore the influence of joint angle on MCI recognition. In the future, we will continue follow-up on this this study by obtaining data before and after healthy subjects develop MCI, which is of great significance for further clarifying the recognition of MCI through gait parameters. Further studies should also improve the efficiency of clinical assessment and diagnosis of MCI by constructing a clinical prediction model through the dual-task gait parameters of MCI patients.

Conclusion

This study examined dual-task three-dimensional gait analysis methods, and the key spatial-temporal parameters for the early diagnosis of MCI were screened through PCA. The results showed that the $DTC_{cadence}$ based on the cognitive-motor dual-task gait analysis has potential application value for the early recognition of MCI. The results could provide theoretical support for improving the clinical diagnosis of MCI.

Data availability statement

The raw data supporting the conclusions of this article will be made available by the corresponding authors, upon reasonable request.

Ethics statement

The studies involving human participants were reviewed and approved by the Fifth Affiliated Hospital of Guangzhou Medical University. The patients/participants provided their written informed consent to participate in this study.

Author contributions

QL, HO, and YZ designed the study. QL, YZ, and SL drafted the manuscript. YZ, SL, JL, and YJ performed data analysis. JL, HC, YJ, BZ, AY, DH, QYL, HL, SC, FX, and HO collected the data. YJ, BZ, QYL, and HL wrote sections of the manuscript. QL and HO approved the final version of the manuscript. All authors contributed to the manuscript revision, read, and approved the submitted version.

Funding

This study was supported by the National Science Foundation of China (No. 81902281), the General Guidance Program of Guangzhou Municipal Health and Family Planning (Nos. 20221A011109, 20211A011106, 20221A011106, and 20211A010079), Guangdong Province Department of Education (No. 2021ZDZX2063), Guangzhou Key Medical Disciplines (2021-2023), Guangzhou and University Foundation (No. 202102010100), Guangzhou Medical University Foundation (No. PX-66221494/02-408-2203-2062), Key Laboratory of Guangdong Higher Education Institutes (No. 2021KSYS009), National Key R&D Program of China (No. 2018YFC2002500), and Guangzhou Clinical Characteristic Technology Construction Project (2023-2025:NO.19).

Acknowledgments

We thank all the undergraduates of Guangzhou Medical University (Rongwei Du, Tingting Peng, Peiling Ou, Guanghui Qiu, and Xiaoqin Zheng) for participating in this study, as well as the employees of the Fifth Affiliated Hospital of Guangzhou Medical University for data collection.

Conflict of interest

The authors declare that the research was conducted in the absence of any commercial or financial relationships that could be construed as a potential conflict of interest.

Publisher's note

All claims expressed in this article are solely those of the authors and do not necessarily represent those of their affiliated organizations, or those of the publisher, the editors and the reviewers. Any product that may be evaluated in this article, or claim that may be made by its manufacturer, is not guaranteed or endorsed by the publisher.

Supplementary material

The Supplementary Material for this article can be found online at: https://www.frontiersin.org/articles/10.3389/fnagi.2022.969822/full#supplementary-material

References

Annweiler, C., Beauchet, O., Celle, S., Roche, F., Annweiler, T., Allali, G., et al. (2012). Contribution of brain imaging to the understanding of gait disorders in Alzheimer's disease: A systematic review. *Am. J. Alzheimers Dis. Other Demen.* 27, 371–380. doi: 10.1177/1533317512454710

Barry, E., Galvin, R., Keogh, C., Horgan, F., and Fahey, T. (2014). Is the Timed Up and Go test a useful predictor of risk of falls in community dwelling older adults: A systematic review and meta-analysis. *BMC Geriatrics* 14:14. doi: 10.1186/1471-2318-14-14

Bayot, M., Dujardin, K., Tard, C., Defebvre, L., Bonnet, C. T., Allart, E., et al. (2018). The interaction between cognition and motor control: A theoretical framework for dual-task interference effects on posture, gait initiation, gait and turning. *Neurophysiol. Clin.* 48, 361–375. doi: 10.1016/j.neucli.2018.10.003

Bishnoi, A., and Hernandez, M. E. (2021). Dual task walking costs in older adults with mild cognitive impairment: A systematic review and meta-analysis. *Aging Ment. Health* 25, 1618–1629. doi: 10.1080/13607863.2020.1802576

Chipi, E., Salvadori, N., Farotti, L., and Parnetti, L. (2019). Biomarker-based signature of Alzheimer's disease in Pre-MCI individuals. *Brain Sci.* 9:213. doi: 10.3390/brainsci9090213

Classification Types and Causes of Diseases. (2018). 2018 Chinese guidelines for diagnosis and treatment of dementia and cognitive impairment V: Diagnosis and treatment of mild cognitive impairment. *Chin. Med. Assoc. J.* 98. doi: 10.1186/s13195-018-0415-6

Doi, T., Shimada, H., Makizako, H., Tsutsumimoto, K., Uemura, K., Anan, Y., et al. (2014). Cognitive function and gait speed under normal and dual-task walking among older adults with mild cognitive impairment. *BMC Neurol.* 14:67. doi: 10.1186/1471-2377-14-67

Grande, G., Triolo, F., Nuara, A., Welmer, A. K., Fratiglioni, L., and Vetrano, D. L. (2019). Measuring gait speed to better identify prodromal dementia. *Exp. Gerontol.* 124:110625. doi: 10.1016/j.exger.2019.05.014

Hunter, S. W., Divine, A., Frengopoulos, C., and Montero Odasso, M. (2018). A framework for secondary cognitive and motor tasks in dual-task gait testing in people with mild cognitive impairment. *BMC Geriatr.* 18:202. doi: 10.1186/s12877-018-0894-0

Jia, L., Du, Y., Chu, L., Zhang, Z., Li, F., Lyu, D., et al. (2020). Prevalence, risk factors, and management of dementia and mild cognitive impairment in adults aged 60 years or older in China: a cross-sectional study. *Lancet. Public Health* 5, e661–e671. doi: 10.1016/S2468-2667(20)30185-7

Julayanont, P., Brousseau, M., Chertkow, H., Phillips, N., and Nasreddine, Z. S. (2014). Montreal cognitive assessment memory index score (MoCA-MIS) as a predictor of conversion from mild cognitive impairment to Alzheimer's disease. *J. Am. Geriatr. Soc.* 62, 679–684. doi: 10.1111/jgs.12742

Kaambwa, B., Bulamu, N. B., Mpundu-Kaambwa, C., and Oppong, R. (2021). Convergent and discriminant validity of the barthel index and the EQ-5D-3L when used on older people in a rehabilitation setting. *Int. J. Environ. Res. Public Health* 18:10314. doi: 10.3390/ijerph181910314

Liao, Y. Y., Chen, I. H., Lin, Y. J., Chen, Y., and Hsu, W. C. (2019). Effects of virtual reality-based physical and cognitive training on executive function and dual-task gait performance in older adults with mild cognitive impairment: A randomized control trial. *Front. Aging Neurosci.* 11:162. doi: 10.3389/fnagi.2019.00162

Liang, J., Guo, Y., Zheng, Y., Lang, S., Chen, H., You, Y., et al. (2019). The lower body positive pressure treadmill for knee osteoarthritis rehabilitation. *J. Vis. Exp. JoVE* 149. doi: 10.3791/59829

Liu-Ambrose, T. Y., Ashe, M. C., Graf, P., Beattie, B. L., and Khan, K. M. (2008). Increased risk of falling in older community-dwelling women with mild cognitive impairment. *Phys. Ther.* 88, 1482–1491. doi: 10.2522/ptj.20080117

McIsaac, T. L., Lamberg, E. M., and Muratori, L. M. (2015). Building a framework for a dual task taxonomy. *Biomed Res. Int.* 2015:591475. doi: 10.1155/2015/591475

Montero-Odasso, M. M., Sarquis-Adamson, Y., Speechley, M., Borrie, M. J., Hachinski, V. C., Wells, J., et al. (2017). Association of dual-task gait with incident dementia in mild cognitive impairment: Results from the gait and brain study. *JAMA Neurol.* 74, 857–865. doi: 10.1001/jamaneurol.2017.0643

Montero-Odasso, M., Casas, A., Hansen, K. T., Bilski, P., Gutmanis, I., Wells, J. L., et al. (2009). Quantitative gait analysis under dual-task in older people with mild cognitive impairment: A reliability study. *J. Neuroeng. Rehabil.* 6:35. doi: 10.1186/1743-0003-6-35

Naidu, A. S., Vasudev, A., Burhan, A. M., Ionson, E., and Montero-Odasso, M. (2019). Does dual-task gait differ in those with late-life depression versus mild cognitive impairment? *Am. J. Geriatr. Psychiatry* 27, 62–72. doi: 10.1016/j.jagp.2018.10.011

Nasreddine, Z. S., Phillips, N. A., Bédirian, V., Charbonneau, S., Whitehead, V., Collin, I., et al. (2005). The montreal cognitive assessment. MoCA: A brief screening tool for mild cognitive impairment. *J. Am. Geriatr. Soc.* 53, 695–699. doi: 10.1111/j.1532-5415.2005.53221.x

Noce Kirkwood, R., de Souza Moreira, B., Mingoti, S. A., Faria, B. F., Sampaio, R. F., and Alves Resende, R. (2018). The slowing down phenomenon: What is the age of major gait velocity decline? *Maturitas* 115, 31–36. doi: 10.1016/j.maturitas.2018.06.005

Oh, C. (2021). Single-Task or Dual-Task? Gait assessment as a potential diagnostic tool for Alzheimer's dementia. *J. Alzheimer's Dis. JAD* 84, 1183–1192. doi: 10.3233/JAD-210690

Ou, H., Lang, S., Zheng, Y., Huang, D., Gao, S., Zheng, M., et al. (2021). Motor dual-tasks for gait analysis and evaluation in post-stroke patients. *J. Vis. Exp. JoVE* 169. doi: 10.3791/62302

Petersen, R. C. (2004). Mild cognitive impairment as a diagnostic entity. *J. Int. Med.* 256, 183–194.

Rosano, C., Brach, J., Longstreth, W. T., and Newman, A. B. (2006). Quantitative measures of gait characteristics indicate prevalence of underlying subclinical structural brain abnormalities in high-functioning older adults. *Neuroepidemiology* 26, 52–60. doi: 10.1159/000089240

Schwenk, M., Sabbagh, M., Lin, I., Morgan, P., Grewal, G. S., Mohler, J., et al. (2016). Sensor-based balance training with motion feedback in people with mild cognitive impairment. *J. Rehabil. Res. Dev.* 53, 945–958. doi: 10.1682/JRRD.2015.05.0089

Shi, L. P., Yao, S. H., and Wang, W. (2022). Prevalence and distribution trends of mild cognitive impairment among Chinese older adults:A Meta-analysis. *Chin. Gen. Prac.* 25, 109–114.

Sun, Z., Zhao, S., Suo, X., and Dou, Y. (2022). Sirt1 protects against hippocampal atrophy and its induced cognitive impairment in middle-aged mice. *BMC Neurosci.* 23:33. doi: 10.1186/s12868-022-00718-8

Tsang, C. S.-L., Wang, S., Miller, T., and Pang, M. Y.-C. (2022). Degree and pattern of dual-task interference during walking vary with component tasks in people after stroke: A systematic review. *J. Physiother.* 68, 26–36. doi: 10.1016/j.jphys.2021.12.009

Tsuchida, W., Kobayashi, Y., Inoue, K., Horie, M., Yoshihara, K., and Ooie, T. (2022). Kinematic characteristics during gait in frail older women identified by principal component analysis. *Sci. Rep.* 12:1676. doi: 10.1038/s41598-022-04801-2

Tyrovolas, S., Koyanagi, A., Lara, E., Santini, Z. I., and Haro, J. M. (2016). Mild cognitive impairment is associated with falls among older adults: Findings from the Irish Longitudinal Study on Ageing (TILDA). *Exp. Gerontol.* 75, 42–47. doi: 10.1016/j.exger.2015.12.008

frontiers | Frontiers in Aging Neuroscience

TYPE Review
PUBLISHED 06 January 2023
DOI 10.3389/fnagi.2022.1028822

OPEN ACCESS

EDITED BY
Le Li,
Northwestern Polytechnical University, China

REVIEWED BY
Shirin Hosseini,
Technische Universitat Braunschweig, Germany
Nasra Ayuob,
Damietta University, Egypt, Egypt
Tuba Aktürk,
Istanbul Medipol University, Turkey

*CORRESPONDENCE
Wei Gu
✉ sam6116@163.com
Xueqiang Wang
✉ wangxueqiang@sus.edu.cn

†These authors have contributed equally to this work and share first authorship

SPECIALTY SECTION
This article was submitted to Neurocognitive Aging and Behavior, a section of the journal Frontiers in Aging Neuroscience

RECEIVED 26 August 2022
ACCEPTED 05 December 2022
PUBLISHED 06 January 2023

CITATION
Wang X, Si K, Gu W and Wang X (2023) Mitigating effects and mechanisms of Tai Chi on mild cognitive impairment in the elderly. Front. Aging Neurosci. 14:1028822. doi: 10.3389/fnagi.2022.1028822

Mitigating effects and mechanisms of Tai Chi on mild cognitive impairment in the elderly

Xin Wang[1†], Keyi Si[2†], Wei Gu[1*] and Xueqiang Wang[3,4*]

[1]Faculty of Traditional Chinese Medicine, Naval Medical University, Shanghai, China, [2]Department of Military Health Statistics, Naval Medical University, Shanghai, China, [3]Department of Sport Rehabilitation, Shanghai University of Sport, Shanghai, China, [4]Department of Rehabilitation Medicine, Shanghai Shangti Orthopaedic Hospital, Shanghai, China

Mild cognitive impairment (MCI) is a major public health concern that endangers health and decreases the quality of life of the elderly around the world. A recent clinical guideline has recommended regular exercise (twice per week) for patients with MCI as part of an overall approach to management. Tai Chi, a form of light-to-moderate-intensity mind-body exercise, is particularly suitable for seniors. This review aims to summarize epidemiological studies related to the effects of Tai Chi on symptom remission in older adults with MCI and reveal the potential mechanisms. Evidence suggested that Tai Chi can improve cognitive functions and alleviate the accompanying symptoms of MCI in the elderly potentially by activating the expression of signals in different brain regions, altering their connectivity, increasing the brain volume, and modulating brain-derived neurotropic and inflammation factors. Studies comparing various types of Tai Chi may contribute to the identification of paradigms that have appropriate intensities and difficulty and exert good effects on older people with MCI. In addition, studies are warranted to determine the frequency and duration of training that can optimize the beneficial effects of Tai Chi on MCI.

KEYWORDS

Tai Chi, mild cognitive impairment, elderly, cognitive function, mechanism

Introduction

Mild cognitive impairment (MCI) is a syndrome of cognitive dysfunction beyond that associated with natural aging but is not severe enough to meet the criteria for dementia. The risk of developing MCI increases significantly with age, with an annual conversion rate from 1% at age 60 to 11% at age 85 (Yesavage et al., 2002). MCI is an independent risk factor for dementia. A meta-analysis estimated that individuals with MCI were 2.3 times more likely to develop dementia than their age-matched counterparts without MCI, and the cumulative dementia incidence was 14.9% in MCI patients aged ≥65 years within a 2-year follow-up (Petersen et al., 2018).

MCI can be divided into single/multiple-domain amnestic MCI and single/multiple-domain non-amnestic MCI (**Figure 1**; Petersen et al., 1997; Petersen, 2004). Amnestic MCI is predominated by a memory deficit, whereas non-amnestic MCI is characterized by disturbances of attention, information processing, psychomotor speed, language, or executive functions (Tannenbaum et al., 2012). Other symptoms may also include a deficit in gait and balance, sleep disturbance, and body pain (Kong et al., 2016; Bahureksa et al., 2017; Hu et al., 2017). Additionally, a systematic review reported that 35%–85% of patients with MCI had at least one neuropsychiatric symptom, with the most common symptoms being depression, anxiety, irritability, and apathy (Martin and Velayudhan, 2020).

To date, no pharmacological treatments specifically for MCI have been approved (Tricco et al., 2013). However, accumulating evidence from randomized clinical trials (RCTs) indicated that physical activity could benefit cognitive functions in patients with MCI (Langa and Levine, 2014; Demurtas et al., 2020). A recent clinical practice guideline has recommended regular exercise (twice per week) as part of MCI management (Petersen et al., 2018).

Tai Chi, a mind-body low-impact exercise, may offer numerous health benefits to individuals with MCI, but related results were not consistent. A systematic review and a meta-analysis of RCTs reported that Tai Chi could significantly improve memory, learning, visuospatial ability, and executive functions in patients with MCI compared with no exercise (Lim et al., 2019; Lin et al., 2021). Furthermore, Tai Chi and cognitive mixed training have shown positive effects on delaying the progression of MCI to dementia (Li et al., 2022). However, one meta-analysis found no associations between Tai Chi and global cognition and memory in older people with cognitive impairment (Wang et al., 2018). Besides, related mechanism studies are still in a nascent stage. Current evidence indicated that as a type of aerobic exercise, Tai Chi might induce some positive neurophysiological changes related to cognitive function improvements, such as increases in hippocampus size, regional cerebral blood flow, and the production of neurotrophic factors (Burdette et al., 2010; Voss et al., 2010; Suzuki et al., 2013). Moreover, some stress-related pathways (e.g., cortisol) associated with depression and anxiety alleviation might be induced by meditation, mental focus, and deep breathing in Tai Chi (Wayne et al., 2014).

Given the light to moderate intensity [about three metabolic equivalents of task (METs)], Tai Chi has attracted people worldwide in pursuit of health and longevity, especially the frail elderly who experience a functional decline (Hui et al., 2016). This article aimed to give a comprehensive review about the impact of Tai Chi on MCI in the elderly and the potential mechanisms.

Amelioration of the clinical symptoms of MCI through Tai Chi in the elderly

Improve memory function

Amnestic MCI is a subtype of MCI manifesting as a decline in various types of memory (Leyhe et al., 2009; Costa et al., 2011; Tuena et al., 2021). The prevalence of amnestic MCI in people aged ≥60 was 7.4% in South Italy and 17.1% in China (Li et al., 2020; Caffo et al., 2022). Older patients with amnestic MCI are more likely to progress to Alzheimer's dementia than those with non-amnestic MCI (Jungwirth et al., 2012). Tai Chi, which calls for a substantial cognitive effort to learn new skills by remembering and performing movements, might prevent or alleviate memory loss in older adults with MCI (Lin et al., 2021).

An RCT from Thailand reported that the increase in logical memory delayed recall score was more pronounced in the 10-form Tai Chi group (three times per week for 6 months) than in the educational control group [mean difference: 0.43; 95% confidence interval (CI): 0.2, 0.7; Sungkarat et al., 2018]. An RCT from China also found that the Mattis memory score was enhanced in the Tai Chi group (three times per week for 40 weeks) in contrast to that in the other three groups (walking, social interaction, or no intervention; Mortimer et al., 2012). In another RCT from China, 389 older participants with MCI were randomized into either the 24-form simplified Tai Chi group or the exercise group (stretching and toning), and both their delayed recall and subjective memory complaints significantly improved after 5 months of intervention, but the positive effect only remained for delayed recall at 1-year post-intervention (Lam et al., 2011, 2012). In contrast, there are also some studies finding no associations between Tai Chi and memory improvement in older people with cognitive impairment compared with health education (Wang et al., 2018). The authors speculated that the beneficial effects of Tai Chi might not be apparent until enough training (60 min per time and three times per week for at least 12 weeks) had been done. In addition, a study found that Taoist Tai Chi + memory intervention program (MIP) was not superior to MIP alone in memory performance (Fogarty et al., 2016).

Improve executive function

The executive function refers to a set of cognitive abilities that help an individual plan, monitor, and achieve a goal, mainly including inhibition and interference control, working memory, and cognitive flexibility (Diamond, 2020). Elderly people with MCI are likely to have some defects in executive functions, which might be alleviated by exercises, such

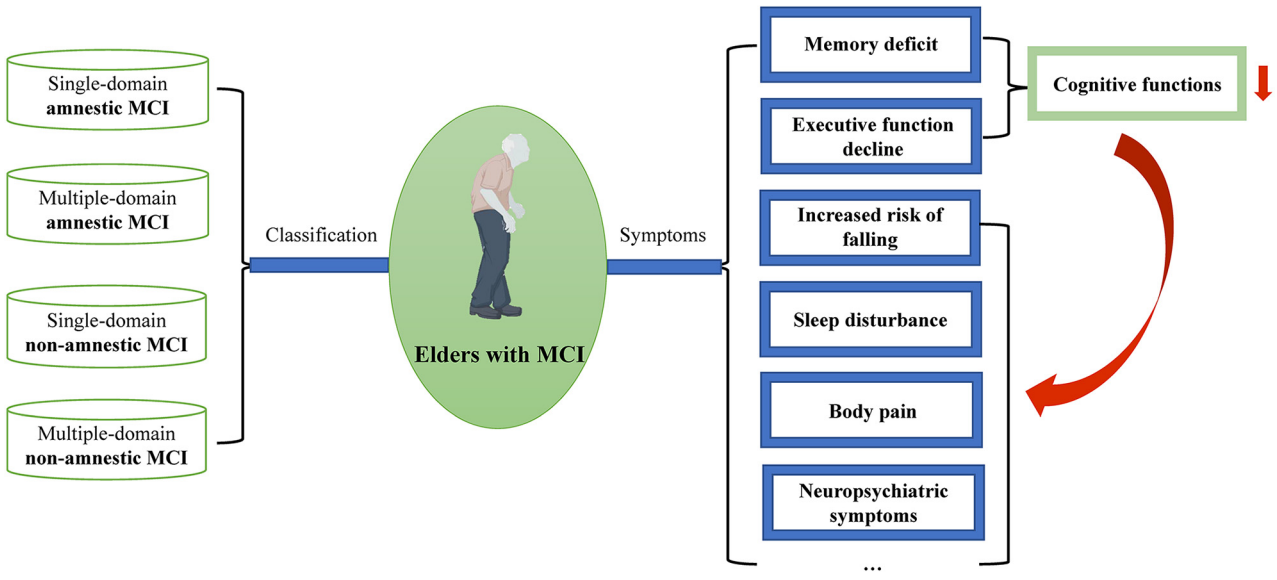

FIGURE 1
Classification and symptoms of mild cognitive impairment (MCI) in the elderly.

as Tai Chi (Law et al., 2020). A systematic review and meta-analysis found that Tai Chi was effective in improving the executive functions of processing speed, attention, and working memory compared with either non-active (health education or no intervention) or active controls (walking or endurance, resistance/strength, and flexibility exercises; Wayne et al., 2014). However, the number of studies was very limited (Tai Chi vs. non-active controls: N = 4; Tai Chi vs. active controls: N = 2). Apart from studies in the meta-analysis, an individual trial showed that 6 months of 10-form Tai Chi training (three times per week) was effective in improving the mental switching component of executive function in older adults with amnestic MCI (Sungkarat et al., 2018). The beneficial effects on executive function in exergaming-based Tai Chi group (modified Yang style), traditional Tai Chi group (simplified 24-form Yang style), and untrained controls were compared (Liu et al., 2022). During the Tai Chi exergames, participants imitated a virtually-presented Tai Chi instructor and made real-time adjustments in response to immediate feedback. These two Tai Chi groups (three times per week for 12 weeks) had similar improvements in executive functions, significantly stronger than the controls. Two RCTs assessing the effects of 24-form or 10-form Tai Chi on components of executive function showed significant improvement in Trail Making Test (task switching) but not the digit span forward and backward test (information updating and monitoring), indicating that the intervention effect of Tai Chi might be specific to certain executive components (Lam et al., 2011; Sungkarat et al., 2018).

Improve global cognitive function

Tai Chi is a light-to-moderate-intensity aerobic exercise, which may offer benefits to global cognitive functions (Bao and Liu, 2019). A 48 times 8-form Tai Chi training within 3 months can significantly improve the MOCA-P (the Peking Union Medical College version of Montreal cognitive assessment) total score of the elders with MCI, especially in its sub-project score (visual space function and long delayed recall) compared with the control group (a 30-min health education about MCI prevention and a related handbook; Wang and Sheng, 2016). The higher the MOCA-P score, the better the global cognitive function is. Systematic reviews demonstrated that compared with non-intervention controls or other active interventions (adapted physical activity and health education, stretching and relaxation exercise, walking, etc.), 12 weeks to 1 year of Tai Chi training could yield small to moderate clinically relevant improvements in global cognitive functions for cognitively impaired older adults (Wayne et al., 2014; Lim et al., 2019; Zhou et al., 2022). A pilot RCT compared the effects of 24-form Yang-style Tai Chi vs. conventional exercise with similar intensity on global cognitive function in adults aged ≥50 years with MCI (Yu et al., 2022). The results indicated that Tai Chi resulted in earlier (12 weeks vs. 24 weeks) and more significant improvements in cognitive flexibility. Notably, Tai Chi had additional positive effects on global cognitive function in comparison to cognitive training alone after 12 months of intervention, but the beneficial effects in both groups gradually disappeared after they stopped training, and only those who

continued to receive the combined training maintained their cognitive performance after another 12 months (Li et al., 2022). Therefore, prolonged training is required to delay cognitive decline. A meta-analysis revealed that as the duration of Tai Chi increased from 20–40 min to 60 min, profound improvement in global cognitive function would be obtained. However, one study found that the cognitive function was not differentially improved in the Taoist Tai Chi + MIP group relative to the MIP-only group over the shorter term (10 weeks) and longer-term (22 weeks; Fogarty et al., 2016). This might be attributed to the instability of the test or the relatively large difference in baseline cognitive functions between the groups.

Reduce the risk of falls

Good performance in maintaining balance and gait not only relies on the health of muscles and bones but also on that of some cognitive functions, such as executive-attentional functions, visuospatial abilities, and memory (Amboni et al., 2013). Degenerated muscles and bones and cognitive impairment often coexist in older adults, increasing the risk of falls (Tamura et al., 2018). A study reported that older people with cognitive impairment were four times more likely to fall than those without these issues (Tinetti et al., 1988).

Tai Chi might be an effective strategy for preventing falls in the elderly with MCI possibly by improving their somatic and cognitive functions related to balance, muscle strength, physical endurance, postural control, and flexibility (Wehner et al., 2021). A meta-analysis summarized that Tai Chi might reduce the incidence of falls by 43% over a short time (<12 months) in older and at-risk adults (Lomas-Vega et al., 2017). Sungkarat et al. (2017) assessed the effect of a combination of center- and home-based 10-form Tai Chi training on the risk of falls in older adults with MCI using various indicators, including knee proprioception, knee extension strength, hand reaction time, postural sway, and Physiological Profile Assessment fall risk index. These indices significantly improved after a 15-week intervention (three times per week). In addition to field training, the effects of Tai Chi online courses on the risk of falls have been explored during the COVID-19 pandemic. Liu et al. (2022) found that the exergaming-based Yang-style Tai Chi and traditional Yang-style Tai Chi groups had comparable improvements in gait performance and cognitive-dual-task cost, both of which were better than those of the untrained control group. Inconsistently, Li et al. (2021) found that though the home-based Tai Chi group performed better on tests of balance, chair stands, and gait performance than the stretching group, no significant reduction in falls (incidence rate ratio: 0.58; 95% CI: 0.32, 1.03) was observed possibly because of the small sample size (N = 15 for each group). Besides, a low-quality study reported that the Taoist Tai Chi + MIP on gait or balance showed no preferential benefit to the elders with MCI than the pure memory training (Fogarty et al., 2016).

Improve sleep quality

Compared with a normal population, MCI patients are more likely to experience sleep disturbances (18.3%–45.4% vs. 10.9%–23.3%), manifesting as greater wake after sleep onset, lower sleep efficiency, and longer rapid eye movement sleep latency (Da, 2015; D'Rozario et al., 2020). Some studies have suggested a bidirectional relationship between sleep problems and cognitive decline (Guarnieri and Sorbi, 2015). Specifically, circadian dysregulation might precede MCI and accelerate its progress to Alzheimer's disease, and different patterns of sleep disorders might result from specific dementias, depending on the areas affected in the brain (Tranah et al., 2011; Roth, 2012).

Tai Chi has been proposed as an effective intervention to mitigate sleep problems in older adults, but the evidence is limited in patients with MCI. In a pilot RCT, older adults with cognitive impairment who attended the 10-form Tai Chi sessions twice a week for 2 months had prolonged sleep duration (+48 min) and increased sleep efficiency (+9.1%) after 6 months, significantly better than those of the untrained group (Chan et al., 2016). A systematic review found that generally healthy older adults had the greatest number of significant improvements in various sleep outcomes after they performed moderate intensity exercise (e.g., Baduanjin, Tai Chi, and yoga) three times per week for at least 3 months (Vanderlinden et al., 2020). Regular exercise, especially Tai Chi training involving deep breathing and meditation, may promote relaxation and raise body temperature in ways that are helpful for initiating and maintaining sleep (Montgomery and Dennis, 2002).

Reduce body pain

MCI in older people is often accompanied by inflammation and chronic pain. A prospective cohort study demonstrated that the prevalence and severity of chronic pain were independently influenced by cognitive measures (attention, visual memory, and executive function) and affective factors (state anxiety, passive coping strategies, and depression; Attal et al., 2014). Systematic reviews and meta-analyses of RCTs demonstrated that Tai Chi was an effective intervention for relieving low back pain and pain caused by osteoporosis, osteoarthritis, and fibromyalgia (Kong et al., 2016). Lauche et al. (2016) showed the effectiveness of 12 weeks of 13-form Yang-style Tai Chi training in improving chronic nonspecific neck pain relative to non-trained controls. A pilot study found that compared with

light physical exercise program, a 12-week 8-form Yang-style Tai Chi training program could significantly lower pain severity and pain interference in older adults with chronic multisite pain (You et al., 2018). The valid duration of Tai Chi for osteoarthritis pain relief was at least 6 weeks as suggested by a systematic review and meta-analysis (Kong et al., 2016). In 2017, a clinical practice guideline from the American College of Physicians recommended patients with chronic low back pain to select Tai Chi or other mind-body exercise as a nonpharmacologic treatment (Qaseem et al., 2017). However, related evidence is limited and has low or moderate quality. Overlaps have been found among the brain regions responsible for pain modulation and cognition, such as the amygdala, prefrontal cortex, and hippocampus (Attal et al., 2014; Shen et al., 2021). When Tai Chi improves cognitive functions through altering these regions, some beneficial effects on pain relief may occur.

Relieve internal bad sentiment and improve the quality of life

Even though senior people with MCI can perform daily activities, they may still face some cognitive, social, or psychological problems that can make them feel anxious and upset, and thus their quality of life is reduced. Older adults with MCI who have low income, depressive symptoms, or poor sleep quality are likely to report low quality of life (Song et al., 2019). Eight weeks of the 10-form Tai Chi training has been linked to improvement in the mental health component of quality of life in older adults with cognitive impairment (Chan et al., 2016). Researchers speculated that such benefits might be attributed to more social interaction and companionship offered by Tai Chi. After a 16-week Yang-style simple Tai Chi training, older patients with MCI scored higher in some subscales of Short-form 12, a measure of the quality of life, than untrained controls (Siu and Lee, 2021). Reduction in depression and anxiety, alleviation of body pain, exaltation on activities of daily living, and improvement in sleep quality may somehow mediate the effects of Tai Chi on the quality of life in patients suffering from MCI (Siu and Lee, 2018; Farhang et al., 2019).

As previously mentioned, many epidemiological studies have identified the beneficial effects of Tai Chi on symptoms of MCI in the elderly, including memory deficit, executive function decline, sleep disturbance, body pain, and emotional disorders (**Table 1**). The soft movement and the postural control in Tai Chi may improve the flexibility of the limb joints and the stability of the posture, while the combination of aerobic exercise, meditation, and breathing control may alleviate emotional distress and improve some cognitive functions, such as the memory function and the executive function (**Figure 2**).

Mechanisms underlying the effects of Tai Chi on cognitive functions

Alter the functional connectivity of different brain regions

The human brain is a large network composed of structurally and functionally interconnected components (Fam et al., 2020). It can be artificially divided into different regions (lobes) in charge of various functions. Accumulating neuroimaging studies have demonstrated that MCI is a disorder characterized by brain dysconnectivity. The beneficial effects of Tai Chi on cognitive functions in older patients with MCI might be mediated by altering the connectivity of the brain network.

The prefrontal cortex, a region controlling the highest levels of cognitive and emotional processes, is extremely vulnerable to aging, and declines in these processes manifest as disrupted connectivity among brain regions (Jones et al., 2019; Yan and Rein, 2022). Research discovered that the resting-state functional connectivity between the medial prefrontal cortex and bilateral hippocampus increased significantly after 12 weeks (5 days per week) of Tai Chi training; the increase was associated with corresponding improvement in memory functions measured by the Wechsler Memory Scale (Li et al., 2014). Similarly, another study reported that a multimodal intervention comprising cognitive training (181-h sessions), Tai Chi (three times per week for 6 weeks), and group counseling (once per week) was efficacious in improving the resting-state functional connectivity between the medial prefrontal cortex and the medial temporal lobe and the strength of the connectivity was positively correlated with changes in cognitive performance assessed by the Category Fluency Test (Tao et al., 2016, 2017a). Hui et al. (2016) monitored the functional connections of different brain regions among experienced Tai Chi practitioners and untrained controls during resting and movement states. They found that Tai Chi could induce the activation of the prefrontal cortex, motor cortex, and occipital cortex, improve the connections among them in myogenic activity, sympathetic nervous system, and endothelial cell metabolic activities, and increase cerebral blood flow, which was associated with improvement in cognitive functions. Other studies have shown that Tai Chi could increase connectivity between the left middle frontal gyrus and the left superior parietal lobule, between the posterior cingulate cortex and the right putamen/caudate, or between the left prefrontal cortex and the right sensorimotor area and reduced connectivity among the bilateral dorsolateral prefrontal cortex, the left superior frontal gyrus, and the anterior cingulate cortex (Tao et al., 2017b; Liu J. et al., 2019; Wang and Lu, 2022).

The status of brain region connections is closely related to the efficiency of information transfer (Sun et al., 2014). Compared with general aerobic exercise, 8 weeks of Tai Chi training could significantly enhance the nodal clustering

TABLE 1 Characteristics of studies related to the effects of Tai Chi on mild cognitive impairment in the elderly.

Studies	Country	Diagnostic criteria	Participants (IG/CG)	Age, mean (SD), year	Intervention	Frequency and duration of Tai Chi	Follow-up	Adverse event	Outcomes/Measurements
Bao and Liu (2019)	China	Amnestic MCI, Global Deterioration Scale: 2–3; CDR score: 2; ADL ≤26	31/31	IG: 68.22 (9.84); CG: 65.62 (9.34)	IG: 24-form Tai Chi; CG: health education	Twice a day, 3 days a week for 6 months	6 months	Not reported	Tai Chi group had higher MMSE and MOCA scores, shorter P300's incubation period, and higher volatility than the control group ($P < 0.05$).
Birimoglu and Deveci (2021)	Turkey	MCI (MMSE and MoCA <25)	20/22	IG: 74.21 (6.93); CG: 74.21 (6.93)	IG: Yang style Tai Chi; CG: not subjected to any physical practice	35–40 min/session, twice a week for 3 months	3 months	Not reported	The scores of cognitive adaptations and changes in level subscales of the fall behavioral scale were significantly increased in the Tai Chi group ($P < 0.01$).
Chan et al. (2016)	China	MCI (MMSE 13–26)	27/25	IG: 78.4 (7.1); CG: 82.2 (6.7)	IG: 10-form Tai Chi; CG: usual activities	60-min session, twice a week for 2 months	6 months	None	Tai Chi group had significantly better results in the Chinese Pittsburgh Sleep Quality Index global score ($P = 0.004$), sleep duration ($P = 0.003$), habitual sleep efficiency ($P = 0.002$), and the Short-form 12 mental health component ($P < 0.001$).
Fogarty et al. (2016)	Canada	Amnestic MCI, MMSE	22/18	CG: 71.55 (9.33); CG: 72.61 (5.78)	IG: Taoist Tai Chi + MIP; CG: MIP	2 × 90 min for 10 weeks	3 months	Not reported	Both groups significantly increased their memory strategy knowledge and use, ratings of physical health, processing speed, everyday memory, and visual attention. No preferential benefit was found for individuals in the MIP + Tai Chi group on cognition, gait, or balance measures.
Kasai et al. (2010)	Brazil	MCI (RBMT ≤10)	13/13	IG: 73.54; CG: 74.54	IG: Yang style Tai Chi; CG: not practice Tai Chi	60-min per session, twice per week for 6 months	6 months	Not reported	Tai Chi group had significant improvement in the RBMT and the SMC ($P = 0.007$ and $P = 0.023$).
Lam et al. (2011)	China	CDR 0.5 or amnestic MCI	135/194	IG: 77.2 (6.3); CG: 78.3 (6.6)	IG: 24-form simplified Tai Chi; CG: stretching and toning exercise	3 × 30 min/week for 8–12 weeks + video CD of Tai Chi + monthly refresher lessons for 5 months	5 months	One fall with minor injury in CG	Tai Chi group had significantly better performance in visual spans and CDR sum of boxes scores ($P < 0.001$) and lower risk of dementia ($P < 0.05$).
Lam et al. (2012)	China	CDR 0.5 or amnestic MCI	92/169	IG: 77.2 (6.3); CG: 78.3 (6.6)	IG: 24-form simplified Tai Chi; CG: stretching and toning exercise	3 × 30 min/week for 4–6 weeks + video CD of Tai Chi + monthly refresher lessons for 12 months	1 year	Death: 1 in IG and 2 in CG; fall with bone fracture: 1 in IG and 1 in CG	Tai Chi group had a lower risk of developing dementia ($P = 0.04$) and a better preservation of CDR sum of boxes scores ($P = 0.04$). Tai Chi group had greater improvement in delay recall ($P = 0.05$) and Cornell Scale for Depression in Dementia scores ($P = 0.02$) in completers-only analyses.
	China	MCI (20 ≤MMSE ≤30)	22/24	IG: 75 (11); CG: 77 (10)	IG: Tai Ji Quan; CG: usual daily physical activities	60-min per session, twice per week for 14 weeks.	14 weeks	None	Tai Chi group had significant improvement on MMSE ($P < 0.001$), physical performance, and balance efficacy measures ($P < 0.05$).

(*Continued*)

10.3389/fnagi.2022.1028822

TABLE 1 (Continued)

Studies	Country	Diagnostic criteria	Participants (IG/CG)	Age, mean (SD), year	Intervention	Frequency and duration of Tai Chi	Follow-up	Adverse event	Outcomes/Measurements
Li et al. (2021)	China	MCI (CDR ≤0.5 and MMSE ≥24)	15/15	IG: 76.13 (6.2); CG: 76.2 (6.3)	IG: Tai Ji Quan; CG: stretching	60-min virtual exercise sessions *via* Zoom, twice weekly for 6 months	6 months	No serious intervention-related adverse events	Tai Chi group did not reduce falls or the number of fallers, but performed consistently better in balance (30-s chair stands and Timed Up and Go under single-task and dual-task conditions).
Li et al. (2022)	China	MCI (detailed medical history, neurological examinations, (CDR = 0.5) and MTA)	48/51	IG: 65.6 (5.6); CG: 65.5 (7.2)	IG: Tai Chi and cognitive training; CG: cognitive training	2 × 120 min/week for 12 months; a subgroup of IG received training for another 12 months	24 months	Not reported	Tai Chi enhanced global cognitive function in MCI. Tai Chi and cognitive mixed exercise showed positive effects on delaying cognitive decline.
Liu et al. (2022)	China	MCI based on Petersen's criteria	16 + 17/17	IG: 74.6 (6.1) and 73.2 (6.3); CG: 73.4 (6.5)	IG: exergaming-based/traditional Tai Chi (24-form Yang style); CG: usual daily physical activities	3 × 50 min/week for 3 months	3 months	None	The exergaming-based and traditional Tai Chi groups performed better than the control group on the Chinese version of the Stroop Color and Word Test, the TMT (A and B), the one-back test, gait speed, and dual-task cost of gait speed in cognitive dual-task conditions. Only the exergaming-based Tai Chi group experienced beneficial effects for the Montreal Cognitive Assessment.
Siu and Lee (2021)	China	MCI (MMSE 19–28)	80/80	IG: 60–74 (78.8%), 75 or above (21.3%); CG:60–74 (55%), 75 or above (45%)	IG: 24-form Yang-style Tai Chi; CG: usual activities	60 min per session, 2 sessions per week for 16 weeks	17–18 weeks	Not reported	Tai Chi group performed better in the physical health component ($P = 0.036$), the mental health component ($P = 0.014$), as well as several subscales of SF-12, namely, the role-physical ($P = 0.044$), the bodily pain ($P < 0.001$) and the vitality ($P = 0.004$) subscales.
Sungkarat et al. (2017)	Thailand	Amnestic MCI, MMSE ≥24 and MoCA <26	33/33	IG: 68.3 (6.7); CG: 67.5 (7.3)	IG: 10-form Tai Chi; CG: health education	3-week center-based + 12-week home-based Tai Chi (50 min per session, 3 times per week)	15 weeks	One ill health, one study-unrelated ankle fracture	Tai Chi group had significantly better performance on Logical Memory, Block Design (visuospatial ability), TMT (B-A; executive function), composite PPA score (fall risk), and PPA parameter scores (knee extension strength, reaction time, postural sway, and lower limb proprioception).
Sungkarat et al. (2018)	Thailand	Amnestic MCI, MMSE ≥24 and MoCA <26	33/33	IG: 68.3 (6.7); CG: 67.5 (7.3)	IG: 10-form Tai Chi; CG: health education	3-week center-based + 6 months home-based Tai Chi (50 min per session, 3 times per week)	27 weeks	One ill health, one study-unrelated ankle fracture	Tai Chi group had significantly better performance on Logical Memory and TMT (B-A), and higher plasma BDNF levels. No significant difference on Block Design scores, Digit Span forward/backward scores (executive function), and plasma TNF-α and interleukin-10 levels were observed.

(*Continued*)

10.3389/fnagi.2022.1028822

TABLE 1 (Continued)

Studies	Country	Diagnostic criteria	Participants (IG/CG)	Age, mean (SD), year	Intervention	Frequency and duration of Tai Chi	Follow-up	Adverse event	Outcomes/Measurements
Tsai et al. (2015)	USA	Moderate, mild, or subtle MCI and knee osteoarthritis (18 ≤ MMSE ≤28 and VDS ≥2 or WOMAC ≥3)	28/27	79	IG: 12-form Sun-style Tai Chi; CG: instructor-led educational activities	3 sessions per week for 20 weeks	20 weeks	None	The VDS and observed pain behaviors were significantly better in the Tai Chi group ($P = 0.008–0.048$).
Wang and Sheng (2016)	China	MCI (MoCA-P ≤25)	43/49	IG: 6–70: 2, 70–80: 30, 80–85: 11; CG: 65–70: 2, 70–80: 30, 80–85: 17	IG: 8-form Tai Chi; CG: health education	At least 40 min each time, at least 4 times a week for 3 months	3 months	One case of accidental fall	The total scores of MoCA-P and the scores of visual space function and long-delayed recall were higher in the Tai Chi group ($P < 0.01$).
Xu et al. (2020)	China	MCI (MoCA-Hong Kong: 19–21)	6/6	IG: 76.43 (4.47); CG: 70.67 (4.23)	IG: 24-form simplified Tai Chi; CG: health advice	12-week training + 12-week practice (30 min per session, 3 times per week)	6 months	One leg pain	Tai Chi group had a significantly lower cost of health service utilization and better performance in DAD score and GAS-20 ($P < 0.05$).
Young (2020)	China	Mild-stage dementia (MMSE ≥18)	41/39	IG: 80.05 (6.17); CG: 80.25 (6.33)	IG: 8-form Tai Chi; CG: usual activities	60 min per session, twice a week, with a total of 14 sessions	7 weeks	Not reported	Tai Chi group was more effective in improving the Dementia Rating Scale and MMSE scores ($P < 0.01$).
Yu et al. (2022)	China	MCI (below the 7th percentile of the normative data using the MoCA-Hong Kong)	10/12	IG: 67.3 (4.2); CG: 67.2 (6.8)	IG: 24-form Yang-style Tai Chi; CG: conventional exercise	3 sessions of 60-min training per week for 6 months	6 months	None	Tai Chi group showed greater improvements in MoCA-Hong Kong score than the exercise group at 12 weeks ($P < 0.001$), but the difference was no longer significant at 24 weeks ($P = 0.061$).

Note: ADL, Activities of Daily Living; BDNF, brain-derived neurotrophic factor; CDR, Clinical Dementia Rating Scale; CG, control group; CPQSI, the Chinese Pittsburgh Sleep Quality Index; DAD, the Disability Assessment for Dementia; GAS-20, the Geriatric Anxiety Scale with a maximum score of 20; GDS, Geriatric Depression Scale; HK-MoCA, Montreal Cognitive Assessment Hong Kong version; IG, intervention group; MCI, mild cognitive impairment; MIP, memory intervention program; MMSE, Mini-Mental State Examination; MoCA, Montreal Cognitive Assessment; MoCA-P, the Peking Union Medical College Version of Montreal Cognitive Assessment; MTA, The Visual Rating Medial Temporal Atrophy Score; PPA, Physiological Profile Assessment; RBMT, Rivermead Behavioral Memory test; SD, standard deviation; SMC, subjective memory complaints; TC, Tai Chi; TNF, tumor necrosis factor; TMT, Trail-Making Test; VDS, Verbal Descriptor Scale; WOMAC, the Western Ontario and MacMaster pain scale.

10.3389/fnagi.2022.1028822

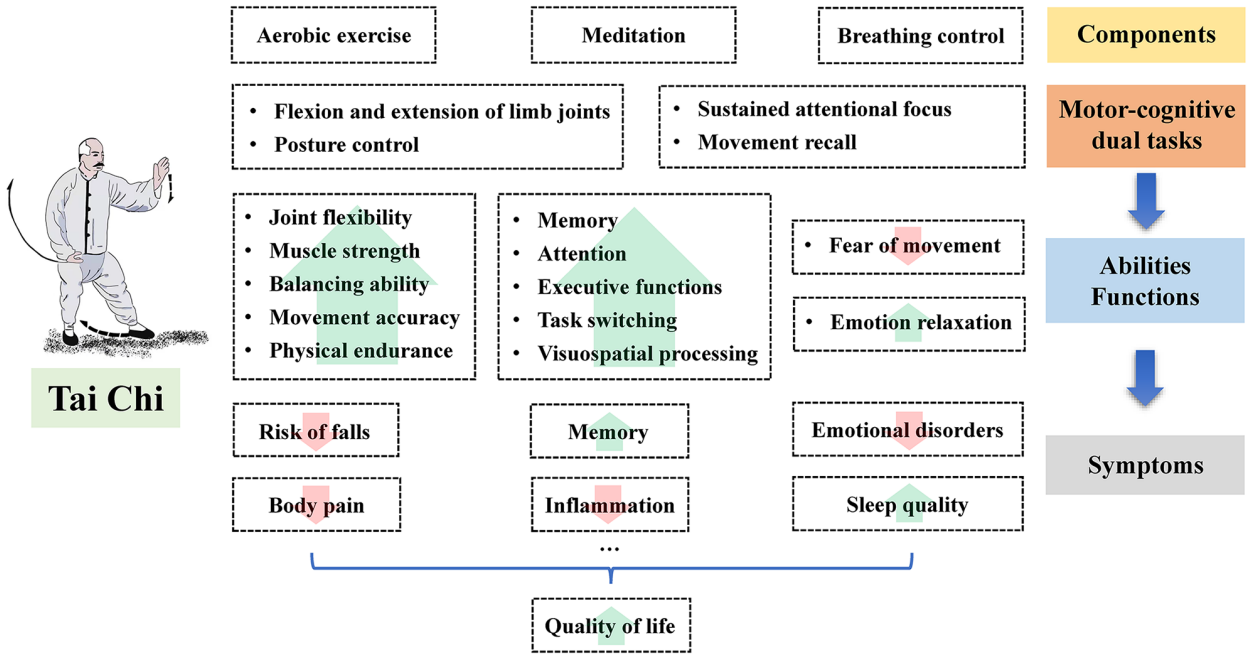

FIGURE 2
The potential benefits of Tai Chi on the symptoms of mild cognitive impairment in the elderly.

coefficient of the left thalamus, an indicator of the ability of information processing and transmission between this region and adjacent brain regions (Cui et al., 2021). This was also reflected as higher cognitive flexibility (smaller reaction time difference between the heterogeneous and homogeneous tasks) in Tai Chi practitioners. Given that the thalamus plays an important role in attention, working memory, and sleep, it is reasonable why Tai Chi can help attenuate the progressive decline of cognitive functions (Mitchell et al., 2014).

Elderly people with MCI are more likely to develop neuropsychiatric disorders, such as anxiety and depression. Tai Chi might be efficacious in alleviating negative feelings by strengthening the fronto-striatal functional connectivity or weakening the connectivity between the dorsolateral prefrontal cortex and the middle frontal gyrus (Liu et al., 2018, 2020).

Increase the activation of the prefrontal cortex

The prefrontal cortex, a brain region involved in many cognitive functions, including working memory, sensory attention, abstraction, planning, value-based decision-making, and motor control, is vulnerable to neurodegeneration associated with aging (Chafee and Heilbronner, 2022). Reduced activation in the dorsolateral prefrontal cortex during memory retrieval may lead to adverse memory performance (Uemura et al., 2016). Tai Chi might reduce the degeneration of the prefrontal cortex caused by aging by increasing its activation. Oxyhemoglobin, a reliable indicator of changes in regional cerebral blood flow, can be used to reflect cortical activation during movement (Perrey, 2008). Lu et al. (2016) reported a case in which the prefrontal oxyhemoglobin level was monitored when a Tai Chi master was asked to perform Tai Chi and cycling on two separate days. They found a greater increase in oxyhemoglobin and total hemoglobin levels (sum of oxygenated and deoxygenated hemoglobin) during the Tai Chi routine, suggesting that the subject had greater prefrontal neuronal activation during Tai Chi exercise than that during cycling, though these two activities had similar intensities (2.6 METs for Tai Chi and 2.3 METs for cycling). This research speculated that the additional activation was due to the mental involvement unique to Tai Chi. Some studies found increased prefrontal activation assessed by functional magnetic resonance imaging or functional near-infrared spectroscopy and increased resting-state activity in the dorsolateral prefrontal cortex evaluated by the fractional amplitude of low-frequency fluctuations in the Tai Chi group (Wu et al., 2018; Xie et al., 2019; Wang S. et al., 2021).

Increase gray matter density and regional homogeneity in the hippocampus

The hippocampus, a region that plays a vital role in learning, memory formation and consolidation, and emotion

regulation, is located within the medial temporal lobe of the brain (Bartsch and Wulff, 2015). A series of alterations in the aging hippocampus, including decreased volume and neuronal density, increased neuroinflammation, and altered intracellular signaling, has been associated with cognitive decline (Driscoll et al., 2003; Bettio et al., 2017). Compared with controls, Tai Chi practitioners were reported to have increased gray matter densities, higher regional homogeneity in the hippocampus, and enhanced memory-related test scores; this finding implied that Tai Chi improves memory functions by altering the hippocampus at structural and functional levels (Yue et al., 2020a). Specifically, participants who regularly performed Tai Chi for at least 6 years had higher gray matter densities in the left hippocampus and left parahippocampal gyrus than those who walked for exercise. Regional homogeneity is a data analysis method of resting-state functional magnetic resonance imaging technique and mainly reflects the consistency of the spontaneous activities of local neurons (Liu et al., 2021). This study also found significantly higher regional homogeneity activation in the hippocampus and a positive relationship between this factor and memory performance in the Tai Chi group, which is consistent with the results of another study with 6 weeks of Tai Chi intervention (Zheng et al., 2015).

Improve the efficiency and microstructure of brain white matter

The white matter serves a critical role in cognitive functions because it connects gray matter regions throughout the brain (Filley and Fields, 2016). The reduced integrity of the white matter during aging is related to a decline in memory, executive function, and general cognition (Coelho et al., 2021). Older patients with MCI and memory deficit exhibited decreased white matter integrity for the bilateral dorsal frontal-striatal tract, left anterior thalamocortical radiations-ventral part, and corpus callosum connecting the bilateral inferior parietal lobule and ventral prefrontal regions (Chang et al., 2021). Compared with older adults who regularly performed walking as exercise for at least 6 years, older adults who performed Tai Chi for a similar period had a smaller small-world attribute (sigma), which indicated higher efficiency of information transfer in the white matter network (Yue et al., 2020b). This attribute is associated with enhanced performance of the updating function in working memory. Apart from the statistical evidence of a small-world network, a study used diffusion tensor imaging to explore the microstructure of the brain white matter of Tai Chi practitioners and their sedentary counterparts (Yao et al., 2019). The results showed that the fractional anisotropy in the splenium of the corpus callosum was significantly higher in the Tai Chi group than in the control group, suggesting the improved integrity of the white matter. Additionally, a meta-analysis of RCTs investigating the role of Tai Chi on cardiorespiratory fitness in elderly people indicated that Tai Chi can significantly increase the maximum rate of oxygen consumption (VO_2max). Meanwhile, white matter microstructure mediates the association of VO_2max with spatial working memory performance (Tan et al., 2022). In summary, Tai Chi might improve cognitive functions by slowing down white matter degeneration.

Increase the brain volume and cortex thickness

Older adults with MCI often exhibit increased brain atrophy rate. Patients with MCI accompanied by hippocampal atrophy, medial temporal lobe atrophy, or entorhinal atrophy are at a high risk of developing Alzheimer's disease (Li et al., 2016). Decreases in the volumes of different brain regions might lead to impairment in cognitive functions. For instance, a decrease in the hippocampal volume has been linked to poor episodic memory, working memory, and executive functioning (Hardcastle et al., 2020). Mortimer et al. (2012) reported that after 40 weeks of Tai Chi training, the whole brain volume increased by 0.47%, significantly higher than that in the walking group (−0.15%) or no intervention group (−0.24%); this finding might partially explain cognitive improvements related to verbal learning, attention, and memory in the Tai Chi group. Compared with general aerobic exercise, 8 weeks of Tai Chi tends to have a stronger effect on brain plasticity, as evidenced by an increase in gray matter volume in the left middle occipital gyrus, left superior temporal gyrus, and right middle temporal gyrus (Cui et al., 2019). These regions are highly correlated with visual information processing, emotion regulation, language/semantic processing, and memory encoding and retrieval (Pico-Perez et al., 2017; Teng et al., 2018; Liu et al., 2021). In addition, increased gray matter volume has been found in the insula, medial temporal lobe, putamen, thalamus, and hippocampus in Tai Chi practitioners (Tao et al., 2017c; Liu S. et al., 2019).

Apart from an increase in brain volume, an increase in cortical thickness was observed in some specific brain regions in the Tai Chi group, such as the precentral gyrus, the middle frontal sulcus, the superior temporal gyrus, and the medial occipito-temporal sulcus, which are responsible for motor execution, emotion and cognition integration, and special navigation (Wei et al., 2013). Similar effects can be induced by meditation or aerobic exercise; hence, these activities might have common mechanisms for brain reshaping (Lazar et al., 2005; Rogge et al., 2018).

Change brain event-related potentials

An ERP refers to an electrical brain response time-locked to a particular stimulus or event, which can be recorded *via*

electroencephalography (Aaronson, 2021). ERPs are commonly used in assessing cognitive processing at a high temporal resolution (Helfrich and Knight, 2019). In this context, ERPs as indicators are more sensitive than behavioral reactions (Fong et al., 2014). P3b and P3 amplitudes are indices of neural resource and cognitive processing capability allocation and have large amplitudes reflecting enhanced processing capability; P3 latency reflects stimulus evaluation time or processing speed, with shorter latency indicating superior performance (Gao et al., 2013). Under a natural condition, P3 amplitude decreases regularly with increasing age at a rate of 0.18 μV per year, whereas its latency increases at a rate of 1.36 ms per year (Picton et al., 1984). Tai Chi might mitigate such a trend. A cross-sectional study reported that Tai Chi practitioners had larger P3b amplitudes than sedentary controls; this result was consistent with that of another study, which showed a larger P3 amplitude in older adults practicing Tai Chi in a task-switching task (Fong et al., 2014; Hawkes et al., 2014). This phenomenon implies that Tai Chi practitioners allocate more attention or other resources to the task given by researchers than individuals that do not perform Tai Chi and thereby have better cognitive performance. The second study found shorter P3 latency in the Tai Chi group than in sedentary counterparts, indicating the faster processing speed of the practitioners. These findings are consistent with the "compensation hypothesis," which suggests that age-related cognitive deterioration can be compensated by the frontal activation of neural networks through learning new skills or exercise (Fong et al., 2014).

Increase concentrations of brain-derived neurotrophic factor

Brain-derived neurotrophic factor (BDNF) is a protein that can regulate a wide range of activities essential for the development and maintenance of normal brain functions (Colucci-D'Amato et al., 2020). It is considered a mediator in the association between an external stimulus (e.g., exercise and enriched environment) and improved neurogenesis and synaptic plasticity in the hippocampus and prefrontal cortex, which is critical for learning and memory (Numakawa et al., 2018). Results of a trial showed that the aerobic exercise-induced upregulation of serum BDNF was associated with increased hippocampal volume and improved memory function (Erickson et al., 2011). An RCT demonstrated that 6 months of the 10-form Tai Chi practice was effective in upregulating plasma BDNF along with improving memory and mental switching in older patients with amnestic MCI (Sungkarat et al., 2018). A similar phenomenon was also observed in another study with 10 weeks of Tai Chi intervention (Solianik et al., 2021).

Decrease plasma amyloid beta (Aβ) and total tau (t-tau) protein levels

The hallmark neuropathological substrates for MCI are β-amyloid (Aβ) plaques and intracellular tau neurofibrillary tangles (NFTs; Chandra et al., 2019). Aβ peptides have been demonstrated to lead to lipid peroxidation in amnestic MCI brains (Butterfield and Boyd-Kimball, 2018). The severity of cognitive symptoms and disease duration are positively correlated with the existence and the amount of hyperphosphorylated tau-based NFT pathology (Gómez-Isla et al., 1997). A mice study found that 8 weeks of aerobic exercise (treadmill) could alleviate memory impairments by reducing tau hyperphosphorylation in the cerebral cortex (Jeong and Kang, 2018). Tai Chi is a type of aerobic exercise and may have a similar effect. Reduced Aβ1–42 was considered evidence of amyloid deposition in the brain (Harris et al., 2015). A positive association was observed between the plasma level of Aβ1–42 and global cognition and hippocampal volume (Poljak et al., 2016). Long-term Tai Chi practice has been shown to increase hippocampal volume (Wei et al., 2013). Besides, Tai Chi was associated with improved cerebral blood flow velocity, which may help inhibit the formation and aggregation of Aβ plaques and intracellular NFTs (Burdette et al., 2010).

Regulate brain inflammatory factors

Inflammation has been implicated in the pathogenesis of chronic neurodegenerative diseases, such as MCI. A meta-analysis has verified several inflammatory markers with significantly different expression levels in patients with MCI compared with healthy controls, such as elevated levels of soluble tumor necrosis factor receptor 2 and interleukin-6 (IL-6; Shen et al., 2019). Some inflammatory markers, such as IL-1 and IL-1β, are directly correlated with the impairment of hippocampal-dependent memory processing (Shaftel et al., 2008). The results of studies focusing on the effects of Tai Chi on inflammation control were inconsistent. Some of them showed reduced levels of IL-6, tumor necrosis factor, and C reactive protein in the Tai Chi group, but some showed no significant changes or even reversed results (Bower and Irwin, 2016). This might be attributed to the complexity of inflammation regulation and the instability of circulating inflammatory markers that can be influenced by many factors apart from Tai Chi. However, RCTs that examined the effects of Tai Chi on inflammation-related gene expression consistently demonstrated reduced activity of nuclear factor kappa B (NF-κB; Bower and Irwin, 2016). NF-κB plays a key role in cognitive performance. A mice experiment indicated that lipopolysaccharides could induce cognitive impairment and neuroinflammation by activating the NF-κB signaling pathway (Zhao et al., 2019). Moreover, another study conducted

on Wistar rats found that aerobic exercise could attenuate age-related memory decline, decreased hippocampal NF-κB levels, and atrophy (Lovatel et al., 2013).

Although many epidemiological studies have identified the beneficial effects of Tai Chi on various cognitive functions, the underlying neural mechanisms have not been investigated in detail. The performance of cognitive processes depends on the condition of a neural substrate. Previous studies have linked cognitive impairment with structural, neuroelectric, and metabolic abnormalities in a range of brain regions, including the hippocampus, prefrontal cortex, and temporal gyrus. Tai Chi might alleviate cognitive decline through altering factors related to these aspects, particularly by altering the functional connectivity of different brain regions, increasing the activation of the prefrontal cortex and hippocampus, changing brain event-related potential (ERP), and regulating brain inflammatory factors (**Figure 3**).

Current problems and prospects

Though guidelines have recommended exercise as an effective nonpharmacologic treatment for preserving cognitive functions in patients with MCI, many older adults are prevented to perform exercises because of physical frailty. Tai Chi may be appealing to elders with MCI because it is a light-to-moderate-intensity aerobic exercise that is safe and friendly to those with different levels of mobility. Furthermore, Tai Chi does not require special equipment or a venue and can thus be performed anywhere at any time.

Tai Chi has its unique advantages over other forms of exercises in improving cognitive functions. First, Tai Chi has many movements. In contrast to general exercises consisting of simple and repetitive movements, Tai Chi requires learning and memorizing different movements and their sequences and formulas, which leads to particularly significant improvements in mental flexibility and immediate recall (Lim et al., 2019). Second, Tai Chi, considered a moving meditation, has a higher level of intellectual involvement. Meditation has been demonstrated to consistently alter some brain regions that are keys to meta-awareness, memory consolidation and reconsolidation, and emotion regulation (Fox et al., 2014). This may shed light on why Tai Chi has stronger effects than general aerobic exercises on brain plasticity and executive functions (Cui et al., 2019; Chen et al., 2020).

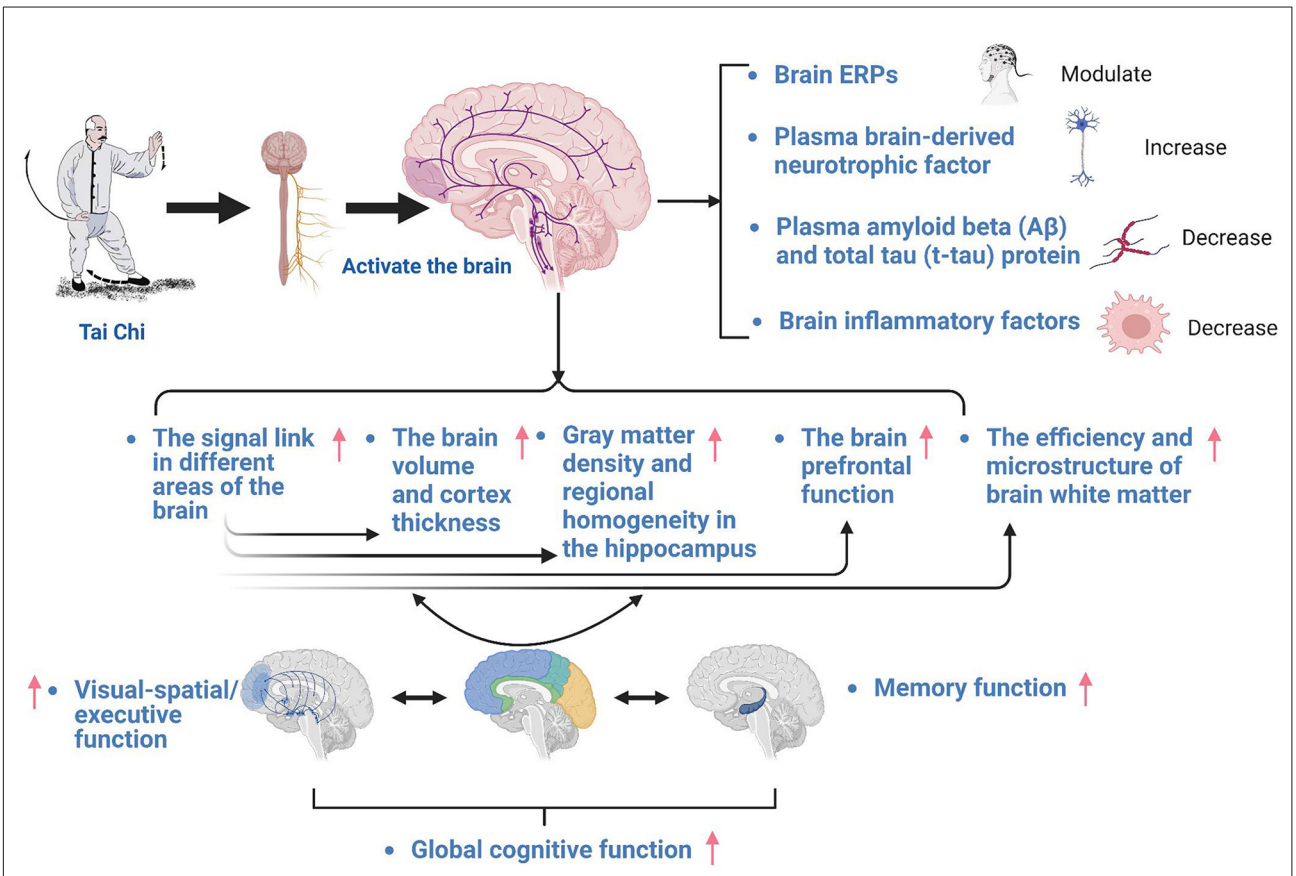

FIGURE 3
The brain function mechanisms of the Tai Chi treatment for mild cognitive dysfunction.

Tai Chi has many types and can be classified either by founding family (Chen style, Yang style, Wu Hao style, Wu style, and Sun style) or by the degree of difficulty (8-style, 16-style, 24-style, 32-style, and 42-style). The stance can be performed at three heights (high, medium, and low). The different types or movements of Tai Chi may require different levels of physical strength and flexibility. Selecting a style that works best for one's condition under the guidance of professionals is important to safety, especially for elders with chronic conditions or disabilities. For example, the lower the stance is, the more power, flexibility, and capacity of balance are needed. Starting Tai Chi from a high stance and gradually moving towards lower ones is preferred for senior beginners. Moreover, the effects of Tai Chi on MCI may vary with style. Most studies used 24-style Tai Chi as the exercise intervention program. Whether other styles can result in better performance is currently unclear. A systematic review indicated that the Yang style tended to be more effective than Sun-style in preventing falls in elders (risk ratio: 0.61 vs. 0.88). More RCTs comparing various Tai Chi styles are needed to determine the most effective one.

Apart from style, duration and frequency may influence the effect size of Tai Chi on MCI. A bibliometric analysis from 2010 to 2020 showed that in most trials with positive effects, Tai Chi was performed for 60 min per time and three times per week for at least 12 weeks (Yang et al., 2021). A recent study speculated that an intervention lasting 6 months to 1 year might lead to further improvements in cognitive functions (Lim et al., 2019). The effect size of Tai Chi on static steady-state balance in older adults was positively correlated with exercise frequency in a meta-analysis (Wang L. C. et al., 2021). Dose-response analyses are needed to optimize the intervention of Tai Chi on MCI.

Tai Chi has been delivered face-to-face by an instructor. Combining Tai Chi with other teaching forms may be an alternative for individuals who prefer to perform Tai Chi at home or who have no access to an instructor. A modified Tai Chi *via* virtual reality has been compared with untrained controls in older adults with cognitive impairment (Hsieh et al., 2018). Significant improvements in cognitive functions were observed in favor of Tai Chi (twice weekly for 6 months) and were closely correlated with the average movement accuracy score. Virtual reality can help practitioners memorize movements by providing verbal and visual cueing and can facilitate standardizing movements by providing immediate feedback.

Though not very consistent, most of the previous epidemiological studies indicated that Tai Chi was a potentially effective strategy for relieving the symptoms of MCI and delaying the progression of MCI to dementia in older adults. The symptoms included but were not limited to memory deficit, executive function decline, sleep disturbance, and body pain. As for the underlying mechanisms, studies demonstrated that Tai Chi can increase connectivity between many brain regions, increase brain volume, and improve the efficiency of the white matter. Additionally, Tai Chi might promote the clearing of neuropathological substrates for MCI and reduce inflammatory factors. Although some of the previous studies appear confusing and even partially contradictory, the combined evidence suggests that Tai Chi may have a positive value in slowing brain aging and rejuvenating brains affected by MCI.

In summary, accumulating evidence from RCTs has suggested Tai Chi as a promising strategy for improving cognitive functions and delaying the onset of dementia in patients with MCI possibly by altering structures and neural activities and regulating other factors (e.g., neurotrophic and inflammatory factors). Future studies are encouraged to compare the different styles of Tai Chi, explore whether a dose-response relationship exists, determine how long an effect can last, and perform subgroup analyses on different types of MCI given that the effects of Tai Chi may vary with specific domain impairment, and investigate potential neural mechanisms by neuroimaging techniques and biochemical markers.

Author contributions

XiW and KS contributed to the conception and design of the study. XiW wrote the first draft. XuW and WG organized the research project and corrected the manuscript. All authors contributed to the article and approved the submitted version.

Funding

This work was supported by the Shanghai Key Lab of Human Performance (Shanghai University of Sport; 11DZ2261100) and the Naval Medical University "Qi Hang" Military Medical Talent Program (2019-QH-12).

Conflict of interest

The authors declare that the research was conducted in the absence of any commercial or financial relationships that could be construed as a potential conflict of interest.

Publisher's note

References

Aaronson, B. (2021). "Event-related potential," in *Encyclopedia of Autism Spectrum Disorders*, ed F. R. Volkmar (Cham: Springer).

Amboni, M., Barone, P., and Hausdorff, J. M. (2013). Cognitive contributions to gait and falls: evidence and implications. *Mov. Disord.* 28, 1520–1533. doi: 10.1002/mds.25674

Attal, N., Masselin-Dubois, A., Martinez, V., Jayr, C., Albi, A., Fermanian, J., et al. (2014). Does cognitive functioning predict chronic pain? Results from a prospective surgical cohort. *Brain* 137, 904–917. doi: 10.1093/brain/awt354

Bahureksa, L., Najafi, B., Saleh, A., Sabbagh, M., Coon, D., Mohler, M. J., et al. (2017). The impact of mild cognitive impairment on gait and balance: a systematic review and meta-analysis of studies using instrumented assessment. *Gerontology* 63, 67–83. doi: 10.1159/000445831

Bao, N., and Liu, C. (2019). Study on the influence of Taijiquan on the cognitive function of patients with amnestic mild cognitive impairment. *Med. Informat.* 32, 115–117. Available online at: https://kns.cnki.net/kcms/detail/detail.aspx?FileName=YXXX201902032&DbName=CJFQ2019.

Bartsch, T., and Wulff, P. (2015). The hippocampus in aging and disease: from plasticity to vulnerability. *Neuroscience* 309, 1–16. doi: 10.1016/j.neuroscience.2015.07.084

Bettio, L., Rajendran, L., and Gil-Mohapel, J. (2017). The effects of aging in the hippocampus and cognitive decline. *Neurosci. Biobehav. Rev.* 79, 66–86. doi: 10.1016/j.neubiorev.2017.04.030

Birimoglu, O. C., and Deveci, E. (2021). The effectiveness of Tai Chi Chuan on fear of movement, prevention of falls, physical activity and cognitive status in older adults with mild cognitive impairment: a randomized controlled trial. *Perspect. Psychiatr. Care* 57, 1273–1281. doi: 10.1111/ppc.12684

Bower, J. E., and Irwin, M. R. (2016). Mind-body therapies and control of inflammatory biology: a descriptive review. *Brain Behav. Immun.* 51, 1–11. doi: 10.1016/j.bbi.2015.06.012

Burdette, J. H., Laurienti, P. J., Espeland, M. A., Morgan, A., Telesford, Q., Vechlekar, C. D., et al. (2010). Using network science to evaluate exercise-associated brain changes in older adults. *Front. Aging Neurosci.* 2:23. doi: 10.3389/fnagi.2010.00023

Butterfield, D. A., and Boyd-Kimball, D. (2018). Oxidative stress, amyloid-β peptide and altered key molecular pathways in the pathogenesis and progression of Alzheimer's disease. *J. Alzheimers Dis.* 62, 1345–1367. doi: 10.3233/JAD-170543

Caffo, A. O., Spano, G., Tinella, L., Lopez, A., Ricciardi, E., Stasolla, F., et al. (2022). The prevalence of amnestic and non-amnestic mild cognitive impairment and its association with different lifestyle factors in a south italian elderly population. *Int. J. Environ. Res. Public Health* 19:3097. doi: 10.3390/ijerph19053097

Chafee, M. V., and Heilbronner, S. R. (2022). Prefrontal cortex. *Curr. Biol.* 32, 346–351. doi: 10.1016/j.cub.2022.02.071

Chan, A. W., Yu, D. S., Choi, K. C., Lee, D. T., Sit, J. W., and Chan, H. Y. (2016). Tai chi qigong as a means to improve night-time sleep quality among older adults with cognitive impairment: a pilot randomized controlled trial. *Clin. Interv. Aging* 11, 1277–1286. doi: 10.2147/CIA.S111927

Chandra, A., Valkimadi, P. E., Pagano, G., Cousins, O., Dervenoulas, G., and Politis, M. (2019). Applications of amyloid, tau and neuroinflammation PET imaging to Alzheimer's disease and mild cognitive impairment. *Hum. Brain Mapp.* 40, 5424–5442. doi: 10.1002/hbm.24782

Chang, Y. L., Chao, R. Y., Hsu, Y. C., Chen, T. F., and Tseng, W. I. (2021). White matter network disruption and cognitive correlates underlying impaired memory awareness in mild cognitive impairment. *Neuroimage Clin.* 30:102626. doi: 10.1016/j.nicl.2021.102626

Chen, F. T., Etnier, J. L., Chan, K. H., Chiu, P. K., Hung, T. M., and Chang, Y. K. (2020). Effects of exercise training interventions on executive function in older adults: a systematic review and meta-analysis. *Sports Med.* 50, 1451–1467. doi: 10.1007/s40279-020-01292-x

Coelho, A., Fernandes, H. M., Magalhaes, R., Moreira, P. S., Marques, P., Soares, J. M., et al. (2021). Signatures of white-matter microstructure degradation during aging and its association with cognitive status. *Sci. Rep.* 11:4517. doi: 10.1038/s41598-021-83983-7

Colucci-D'Amato, L., Speranza, L., and Volpicelli, F. (2020). Neurotrophic factor BDNF, physiological functions and therapeutic potential in depression, neurodegeneration and brain cancer. *Int. J. Mol. Sci.* 21:7777. doi: 10.3390/ijms21207777

Costa, A., Caltagirone, C., and Carlesimo, G. A. (2011). Prospective memory impairment in mild cognitive impairment: an analytical review. *Neuropsychol. Rev.* 21, 390–404. doi: 10.1007/s11065-011-9172-z

Cui, L., Tao, S., Yin, H. C., Shen, Q. Q., Wang, Y., Zhu, L. N., et al. (2021). Tai chi chuan alters brain functional network plasticity and promotes cognitive flexibility. *Front. Psychol.* 12:665419. doi: 10.3389/fpsyg.2021.665419

Cui, L., Yin, H., Lyu, S., Shen, Q., Wang, Y., Li, X., et al. (2019). Tai chi chuan vs general aerobic exercise in brain plasticity: a multimodal MRI study. *Sci. Rep.* 9:17264. doi: 10.1038/s41598-019-53731-z

Da, S. R. (2015). Sleep disturbances and mild cognitive impairment: a review. *Sleep Sci.* 8, 36–41. doi: 10.1016/j.slsci.2015.02.001

Demurtas, J., Schoene, D., Torbahn, G., Marengoni, A., Grande, G., Zou, L., et al. (2020). Physical activity and exercise in mild cognitive impairment and dementia: an umbrella review of intervention and observational studies. *J. Am. Med. Dir. Assoc.* 21, 1415–1422. doi: 10.1016/j.jamda.2020.08.031

Diamond, A. (2020). Executive functions. *Handb. Clin. Neurol.* 173, 225–240. doi: 10.1016/B978-0-444-64150-2.00020-4

Driscoll, I., Hamilton, D. A., Petropoulos, H., Yeo, R. A., Brooks, W. M., Baumgartner, R. N., et al. (2003). The aging hippocampus: cognitive, biochemical and structural findings. *Cereb. Cortex* 13, 1344–1351. doi: 10.1093/cercor/bhg081

D'Rozario, A. L., Chapman, J. L., Phillips, C. L., Palmer, J. R., Hoyos, C. M., Mowszowski, L., et al. (2020). Objective measurement of sleep in mild cognitive impairment: a systematic review and meta-analysis. *Sleep Med. Rev* 52:101308. doi: 10.1016/j.smrv.2020.101308

Erickson, K. I., Voss, M. W., Prakash, R. S., Basak, C., Szabo, A., Chaddock, L., et al. (2011). Exercise training increases size of hippocampus and improves memory. *Proc. Natl. Acad. Sci. U S A* 108, 3017–3022. doi: 10.1073/pnas.1015950108

Fam, J., Sun, Y., Qi, P., Lau, R. C., Feng, L., Kua, E. H., et al. (2020). Mindfulness practice alters brain connectivity in community-living elders with mild cognitive impairment. *Psychiatry Clin. Neurosci.* 74, 257–262. doi: 10.1111/pcn.12972

Farhang, M., Miranda-Castillo, C., Rubio, M., and Furtado, G. (2019). Impact of mind-body interventions in older adults with mild cognitive impairment: a systematic review. *Int. Psychogeriatr.* 31, 643–666. doi: 10.1017/S1041610218002302

Filley, C. M., and Fields, R. D. (2016). White matter and cognition: making the connection. *J. Neurophysiol.* 116, 2093–2104. doi: 10.1152/jn.00221.2016

Fogarty, J. N., Murphy, K. J., McFarlane, B., Montero-Odasso, M., Wells, J., Troyer, A. K., et al. (2016). Taoist tai chi(R) and memory intervention for individuals with mild cognitive impairment. *J. Aging Phys. Activ.* 24, 169–180. doi: 10.1123/japa.2014-0062

Fong, D. Y., Chi, L. K., Li, F., and Chang, Y. K. (2014). The benefits of endurance exercise and tai chi chuan for the task-switching aspect of executive function in older adults: an ERP study. *Front. Aging Neurosci.* 6:295. doi: 10.3389/fnagi.2014.00295

Fox, K. C., Nijeboer, S., Dixon, M. L., Floman, J. L., Ellamil, M., Rumak, S. P., et al. (2014). Is meditation associated with altered brain structure? a systematic review and meta-analysis of morphometric neuroimaging in meditation practitioners. *Neurosci. Biobehav. Rev.* 43, 48–73. doi: 10.1016/j.neubiorev.2014.03.016

Gao, Y., Raine, A., Venables, P. H., and Mednick, S. A. (2013). The association between p3 amplitude at age 11 and criminal offending at age 23. *J. Clin. Child Adolesc. Psychol.* 42, 120–130. doi: 10.1080/15374416.2012.719458

Gómez-Isla, T., Hollister, R., West, H., Mui, S., Growdon, J. H., Petersen, R. C., et al. (1997). Neuronal loss correlates with but exceeds neurofibrillary tangles in Alzheimer's disease. *Ann. Neurol.* 41, 17–24. doi: 10.1039/d2nr04021b

Guarnieri, B., and Sorbi, S. (2015). Sleep and cognitive decline: a strong bidirectional relationship. it is time for specific recommendations on routine assessment and the management of sleep disorders in patients with mild cognitive impairment and dementia. *Eur. Neurol.* 74, 43–48. doi: 10.1159/000434629

Hardcastle, C., O'Shea, A., Kraft, J. N., Albizu, A., Evangelista, N. D., Hausman, H. K., et al. (2020). Contributions of hippocampal volume to cognition in healthy older adults. *Front. Aging Neurosci.* 12:593833. doi: 10.3389/fnagi.2020.593833

Harris, P., Fernandez, S. M., Surace, E. I., Chrem, M. P., Martin, M. E., Clarens, M. F., et al. (2015). Cognitive reserve and Aβ1–42 in mild cognitive impairment (argentina-Alzheimer's disease neuroimaging initiative). *Neuropsychiatr. Dis. Treat.* 11, 2599–2604.

Hawkes, T. D., Manselle, W., and Woollacott, M. H. (2014). Tai Chi and meditation-plus-exercise benefit neural substrates of executive function: a cross-sectional, controlled study. *J. Complement. Integr. Med.* 11, 279–288. doi: 10.1515/jcim-2013-0031

Helfrich, R. F., and Knight, R. T. (2019). Cognitive neurophysiology: event-related potentials. *Handb. Clin. Neurol.* 160, 543–558. doi: 10.1016/B978-0-444-64032-1.00036-9

Hsieh, C. C., Lin, P. S., Hsu, W. C., Wang, J. S., Huang, Y. C., Lim, A. Y., et al. (2018). The effectiveness of a virtual reality-based tai chi exercise on cognitive and physical function in older adults with cognitive impairment. *Dement. Geriatr. Cogn. Disord.* 46, 358–370. doi: 10.1159/000494659

Hu, M., Zhang, P., Li, C., Tan, Y., Li, G., Xu, D., et al. (2017). Sleep disturbance in mild cognitive impairment: a systematic review of objective measures. *Neurol. Sci.* 38, 1363–1371. doi: 10.1007/s10072-017-2975-9

Hui, S. S., Xie, Y. J., Woo, J., and Kwok, T. C. (2016). Practicing tai chi had lower energy metabolism than walking but similar health benefits in terms of aerobic fitness, resting energy expenditure, body composition and self-perceived physical health. *Complement. Ther. Med.* 27, 43–50. doi: 10.1016/j.ctim.2016.05.006

Jeong, J. H., and Kang, E. B. (2018). Effects of treadmill exercise on PI3K/AKT/GSK-3beta pathway and tau protein in high-fat diet-fed rats. *J. Exerc. Nutr. Biochem.* 22, 9–14. doi: 10.20463/jenb.2018.0002

Jones, S. A., De Marco, M., Manca, R., Bell, S. M., Blackburn, D. J., Wilkinson, I. D., et al. (2019). Altered frontal and insular functional connectivity as pivotal mechanisms for apathy in Alzheimer's disease. *Cortex* 119, 100–110. doi: 10.1016/j.cortex.2019.04.008

Jungwirth, S., Zehetmayer, S., Hinterberger, M., Tragl, K. H., and Fischer, P. (2012). The validity of amnestic MCI and non-amnestic MCI at age 75 in the pred iction of Alzheimer's dementia and vascular dementia. *Int. Psychogeriatr.* 24, 959–966. doi: 10.1017/S1041610211002870

Kasai, J. Y., Busse, A. L., Magaldi, R. M., Soci, M. A., Rosa, P. M., Curiati, J. A., et al. (2010). Effects of tai chi chuan on cognition of elderly women with mild cognitive impairment. *Einstein (Sao Paulo).* 8, 40–45. doi: 10.1590/S1679-45082010AO1470

Kong, L. J., Lauche, R., Klose, P., Bu, J. H., Yang, X. C., Guo, C. Q., et al. (2016). Tai chi for chronic pain conditions: a systematic review and meta-analysis of randomized controlled trials. *Sci. Rep.* 6:25325. doi: 10.1038/srep25325

Lam, L. C., Chau, R. C., Wong, B. M., Fung, A. W., Lui, V. W., Tam, C. C., et al. (2011). Interim follow-up of a randomized controlled trial comparing Chinese style mind body (tai chi) and stretching exercises on cognitive function in subjects at risk of progressive cognitive decline. *Int. J. Geriatr. Psychiatry* 26, 733–740. doi: 10.1002/gps.2602

Lam, L. C., Chau, R. C., Wong, B. M., Fung, A. W., Tam, C. W., Leung, G. T., et al. (2012). A 1-year randomized controlled trial comparing mind body exercise (tai chi) with stretching and toning exercise on cognitive function in older Chinese adults at risk of cognitive decline. *J. Am. Med. Dir. Assoc.* 13, 515–568. doi: 10.1016/j.jamda.2012.03.008

Langa, K. M., and Levine, D. A. (2014). The diagnosis and management of mild cognitive impairment: a clinical review. *JAMA* 312, 2551–2561. doi: 10.1001/jama.2014.13806

Lauche, R., Stumpe, C., Fehr, J., Cramer, H., Cheng, Y. W., Wayne, P. M., et al. (2016). The effects of tai chi and neck exercises in the treatment of chronic nonspecific neck pain: a randomized controlled trial. *J. Pain* 17, 1013–1027. doi: 10.1016/j.jpain.2016.06.004

Law, C. K., Lam, F. M., Chung, R. C., and Pang, M. Y. (2020). Physical exercise attenuates cognitive decline and reduces behavioural problems in people with mild cognitive impairment and dementia: a systematic review. *J. Physiother.* 66, 9–18. doi: 10.1016/j.jphys.2019.11.014

Lazar, S. W., Kerr, C. E., Wasserman, R. H., Gray, J. R., Greve, D. N., Treadway, M. T., et al. (2005). Meditation experience is associated with increased cortical thickness. *Neuroreport* 16, 1893–1897. doi: 10.1097/01.wnr.0000186598.66243.19

Leyhe, T., Muller, S., Milian, M., Eschweiler, G. W., and Saur, R. (2009). Impairment of episodic and semantic autobiographical memory in patients with mild cognitive impairment and early Alzheimer's disease. *Neuropsychologia* 47, 2464–2469. doi: 10.1016/j.neuropsychologia.2009.04.018

Li, F., Harmer, P., Voit, J., and Chou, L. S. (2021). Implementing an online virtual falls prevention intervention during a public health pandemic for older adults with mild cognitive impairment: a feasibility trial. *Clin. Interv. Aging* 16, 973–983. doi: 10.2147/CIA.S306431

Li, W., Sun, L., and Xiao, S. (2020). Prevalence, incidence, influence factors and cognitive characteristics of amnestic mild cognitive impairment among older adult: a 1-year follow-up study in china. *Front. Psychiatry* 11:75. doi: 10.3389/fpsyt.2020.00075

Li, J. Q., Tan, L., Wang, H. F., Tan, M. S., Tan, L., Xu, W., et al. (2016). Risk factors for predicting progression from mild cognitive impairment to Alzheimer's disease: a systematic review and meta-analysis of cohort studies. *J. Neurol. Neurosurg. Psychiatry* 87, 476–484. doi: 10.1136/jnnp-2014-310095

Li, B., Tang, H., He, G., Jin, Z., He, Y., Huang, P., et al. (2022). Tai Chi enhances cognitive training effects on delaying cognitive decline in mild cognitive impairment. *Alzheimers Dement.* doi: 10.1002/alz.12658. [Online ahead of print].

Li, R., Zhu, X., Yin, S., Niu, Y., Zheng, Z., Huang, X., et al. (2014). Multimodal intervention in older adults improves resting-state functional connectivity between the medial prefrontal cortex and medial temporal lobe. *Front. Aging Neurosci.* 6:39. doi: 10.3389/fnagi.2014.00039

Lim, K. H., Pysklywec, A., Plante, M., and Demers, L. (2019). The effectiveness of Tai Chi for short-term cognitive function improvement in the early stages of dementia in the elderly: a systematic literature review. *Clin. Interv. Aging* 14, 827–839. doi: 10.2147/CIA.S202055

Lin, R., Cui, S., Yang, J., Yang, H., Feng, Z., Wahner-Roedler, D. L., et al. (2021). Effects of tai chi on patients with mild cognitive impairment: a systematic review and meta-analysis of randomized controlled trials. *Biomed. Res. Int.* 2021:5530149. doi: 10.1155/2021/5530149

Liu, C. L., Cheng, F. Y., Wei, M. J., and Liao, Y. Y. (2022). Effects of exergaming-based tai chi on cognitive function and dual-task gait performance in older adults with mild cognitive impairment: a randomized control trial. *Front. Aging Neurosci.* 14:761053. doi: 10.3389/fnagi.2022.761053

Liu, L., Jiang, H., Wang, D., and Zhao, X. F. (2021). A study of regional homogeneity of resting-state functional magnetic resonance imaging in mild cognitive impairment. *Behav. Brain Res.* 402:113103. doi: 10.1016/j.bbr.2020.113103

Liu, S., Li, L., Liu, Z., and Guo, X. (2019). Long-term tai chi experience promotes emotional stability and slows gray matter atrophy for elders. *Front. Psychol.* 10:91. doi: 10.3389/fpsyg.2019.00091

Liu, Z., Li, L., Liu, S., Sun, Y., Li, S., Yi, M., et al. (2020). Reduced feelings of regret and enhanced fronto-striatal connectivity in elders with long-term tai chi experience. *Soc. Cogn. Affect. Neurosci.* 15, 861–873. doi: 10.1093/scan/nsaa111

Liu, J., Tao, J., Liu, W., Huang, J., Xue, X., Li, M., et al. (2019). Different modulation effects of tai chi chuan and baduanjin on resting-state functional connectivity of the default mode network in older adults. *Soc. Cogn. Affect. Neurosci.* 14, 217–224. doi: 10.1093/scan/nsz001

Liu, Z., Wu, Y., Li, L., and Guo, X. (2018). Functional connectivity within the executive control network mediates the effects of long-term tai chi exercise on elders' emotion regulation. *Front. Aging Neurosci.* 10:315. doi: 10.3389/fnagi.2018.00315

Lomas-Vega, R., Obrero-Gaitan, E., Molina-Ortega, F. J., and Del-Pino-Casado, R. (2017). Tai chi for risk of falls. a meta-analysis. *J. Am. Geriatr. Soc.* 65, 2037–2043. doi: 10.1111/jgs.15008

Lovatel, G. A., Elsner, V. R., Bertoldi, K., Vanzella, C., Moyses, F. S., Vizuete, A., et al. (2013). Treadmill exercise induces age-related changes in aversive memory, neuroinflammatory and epigenetic processes in the rat hippocampus. *Neurobiol. Learn. Mem* 101, 94–102. doi: 10.1016/j.nlm.2013.01.007

Lu, X., Hui-Chan, C. W., and Tsang, W. W. (2016). Changes of heart rate variability and prefrontal oxygenation during tai chi practice versus arm ergometer cycling. *J. Phys. Ther. Sci.* 28, 3243–3248. doi: 10.1589/jpts.28.3243

Martin, E., and Velayudhan, L. (2020). Neuropsychiatric symptoms in mild cognitive impairment: a literature review. *Dement. Geriatr. Cogn. Disord.* 49, 146–155. doi: 10.1159/000507078

Mitchell, A. S., Sherman, S. M., Sommer, M. A., Mair, R. G., Vertes, R. P., and Chudasama, Y. (2014). Advances in understanding mechanisms of thalamic relays in cognition and behavior. *J. Neurosci.* 34, 15340–15346. doi: 10.1523/JNEUROSCI.3289-14.2014

Montgomery, P., and Dennis, J. (2002). Physical exercise for sleep problems in adults aged 60+. *Cochrane Database Syst. Rev.* 2002:CD003404. doi: 10.1002/14651858.CD003404

Mortimer, J. A., Ding, D., Borenstein, A. R., DeCarli, C., Guo, Q., Wu, Y., et al. (2012). Changes in brain volume and cognition in a randomized trial of exercise and social interaction in a community-based sample of non-demented Chinese elders. *J. Alzheimers Dis* 30, 757–766. doi: 10.3233/JAD-2012-120079

Numakawa, T., Odaka, H., and Adachi, N. (2018). Actions of brain-derived neurotrophin factor in the neurogenesis and neuronal function and its

involvement in the pathophysiology of brain diseases. *Int. J. Mol. Sci.* 19:3650. doi: 10.3390/ijms19113650

Perrey, S. (2008). Non-invasive NIR spectroscopy of human brain function during exercise. *Methods* 45, 289–299. doi: 10.1016/j.ymeth.2008.04.005

Petersen, R. C. (2004). Mild cognitive impairment as a diagnostic entity. *J. Intern. Med.* 256, 183–194. doi: 10.1111/j.1365-2796.2004.01388.x

Petersen, R. C., Lopez, O., Armstrong, M. J., Getchius, T., Ganguli, M., Gloss, D., et al. (2018). Practice guideline update summary: mild cognitive impairment: report of the guideline development, dissemination and implementation subcommittee of the american academy of neurology. *Neurology* 90, 126–135. doi: 10.1212/WNL.0000000000004826

Petersen, R. C., Smith, G. E., Waring, S. C., Ivnik, R. J., Kokmen, E., and Tangelos, E. G. (1997). Aging, memory and mild cognitive impairment. *Int. Psychogeriatr.* 9, 65–69.

Pico-Perez, M., Radua, J., Steward, T., Menchon, J. M., and Soriano-Mas, C. (2017). Emotion regulation in mood and anxiety disorders: a meta-analysis of fMRI cognitive reappraisal studies. *Prog. Neuropsychopharmacol. Biol. Psychiatry* 79, 96–104. doi: 10.1016/j.pnpbp.2017.06.001

Picton, T. W., Stuss, D. T., Champagne, S. C., and Nelson, R. F. (1984). The effects of age on human event-related potentials. *Psychophysiology* 21, 312–325. doi: 10.1111/j.1469-8986.1984.tb02941.x

Poljak, A., Crawford, J. D., Smythe, G. A., Brodaty, H., Slavin, M. J., Kochan, N. A., et al. (2016). The relationship between plasma abeta levels, cognitive function and brain volumetrics: sydney memory and ageing study. *Curr. Alzheimer Res.* 13, 243–255. doi: 10.2174/1567205013666151218150202

Qaseem, A., Wilt, T. J., McLean, R. M., Forciea, M. A., Denberg, T. D., Barry, M. J., et al. (2017). Noninvasive treatments for acute, subacute and chronic low back pain: a clinical practice guideline from the american college of physicians. *Ann. Intern. Med.* 166, 514–530. doi: 10.7326/M16-2367

Rogge, A. K., Roder, B., Zech, A., and Hotting, K. (2018). Exercise-induced neuroplasticity: balance training increases cortical thickness in visual and vestibular cortical regions. *Neuroimage* 179, 471–479. doi: 10.1016/j.neuroimage.2018.06.065

Roth, H. L. (2012). Dementia and sleep. *Neurol. Clin.* 30, 1213–1248. doi: 10.1016/j.ncl.2012.08.013

Shaftel, S. S., Griffin, W. S., and O'Banion, M. K. (2008). The role of interleukin-1 in neuroinflammation and Alzheimer disease: an evolving perspective. *J. Neuroinflammation* 5:7. doi: 10.1186/1742-2094-5-7

Shen, X. N., Niu, L. D., Wang, Y. J., Cao, X. P., Liu, Q., Tan, L., et al. (2019). Inflammatory markers in Alzheimer's disease and mild cognitive impairment: a meta-analysis and systematic review of 170 studies. *J. Neurol. Neurosurg. Psychiatry* 90, 590–598. doi: 10.1136/jnnp-2018-319148

Shen, C. L., Watkins, B. A., Kahathuduwa, C., Chyu, M. C., Zabet-Moghaddam, M., Elmassry, M. M., et al. (2021). Tai chi improves brain functional connectivity and plasma lysophosphatidylcholines in postmenopausal women with knee osteoarthritis: an exploratory pilot study. *Front. Med. (Lausanne)* 8:775344. doi: 10.3389/fmed.2021.775344

Siu, M. Y., and Lee, D. (2018). Effects of tai chi on cognition and instrumental activities of daily living in community dwelling older people with mild cognitive impairment. *BMC Geriatr.* 18:37. doi: 10.1186/s12877-018-0720-8

Siu, M. Y., and Lee, D. (2021). Is tai chi an effective intervention for enhancing health-related quality of life in older people with mild cognitive impairment? an interventional study. *Int. J. Older People Nurs.* 16:e12400. doi: 10.1111/opn.12400

Solianik, R., Mickeviciene, D., Zlibinaite, L., and Cekanauskaite, A. (2021). Tai chi improves psychoemotional state, cognition and motor learning in older adults during the COVID-19 pandemic. *Exp. Gerontol.* 150:111363. doi: 10.1016/j.exger.2021.111363

Song, D., Yu, D. S., Li, P. W., He, G., and Sun, Q. (2019). Correlates of health-related quality of life among chinese older adults with mild cognitive impairment. *Clin. Interv. Aging* 14, 2205–2212. doi: 10.2147/CIA.S227767

Sun, Y., Yin, Q., Fang, R., Yan, X., Wang, Y., Bezerianos, A., et al. (2014). Disrupted functional brain connectivity and its association to structural connectivity in amnestic mild cognitive impairment and Alzheimer's disease. *PLoS One* 9:e96505. doi: 10.1371/journal.pone.0096505

Sungkarat, S., Boripuntakul, S., Chattipakorn, N., Watcharasaksilp, K., and Lord, S. R. (2017). Effects of tai chi on cognition and fall risk in older adults with mild cognitive impairment: a randomized controlled trial. *J. Am. Geriatr. Soc* 65, 721–727. doi: 10.1111/jgs.14594

Sungkarat, S., Boripuntakul, S., Kumfu, S., Lord, S. R., and Chattipakorn, N. (2018). Tai Chi improves cognition and plasma BDNF in older adults with mild cognitive impairment: a randomized controlled trial. *Neurorehabil. Neural Repair* 32, 142–149. doi: 10.1177/1545968317753682

Suzuki, T., Shimada, H., Makizako, H., Doi, T., Yoshida, D., Ito, K., et al. (2013). A randomized controlled trial of multicomponent exercise in older adults with mild cognitive impairment. *PLoS One* 8:e61483. doi: 10.1371/journal.pone.0061483

Tamura, Y., Ishikawa, J., Fujiwara, Y., Tanaka, M., Kanazawa, N., Chiba, Y., et al. (2018). Prevalence of frailty, cognitive impairment and sarcopenia in outpatients with cardiometabolic disease in a frailty clinic. *BMC Geriatr.* 18:264. doi: 10.1186/s12877-018-0955-4

Tan, T., Meng, Y., Lyu, J. L., Zhang, C., Wang, C., Liu, M., et al. (2022). A systematic review and meta-analysis of tai chi training in cardiorespiratory fitness of elderly people. *Evid. Based Complement. Alternat. Med.* 2022:4041612. doi: 10.1155/2022/4041612

Tannenbaum, C., Paquette, A., Hilmer, S., Holroyd-Leduc, J., and Carnahan, R. (2012). A systematic review of amnestic and non-amnestic mild cognitive impairment induced by anticholinergic, antihistamine, GABAergic and opioid drugs. *Drugs Aging* 29, 639–658. doi: 10.1007/BF03262280

Tao, J., Chen, X., Liu, J., Egorova, N., Xue, X., Liu, W., et al. (2017a). Tai chi chuan and baduanjin mind-body training changes resting-state low-frequency fluctuations in the frontal lobe of older adults: a resting-state fMRI study. *Front. Hum. Neurosci.* 11: 514. doi: 10.3389/fnhum.2017.00514

Tao, J., Chen, X., Egorova, N., Liu, J., Xue, X., Wang, Q., et al. (2017b). Tai chi chuan and baduanjin practice modulates functional connectivity of the cognitive control network in older adults. *Sci. Rep.* 7:41581. doi: 10.1038/srep41581

Tao, J., Liu, J., Egorova, N., Chen, X., Sun, S., Xue, X., et al. (2016). Increased hippocampus-medial prefrontal cortex resting-state functional connectivity and memory function after tai chi chuan practice in elder adults. *Front. Aging Neurosci.* 8:25. doi: 10.3389/fnagi.2016.00025

Tao, J., Liu, J., Liu, W., Huang, J., Xue, X., Chen, X., et al. (2017c). Tai chi chuan and baduanjin increase grey matter volume in older adults: a brain imaging study. *J. Alzheimers Dis.* 60, 389–400. doi: 10.3233/JAD-170477

Teng, C., Zhou, J., Ma, H., Tan, Y., Wu, X., Guan, C., et al. (2018). Abnormal resting state activity of left middle occipital gyrus and its functional connectivity in female patients with major depressive disorder. *BMC Psychiatry* 18:370. doi: 10.1186/s12888-018-1955-9

Tinetti, M. E., Speechley, M., and Ginter, S. F. (1988). Risk factors for falls among elderly persons living in the community. *N. Engl. J. Med.* 319, 1701–1707. doi: 10.1056/NEJM198812293192604

Tranah, G. J., Blackwell, T., Stone, K. L., Ancoli-Israel, S., Paudel, M. L., Ensrud, K. E., et al. (2011). Circadian activity rhythms and risk of incident dementia and mild cognitive impairment in older women. *Ann. Neurol.* 70, 722–732. doi: 10.1002/ana.22468

Tricco, A. C., Soobiah, C., Berliner, S., Ho, J. M., Ng, C. H., Ashoor, H. M., et al. (2013). Efficacy and safety of cognitive enhancers for patients with mild cognitive impairment: a systematic review and meta-analysis. *CMAJ* 185, 1393–1401. doi: 10.1503/cmaj.130451

Tsai, P. F., Chang, J. Y., Beck, C., Kuo, Y. F., Keefe, F. J., and Rosengren, K. (2015). A supplemental report to a randomized cluster trial of a 20-week sun-style tai chi for osteoarthritic knee pain in elders with cognitive impairment. *Complement. Ther. Med* 23, 570–576. doi: 10.1016/j.ctim.2015.06.001

Tuena, C., Mancuso, V., Stramba-Badiale, C., Pedroli, E., Stramba-Badiale, M., Riva, G., et al. (2021). Egocentric and allocentric spatial memory in mild cognitive impairment with real-world and virtual navigation tasks: a systematic review. *J. Alzheimers Dis.* 79, 95–116. doi: 10.3233/JAD-201017

Uemura, K., Shimada, H., Doi, T., Makizako, H., Tsutsumimoto, K., Park, H., et al. (2016). Reduced prefrontal oxygenation in mild cognitive impairment during memory retrieval. *Int. J. Geriatr. Psychiatry.* 31, 583–591. doi: 10.1002/gps.4363

Vanderlinden, J., Boen, F., and van Uffelen, J. (2020). Effects of physical activity programs on sleep outcomes in older adults: a systematic review. *Int. J. Behav. Nutr. Phys. Act.* 17:11. doi: 10.1186/s12966-020-0913-3

Voss, M. W., Prakash, R. S., Erickson, K. I., Basak, C., Chaddock, L., Kim, J. S., et al. (2010). Plasticity of brain networks in a randomized intervention trial of exercise training in older adults. *Front. Aging Neurosci.* 2:32. doi: 10.3389/fnagi.2010.00032

Wang, S., and Lu, S. (2022). Brain functional connectivity in the resting state and the exercise state in elite tai chi chuan athletes: an fNIRS study. *Front. Hum. Neurosci.* 16:913108. doi: 10.3389/fnhum.2022.913108

Wang, S., Rao, B., Chen, L., Chen, Z., Fang, P., Miao, G., et al. (2021). Using fractional amplitude of low-frequency fluctuations and functional connectivity in patients with post-stroke cognitive impairment for a simulated stimulation program. *Front. Aging Neurosci* 13:724267. doi: 10.3389/fnagi.2021.724267

Wang, Q., and Sheng, Y. (2016). Time effect analysis of Taijiquan on cognitive function of patients with mild cognitive impairment. *Nursing Manage.* 19, 141–145. doi: 10.1136/bmjopen-2020-042177

Wang, L. C., Ye, M. Z., Xiong, J., Wang, X. Q., and Wu, J. W.. (2021). Optimal exercise parameters of tai chi for balance performance in older adults: a meta-analysis. *J. Am. Geriatr. Soc.* 69, 2000–2010. doi: 10.1111/jgs.17094

Wang, S., Yin, H., Jia, Y., Zhao, L., Wang, L., and Chen, L. (2018). Effects of mind-body exercise on cognitive function in older adults with cognitive impairment: a systematic review and meta-analysis. *J. Nerv. Ment. Dis* 206, 913–924. doi: 10.1097/NMD.0000000000000912

Wayne, P. M., Walsh, J. N., Taylor-Piliae, R. E., Wells, R. E., Papp, K. V., Donovan, N. J., et al. (2014). Effect of tai chi on cognitive performance in older adults: systematic review and meta-analysis. *J. Am. Geriatr. Soc.* 62, 25–39. doi: 10.1111/jgs.12611

Wehner, C., Blank, C., Arvandi, M., Wehner, C., and Schobersberger, W. (2021). Effect of tai chi on muscle strength, physical endurance, postural balance and flexibility: a systematic review and meta-analysis. *BMJ Open Sport. Exerc. Med.* 7:e817. doi: 10.1136/bmjsem-2020-000817

Wei, G. X., Xu, T., Fan, F. M., Dong, H. M., Jiang, L. L., Li, H. J., et al. (2013). Can tai chi reshape the brain? A brain morphometry study. *PLoS One* 8:e61038. doi: 10.1371/journal.pone.0061038

Wu, M. T., Tang, P. F., Goh, J., Chou, T. L., Chang, Y. K., Hsu, Y. C., et al. (2018). Task-switching performance improvements after tai chi chuan training are associated with greater prefrontal activation in older adults. *Front. Aging Neurosci.* 10:280. doi: 10.3389/fnagi.2018.00280

Xie, H., Zhang, M., Huo, C., Xu, G., Li, Z., and Fan, Y. (2019). Tai chi chuan exercise related change in brain function as assessed by functional near-infrared spectroscopy. *Sci. Rep.* 9:13198. doi: 10.1038/s41598-019-49401-9

Xu, Z., Zhang, D., Lee, A. T. C., Sit, R. W. S., Wong, C., Lee, E. K. P., et al. (2020). A pilot feasibility randomized controlled trial on combining mind-body physical exercise, cognitive training and nurse-led risk factor modification to reduce cognitive decline among older adults with mild cognitive impairment in primary care. *PeerJ.* 8:e9845. doi: 10.7717/peerj.9845

Yan, Z., and Rein, B. (2022). Mechanisms of synaptic transmission dysregulation in the prefrontal cortex: pathophysiological implications. *Mol. Psychiatry* 27, 445–465. doi: 10.1038/s41380-021-01092-3

Yang, G. Y., Sabag, A., Hao, W. L., Zhang, L. N., Jia, M. X., Dai, N., et al. (2021). Tai chi for health and well-being: a bibliometric analysis of published clinical studies between 2010 and 2020. *Complement. Ther. Med.* 60:102748. doi: 10.1016/j.ctim.2021.102748

Yao, J., Song, Q., Zhang, K., Hong, Y., Li, W., Mao, D., et al. (2019). The effect of Tai Chi practice on brain white matter structure: a diffusion tensor magnetic resonance imaging study. *Res. Sports Med.* 27, 121–130. doi: 10.1080/15438627.2018.1502184

Yesavage, J. A., O'Hara, R., Kraemer, H., Noda, A., Taylor, J. L., Ferris, S., et al. (2002). Modeling the prevalence and incidence of Alzheimer's disease and mild cognitive impairment. *J. Psychiatr. Res.* 36, 281–286. doi: 10.1016/s0022-3956(02)00020-1

You, T., Ogawa, E. F., Thapa, S., Cai, Y., Zhang, H., Nagae, S., et al. (2018). Tai chi for older adults with chronic multisite pain: a randomized controlled pilot study. *Aging. Clin. Exp. Res.* 30, 1335–1343. doi: 10.1007/s40520-018-0922-0

Young, D. K. (2020). Multicomponent intervention combining a cognitive stimulation group and tai chi to reduce cognitive decline among community-dwelling older adults with probable dementia: a multi-center, randomized controlled trial. *Dementia (London)* 19, 2073–2089. doi: 10.1177/1471301218814637

Yu, A. P., Chin, E. C., Yu, D. J., Fong, D. Y., Cheng, C. P., Hu, X., et al. (2022). Tai chi versus conventional exercise for improving cognitive function in older adults: a pilot randomized controlled trial. *Sci. Rep.* 12:8868. doi: 10.1038/s41598-022-12526-5

Yue, C., Yu, Q., Zhang, Y., Herold, F., Mei, J., Kong, Z., et al. (2020a). Regular tai chi practice is associated with improved memory as well as structural and functional alterations of the hippocampus in the elderly. *Front. Aging Neurosci.* 12:586770. doi: 10.3389/fnagi.2020.586770

Yue, C., Zou, L., Mei, J., Moore, D., Herold, F., Muller, P., et al. (2020b). Tai chi training evokes significant changes in brain white matter network in older women. *Healthcare (Basel)* 8:57. doi: 10.3390/healthcare8010057

Zhao, J., Bi, W., Xiao, S., Lan, X., Cheng, X., Zhang, J., et al. (2019). Neuroinflammation induced by lipopolysaccharide causes cognitive impairment in mice. *Sci. Rep.* 9:5790. doi: 10.1038/s41598-019-42286-8

Zheng, Z., Zhu, X., Yin, S., Wang, B., Niu, Y., Huang, X., et al. (2015). Combined cognitive-psychological-physical intervention induces reorganization of intrinsic functional brain architecture in older adults. *Neural Plast.* 2015:713104. doi: 10.1155/2015/713104

Zhou, K., Liu, M., Bao, D., and Zhou, J. (2022). Effects of traditional chinese exercises on cognitive function in older adults with mild cognitive impairment: a systematic review and meta-analysis. *Front. Hum. Neurosci.* 16:849530. doi: 10.3389/fnhum.2022.849530

Frontiers in
Aging Neuroscience

Explores the mechanisms of central nervous system aging and age-related neural disease

The third most-cited journal in the field of geriatrics and gerontology, with a focus on understanding the mechanistic processes associated with central nervous system aging.

Discover the latest Research Topics

See more →

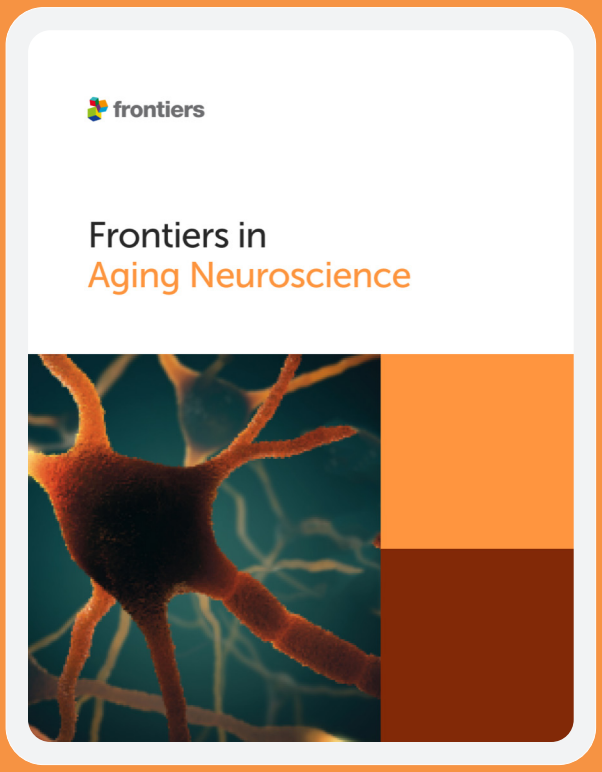

Frontiers

Avenue du Tribunal-Fédéral 34
1005 Lausanne, Switzerland
frontiersin.org

Contact us

+41 (0)21 510 17 00
frontiersin.org/about/contact